Research Infrastructure Quality Assurance

GAW Report No. 284

Report of the Third International Solar UV Radiometer Calibration Campaign (UVC-III)

13 June to 26 August 2022
Davos, Switzerland

WEATHER CLIMATE WATER

WORLD METEOROLOGICAL ORGANIZATION

GLOBAL ATMOSPHERE WATCH

Report of the Third International Solar UV Radiometer Calibration Campaign (UVC-III)

PMOD/WRC, WCC-UV

Davos, Switzerland
13 June to 26 August 2022

G. Hülsen and J. Gröbner

Chair, Publications Board
World Meteorological Organization (WMO)
7 bis, avenue de la Paix
P.O. Box 2300
CH-1211 Geneva 2, Switzerland

Tel.: +41 (0) 22 730 84 03
Email: publications@wmo.int

CONTENTS

Summary

The main task of the World Calibration Centre for UV (WCC-UV) is to assist WMO Members operating WMO/Global Atmosphere Watch (GAW) stations to link their solar UV radiation observations to the WMO/GAW reference scale through comparisons of the station instruments with the reference instruments operated by the Physical Meteorological Observatory and World Radiation Centre (PMOD/WRC). Therefore an "International Solar UV Radiometer Calibration Campaign" was organized at the WCC-UV of PMOD/WRC from 13 June to 26 August 2022.

A total of 74 solar UV radiometers from 29 countries participated in the campaign, of which 17 were from Europe. The nine different radiometer types represented at the campaign were Kipp & Zonen UV-S (18), CUV5 (3) and SUV (5), Yankee UVB-1 (7), analogue and digital Solar Light V. 501 (16/10), EKO MS (5) and five other miscellaneous types. The broadband filter weighting functions were mostly an approximation to the erythemal action spectrum, with a few designated UVB, UVA and UVG.

The two reference spectroradiometers QASUME and QASUMEII of the WCC-UV that operated during the campaign agreed within ±2%. The atmospheric conditions during the campaign varied between fully overcast to clear skies and allowed a reliable calibration for all instruments.

The calibration procedure used the spectral and the angular response functions measured in the laboratory, while the signal responsivity was obtained by an outdoor comparison of solar UV measurements with the reference spectroradiometers, yielding expanded uncertainties (k=2) of 3.1% to 12%.

The measurements of the solar UV radiometers were analysed both with the calibration obtained during this campaign and with the calibration previously used by the home institutes. The average age of the user calibration was three years prior to this campaign (e.g. 2019) and 34 out of the 74 instruments used a single calibration factor, instead of the suggested calibration matrix [5, 7, 8]. The relative differences between the measurements using the user calibration and the one from this campaign varied between 0.8% to more than 50% for specific instruments. Before the calibration 28 radiometers measured the UV irradiance within ±5%, 37 within ±10% and 23 with a higher measurement error. For 15 radiometers no initial calibration was supplied. After the calibration all radiometers measured within 5%.

1. INTRODUCTION

The international solar UV radiometer calibration campaign was held at the World Calibration Centre for UV (WCC-UV) of the Physikalisch-Meteorologisches Observatorium Davos, World Radiation Centre (PMOD/WRC) from 13 June to 26 August 2022.

The campaign was organized to fulfil the main task of the WCC-UV, which is to assist WMO Members operating WMO/GAW stations to link their solar UV radiation observations to the WMO/GAW reference scale through comparisons of the station instruments with the reference instruments operated by PMOD/WRC. The absolute calibration of the WCC-UV is supported by calibration and measurement capabilities (CMC's) within the CIPM MRA[1].

The objective of the campaign was to provide a calibration traceable to the WCC-UV reference for all participating radiometers, with the aim of homogenizing solar UV measurements in all participating countries.

The specific tasks of the campaign were: (a) to individually characterize each radiometer with respect to the relative spectral and angular responsivity in the laboratory following the standard operating procedures of the WCC-UV, and (b) to provide an absolute calibration factor that was obtained by direct comparison of solar irradiance measurements with the WCC-UV reference spectroradiometers on the roof platform of PMOD/WRC.

This solar UV radiometer calibration campaign followed four similar campaigns held in:

- 1995 in Helsinki, Finland [1]
- 1999 in Thessaloniki, Greece [2]
- 2006 in Davos, Switzerland [3] and 2017 also in Davos [10, 11]

74 solar UV radiometers from 42 institutes participated at this calibration campaign. Most radiometers were reference instruments within their respective regional or national networks.

The measurement campaign at PMOD/WRC allowed the original calibration to be compared with the WCC-UV-traceable calibration. It also is an estimation of the variability between solar UV radiometer measurements based on calibrations originating from different sources (manufacturer or national calibration laboratories).

The result of the campaign was the release of calibration certificates for all participating instruments traceable to the international system of units (SI) via the WCC-UV reference.

[1] PMOD/WRC follows the requirements for the competence of testing and calibration laboratories according to ISO/IEC 17025. PMOD/WRC is a designated institute for solar irradiance of the Swiss Federal Office of Metrology, the Swiss signatory of the CIPM MRA (International Committee for Weights and Measures – Mutual Recognition Arrangement).

2. SETUP AND MEASUREMENTS

The calibration and intercomparison campaign took place at PMOD/WRC, Switzerland. The period from 13 June to 26 August 2022 was selected for the calibration. The measurement platform is located on the roof of PMOD/WRC at 1610 m a.s.l., latitude 46.8 N, longitude 9.83 E. The measurement site is in the Swiss Alps and its horizon is limited by mountains; the Davos valley runs NE to SW.

Figure 1. Roof platform of PMOD/WRC.

The laboratory characterizations – spectral and angular responsivity measurements – were completed at the beginning of the campaign. Then the radiometers were installed on the roof platform of PMOD/WRC. Most radiometers arrived at the beginning of June. Late arrivals could participate in the last days of the scheduled campaign period.

The QasumeII [4] spectroradiometer was installed in April 2022 and operated continuously until the beginning of October. In addition, the Qasume spectroradiometer was installed from 12 to 14 July for comparison.

The measurements used for the calibration were obtained in the period 29 June to 25 August, totalling 58 measurement days. The measurement conditions in summer 2022 were very variable, with periods of clear sky, clouds, rain and snow. Figures 2 and 3 show the temperature, precipitation and the UV Index at Davos during the period of the campaign.

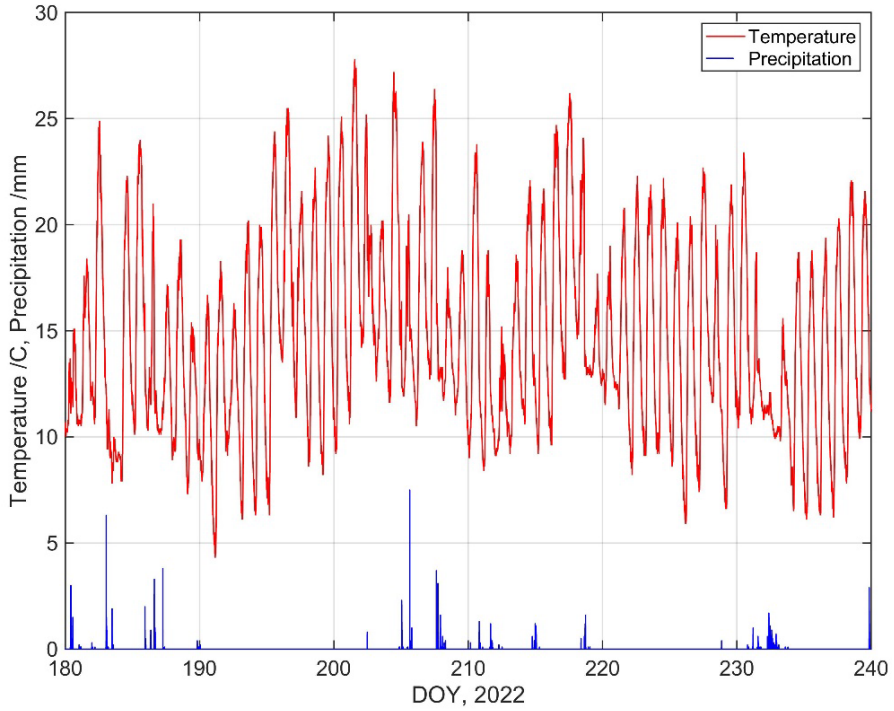

Figure 2. Temperature and precipitation during the period of the campaign.

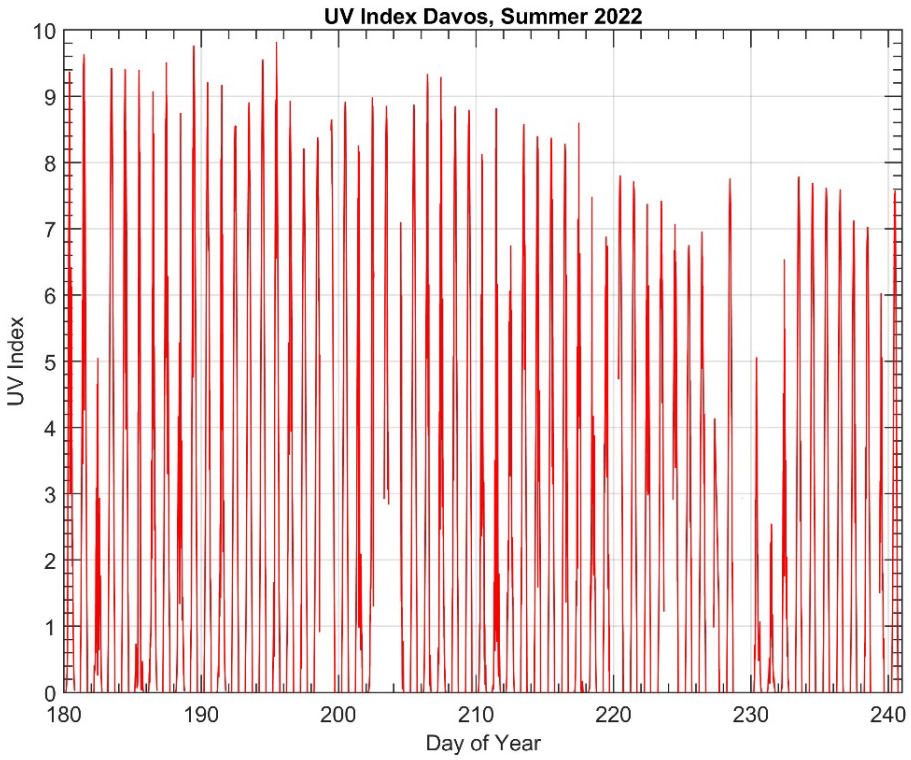

Figure 3. UVI index at Davos during the period of the campaign.

The total column ozone was obtained from Brewer spectrophotometer #163 located on the roof platform of PMOD/WRC, next to QASUMEII. The total column ozone varied between 240 DU and 371 DU with a mean value of 302 DU over the measurement period. All available measurements during the campaign period are shown in Figure 4.

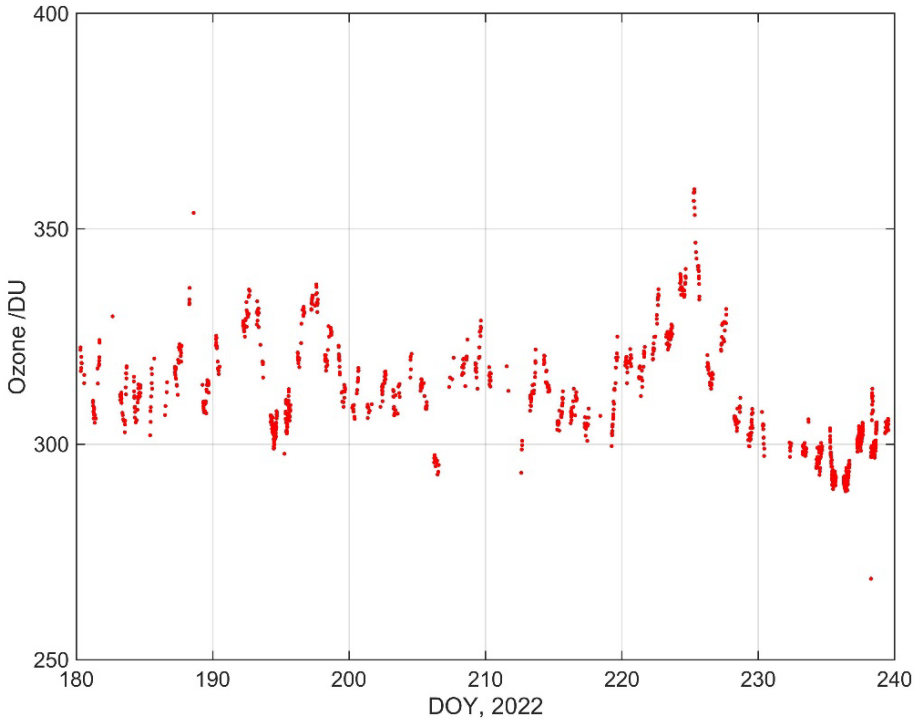

Figure 4. Total column ozone over Davos during the period of the campaign.

3. INSTRUMENTATION FOR THE ABSOLUTE CALIBRATION

The 74 solar UV radiometers from 42 institutes of 29 countries that took part in this campaign are shown in Table 1. The standard product of these instruments is solar irradiance weighted by the respective functions shown in the last column of Table 1: UVE (erythemal) [5], UVB (uniform weighting between 280 nm and 315 nm), UVB320 (uniform weighting between 280 nm and 320 nm), UVA (uniform weighting between 315 nm 400 nm) and UVG (uniform weighting between 280 nm and 400 nm).

Table 1. Summary of participating radiometers.

Number	Manufacturer	Type	Weighting
10	Kipp & Zonen	UV-S-E-T	UVE
2	Kipp & Zonen	UV-S-B-T	UVB
3	Kipp & Zonen	UV-S-A-T	UVA
3	Kipp & Zonen	UV-S-AE-T	UVA+UVE
3	Kipp & Zonen	CUV5	UVG
6	Kipp & Zonen	SUV-E	UVE
1	Kipp & Zonen	SUV-B	UVB
1	Kipp & Zonen	SUV-A	UVA
13	Solar Light	501A UVE	UVE
3	Solar Light	501A UVA	UVA
7	Solar Light	501A-Digital UVE	UVE
3	Solar Light	501A-Digital UVA	UVA
6	Yankee Environmental Systems	UVB-1	UVE
1	Yankee Environmental Systems	UVB-1	UVB320
3	EKO Instruments Co.	MS-11S UVB	UVB
1	EKO Instruments Co.	MS-11S UVA	UVA
1	EKO Instruments Co.	MS-212W	UVE
1	Aerospace Newsky Technology Co.	FS-UVA9	UVA
1	Aerospace Newsky Technology Co.	FS-UVB9	UVB
1	CMS Schreder	CMS-UV-E-T	UVE
1	Deltha Ohm	DELTA-LP UVB 02	UVE
1	Indium Sensor GmbH	IS-1E.1W-081	UVE
1	Sglux GmbH	SGLUX	UVE
1	Scienterra Ltd.	Dosimeter	UVA+UVE
1	UVIOS	Model	UVE

The analogue voltages of the radiometers were acquired with a Campbell CR7 logger (reference: Fluke 5720A Calibrator; calibration date: 18 February 2022) every 10 s. The EKO MS-212W radiometers used their own data acquisition system. The data from the digital SL-501 data acquisition recorders were read out using a custom interface with an interval of 2 s. Their gain factor was set to 10 to improve their resolution.

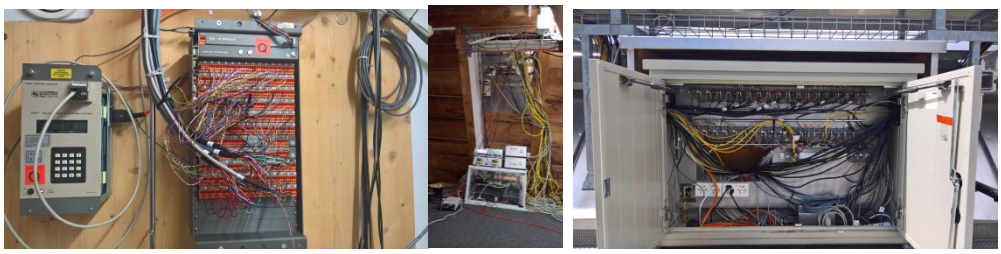

Figure 5. CR7 logger (left) and connection panels 1 and 2.

The data of the spectroradiometer QASUMEII provided the reference for the outdoor measurements. The spectroradiometer measured solar irradiance spectra in the range 290 nm to 420 nm every 15 or 30 minutes.

Figure 6. Picture of some of the participating radiometers prior to installation on the roof platform.

Table 2. List of participating radiometers.
The radiometers belonging to PMOD/WRC are shown in green.

Type	SN	Country	Institute	Calibration methodology
KZ UV-S-E-T	560	Switzerland	PMOD/WRC	C, f_n, Coscor
KZ UV-S-E-T	110053	Spain	National Institute for Aerospace Technology – INTA	C
KZ UV-S-E-T	150110	Estonia	Republic of Estonia Environment Agency	C, f_n, Coscor
KZ UV-S-E-T	160158	France	Université de la Réunion – LACy	C, f_n, Coscor
KZ UV-S-E-T	170200	France	Sécurité Solaire	C
KZ UV-S-E-T	170201	France	Reuniwatt	C
KZ UV-S-E-T	170204	South Africa	NMISA	C, f_n, Coscor
KZ UV-S-E-T	170213	Argentina	Servicio Meteorologico Nacional	C
KZ UV-S-E-T	160142	Spain	Agencia Estatal de Meteorología (AEMET)	C, f_n, Coscor
KZ UV-S-E-T	070643	Spain	Universidad de Extremadura, Departamento de Fisica	C, f_n, Coscor
KZ UV-S-B-T	090015	France	Météo-France	C, f_n, Coscor
KZ UV-S-B-T	150127	Greece	National Observatory of Athens	C
KZ UV-S-A-T	170143	Argentina	Servicio Meteorologico Nacional	C
KZ UV-S-A-T	080005	Spain	Izaña Atmospehric Research Centre (IARC)	C, f_n, Coscor
KZ UV-S-A-T	150084	Greece	National Observatory of Athens	C
KZ UV-S-AE-T	120023	Ecuador	Instituto Nacional de Meteorología e Hidrología	C, f_n, Coscor
KZ UV-S-AE-T	140040	France	ENERGY-Lab (University of La Réunion)	C, f_n, Coscor
KZ UV-S-AE-T	080003	Italy	Arpa Piemonte	C, f_n, Coscor
KZ CUV5	2022	Netherlands	OTT Hydromet	C
KZ CUV5	100114	China	China Meteorological Administration	C
KZ CUV5	200723	China	Zhonghuan TIG (Tianjin) Meteorological Instruments Co., Ltd	C
SUV-E	160003	Netherlands	OTT Hydromet	C
SUV-E	180005	Germany	Meteorologisches Institut München, LMU	C
SUV-E	200082	Hong Kong	Hong Kong Observatory	C
SUV-E	200083	Hong Kong	Hong Kong Observatory	C
SUV-E	200090	Netherlands	OTT Hydromet	C
SUV-E	200095	Italy	ARPA Valle d'Aosta	C, f_n
SUV-B	210285	China	Zhonghuan TIG (Tianjin) Meteorological Instruments Co.,Ltd	C
SUV-A	210194	China	Zhonghuan TIG (Tianjin) Meteorological Instruments Co.,Ltd	C
SL501A UVE	1453	Finland	Finnish Meteorological Institute	C, f_n, Coscor
SL501A UVE	1492	Switzerland	PMOD/WRC	C, f_n, Coscor
SL501A UVE	1493	Switzerland	PMOD/WRC	C, f_n, Coscor
SL501A UVE	1905	Switzerland	Federal Office of Meteorology and Climatology MeteoSwiss	C, f_n, Coscor
SL501A UVE	2872	Switzerland	PMOD/WRC	C, f_n, Coscor

Type	SN	Country	Institute	Calibration methodology
SL501A UVE	3860	Switzerland	PMOD/WRC	C, f_n, Coscor
SL501A UVE	3862	Switzerland	PMOD/WRC	C, f_n, Coscor
SL501A UVE	3863	Switzerland	PMOD/WRC	C, f_n, Coscor
SL501A UVE	3864	Switzerland	PMOD/WRC	C, f_n, Coscor
SL501A UVE	3865	Switzerland	PMOD/WRC	C, f_n, Coscor
SL501A UVE	19488	Mexico	Institute de Geofísica, Universidad Nacional Autónoma de México	C, f_n, Coscor
SL501A UVE	23169	USA	National Renewable Energy Laboratory	C
SL501A UVE	26780	Chile	Dirección Meteorológica de Chile	C
SL501A UVA	2875	Switzerland	PMOD/WRC	C, f_n, Coscor
SL501A UVA	2876	Switzerland	PMOD/WRC	C, f_n, Coscor
SL501A UVA	2877	Switzerland	PMOD/WRC	C, f_n, Coscor
501A-Digital UVE	0922	Sweden	Swedish Meteorological and Hydrological Institute (SMHI)	C, f_n, Coscor
501A-Digital UVE	0936	Poland	IMGW-PIB	C, f_n, Coscor
501A-Digital UVE	1120	Poland	IMGW-PIB	C, f_n, Coscor
501A-Digital UVE	2733	Czech Republic	CHMI, Solar and Ozone Observatory	C, f_n, Coscor
501A-Digital UVE	4811	Slovakia	Slovak Hydrometeorological Institute	C, f_n, Coscor
501A-Digital UVE	16723	Argentina	Servicio Meteorologico Nacional	C, f_n, Coscor
501A-Digital UVE	21883	Korea	National Institute of Meteorological Sciences	C
501A-Digital UVA	16724	Korea	National Institute of Meteorological Sciences	C
501A-Digital UVA	16725	Korea	National Institute of Meteorological Sciences	C
501A-Digital UVA	21904	Korea	National Institute of Meteorological Sciences	C
YES UVB-1	000904	USA	NOAA	C, f_n, Coscor
YES UVB-1	010938	Switzerland	PMOD/WRC	C, f_n, Coscor
YES UVB-1	030520	Spain	Agencia Estatal de Meteorología (AEMET)	C, f_n, Coscor
YES UVB-1	010925	Serbia	University Navi Sad	C
YES UVB-1	150703	Spain	Izaña Atmospehric Research Centre (IARC)	C
YES UVB-1	920906	France	LOA/CNRS/University of Lille	C, f_n, Coscor
YES UVB-1	990506	Hong Kong	Hong Kong Observatory	C, f_n, Coscor
MS-11S UVB	2200102	Netherlands	EKO Instruments	C
MS-11S UVB	2200103	China	Macao Meteorological and Geophysical Bureau	C
MS-11S UVB	21346007	China	Macao Meteorological and Geophysical Bureau	C

Type	SN	Country	Institute	Calibration methodology
MS-10S UVA	10S220010	Japan	EKO Instruments	C
MS-212W	S11044.01	Belgium	BIRA IASB	C, f_n, Coscor
FS-UVA9	5239	China	Aerospace Newsky Technology Co., Ltd.	C
FS-UVB9	3214	China	Aerospace Newsky Technology Co., Ltd.	C
CMS-UV-E-T	CMS16113	Austria	Institute of Biomedical Physics, Innsbruck Medical University	C, fn
DELTA-LP UVB 02	11028751	Italy	Centro Tecnico per la Meteorología	C
IS-1E.1W-081	16799/22	Germany	Indium Sensor GmbH	C
SGLUX	3001	Germany	The Federal Office for Radiation Protection	C
Dosimeter	3000	New Zealand	Scienterra Ltd.	None
Model	UVIOS2	Greece/ Switzerland	National Observatory of Athens and PMOD/WRC	

4. LABORATORY CHARACTERIZATION

The spectral and angular responsivity functions (SRF and ARF) of the radiometers were measured in the WCC-UV laboratory at PMOD/WRC. The method is described in the following four quality management documents: QM-PD-UV-0045 and QM-SOP-UV-0062 (SRF); QM-PD-UV-0043 and QM-SOP-UV-0060 (ARF)[2].

4.1 Relative spectral response facility

The relative spectral response facility consists of an Acton SP2500 double monochromator with gratings of 2400 lines/mm. The wavelength can be selected within the range 200 nm to 1200 nm and the chosen slit width yields a nearly triangular slit function with a full width at half maximum of 2.0 nm. The radiation of a 500 W Xenon lamp is focused onto the entrance slit. A microlens array installed after the exit slit produces a homogeneous 12 mm x 12 mm reference plane.

Behind the microlens array, a quartz plate mounted at 45° (relative to the vertical) transmits about 92% of the radiation towards the test detector and about 8% is deflected towards a photodiode, which is used to monitor the stability of the monochromator signal.

Due to the large receiving surfaces of the radiometers only part of those detectors could be illuminated by the monochromatic light source. Thus, spatial inhomogeneities of the receiving surface of the radiometer were not considered during the SRF measurement.

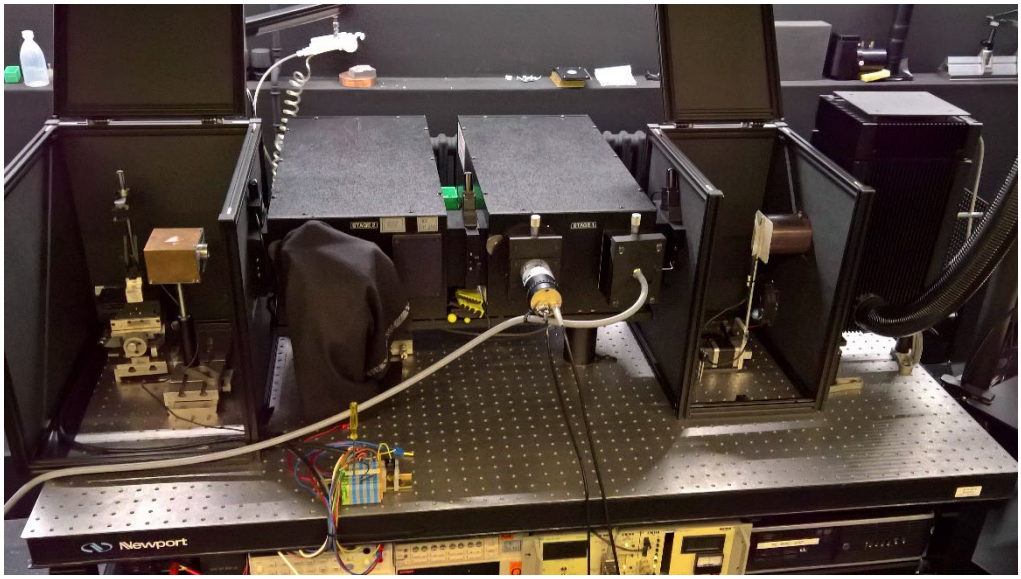

Figure 7. Spectral Response Setup of the WCC-UV.

The relative spectral throughput was determined by measuring the outgoing radiation with a reference silicon diode and was verified using the QASUME spectroradiometer between 270 nm and 420 nm, with a step of 2 nm.

The wavelength scale of the SRF setup was determined by two methods which produced equivalent results:

- A mercury discharge lamp was placed at the entrance of the monochromator and the throughput measured with a photodiode was used to determine the slit function and thus the wavelength offset.

[2] The QM documents mentioned in the manuscript are available on request.

- The slit function measurements of the complete setup (with Xe-Lamp source) with the QASUME spectroradiometer allowed the determination of the wavelength dispersion.

The variability of the radiometer dark signal was monitored for five minutes prior to the SRF measurement, as an indicator of the minimum signal to noise ratio of the radiometer. The SRF measurement itself was obtained over the wavelength range 420 nm down to 270 nm with a step size of 2 nm.

The Solar Light data-loggers of the digital SL501 radiometers were set to a sensitivity of 10 to increase the resolution of the stored measurements. To further increase the signal to noise ratio, the output signal was sampled ten to twenty times at each wavelength setting of the monochromatic light source.

The SRF was obtained from the measurements by subtracting the dark signal measured before initiating the wavelength scan, dividing the result by the relative spectral throughput of the setup and normalizing it to the maximum signal. A sample SRF of a typical radiometer is shown in Figure 8.

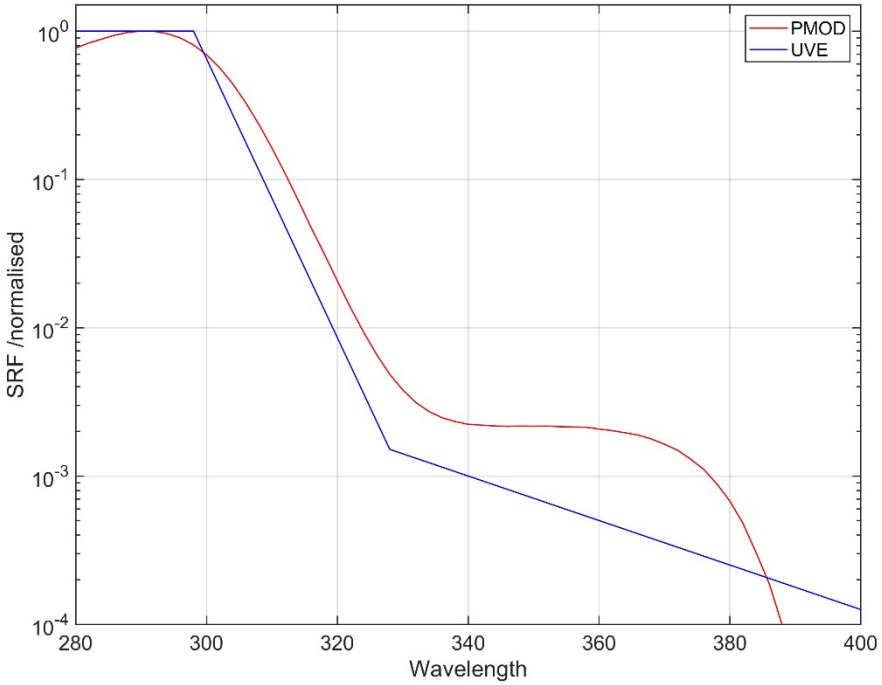

Figure 8. SRF of a KZ radiometer and the CIE erythema action spectrum (UVE).

4.2 Angular response facility

The angular response function of the radiometers was measured on a 3 m long optical bench. A 1000 W Xenon lamp was mounted at one end of the optical bench and produced a collimated radiation source. The detector was mounted on a goniometer at the other end with the vertical rotation axis passing through the plane of the receiving surface of the radiometer. The resolution of the rotation stage was 29642 steps per degree, e.g. 0.012°. The homogeneity of the radiation at the detector reference plane was measured and optimized to better than 1% over the receiving surface area of the detector. A baffle was placed in the beam path to reduce stray light and a WG305 filter with a 50% cut off at 303 nm removed radiation below approx. 300 nm.

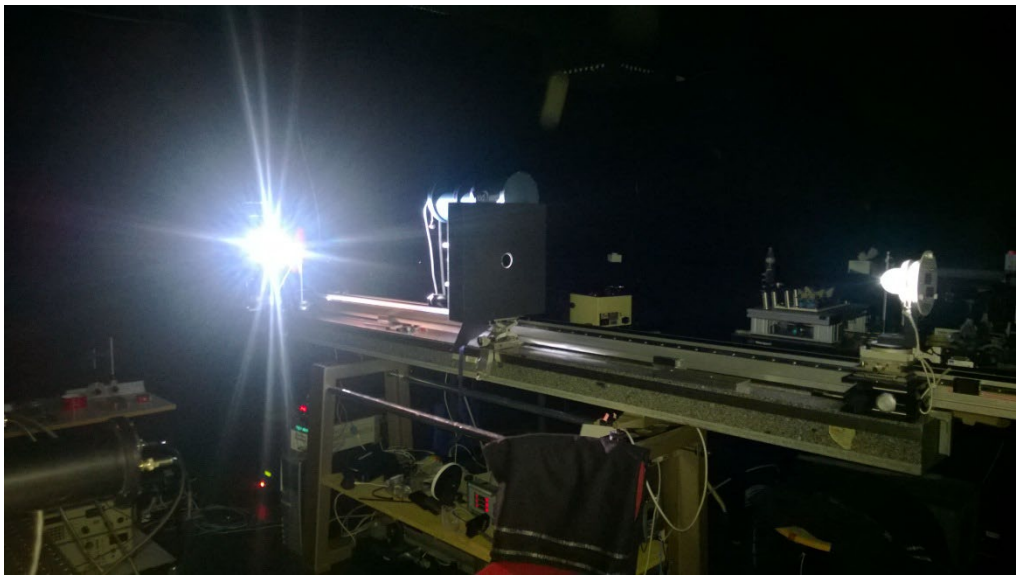

Figure 9. Angular response setup of the WCC-UV.

The alignment of the radiometer used a mirror tool, which reflected a laser beam along the optical axis. This method provided an adjustment precision of better than 0.1°.

The measurements were performed in two orientations of the detector so that the angular response function could be determined for the four quadrants N, S, E, W; the N orientation being defined by the connector of the radiometer.

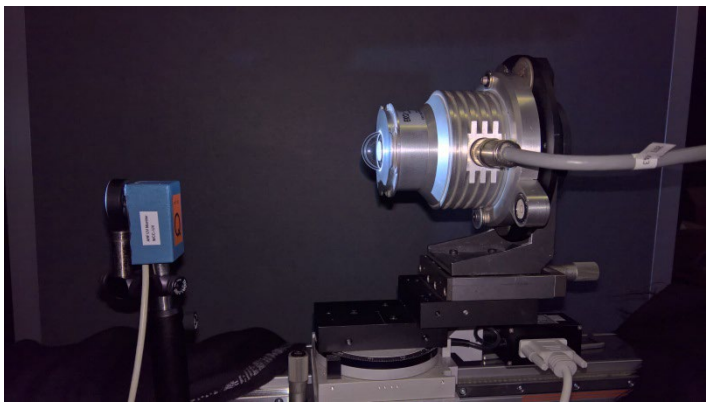

Figure 10. Mounting of an EKO MS-212W radiometer onto the ARF setup.

The ARF for each quadrant was obtained by normalizing the measurements at each angle to the reference measurement at normal incidence. The final ARF was obtained by averaging the measurements of the four quadrants. The cosine error was calculated from the ARF by assuming an isotropic radiation distribution and integrating it over the whole hemisphere. Some instruments showed deviations between the four quadrants, which could be an indication of a tilt of the internal detector relative to the optical axis. Depending on the mounting of the radiometer this tilt led to systematic diurnal variations of the solar measurements.

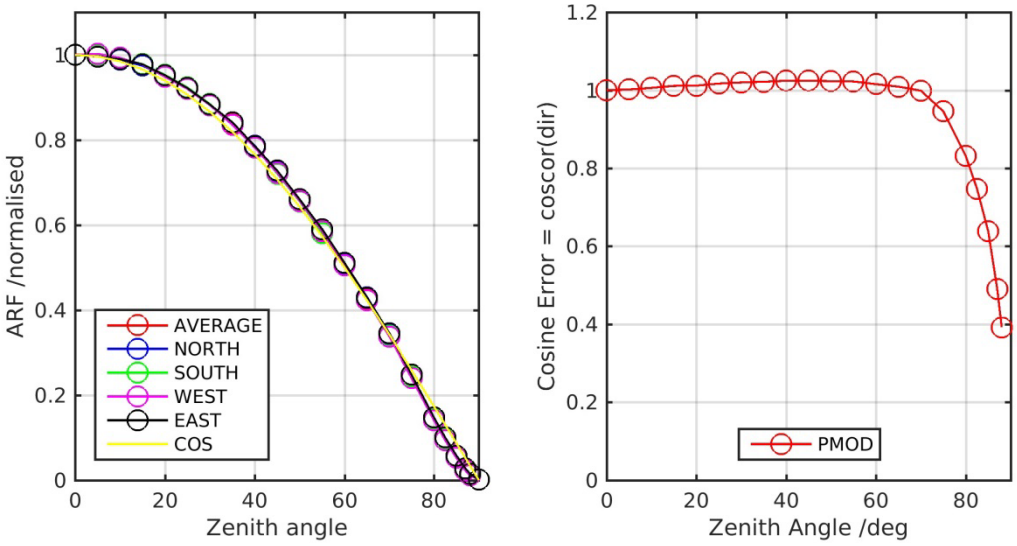

Figure 11. ARF of a KZ radiometer (left) and the corresponding cosine error (right).

5. CALCULATION OF THE CALIBRATION FACTORS

The absolute calibration measurements were carried out on the roof of PMOD/WRC. The method is described in the two quality management documents QM-PD-UV-0041 and QM-SOP-UV-0058. A detailed description can be found in [6]. In the following the main steps of the procedure are summarized.

The calculation of the weighted irradiance, E_{CIE}, from the radiometer data follows the equation published in [6, 7]:

$$E_{CIE} = (U_d - U_{offset}) \cdot C \cdot f_n(SZA, TO_3) \cdot Coscor \qquad \textbf{(1)}$$

where U_d and U_{offset} are the raw and dark signals from the radiometer respectively; C represents the absolute calibration factor determined for a solar zenith angle, SZA, of 40° and total column ozone, TO_3, of 300 DU. The conversion function, f_n, converts the detector responsivity weighted solar irradiance to erythemal weighted irradiance (or other weighting function, see Section 3)[3]. By definition the function f_n is normalized to unity for a total ozone column of 300 DU and a solar zenith angle of 40°. *Coscor* corrects for the detector cosine error. The dark offset, U_{offset}, is determined during every night as the average over all measurements. For the campaign, a fixed time window between 0 to 4 UT and 20 to 24 UT was chosen.

5.1 Spectral correction function, fn

The conversion function, f_n, accounts for the mismatch of the detector spectral responsivity and the nominal weighting function and is calculated as

$$f(SZA, TO_3) = \frac{\int CIE(\lambda) E_{glo}(\lambda) d\lambda}{\int SRF(\lambda) E_{glo}(\lambda) d\lambda} = f_n \cdot f(40°, 300\ DU) \qquad \textbf{(2)}$$

where E_{glo} represents a set of solar spectra calculated with a radiative transfer model[4] for different *SZA* and TO_3. The SRF is obtained from the laboratory measurement described above, and CIE represents the selected action spectrum.

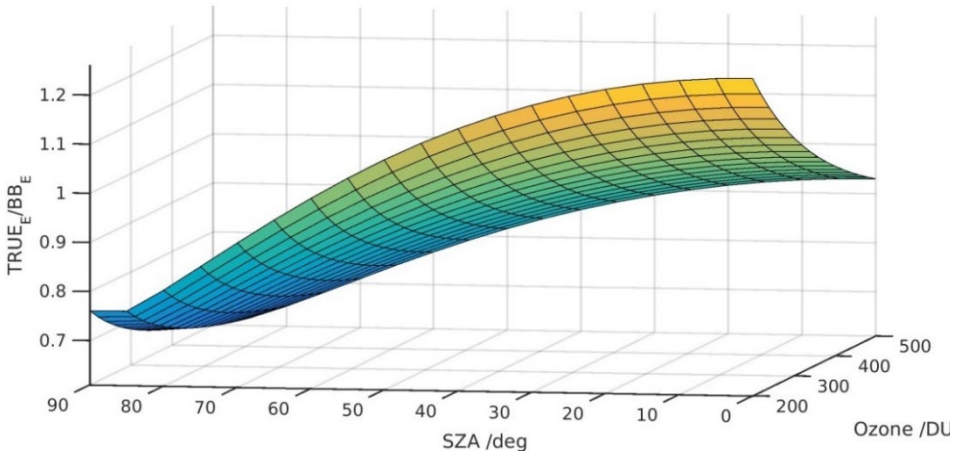

Figure 12. Spectral correction function fn of a KZ radiometer.

[3] Some users calculate f_n^* with a cosine correction function included.
[4] Model spectra were obtained using the sdisort solver of libRadtran 1.1 with the following input parameters: 16 Streams, Standard atmosphere midlatitude summer (afglms), Albedo 0.035, AOD: α=1.6 β=0.01, Altitude 0 m a.s.l., Pressure 1013.25 mbar, SSA 0.95, g 0.76, total ozone column 300 DU.

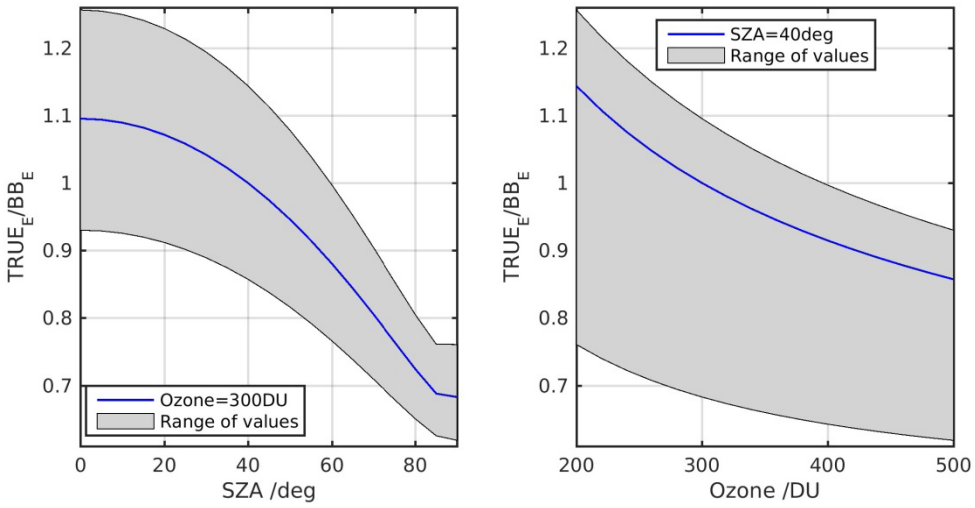

Figure 13. Spectral correction function fn of a KZ radiometer relative to the SZA (left) for a range of total ozone(0 DU – 500 DU) and total ozone column (right) for a range of SZA (0 deg – 90 deg).

5.2 Cosine correction function, Coscor

The angular response of solar UV radiometers usually deviates significantly from the nominal cosine response. The cosine correction function, *Coscor,* is used to correct the data for this effect. The following equations illustrate the derivation of *Coscor*:

$$f_{dir} = \frac{ARF(\theta)}{cos(\theta)}, \quad \textbf{(3)}$$

$$f_{dif} = 2 \cdot \int_0^{pi/2} ARF(\theta)\, sin(\theta) d\theta, \quad \textbf{(4)}$$

$$f_{glo} = f_{dir} \frac{E_{dir}}{E_{glo}} + f_{dif} \frac{E_{dif}}{E_{glo}}, \quad \textbf{(5)}$$

where f_{dir} is the direct cosine error of the radiometer for SZA θ, f_{dif} represents the diffuse cosine error and f_{glo} the global cosine error of the radiometer. E_{glo} is the same set of solar spectra as used in Equation 2. E_{dir} and E_{dif} are the direct and diffuse components of the solar radiation.

This correction depends on the radiation distribution impinging on the radiometer. For solar UV radiation, the cosine correction function depends on the relative fraction of direct and diffuse radiation, and thus on the atmospheric conditions and the solar zenith angle. The cosine correction function calculated for the radiometers assumed an isotropic diffuse radiation distribution since no measurements of the radiation distribution were performed; the fraction of direct, E_{dir}, and diffuse radiation, E_{dif}, was modelled by a radiative transfer model[5] as a function of the solar zenith angle. For the determination of the calibration factor during the campaign, two cases were distinguished:

- Clear sky: A cosine correction function *Coscor*=1/f_{glo} dependent on the SZA was used
- Diffuse sky: Only the diffuse cosine correction factor *Coscor*=1/f_{dif} was applied to the calibration

This simple approximation results in substantial uncertainties especially during rapidly changing cloud conditions. Therefore, only the clear or completely overcast sky data were used for the calibration.

[5] Identical model parameters as defined in Section 5.1

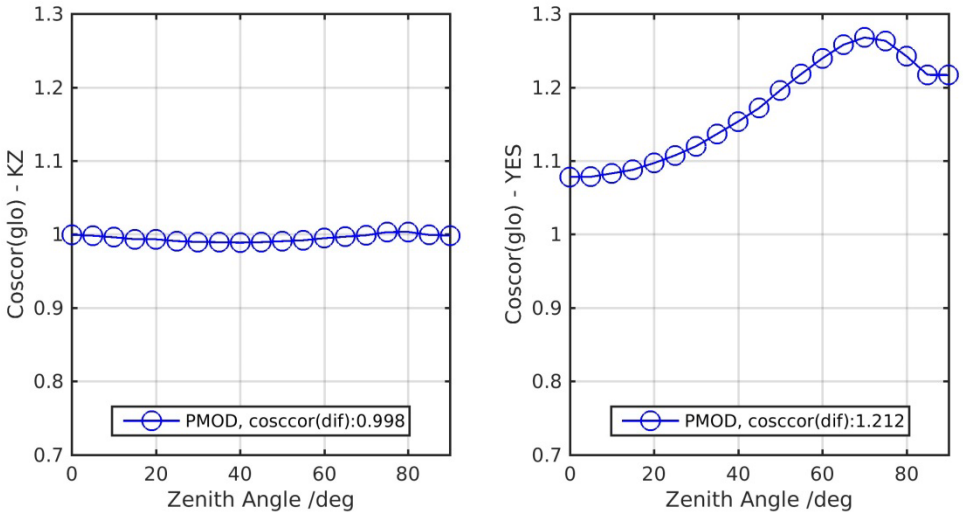

Figure 14. Clear sky cosine correction function (fglo) of a KZ (left) and a YES radiometer (right).

5.3 Absolute calibration factor C

The calibration factor *C,* is obtained by comparison to the solar spectrum measured by the spectroradiometer weighted with the SRF of the radiometer (E_d). Thus,

$$C_i = \frac{E_d}{U_d - U_{offset}} \cdot \frac{1}{Coscor} \cdot f(40°, 300DU), \qquad \textbf{(6)}$$

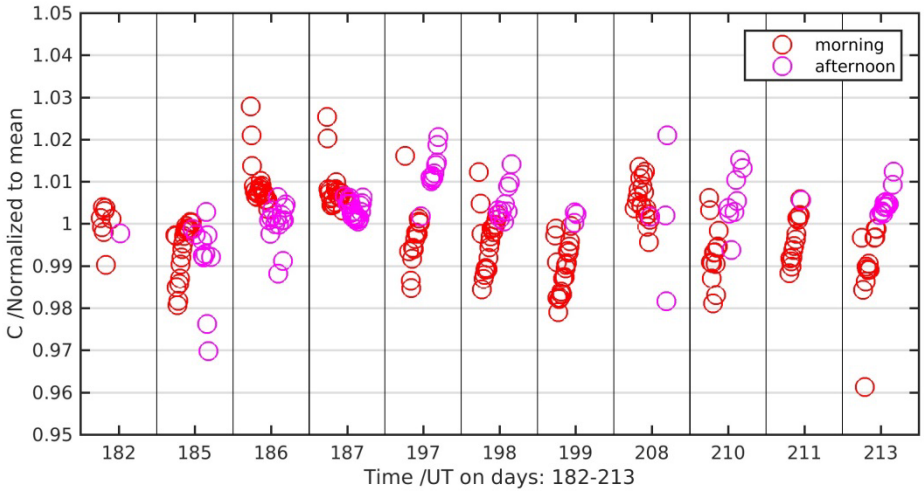

Figure 15. Calibration factors Ci determined for the campaign period for a KZ radiometer. The plots show the inverse of Ci as defined in Equation (6) to facilitate the interpretation. A smaller calibration factor means a smaller signal measured with the radiometer.

Figure 15 shows the variability in calibration factor, C_i, derived from a series of measurements throughout the campaign and used in the uncertainty evaluation. The total absolute calibration factor, *C*, is the mean over C_i.

6. UNCERTAINTY BUDGET

6.1 WCC-UV solar UV radiometer calibration

The uncertainty budget for the calibration of solar UV radiometers is defined in the quality management document QM-OA-UV-0036 and published in [11]. The expanded uncertainty is composed of the following uncertainty contributions according to Equation 6:

- $\mathbf{E_d}$ is the detector weighted spectrum, recorded by the reference spectroradiometer (see Table 4)
- $\mathbf{U_d}$ is the signal of the solar UV radiometer, averaged over the recording time of the spectroradiometer
- $\mathbf{U_{offset}}$ is the dark signal of the solar UV radiometer; calculated daily
- **Cd** is the variability of the calibration factor during the calibration period (see Figure 15 as example)
- **fvar** accounts for the mismatch of the measured and modelled correction function, ***fn***
- **dSRF**: The uncertainty of the SRF measurement is composed of the extrapolation to 400 nm as well as the measurement uncertainty of the SRF itself

The uncertainty of the cosine correction (***Coscor***) does not add to the total uncertainty because it is included through the diurnal variability of the calibration factor C (**Cd**).

The nominal uncertainty budget is summarized in Table 3 according to [14].
The expanded uncertainties stated on the individual certificates issued for the campaign are calculated from the actual data of the specific radiometer calibration and these deviate slightly from the values shown in Table 3. In the table, xi represents the value or range of the measurand, [E] represents the corresponding unit, Type A/B represents the type of uncertainty evaluation, nui the number of degrees of freedom, and u(xi) the corresponding uncertainty.

Table 3. Uncertainty budget for the calibration of solar UV radiometers.

Quantity	xi	[E]	Type	Distribution	nui	u(xi)	[E]
E_d	1–10	UVI	B	Normal	inf	1.1	%
U_d	0–1	V	B	Rectangular	inf	0.2	%
U_{offset}		V	B	Rectangular	inf	0.25	%
Cd	0.2	$Wm^{-2}nm^{-1}V^{-1}$	A	Normal	~3	0.6	%
fvar			B	Rectangular	inf	0.6	%
dSRF			B	Rectangular	Inf	0.6	%
					u(C)	**1.55**	**%**
					u(C)95	**3.1**	**%**

6.2 Manufacturer calibrated solar UV radiometers

Most solar UV radiometers are delivered to the customers either with a certificate of calibration or with their electronic amplifier adjusted to set a nominal relationship between UV irradiance and radiometer output signal. At the campaign some participants sent the radiometer together with this certificate where the uncertainty of the calibration should have been stated, which was not always the case.

6.3 Reference spectroradiometer QASUMEII

The uncertainty budget for spectral solar UV irradiance measurements using QASUME and QASUMEII is summarized in Table 4. The estimation of the various uncertainty components is based on the procedure outlined in Gröbner at al. 2005 [7], with reduced uncertainty values due to the improved characterizations and calibrations developed during the European Joint Research Project "Traceability for surface spectral solar ultraviolet radiation".
The uncertainty contributions shown in the table are described in [4].

Table 4. Uncertainty budget for solar UV measurements using QASUME and QASUMEII; wavelength range: 310 nm to 400 nm (if not stated otherwise).

Uncertainty Parameter	Relative Std Uncertainty/%	
	QASUME	**QASUMEII**
Radiometric calibration (λ≥300 nm)	0.55	
250 W lamp stability (one year)	0.10	
Nonlinearity (PMTor PC)	0.1	0.17
ND filter transmission	n/a	0.3
Stability	0.2	
Temperature dependence	0.2	
Angular response (clear sky / overcast sky)	0.6 / 0.3	
Integrated cosine error	0.3	
Measurement noise	0.2	
Measurement noise (λ=300 nm; SZA=75°)	3.5	
Wavelength shift (after matSHIC)	0.1, 0.5 (λ=300 nm)	

Uncertainty Parameter	Relative Std Uncertainty/%	
	QASUME	QASUMEII
Combined uncertainty	0.95	1.01
Combined uncertainty (overcast sky)	0.80	0.86
Combined uncertainty (λ=300 nm)	3.65	3.67
Expanded uncertainty (k=2, clear sky)	**1.90**	**2.01**
Expanded uncertainty (k=2, overcast sky)	**1.60**	**1.72**
Expanded uncertainty (k=2, λ=300 nm)	**7.30**	**7.34**

7. CAMPAIGN RESULTS

7.1 Spectroradiometer intercomparison

The two reference spectroradiometers QASUME and QASUMEII measured synchronized solar irradiance spectra in the range 290 nm to 400 nm with step 0.25 nm every 15/30 minutes. The instrument entrance optics were located within less than 50 cm from each other at the same height and their distance from the broadband radiometers varied from 1 m to 12 m.

Figure 16. Entrance optics of QASUME (right) and QASUMEII (left).

The comparison of the solar irradiance spectra followed the standard operating procedure of a QASUME intercomparison, i.e. the spectra were convolved to a 1 nm slit width (FWHM) and wavelength adjusted to a common wavelength scale using the matSHIC algorithm. The comparison of all measurements at selected wavelengths and the average over the measurement period is shown in Figures 17 and 18.

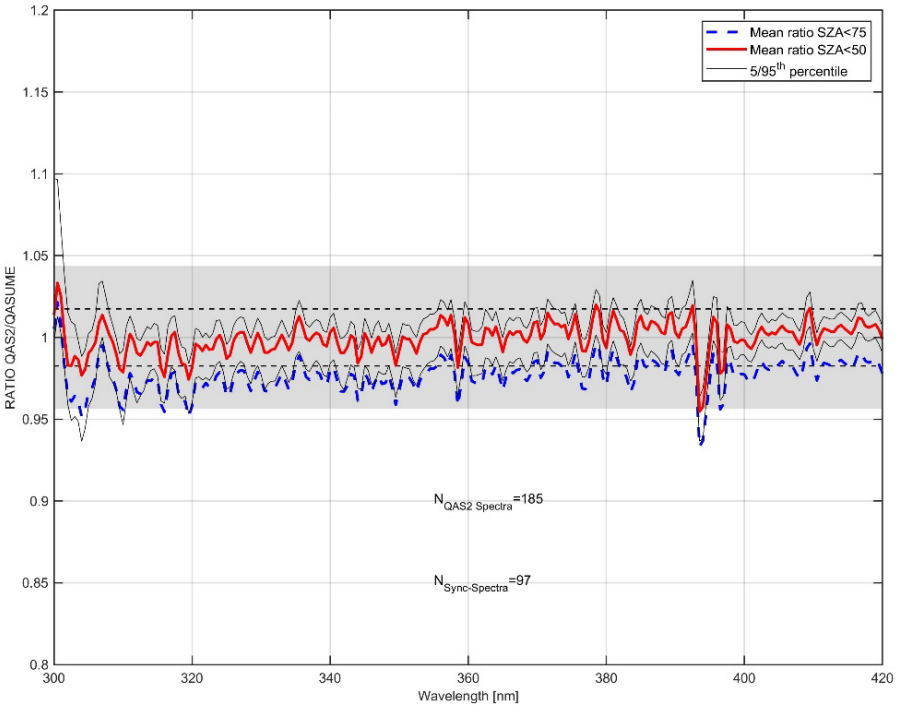

Figure 17. Mean spectral ratio of QASUMEII / QASUME (clear sky data), for the period 12 July 2022 (193) to 14 July 2022 (195).

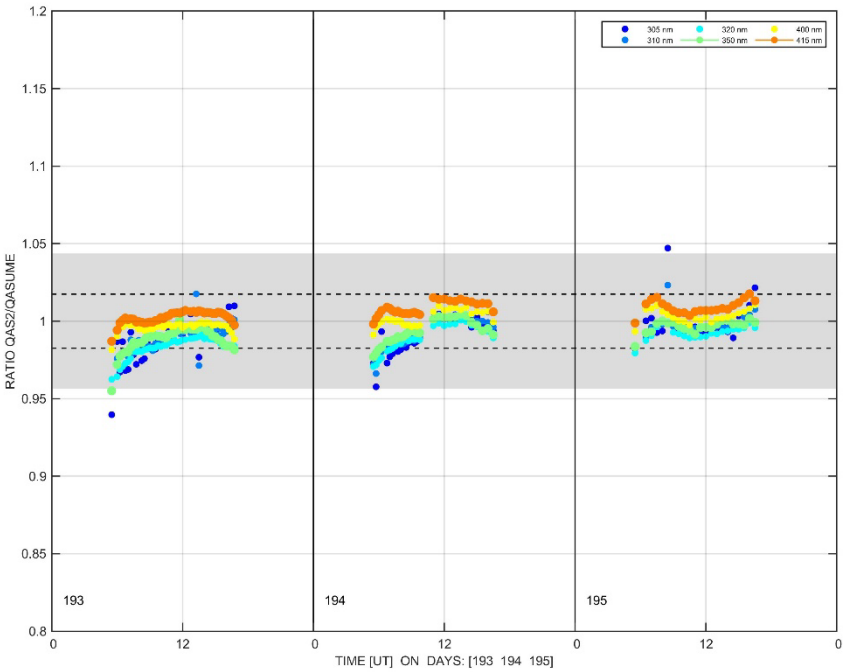

Figure 18. Ratio of QASUMEII / QASUME for selected spectral ranges versus time, for clear sky data, for the period 12 July 2022 (193) to 14 July 2022 (195).

As can be seen in the figure the difference between the two instruments is well within the uncertainty budget defined in Table 4 with an average difference of 0% and a variability of less than or equal to 3%.

The QASUMEII data was used as reference for the calibration of the broadband radiometers. This system was calibrated several times during the comparison period using a portable calibration system with 250 W lamps. The spectroradiometers remained stable within ±1% for the campaign period (see Figure 19). The temperature of the monochromator was stabilized to 27.1 ± 0.2 °C and the diffuser head was heated to a temperature of 28.7 ± 0.7 °C (see Figure 20).

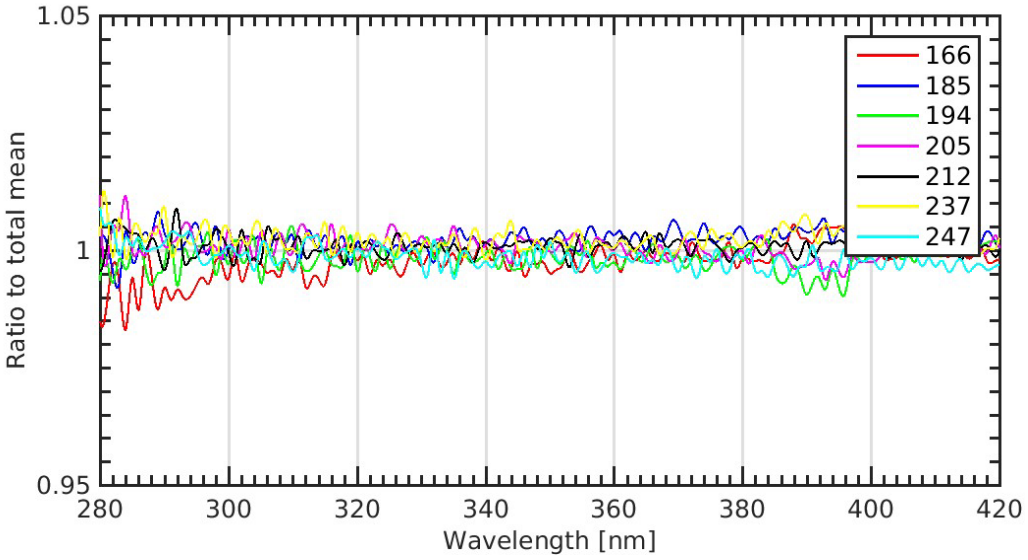

Figure 19. QASUMEII responsivity change based on T68523 lamp measurements on different days of the campaign.

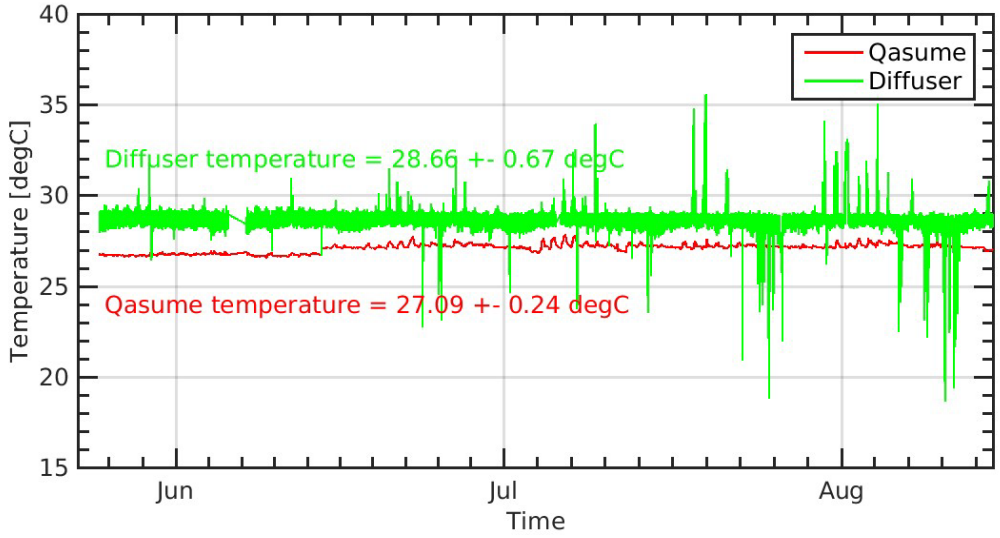

Figure 20. QASUMEII temperature stability of the monochromator and the input optics during the period of the campaign.

7.2 Radiometer calibration

The raw data of the broadband UV radiometers of the whole campaign (all sky conditions, without precipitation) were converted to weighted solar irradiance using the "PMOD" calibration factors on the one hand, and the "USER" supplied original calibration factors[6] on the other. Figures 21 and 22 show an example of the relative ratio between the two data sets with respect to the reference measurements obtained from the reference spectroradiometer QASUMEII.

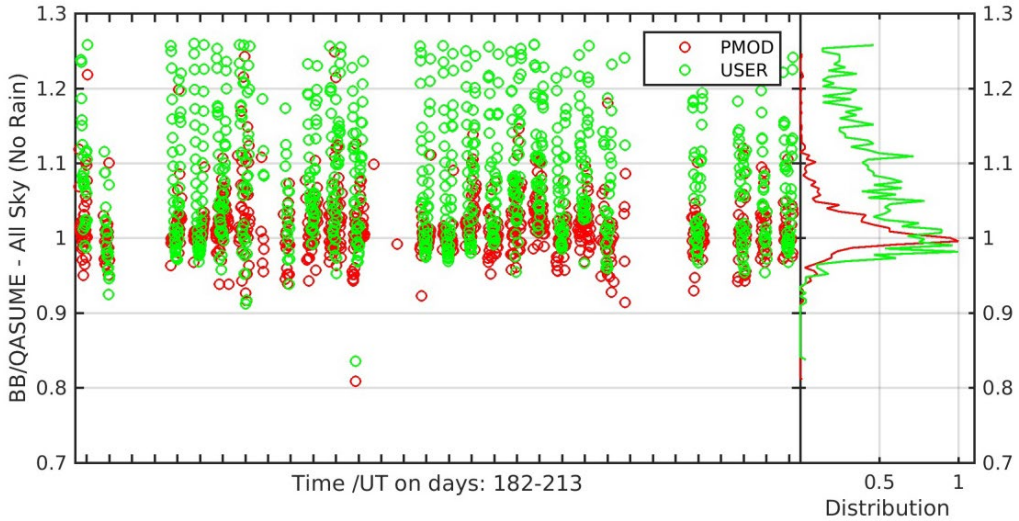

Figure 21. Erythemal weighted broadband irradiance vs. QASUMEII reference data – plotted against the time (left) and as a histogram distribution (right). In this example the data of UVE channel of KZ120023 was used.

[6] Most calibration factors from the participants entered the database of the WCC-UV before the start of the campaign, which enabled a "blind" comparison.

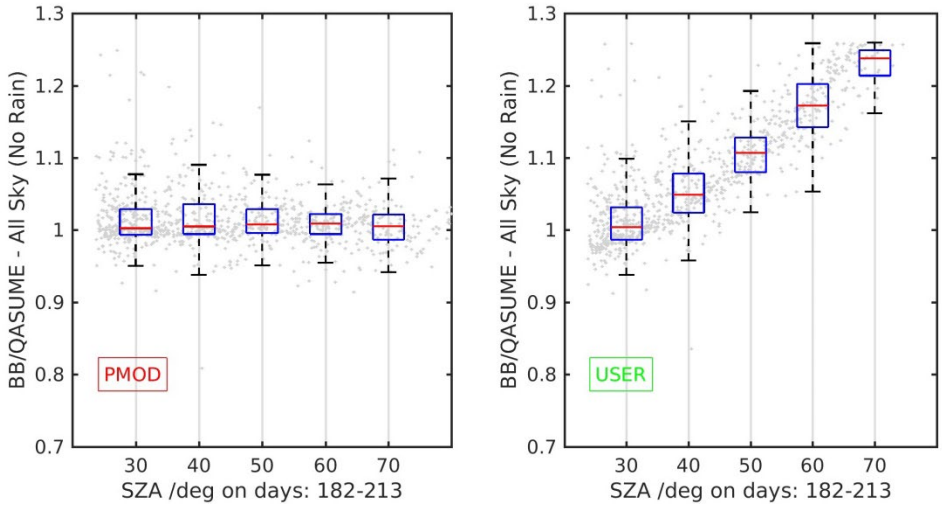

Figure 22. Erythemal weighted broadband irradiance vs. QASUMEII reference data – plotted against the solar zenith angle.
Left: PMOD calibration; right: USER calibration.
In this example the data of UVE channel of KZ120023 was used[7].

Figure 23 summarizes the comparison of the PMOD and USER calibrations relative to the reference. Displayed is the median of the ratio for the calibration period as well as the 2.5th and 97.5th percentile for each instrument (95% coverage). The last point in the figure shows the performance of the UVIOS model simulation [12] relative to the reference data set derived from the QASUME measurements. For this period of the year the median value of this model agreed remarkably well with the measurements of QASUME, while its variability was rather large.

[7] On each box, the central mark indicates the median, and the bottom and top edges of the box indicate the 25th and 75th percentiles, respectively. The whiskers extend to the most extreme data points not considering outliers. Outliers are defined as data points outside the 99.3 % confidence interval, assuming a normal probability distribution [13]

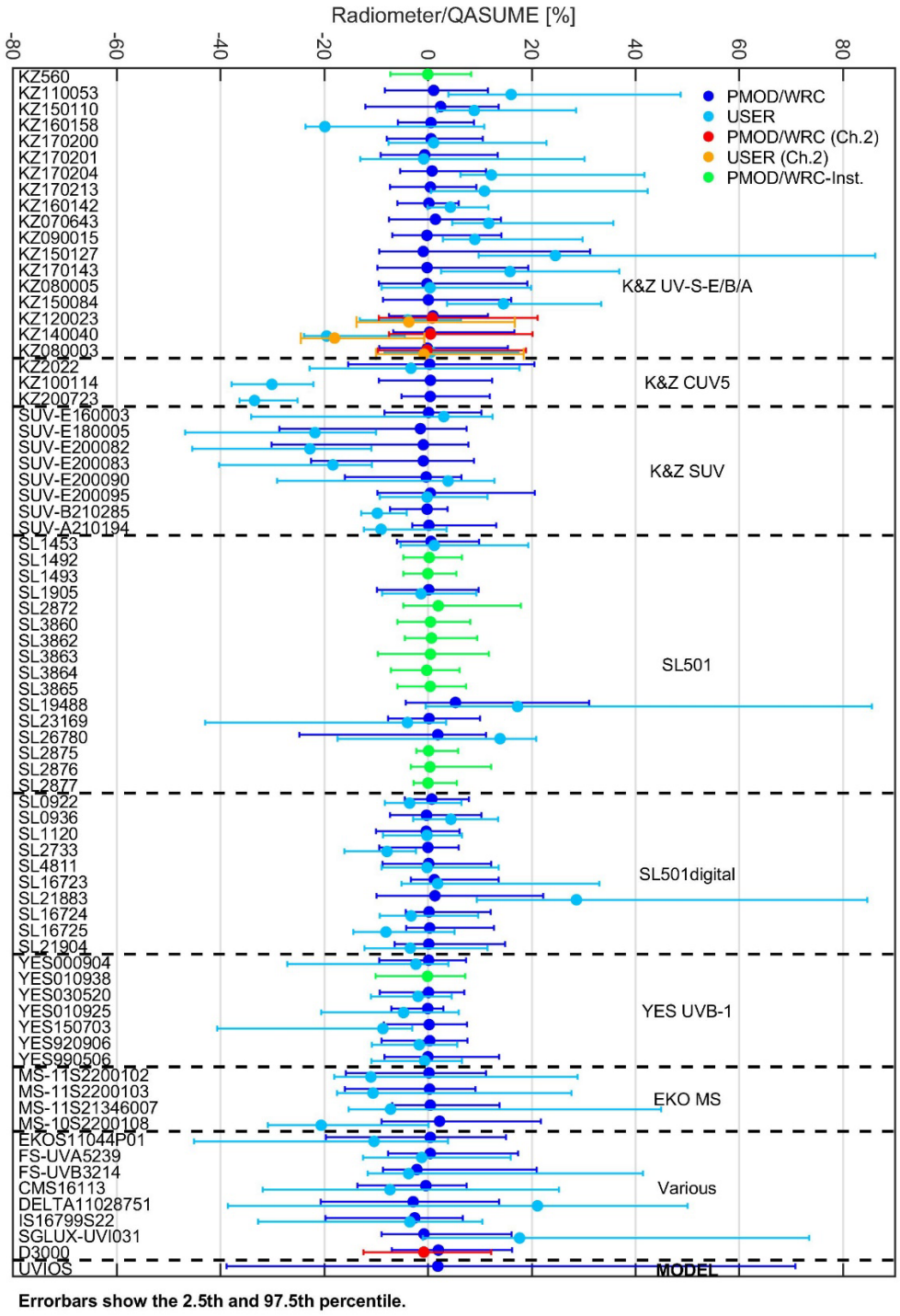

Figure 23. Comparison of the original (USER) and the new (PMOD) calibration.

For some instruments a history of calibrations is available in the WCC-UV database. One example is shown in Figure 24, indicating a gradual shift in the calibration factor since 2009.

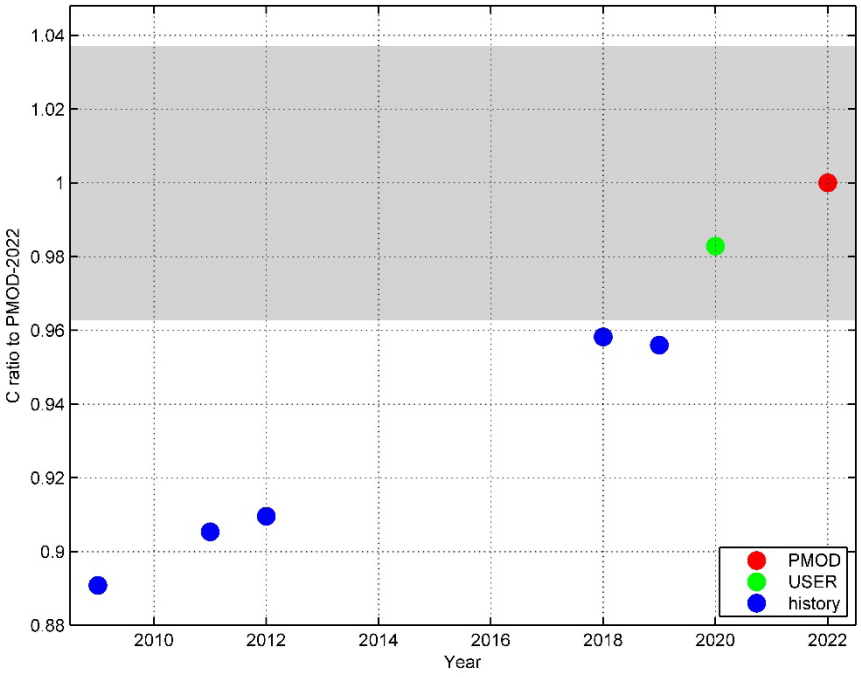

Figure 24. History of the calibration factor C for a SL501 radiometer. The grey shaded area represents the expanded uncertainty of the last calibration factor (red point).

Many participants sent the SRF and ARF derived from the manufacturer or from their own measurements. These data were included in the comparisons – when available. The individual results of all radiometers are listed in the annex.

8. DISCUSSION

Two factors should be pointed out which dominate the quality of the final product of solar UV radiometers. First, the maintenance of the instrument itself and second, the calibration and data processing of the raw data. In the following these two factors are discussed.

8.1 Data processing

Since 2007 several publications give practical guides for broadband instruments measuring solar UV radiation [6, 8, 9]. The most important point mentioned in these investigations is that using a common calibration factor for all atmospheric conditions will result in very high uncertainties of the solar irradiance data weighted with a specific weighting function. However, the data of most of the participating radiometers (34 out of 74) where processed using a single calibration factor prior to the campaign.
The calibration methodology for each participating radiometer can be found in Table 2.

From the variability of the normalized additional factors f_n and *Coscor* the resulting error arising from neglecting these factors in Equation 1 can be estimated. This will be illustrated in the following two sections.

8.1.1 Neglecting the spectral mismatch between the instrument spectral response and the nominal action spectrum

The three panels of Figure 25 show for a clear sky day the diurnal variability of the ratio broadband radiometer vs. reference data for KZ560, SL1493 and YES010938, representing the three main types of radiometers participating at the campaign. The data of the broadband radiometers were calculated using Equation 1 with f_n equal to unity, i.e. neglecting the f_n. The inverse of the correction function, f_n, is shown separately in green and follows the ratio to a high degree. For this typical summer day, the maximal of the correction function is 20% for the KZ, 10% for the SL and 10% for the YES radiometer.

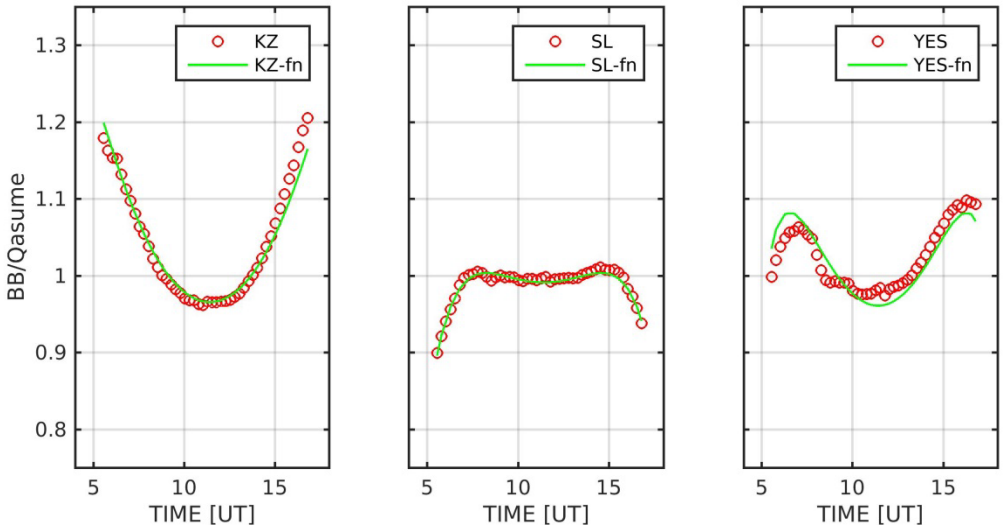

Figure 25. Diurnal variability on DOY 187, 2017, of a KZ (left), SL (middle) and YES (right) radiometer, caused by neglecting the correction matrix f_n. This function is added to the figures in green.

8.1.2 Neglecting the mismatch between the instrument angular response and the nominal cosine response

Similar to the previous section, the three panels of Figure 26 show the diurnal variability on a clear sky day of the same data, however the data of the broadband radiometer were now calculated using Equation 1 with *Coscor* equal to unity, i.e. neglecting the departure of the instrument angular response function from a Lambertian receiver. The inverse of the cosine correction function is shown in green. For this typical summer day, the maximal correction is 3% for the KZ, 6% for the SL and 10% for the YES radiometer. For a diffuse sky day, the corresponding diffuse cosine correction factors are 0.97, 1.09 and 1.21, for KZ, SL, and YES radiometers respectively.

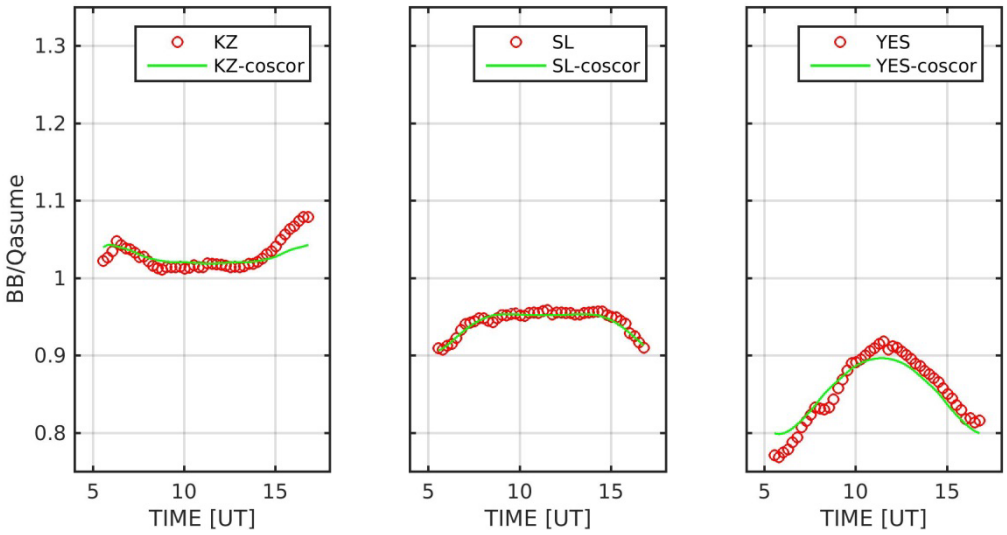

Figure 26. Diurnal variability on DOY 187, 2017, of a KZ (left), SL (middle) and YES (right) radiometer, caused by neglecting the cosine correction function *Coscor*. This function is added to the figures in green

8.2 Instrument humidity

Humidity inside the radiometers is the environmental factor which has a significant impact on the sensitivity of most solar UV radiometers through the susceptibility of the filters used to produce the desired spectral response function.

SL19488 can act as a good example to illustrate the response of an instrument from high to low internal humidity, i.e. the renewal of the desiccant at the beginning of the period (see Figure below). It took around 15 days to dry out. During this drying period the calibration factor changed by about 20%.

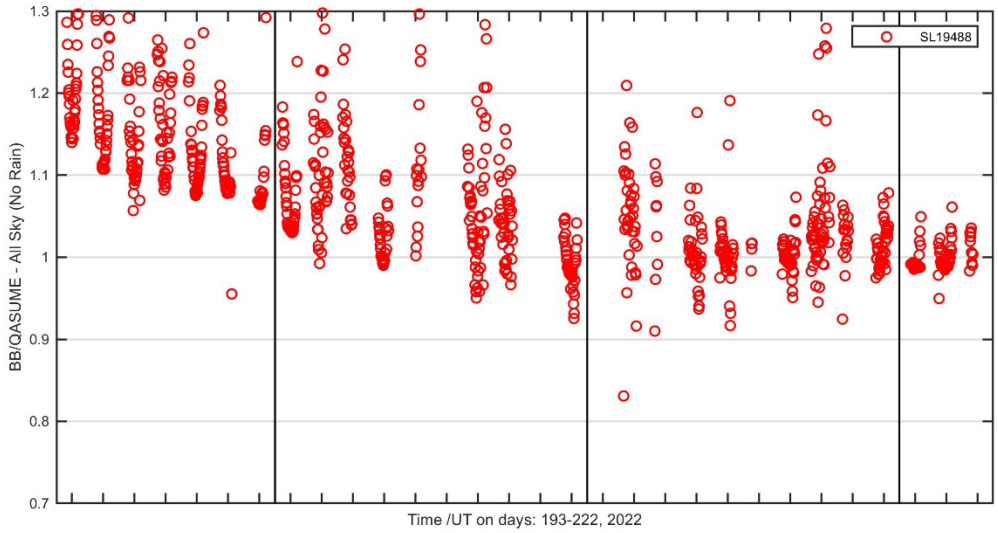

Figure 27. The ratio of the SL19488 irradiance data relative to the reference reveals the sensitivity change after the renewal of the desiccant on DOY 190, 2022.

8.3 History

The calibration frequency of an instrument is an essential element in assessing the uncertainty of solar UV measurements. Only by knowing the instrument calibration before and after a measurement period can the data be quality assessed and produce traceable solar UV irradiance data. From the history of past calibrations, one can estimate typical degradation timescales of radiometers measuring solar UV irradiance. The following radiometers – most belong to PMOD/WRC – have been calibrated annually since 2006: SL1492, SL1493, SL1903, SL3860, KZ560, YES010938.

Figure 28 shows that the calibration factors typically increase by 1.5% to 3% per year for the Solar Light radiometers, which means that the responsivity decreases by the same rate. This requires a calibration at least every four years to achieve an uncertainty of less than 10%. The KZ560 shows unpredictable sensitivity changes in the order 10% between subsequent calibrations. This is probably due to high intake of humidity by the radiometer. On the opposite, SL1903 shows only a very small variability of its sensitivity. The reason is very likely the custom-made sealing of the instrument and annual nitrogen purging procedure.

The GAW-COST726 document by Webb et al. [8] recommends an annual recalibration because of well-known sensitivity changes of solar UV radiometers. The average date of the last calibration year for the 74 radiometers is 2019. The oldest calibration was fifteen years old.

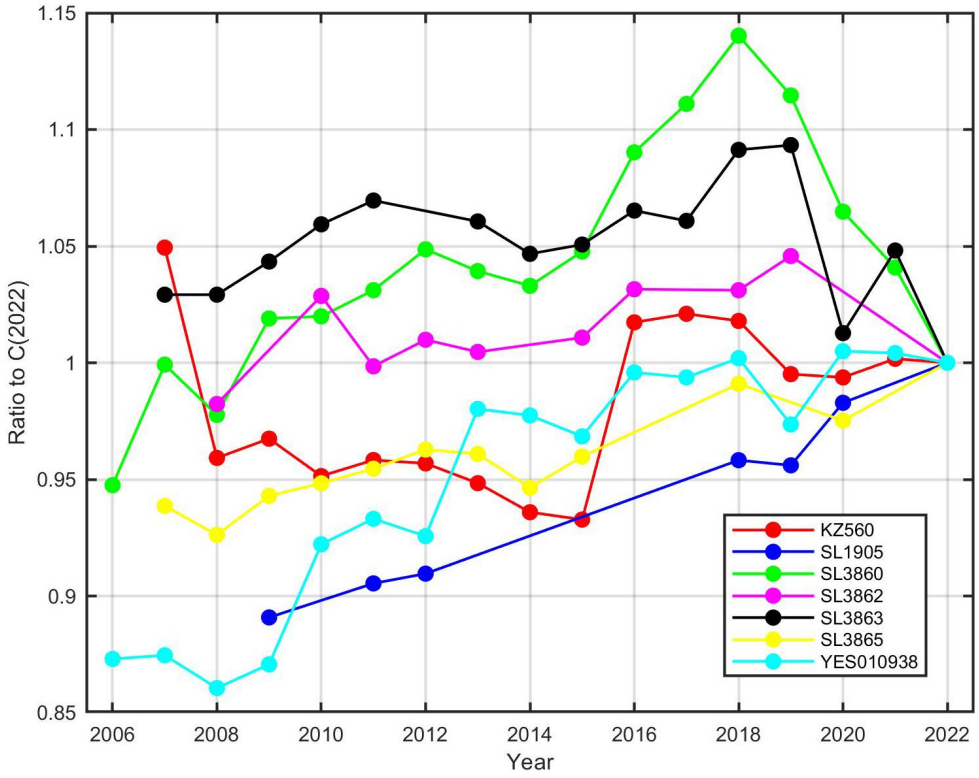

Figure 28. History of calibration of selected solar UV radiometers. Calibration factor normalized to the factor determined during the UVC-III campaign.

8.4 Summary

To summarize – one can extract three components affecting the overall measurement uncertainty of solar UV measurements using broadband filter radiometers on different timescales:

Short term (diurnal)	usage of the correction factors f_n and ***Coscor***
Midterm (months)	Control of the humidity inside the radiometer
Long term (years)	Recalibration frequency

The reported relative expanded uncertainty of measurement of the calibration factor is stated as the standard relative uncertainty of measurement multiplied by the coverage factor k=2, which for a normal distribution corresponds to a coverage probability of approximately 95%. An uncertainty of e.g. 20% (see Section 6.2) over or under estimates UV irradiance by up to this amount. Before the calibration 28 (out of 74) radiometers measured the UV irradiance within ±5%, 37 within ±10% and 23 with a higher measurement error. For 14 radiometers no initial calibration was supplied. After the calibration all radiometers measured within 5%.

9. COMMENTS

9.1 Radiometer maintenance

The campaign was intended to investigate the performance of "reference" radiometers of solar UV broadband networks around the globe. In general, most of the participating radiometers arrived in very good shape at the WCC-UV. A complete list of the observations is given below.

(1) High humidity inside the radiometer can cause transmission changes of the filter and is therefore a crucial condition for the radiometer's sensitivity. We checked the status of the radiometers for:

- (a) Very old drying agent;
- (b) Visible humidity inside;
- (c) Large sensitivity drift after the renewal of the desiccant.

(2) Most solar UV radiometers are temperature stabilized because the sensitivity is a function of the filter and sensor temperature. Therefore, the temperature signal was used to check instabilities of the temperature stabilization;

(3) In addition, we checked the radiometers for:

- (a) Cable Code mutations;
- (b) Corrosion at the cables or electronic;
- (c) A visible filter degradation;
- (d) Contamination on the dome (outside and/or inside);
- (e) Mounting and alignment problems of the radiometers.

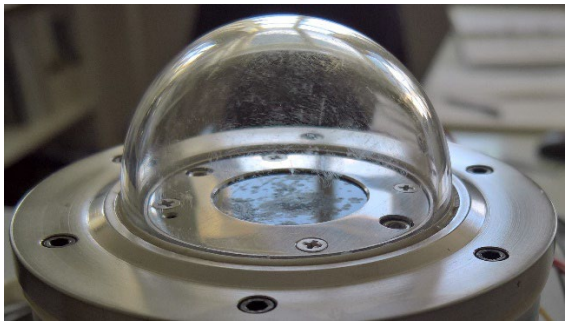

Figure 29. Example of Filter degradation and dome contamination of a radiometer.

ACKNOWLEDGEMENTS

We would like to acknowledge the active support of the PMOD/WRC staff in the preparation and organization of the calibration campaign. The instrument owners provided the calibrated data for the intercomparison period using their home calibration.

Special thanks to Christian Thomann and Jakob Föller for their help in installing the radiometers and the staff of our administrative department for organizing the shipping of the instruments. Many thanks to Jakob Föller and Vattioni Sandro for the angular and spectral responsivity measurements and Pascal Gamma for the data analysis and preparation of this report.

REFERENCES

[1] K. Leszczynski, K. Jokela, L. Ylianttila, R. Visuri and M. Blumthaler, "Erythemally weighted radiometers in solar UV monitoring: Results from the WMO/STUK Intercomparison," Photochem. Photobiol. 67, 212–221, 1998.

[2] *WMO/GAW No. 141* (WMO/TD No. 1051): Report of the LAP/COST/WMO Intercomparison of Erythemal radiometers, Thessaloniki, Greece, 1999.

[3] J. Gröbner, G. Hülsen, L. Vuilleumier, M. Blumthaler, J. M. Vilaplana, D. Walker, and J. E. Gil, "COST 726 – Report of the PMOD/WRC-COST Calibration and Intercomparison of erythemal Radiometers," COST Office, 2009.

[4] G. Hülsen, J. Gröbner, S. Nevas, P. Sperfeld, L. Egli, G. Porrovecchio, and M. Smid, "Traceability of solar UV measurements using the Qasume reference spectroradiometer," Appl. Opt. 55, 7265-7275, 2016.

[5] A.R. Webb, H. Slaper, P. Koepke, and A.W. Schmalwieser, "Know your standard: clarifying the CIE erythema action spectrum," Photochemistry and Photobiology 87: 483-486., 2011.

[6] G. Hülsen, and J. Gröbner, "Characterisation and calibration of ultraviolet broadband radiometers measuring erythemally weighted irradiance," Appl. Opt. 46, 5877-5886, 2007.

[7] J. Gröbner, J. Schreder, S. Kazadzis, A. F. Bais, M. Blumthaler, P. Görts, R. Tax, T. Koskela, G. Seckmeyer, A. R. Webb, and D. Rembges, "Traveling reference spectroradiometer for routine quality assurance of spectral solar ultraviolet irradiance measurements," Appl. Opt. 44, 5321– 5331, 2005.

[8] A. Webb, J. Gröbner, and M. Blumthaler, "A Practical Guide to Operating Broadband Instruments Measuring Erythemally Weighted Irradiance," 2007. EUR 22595, ISBN 92-898-0032-1.

[9] G. Seckmeyer, A. F. Bais, G. Bernhard, M. Blumthaler, C. R. Booth, R.L. Lantz, R.L. McKenzie, P. Disterhoft, and A. Webb, "Instruments to measure solar ultraviolet radiation. Part 2: Broadband Instruments Measuring Erythemally Weighted Solar Irradiance," *WMO/GAW No. 164* World Meteorological Organization, Geneva, 2007 (WMO/TD 1289).

[10] Hülsen G., and Gröbner J., Report of the Second International UV Filter Radiometer Calibration Campaign UVC-II, GAW Report- No. 240, WMO, 2018.

[11] Hülsen G., et al., Second solar ultraviolet radiometer comparison campaign UVC-II, Metrologia 57. 2020.

[12] Kosmopoulos, P. G. et al., Real-time UV index retrieval in Europe using Earth observation-based techniques: system description and quality assessment, Atmospheric Measurement Techniques 14, 2021.

[13] MathWorks: Documentation, Box Plot, https://ch.mathworks.com/help/stats/boxplot.html, 2020.

[14] Evaluation of measurement data – Guide to the expression of uncertainty in measurement, JCGM 100:2008, https://www.bipm.org/en/committees/jc/jcgm/publications

ANNEX

Calibration Results

Individual results for each instrument participating at the calibration and intercomparison campaign at PMOD/WRC, Davos, Switzerland from 13 June to 26 August 2022.

Calibration Results of KZ560 (UVE)

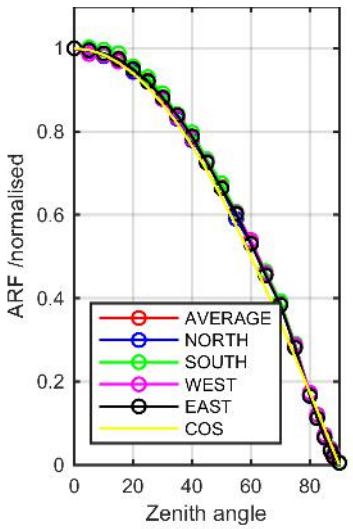

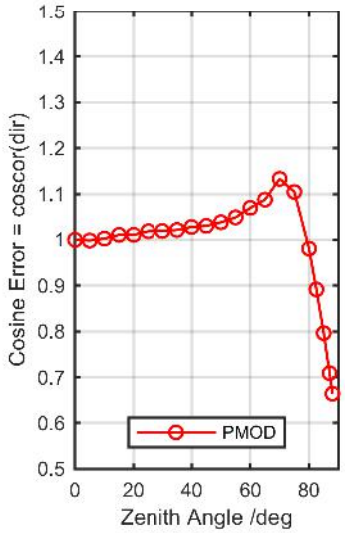

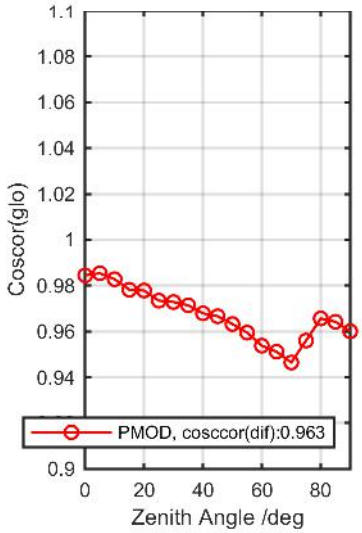

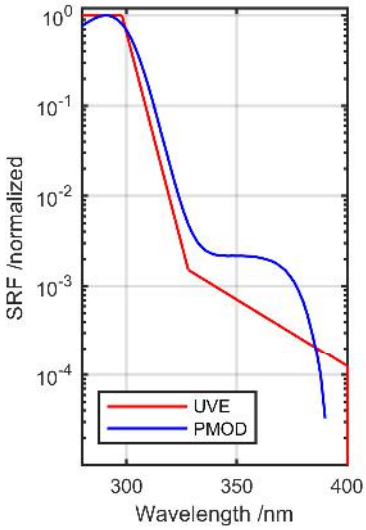

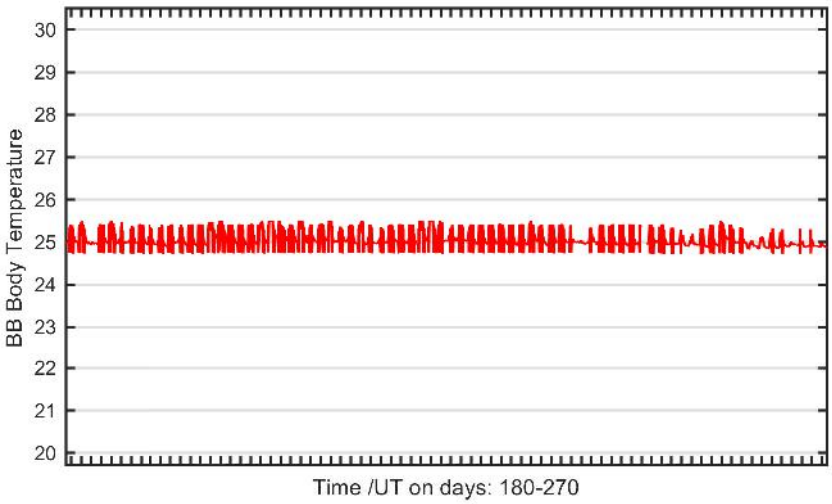

Calibration Matrix fn; Model sdisortPMODmsO3; f0=0.4718

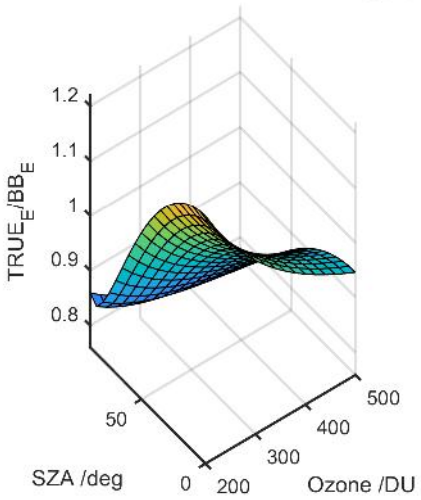

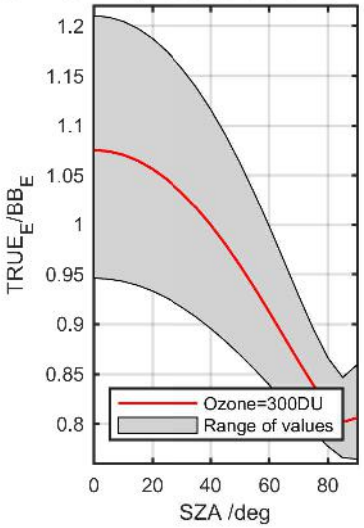

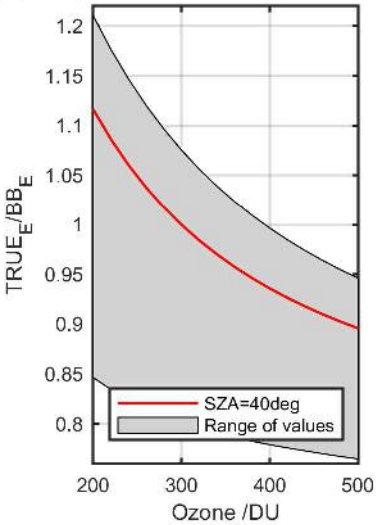

Calibration Results of KZ560 (UVE)

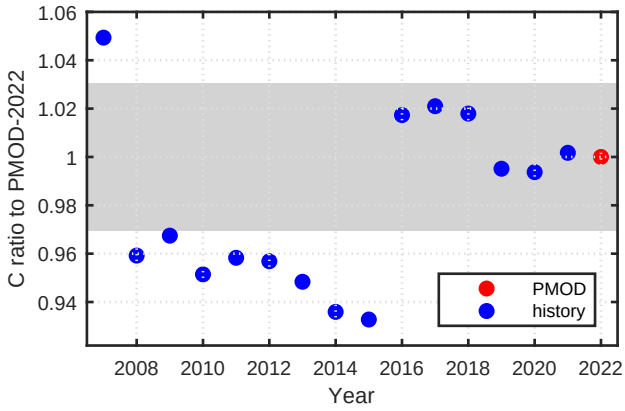

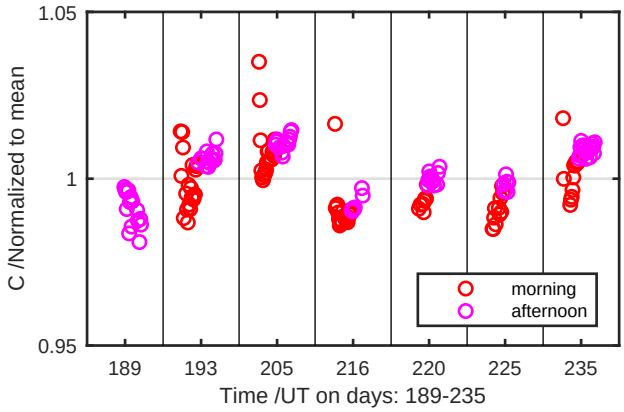

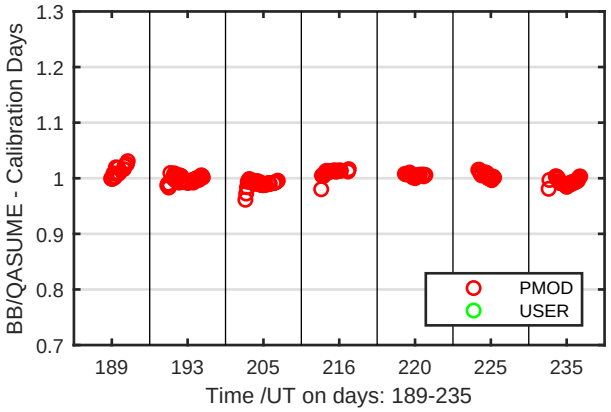

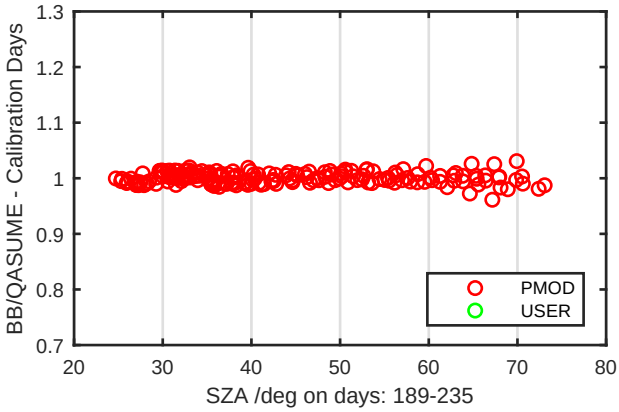

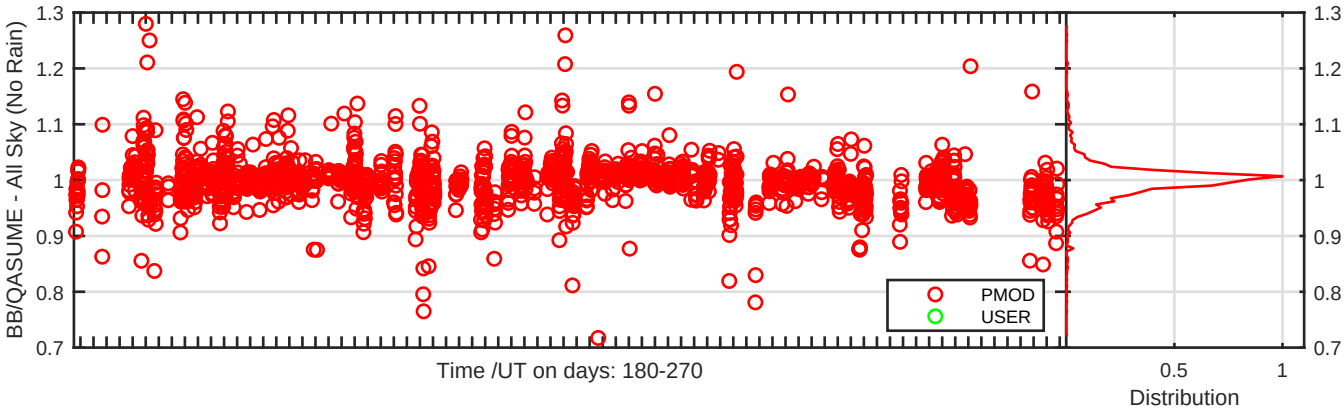

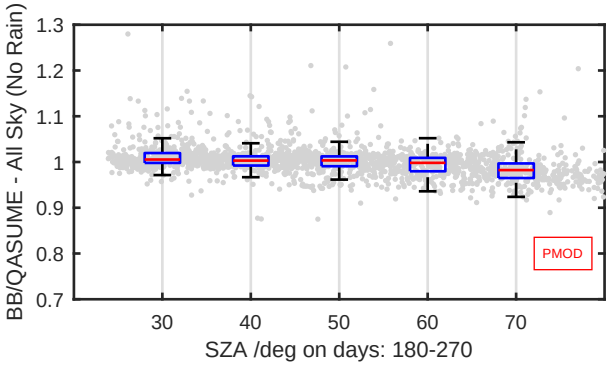

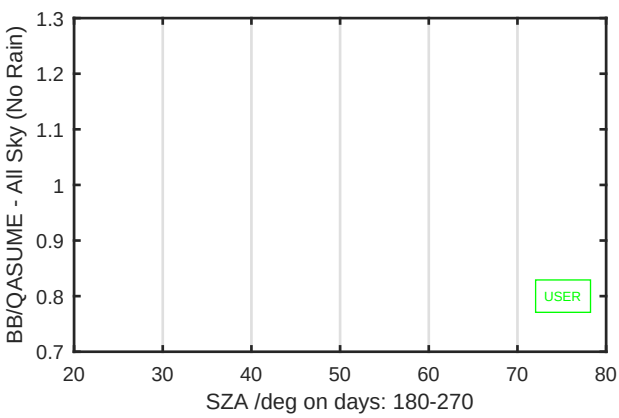

Calibration Results of KZ110053 (UVE)

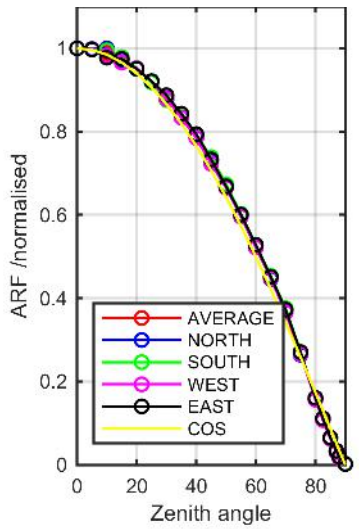

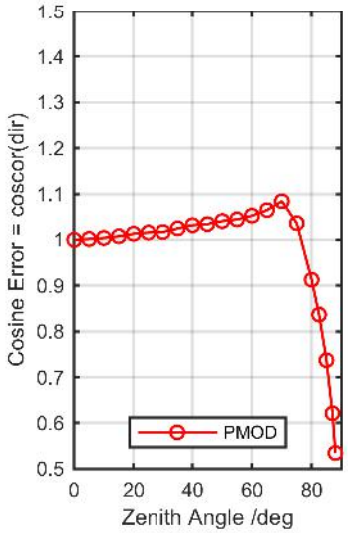

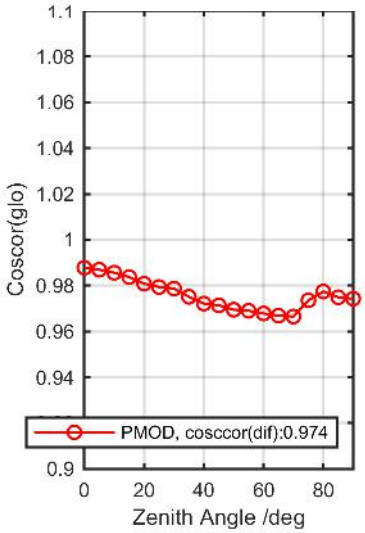

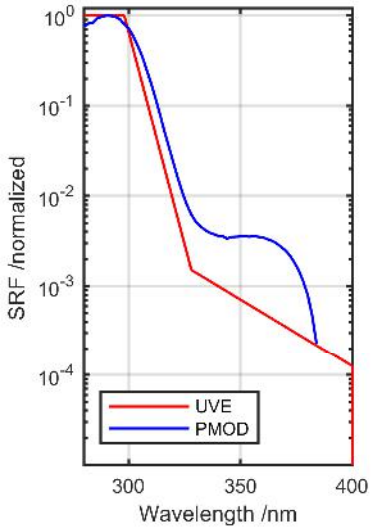

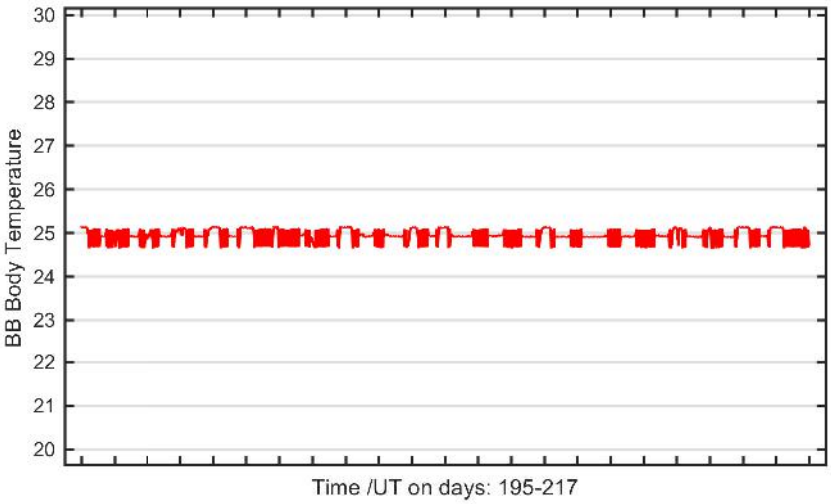

Calibration Matrix fn; Model sdisortREFms2009; f0=0.4022

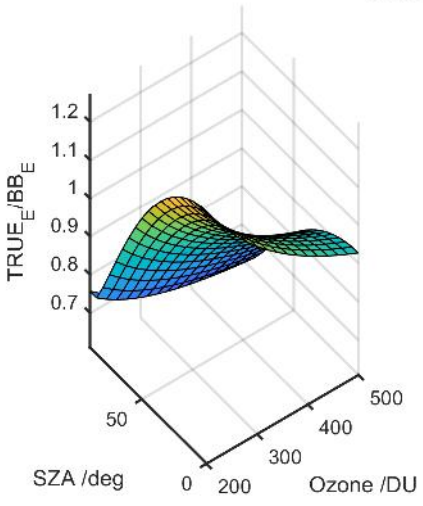

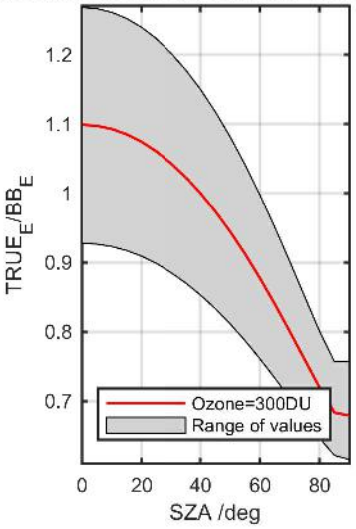

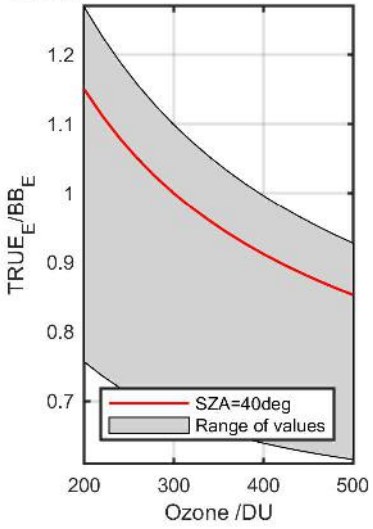

Calibration Results of KZ110053 (UVE)

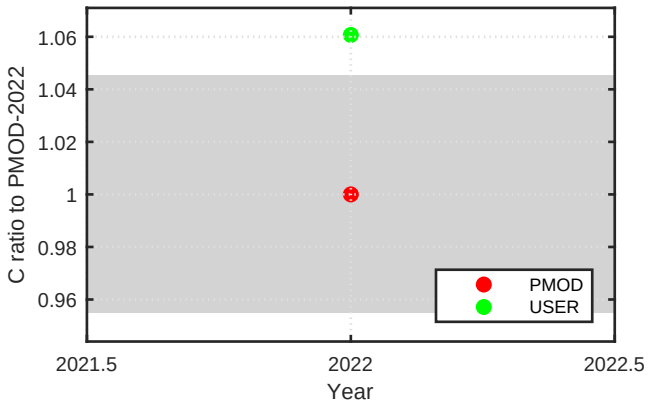

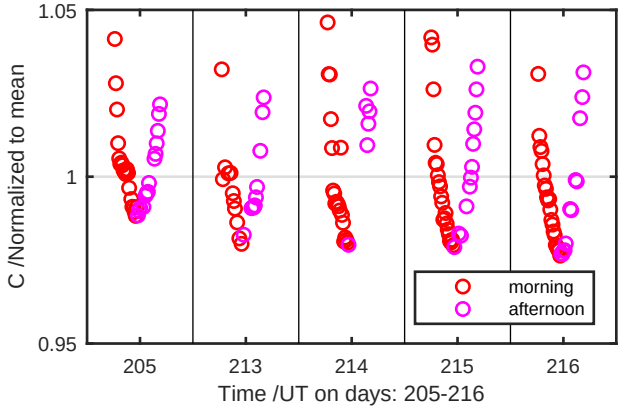

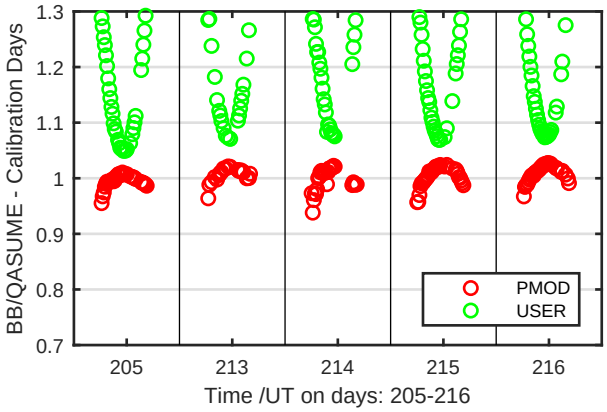

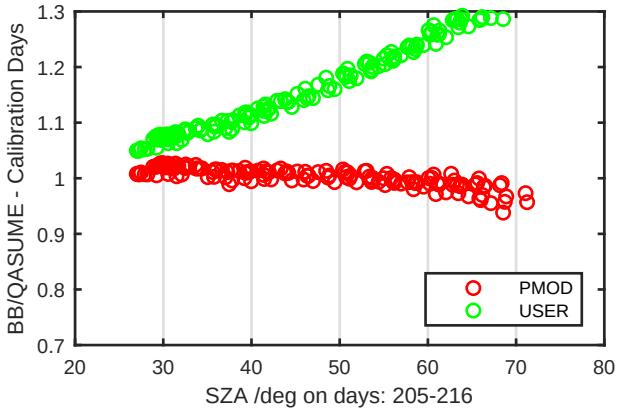

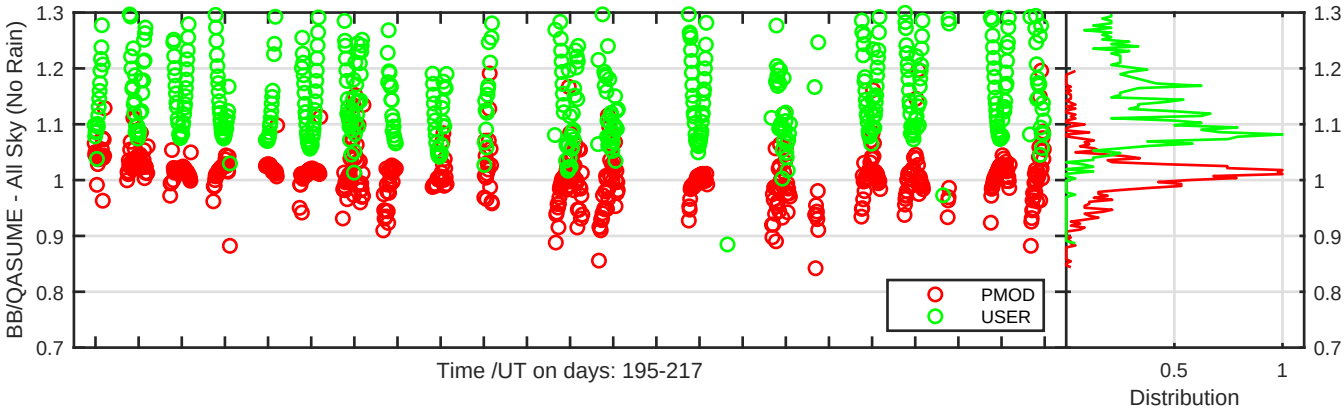

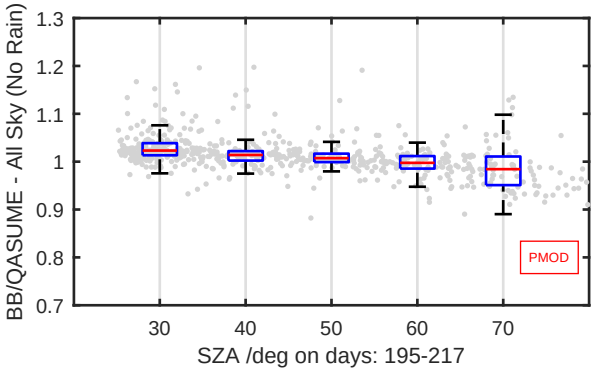

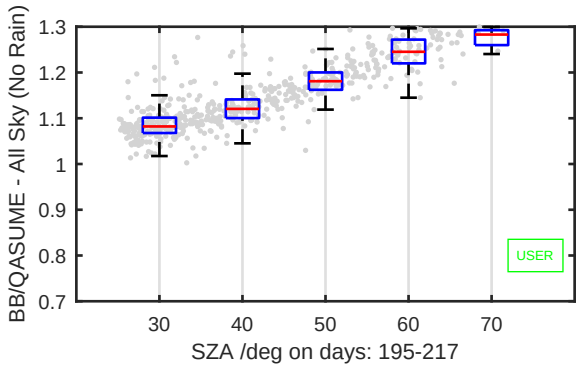

Calibration Results of KZ150110 (UVE)

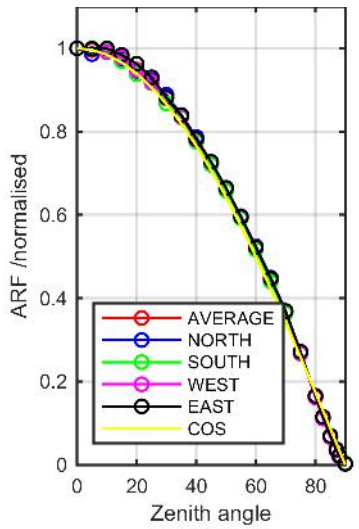

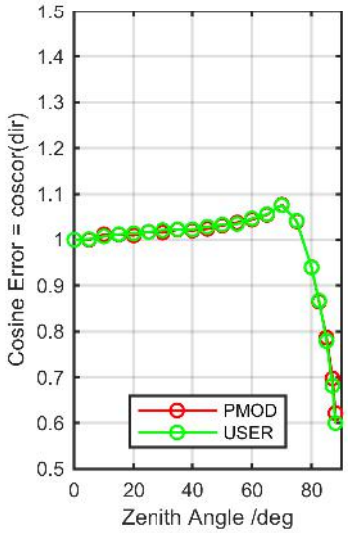

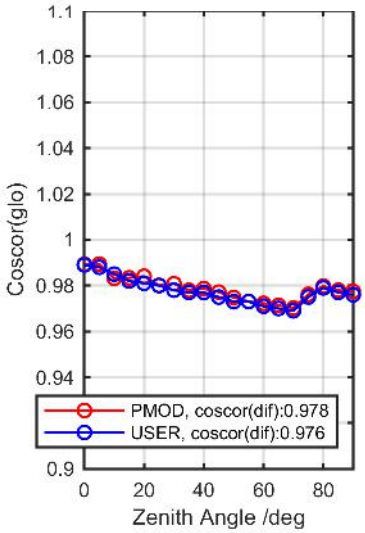

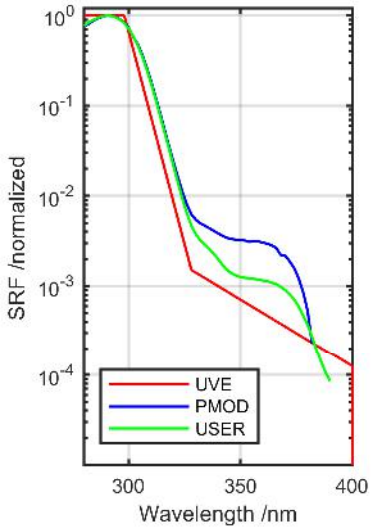

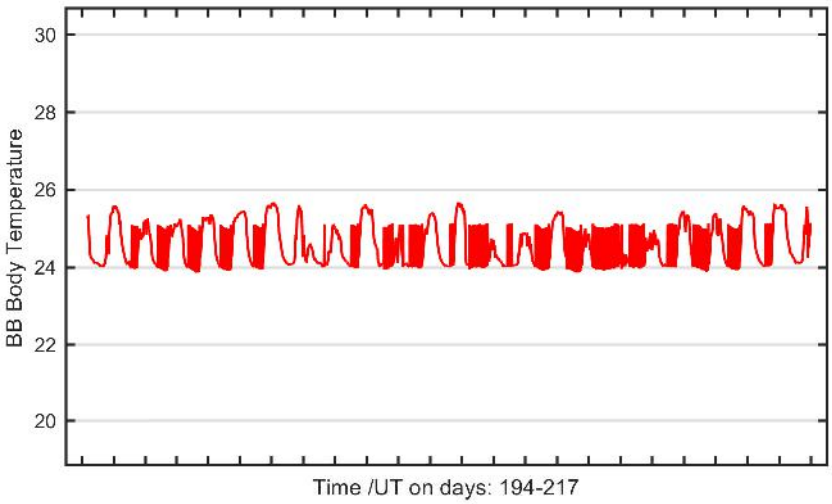

Calibration Matrix fn; Model sdisortREFms2009; f0=0.3957

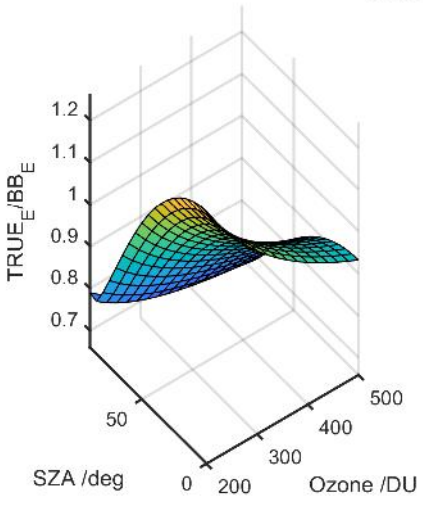

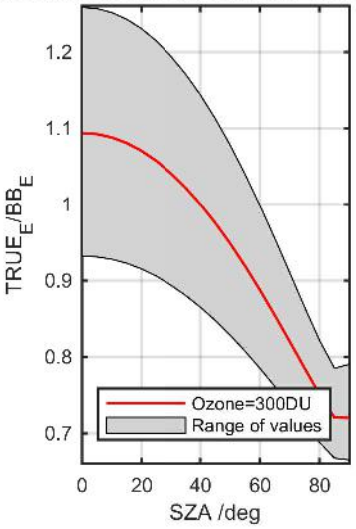

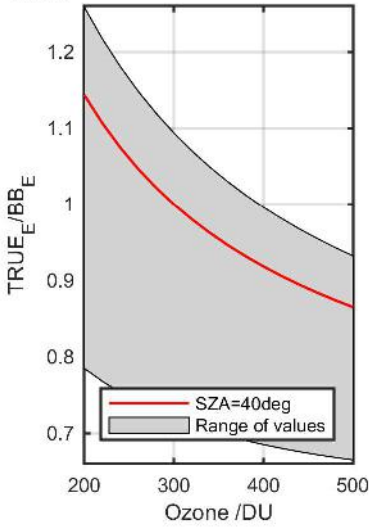

Calibration Results of KZ150110 (UVE)

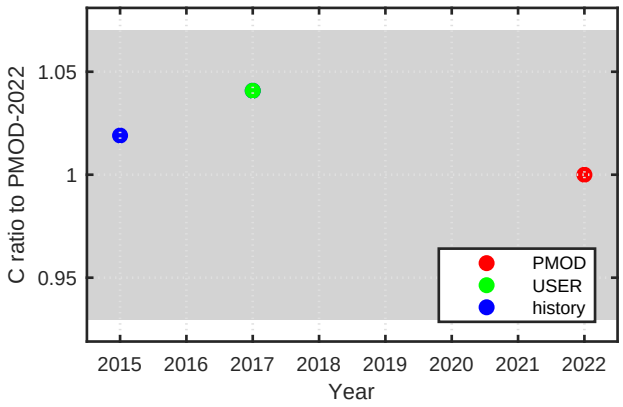

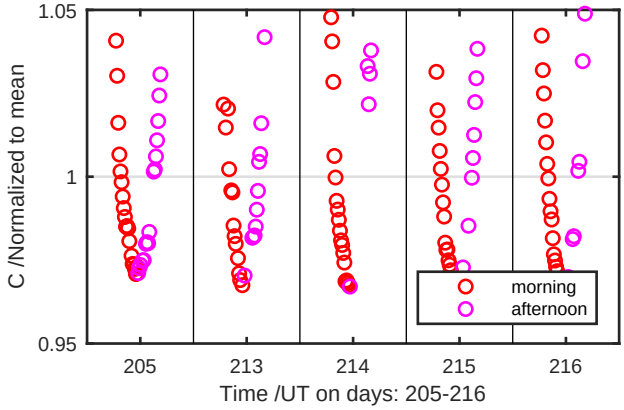

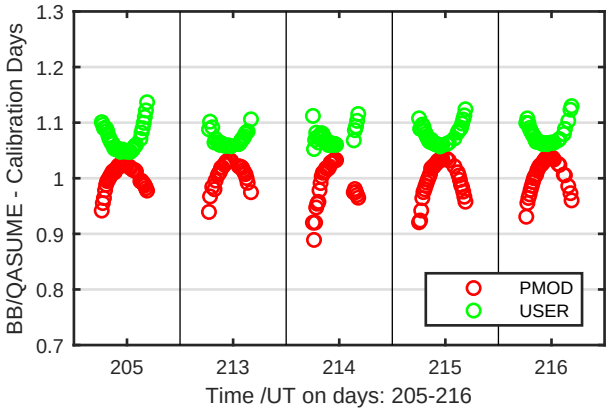

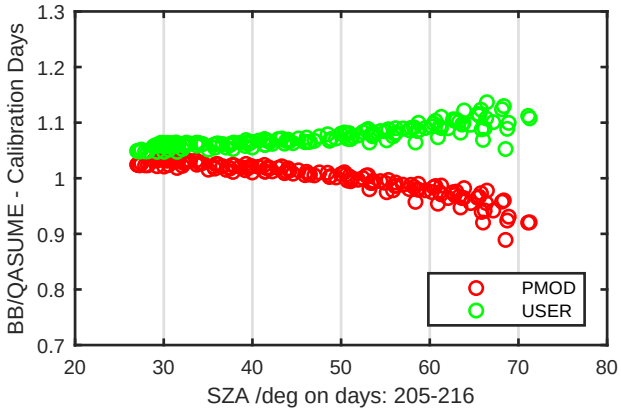

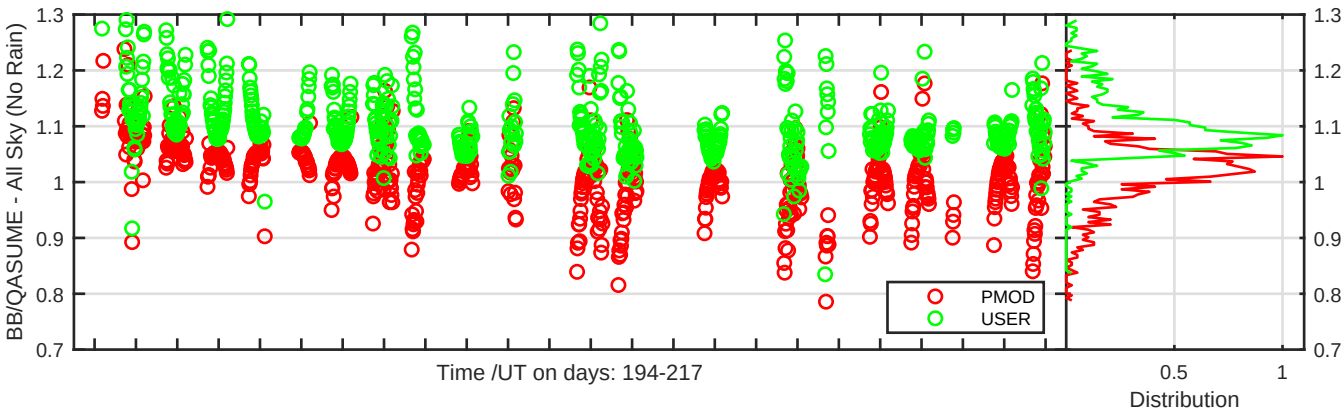

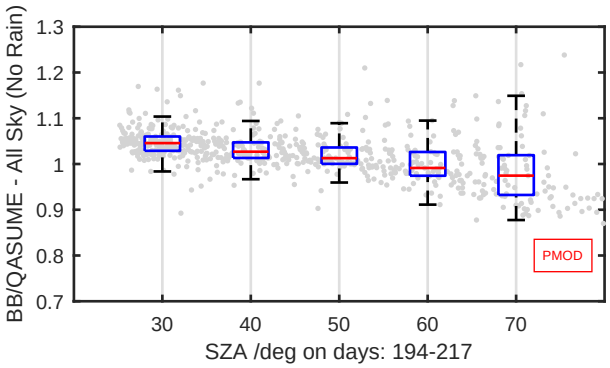

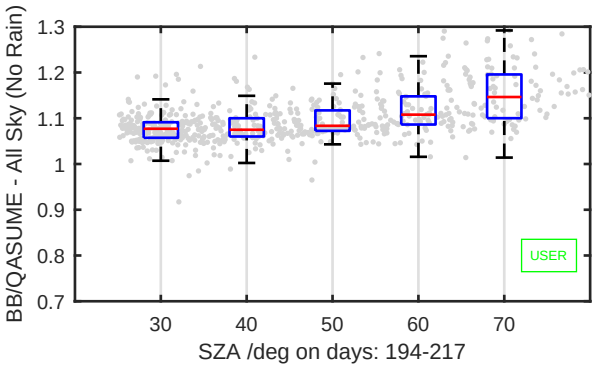

Calibration Results of KZ160158 (UVE)

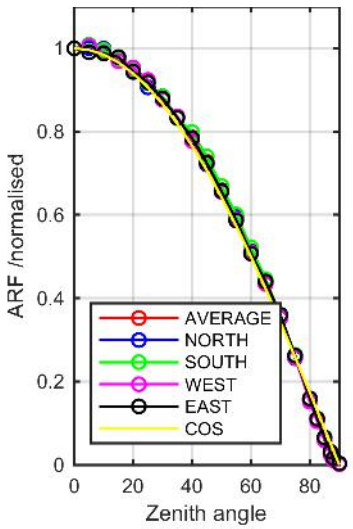

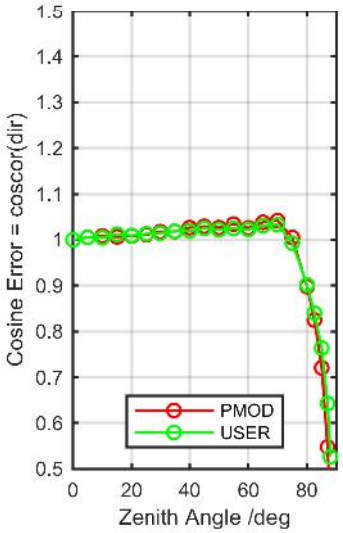

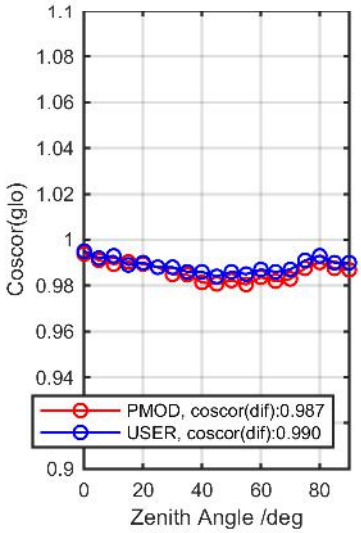

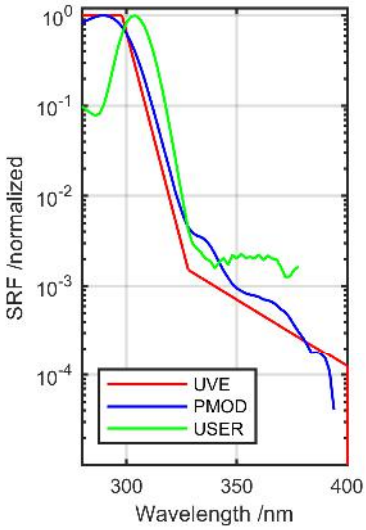

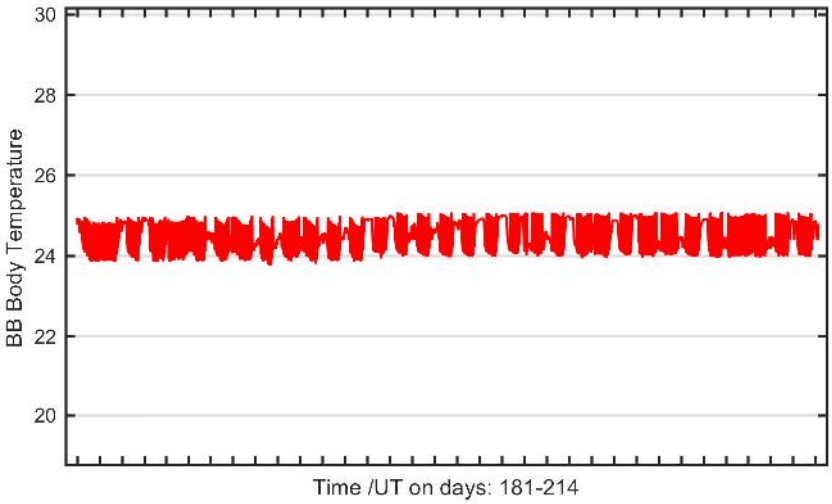

Calibration Matrix fn; Model sdisortREFms2009; f0=0.5703

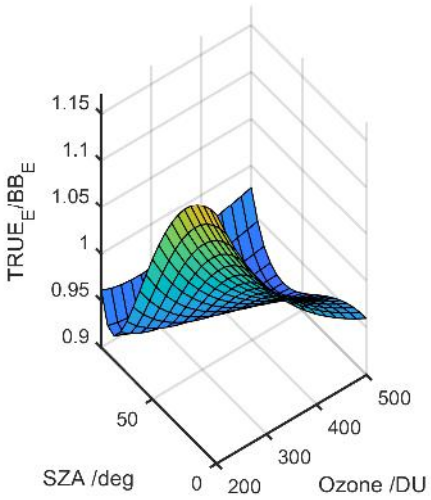

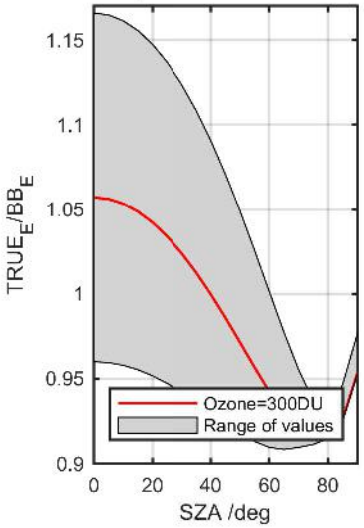

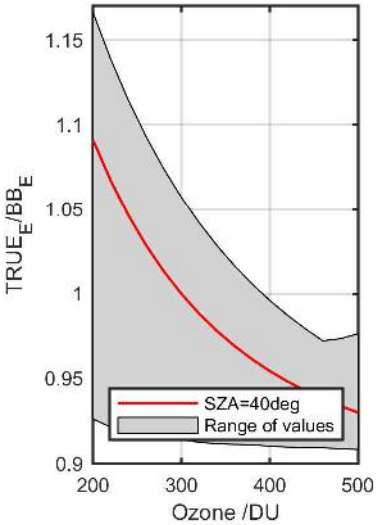

Calibration Results of KZ160158 (UVE)

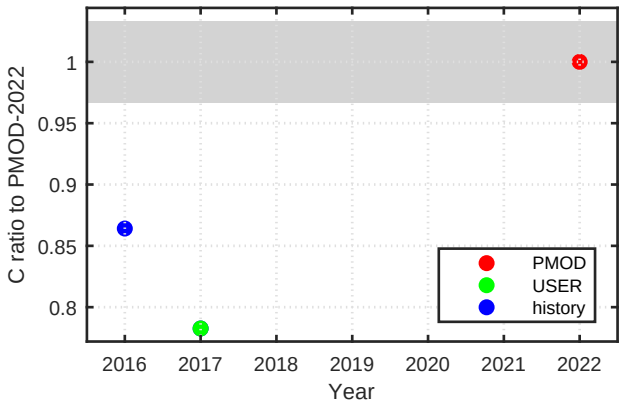

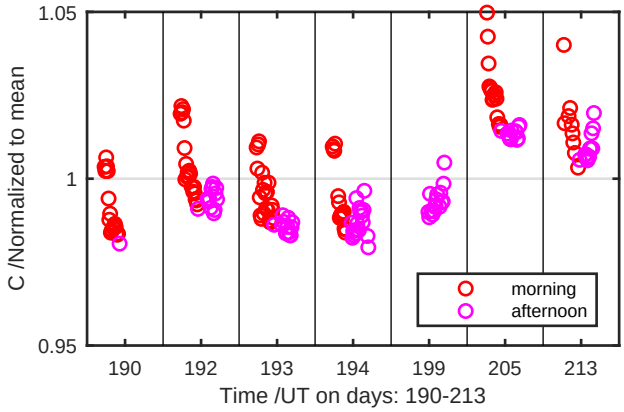

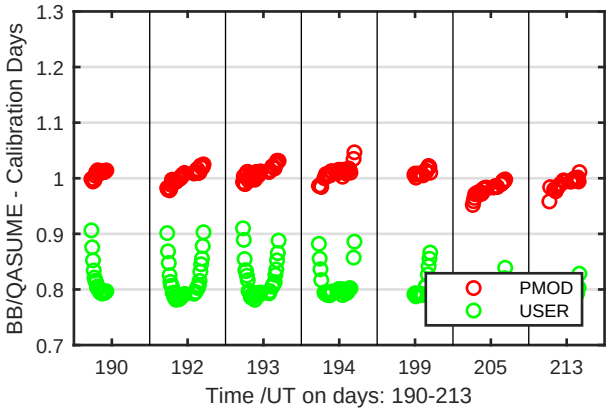

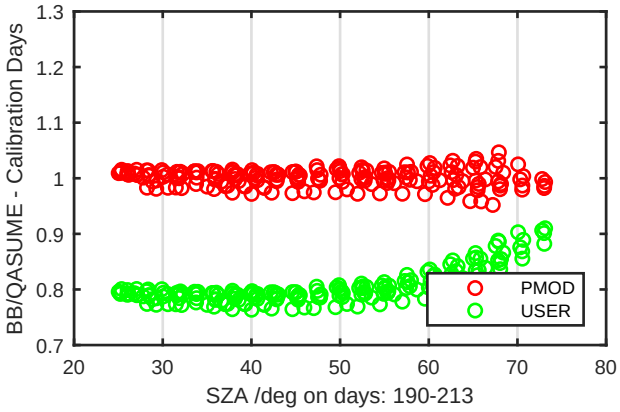

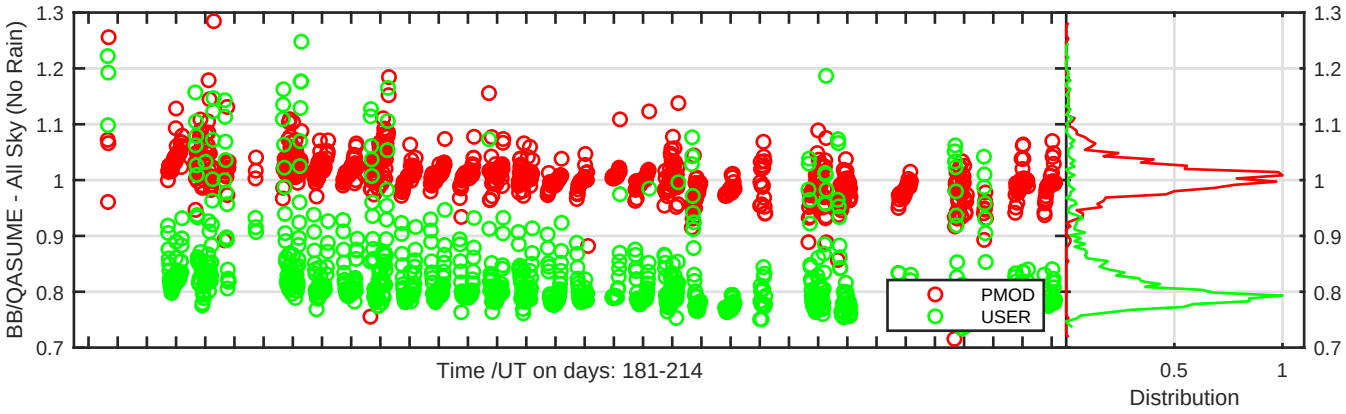

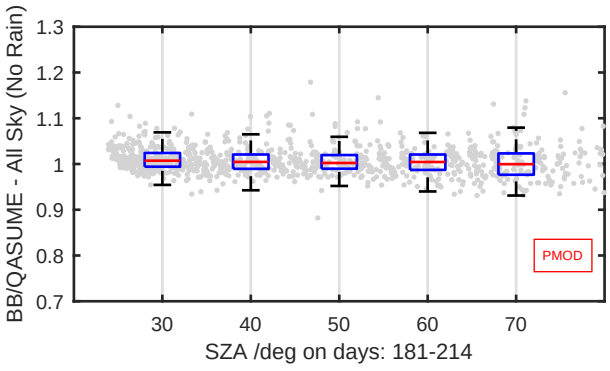

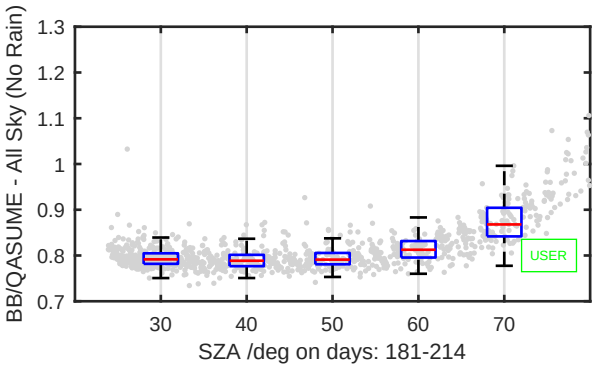

Calibration Results of KZ170200 (UVE)

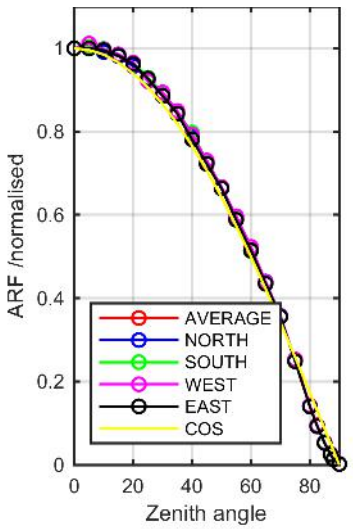

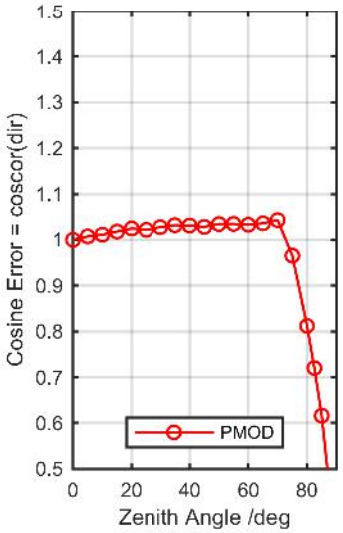

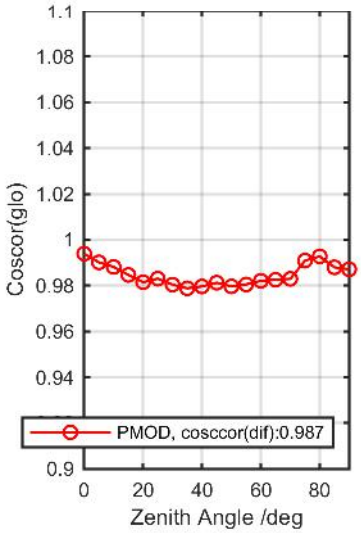

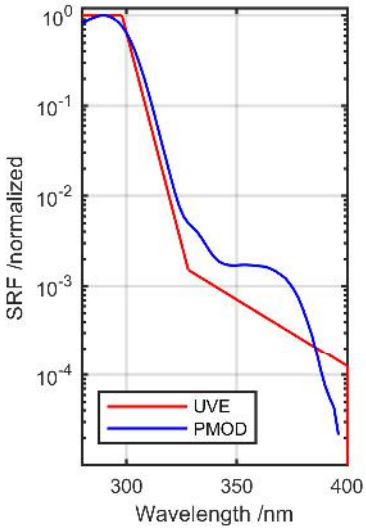

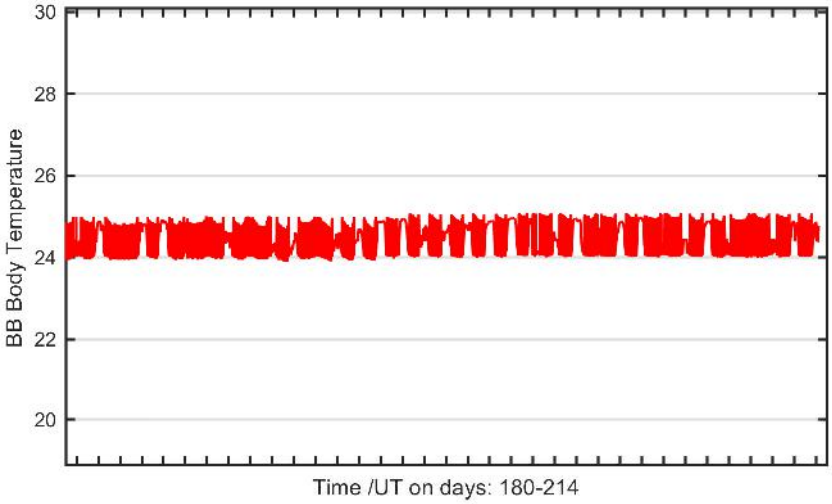

Calibration Matrix fn; Model sdisortREFms2009; f0=0.5447

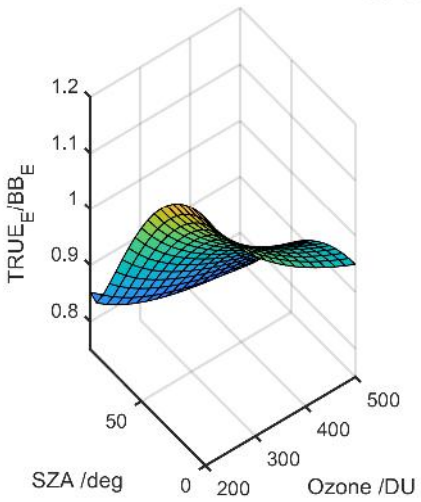

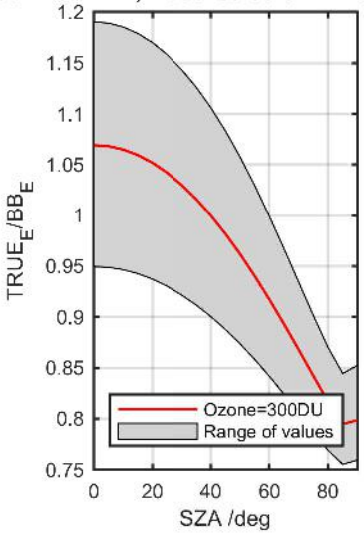

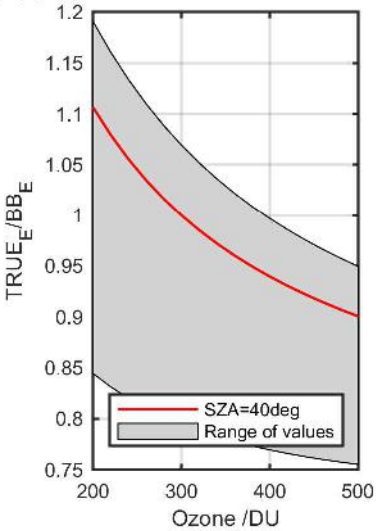

Calibration Results of KZ170200 (UVE)

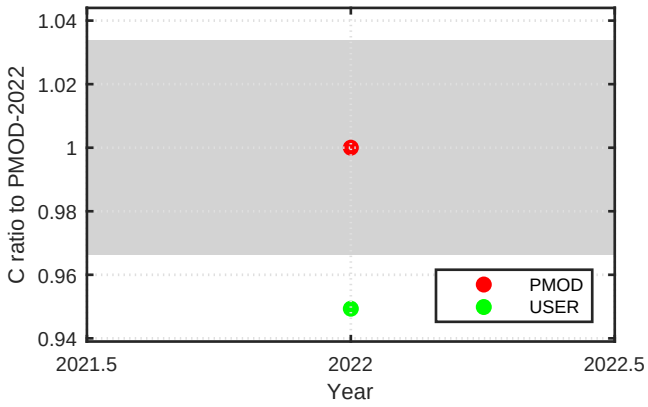

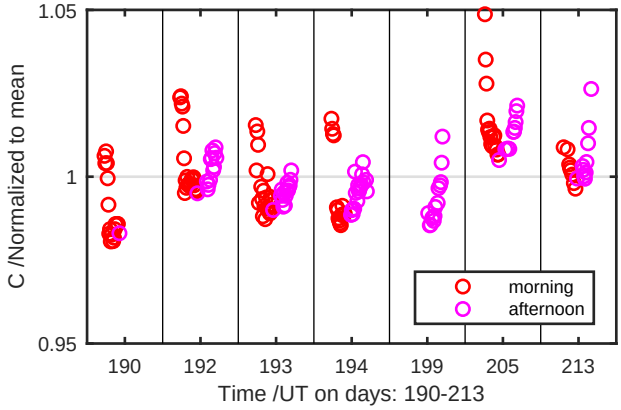

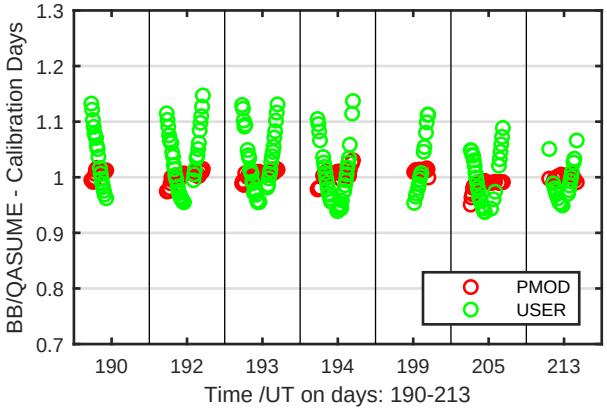

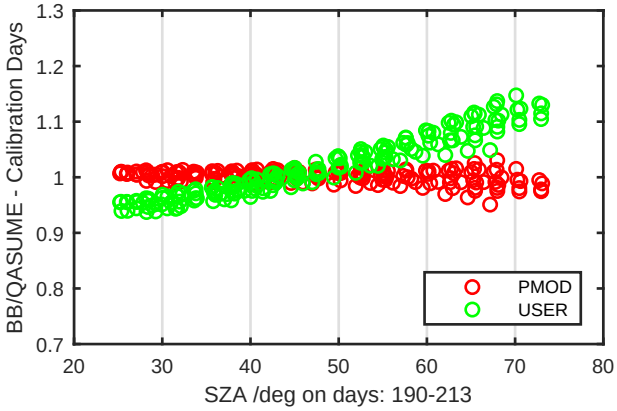

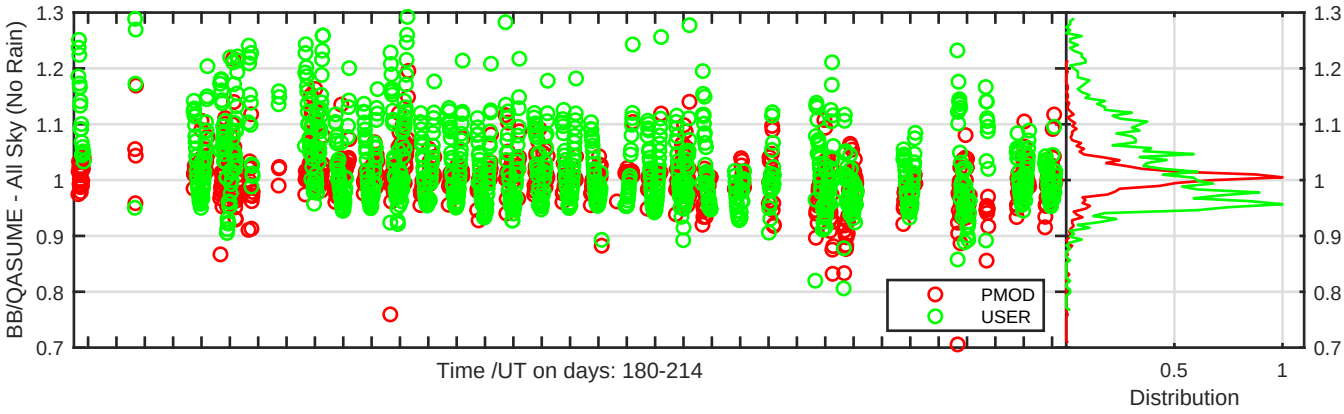

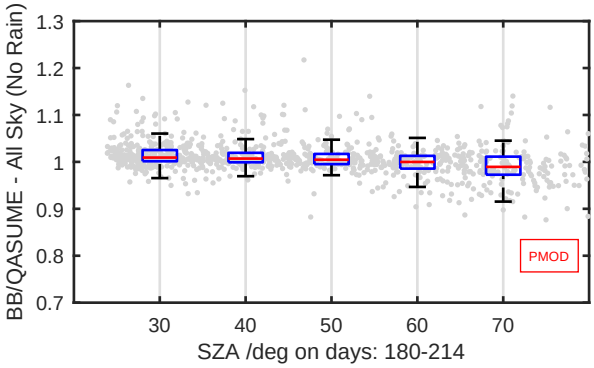

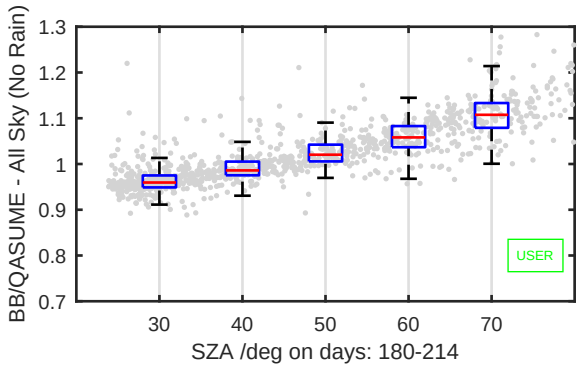

Calibration Results of KZ170201 (UVE)

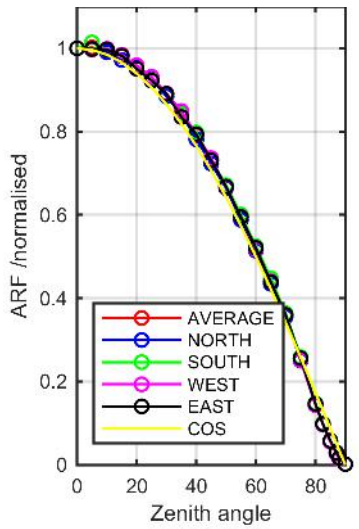

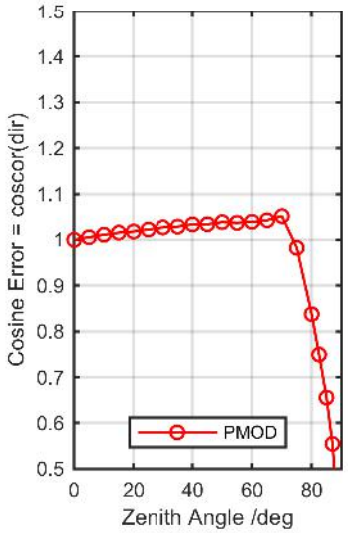

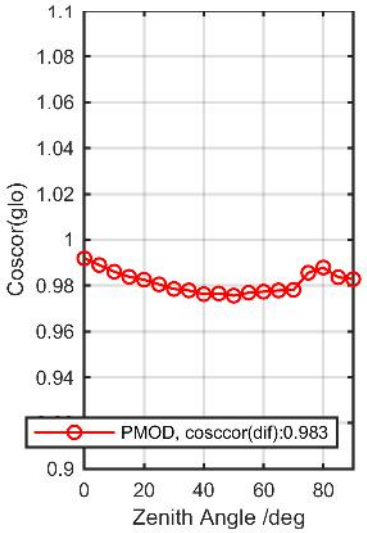

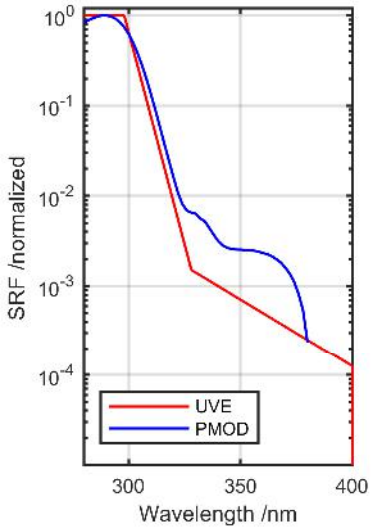

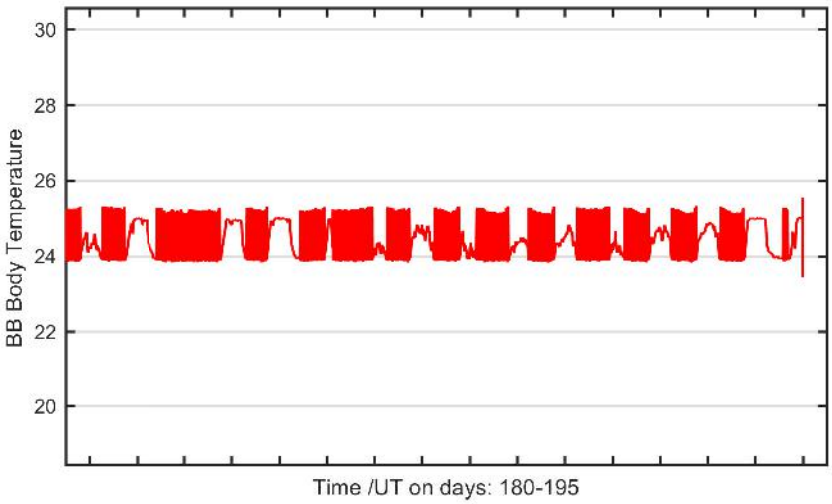

Calibration Matrix fn; Model sdisortREFms2009; f0=0.5225

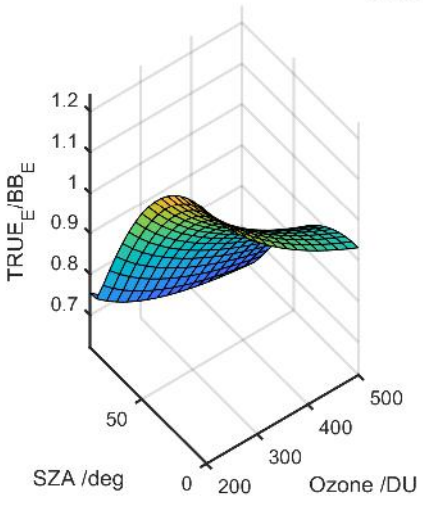

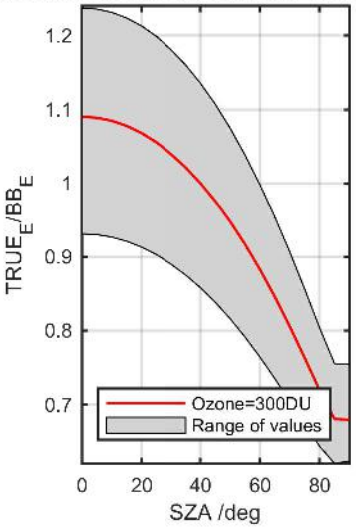

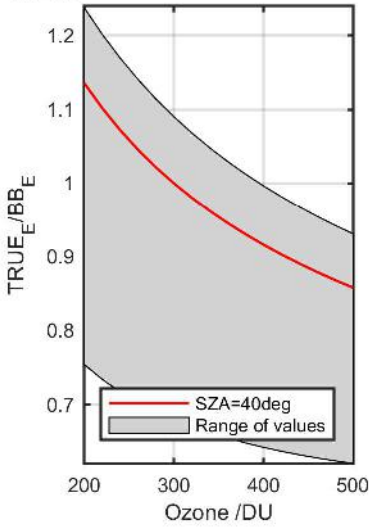

Calibration Results of KZ170201 (UVE)

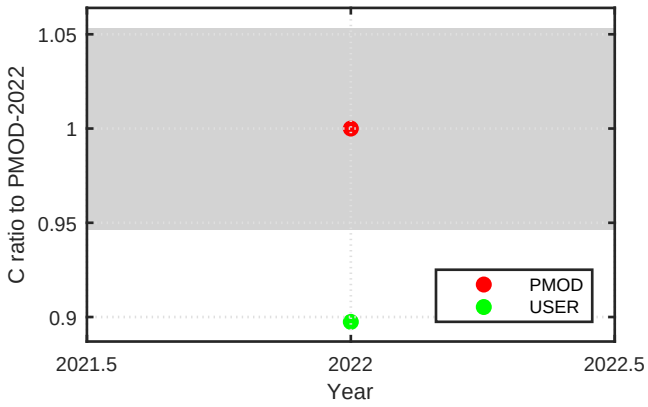

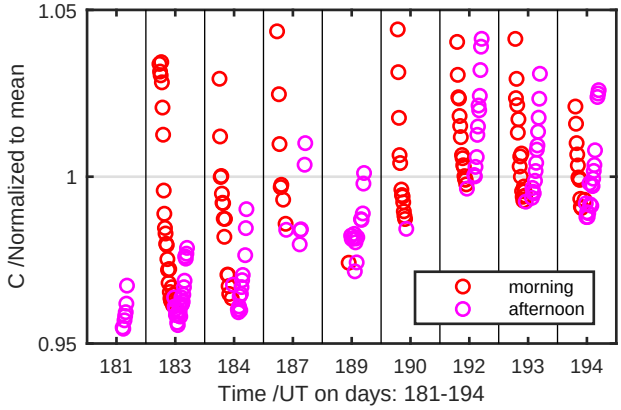

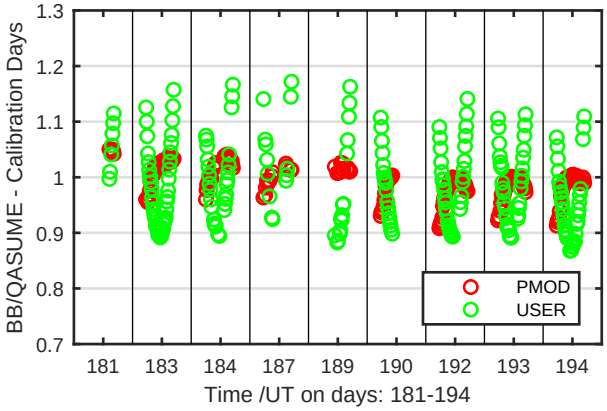

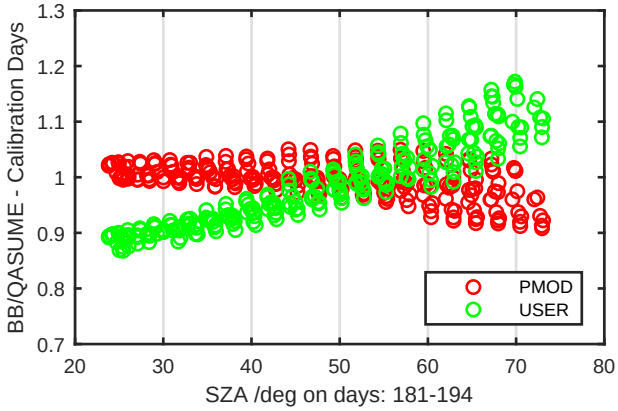

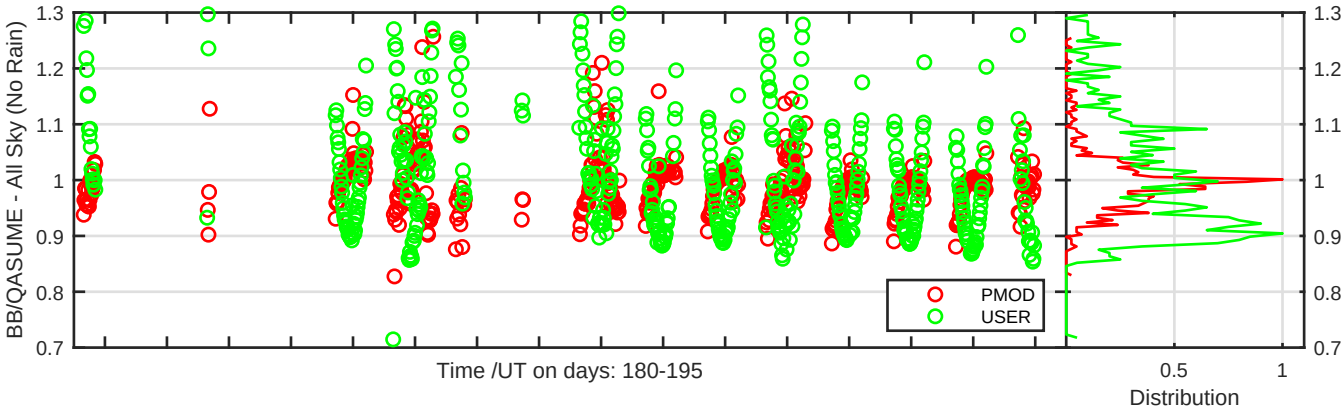

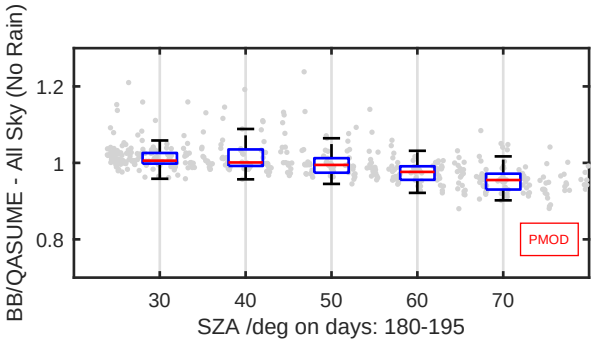

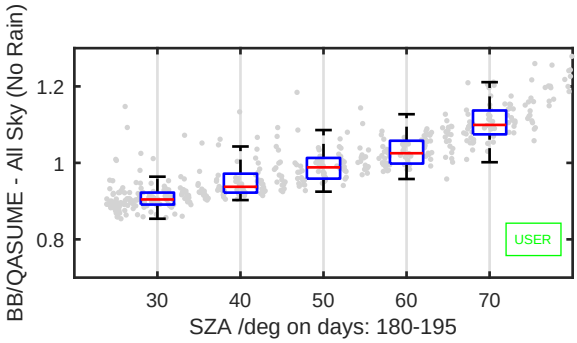

Calibration Results of KZ170204 (UVE)

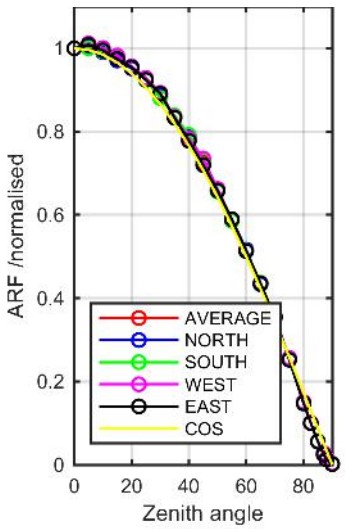

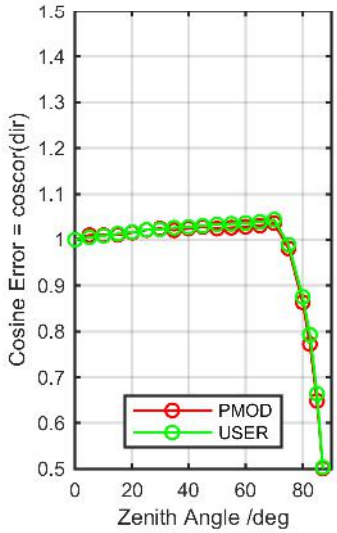

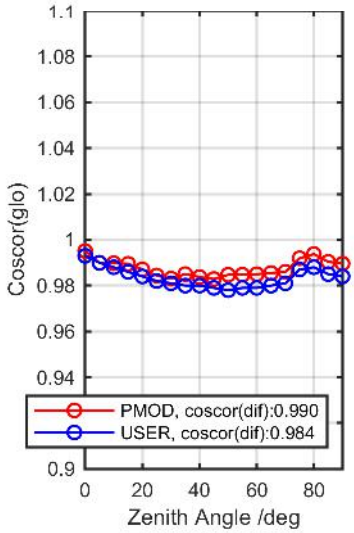

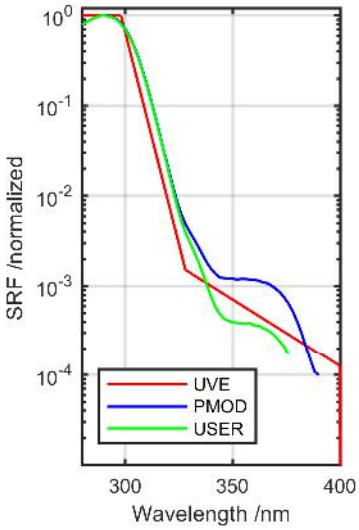

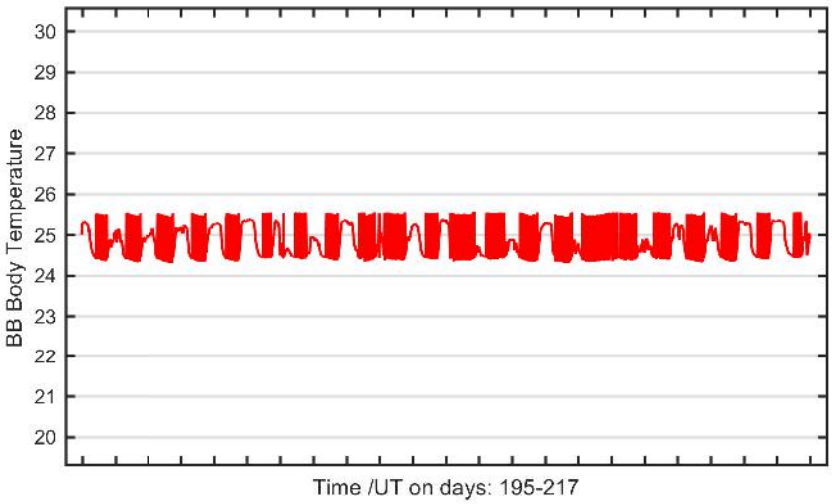

Calibration Matrix fn; Model sdisortREFms2009; f0=0.4833

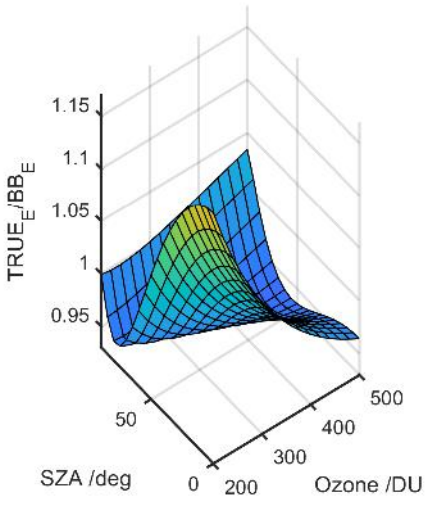

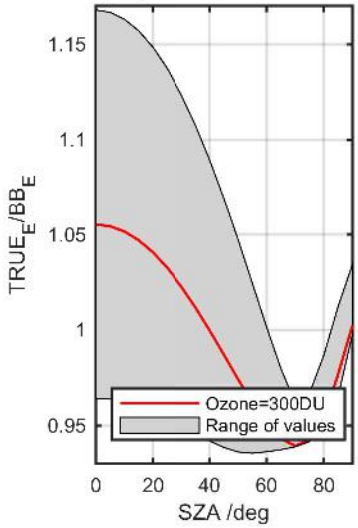

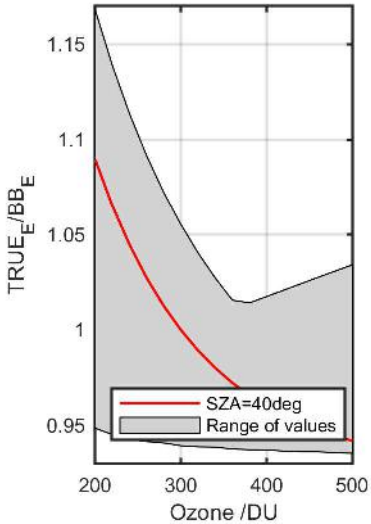

Calibration Results of KZ170204 (UVE)

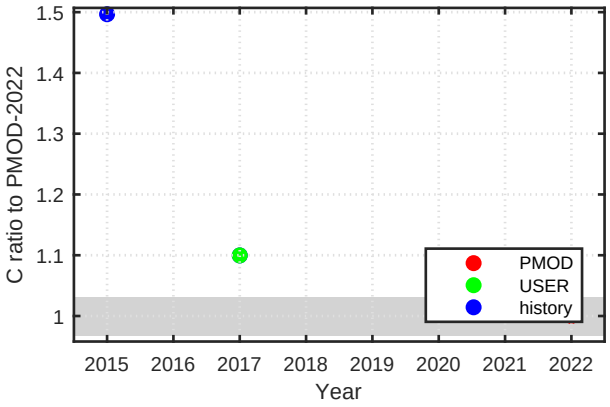

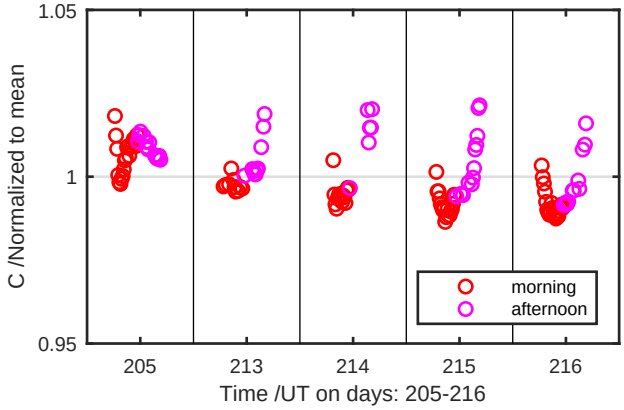

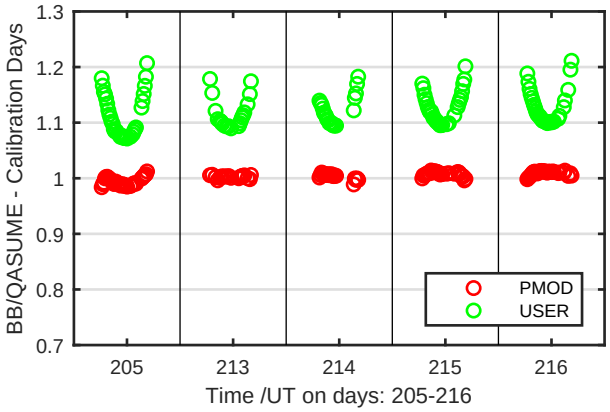

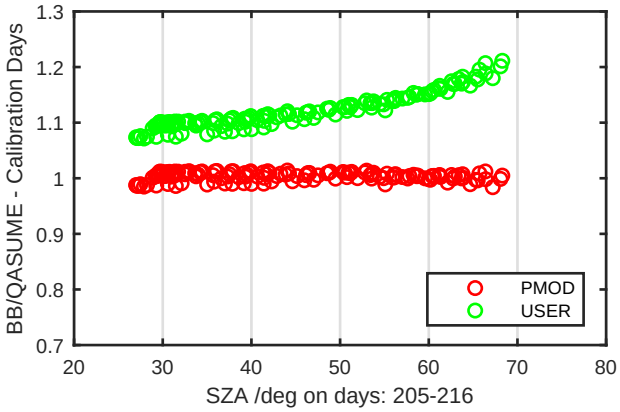

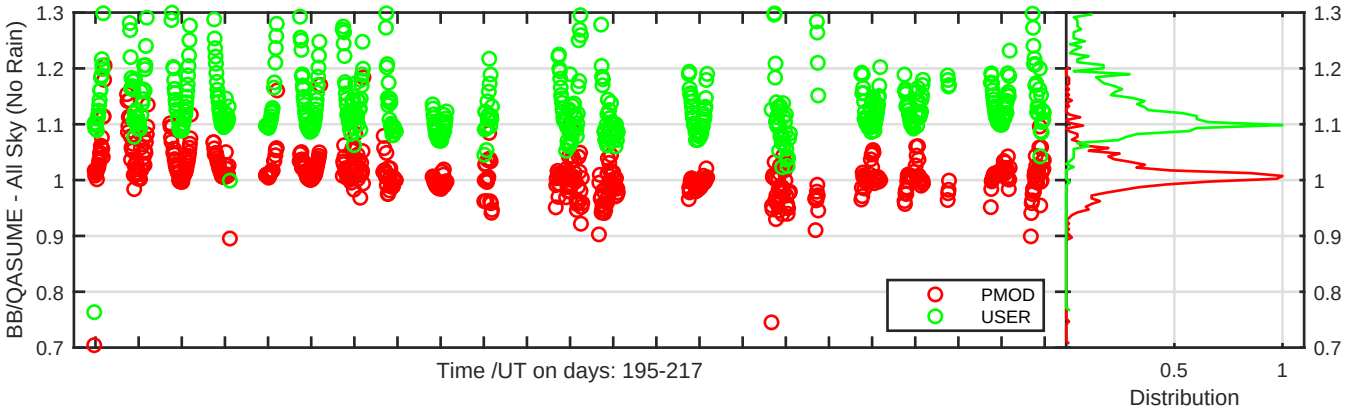

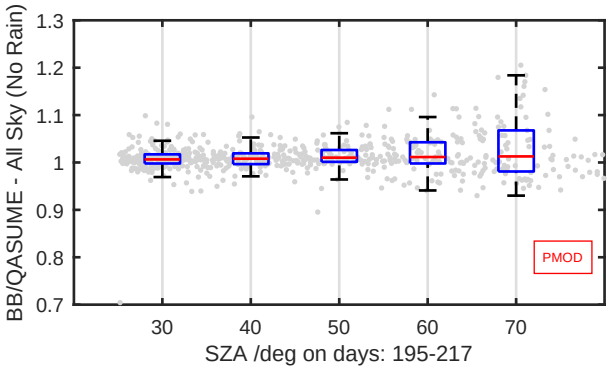

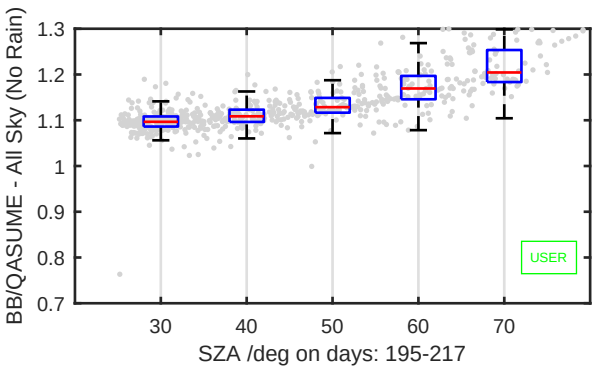

Calibration Results of KZ170213 (UVE)

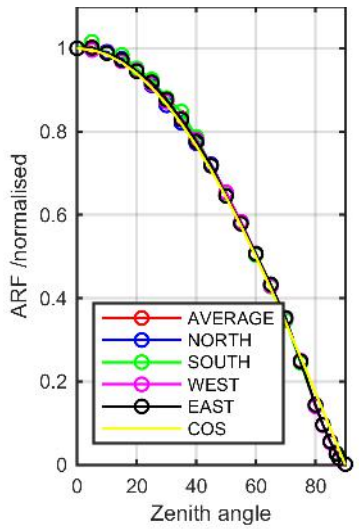

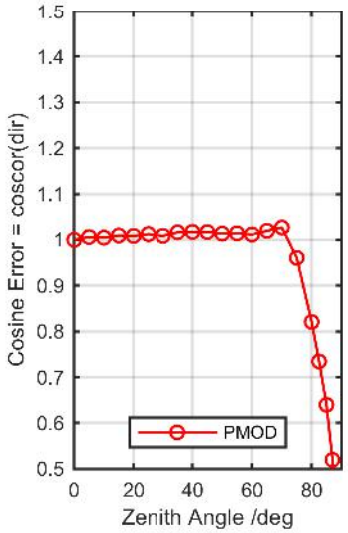

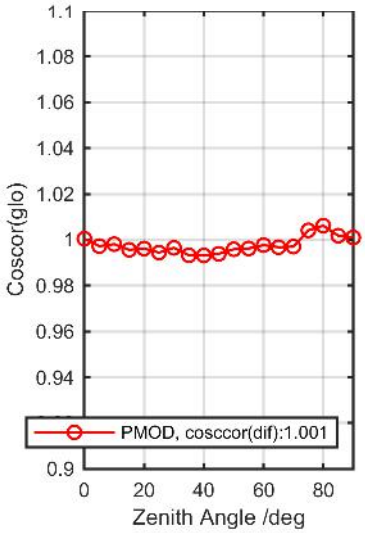

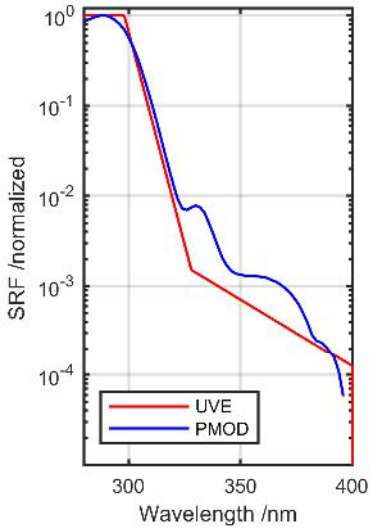

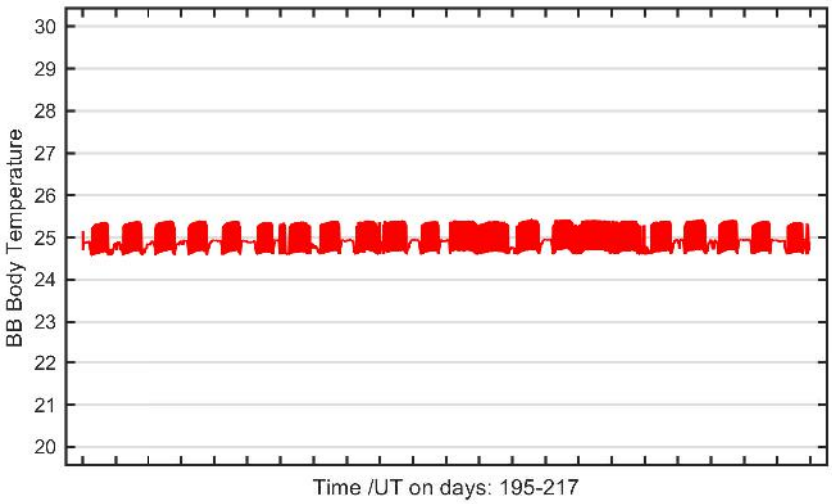

Calibration Matrix fn; Model sdisortREFms2009; f0=0.6107

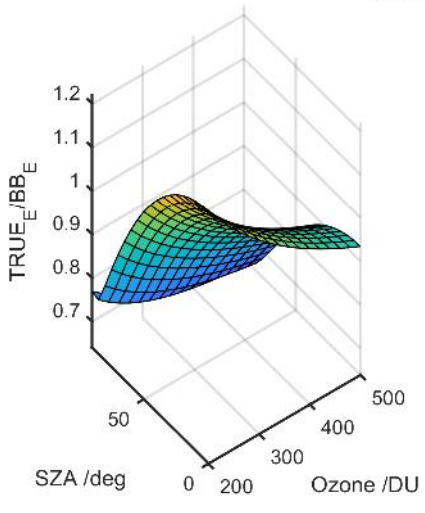

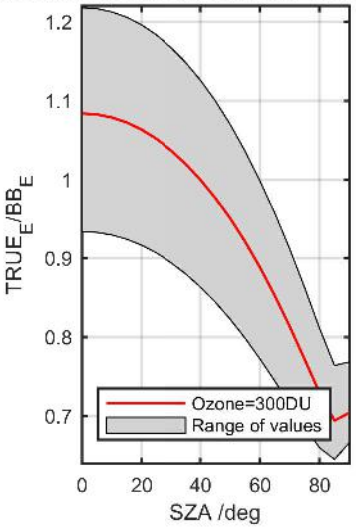

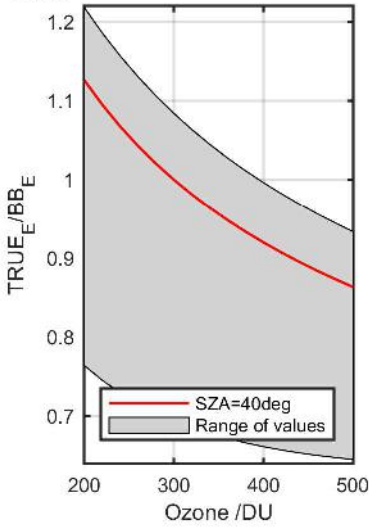

Calibration Results of KZ170213 (UVE)

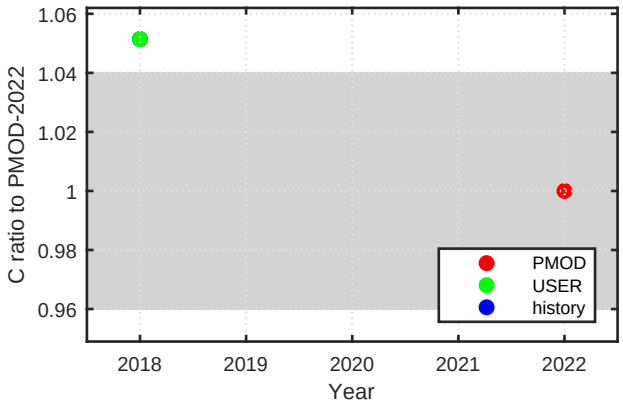

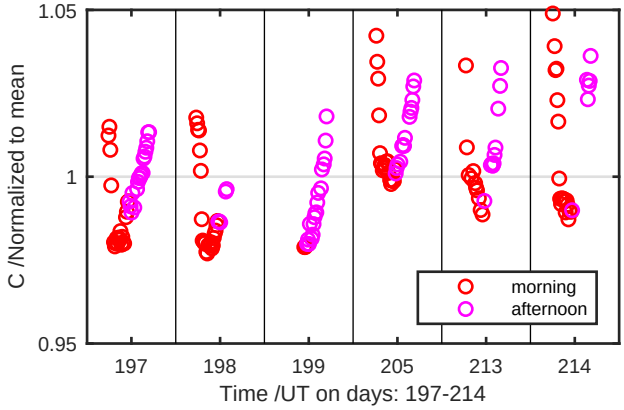

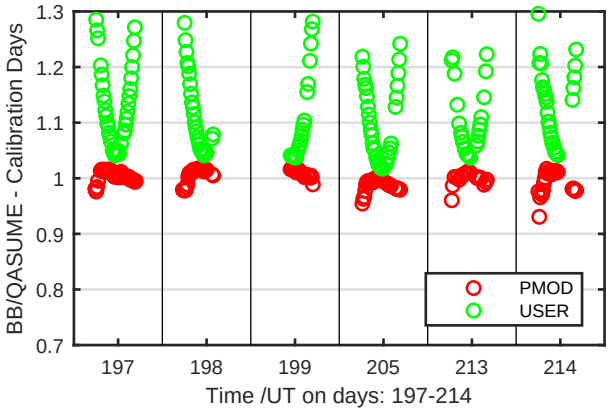

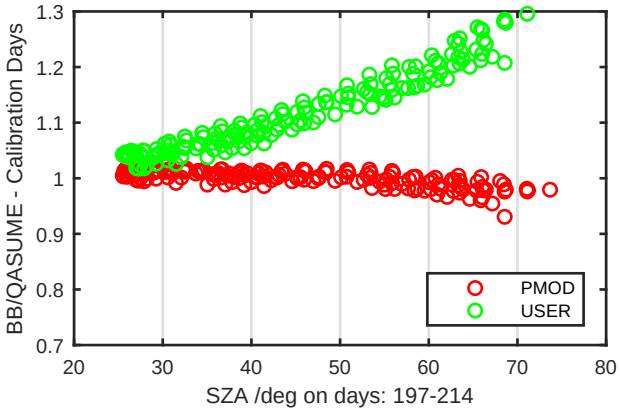

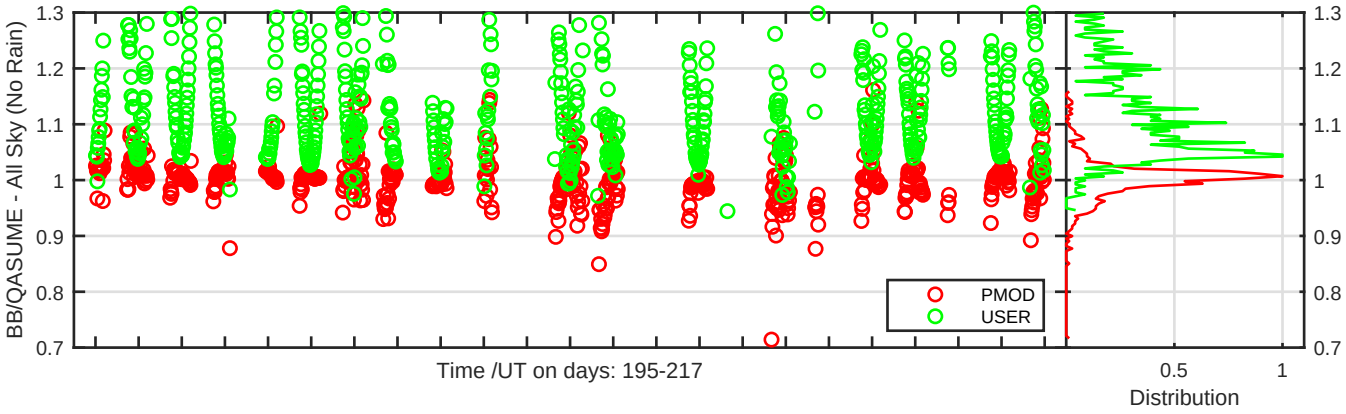

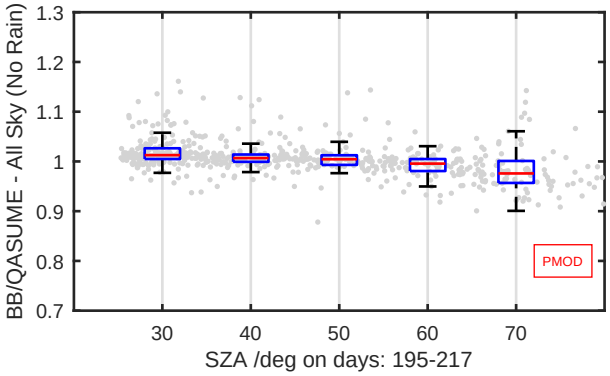

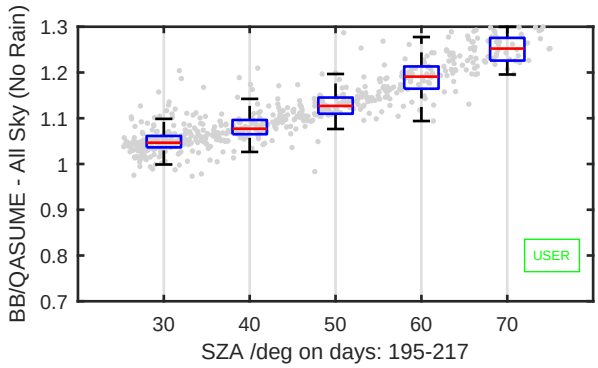

Calibration Results of KZ160142 (UVE)

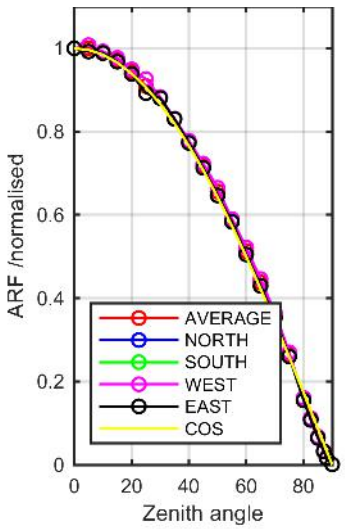

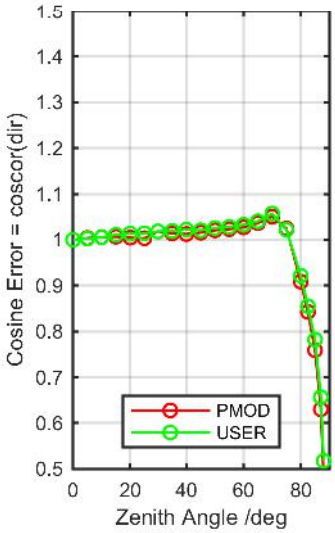

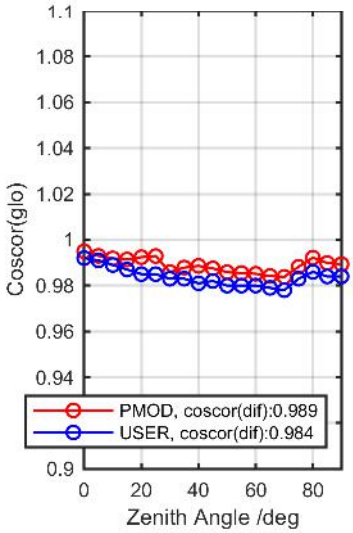

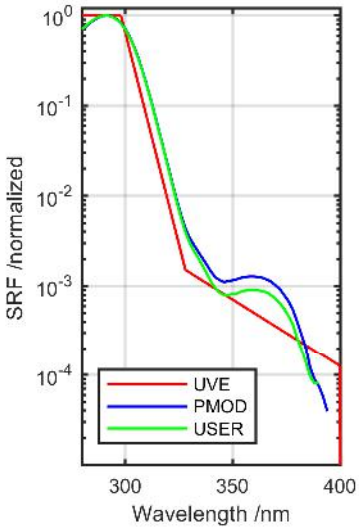

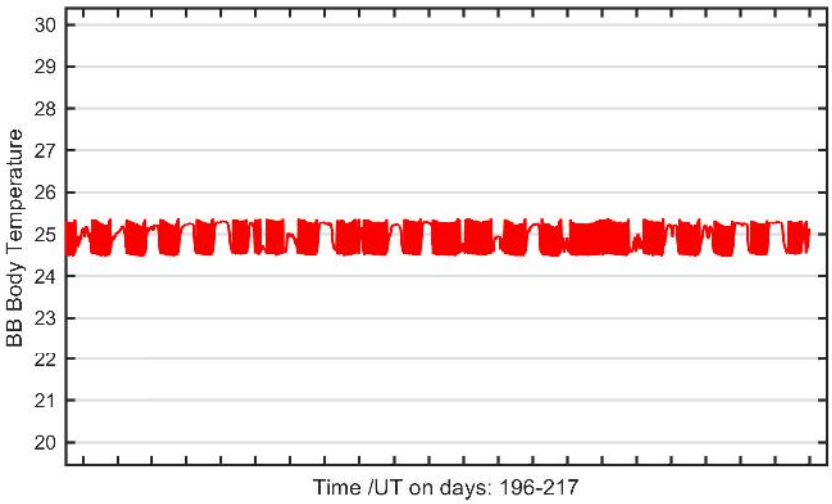

Calibration Matrix fn; Model sdisortREFms2009; f0=0.4869

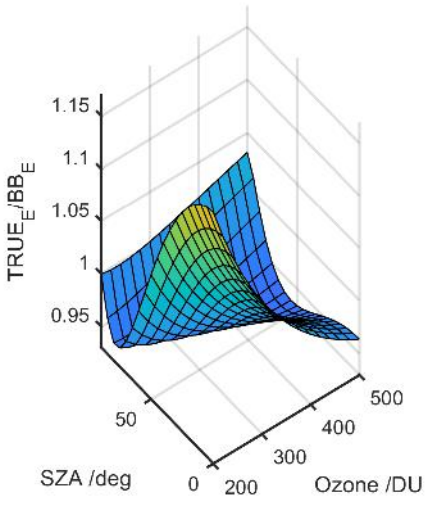

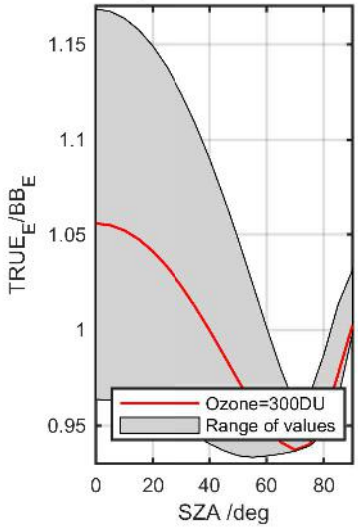

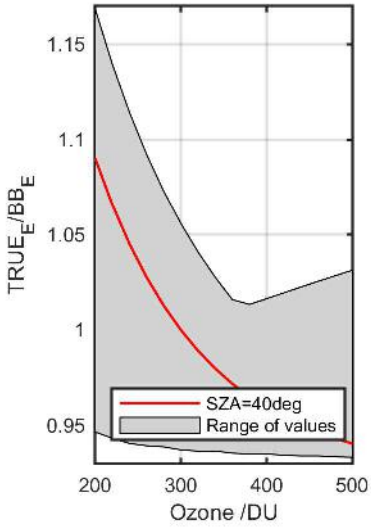

Calibration Results of KZ160142 (UVE)

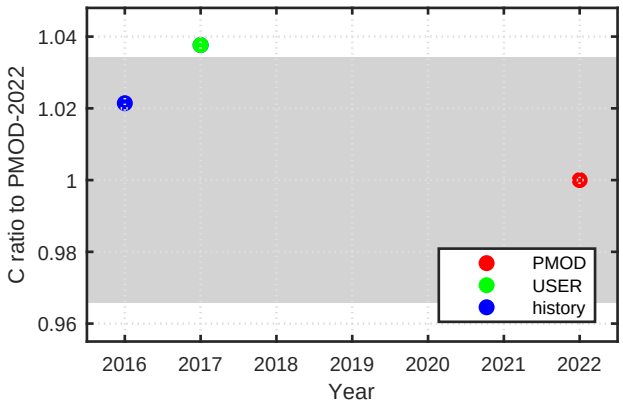

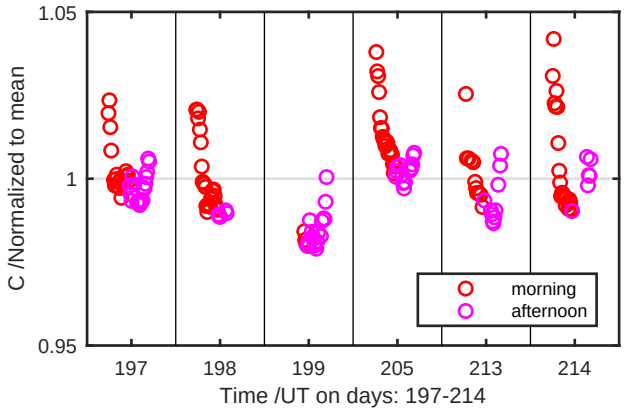

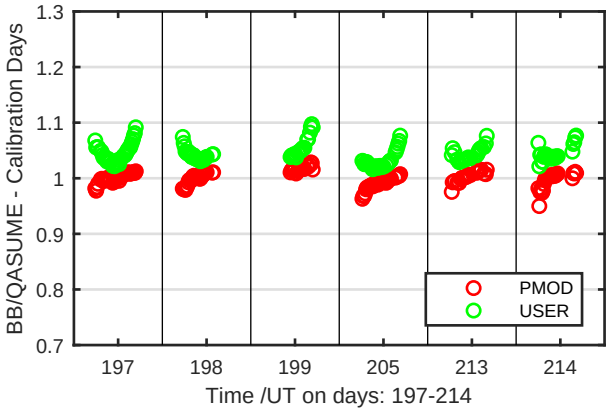

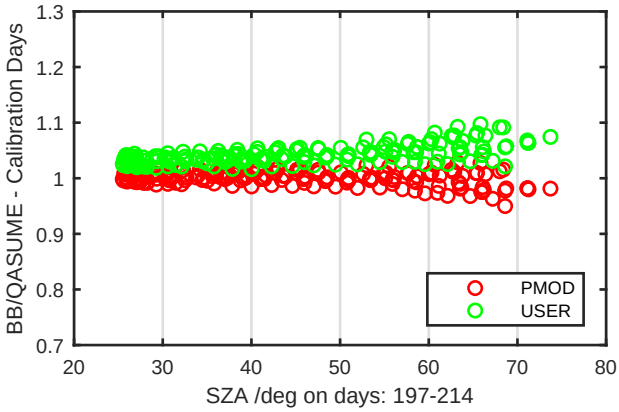

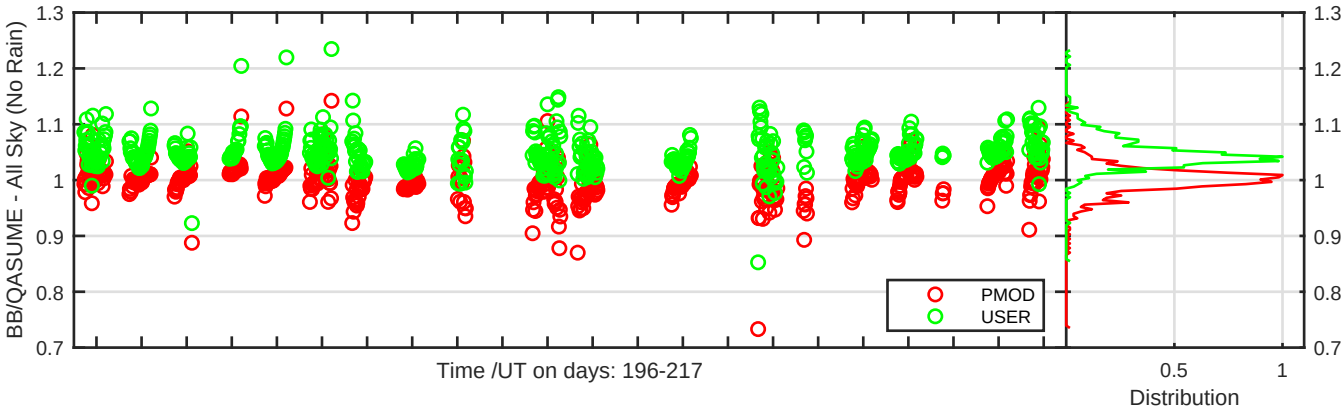

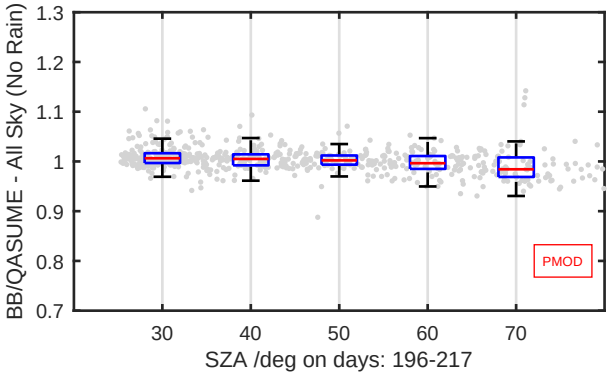

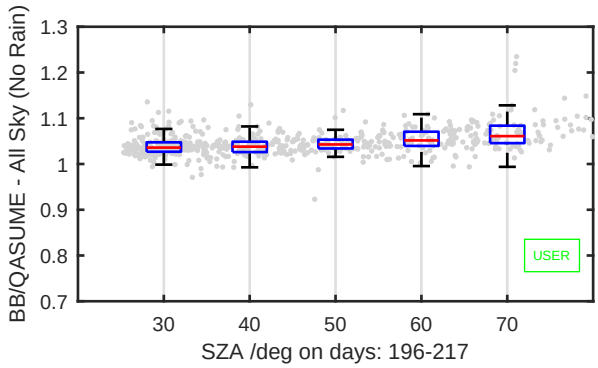

Calibration Results of KZ070643 (UVE)

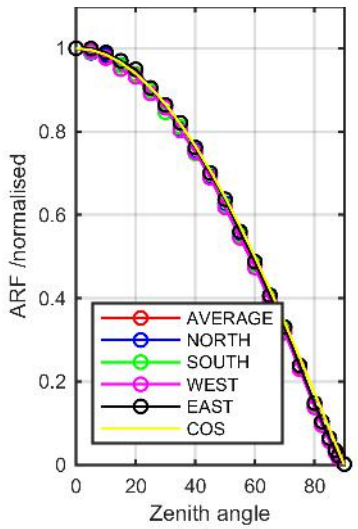

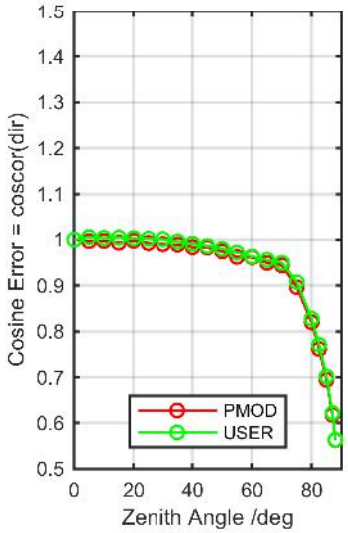

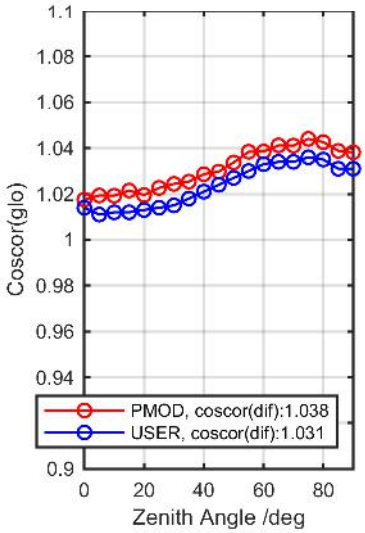

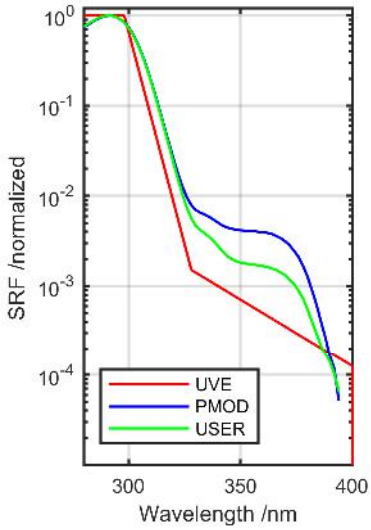

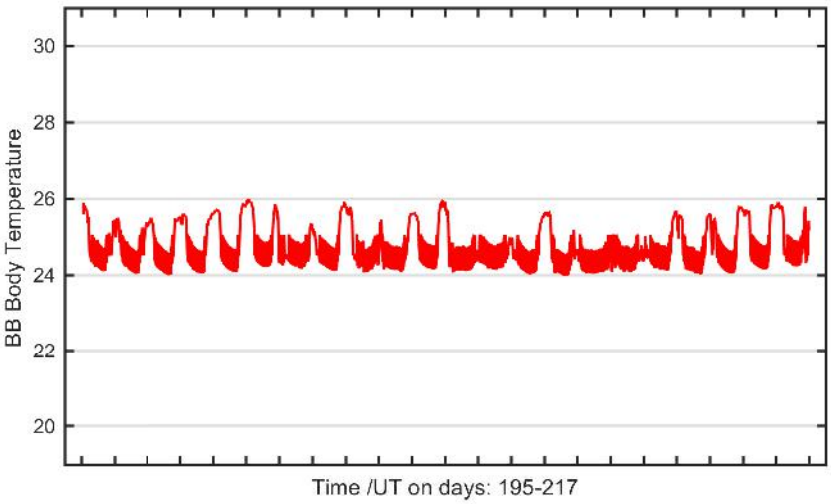

Calibration Matrix fn; Model sdisortREFms2009; f0=0.3563

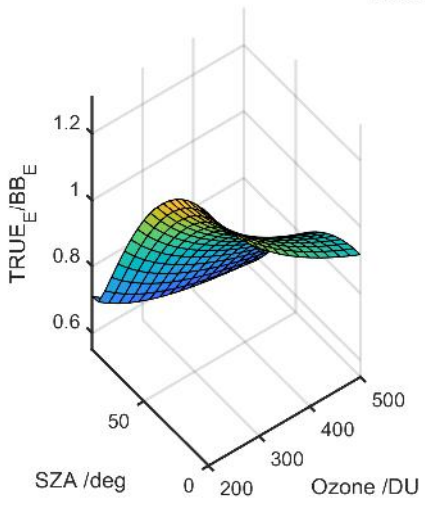

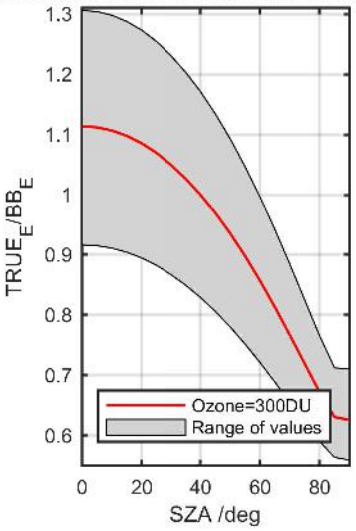

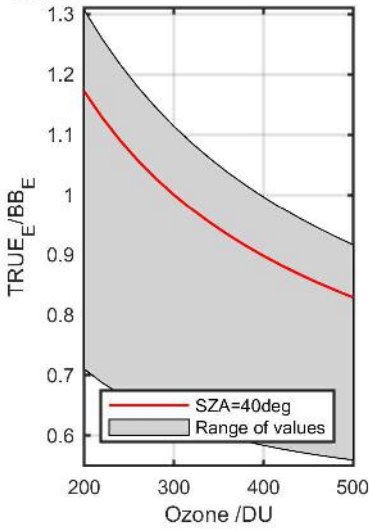

Calibration Results of KZ070643 (UVE)

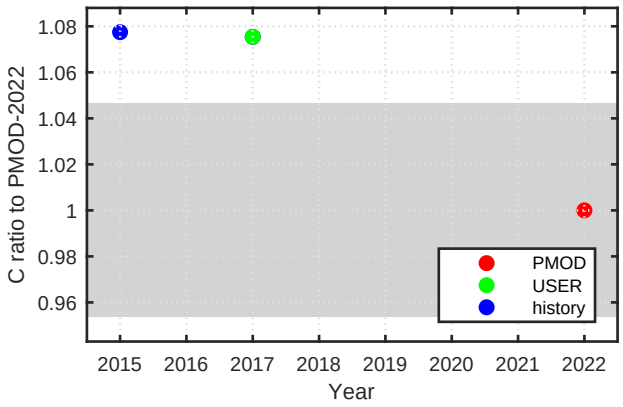

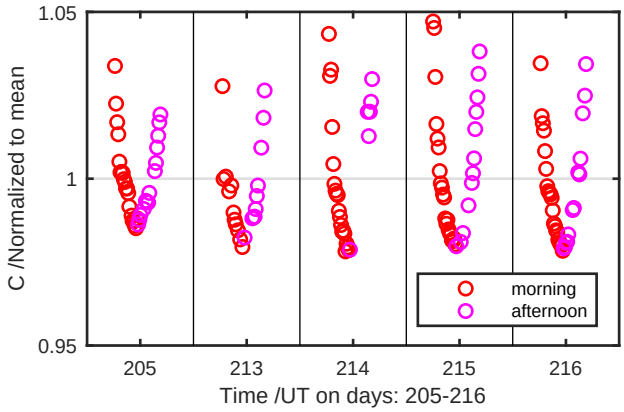

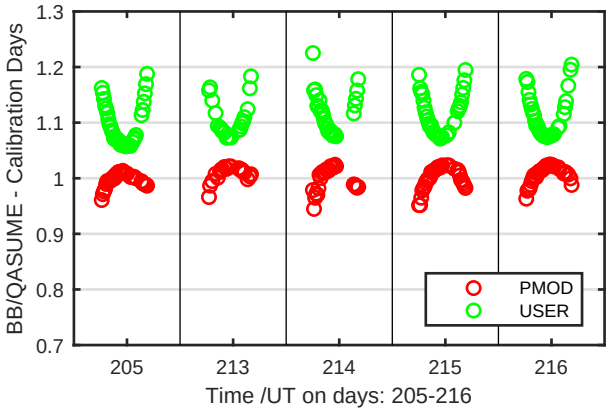

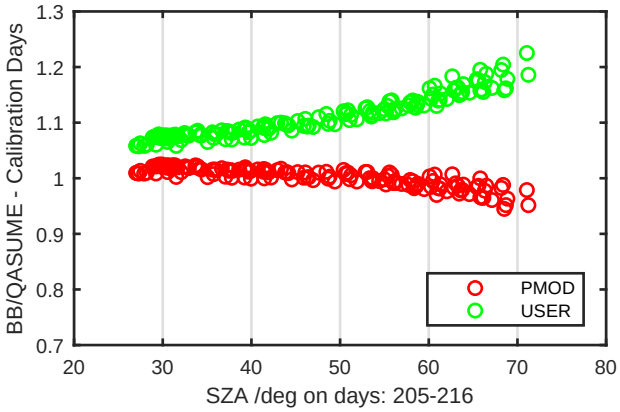

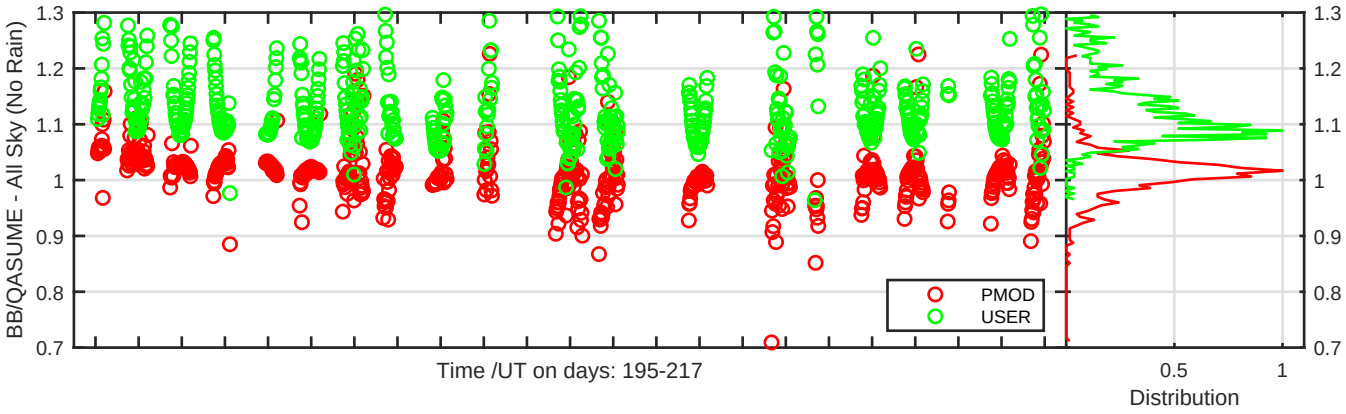

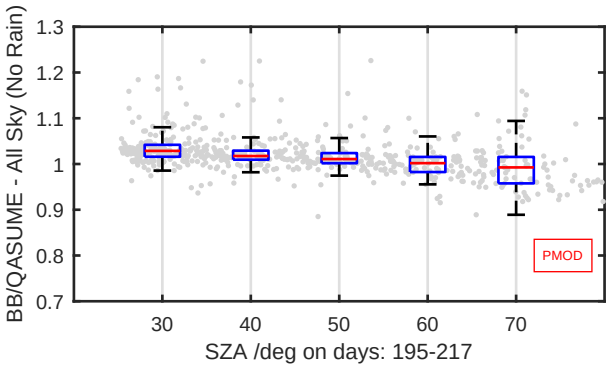

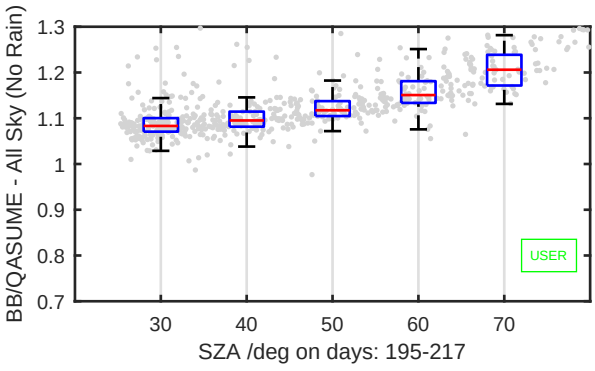

Calibration Results of KZ090015 (UVB)

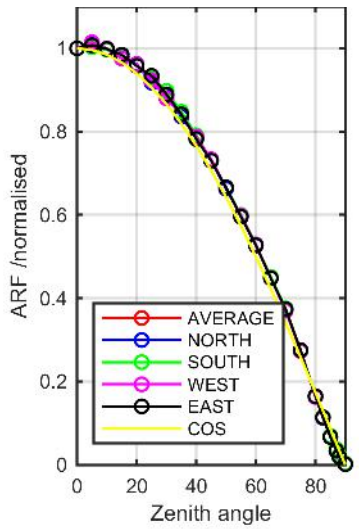

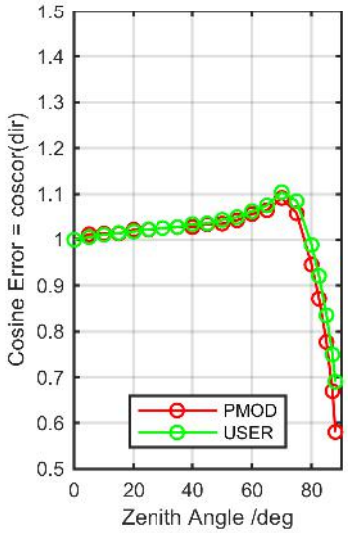

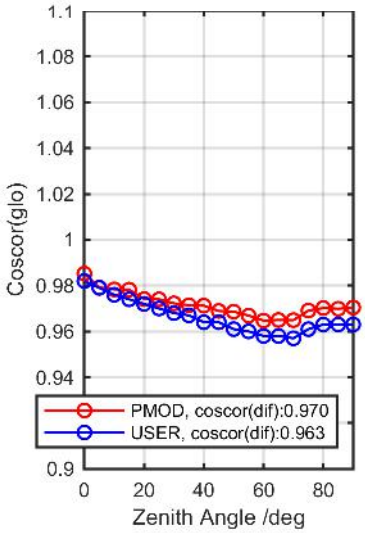

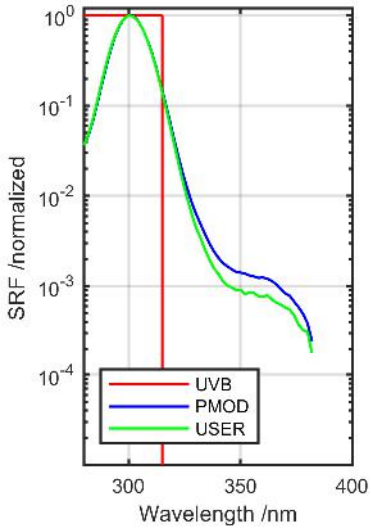

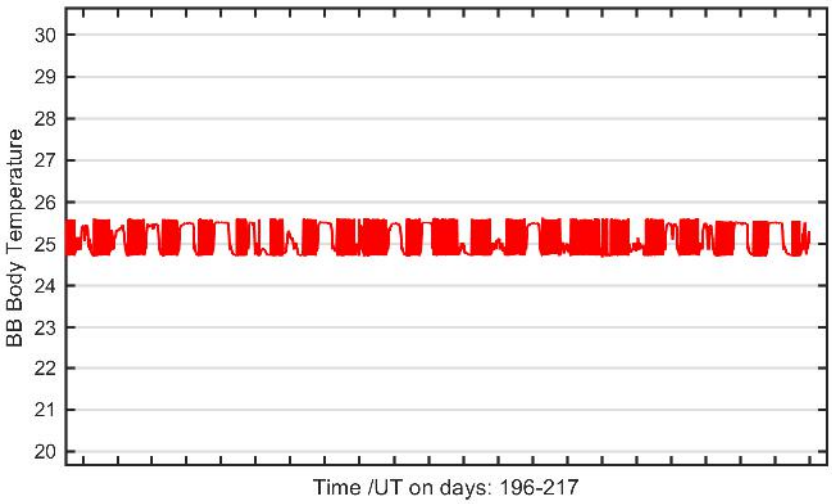

Calibration Matrix fn; Model sdisortREFms2009; f0=1.7977

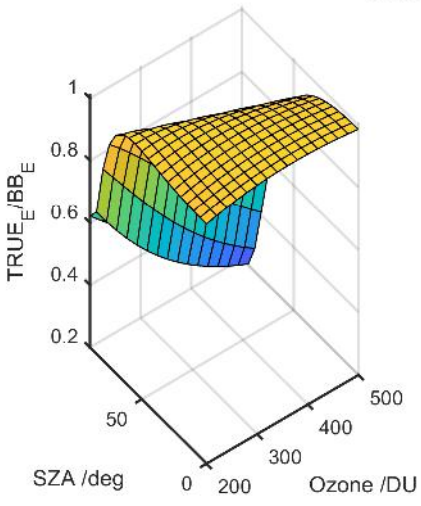

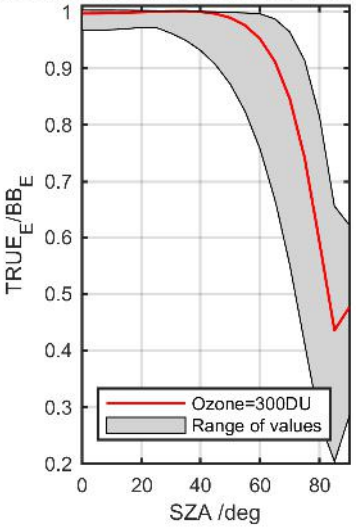

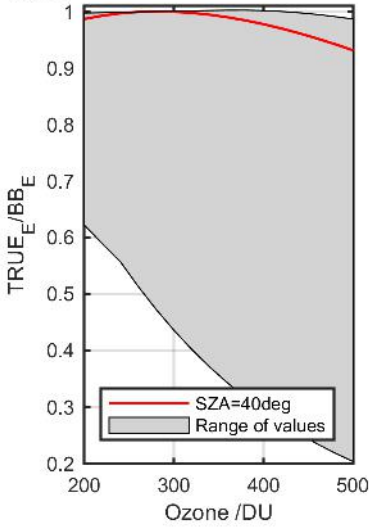

Calibration Results of KZ090015 (UVB)

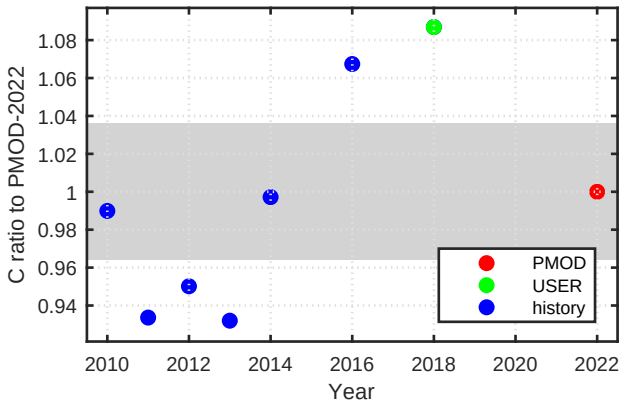

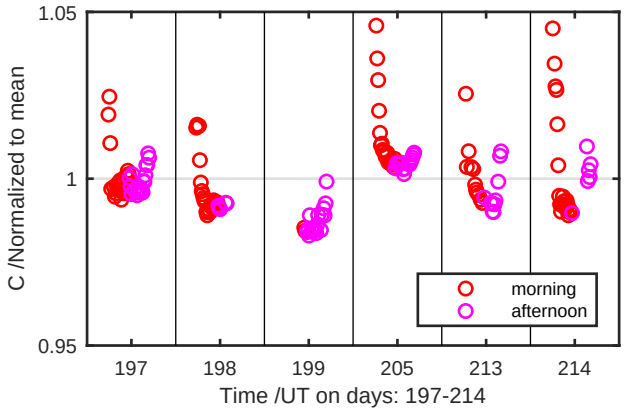

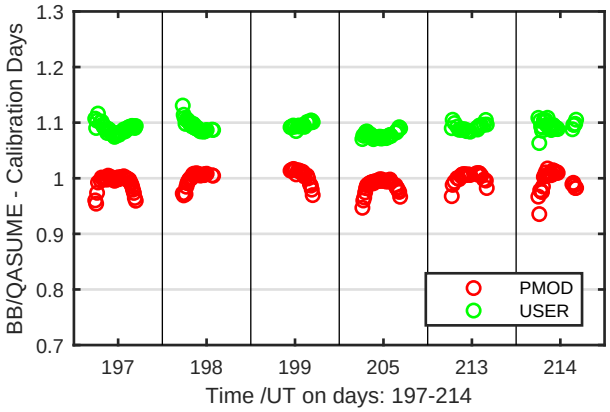

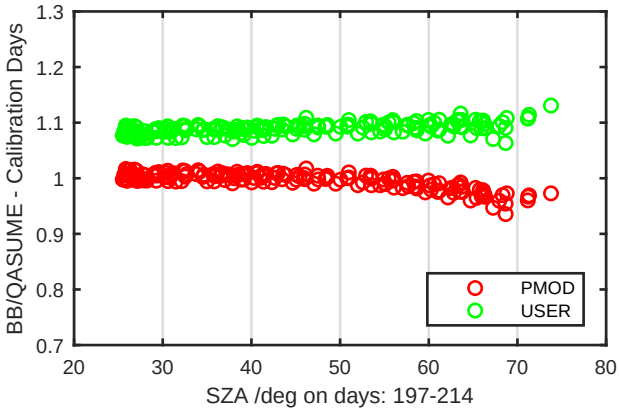

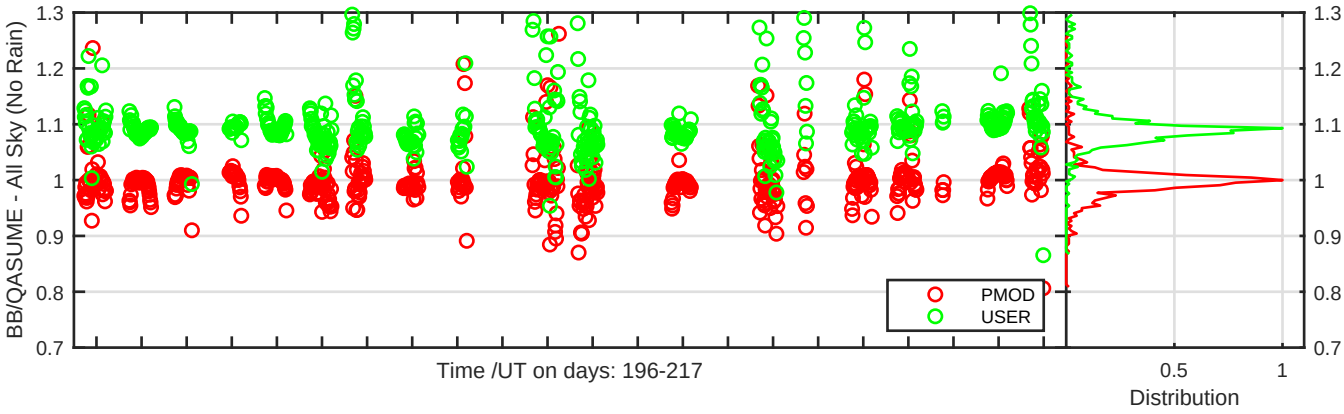

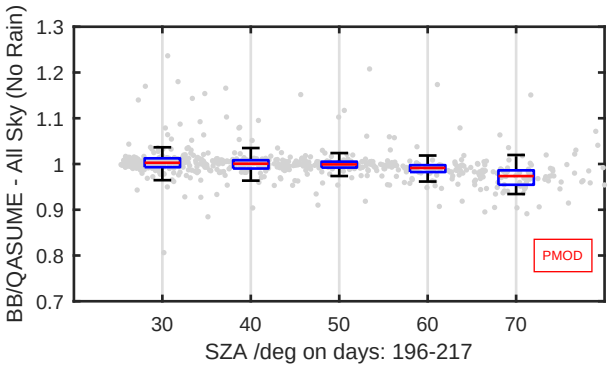

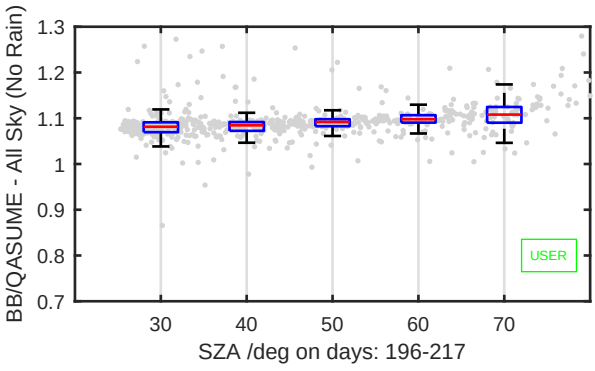

Calibration Results of KZ150127 (UVB)

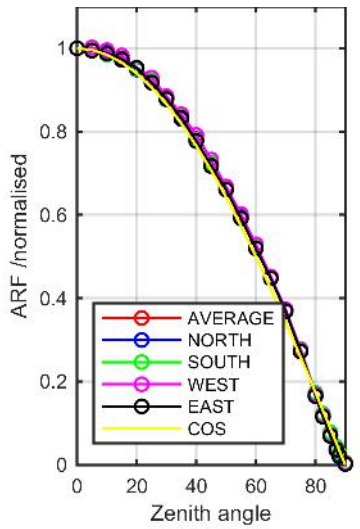

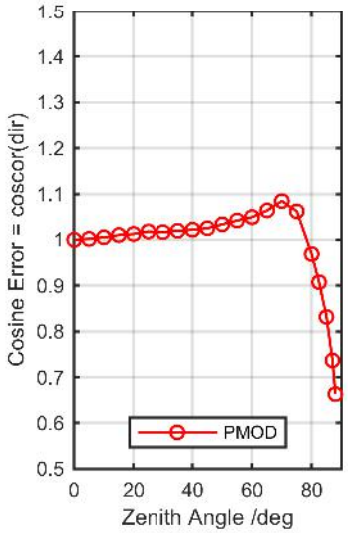

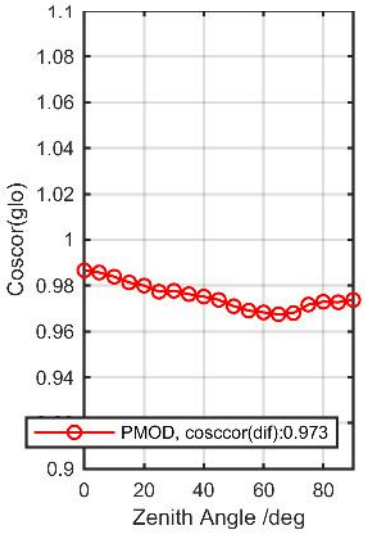

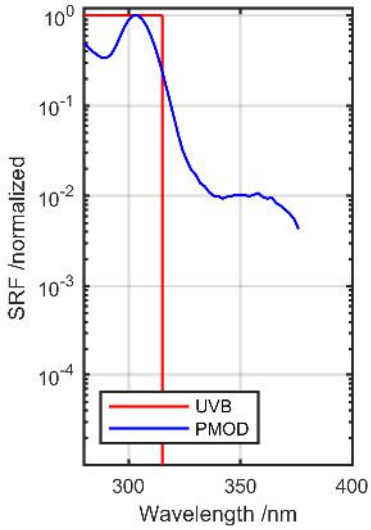

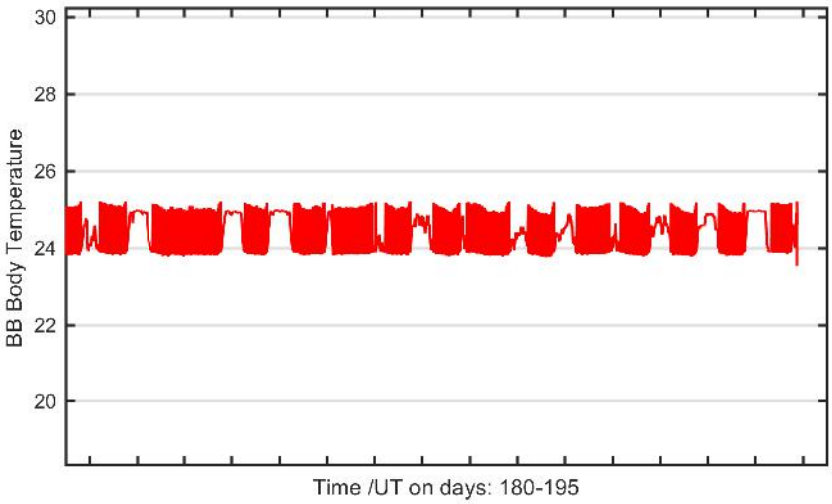

Calibration Matrix fn; Model sdisortREFms2009; f0=1.0386

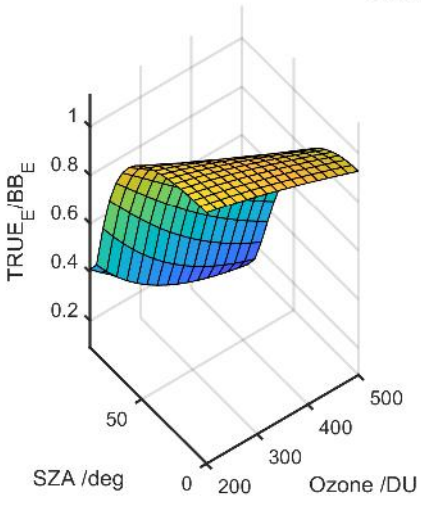

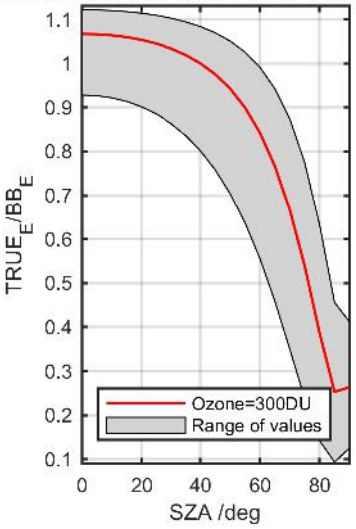

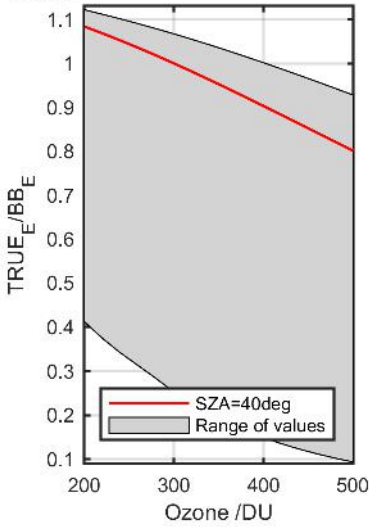

Calibration Results of KZ150127 (UVB)

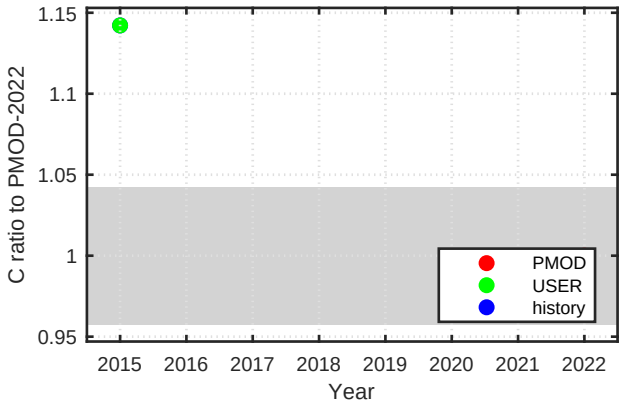

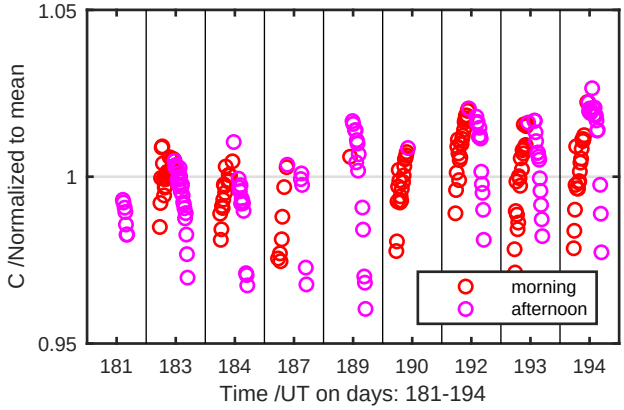

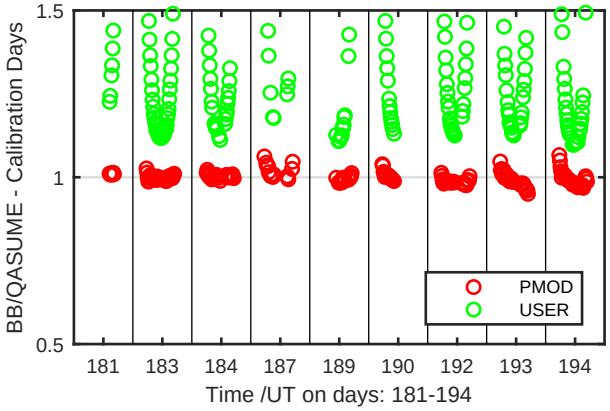

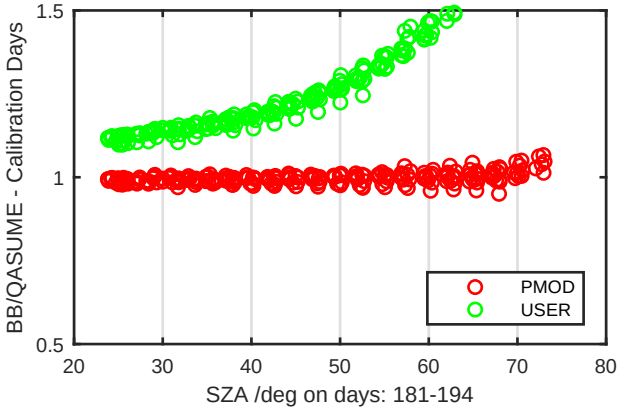

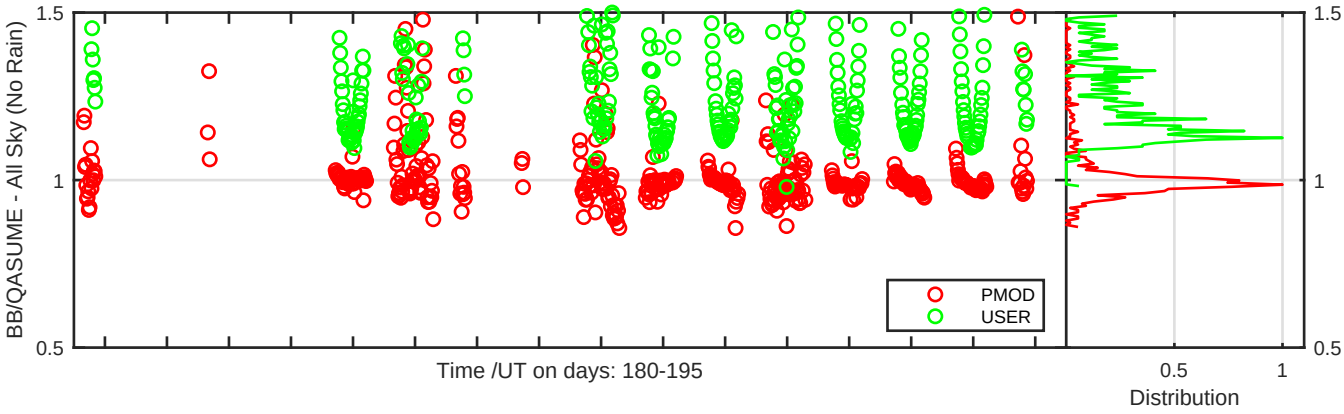

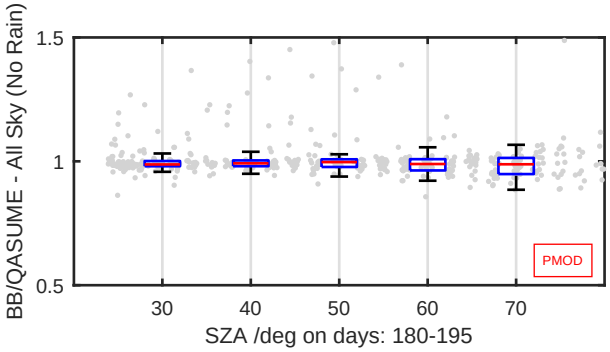

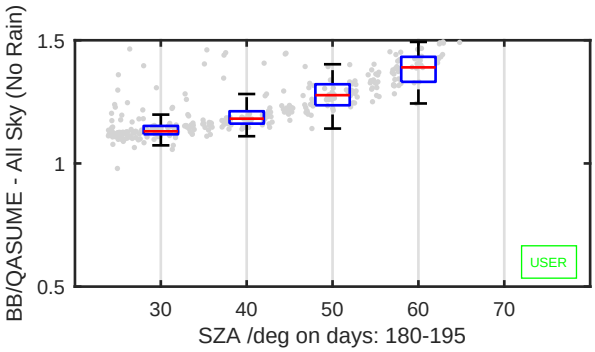

Calibration Results of KZ170143 (UVA)

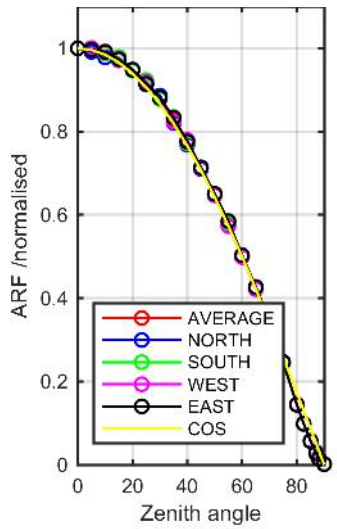

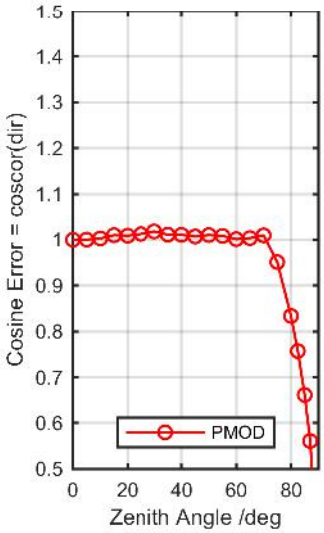

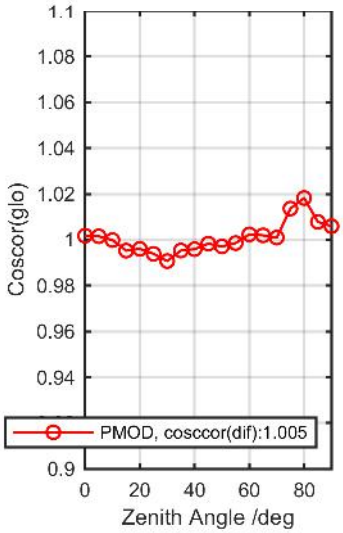

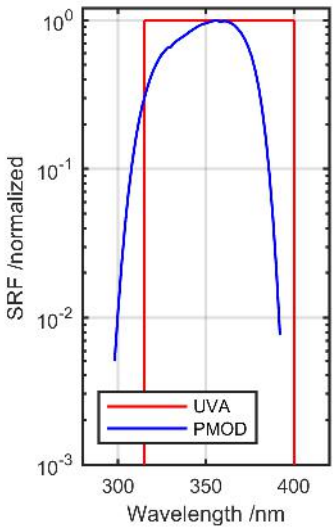

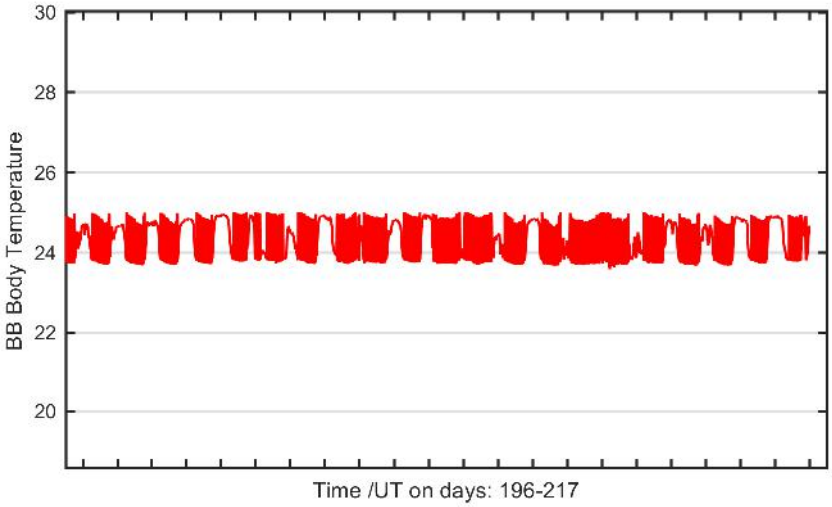

Calibration Matrix fn; Model sdisortREFms2009; f0=1.7185

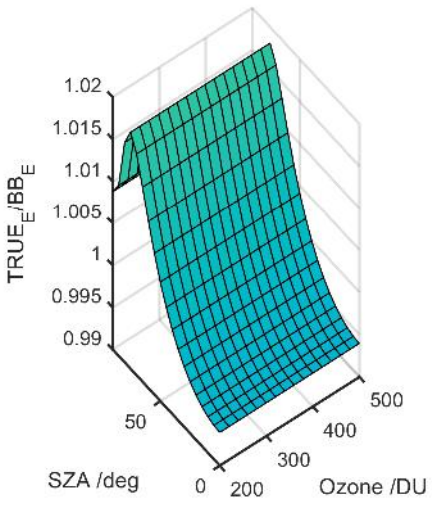

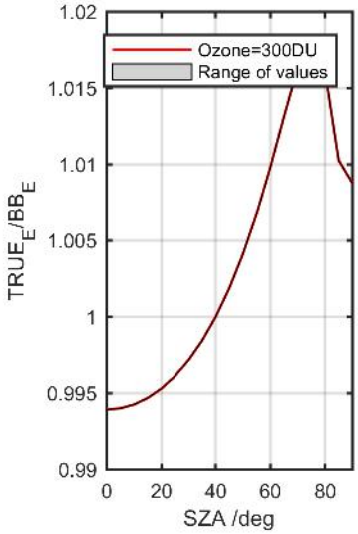

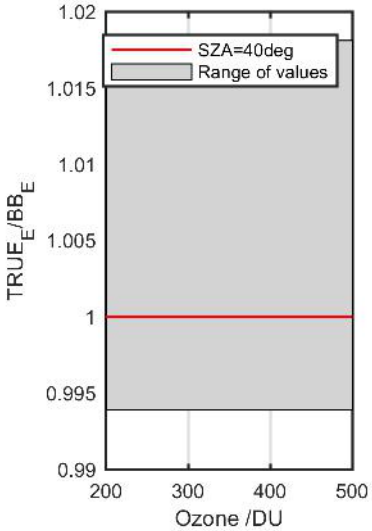

Calibration Results of KZ170143 (UVA)

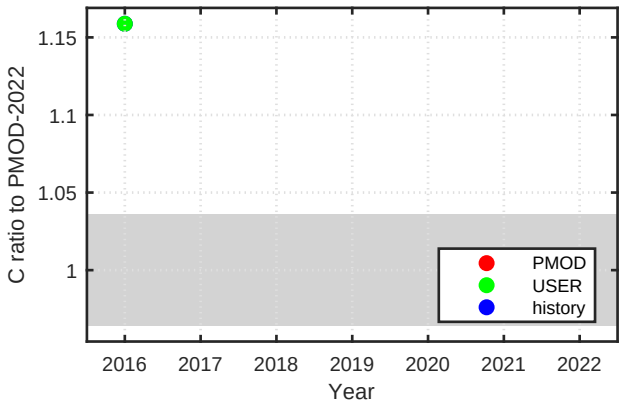

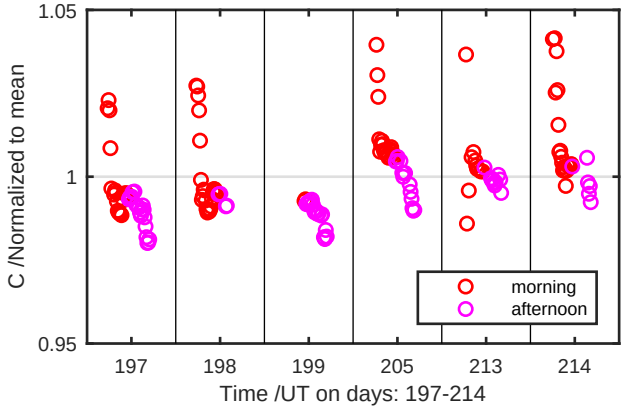

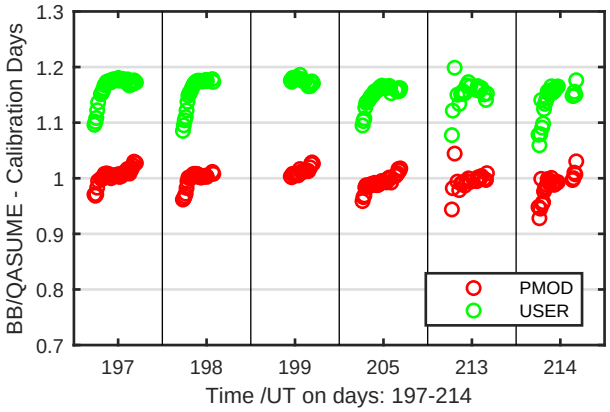

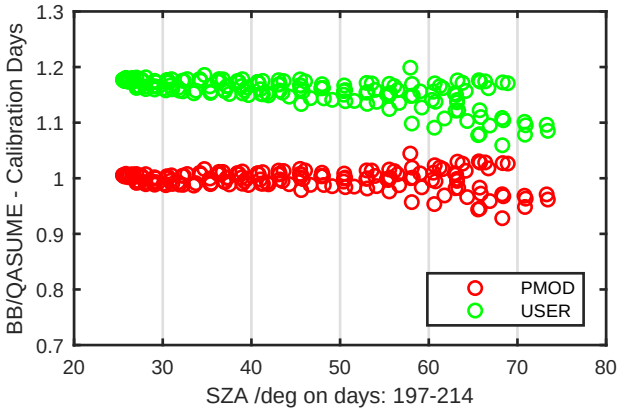

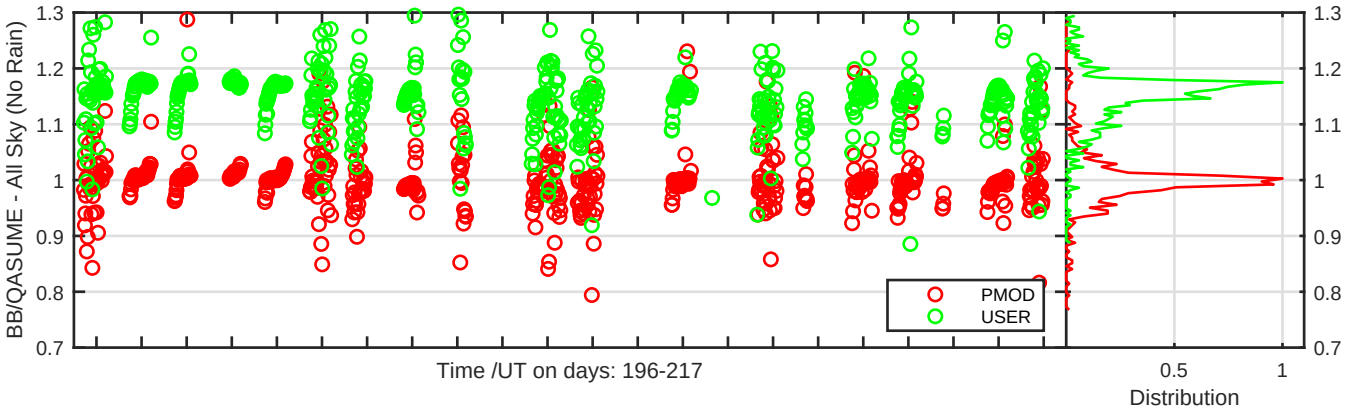

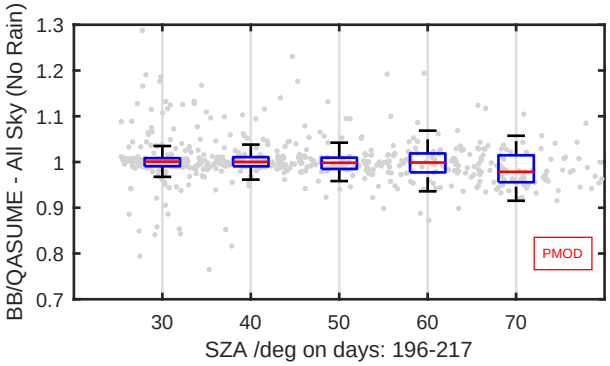

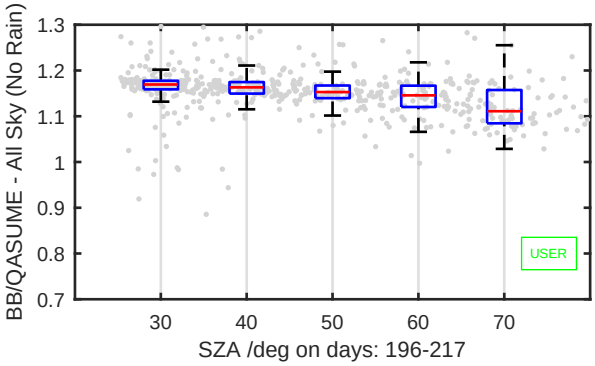

Calibration Results of KZ080005 (UVA)

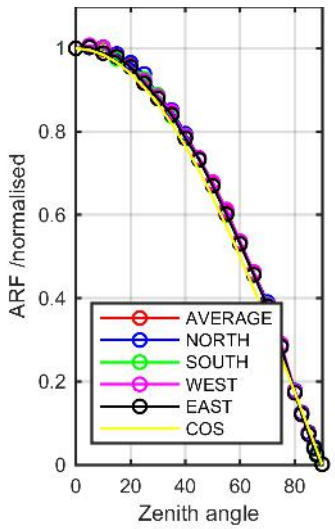

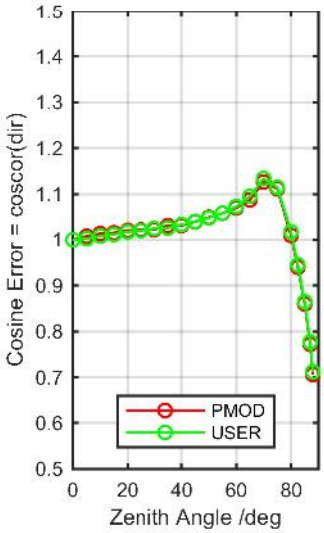

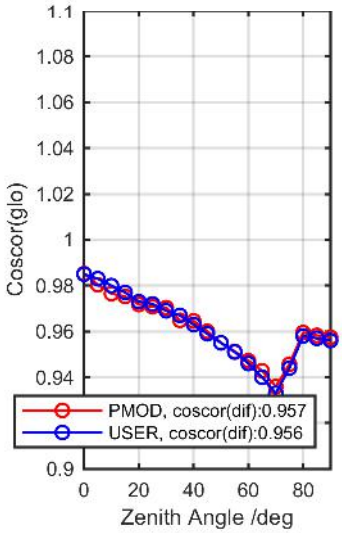

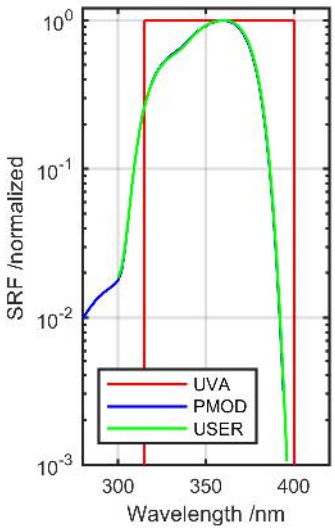

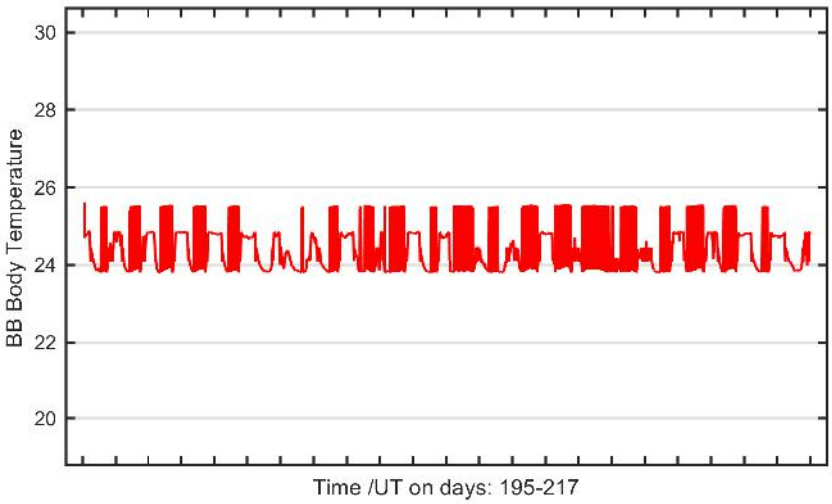

Calibration Matrix fn; Model sdisortREFms2009; f0=1.7724

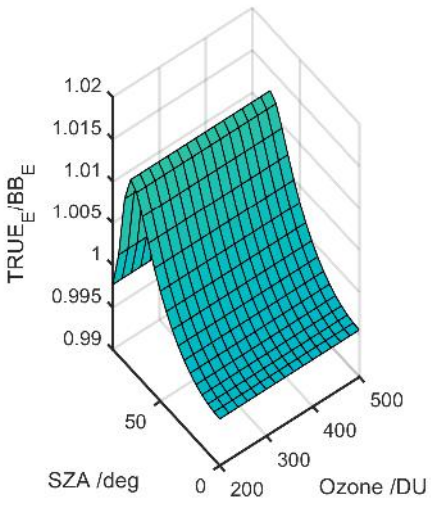

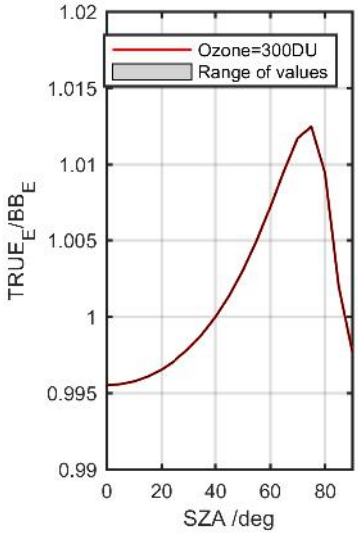

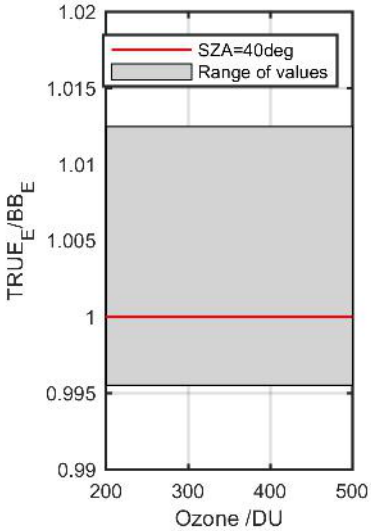

Calibration Results of KZ080005 (UVA)

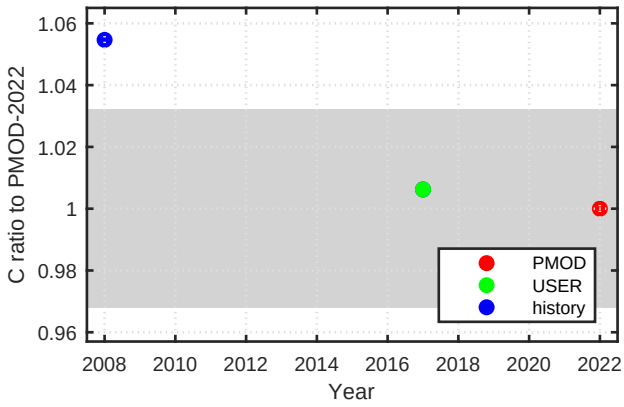

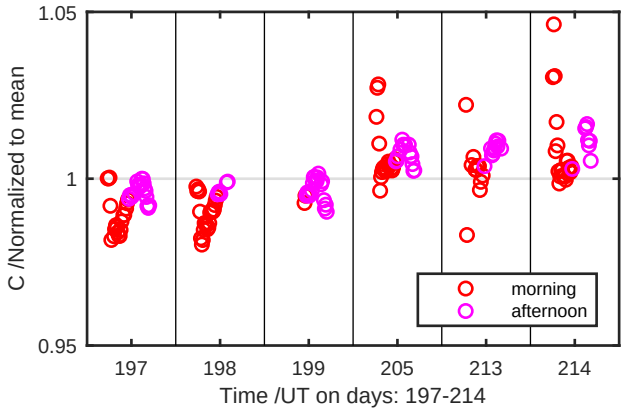

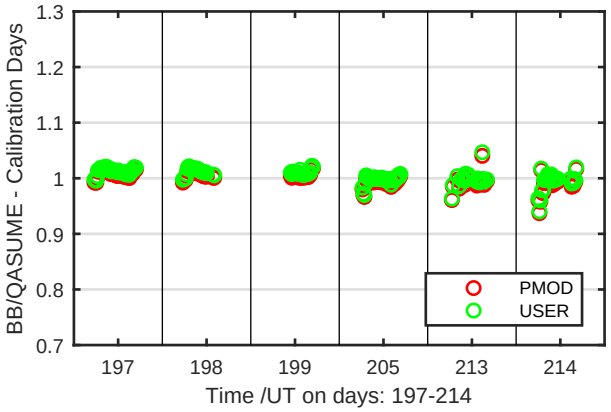

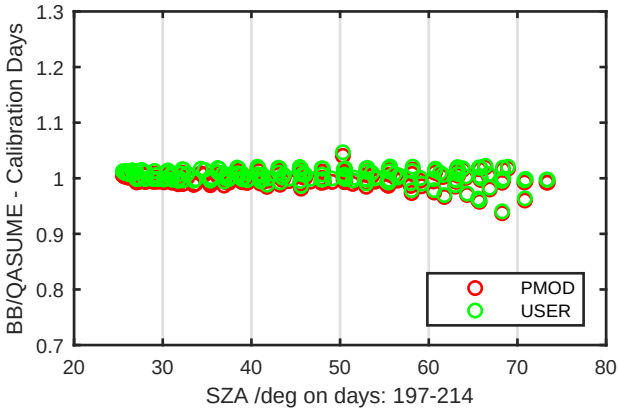

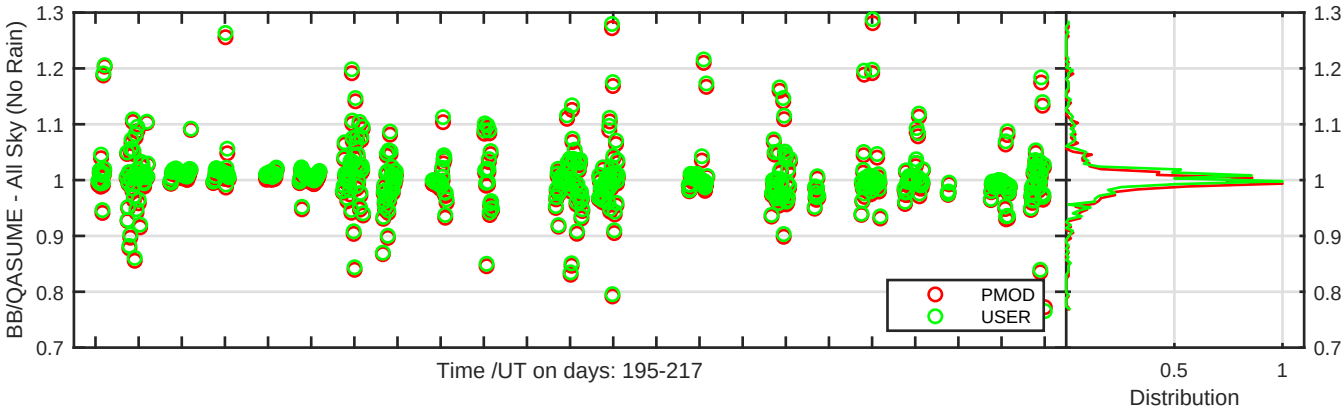

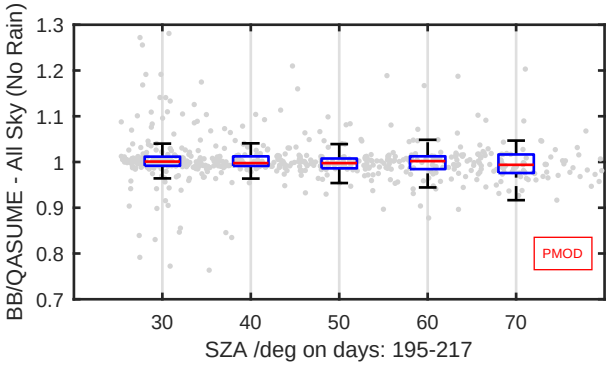

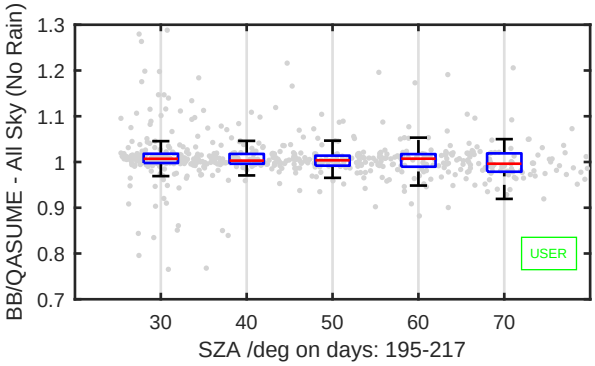

Calibration Results of KZ150084 (UVA)

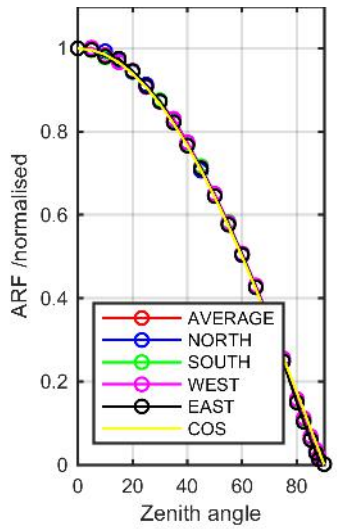

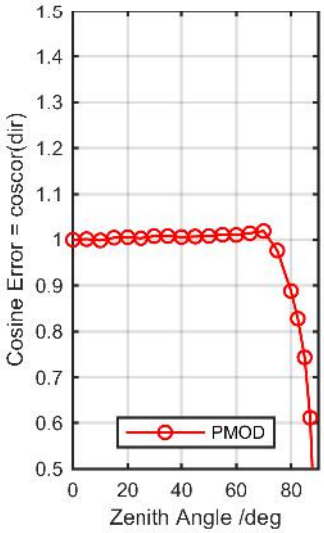

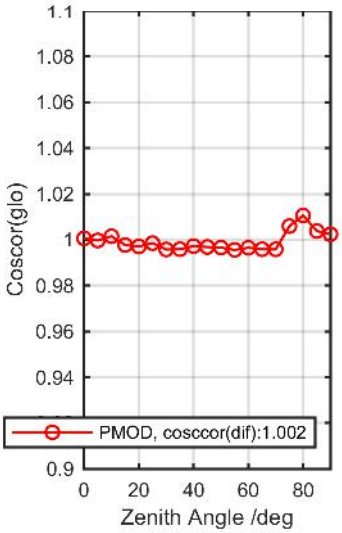

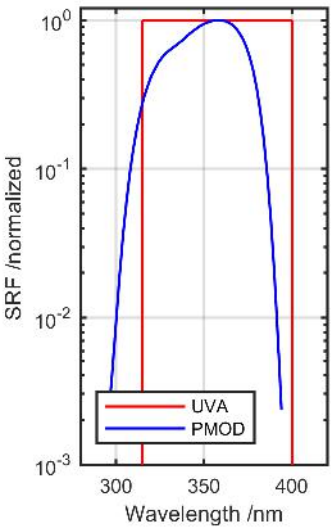

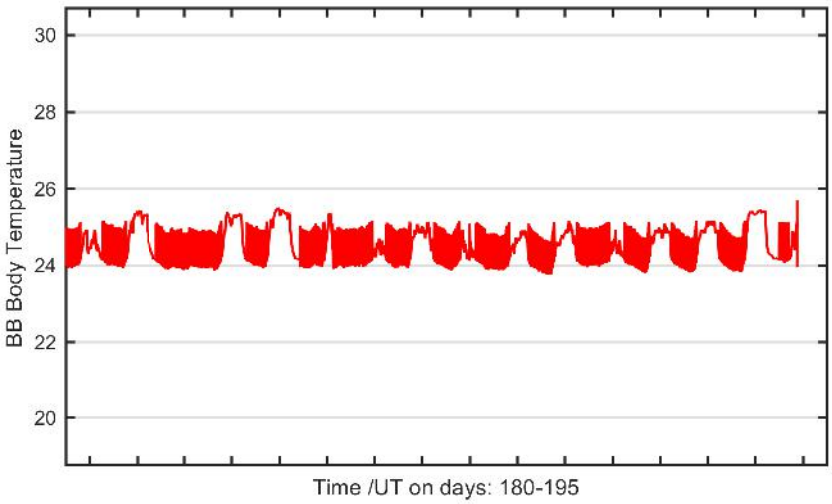

Calibration Matrix fn; Model sdisortREFms2009; f0=1.7596

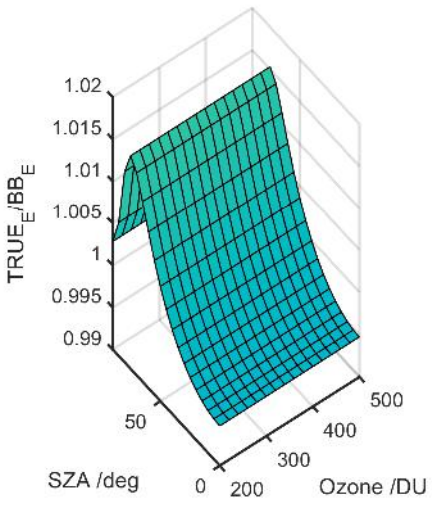

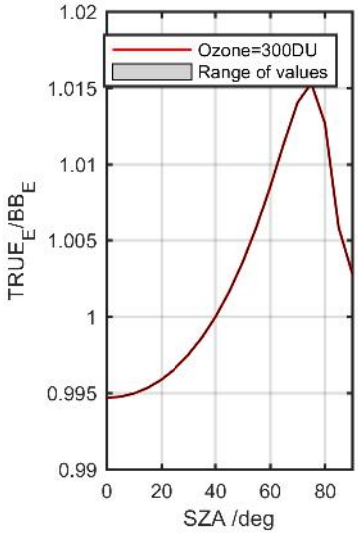

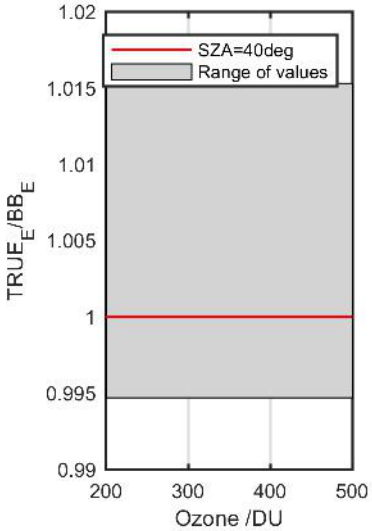

Calibration Results of KZ150084 (UVA)

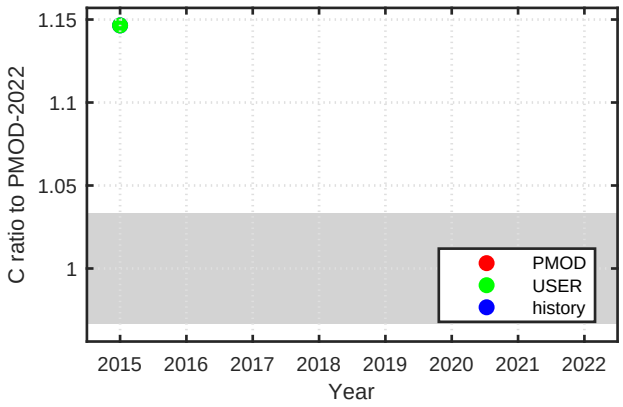

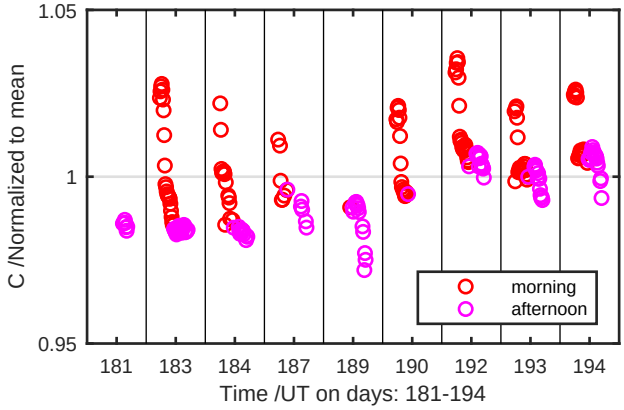

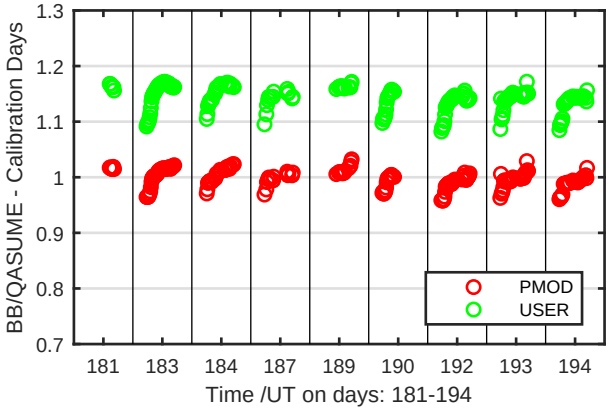

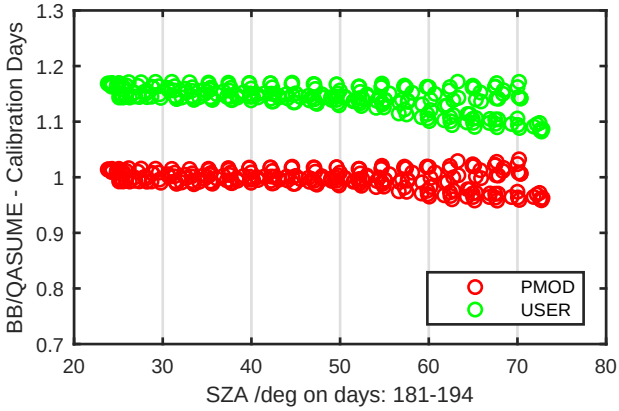

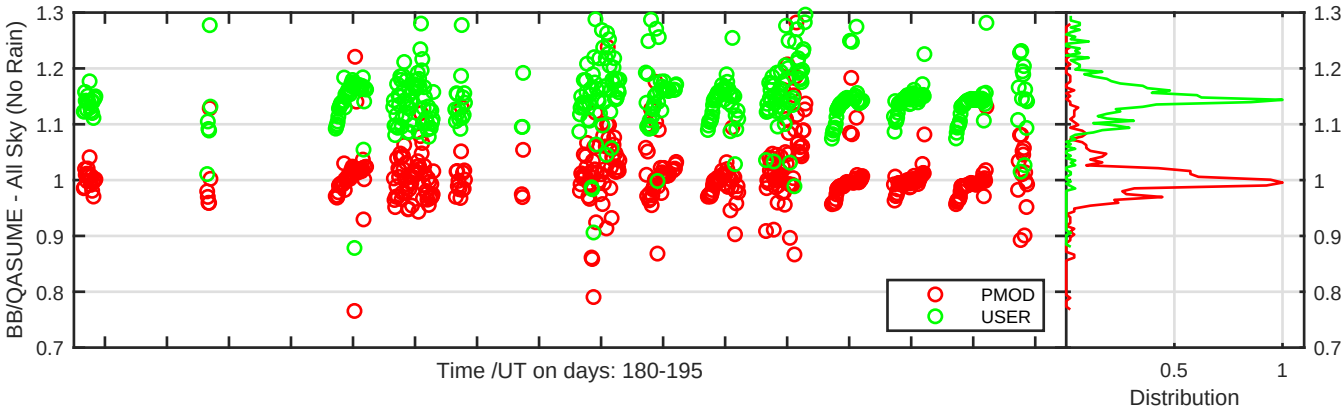

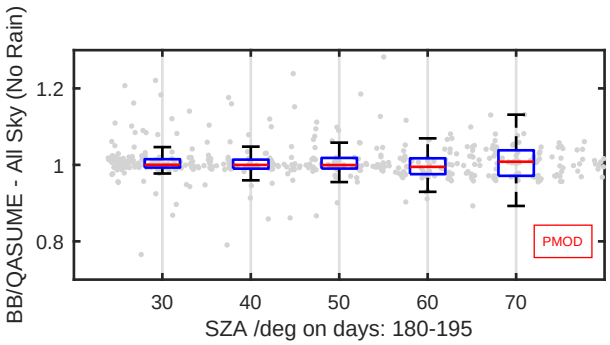

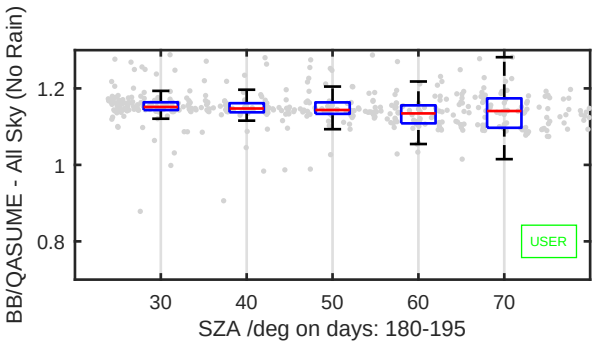

Calibration Results of KZ120023 (UVE)

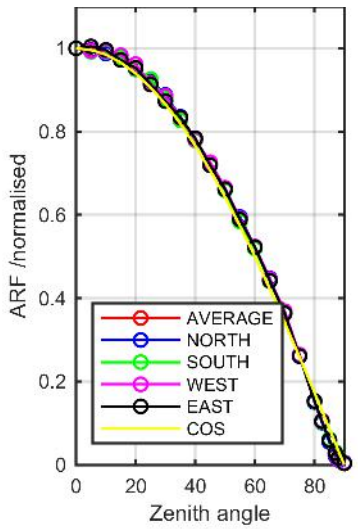

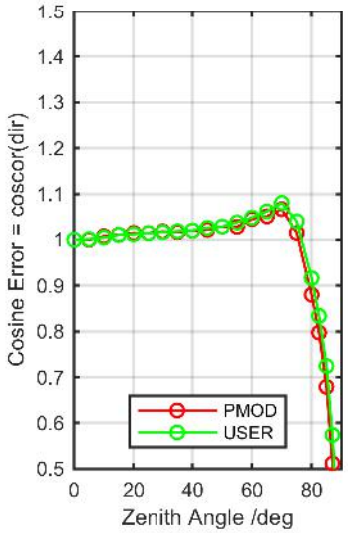

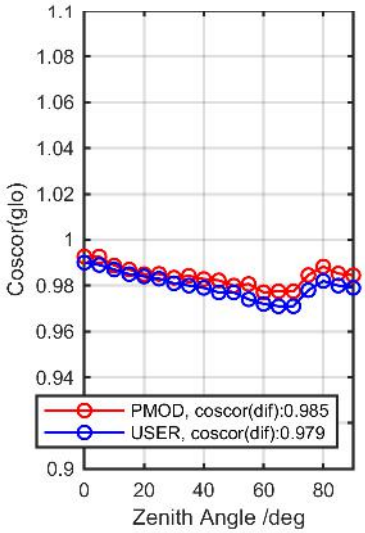

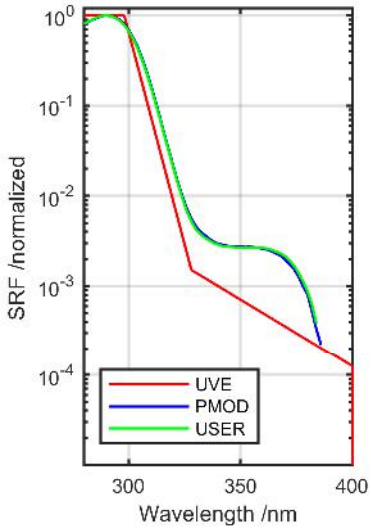

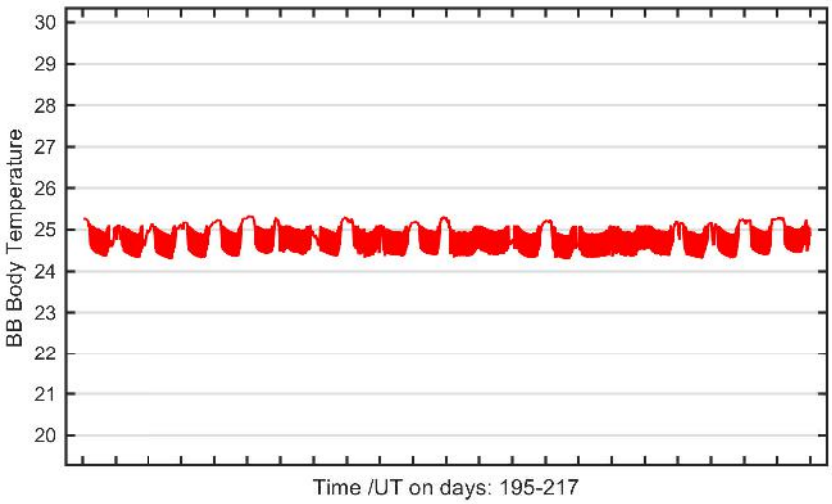

Calibration Matrix fn; Model sdisortREFms2009; f0=0.4428

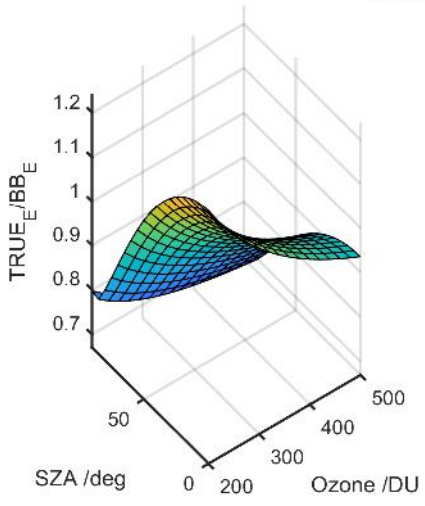

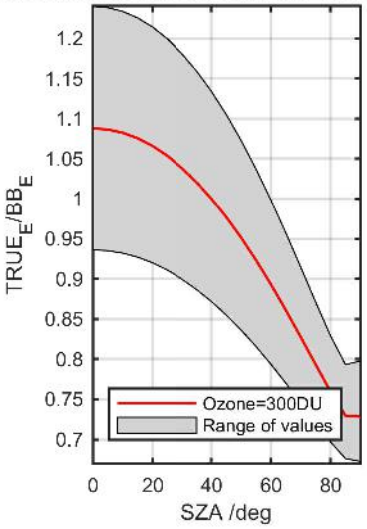

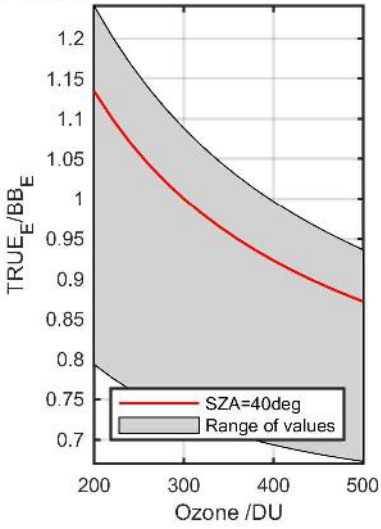

Calibration Results of KZ120023 (UVE)

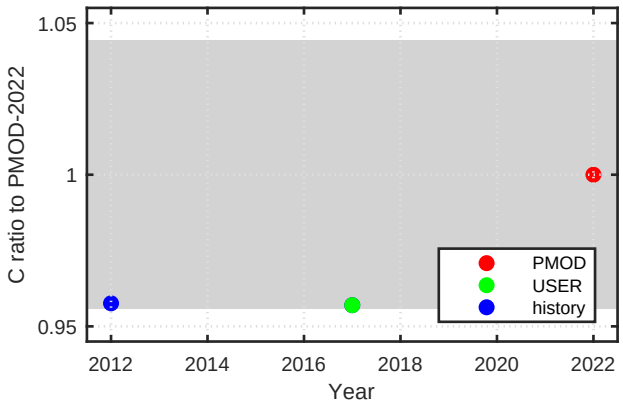

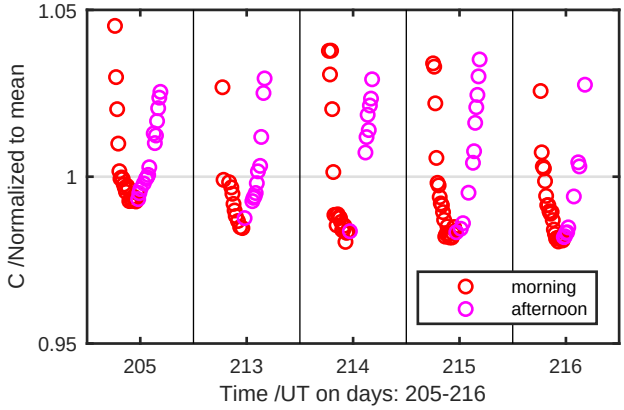

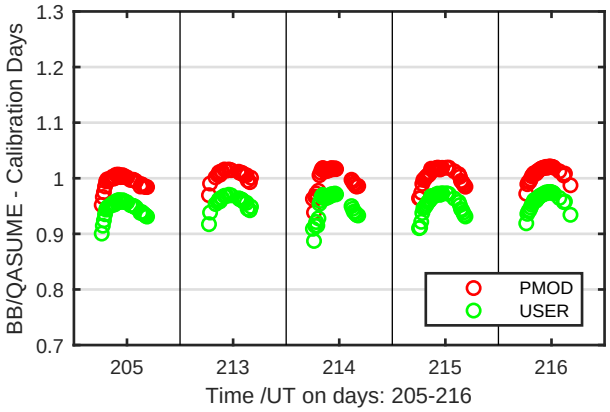

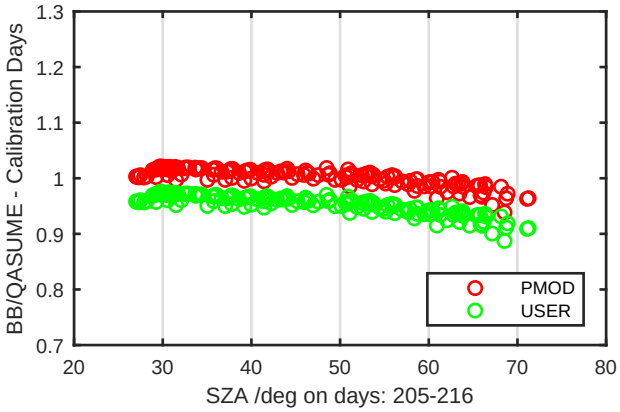

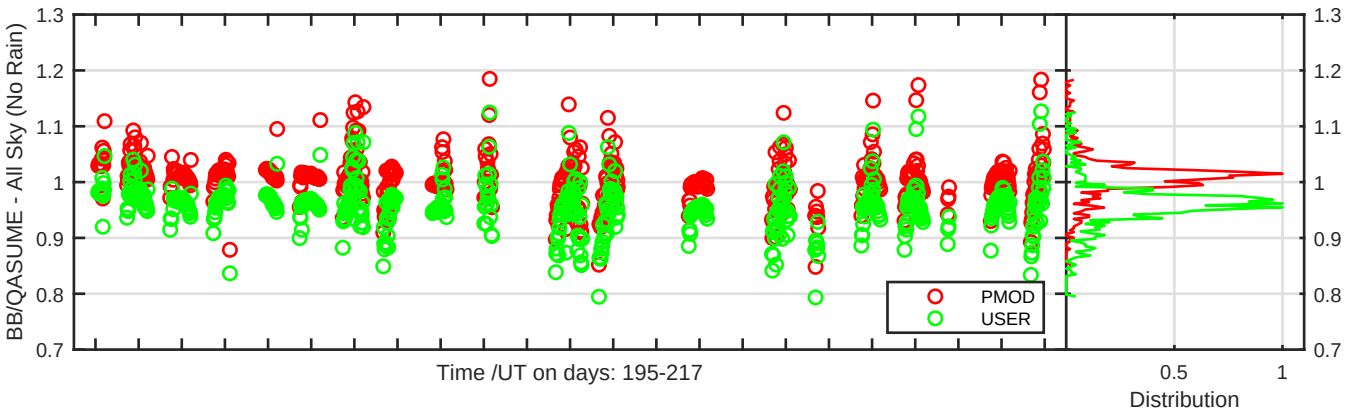

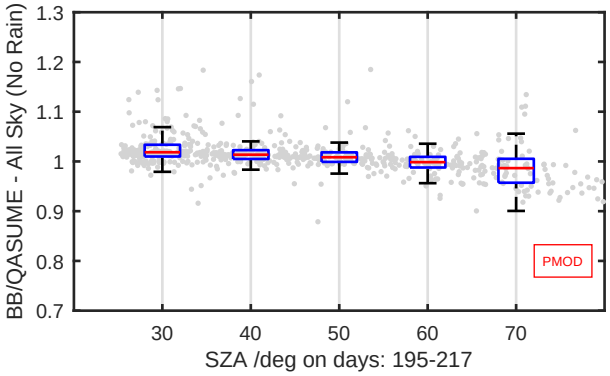

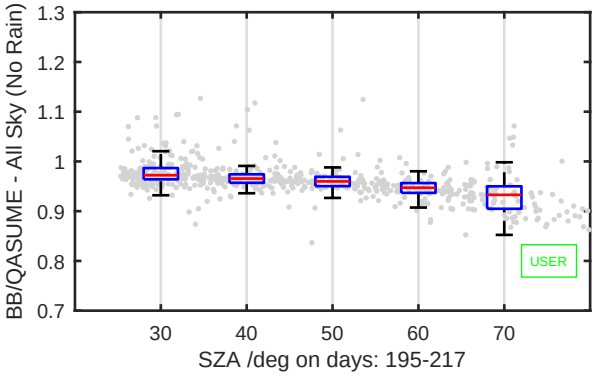

Calibration Results of KZ120023 (UVA)

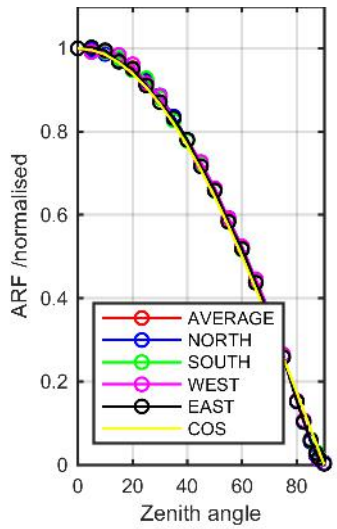

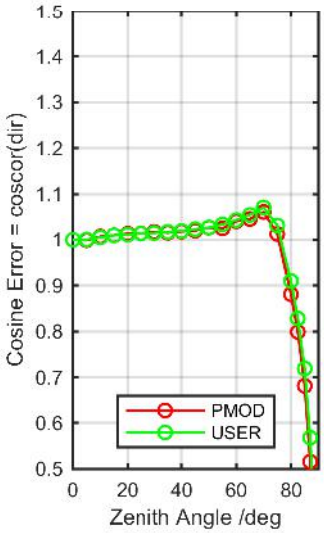

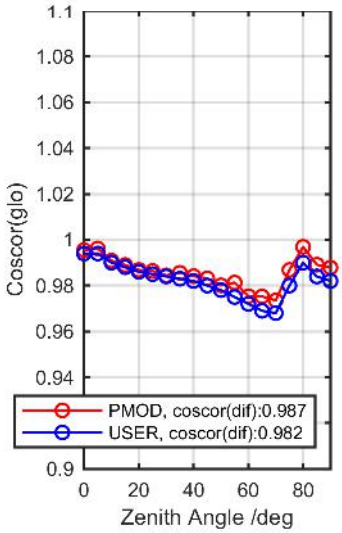

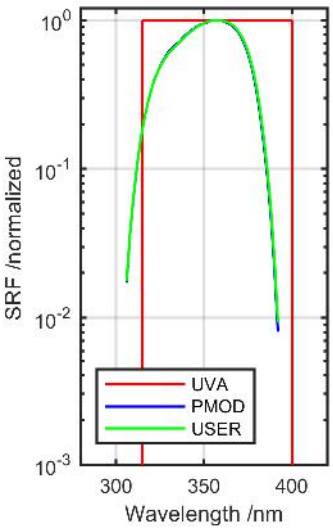

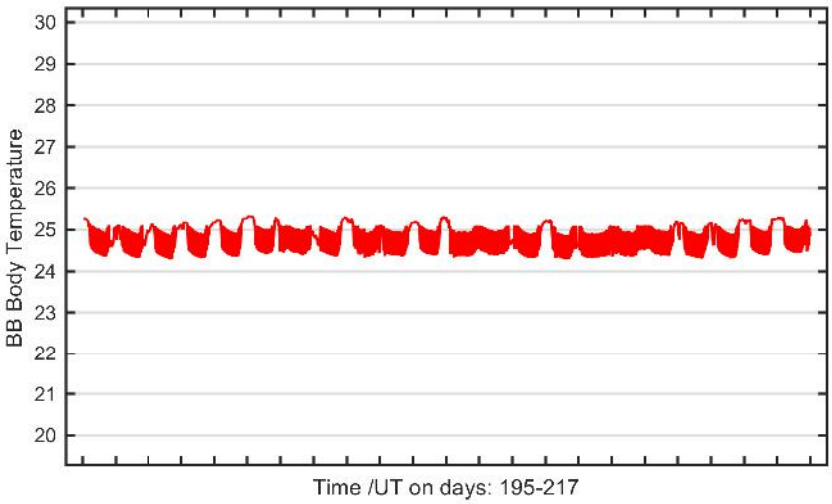

Calibration Matrix fn; Model sdisortREFms2009; f0=1.7883

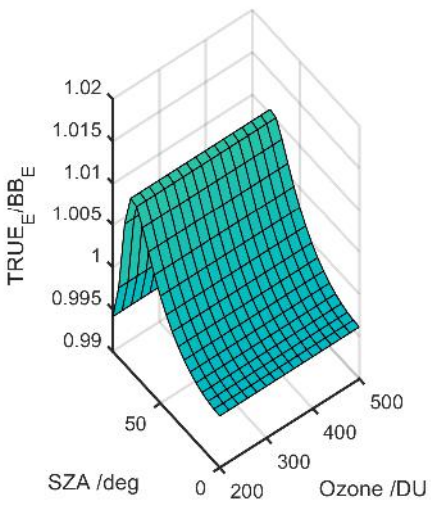

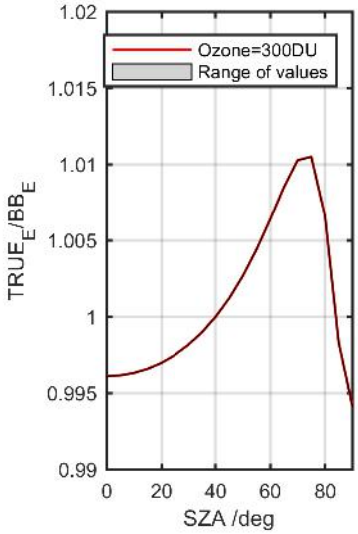

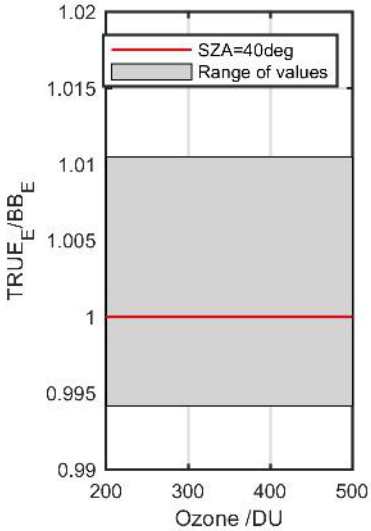

Calibration Results of KZ120023 (UVA)

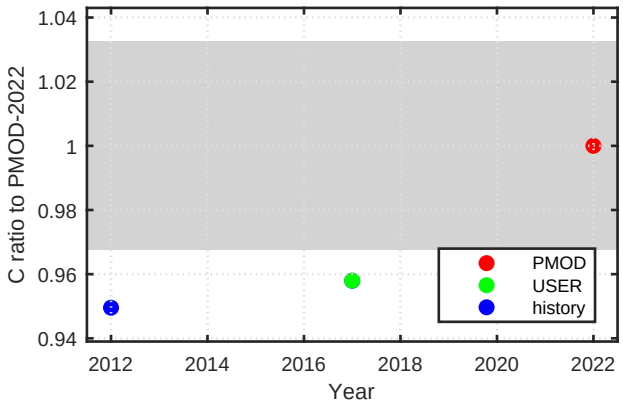

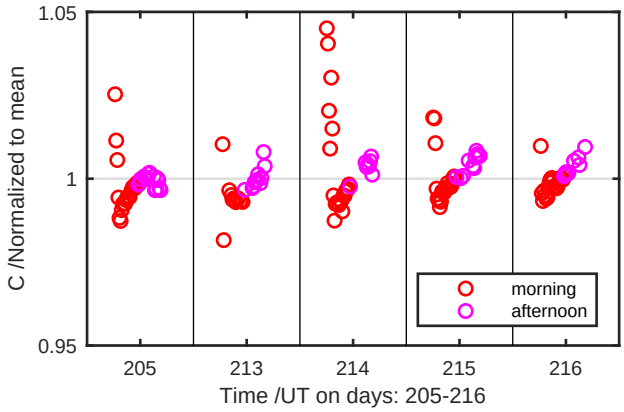

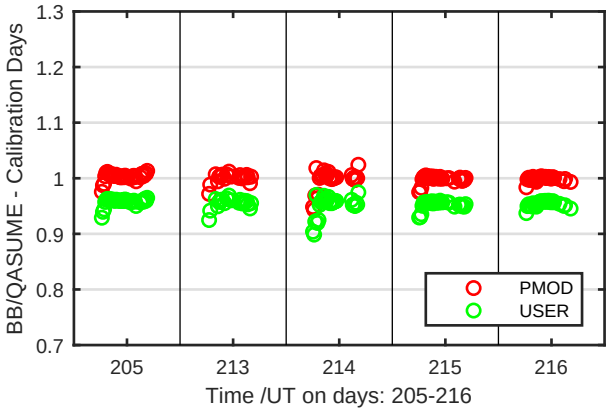

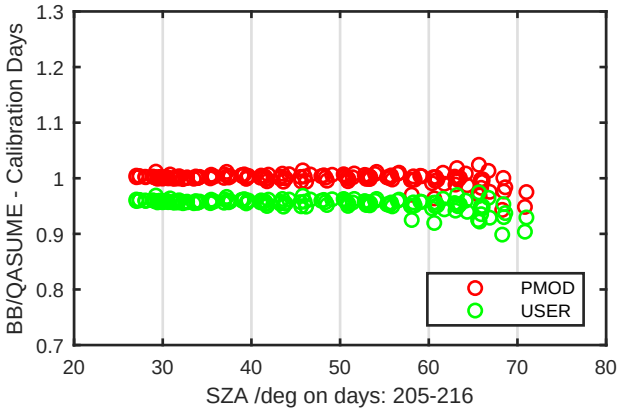

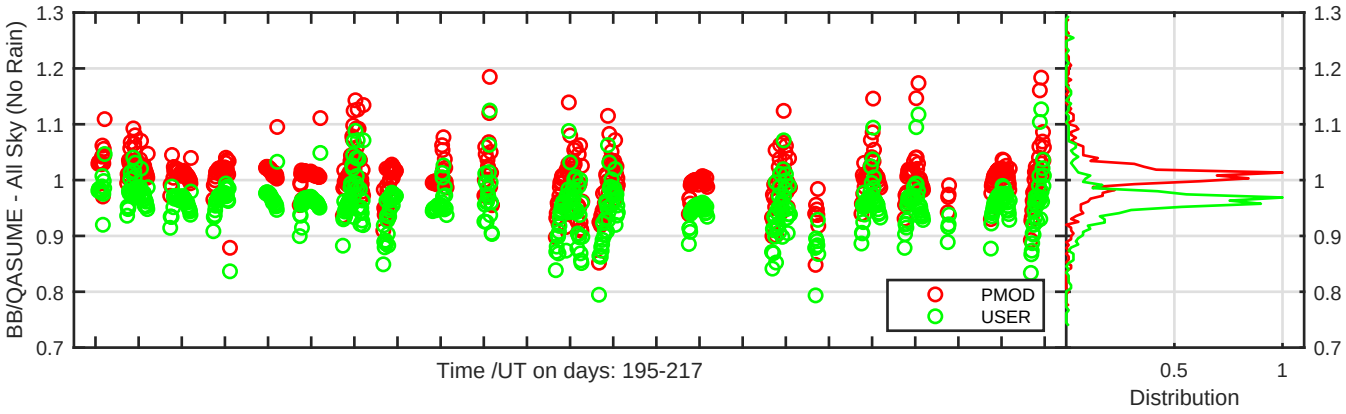

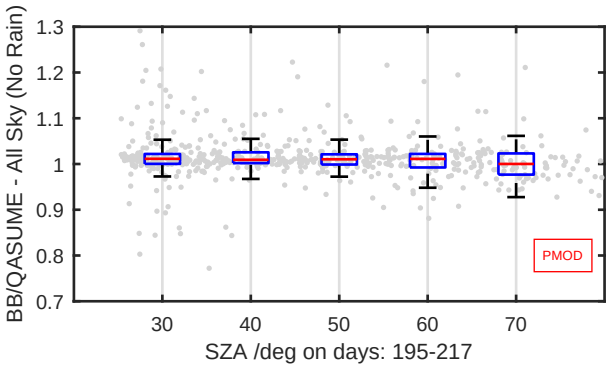

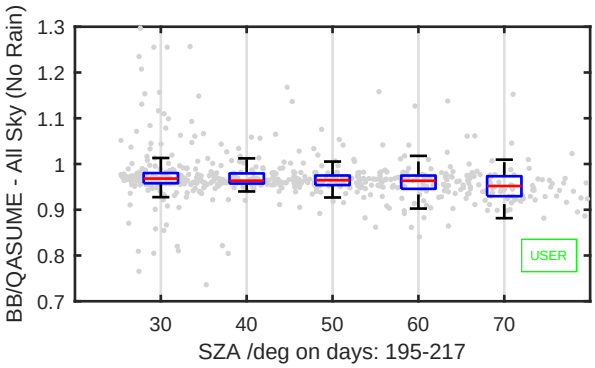

Calibration Results of KZ140040 (UVE)

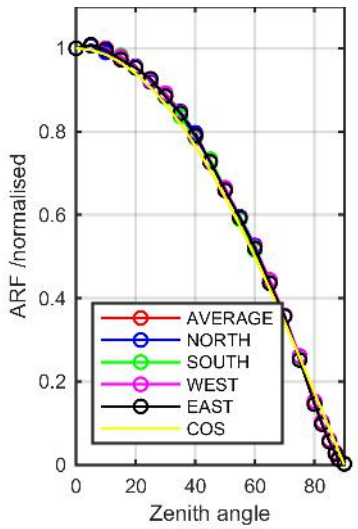

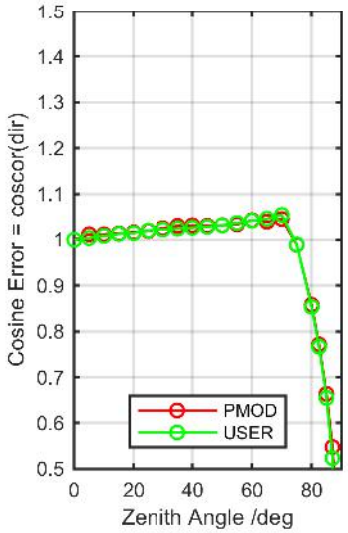

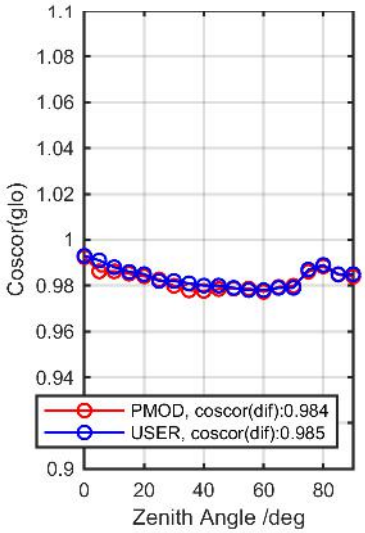

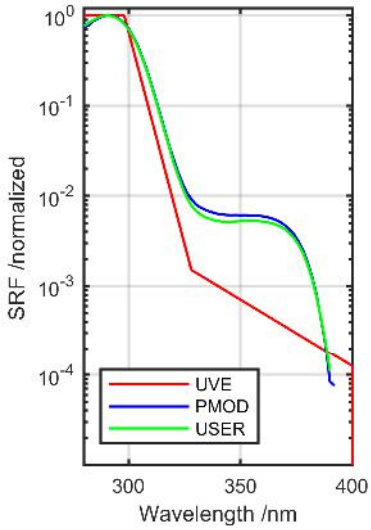

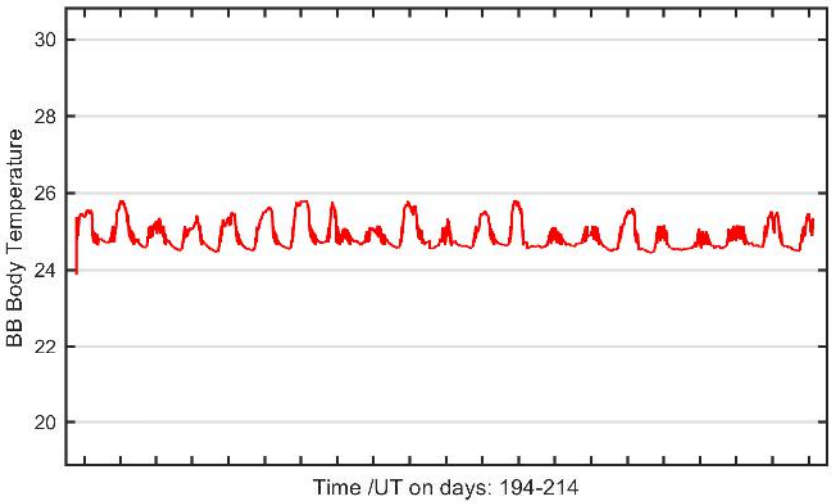

Calibration Matrix fn; Model sdisortREFms2009; f0=0.3307

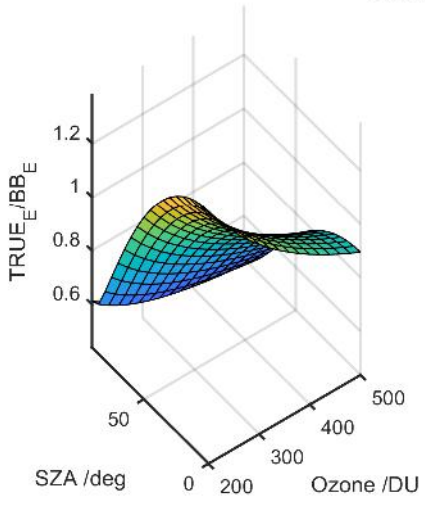

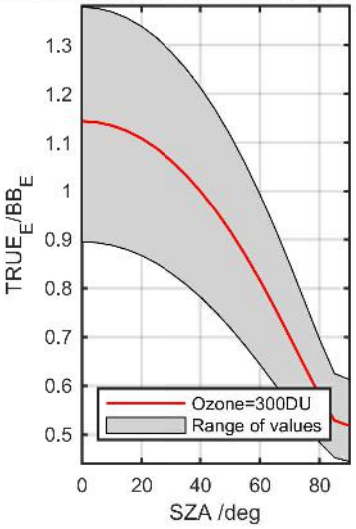

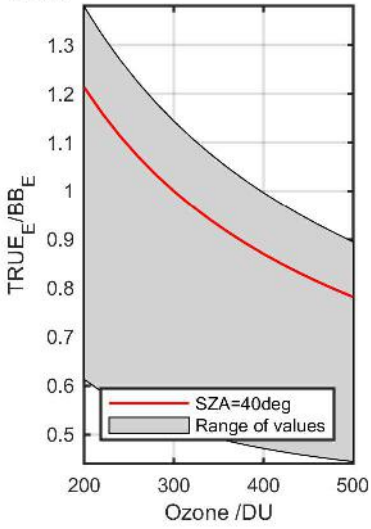

Calibration Results of KZ140040 (UVE)

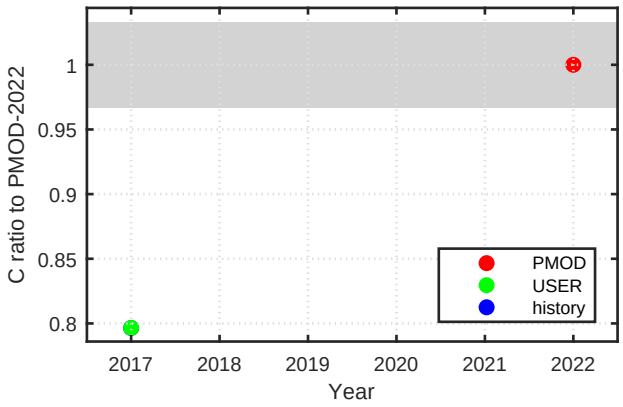

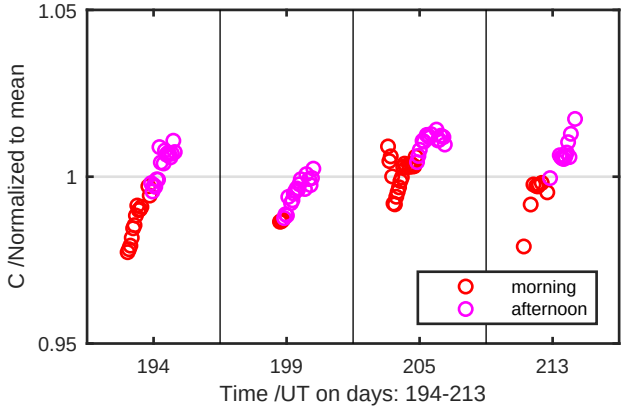

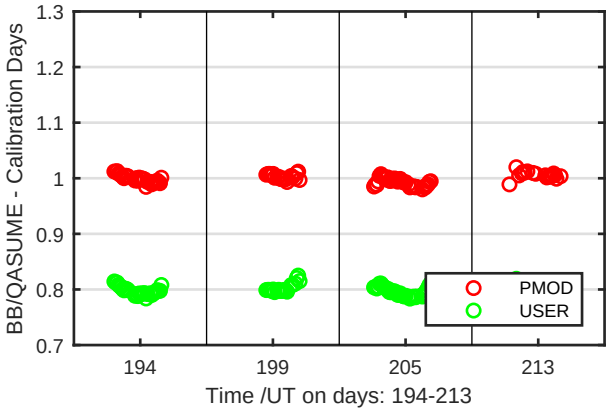

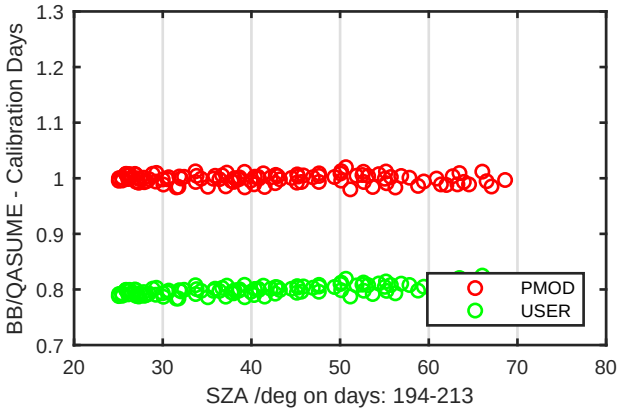

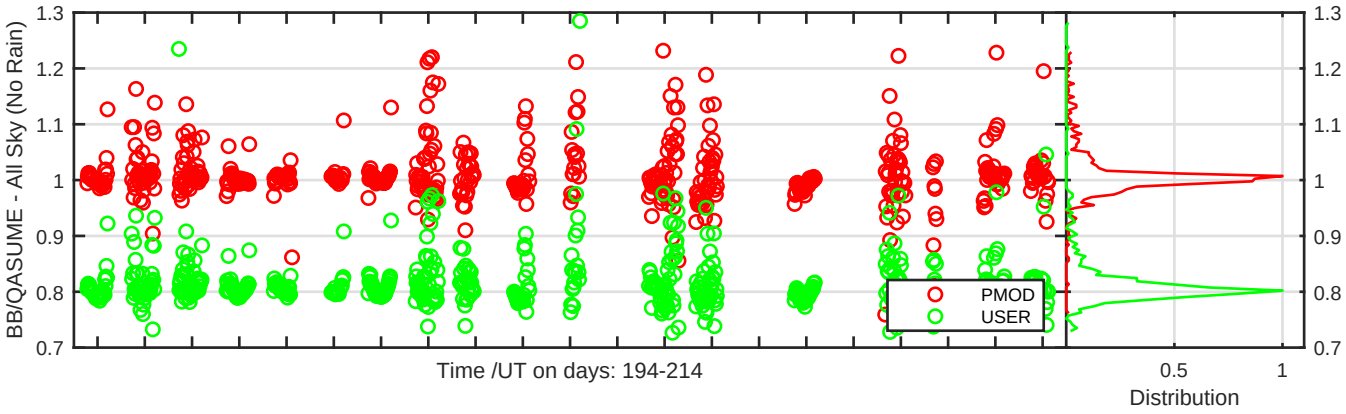

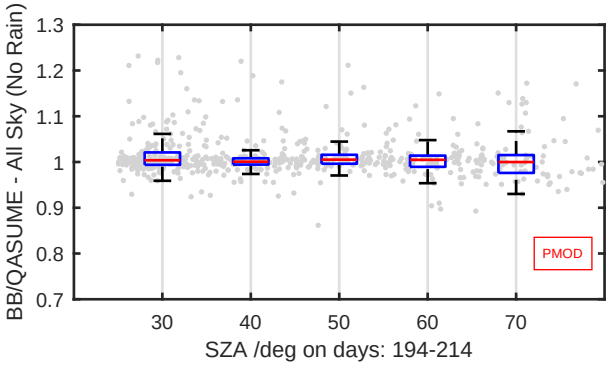

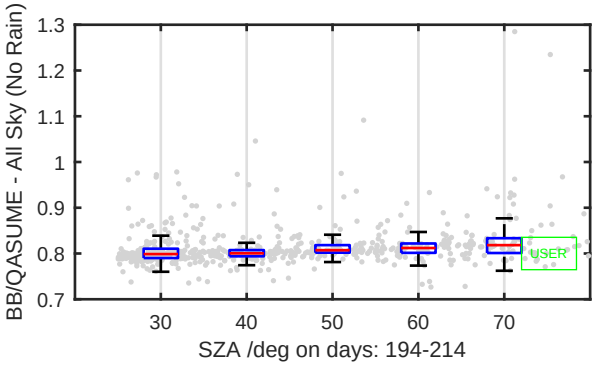

Calibration Results of KZ140040 (UVA)

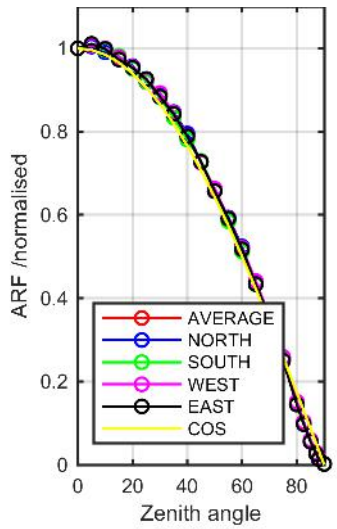

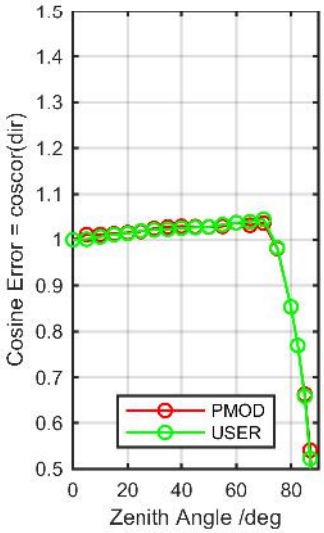

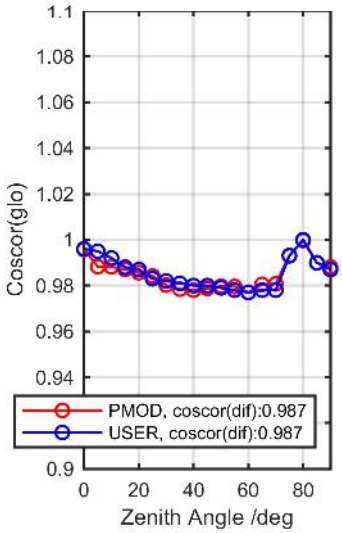

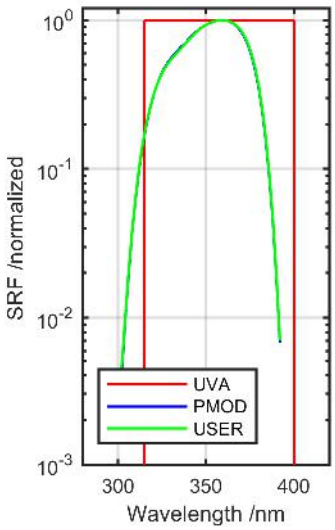

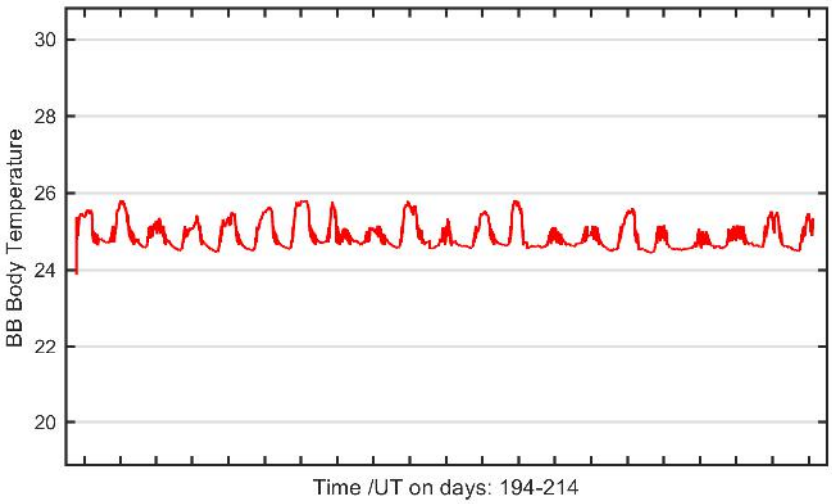

Calibration Matrix fn; Model sdisortREFms2009; f0=1.8150

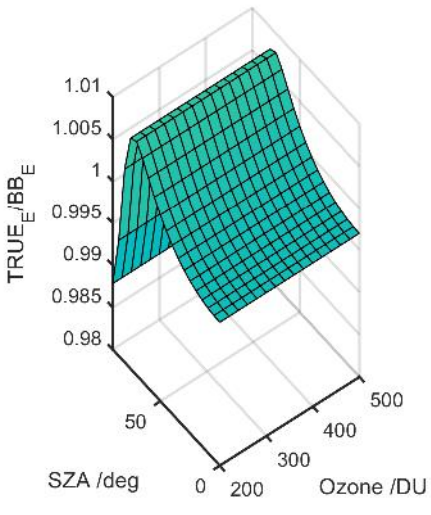

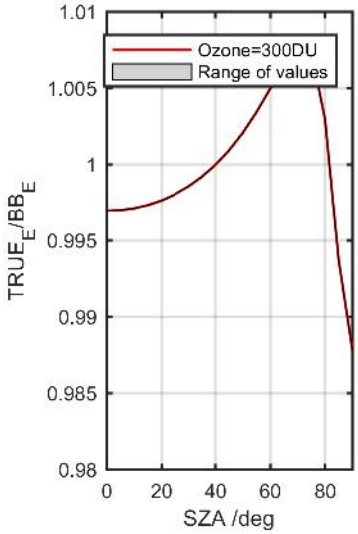

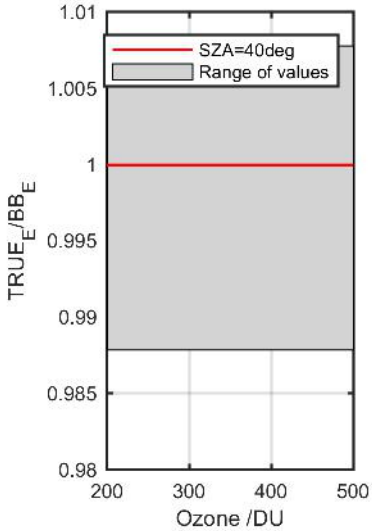

Calibration Results of KZ140040 (UVA)

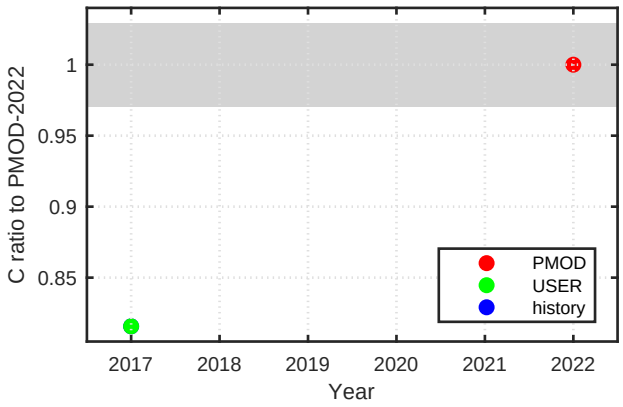

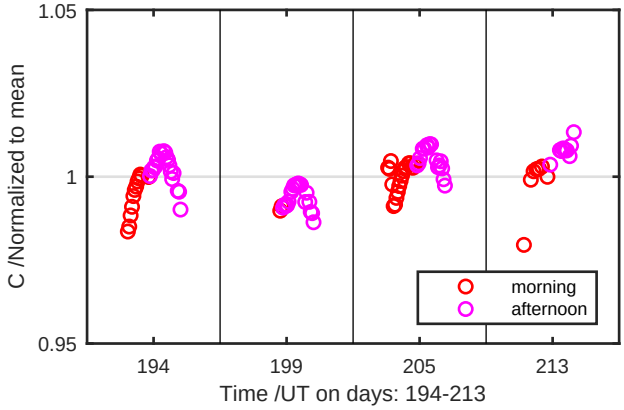

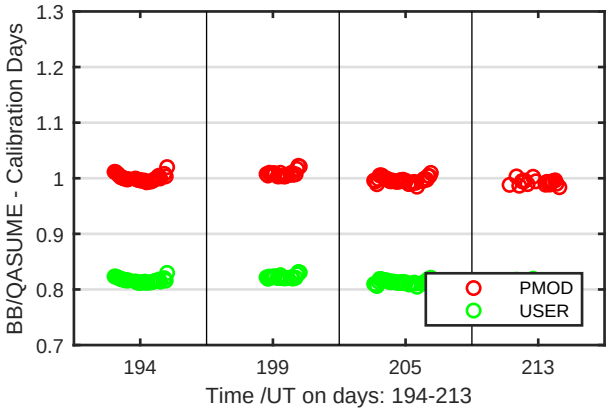

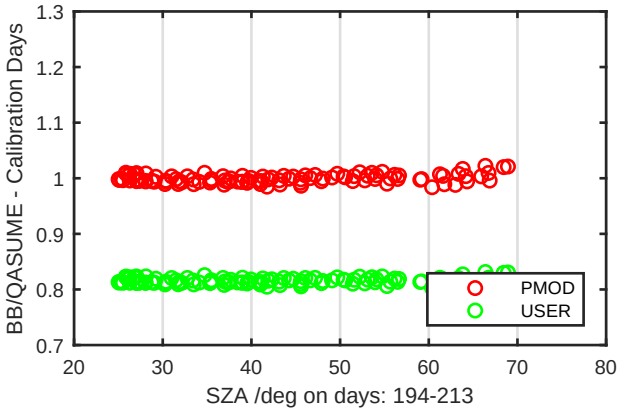

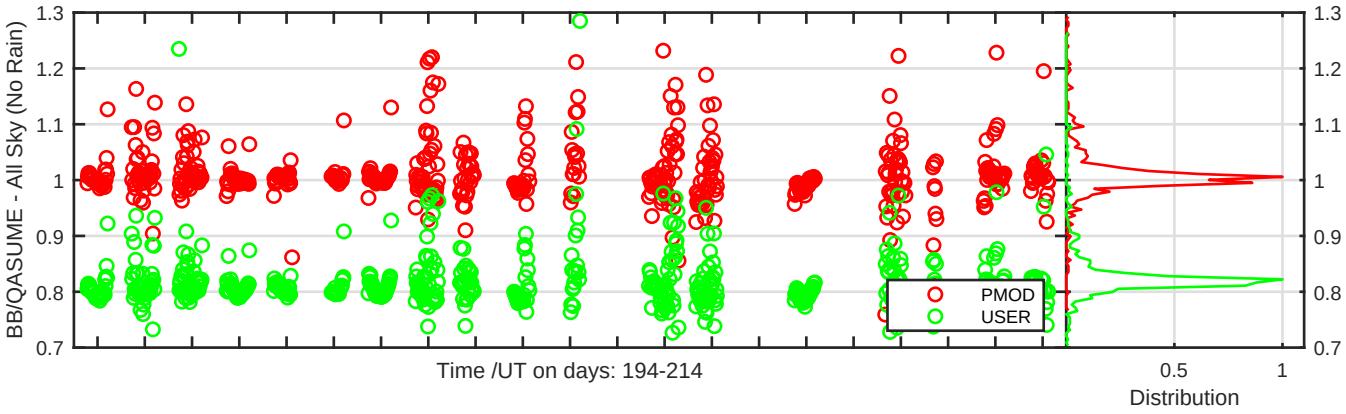

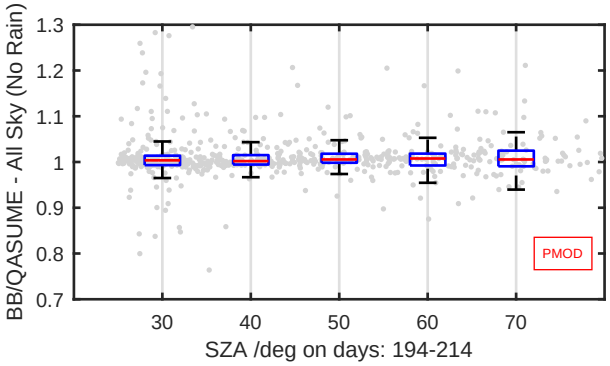

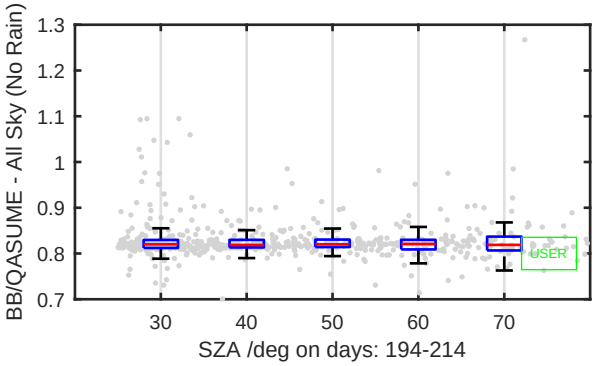

Calibration Results of KZ080003 (UVE)

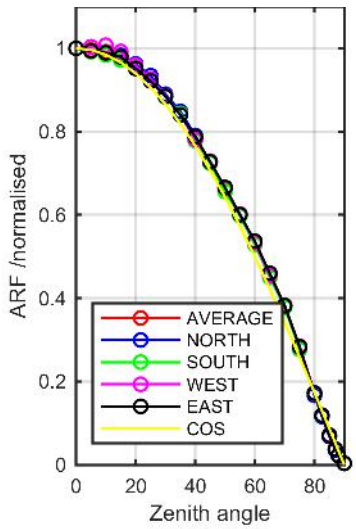

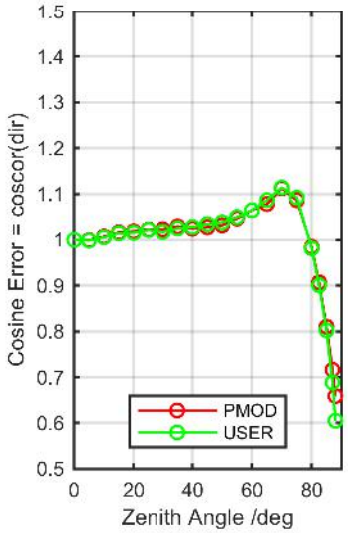

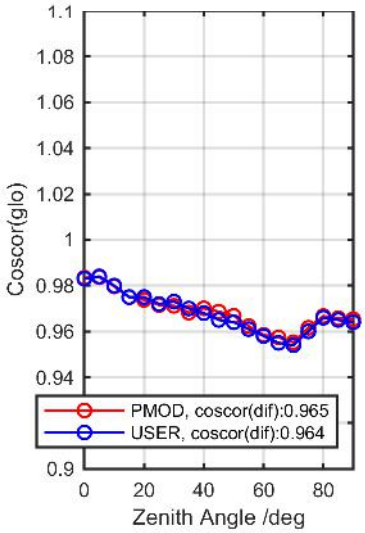

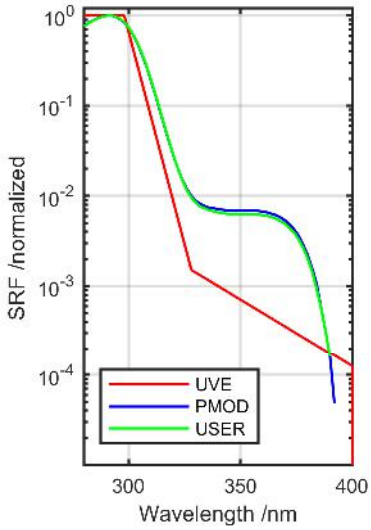

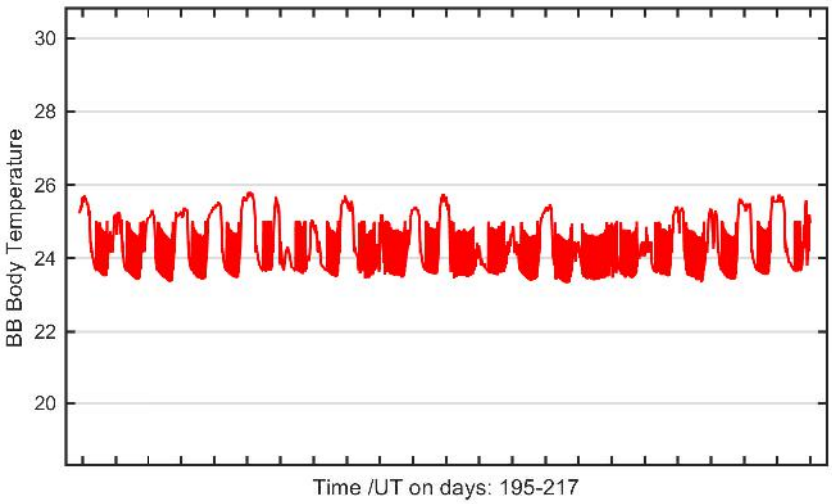

Calibration Matrix fn; Model sdisortREFms2009; f0=0.3045

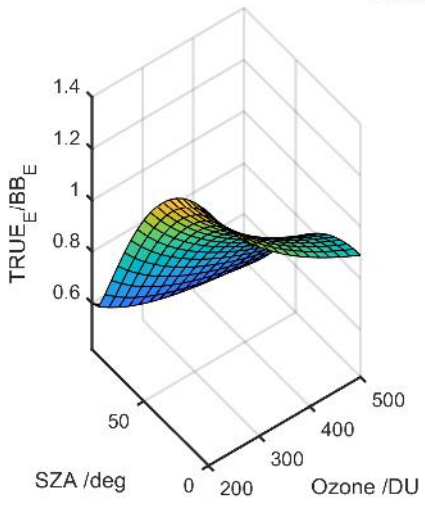

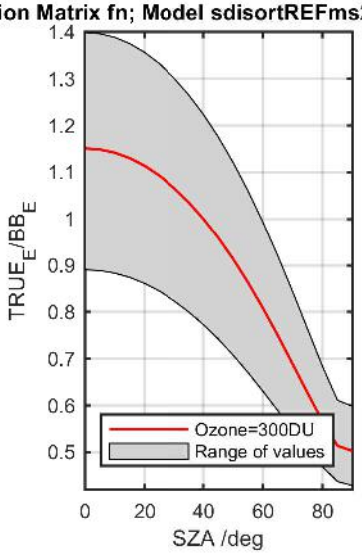

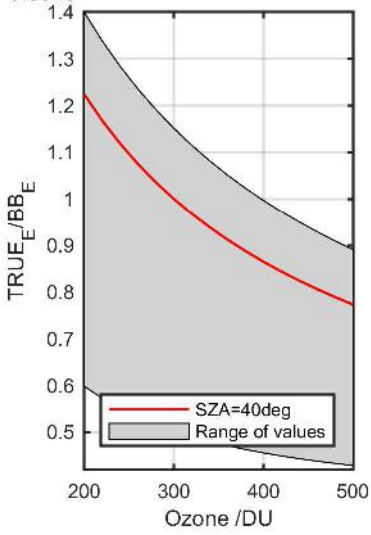

Calibration Results of KZ080003 (UVE)

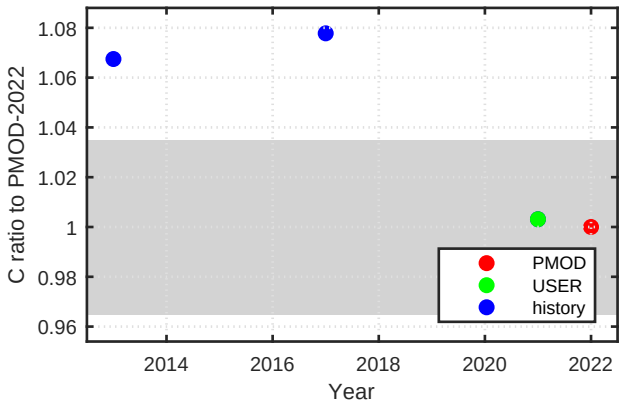

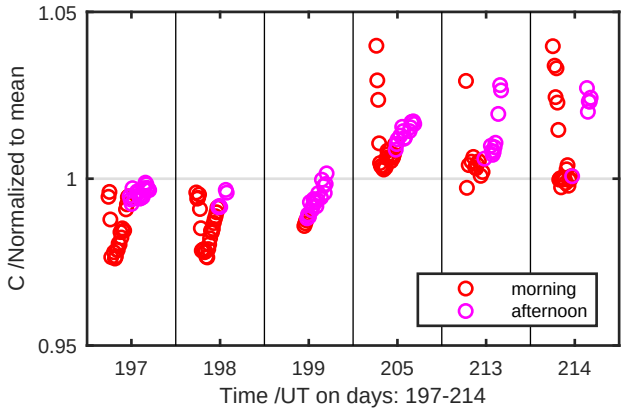

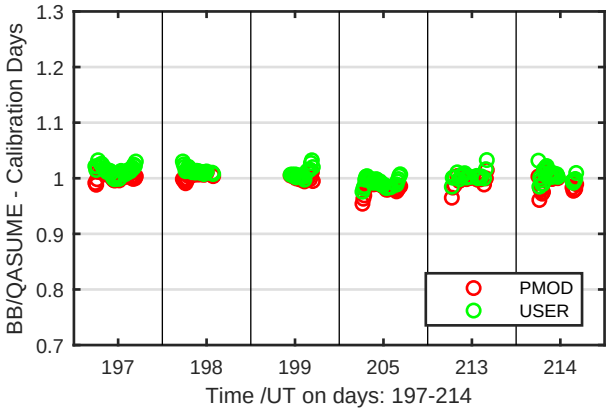

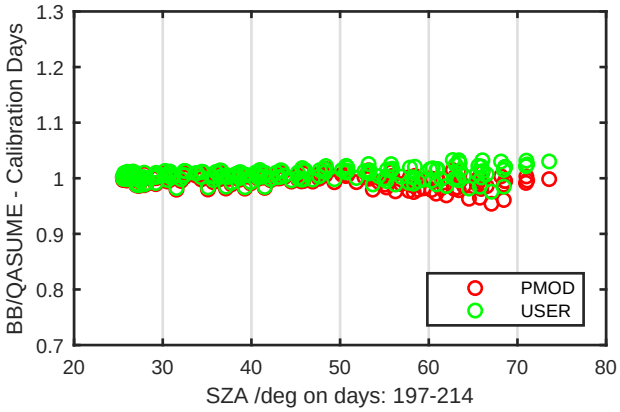

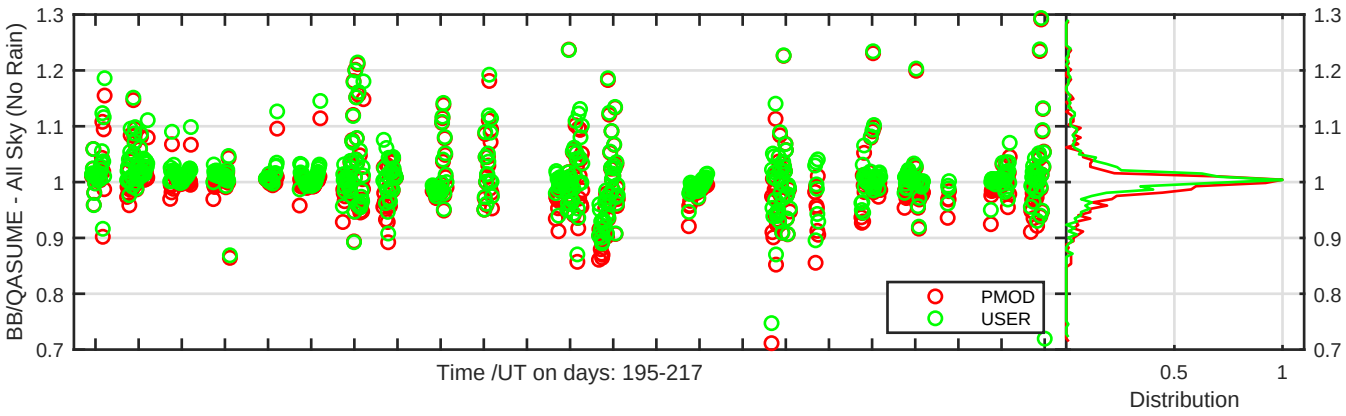

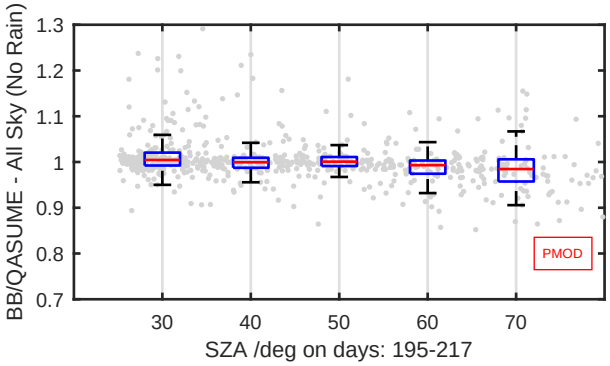

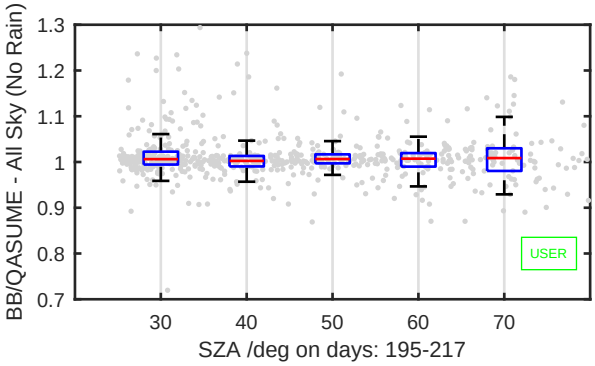

Calibration Results of KZ080003 (UVA)

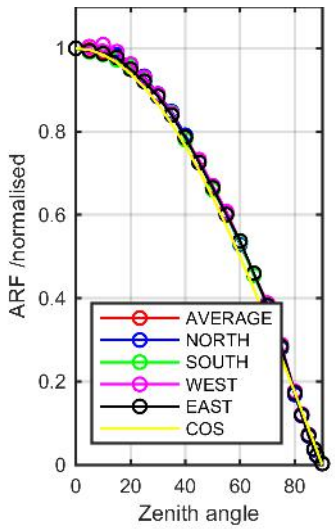

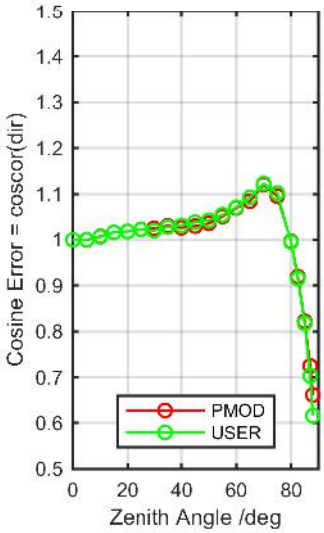

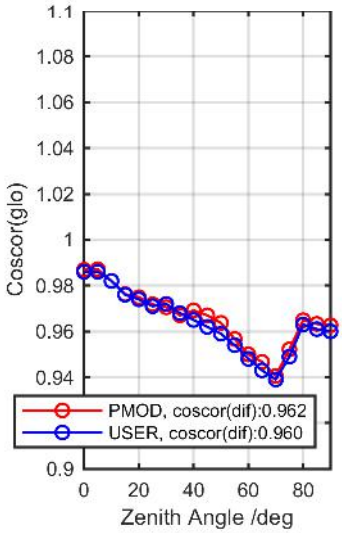

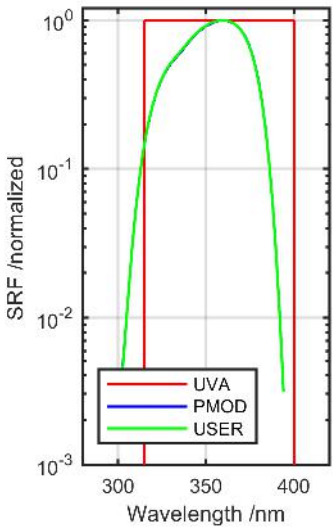

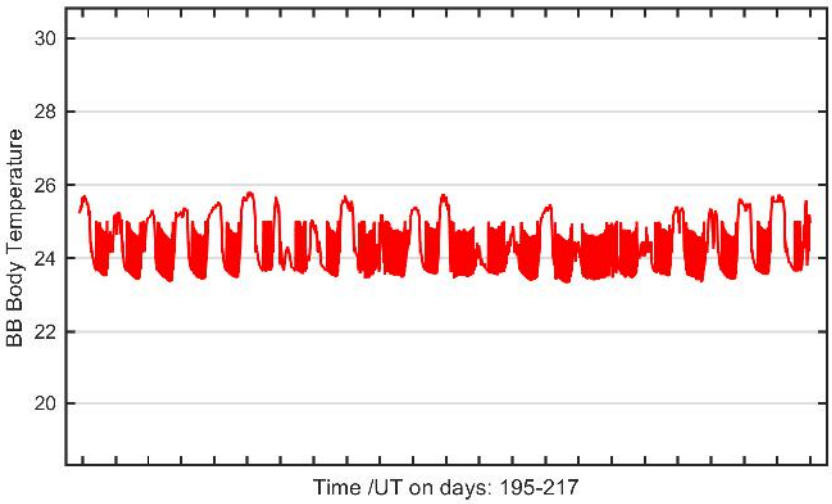

Calibration Matrix fn; Model sdisortREFms2009; f0=1.8305

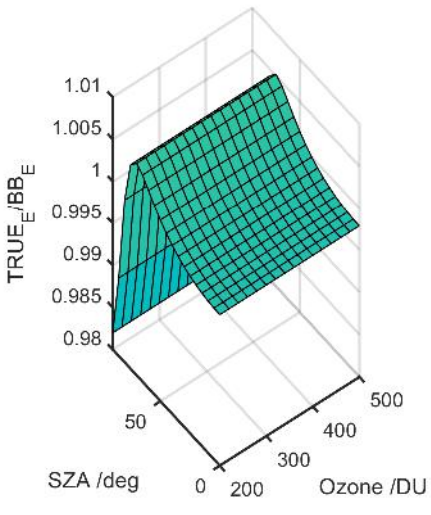

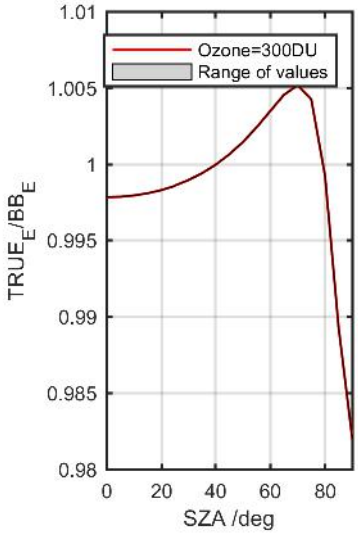

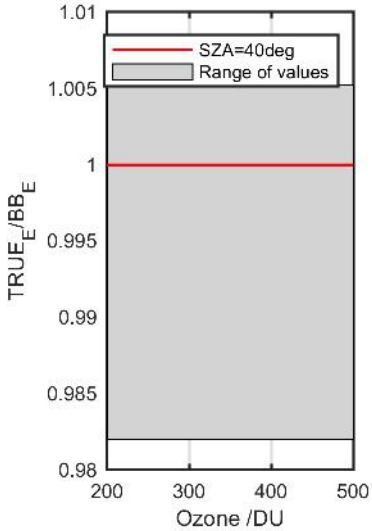

Calibration Results of KZ080003 (UVA)

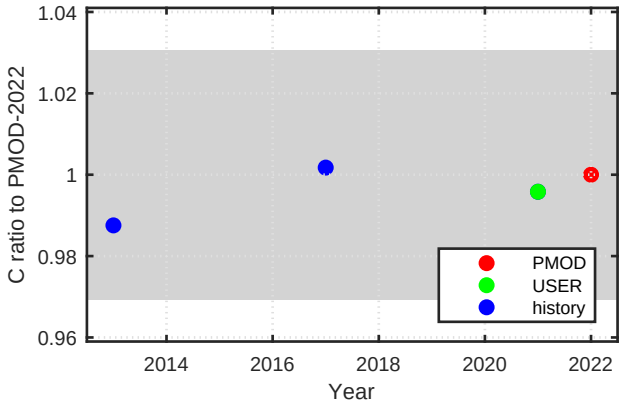

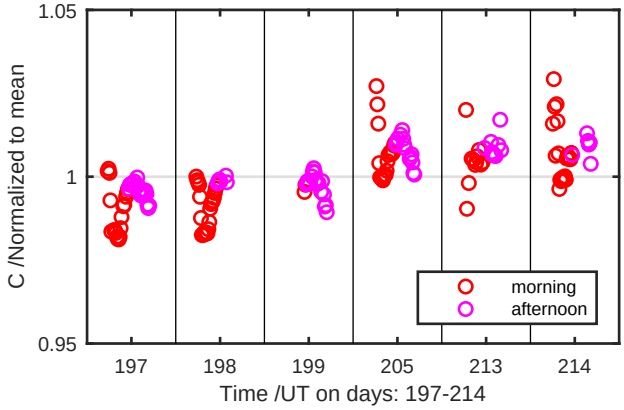

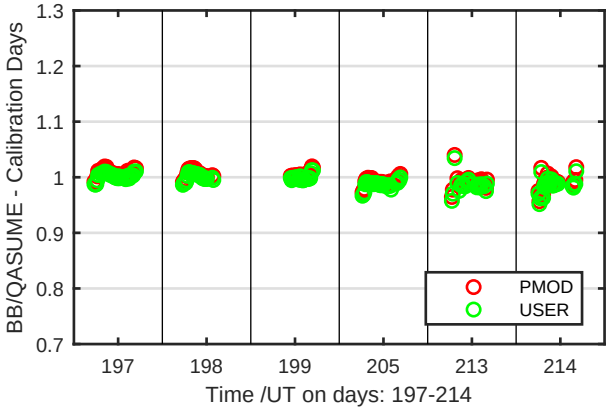

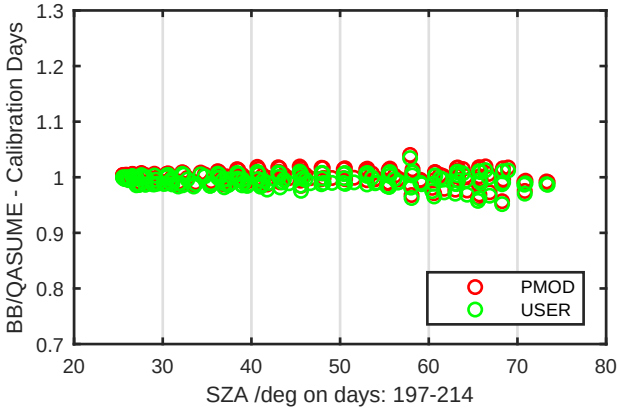

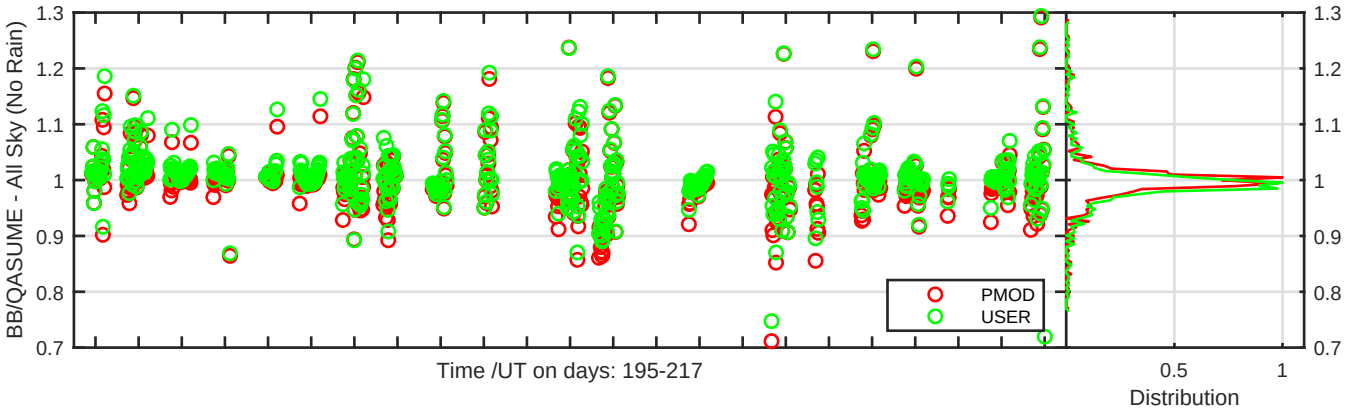

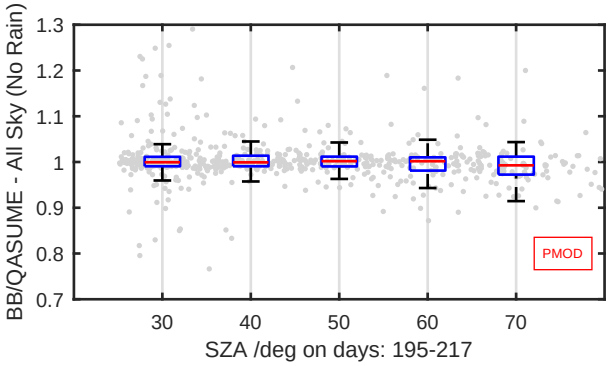

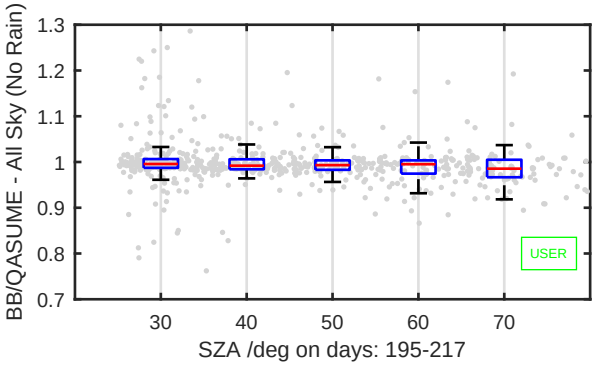

Calibration Results of KZ2022 (UVG)

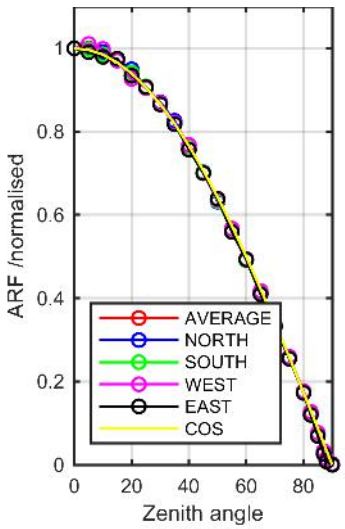

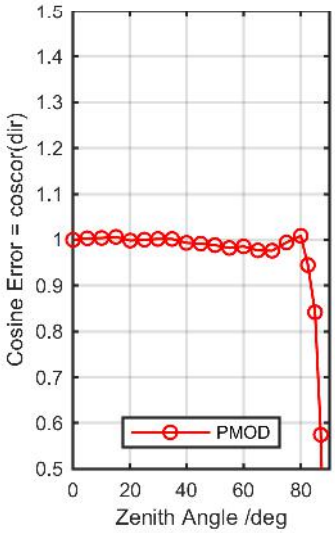

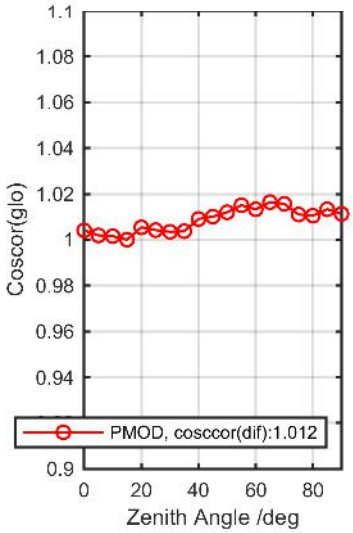

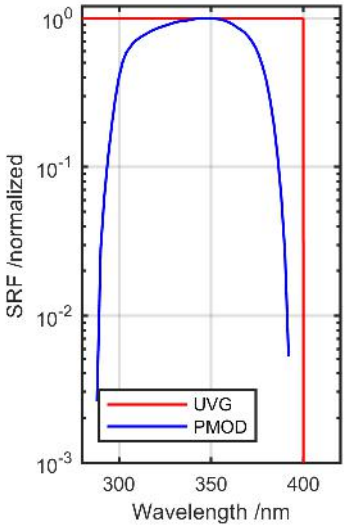

Calibration Matrix fn; Model sdisortREFms2009; f0=1.5716

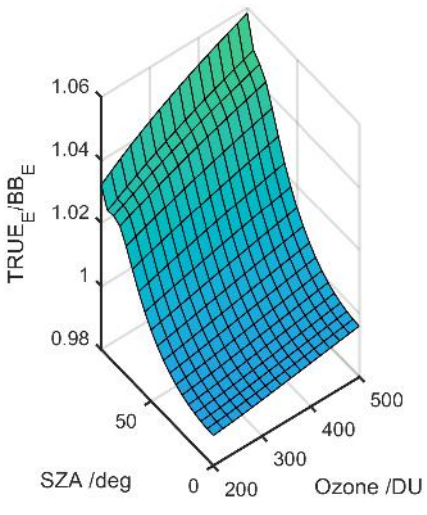

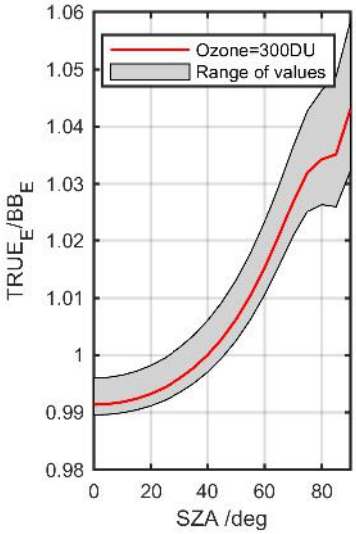

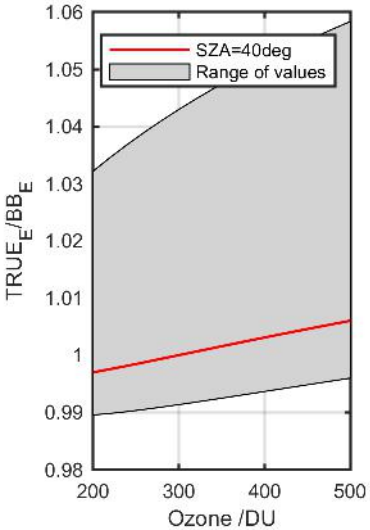

Calibration Results of KZ2022 (UVG)

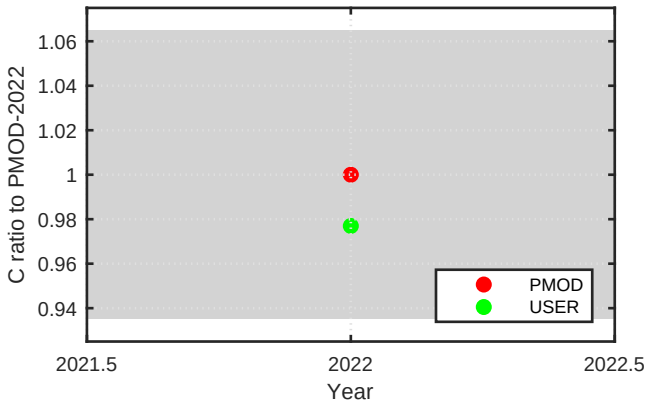

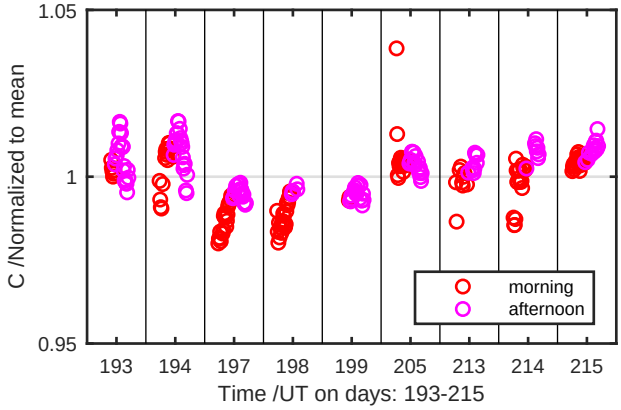

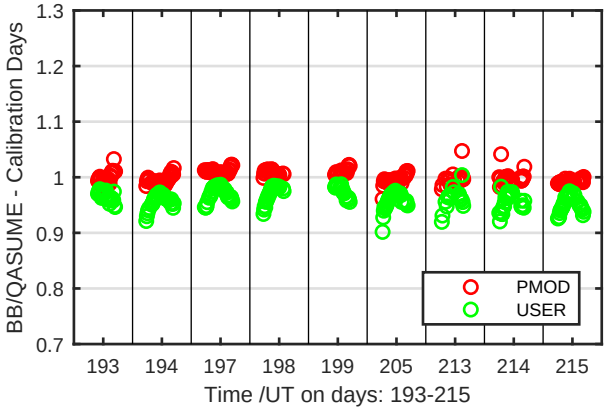

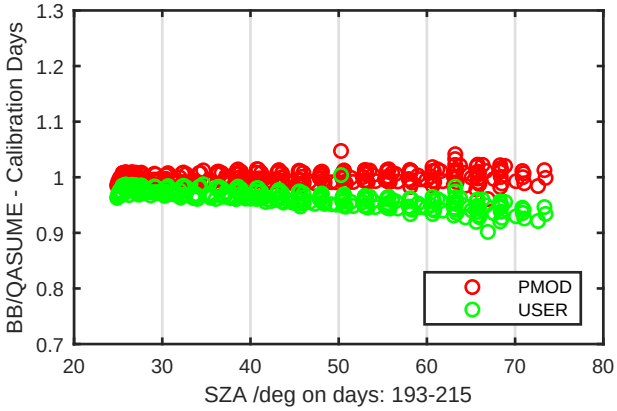

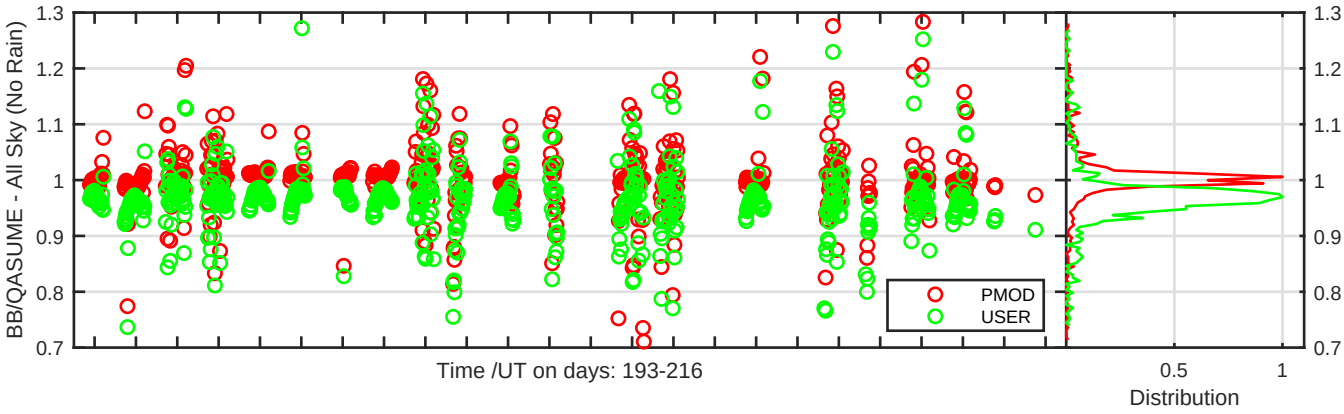

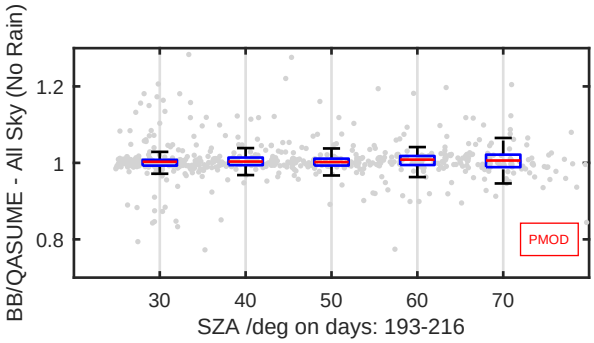

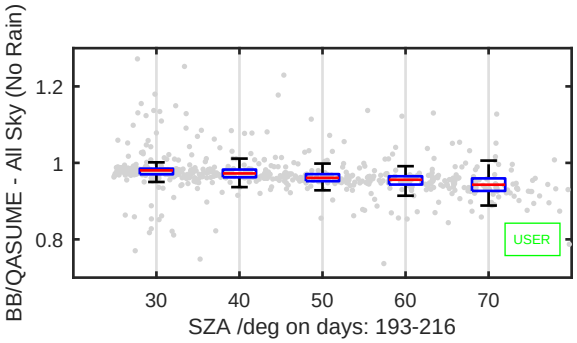

Calibration Results of KZ100114 (UVG)

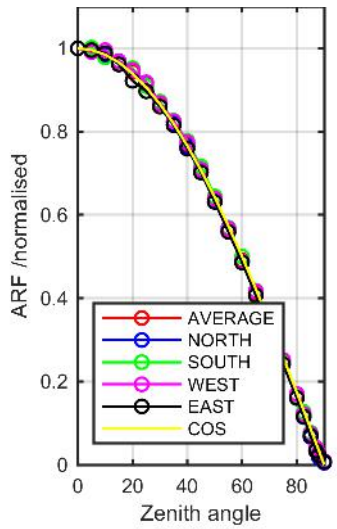

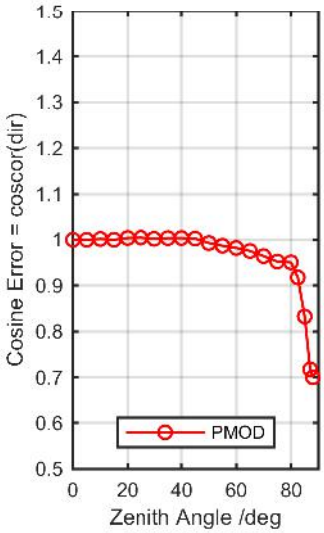

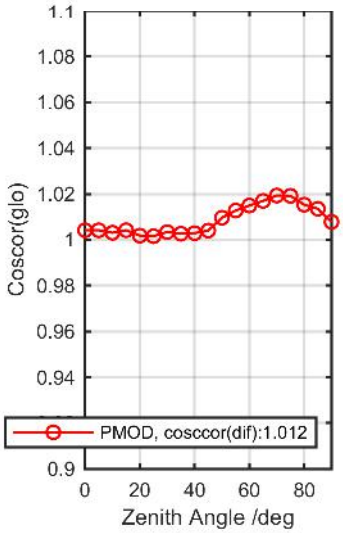

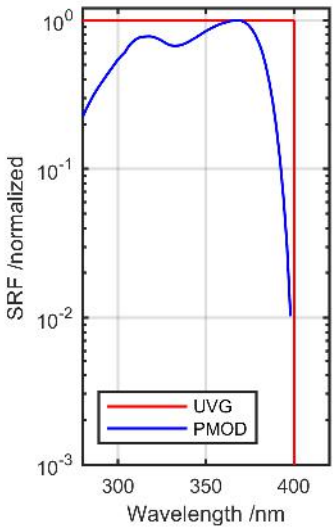

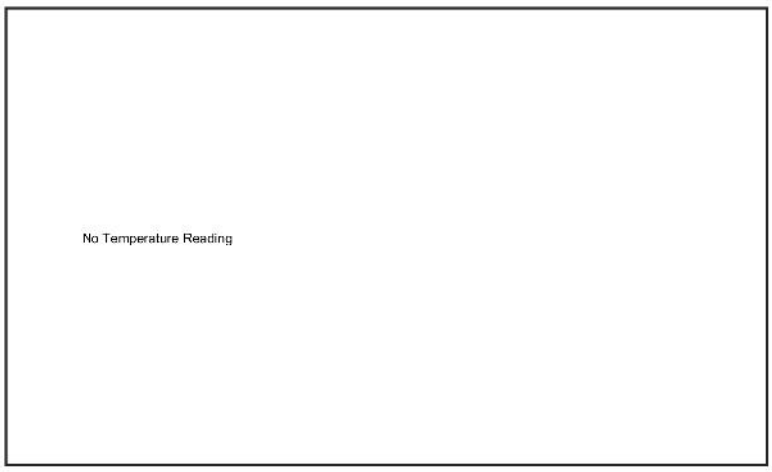

Calibration Matrix fn; Model sdisortREFms2009; f0=1.5003

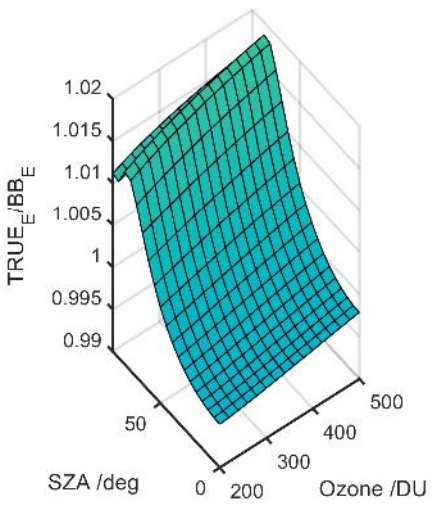

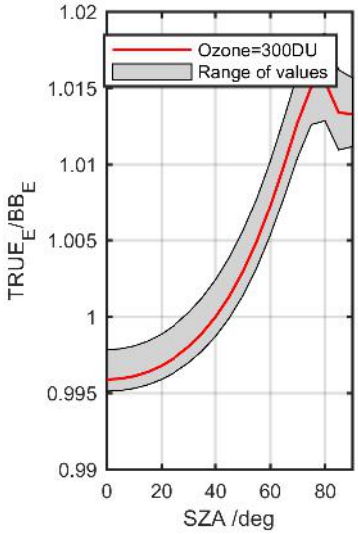

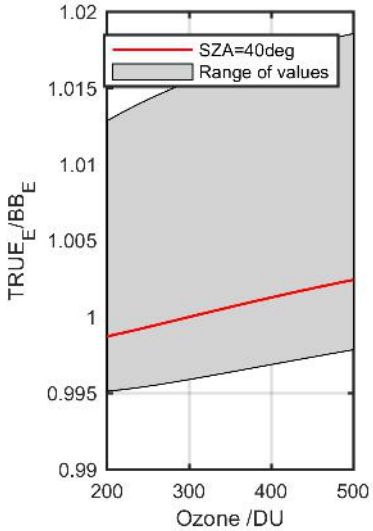

Calibration Results of KZ100114 (UVG)

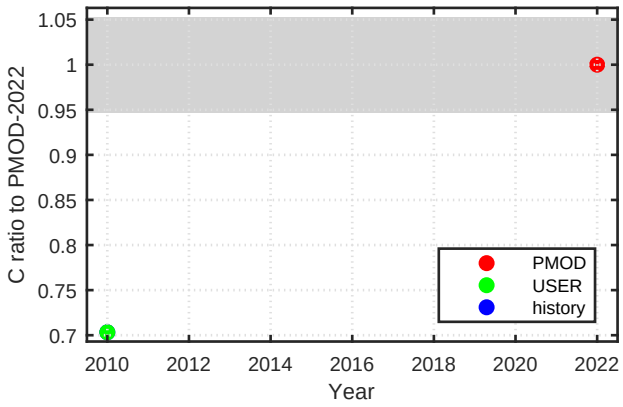

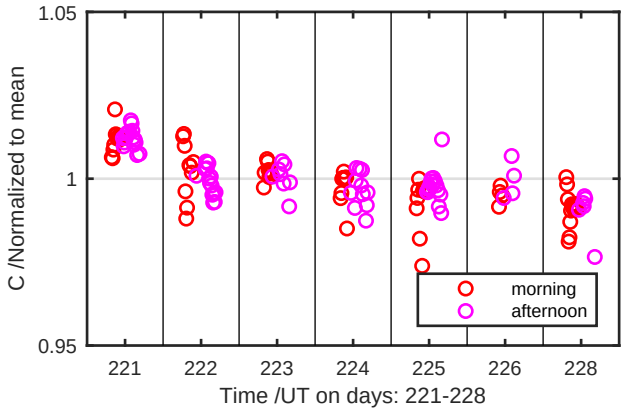

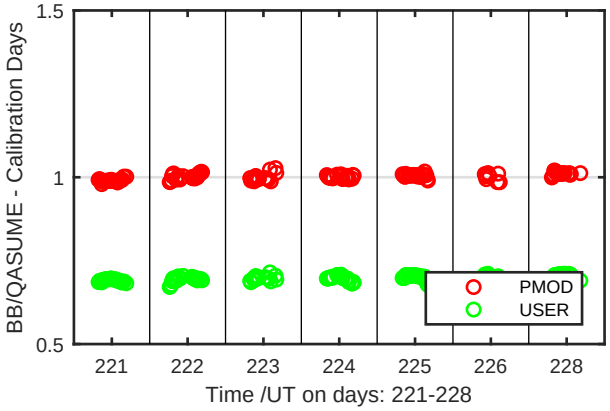

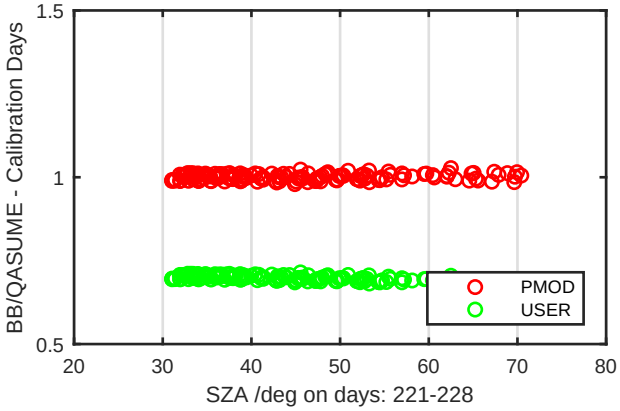

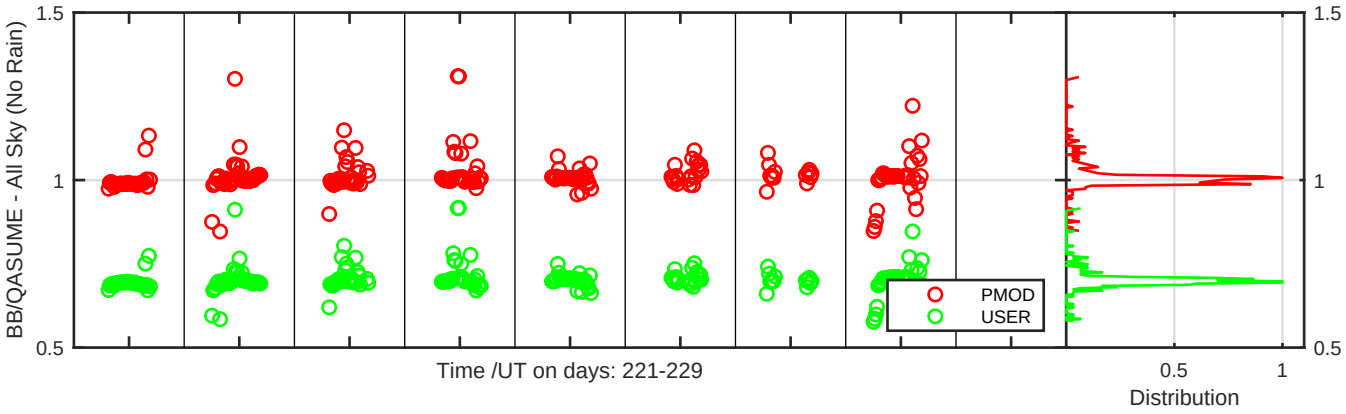

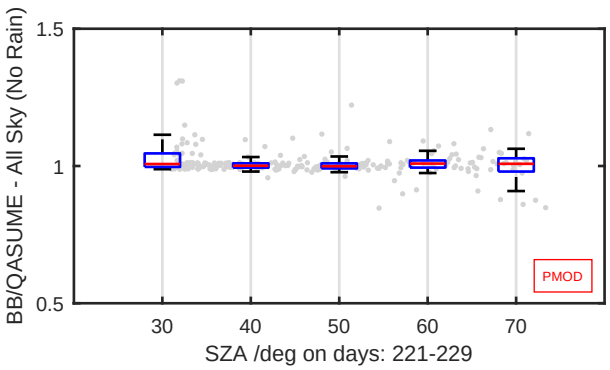

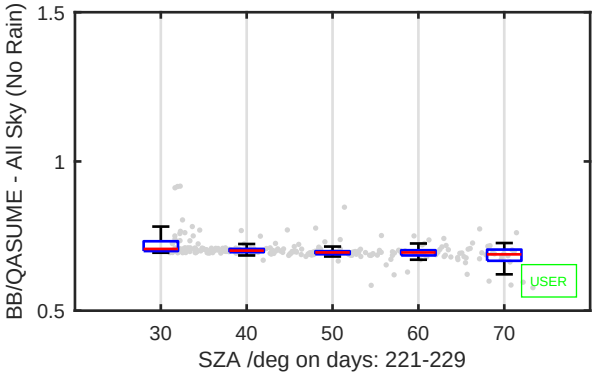

Calibration Results of KZ200723 (UVG)

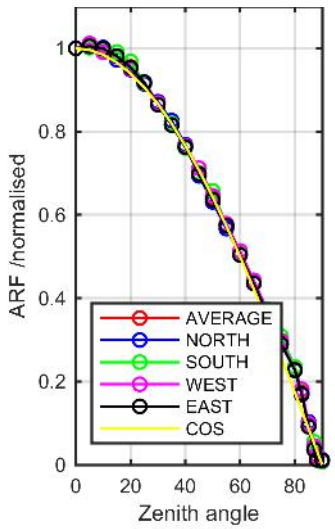

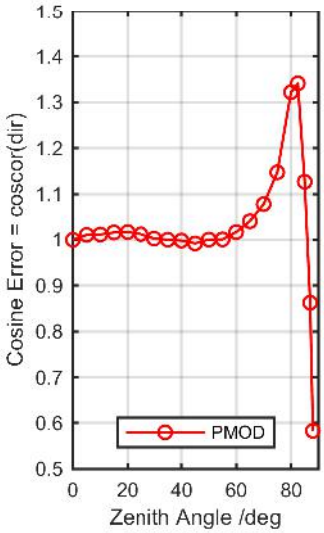

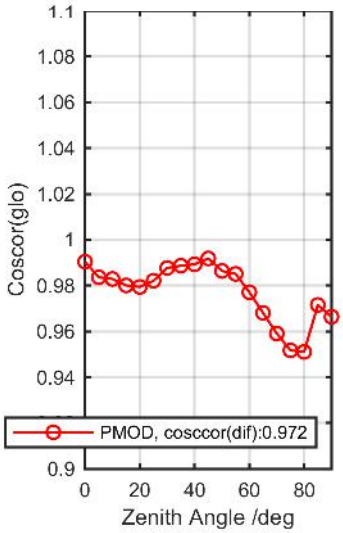

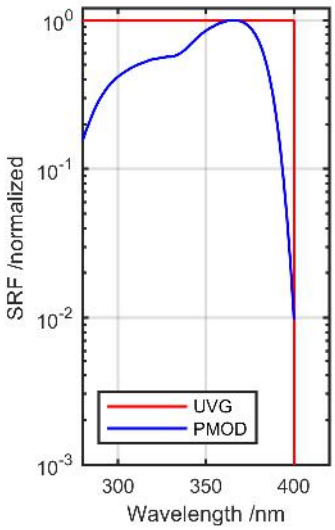

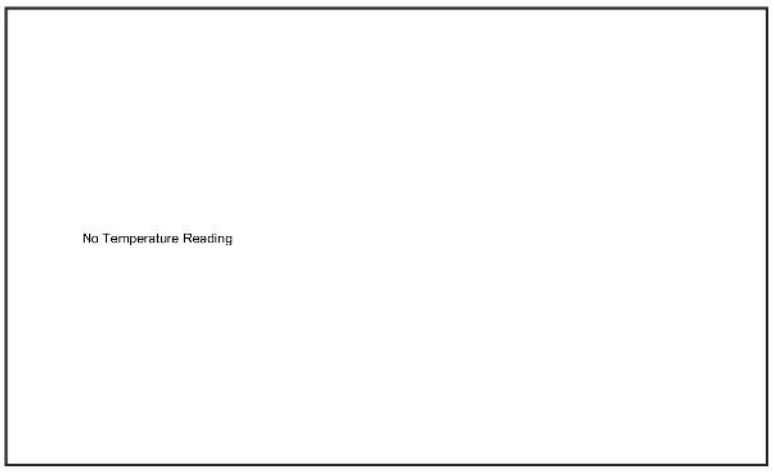

Calibration Matrix fn; Model sdisortREFms2009; f0=1.5599

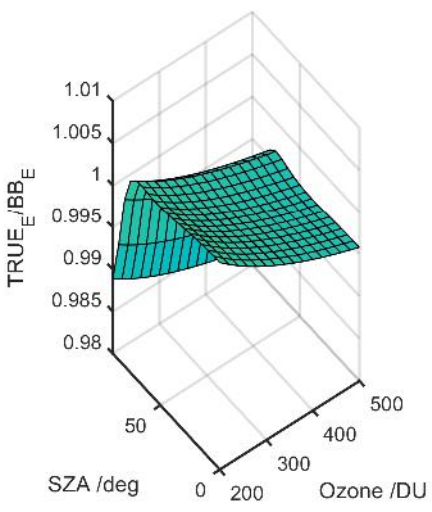

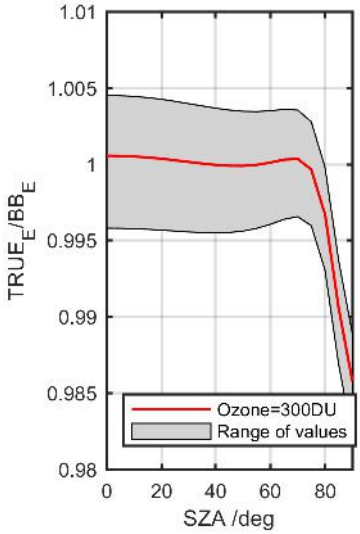

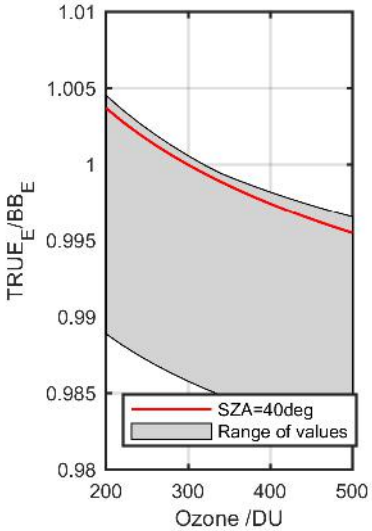

Calibration Results of KZ200723 (UVG)

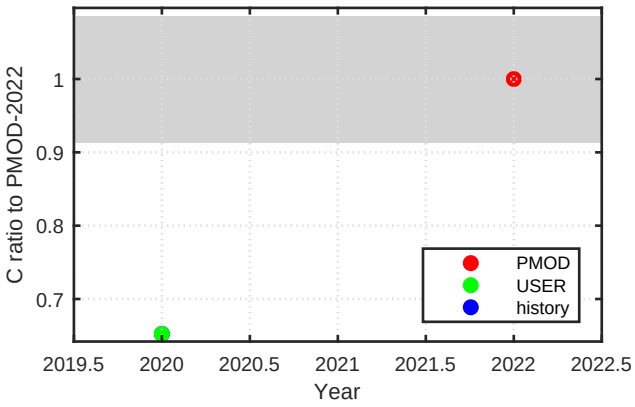

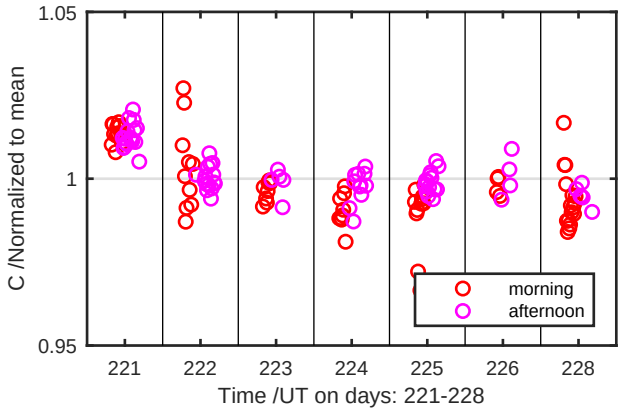

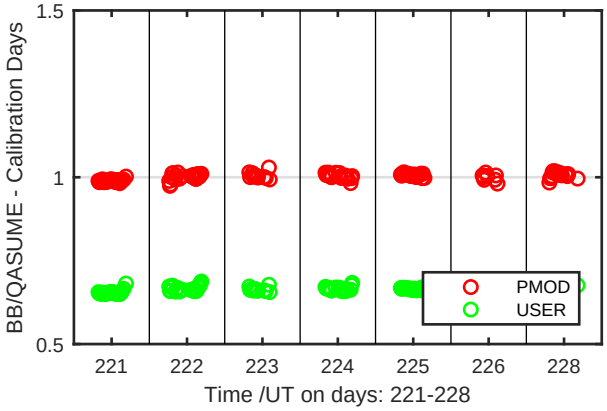

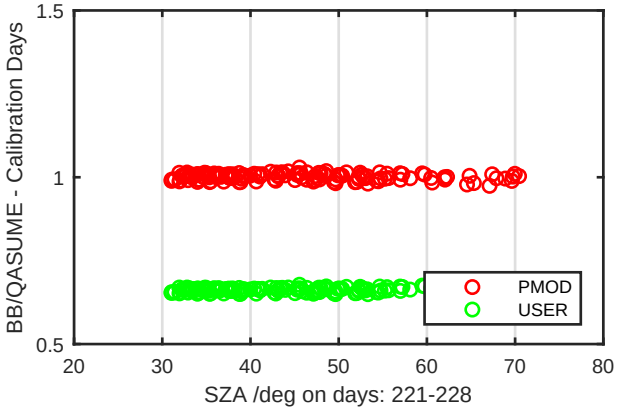

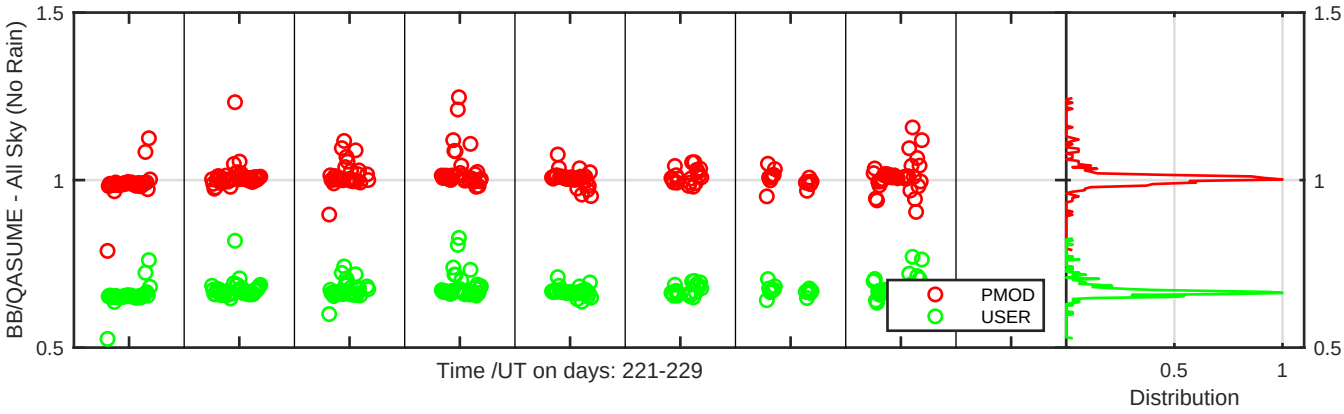

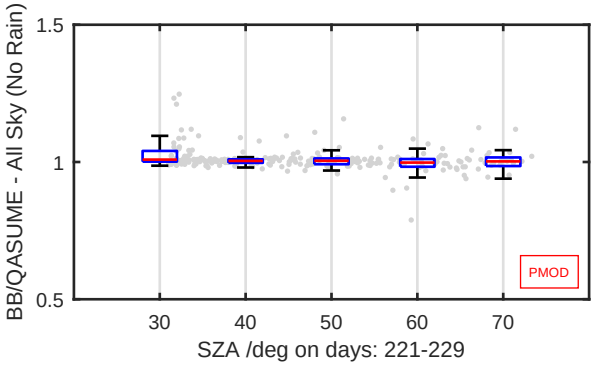

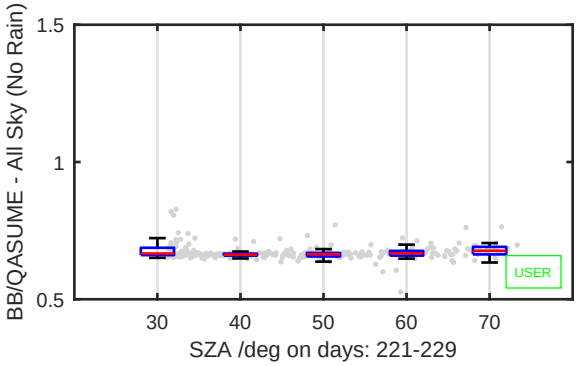

Calibration Results of SUV-E160003 (UVE)

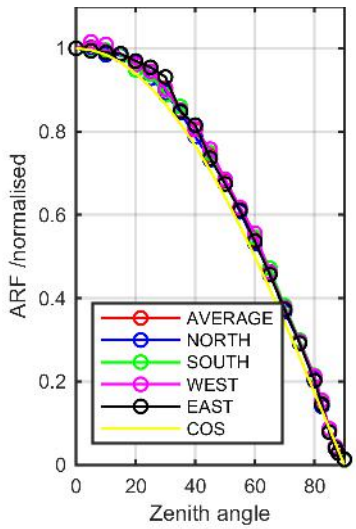

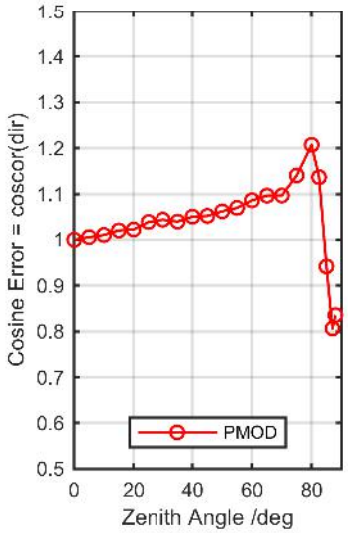

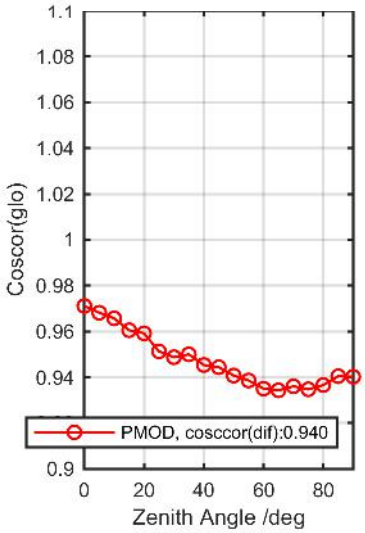

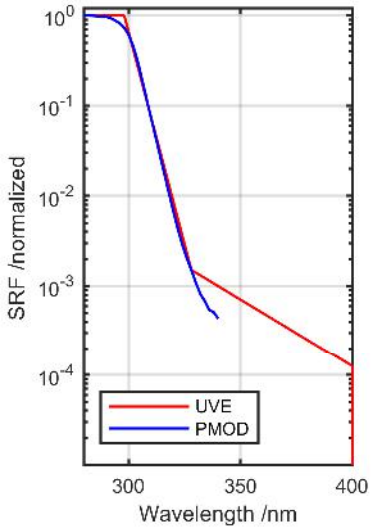

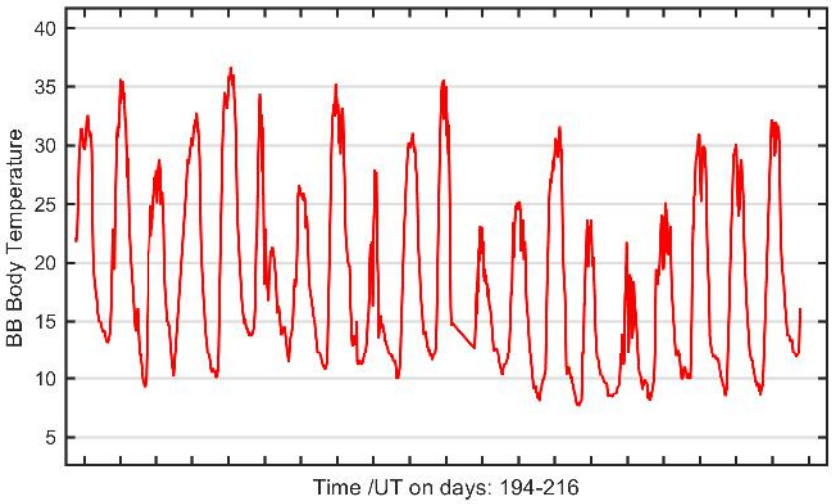

Calibration Matrix fn; Model sdisortREFms2009; f0=1.1384

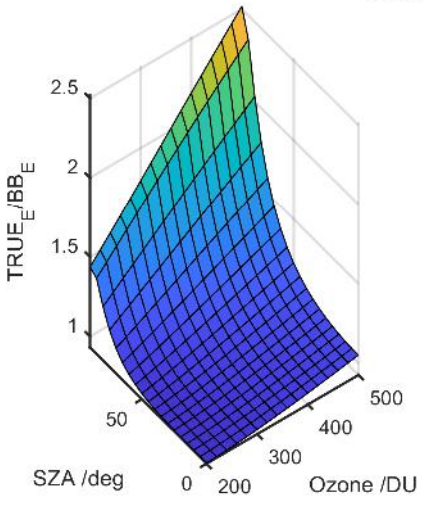

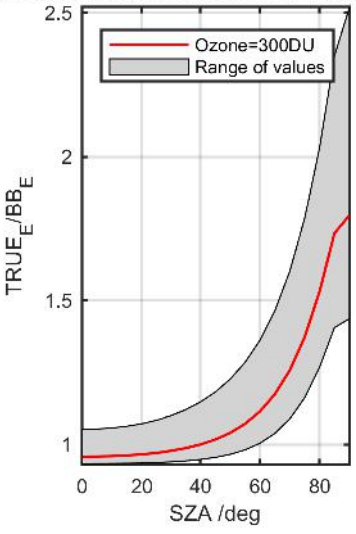

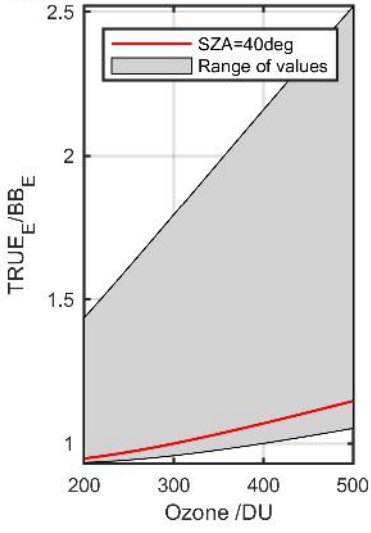

Calibration Results of SUV-E160003 (UVE)

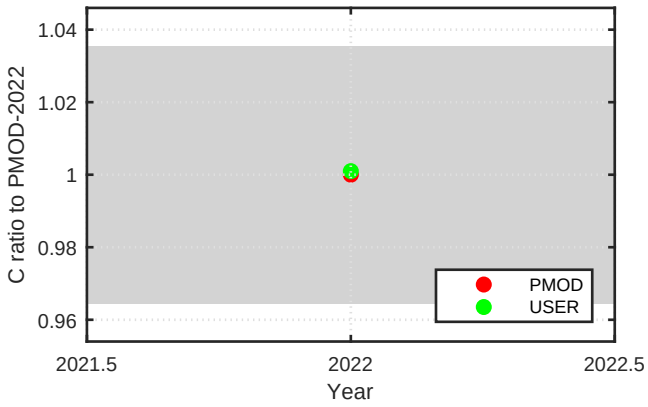

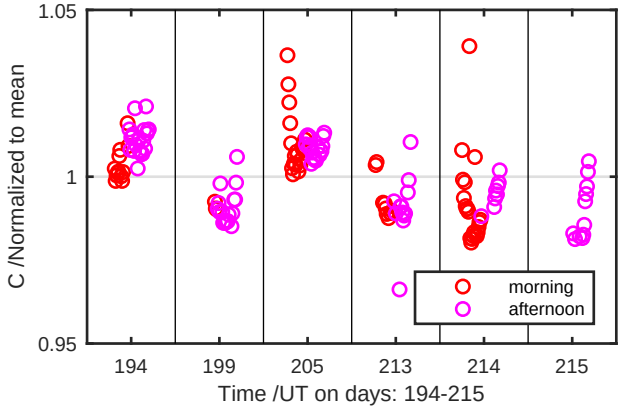

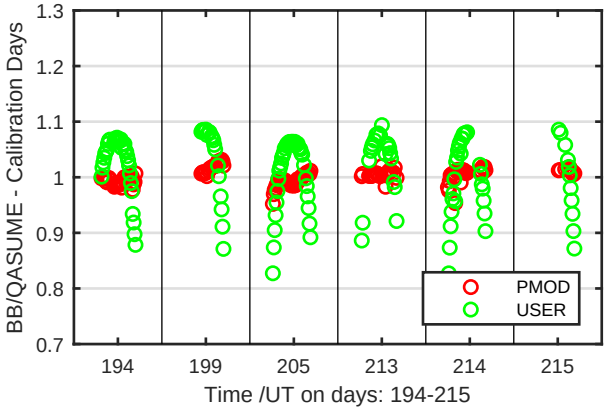

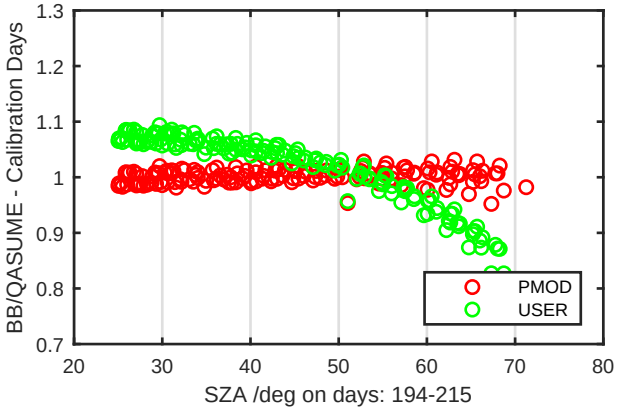

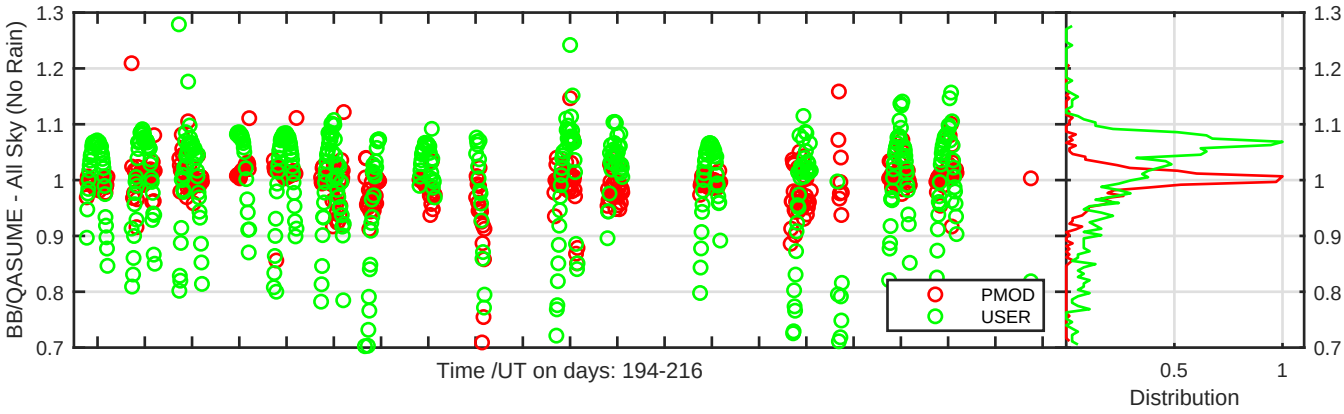

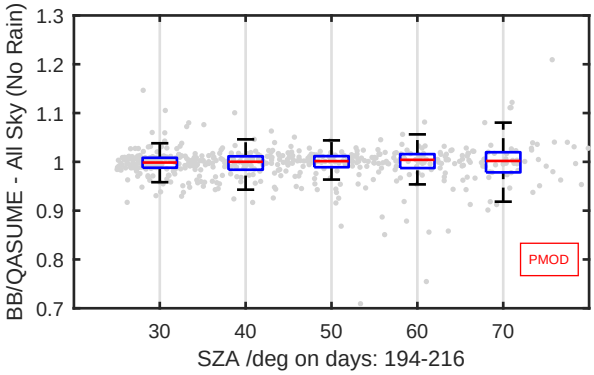

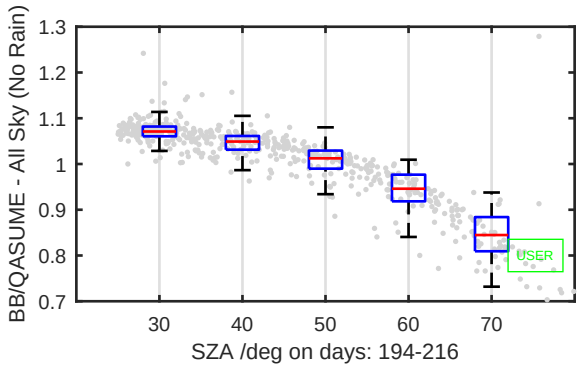

Calibration Results of SUV-E180005 (UVE)

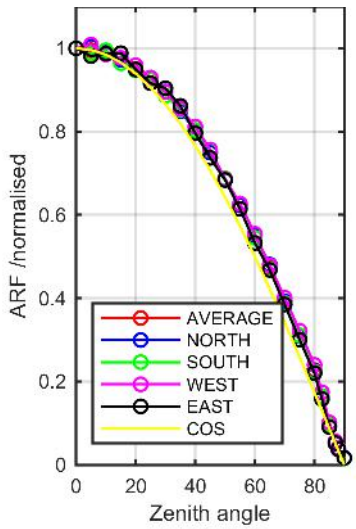

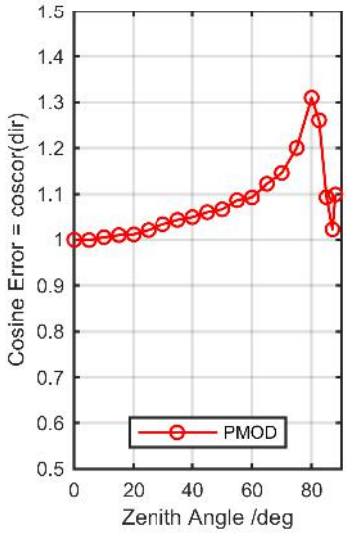

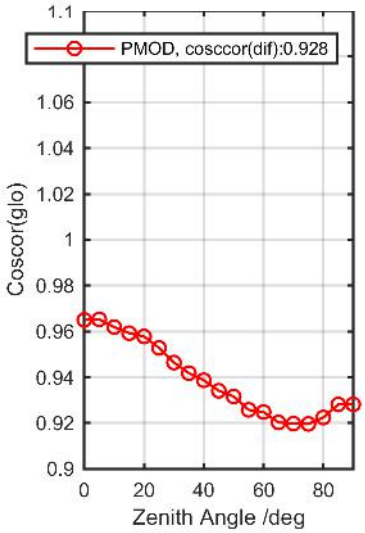

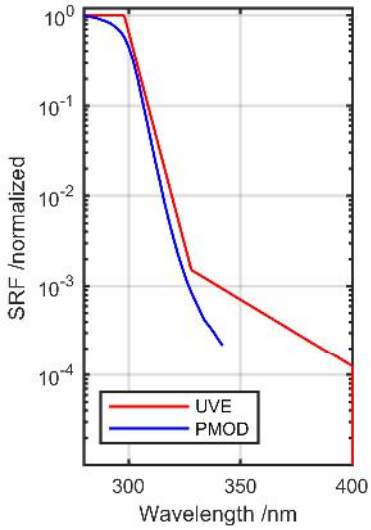

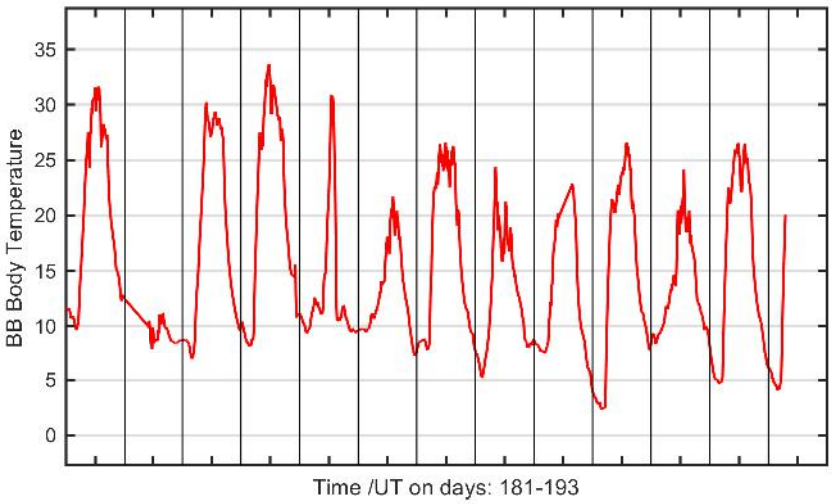

Calibration Matrix fn; Model sdisortREFms2009; f0=1.9369

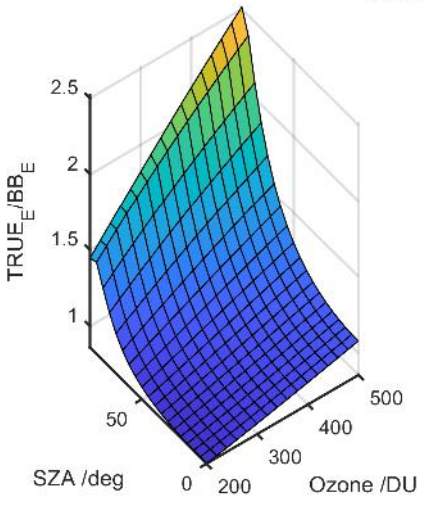

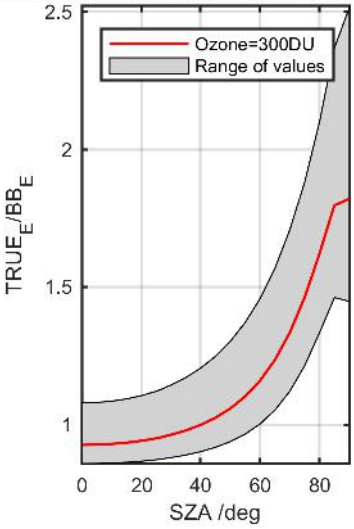

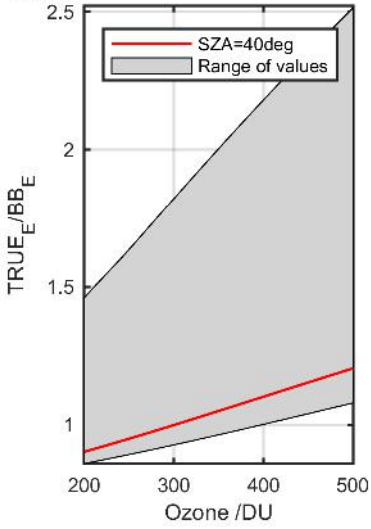

Calibration Results of SUV-E180005 (UVE)

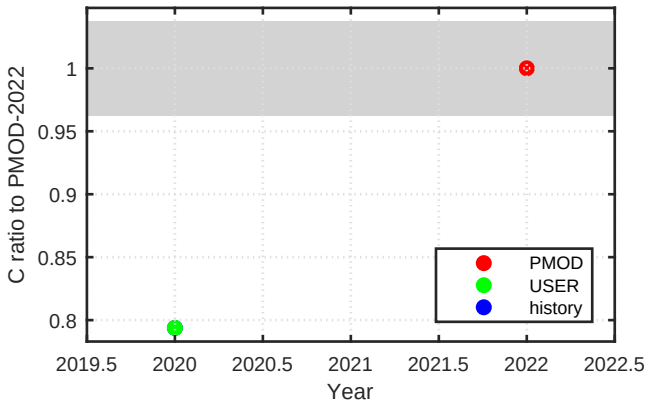

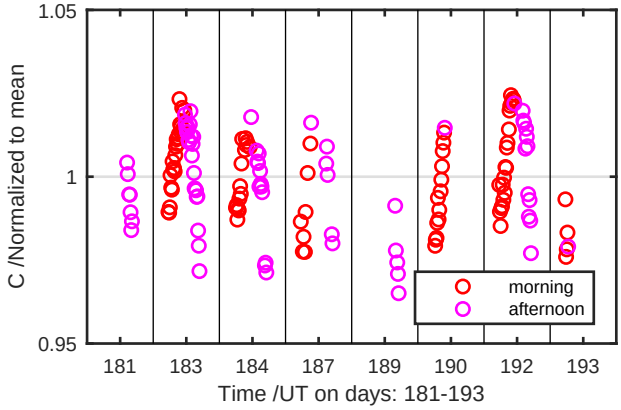

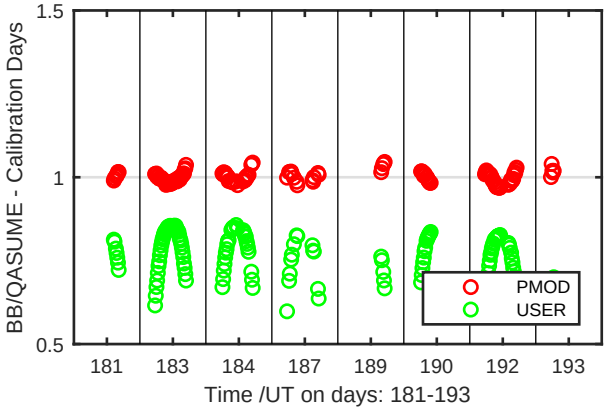

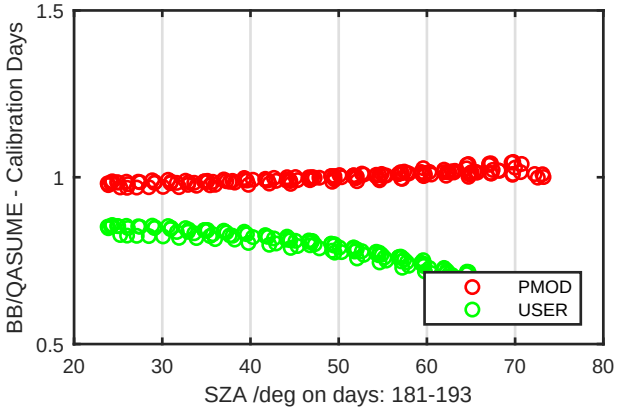

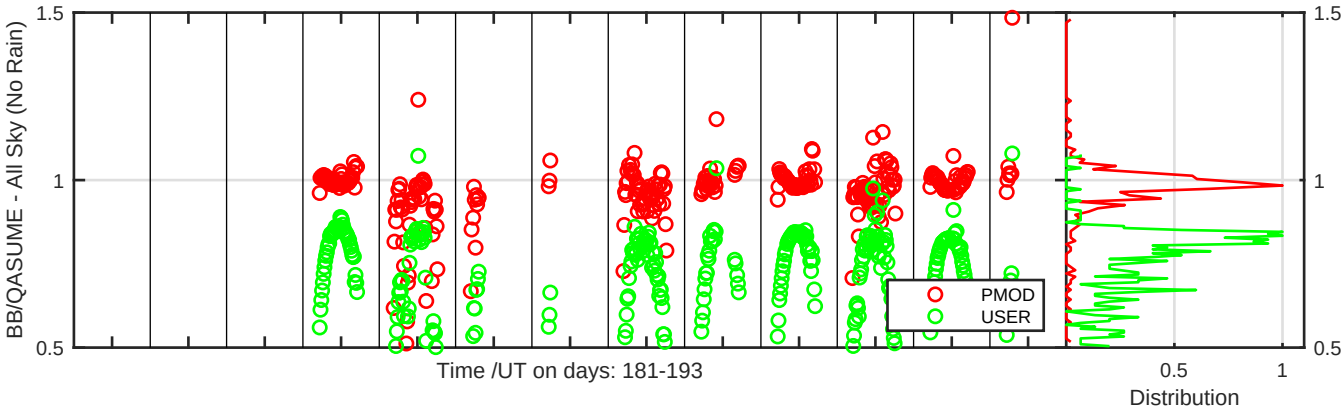

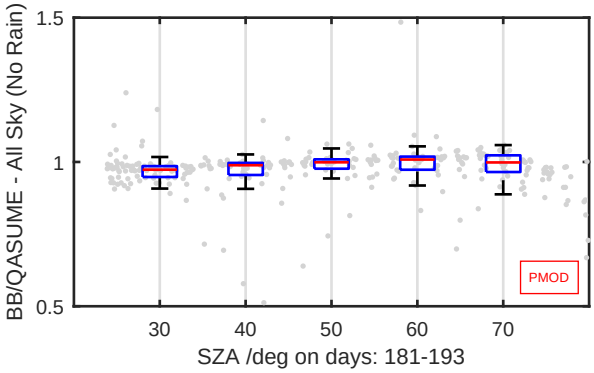

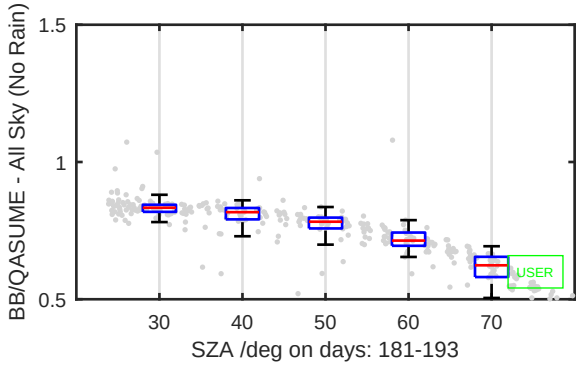

Calibration Results of SUV-E200082 (UVE)

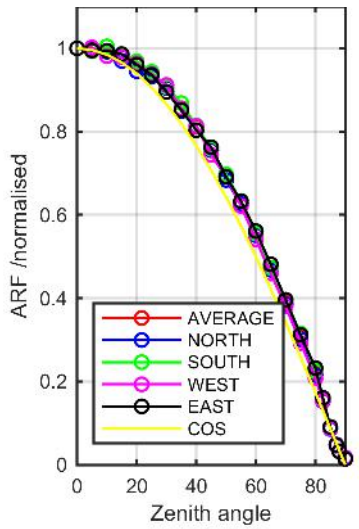

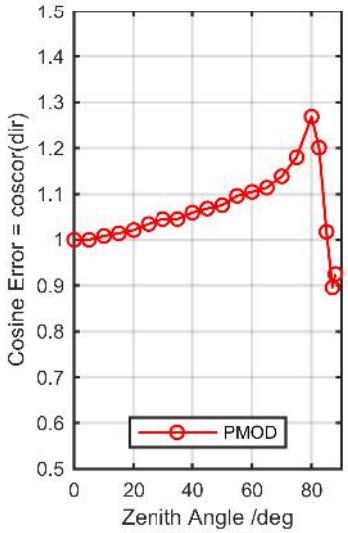

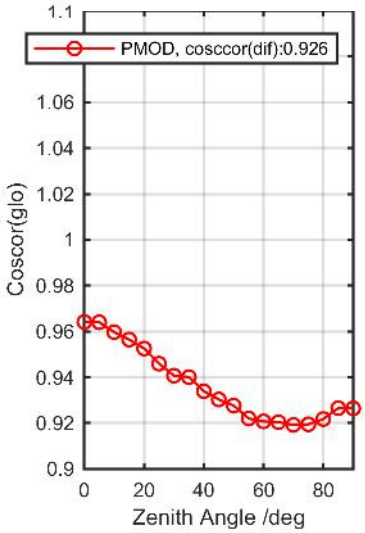

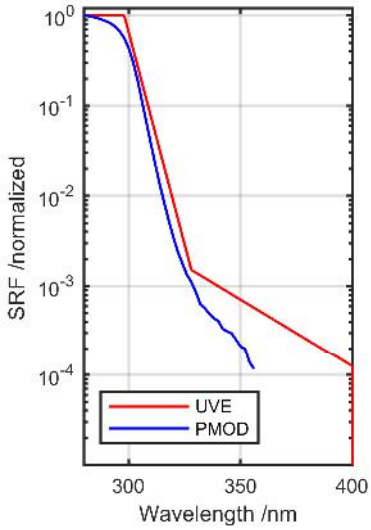

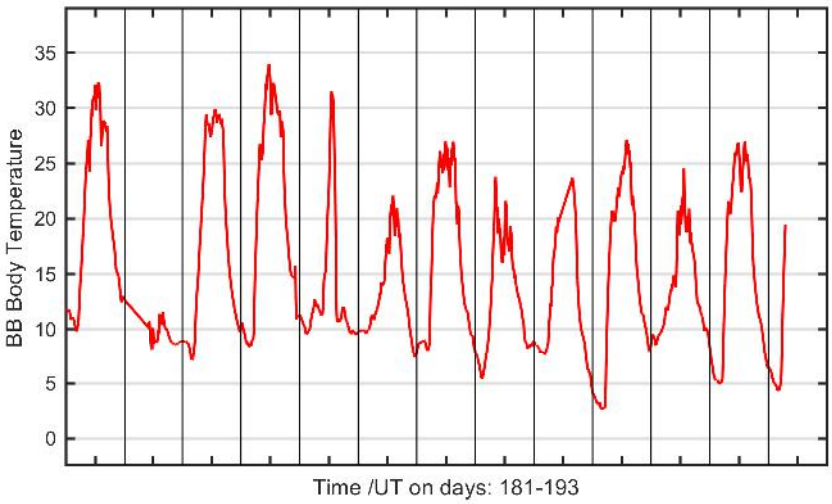

Calibration Matrix fn; Model sdisortREFms2009; f0=1.9710

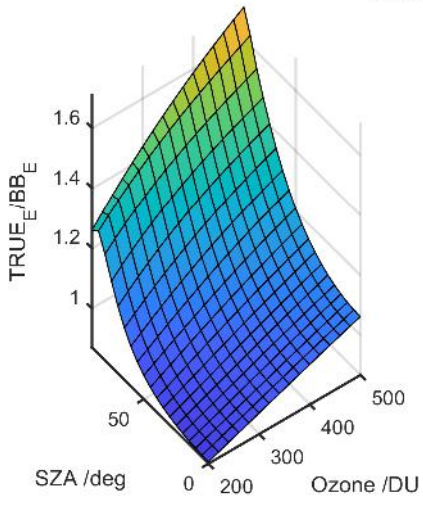

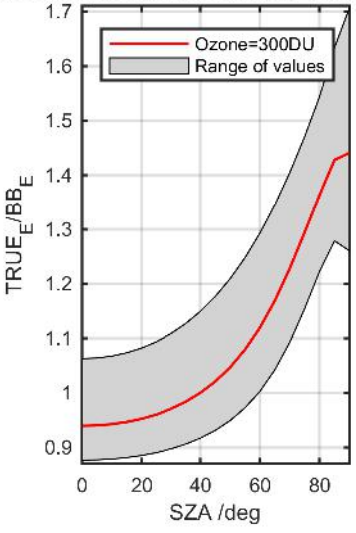

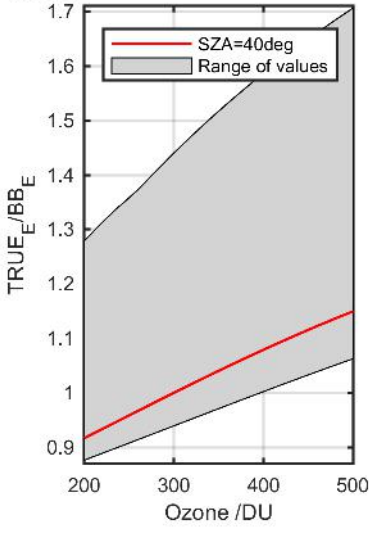

Calibration Results of SUV-E200082 (UVE)

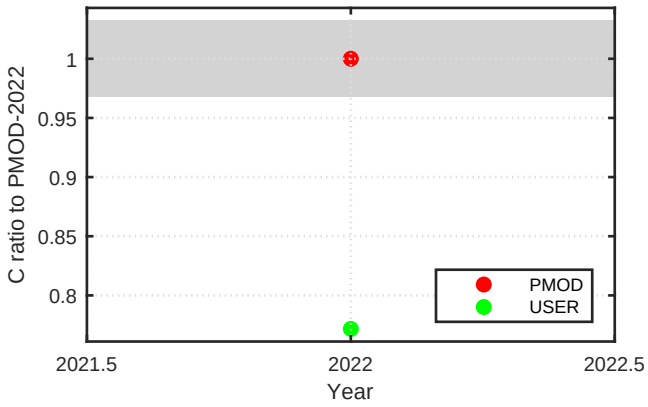

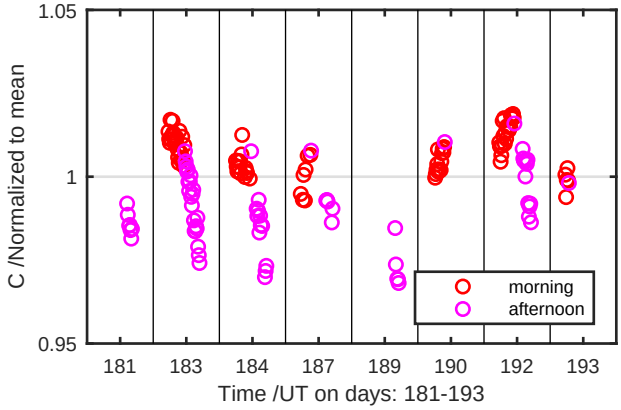

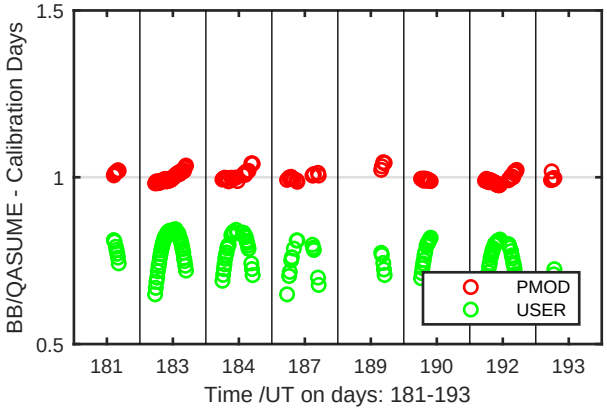

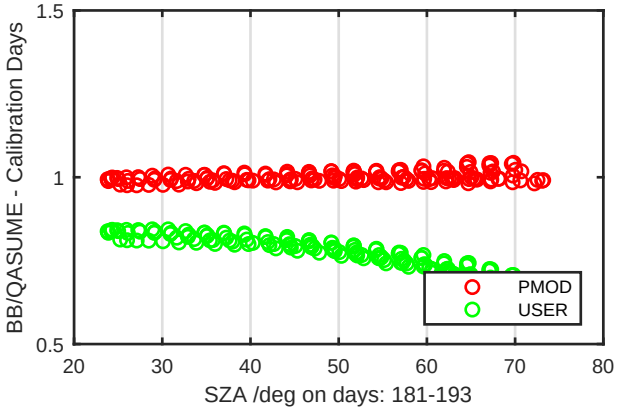

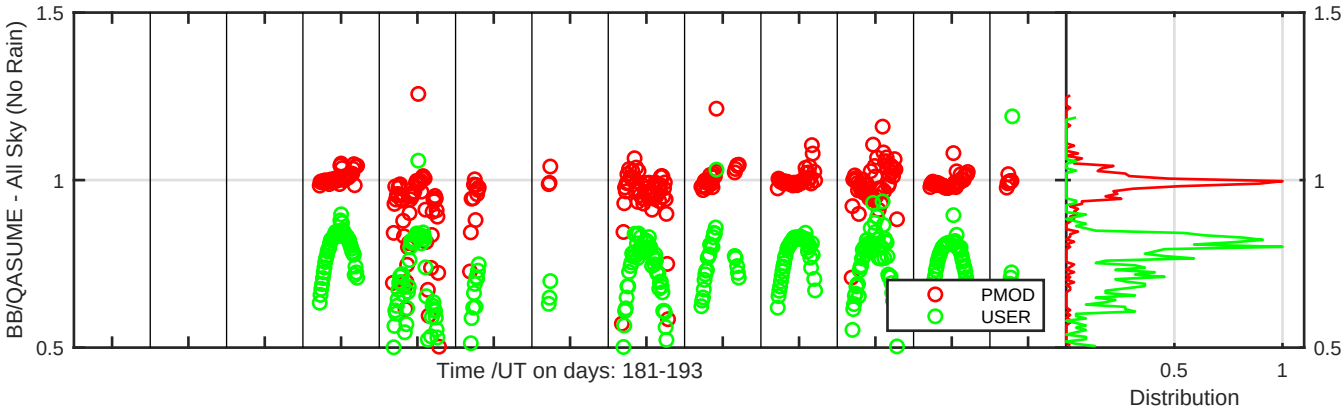

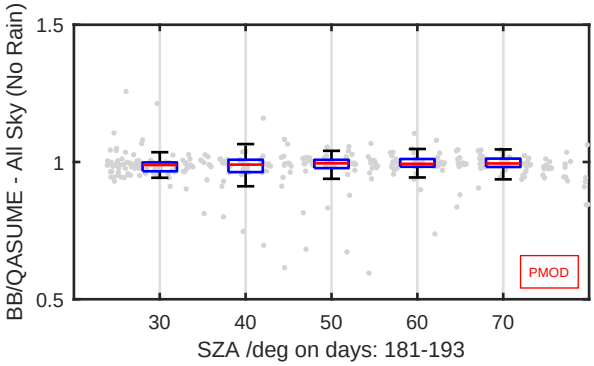

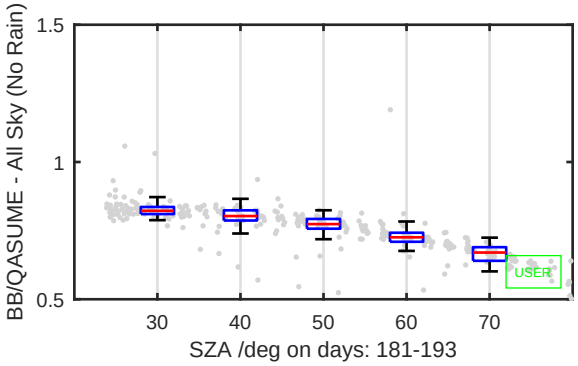

Calibration Results of SUV-E200083 (UVE)

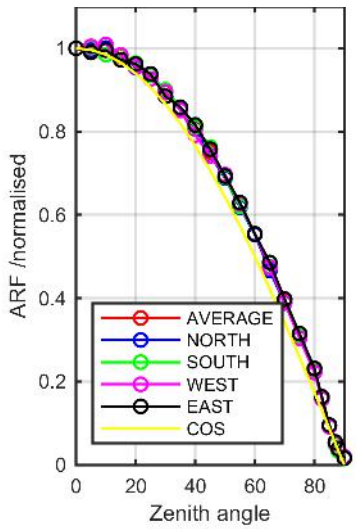

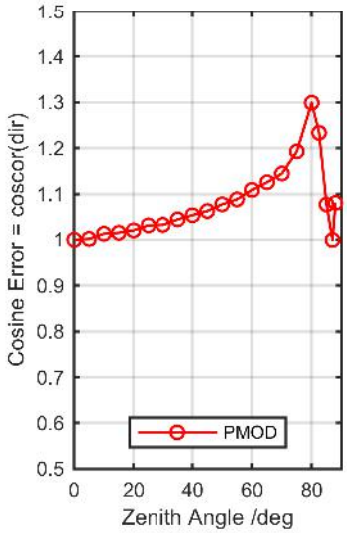

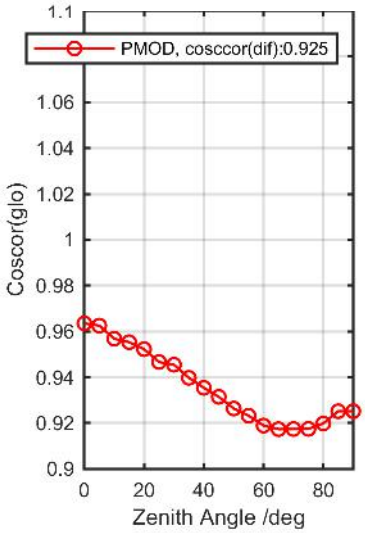

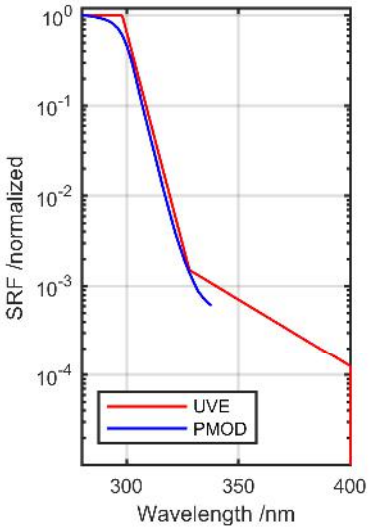

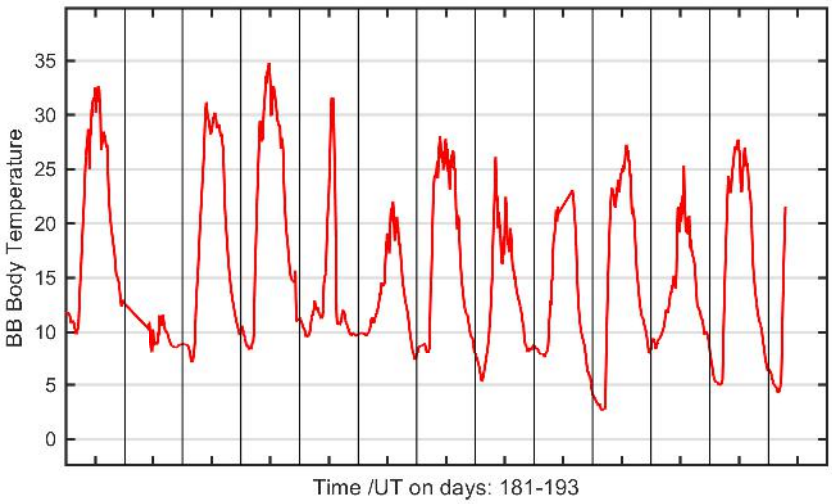

Calibration Matrix fn; Model sdisortREFms2009; f0=1.5684

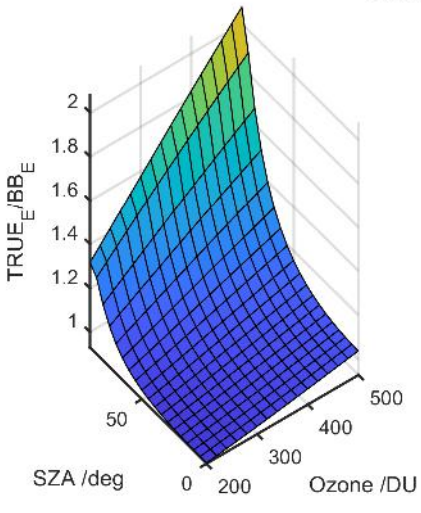

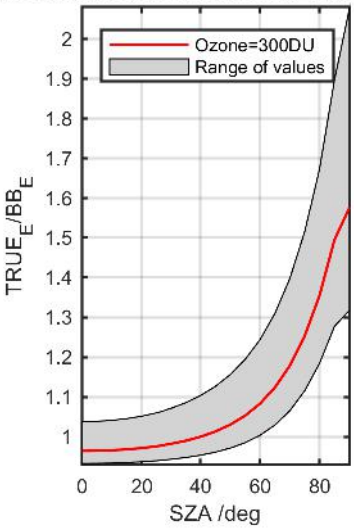

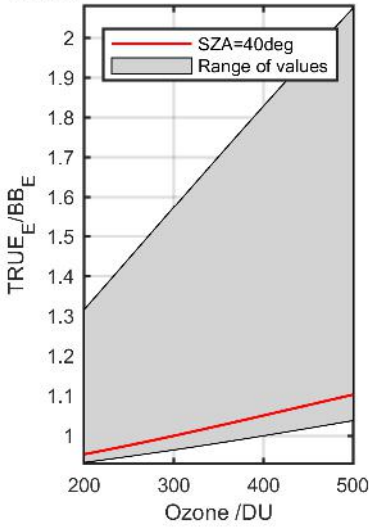

Calibration Results of SUV-E200083 (UVE)

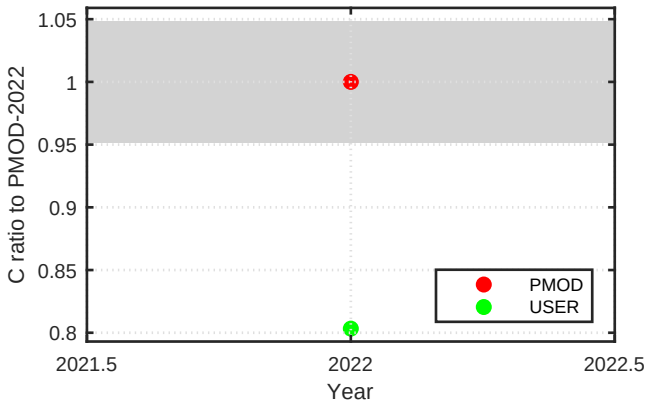

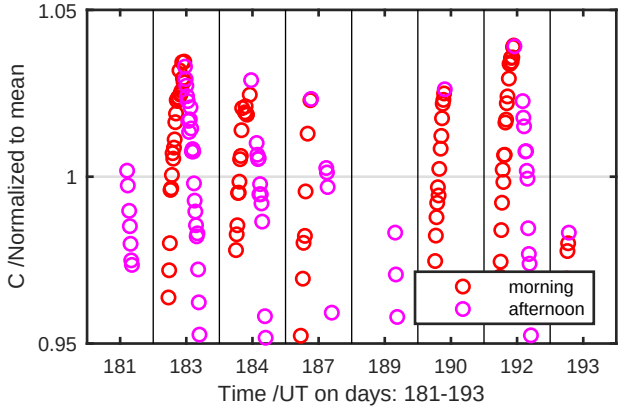

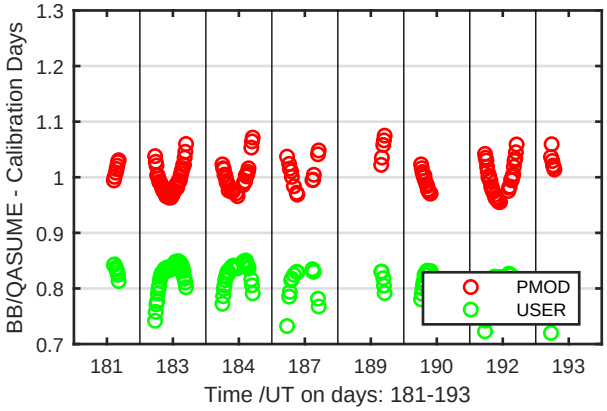

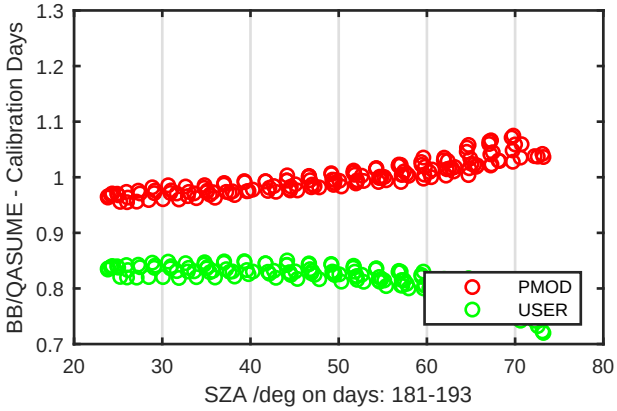

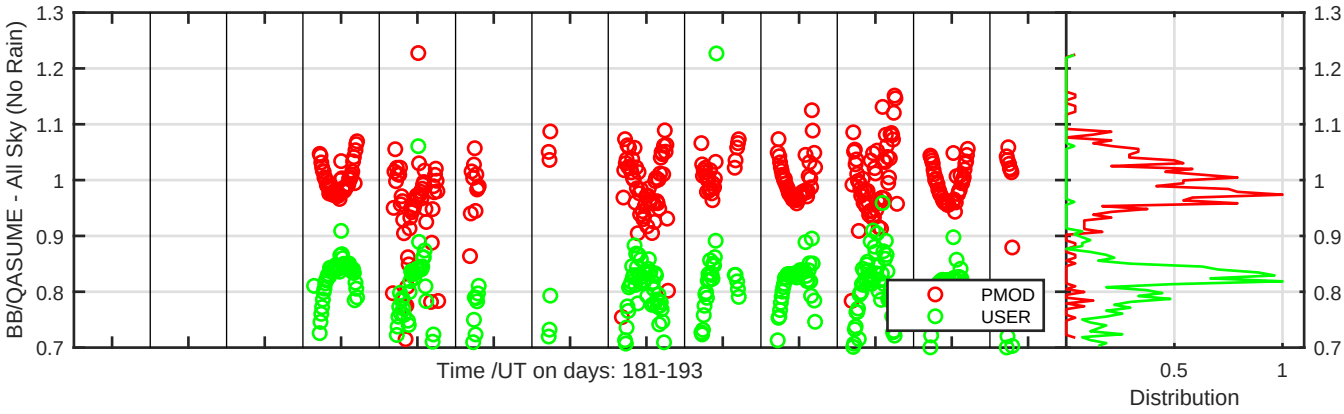

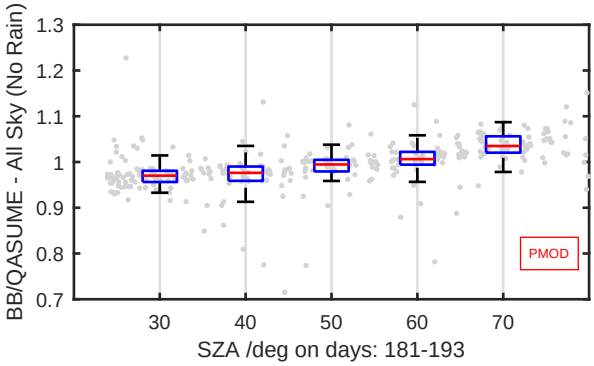

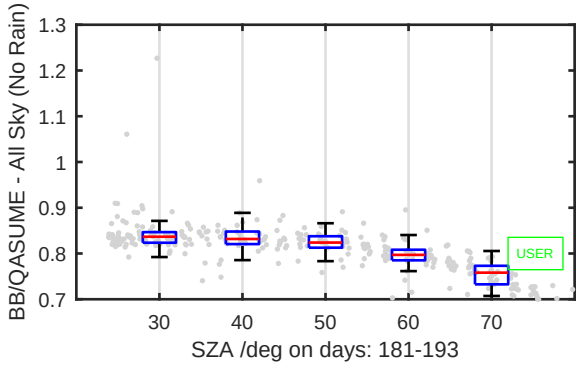

Calibration Results of SUV-E200090 (UVE)

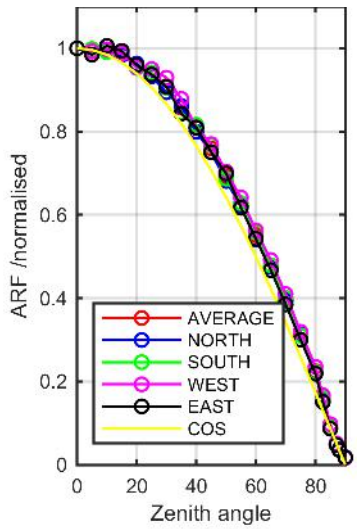

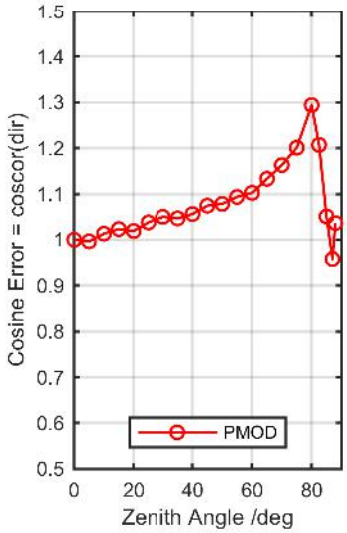

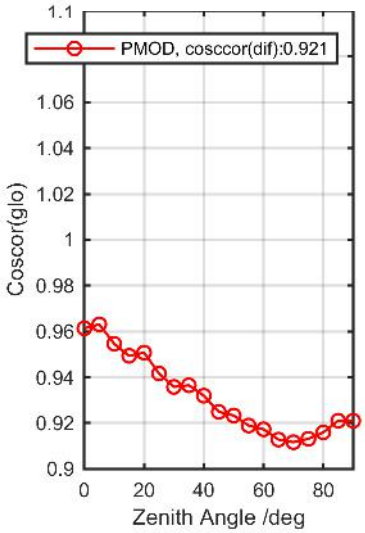

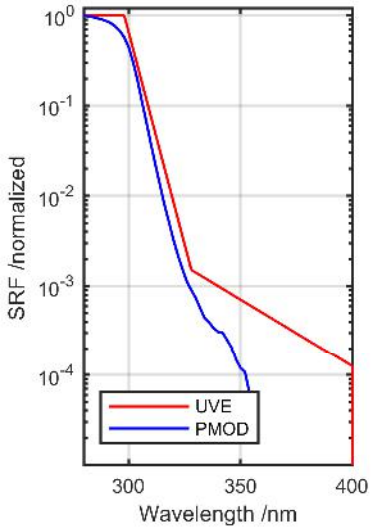

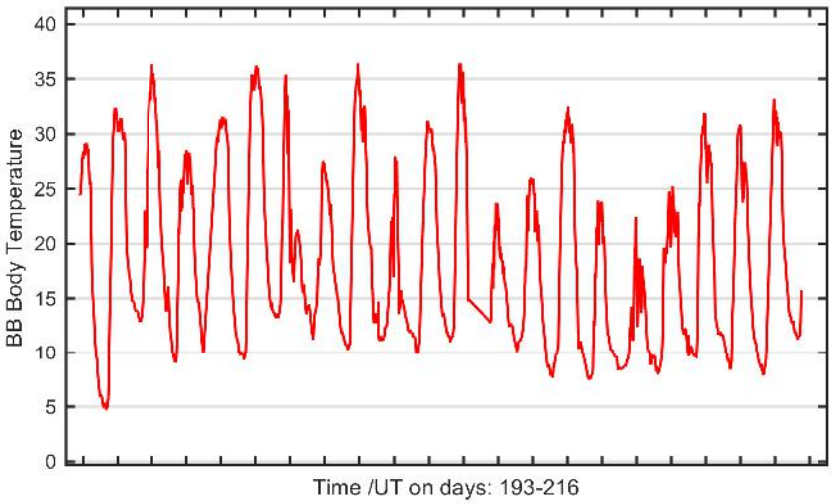

Calibration Matrix fn; Model sdisortREFms2009; f0=2.0301

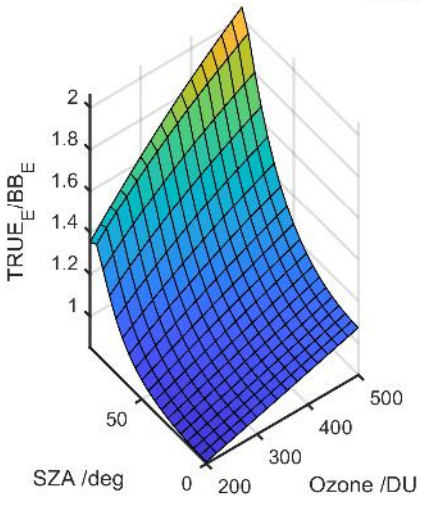

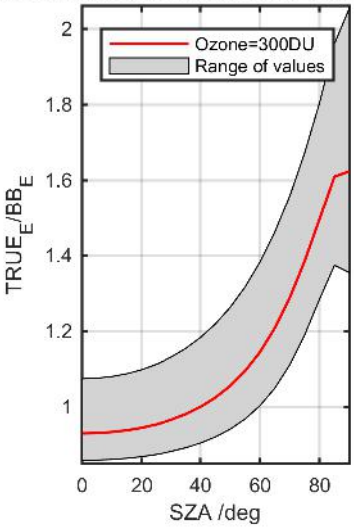

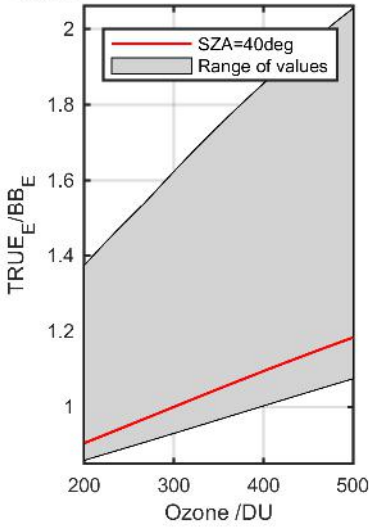

Calibration Results of SUV-E200090 (UVE)

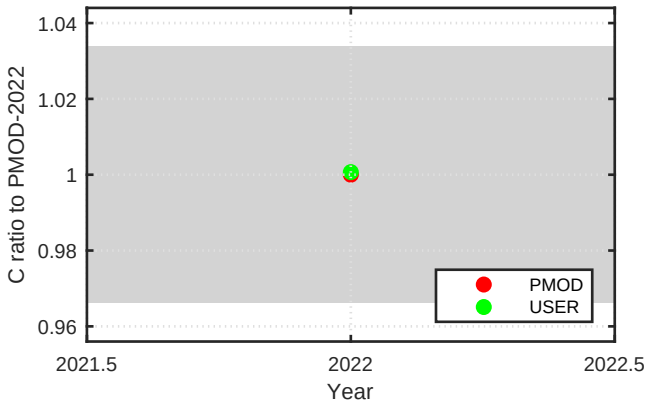

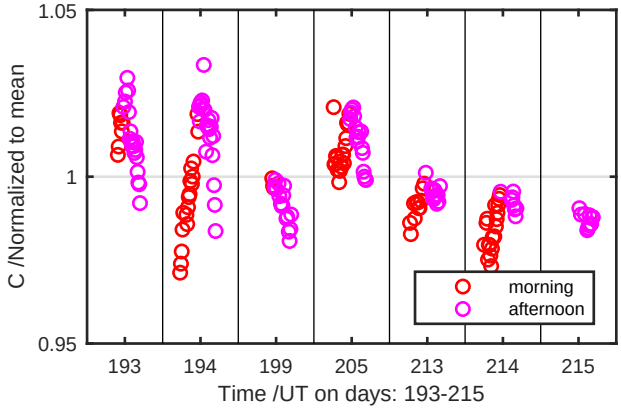

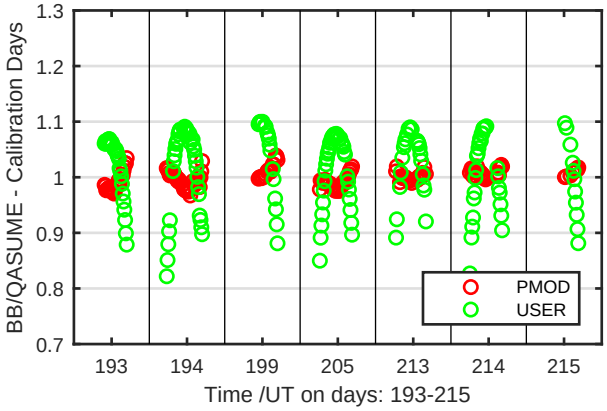

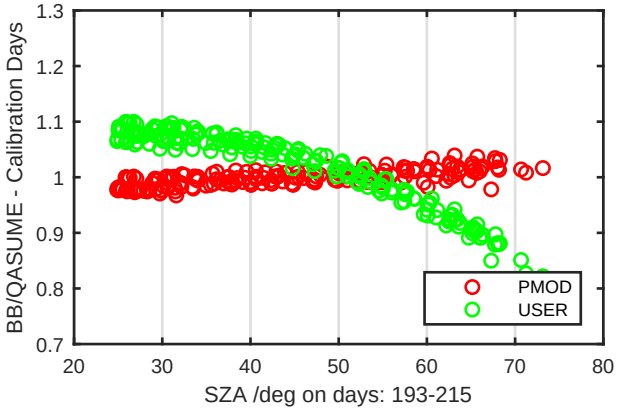

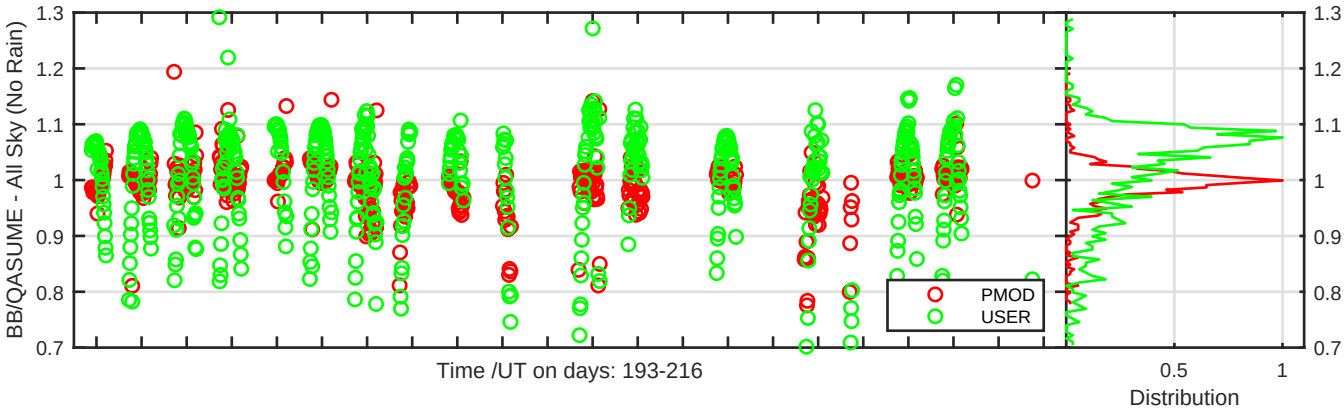

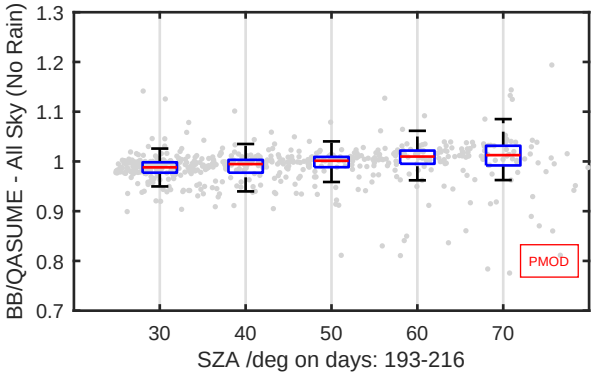

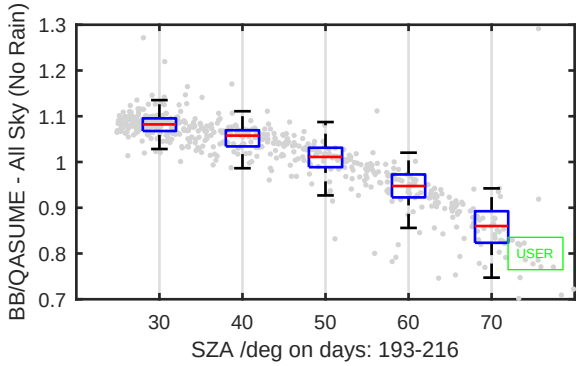

Calibration Results of SUV-E200095 (UVE)

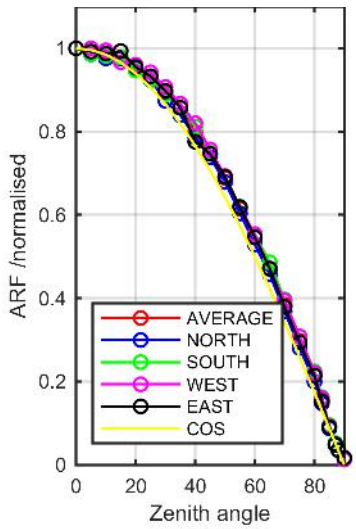

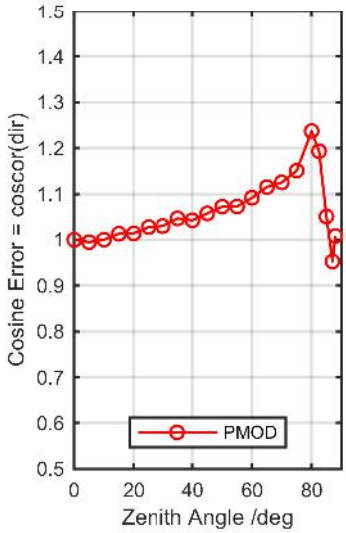

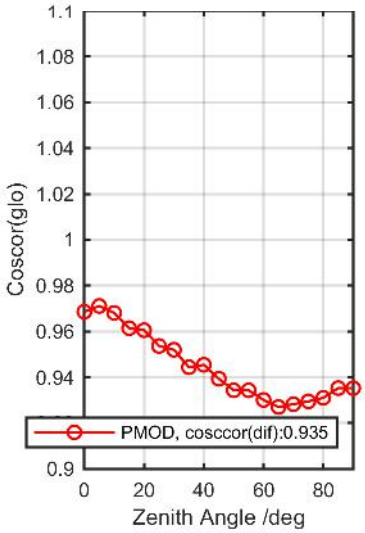

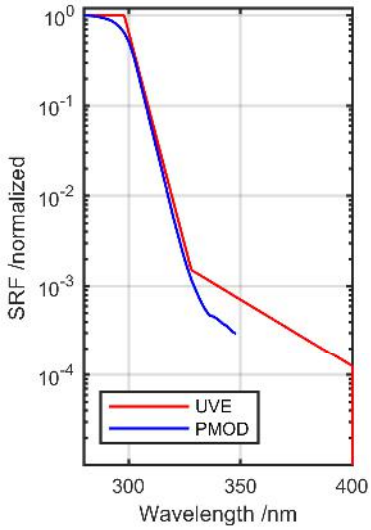

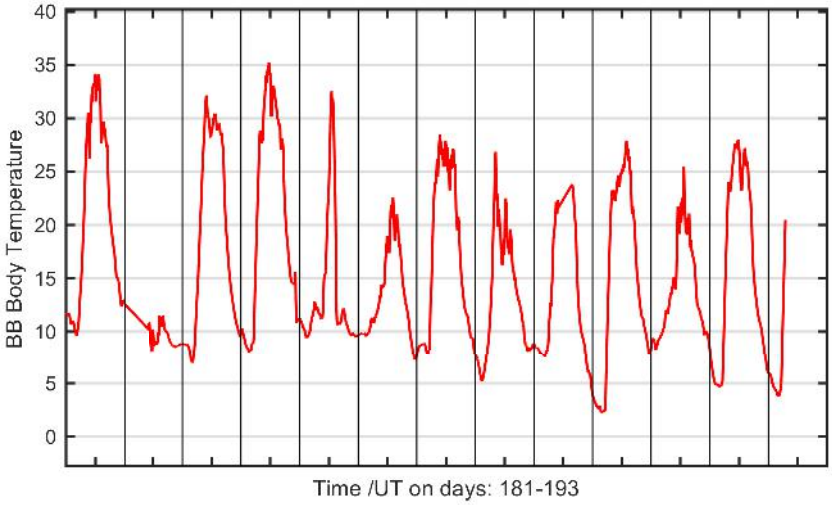

Calibration Matrix fn; Model sdisortREFms2009; f0=1.3872

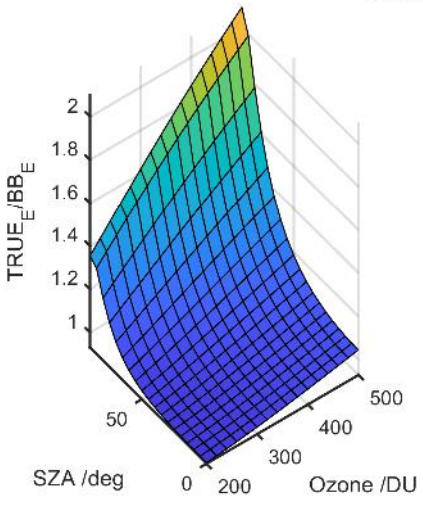

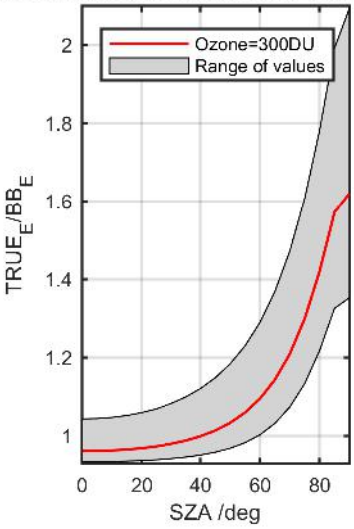

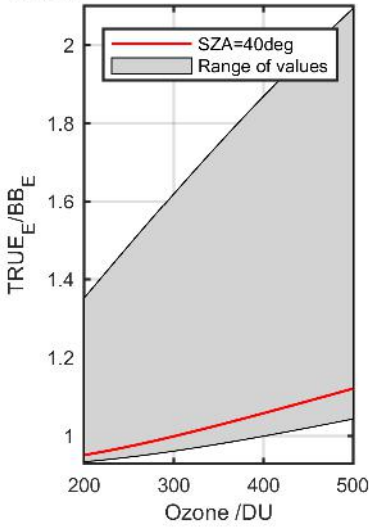

Calibration Results of SUV-E200095 (UVE)

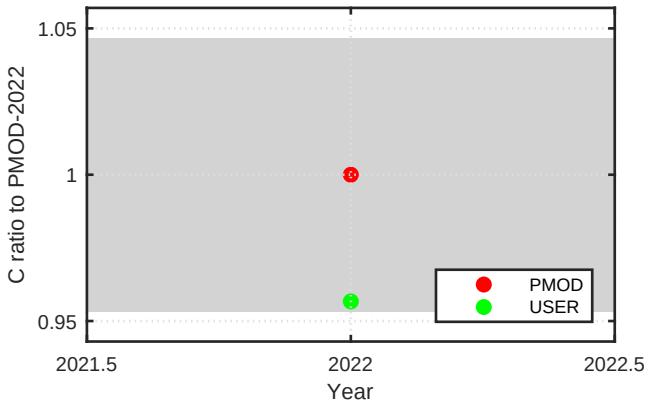

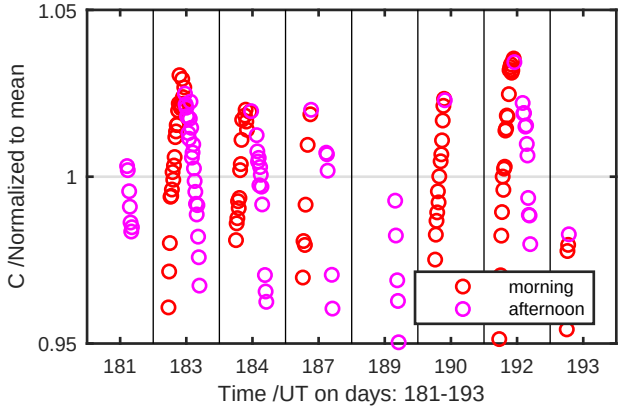

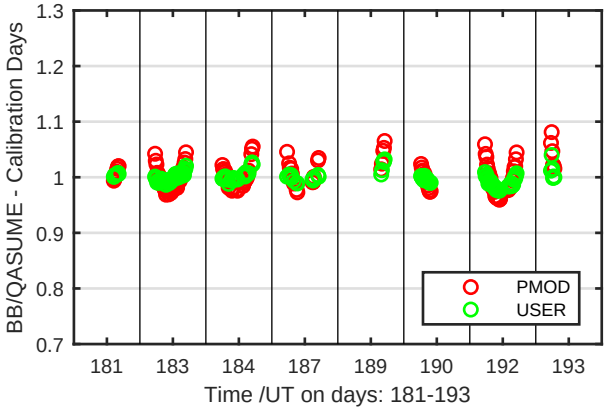

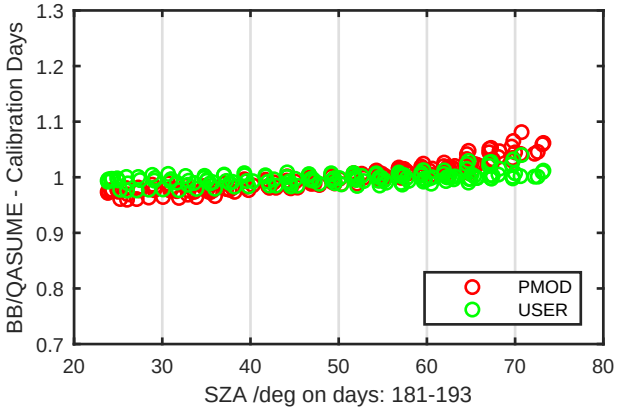

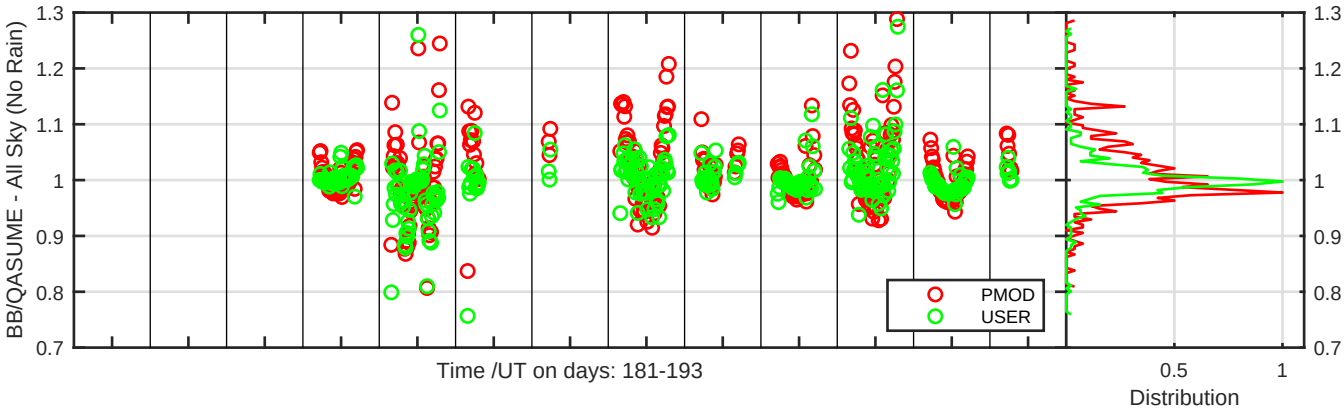

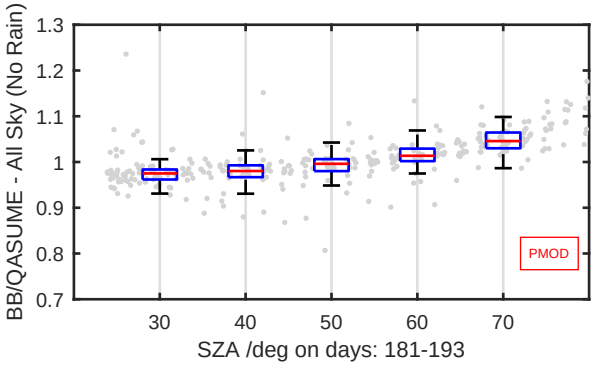

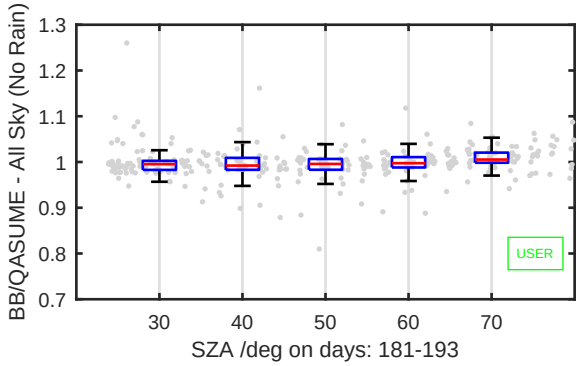

Calibration Results of SUV-B210285 (UVB)

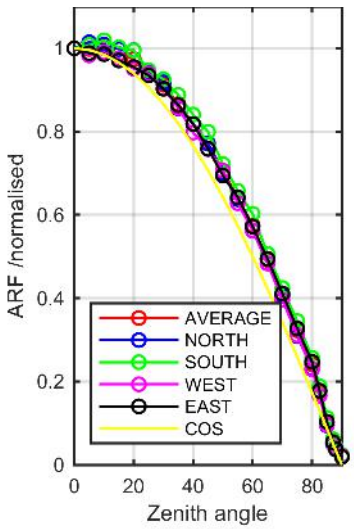

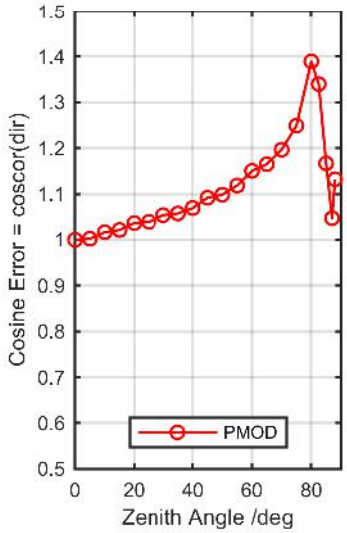

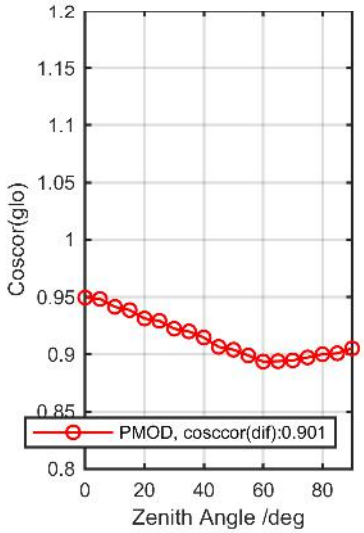

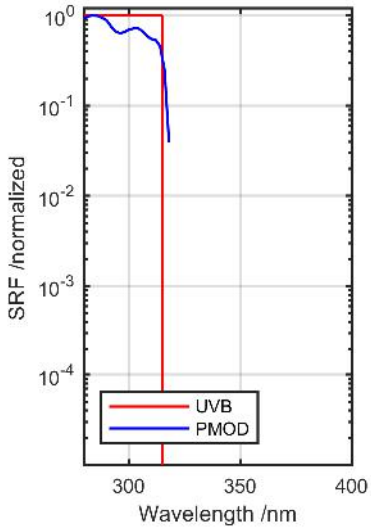

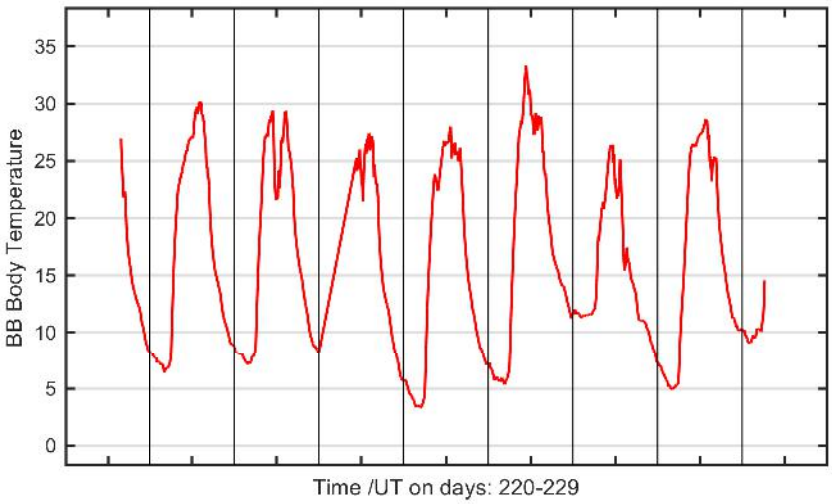

Calibration Matrix fn; Model sdisortREFms2009; f0=1.5073

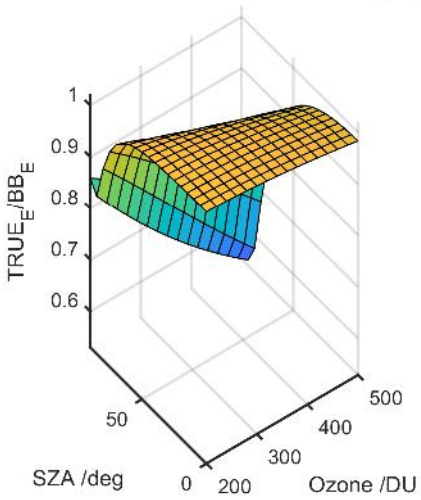

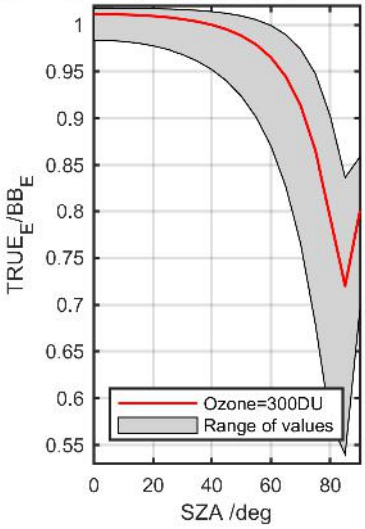

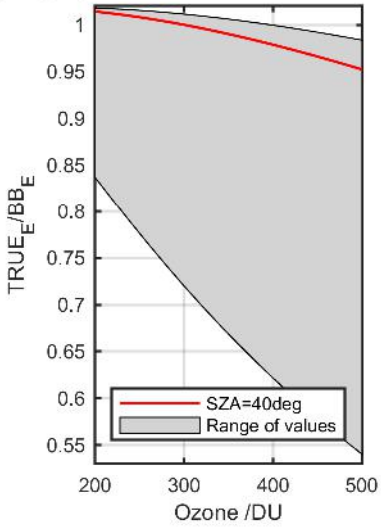

Calibration Results of SUV-B210285 (UVB)

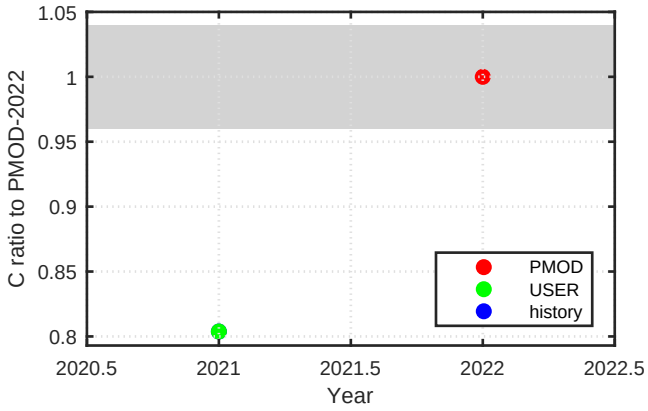

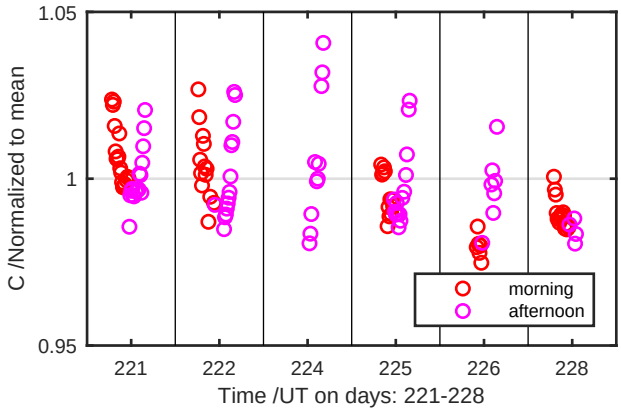

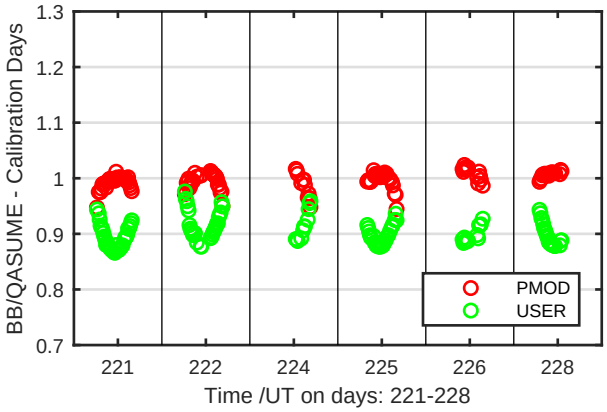

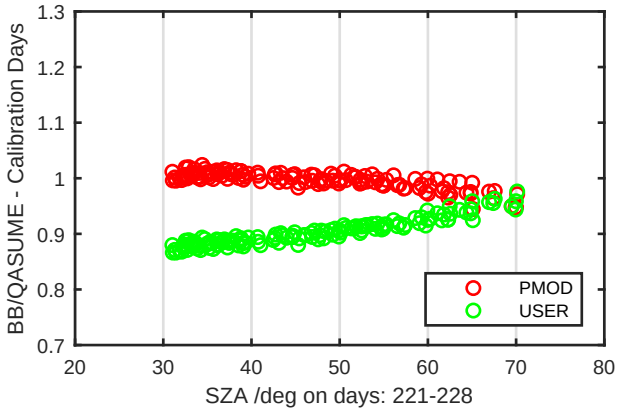

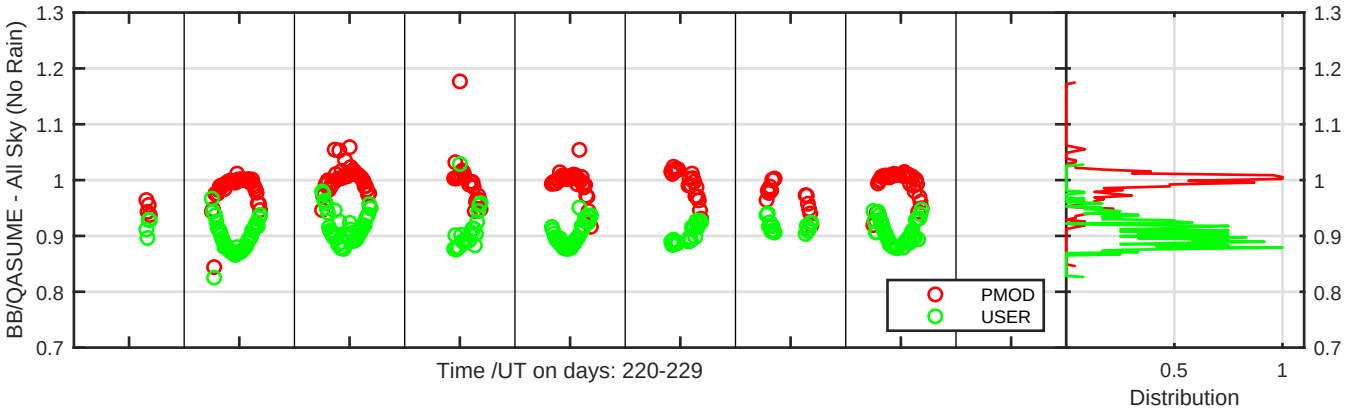

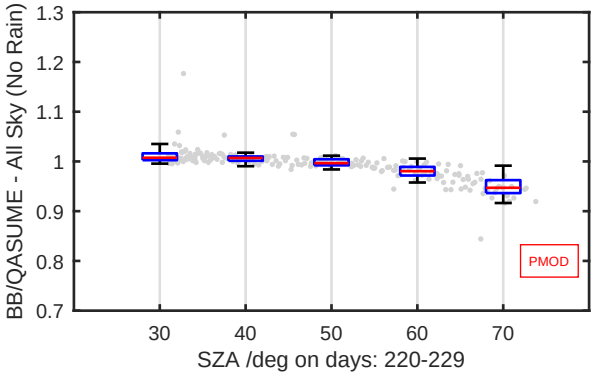

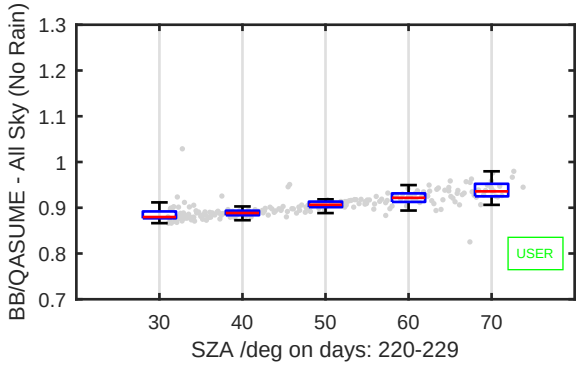

Calibration Results of SUV-A210194 (UVA)

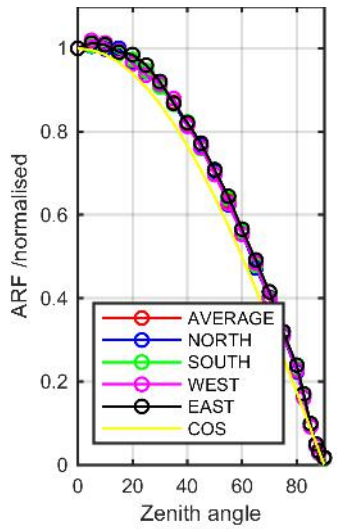

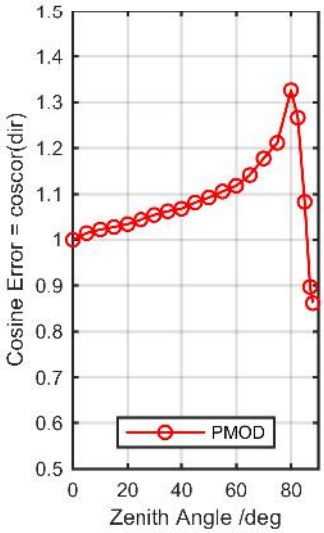

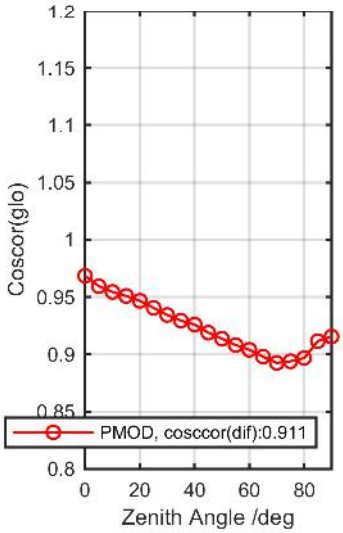

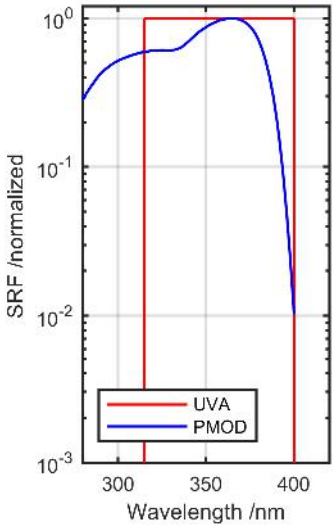

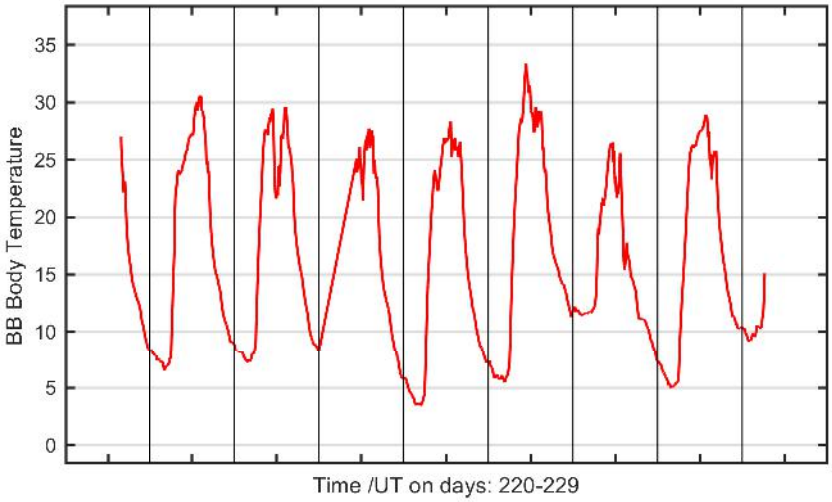

Calibration Matrix fn; Model sdisortREFms2009; f0=1.4953

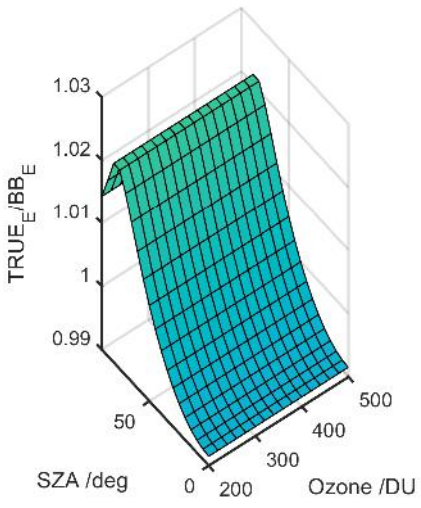

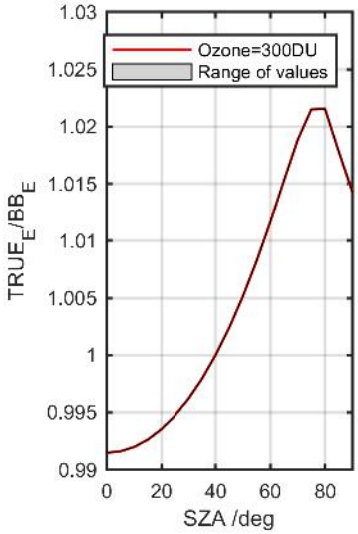

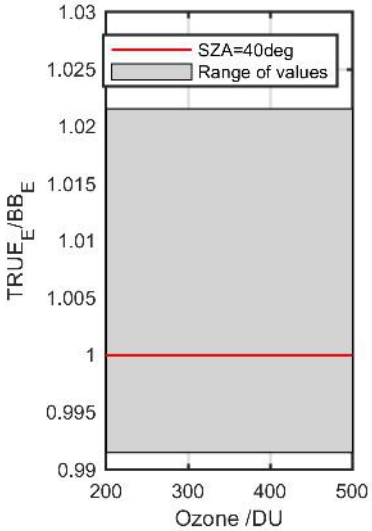

Calibration Results of SUV-A210194 (UVA)

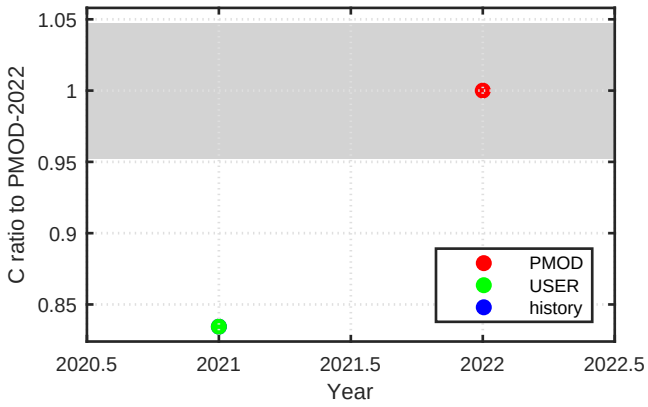

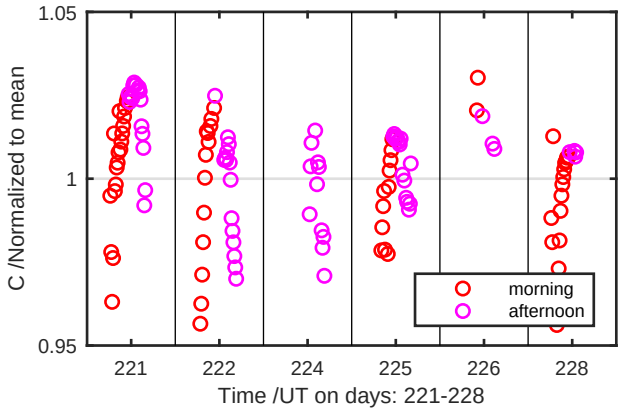

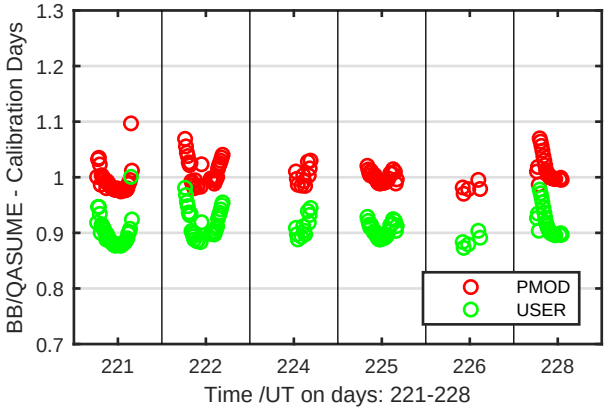

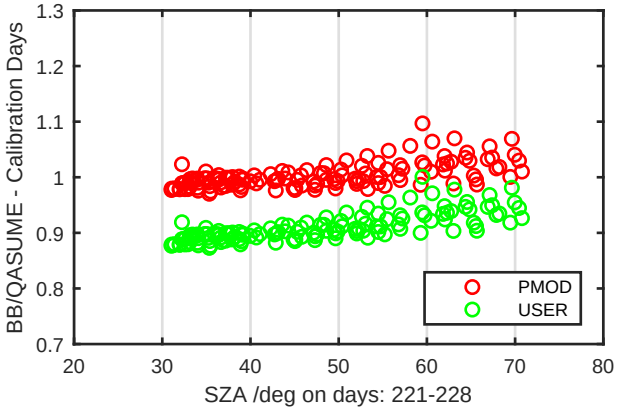

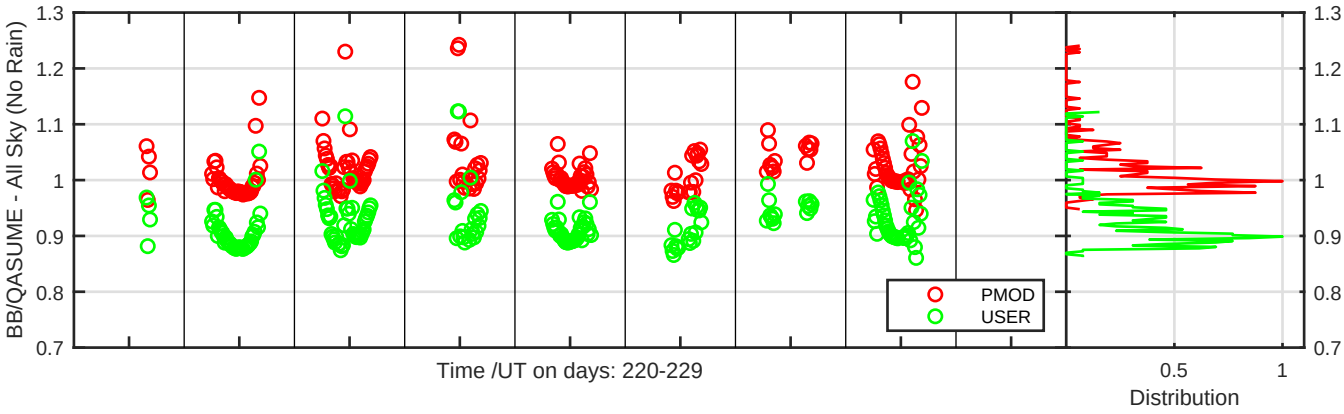

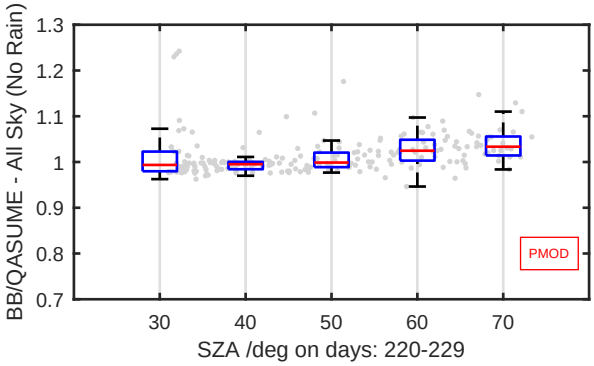

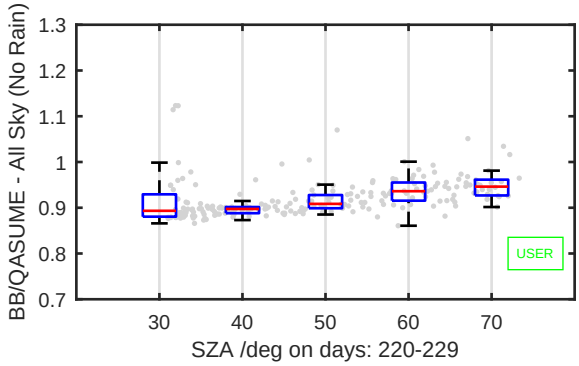

Calibration Results of SL1453 (UVE)

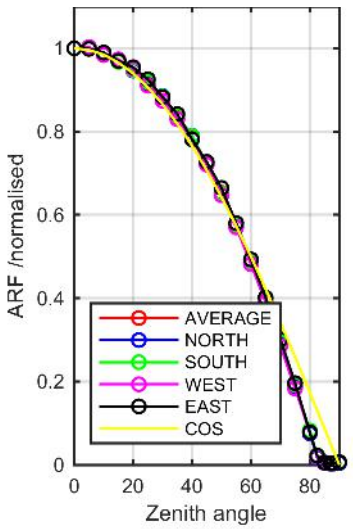

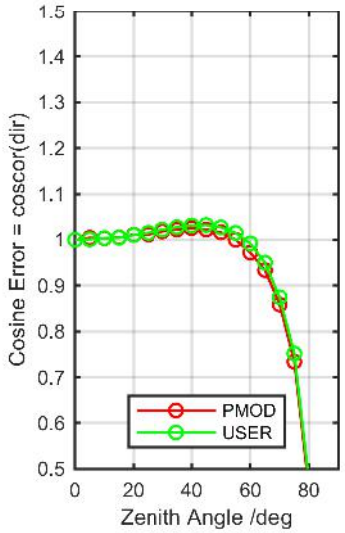

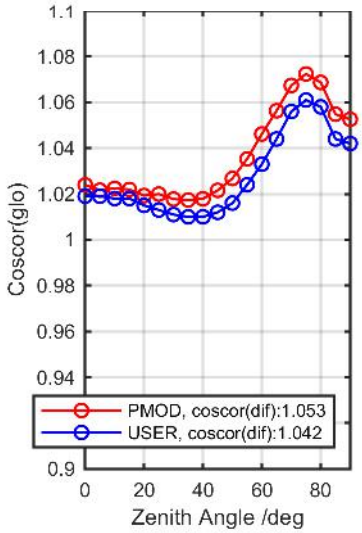

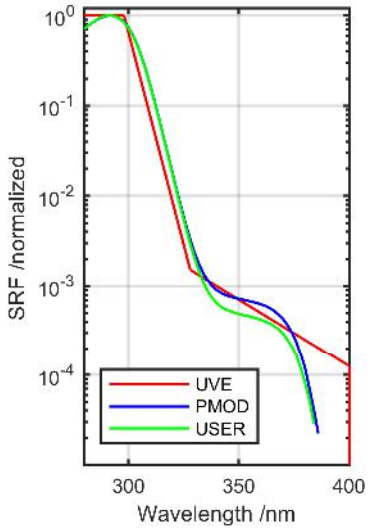

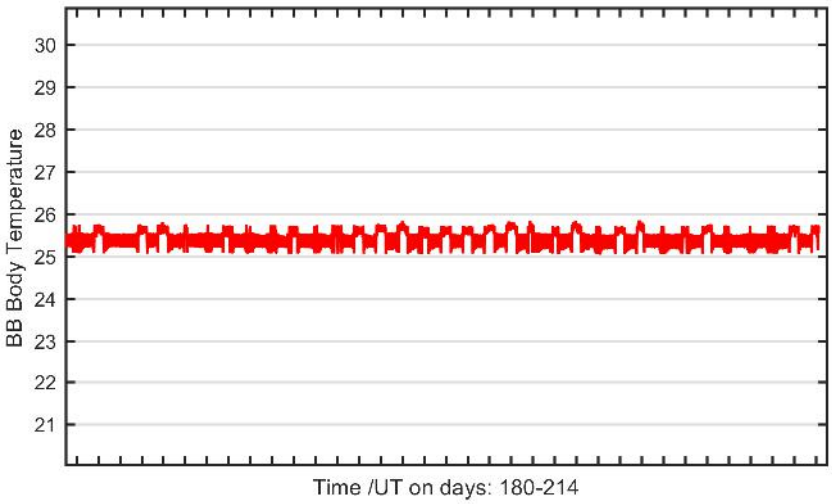

Calibration Matrix fn; Model sdisortREFms2009; f0=0.5406

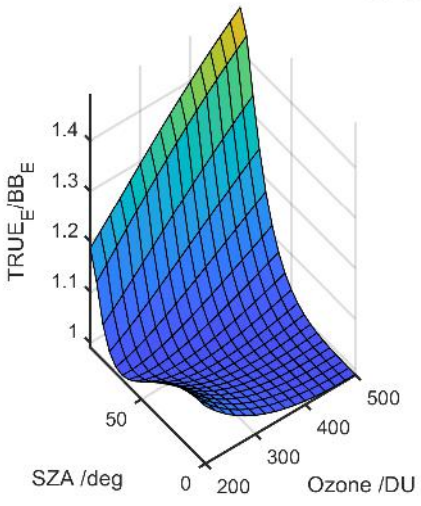

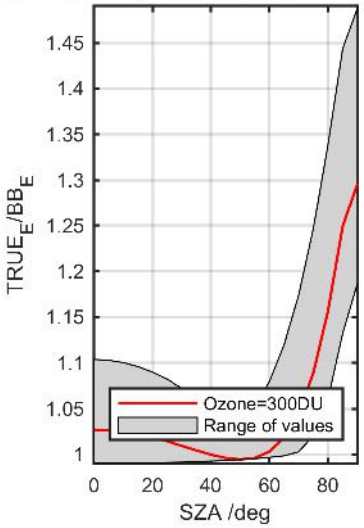

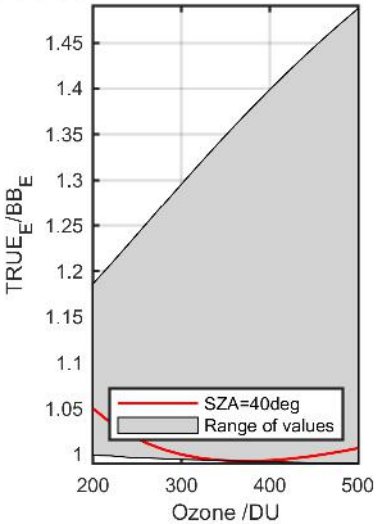

Calibration Results of SL1453 (UVE)

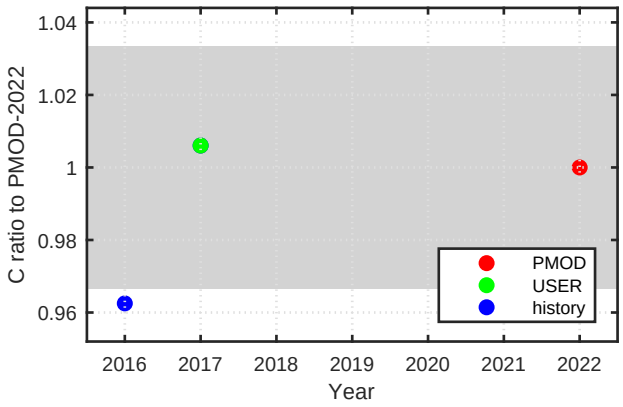

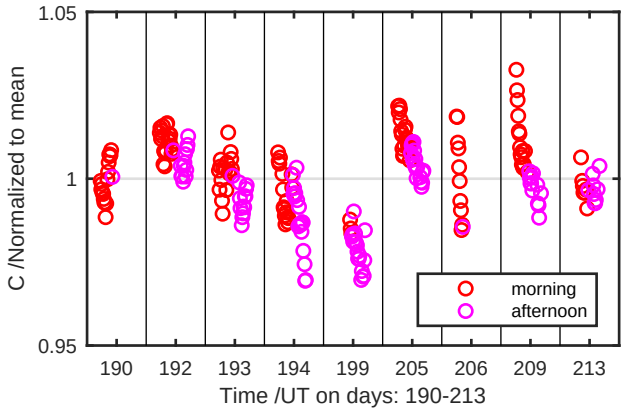

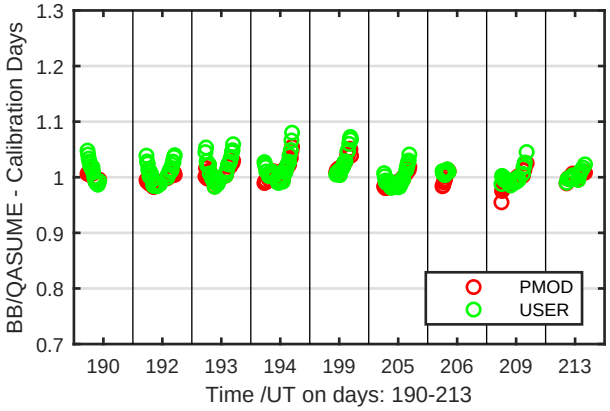

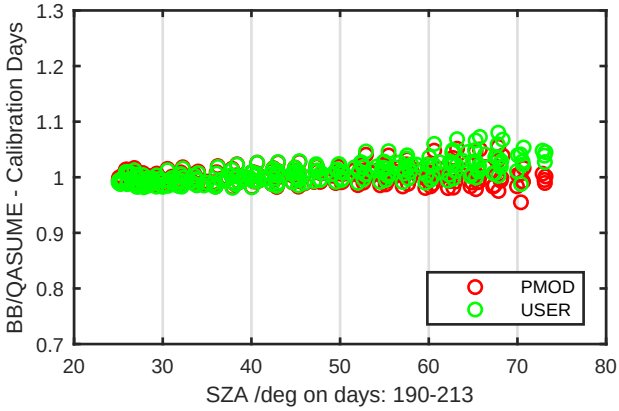

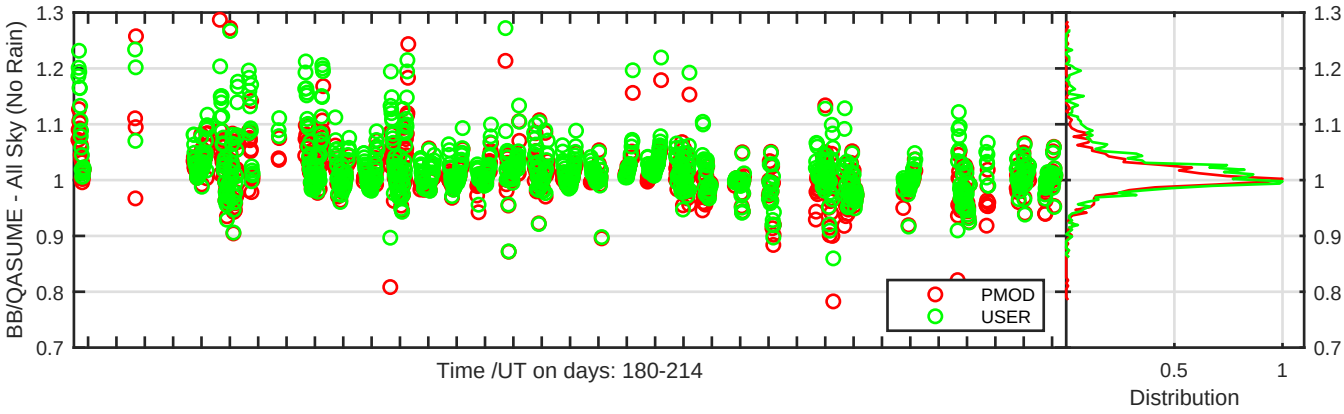

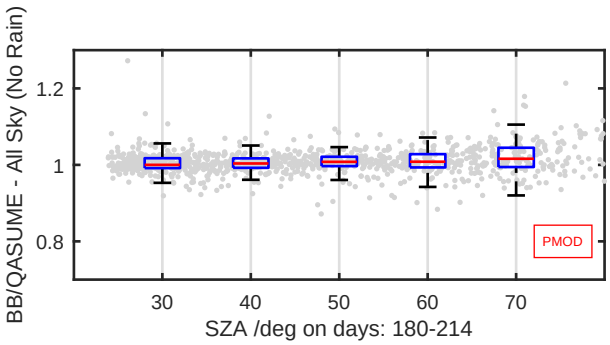

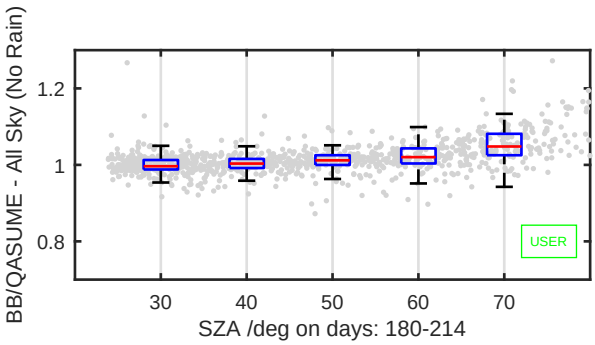

Calibration Results of SL1492 (UVE)

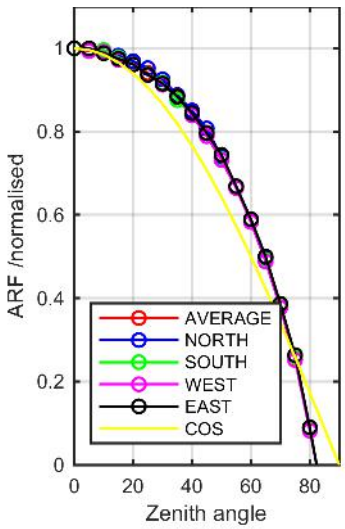

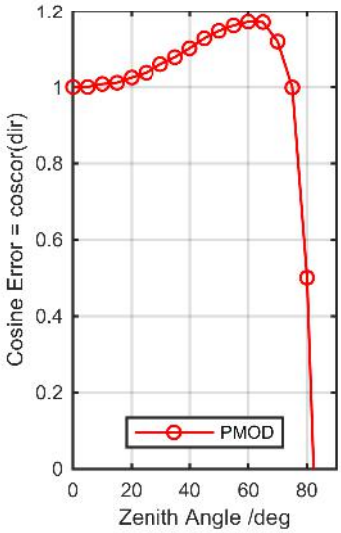

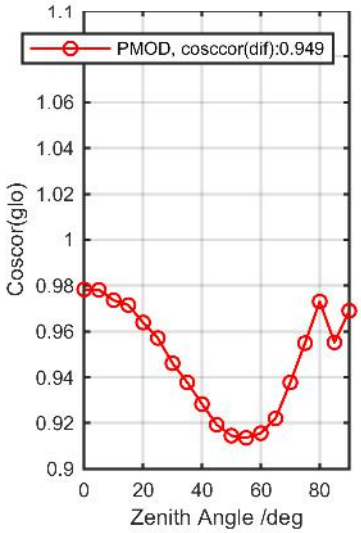

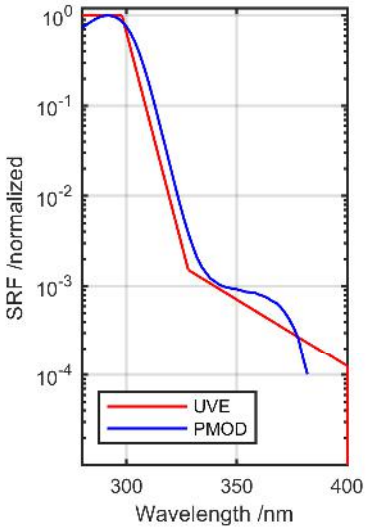

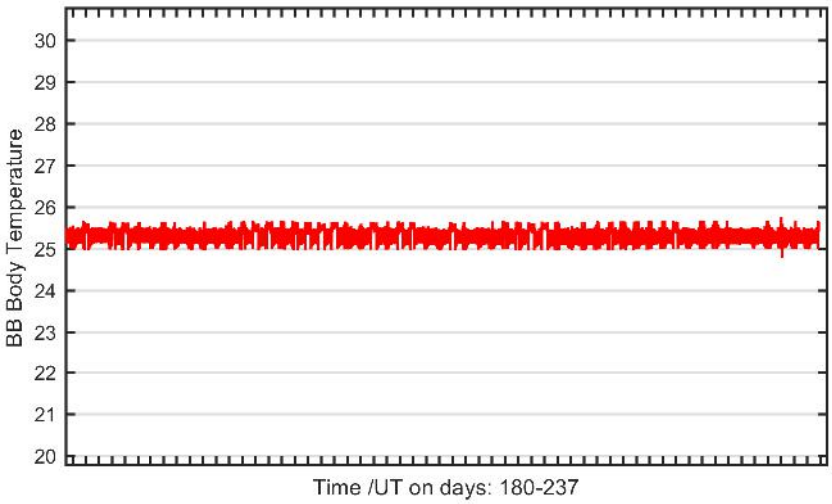

Calibration Matrix fn; Model sdisortPMODmsO3; f0=0.4849

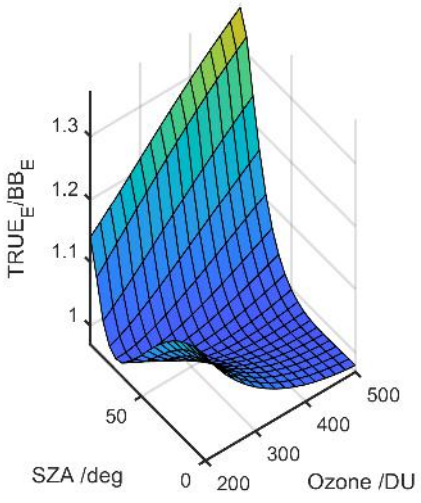

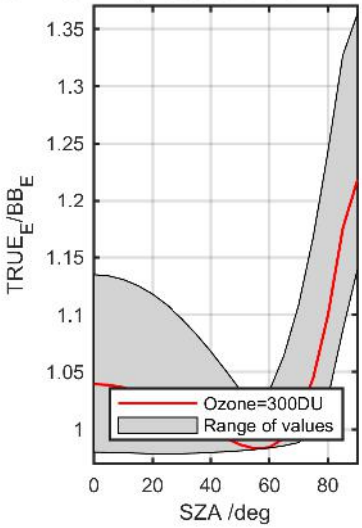

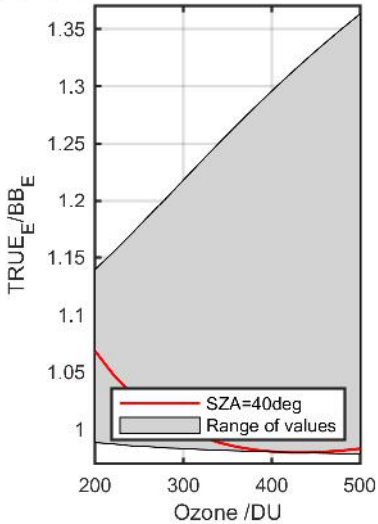

Calibration Results of SL1492 (UVE)

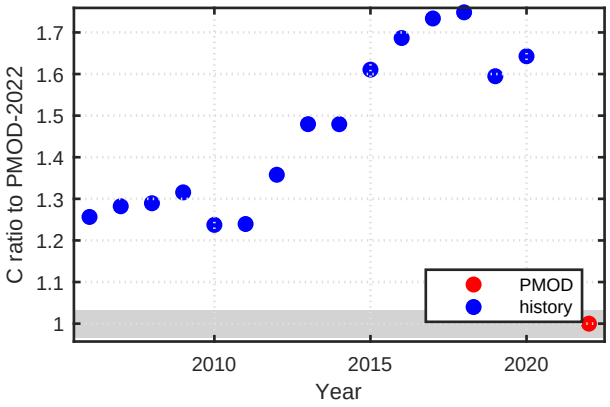

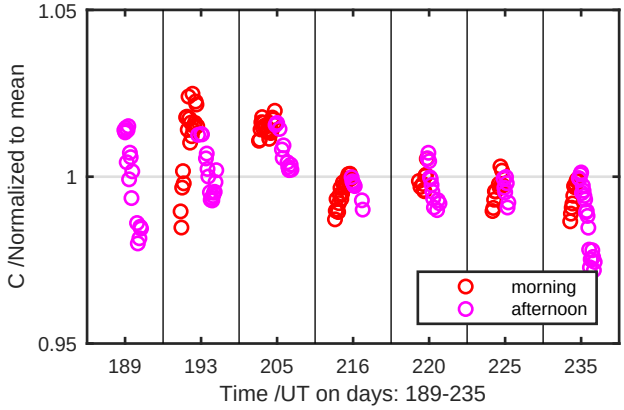

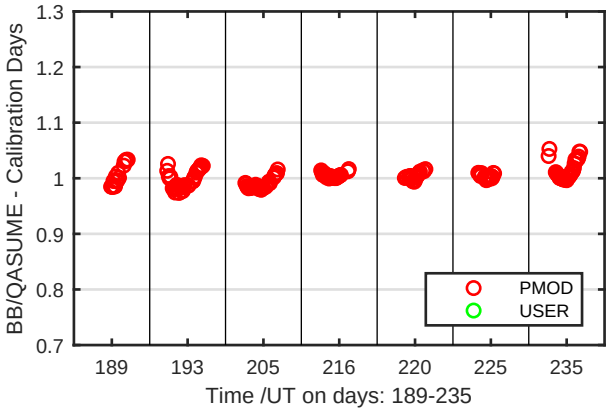

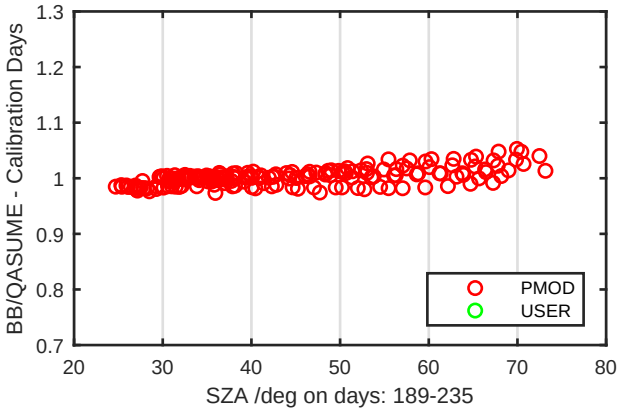

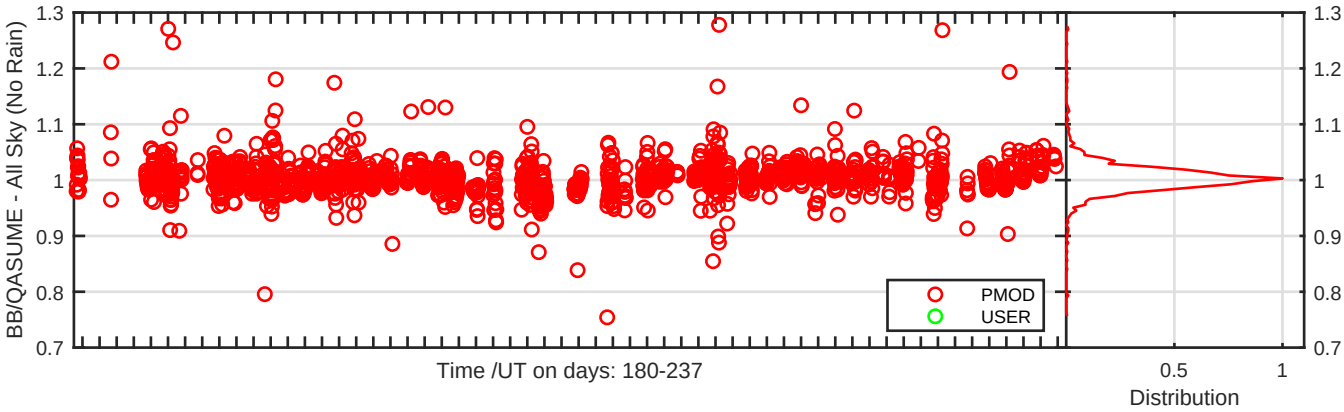

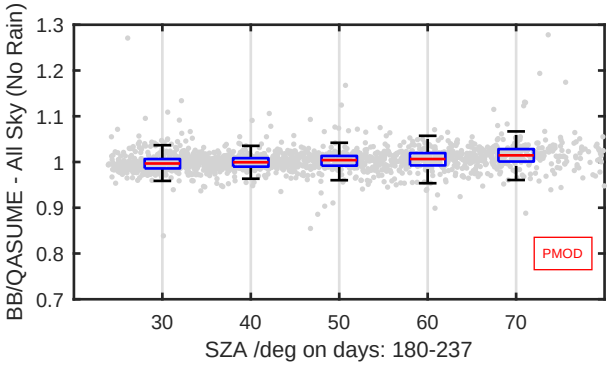

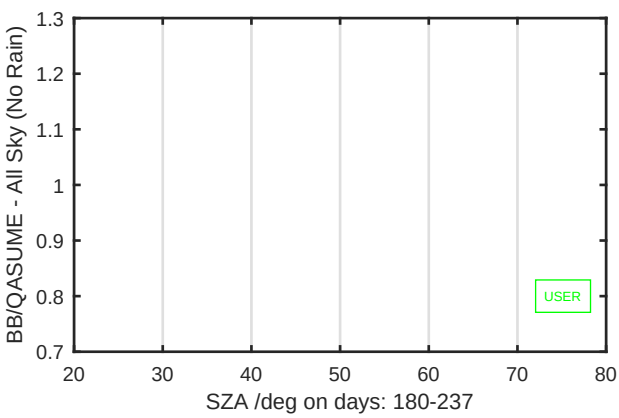

Calibration Results of SL1493 (UVE)

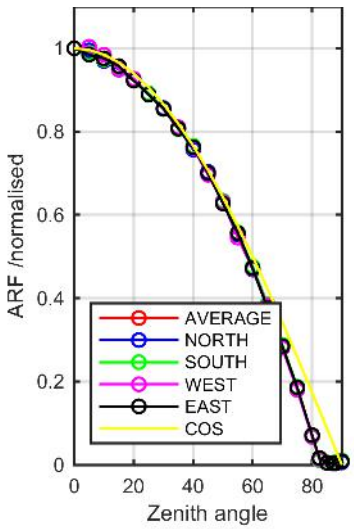

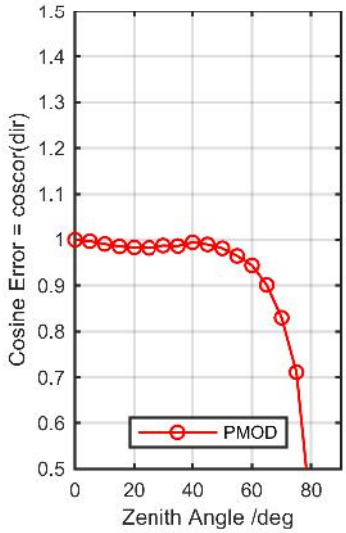

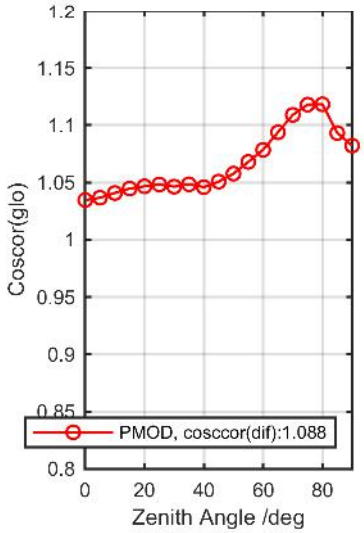

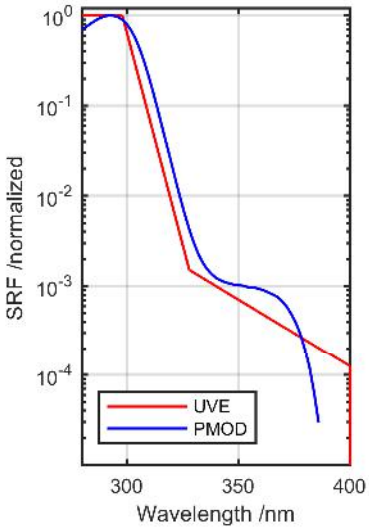

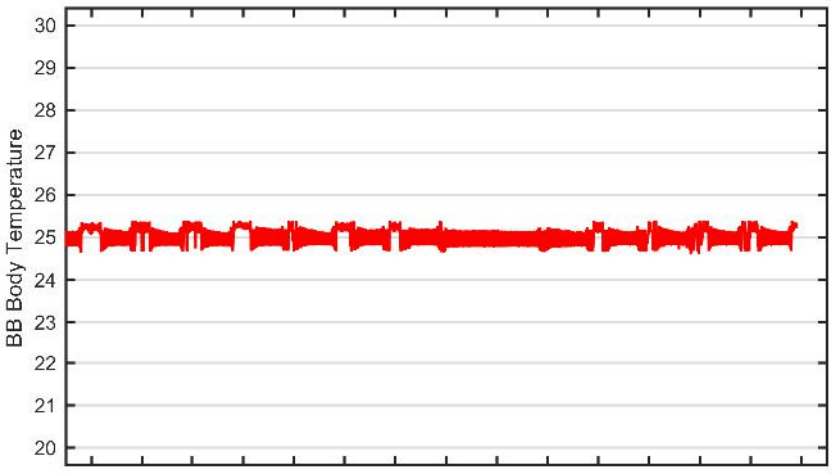

Calibration Matrix fn; Model sdisortPMODmsO3; f0=0.4390

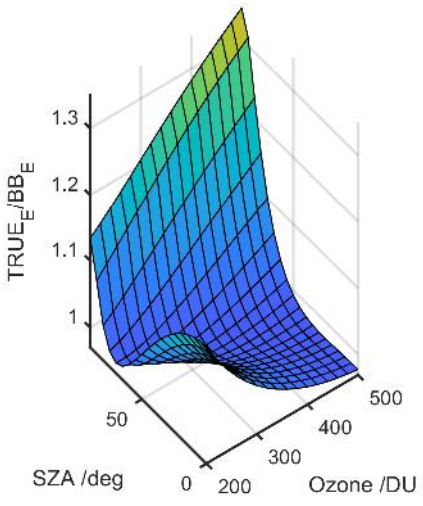

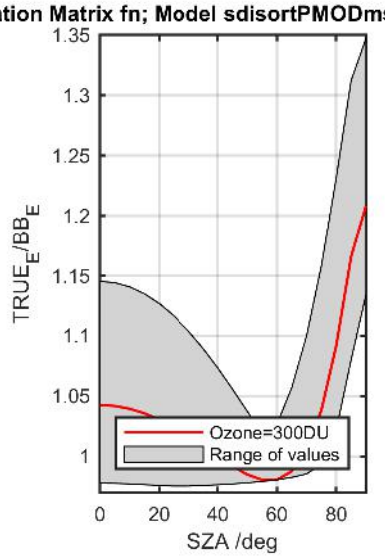

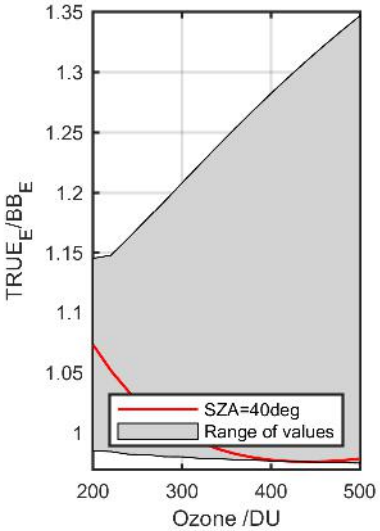

Calibration Results of SL1493 (UVE)

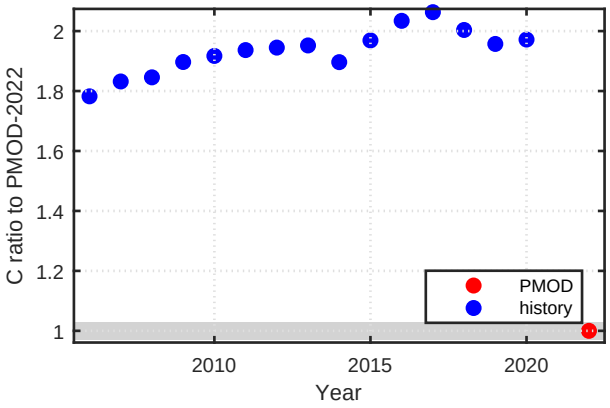

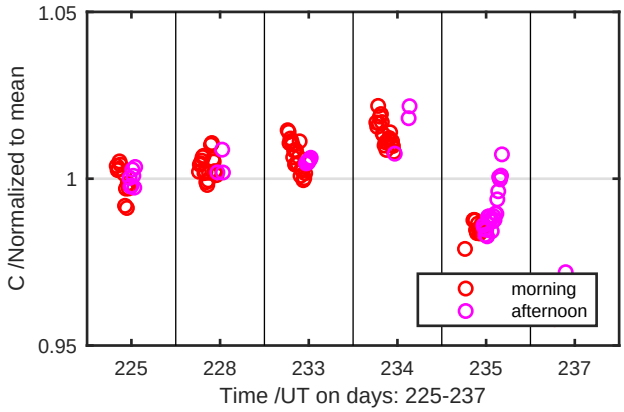

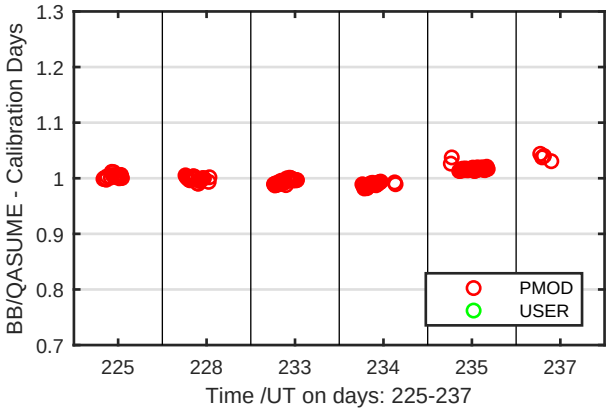

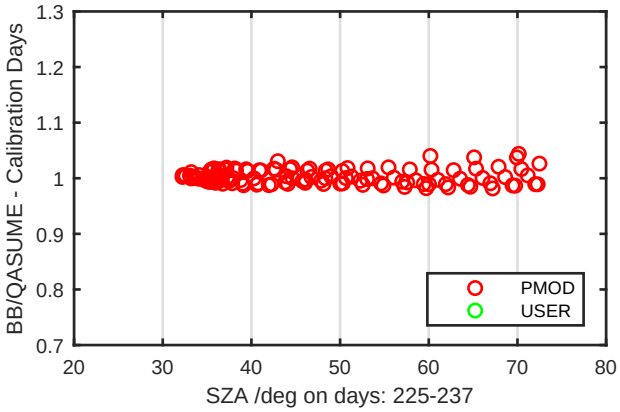

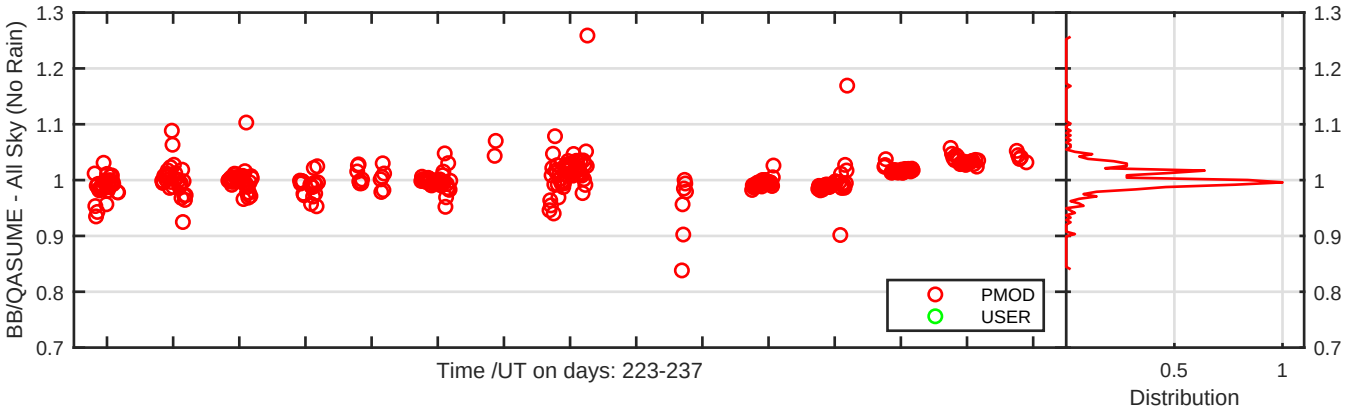

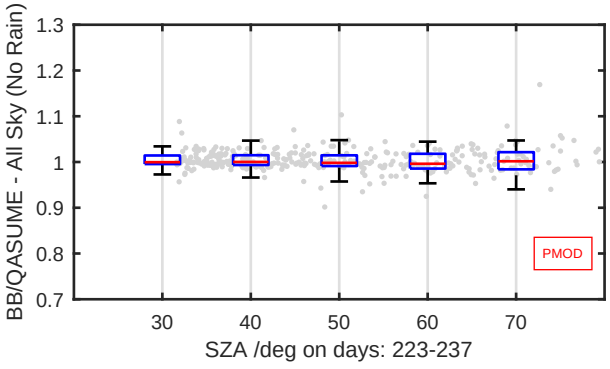

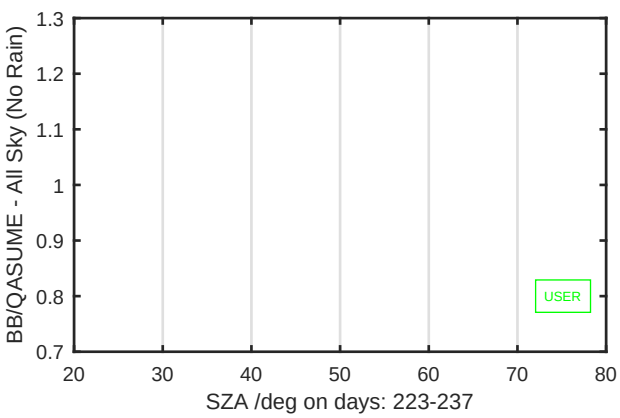

Calibration Results of SL1905 (UVE)

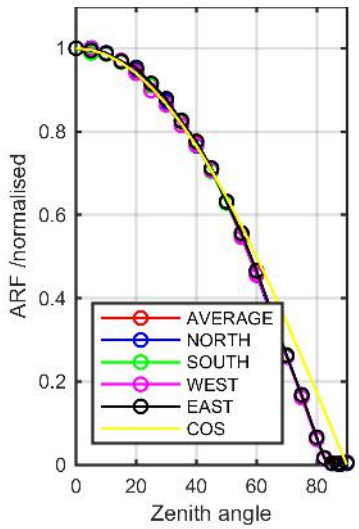

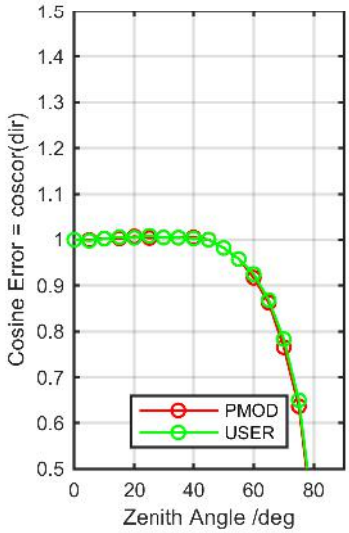

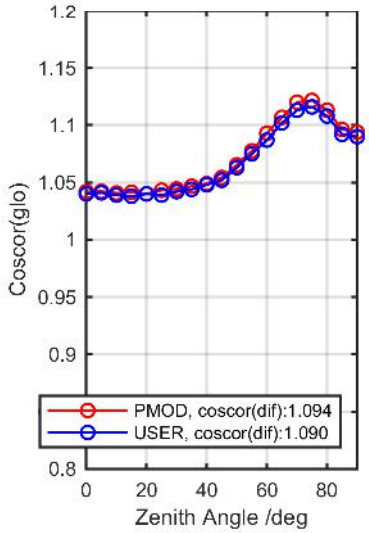

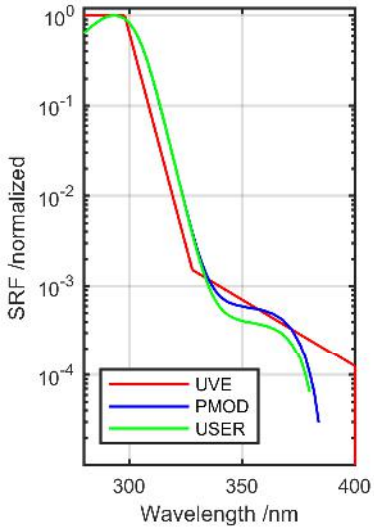

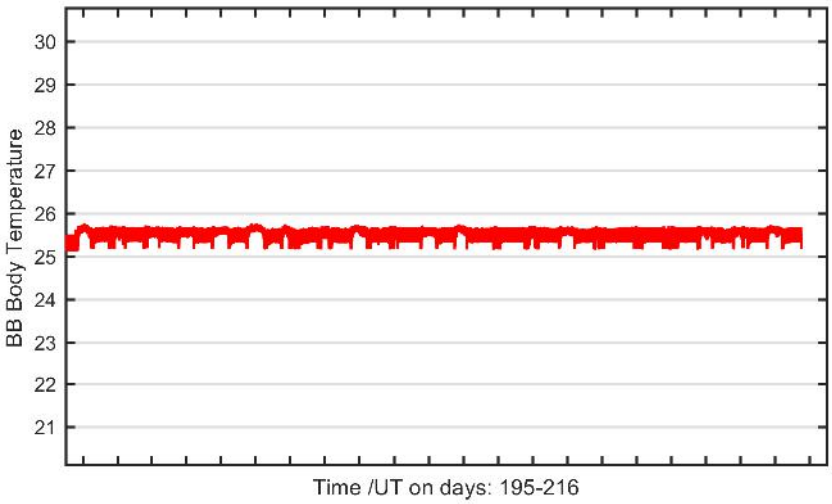

Calibration Matrix fn; Model sdisortREFms2009; f0=0.4310

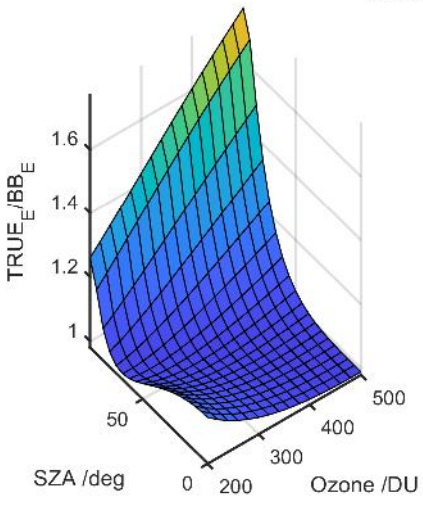

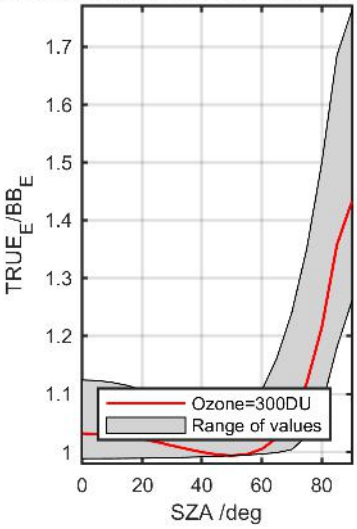

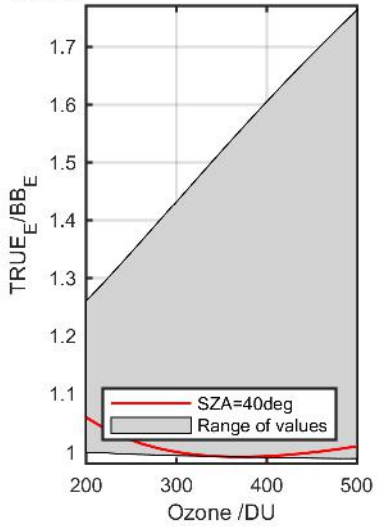

Calibration Results of SL1905 (UVE)

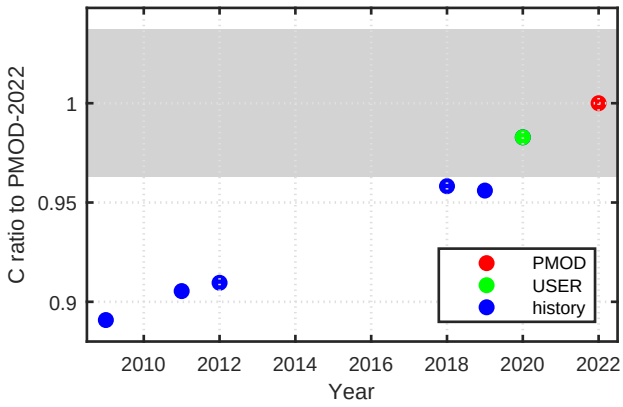

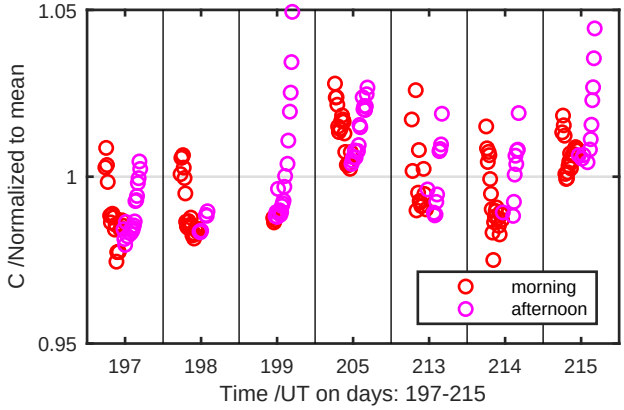

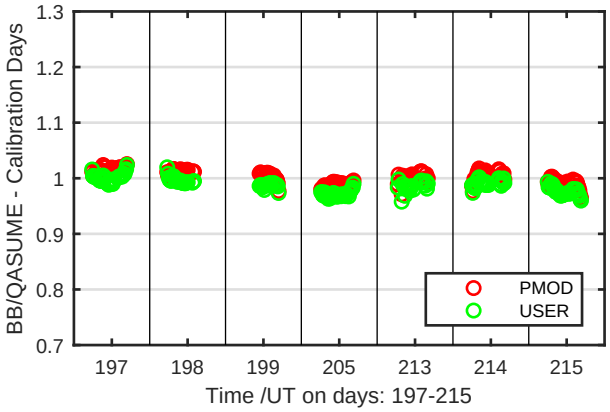

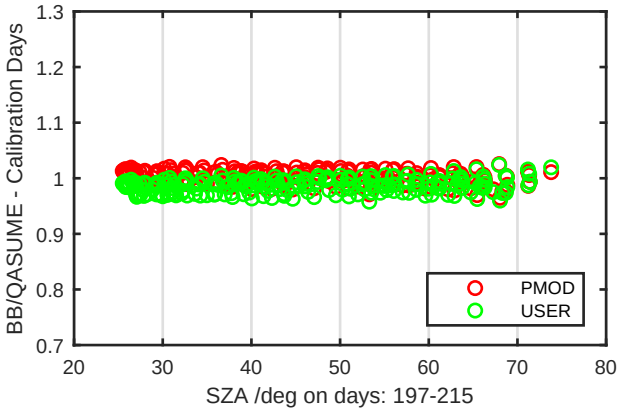

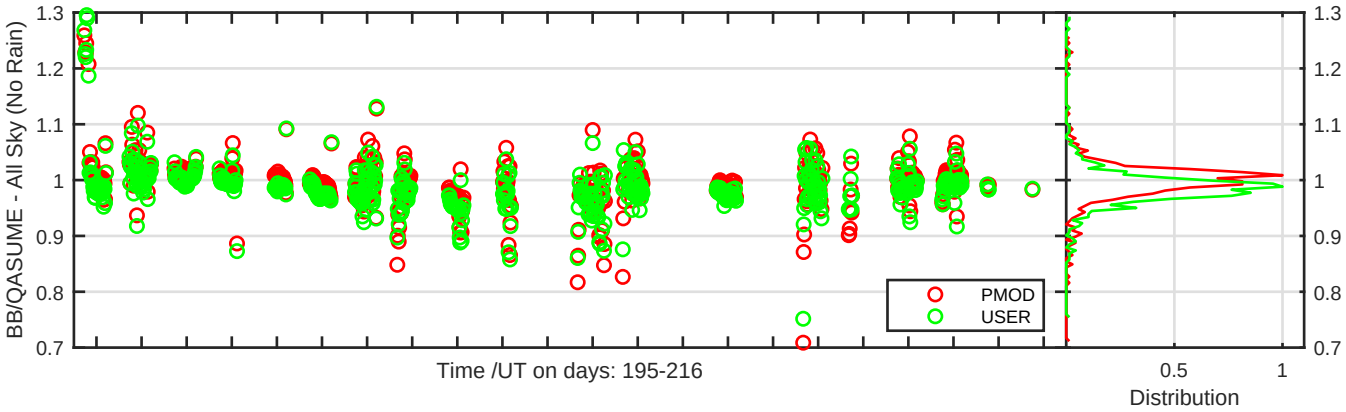

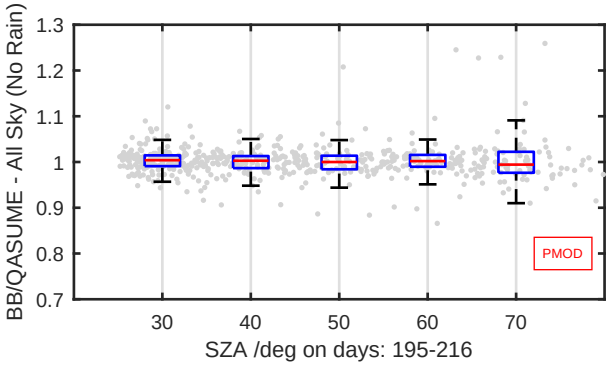

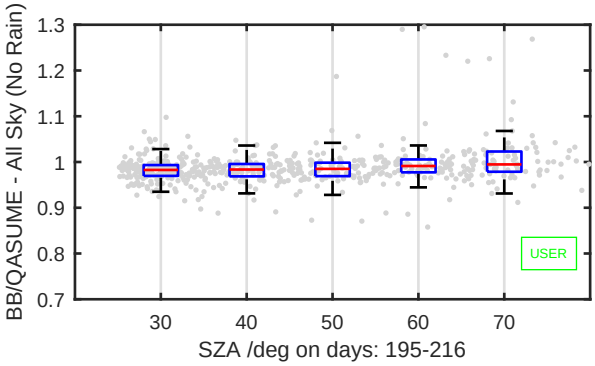

Calibration Results of SL2872 (UVE)

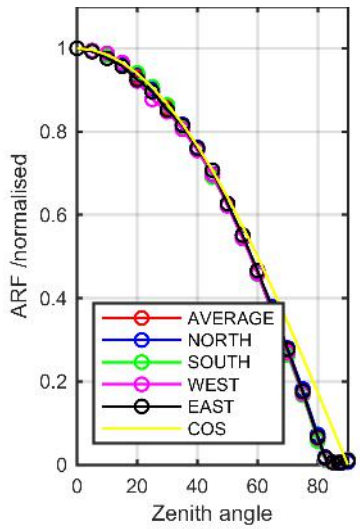

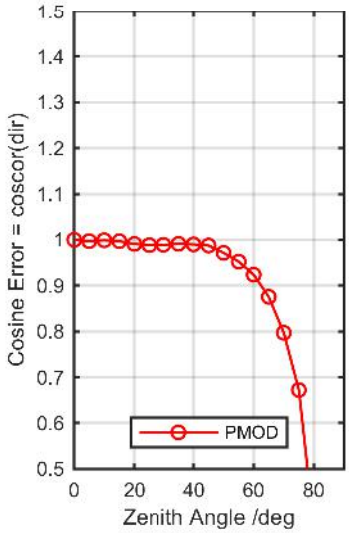

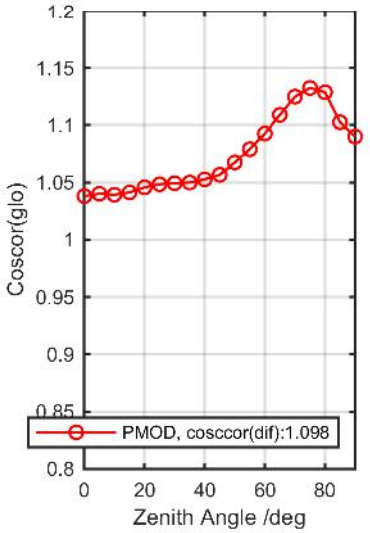

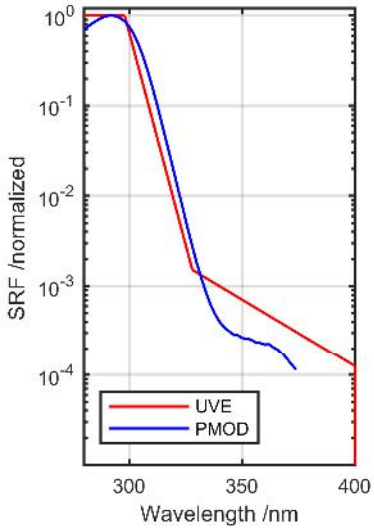

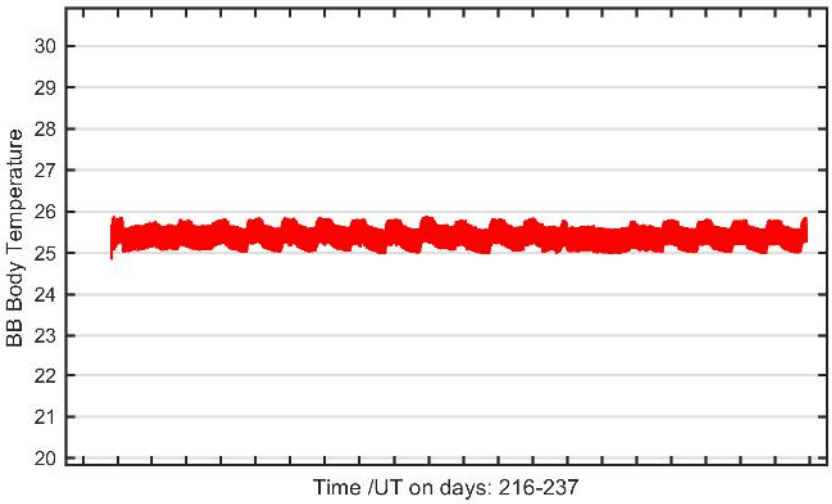

Calibration Matrix fn; Model sdisortPMODmsO3; f0=0.5516

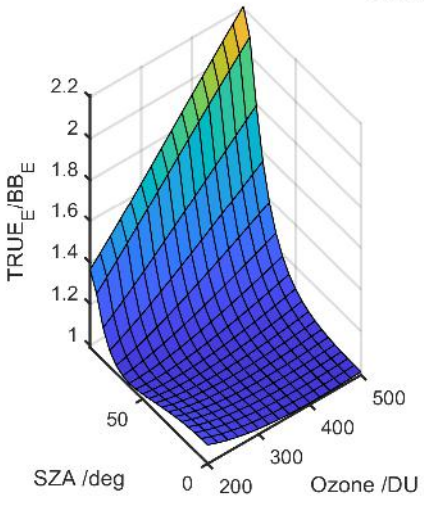

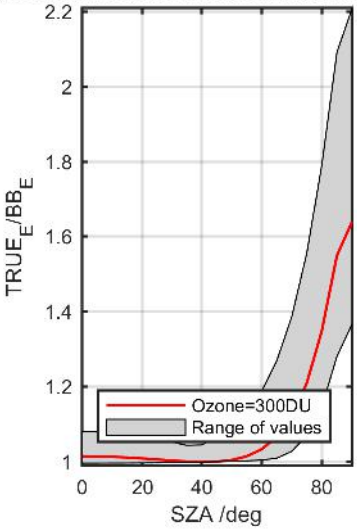

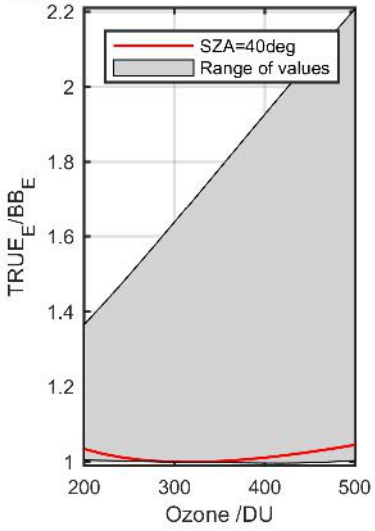

Calibration Results of SL2872 (UVE)

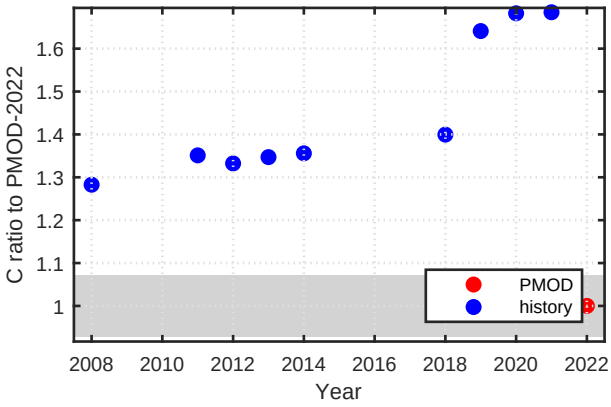

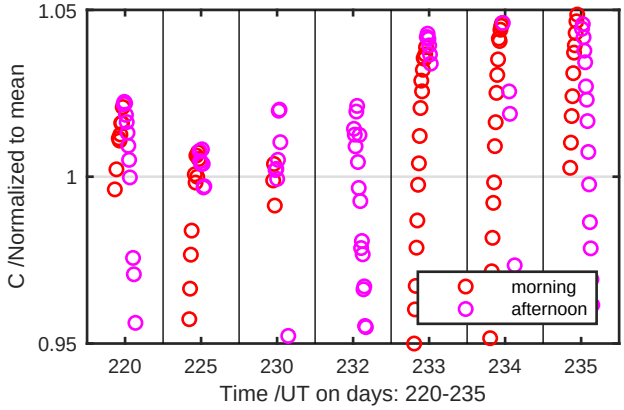

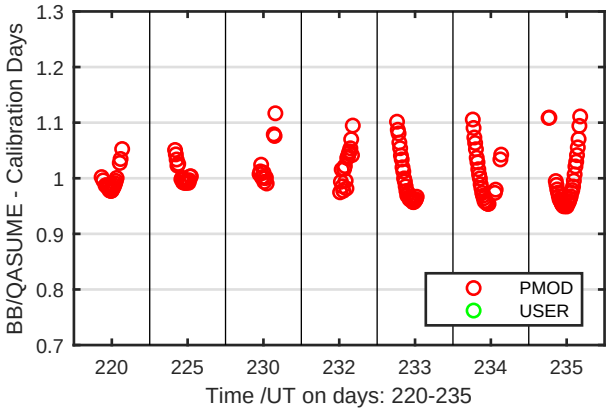

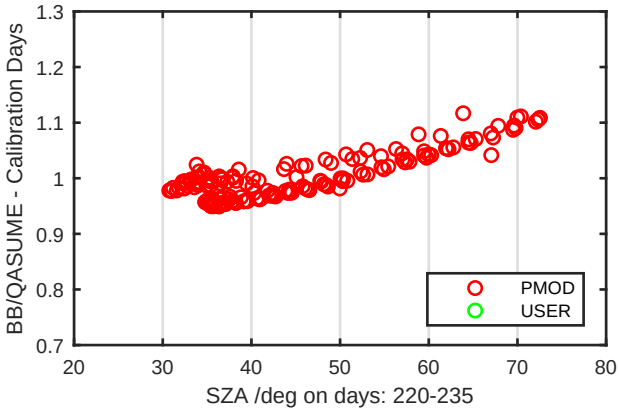

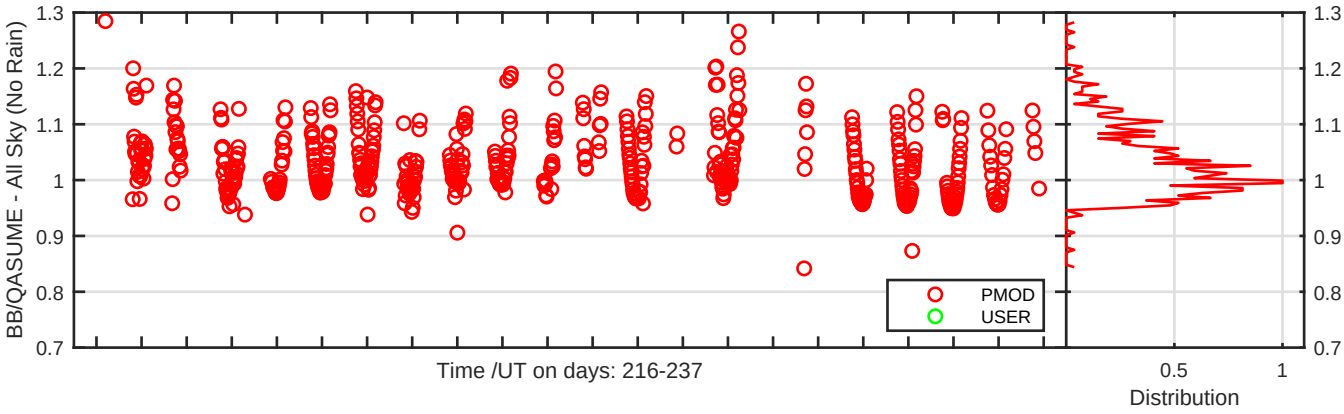

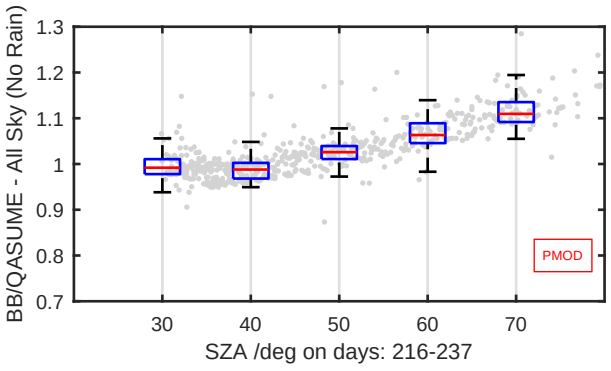

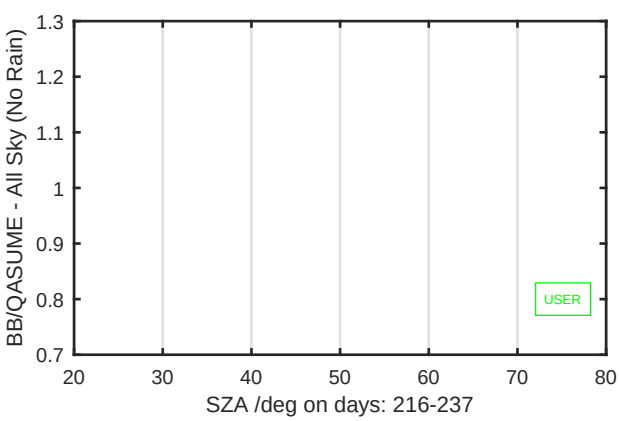

Calibration Results of SL3860 (UVE)

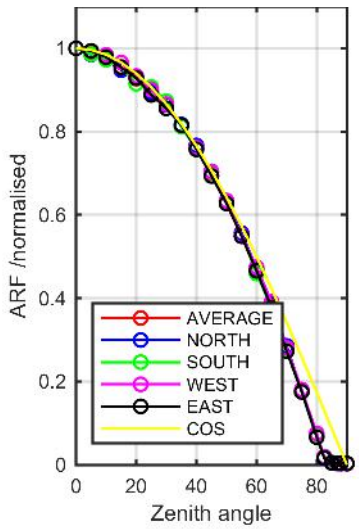

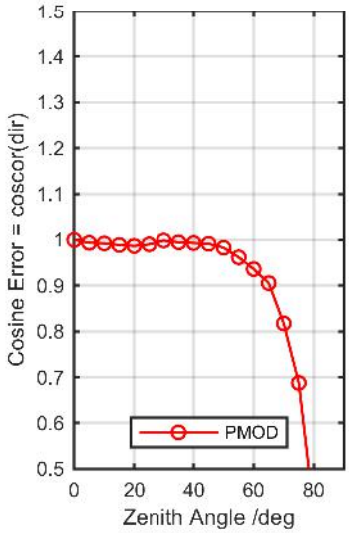

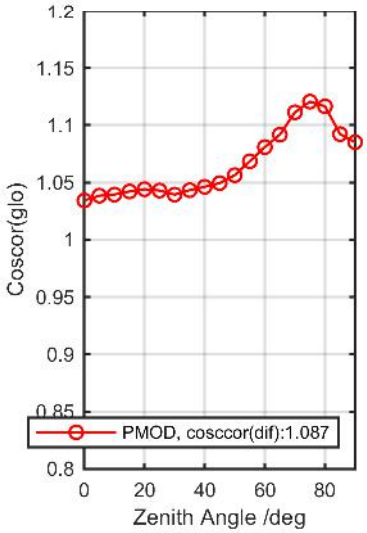

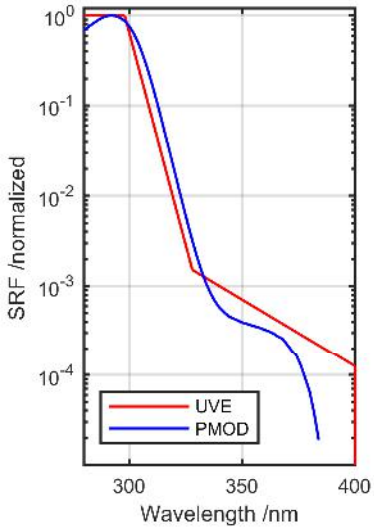

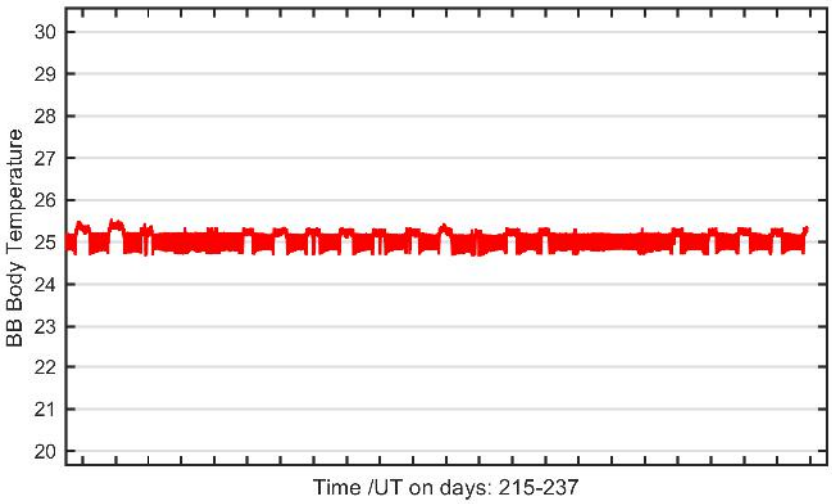

Calibration Matrix fn; Model sdisortPMODmsO3; f0=0.5199

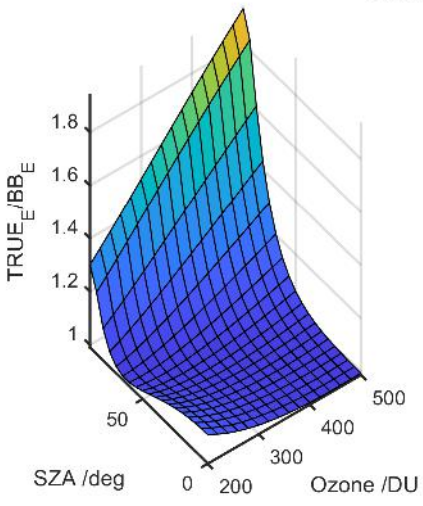

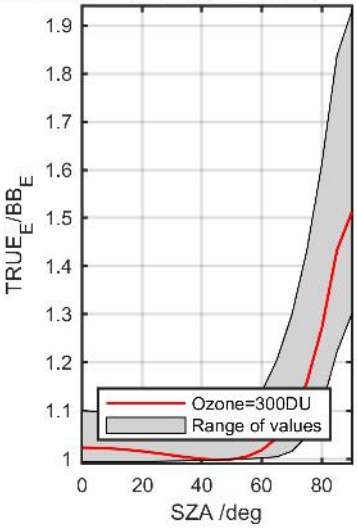

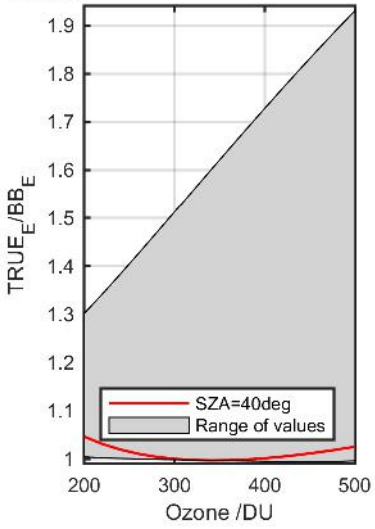

Calibration Results of SL3860 (UVE)

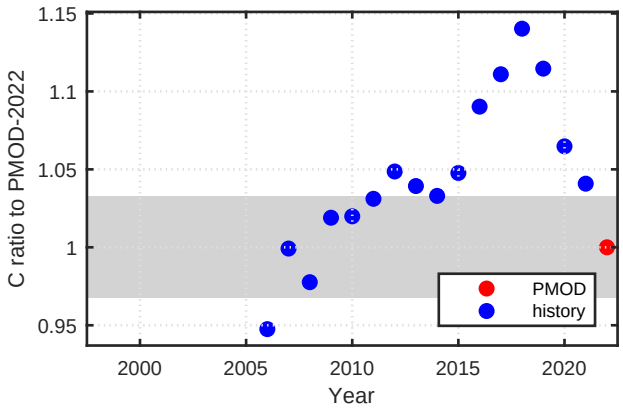

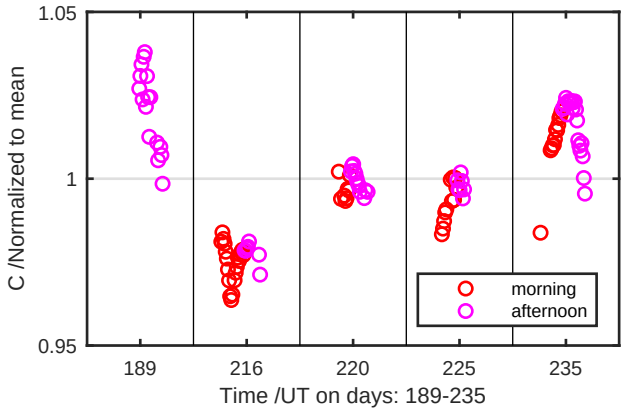

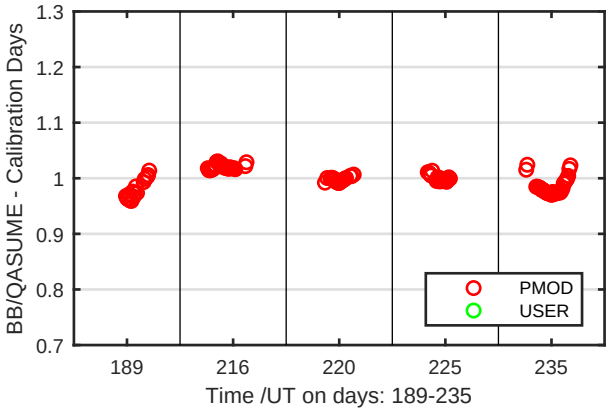

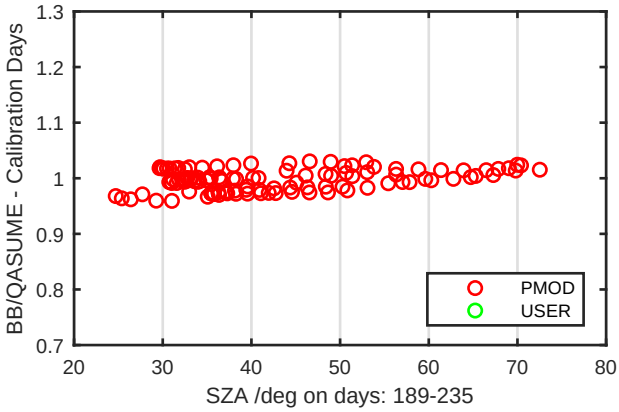

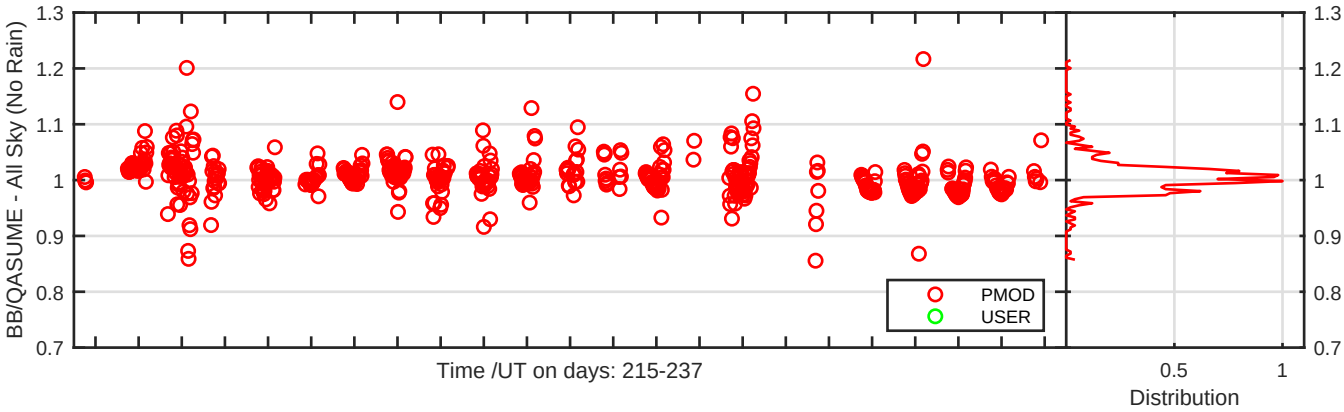

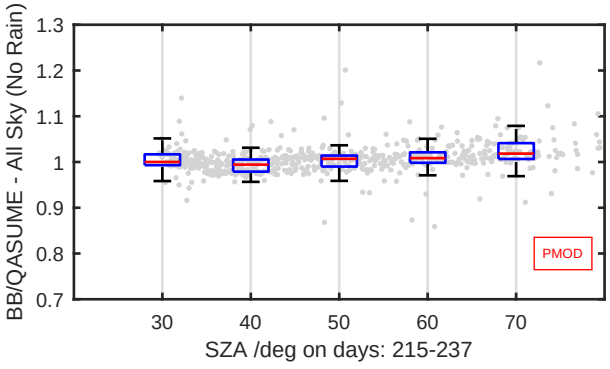

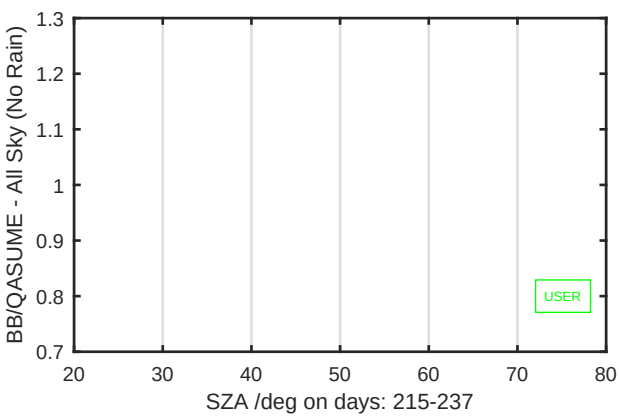

Calibration Results of SL3862 (UVE)

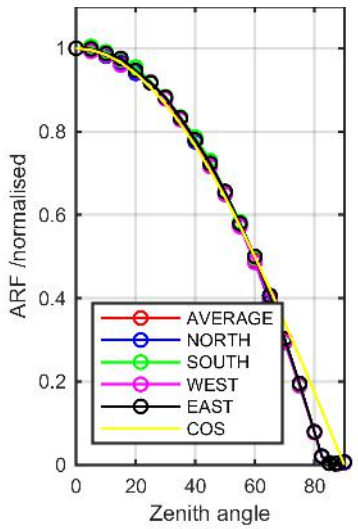

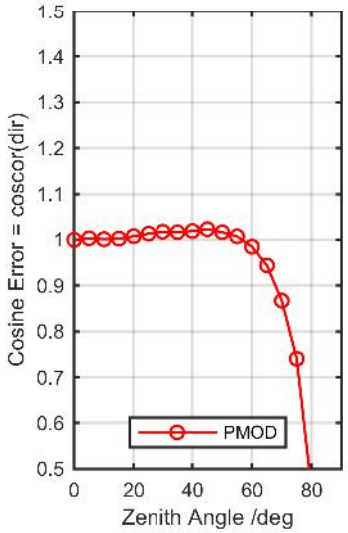

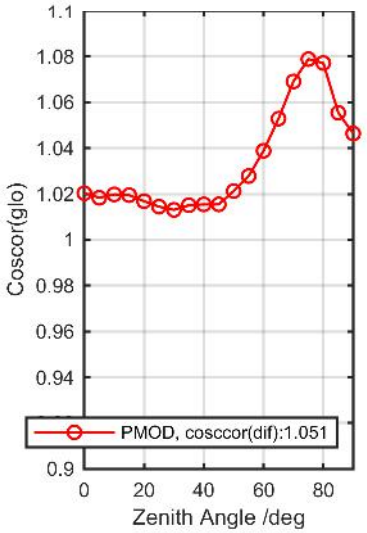

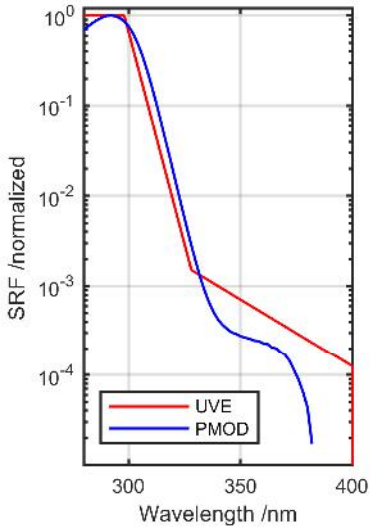

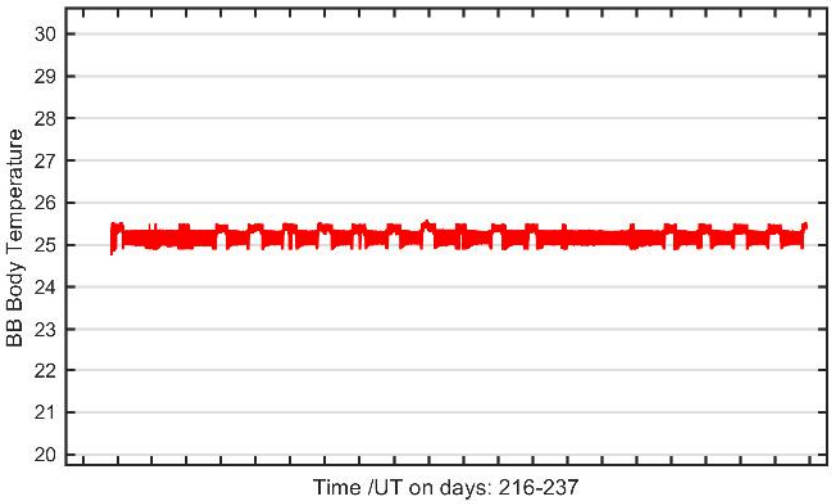

Calibration Matrix fn; Model sdisortPMODmsO3; f0=0.5407

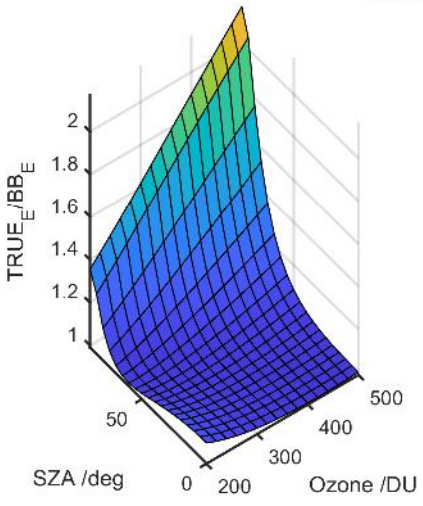

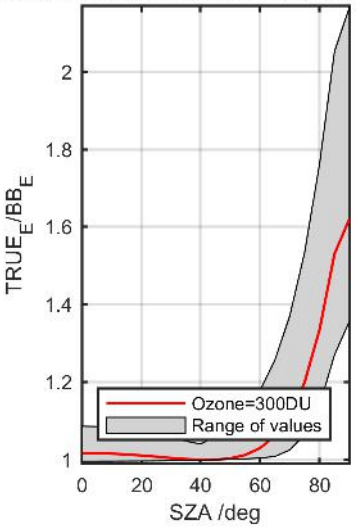

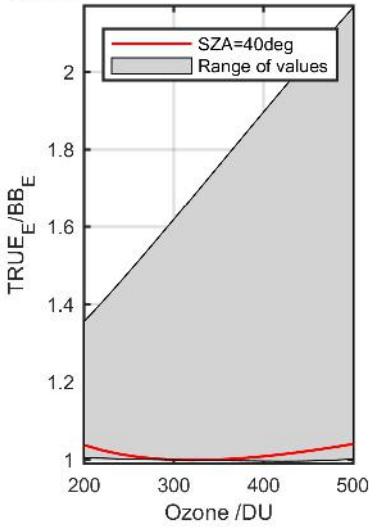

Calibration Results of SL3862 (UVE)

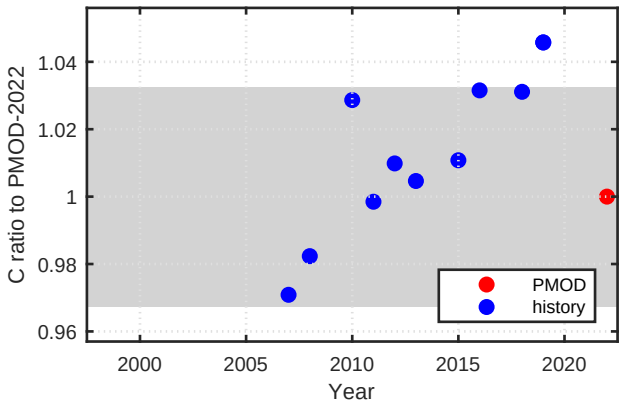

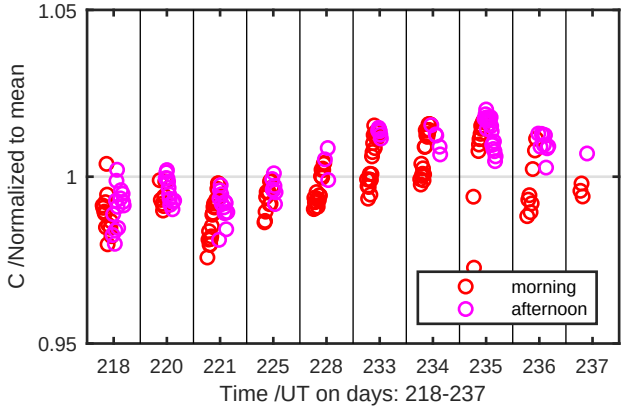

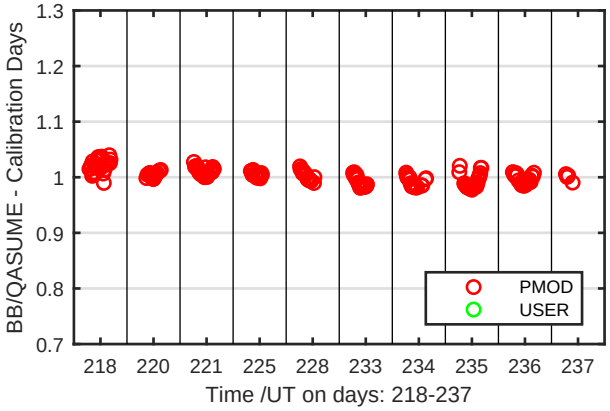

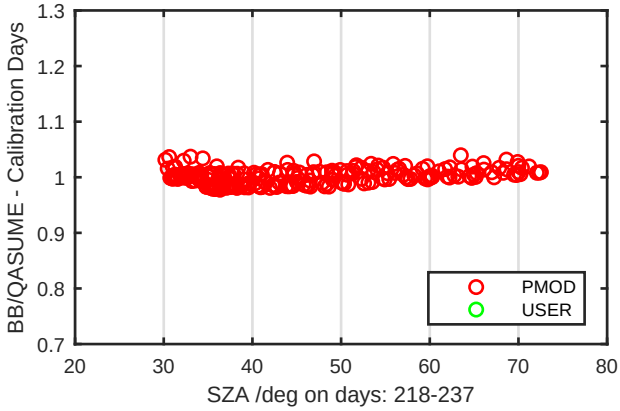

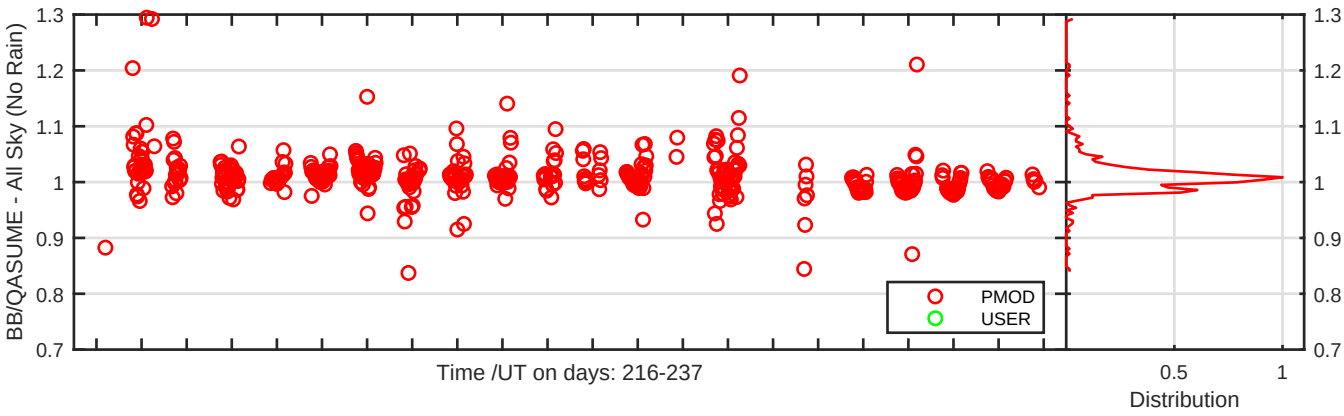

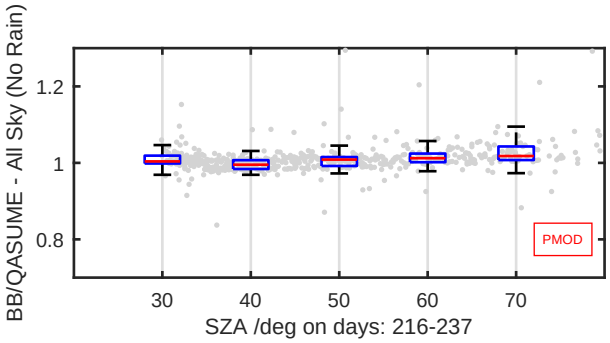

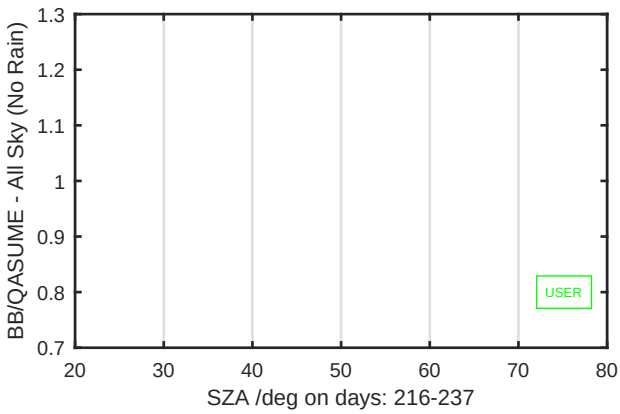

Calibration Results of SL3863 (UVE)

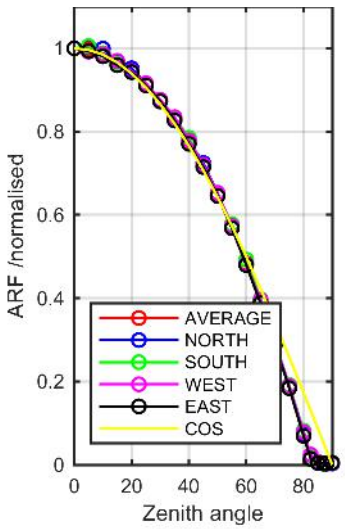

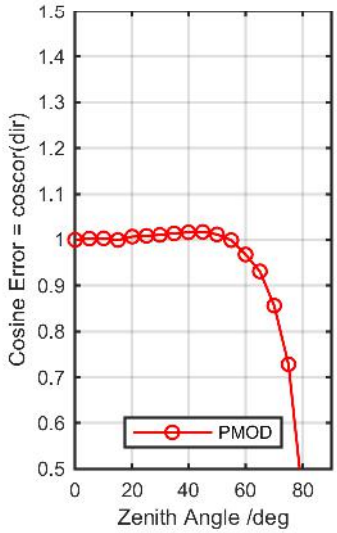

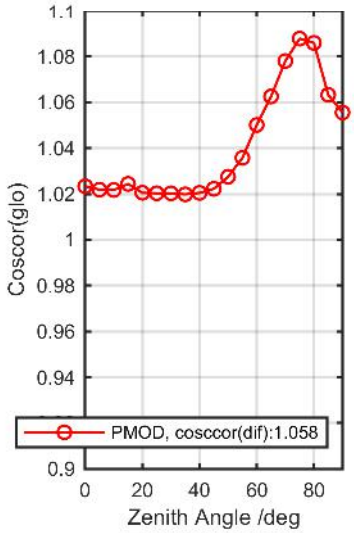

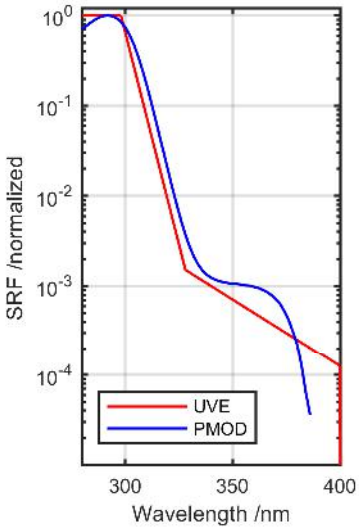

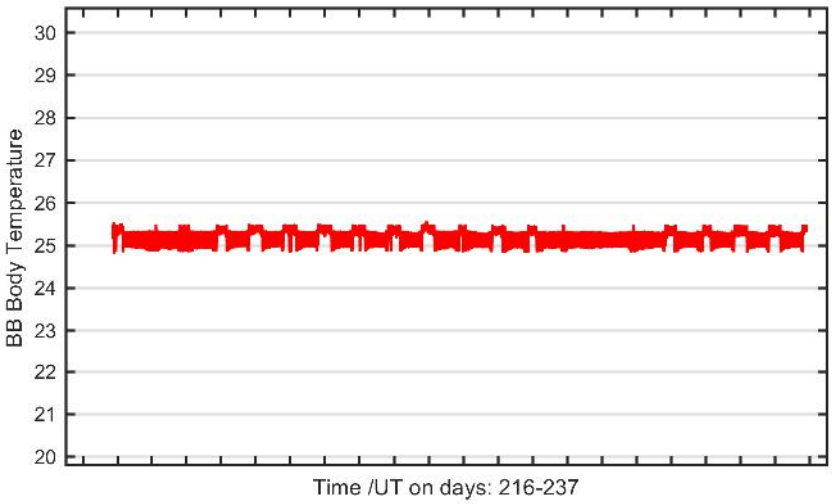

Calibration Matrix fn; Model sdisortPMODmsO3; f0=0.5120

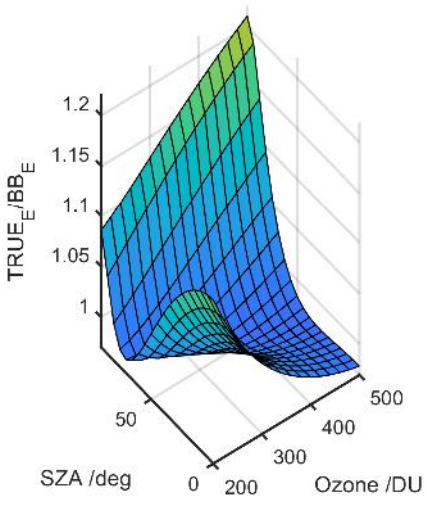

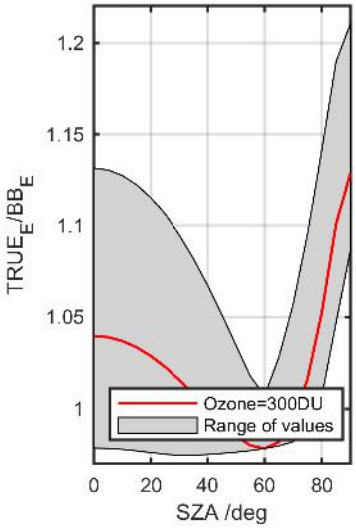

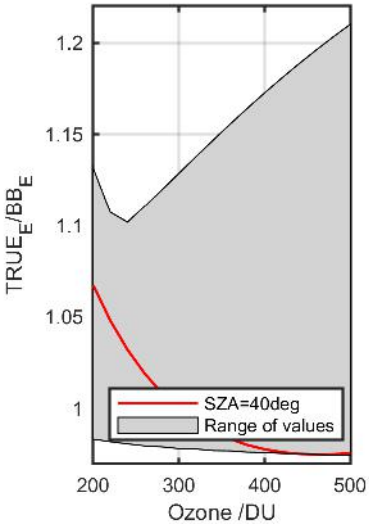

Calibration Results of SL3863 (UVE)

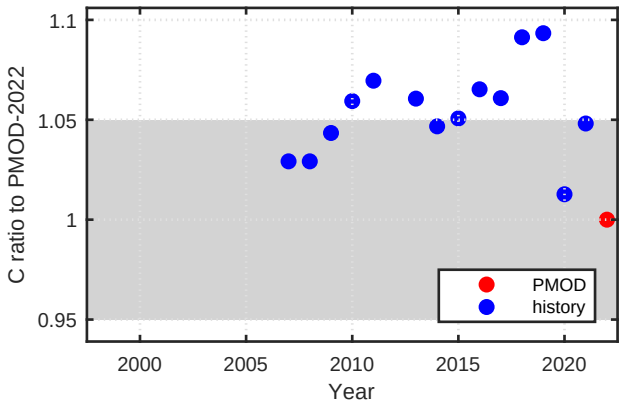

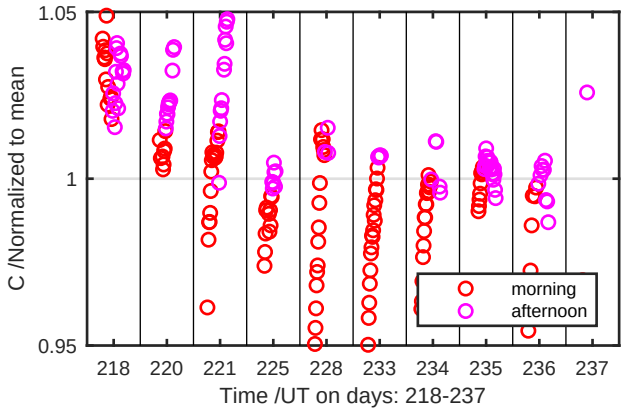

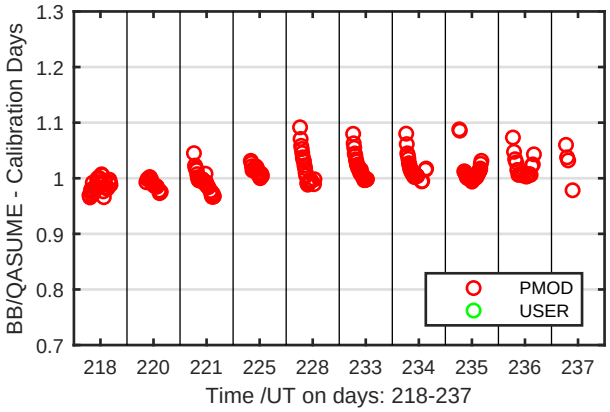

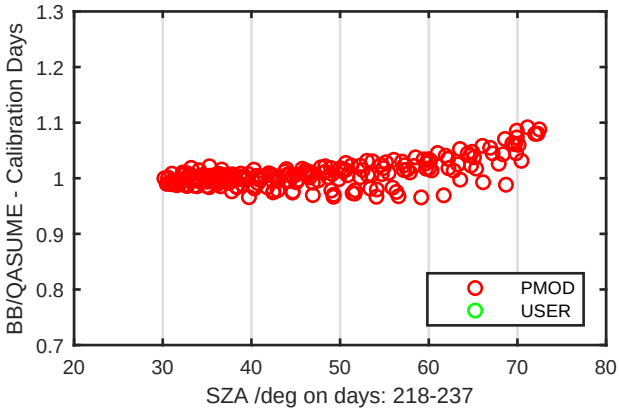

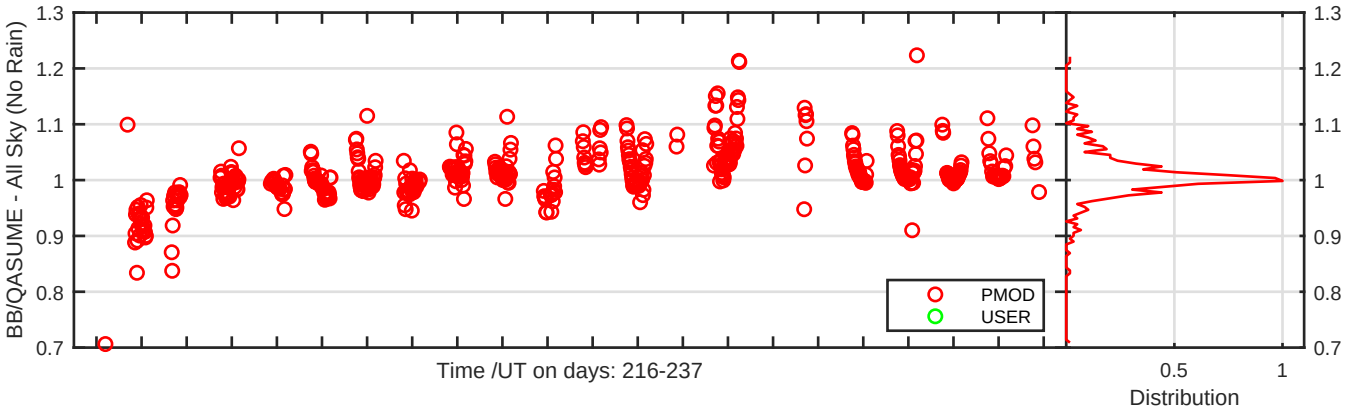

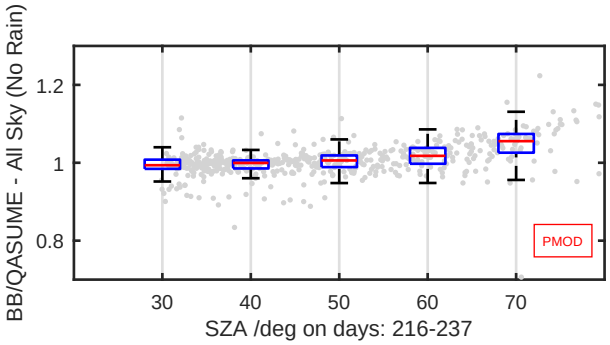

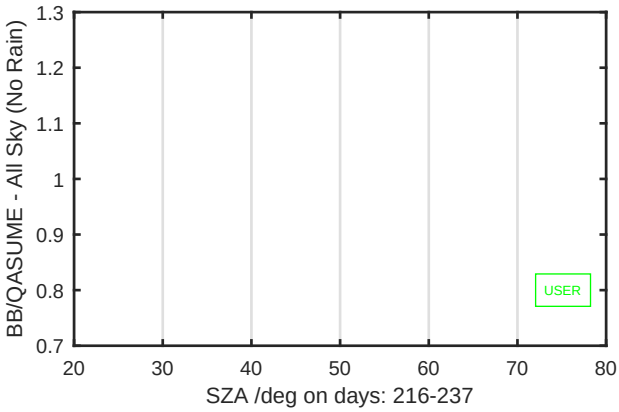

Calibration Results of SL3864 (UVE)

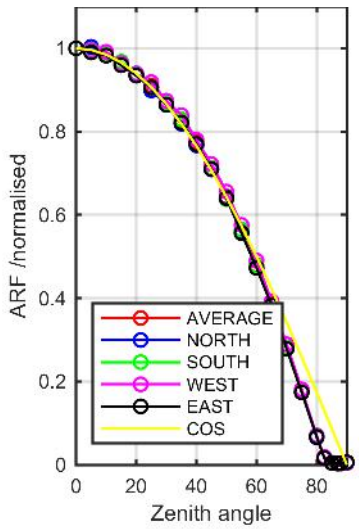

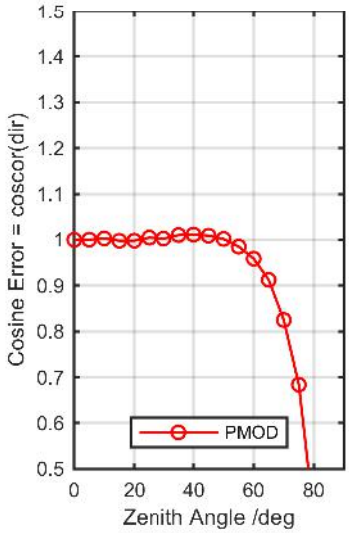

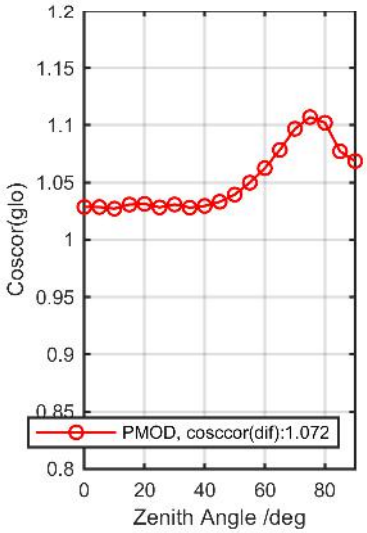

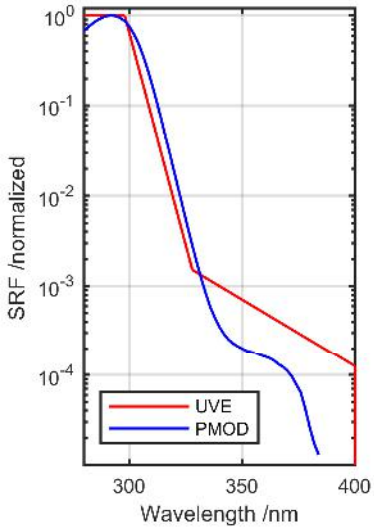

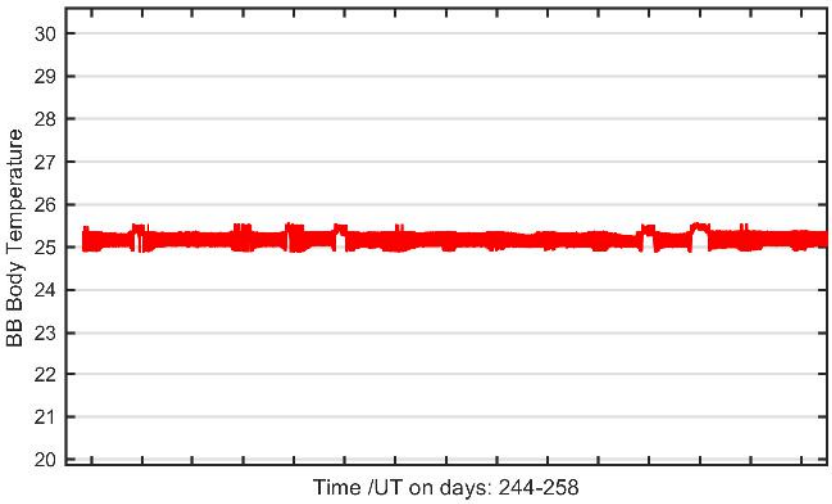

Calibration Matrix fn; Model sdisortPMODmsO3; f0=0.5370

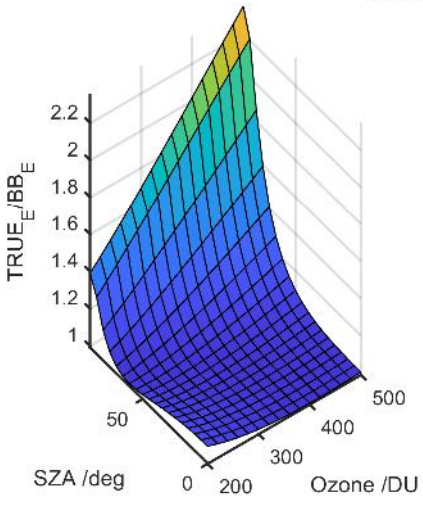

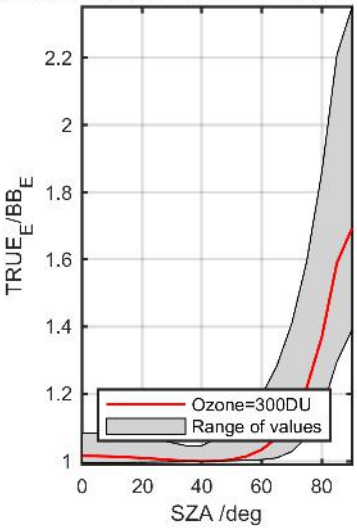

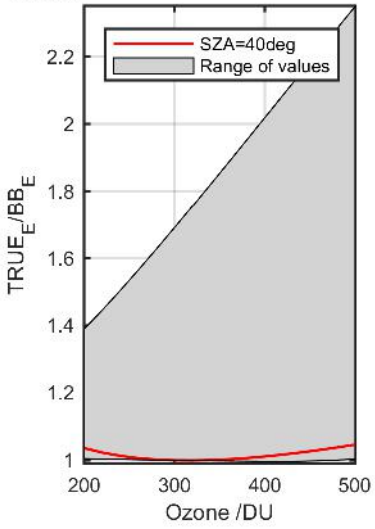

Calibration Results of SL3864 (UVE)

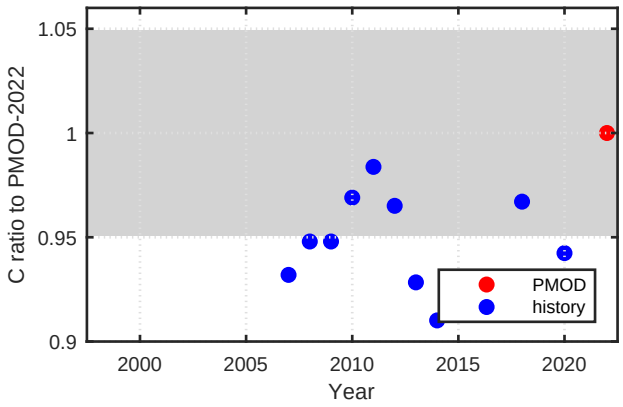

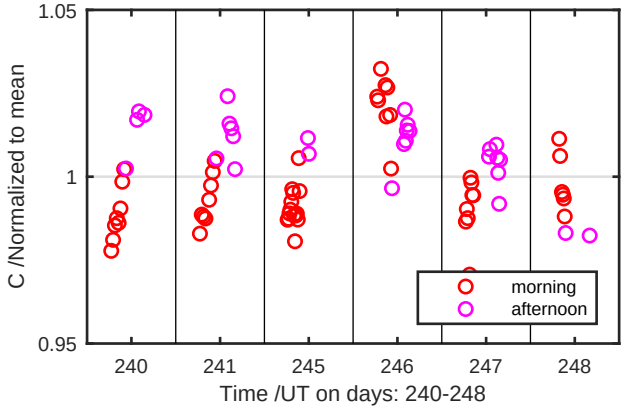

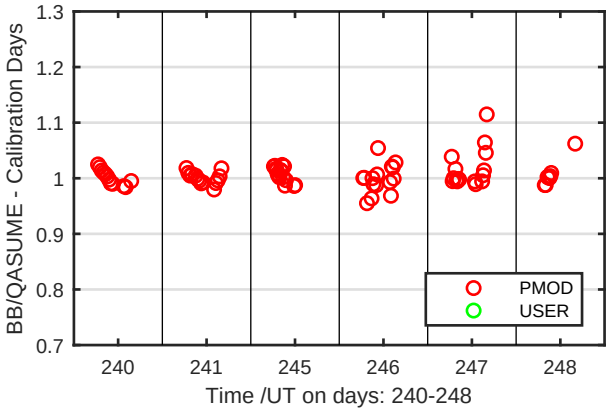

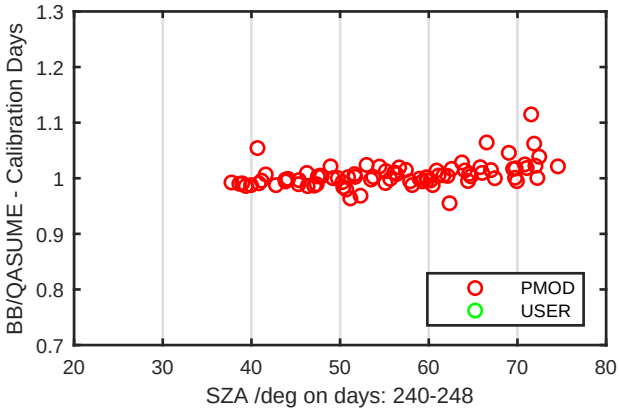

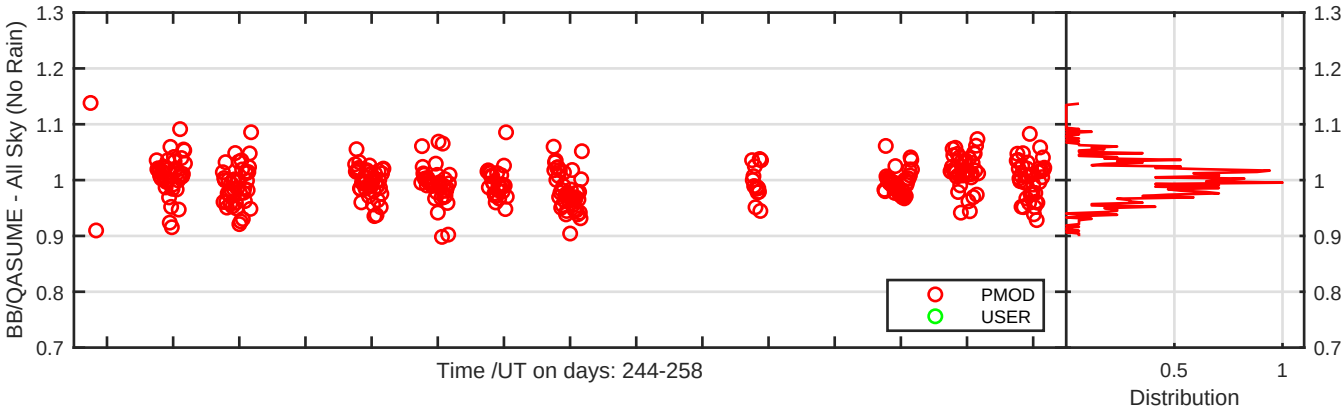

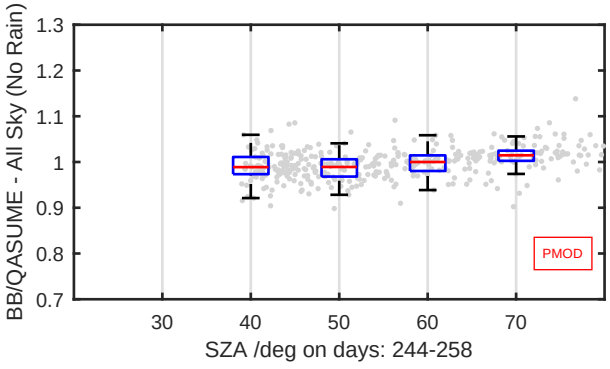

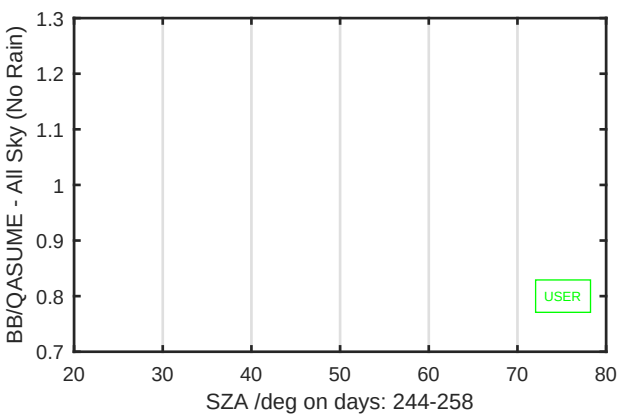

Calibration Results of SL3865 (UVE)

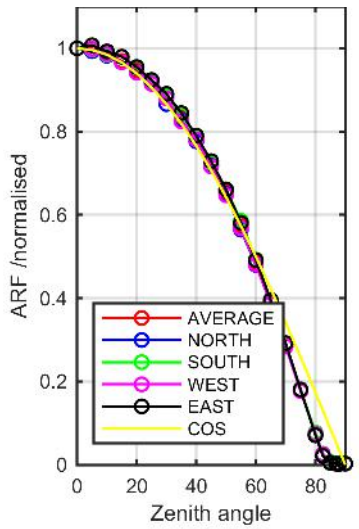

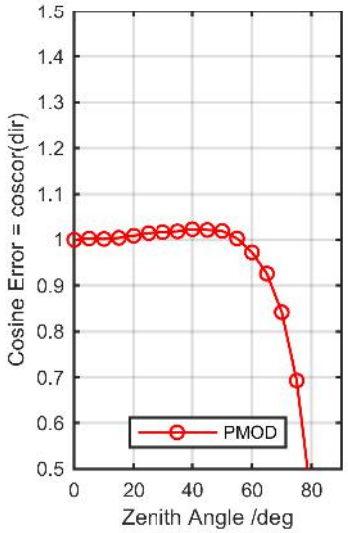

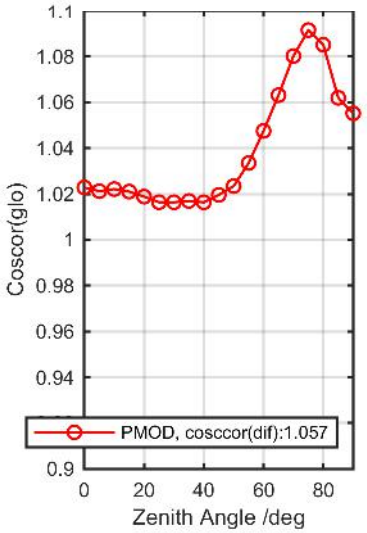

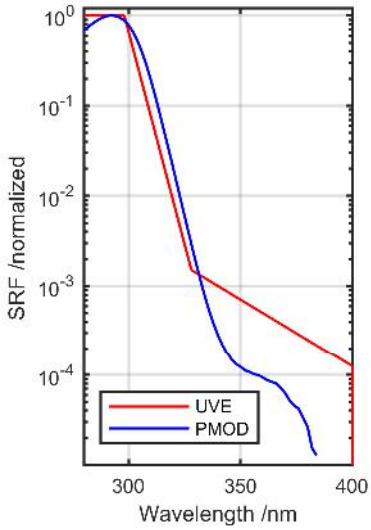

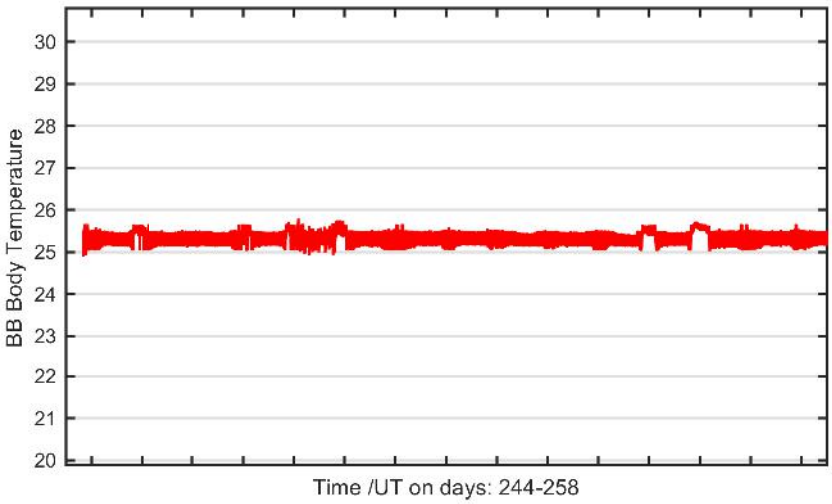

Calibration Matrix fn; Model sdisortPMODmsO3; f0=0.5104

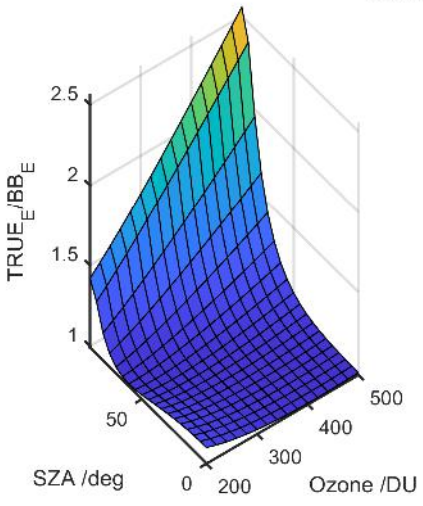

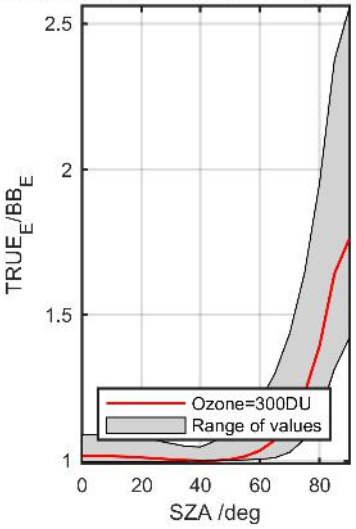

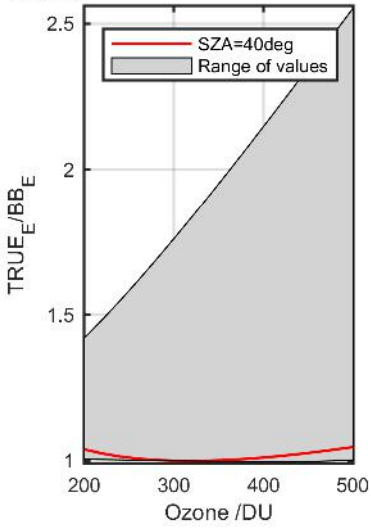

Calibration Results of SL3865 (UVE)

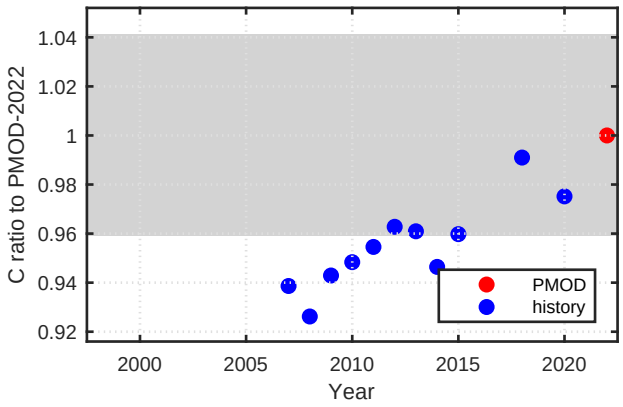

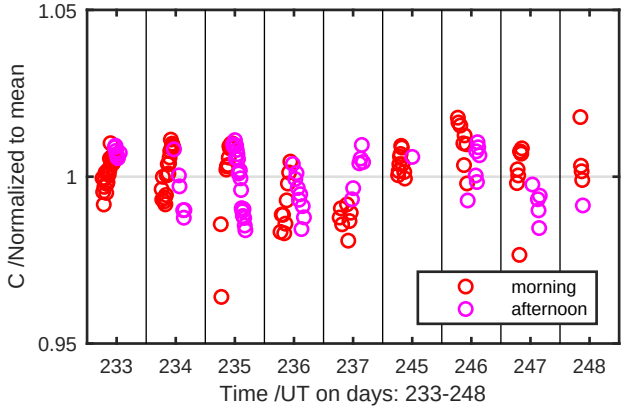

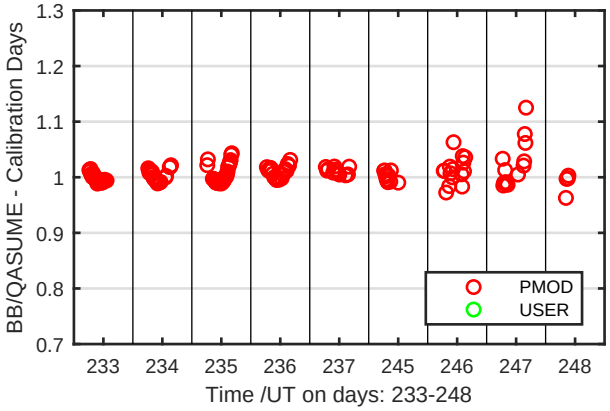

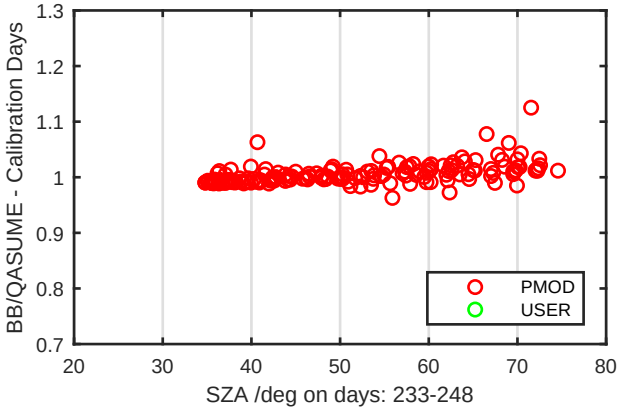

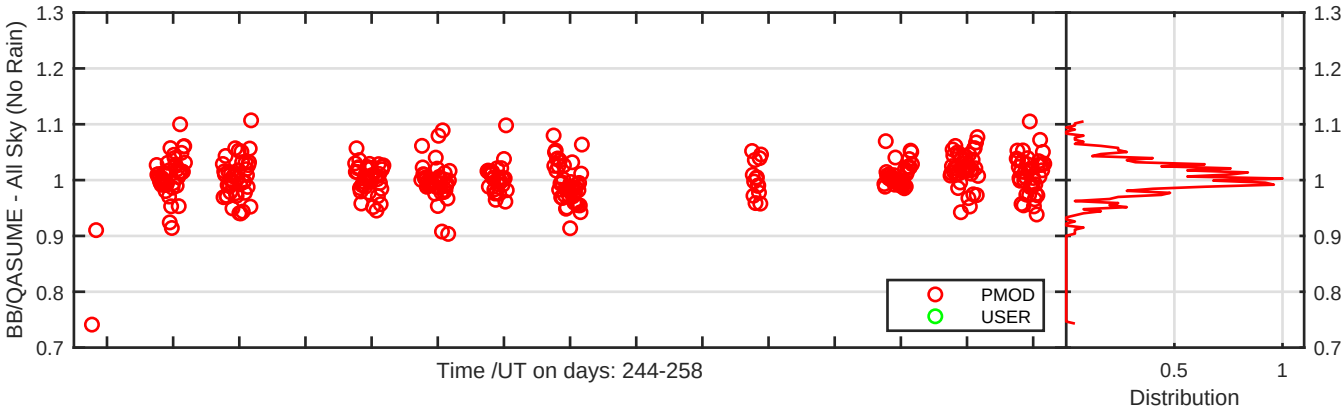

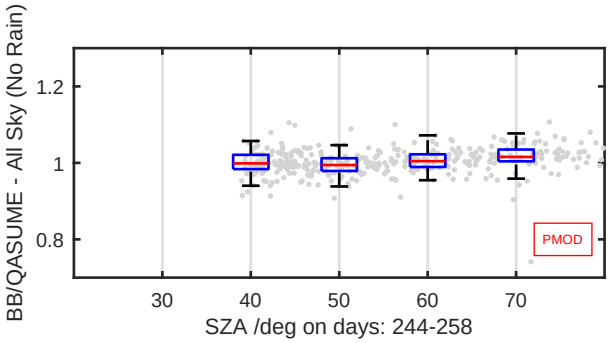

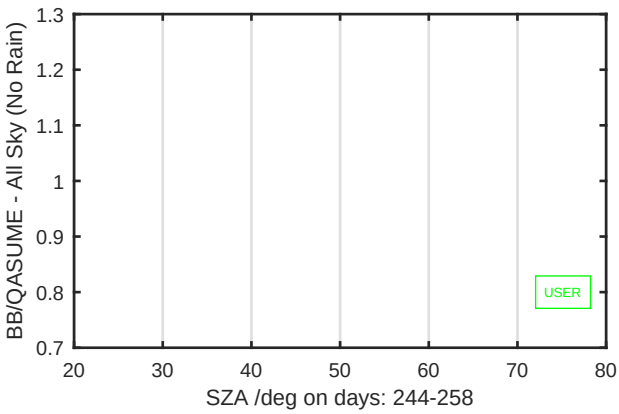

Calibration Results of SL19488 (UVE)

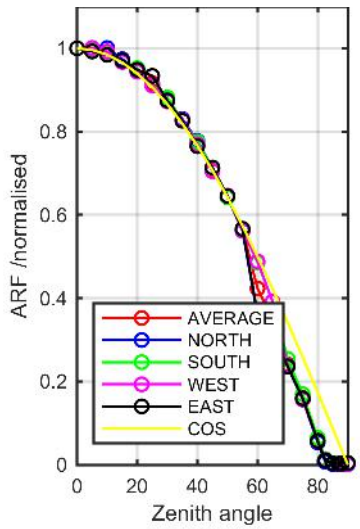

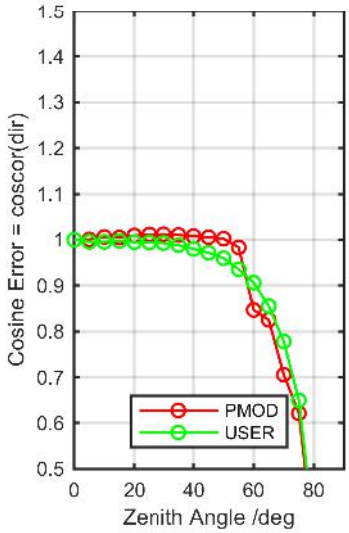

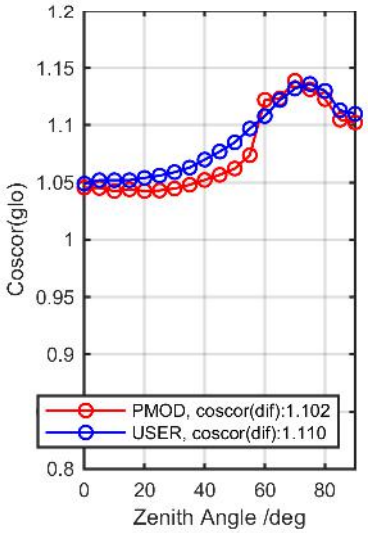

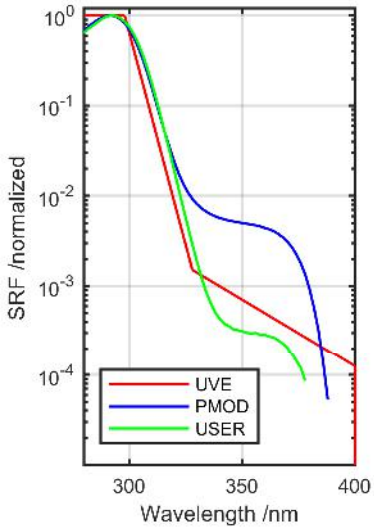

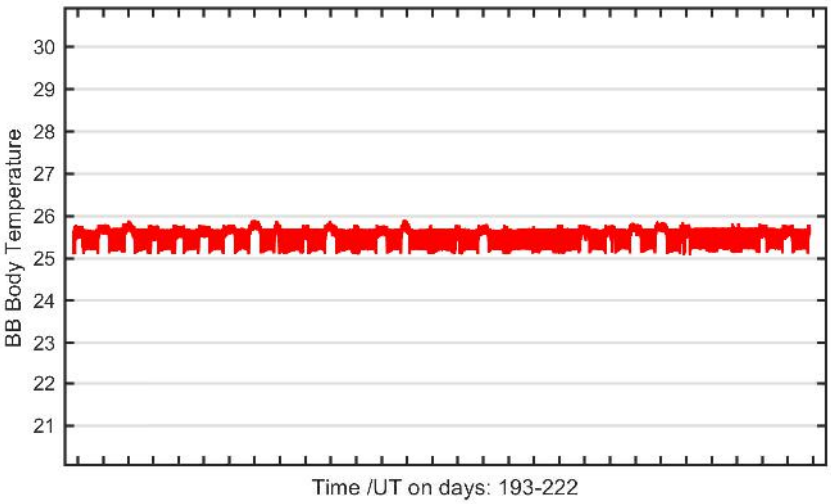

Calibration Matrix fn; Model sdisortREFms2009; f0=0.3750

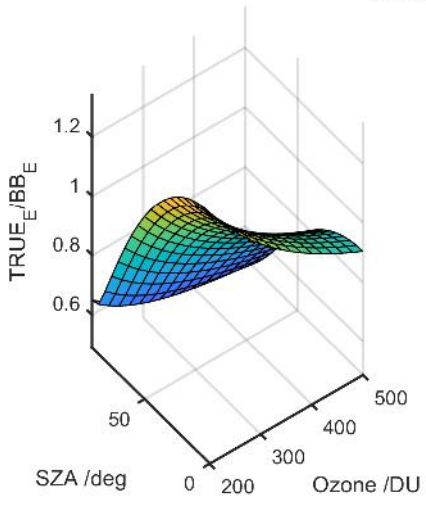

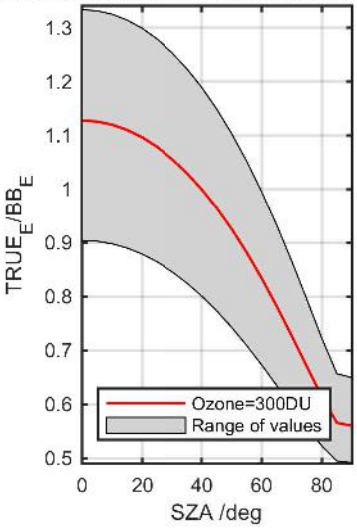

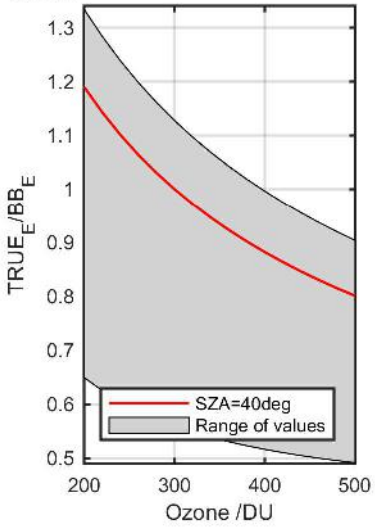

Calibration Results of SL19488 (UVE)

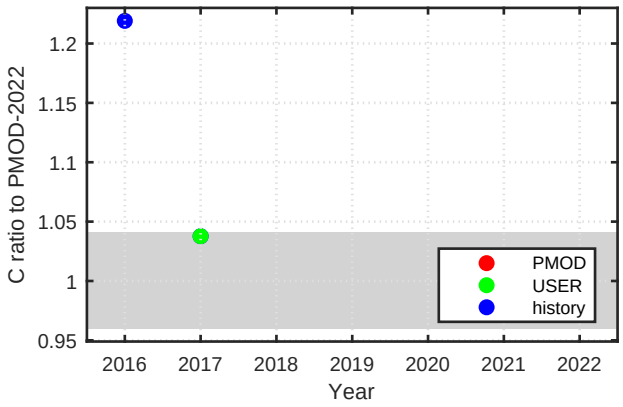

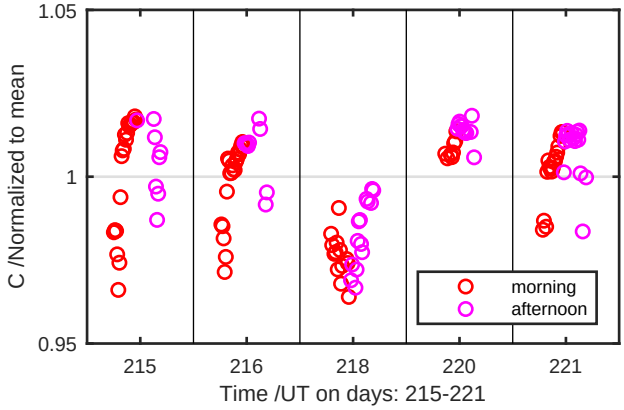

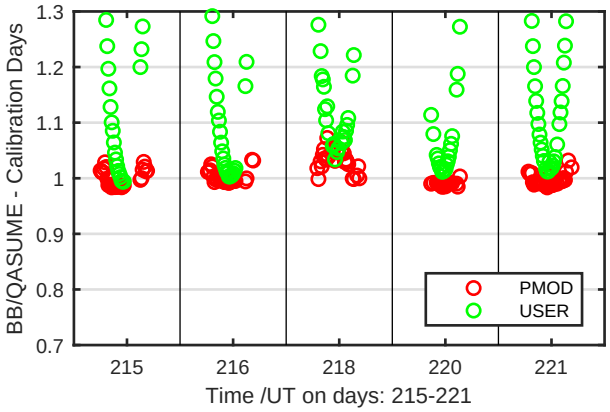

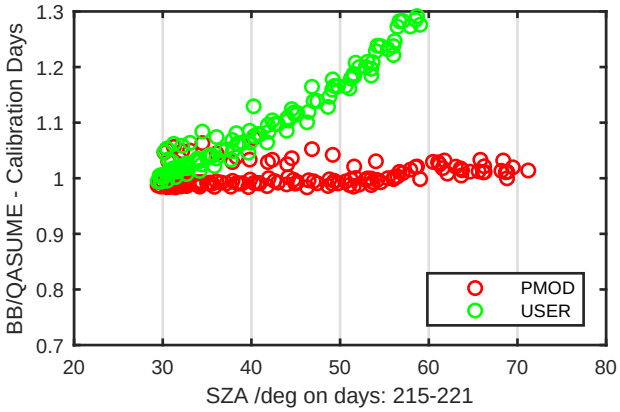

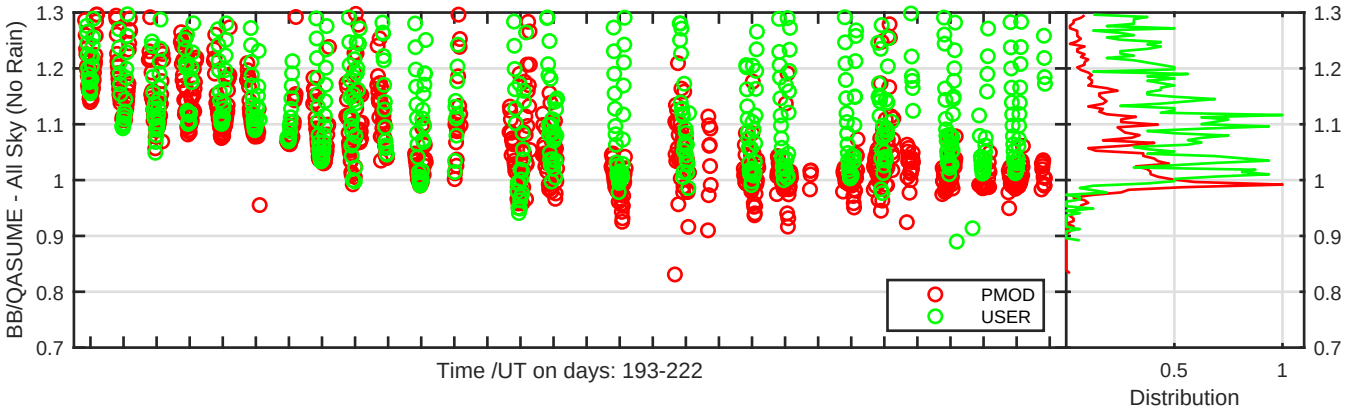

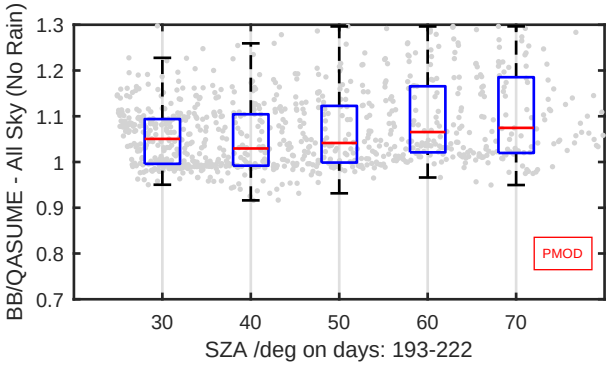

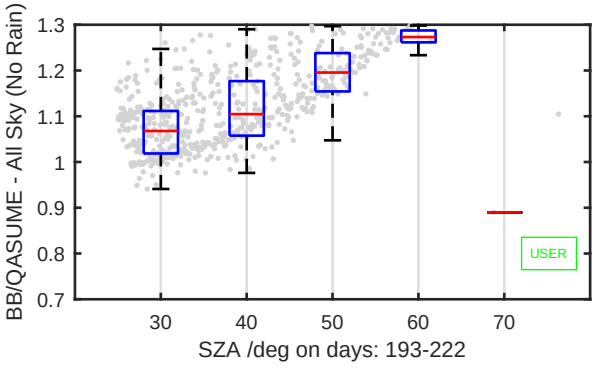

Calibration Results of SL23169 (UVE)

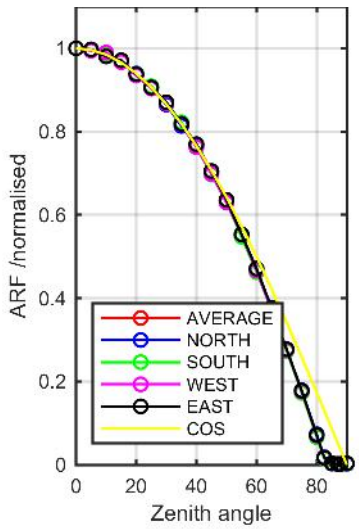

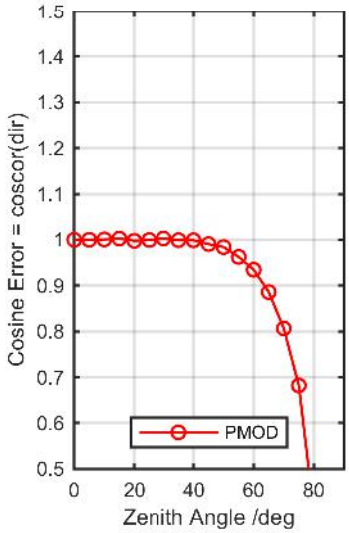

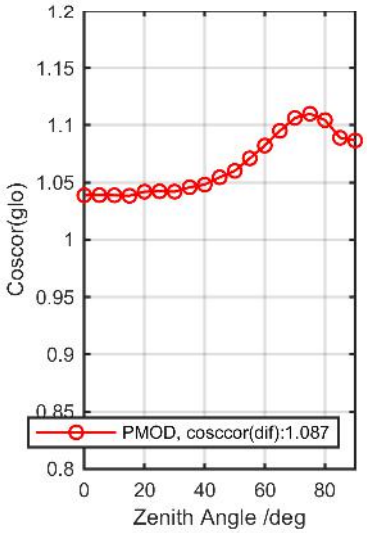

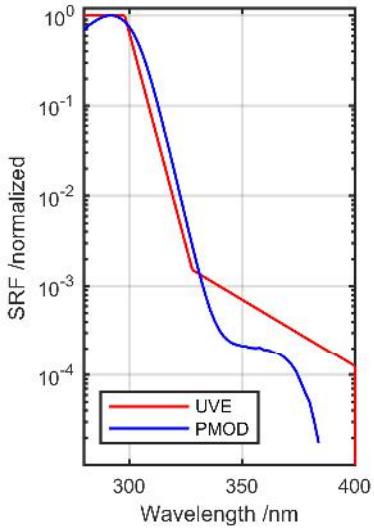

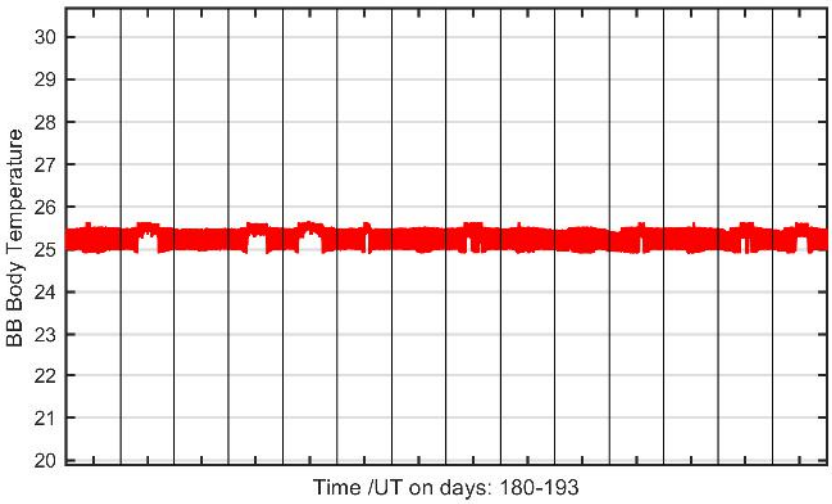

Calibration Matrix fn; Model sdisortREFms2009; f0=0.5274

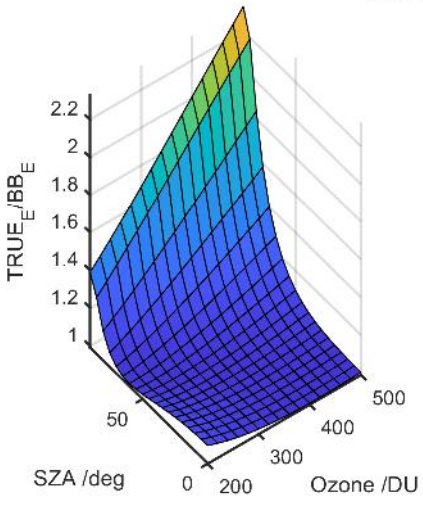

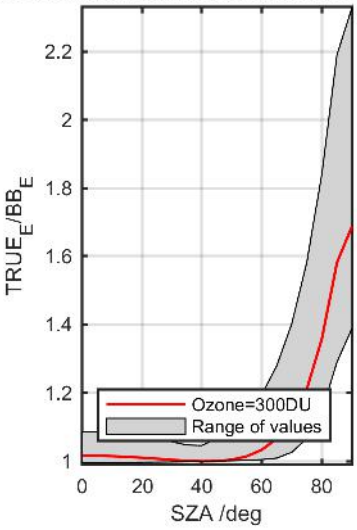

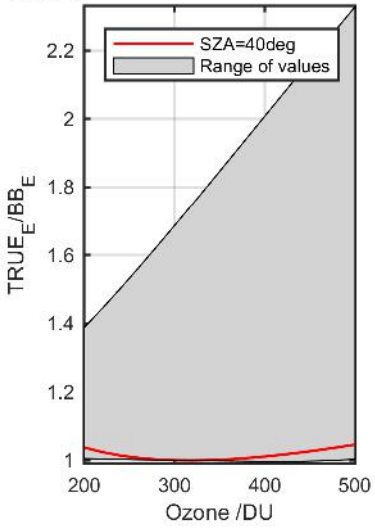

Calibration Results of SL23169 (UVE)

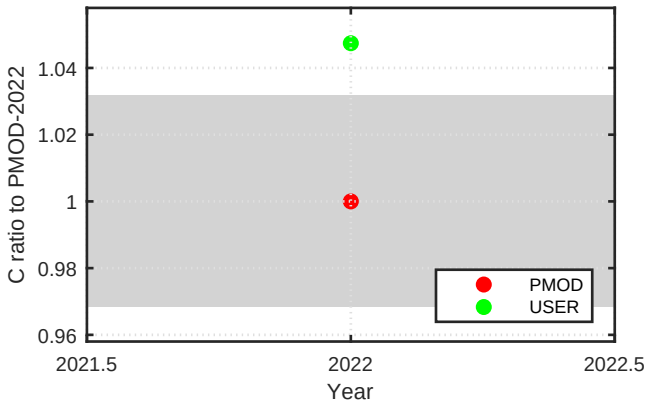

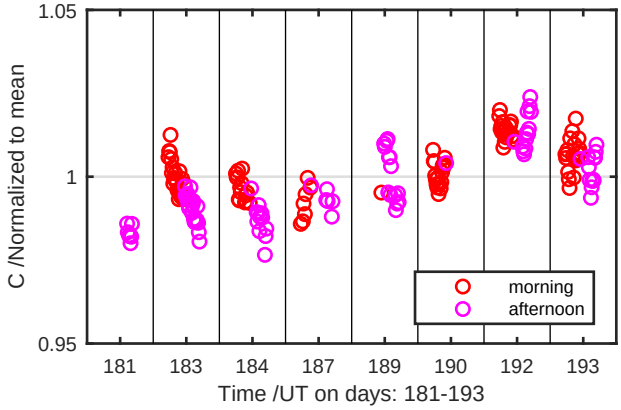

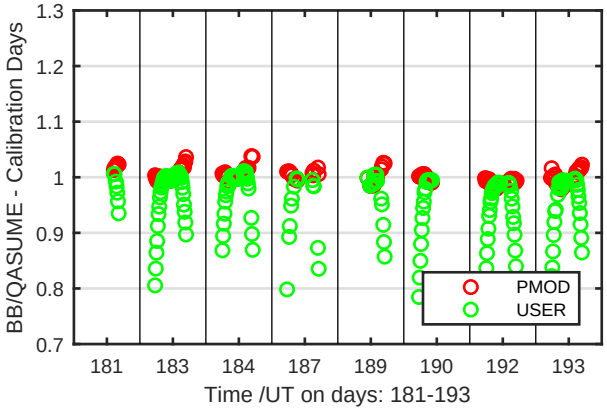

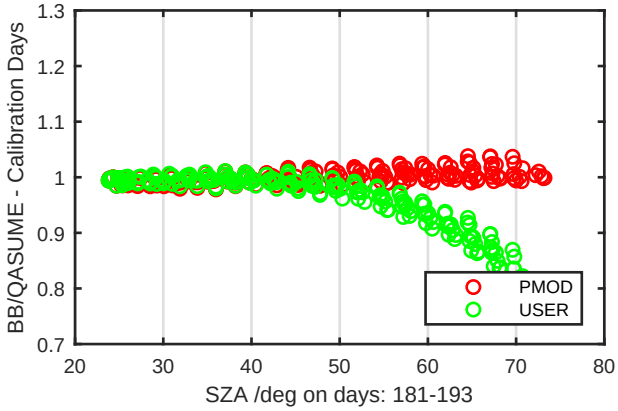

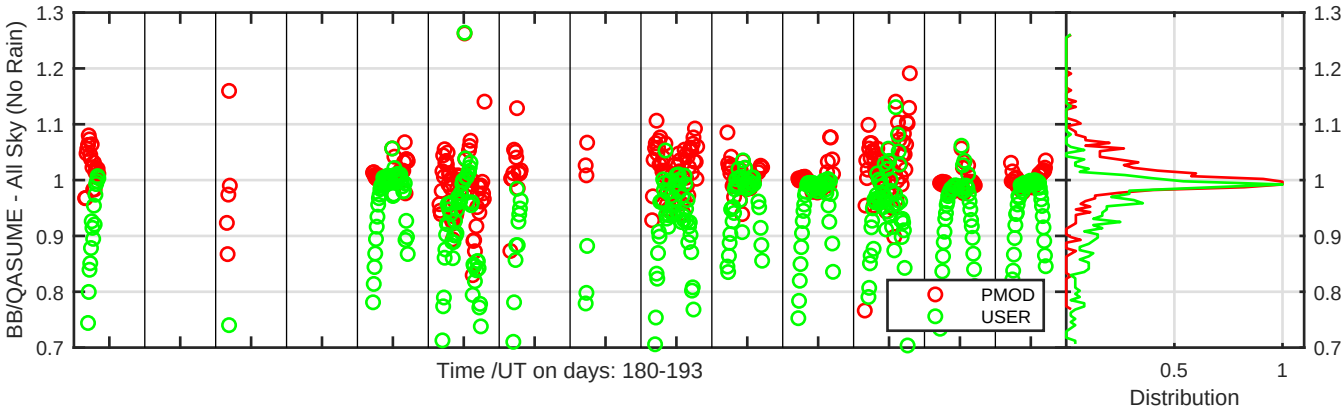

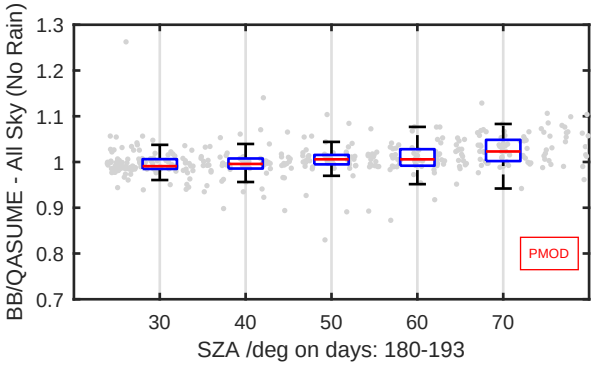

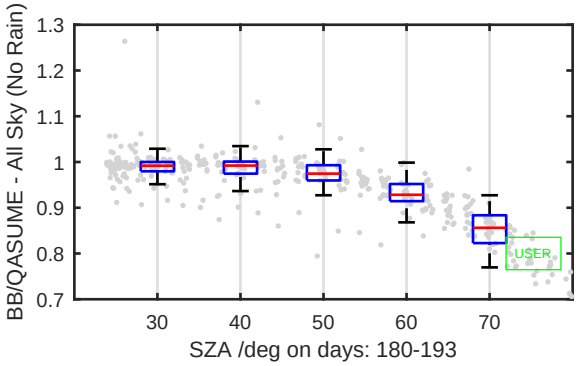

Calibration Results of SL26780 (UVE)

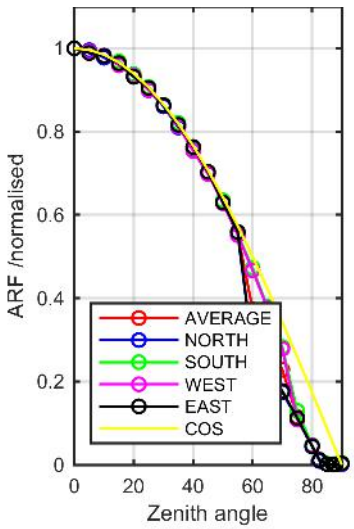

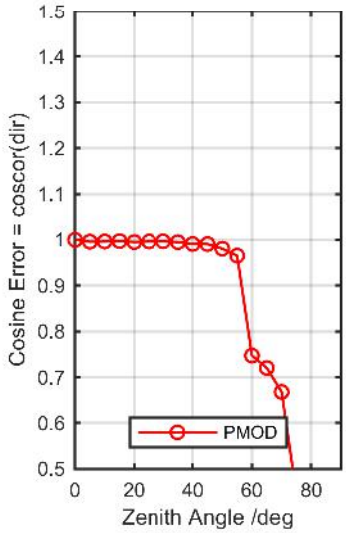

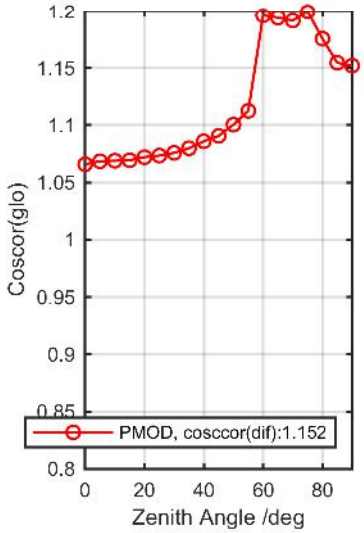

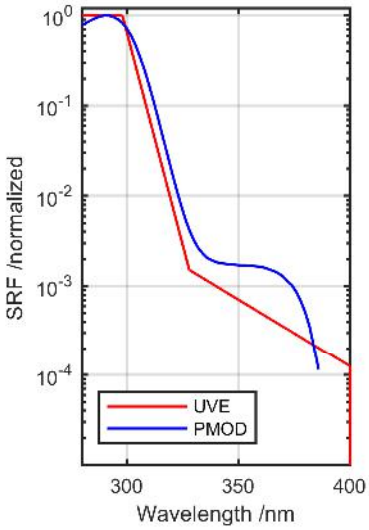

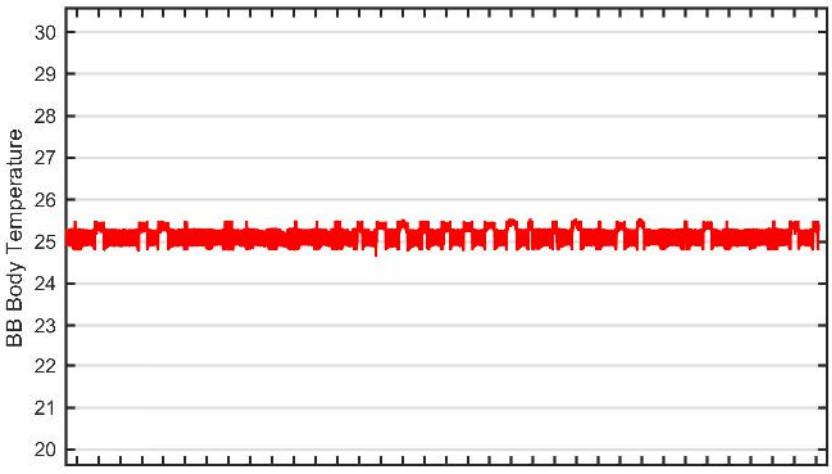

Calibration Matrix fn; Model sdisortREFms2009; f0=0.4847

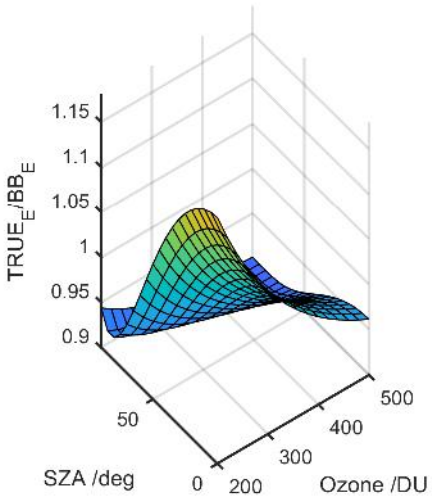

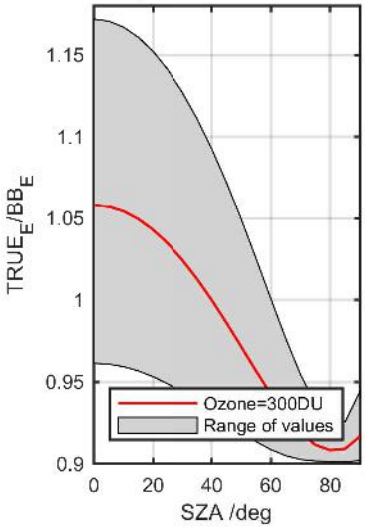

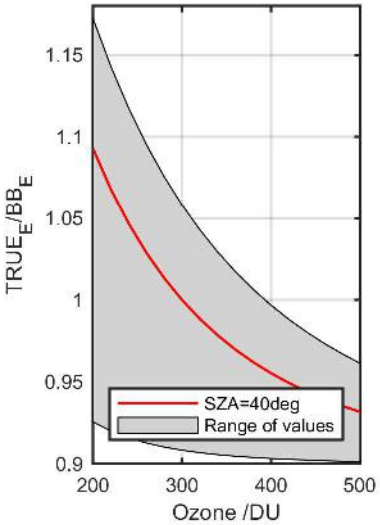

Calibration Results of SL26780 (UVE)

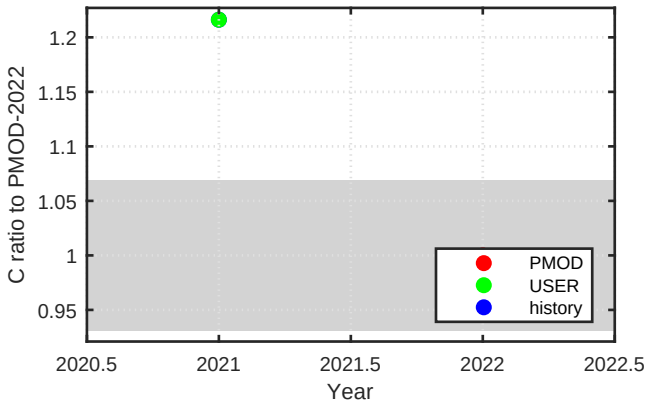

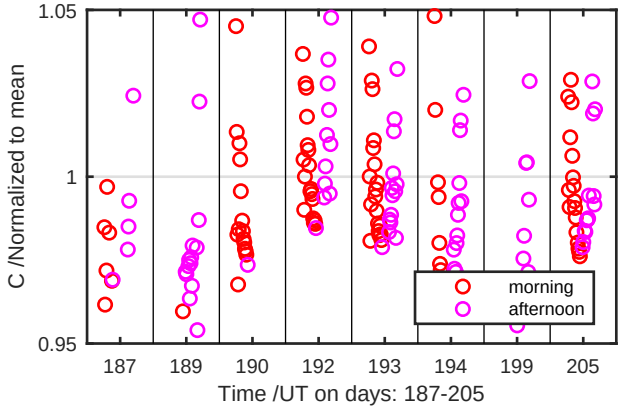

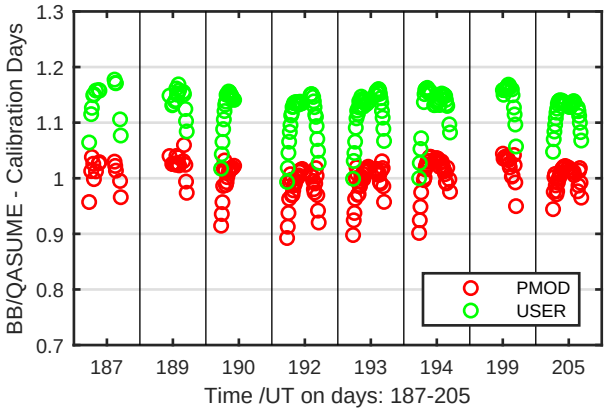

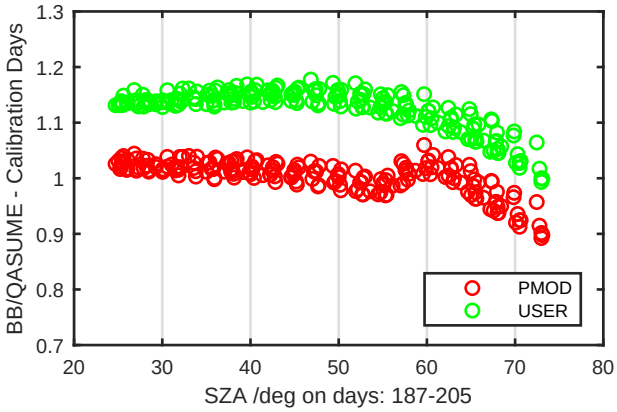

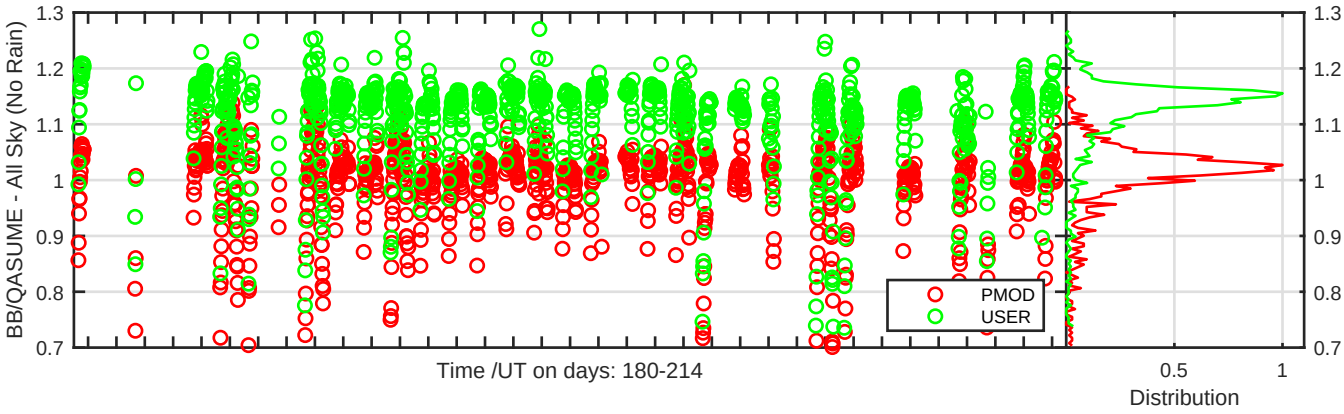

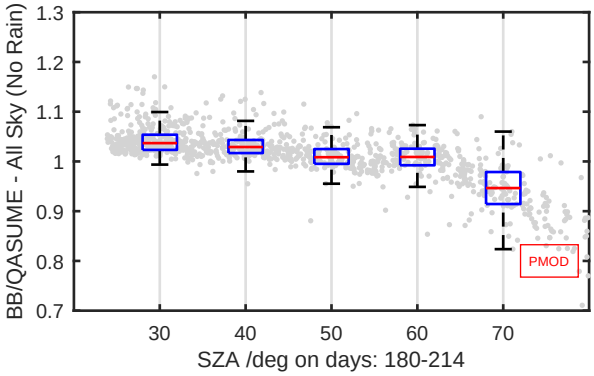

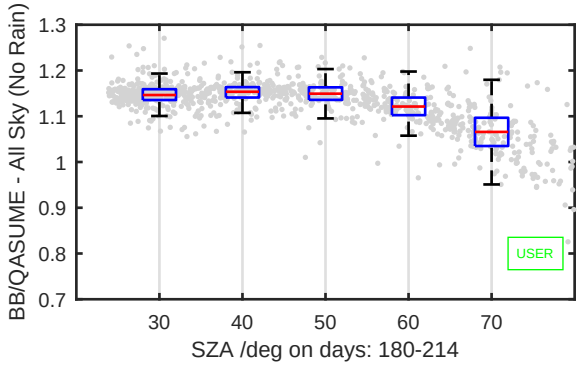

Calibration Results of SL2875 (UVA)

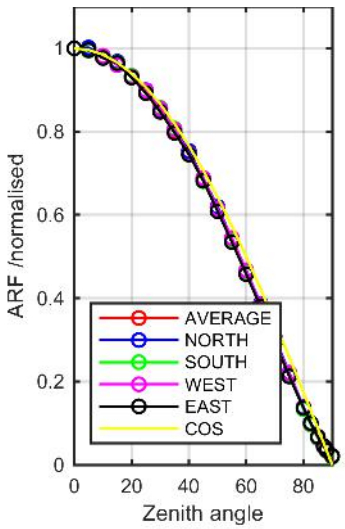

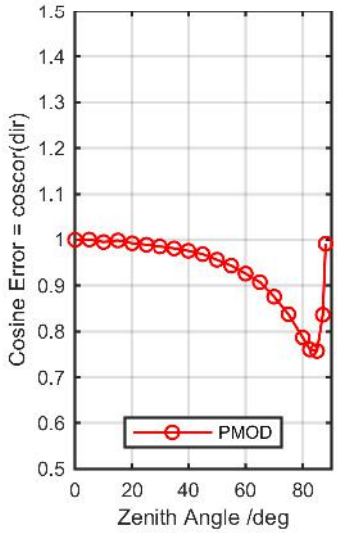

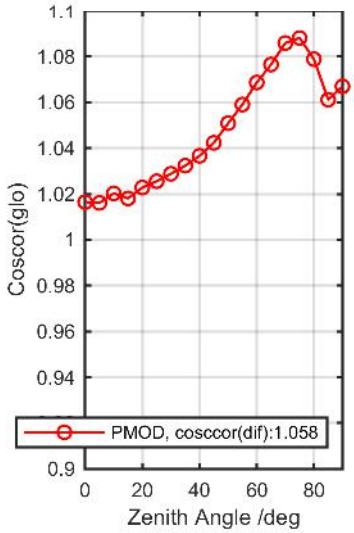

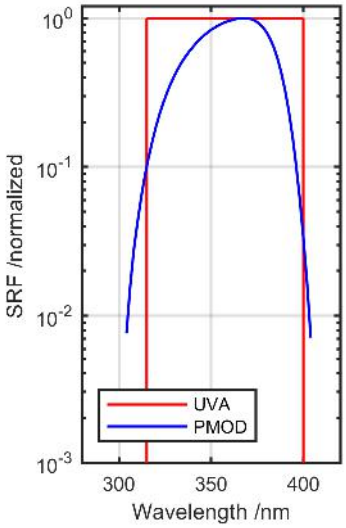

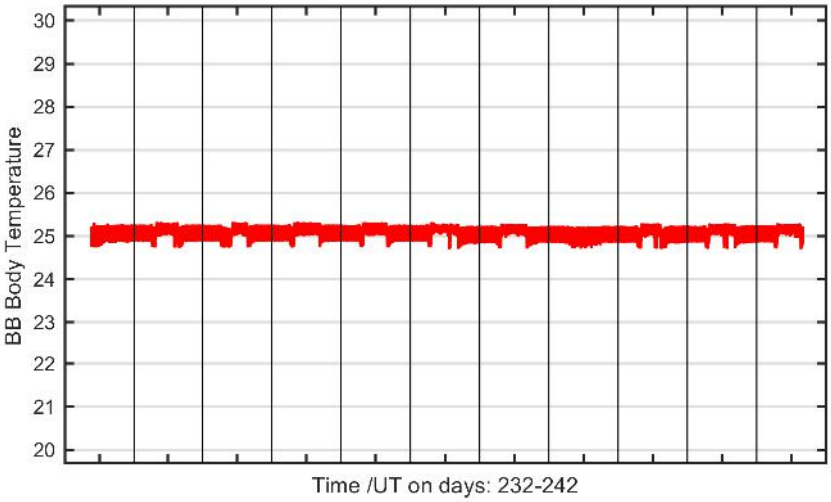

Calibration Matrix fn; Model sdisortPMODmsO3; f0=1.5680

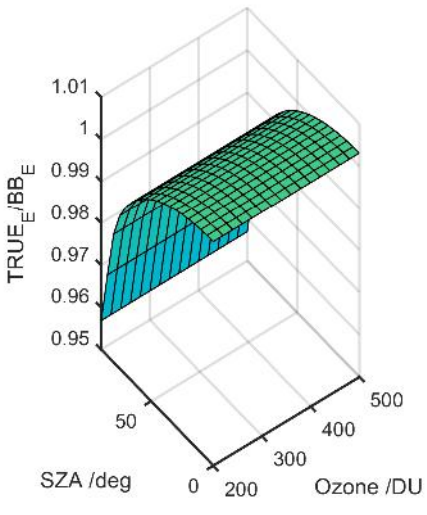

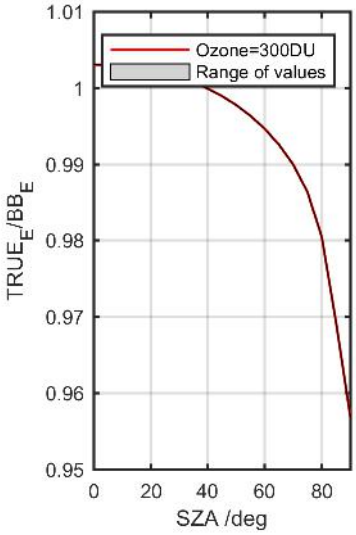

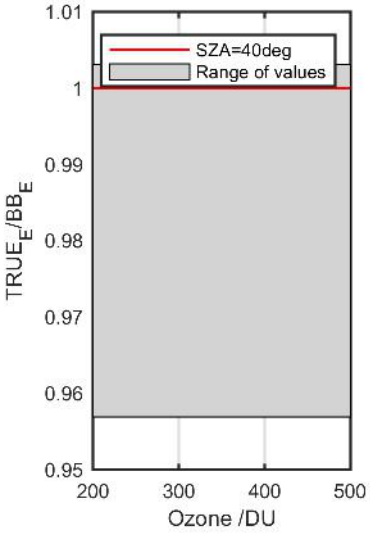

Calibration Results of SL2875 (UVA)

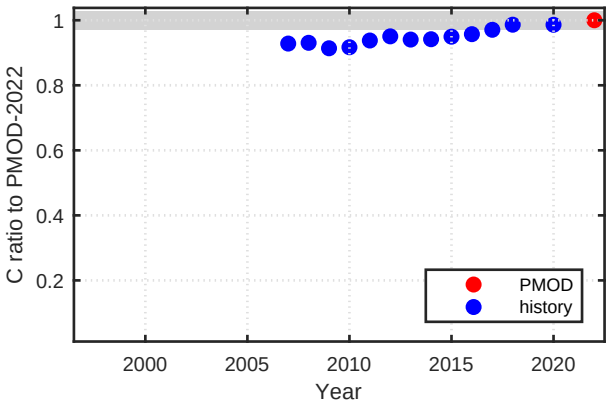

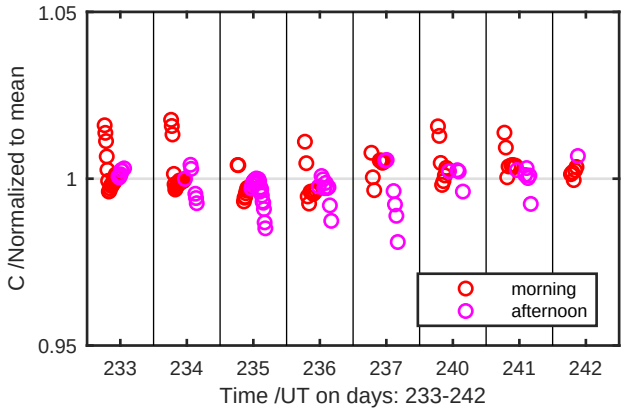

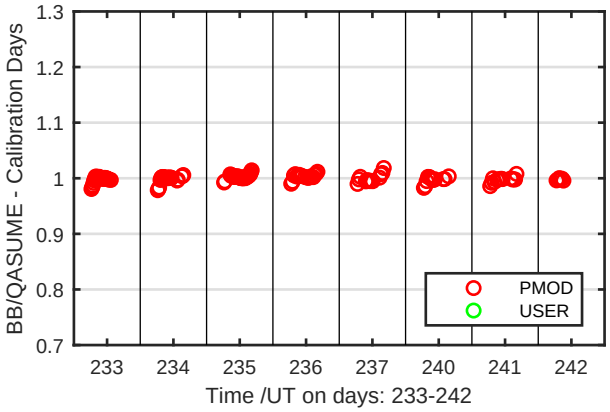

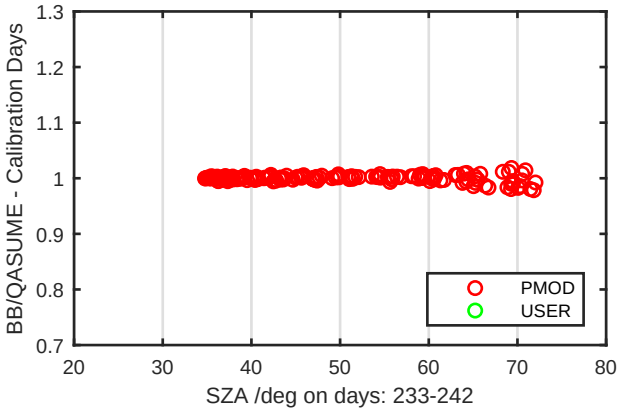

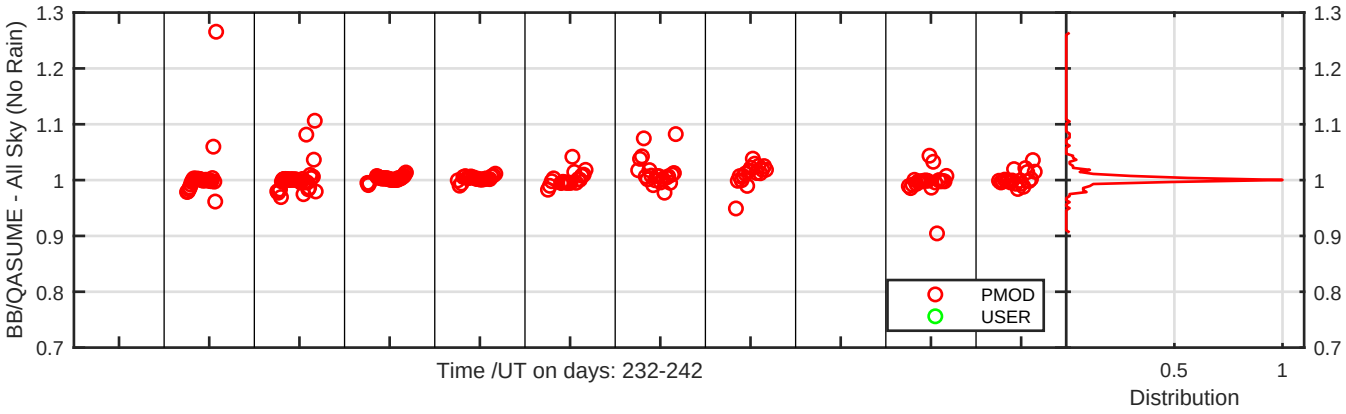

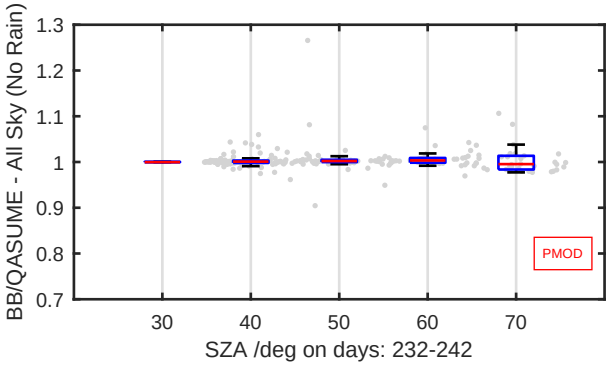

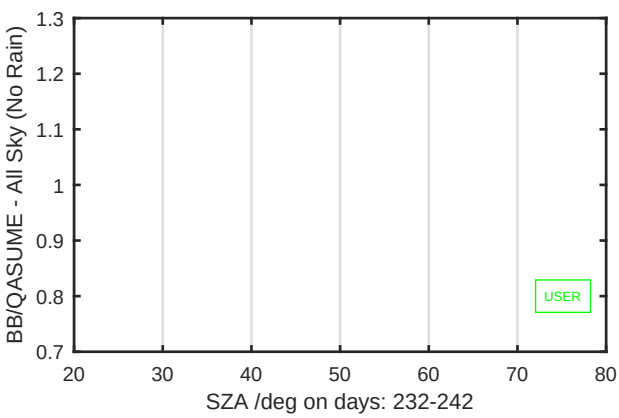

Calibration Results of SL2876 (UVA)

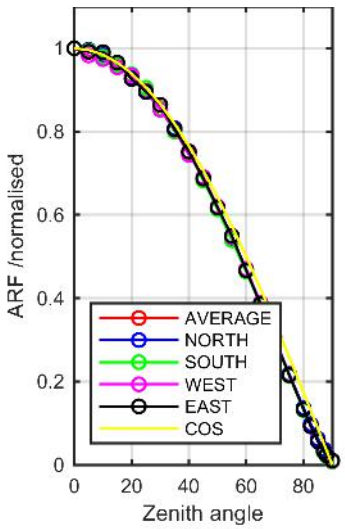

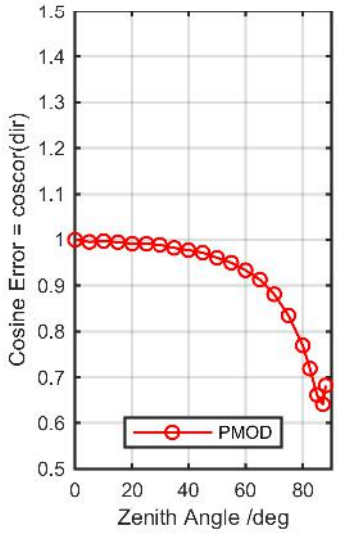

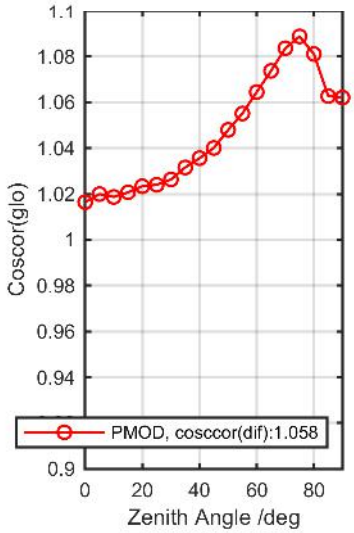

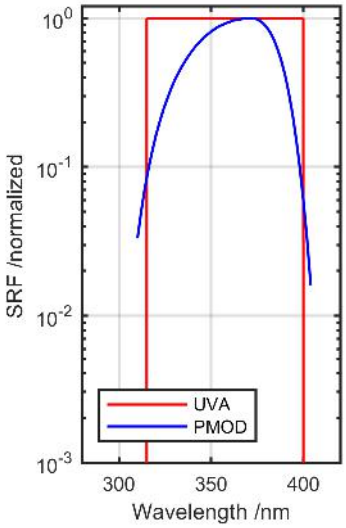

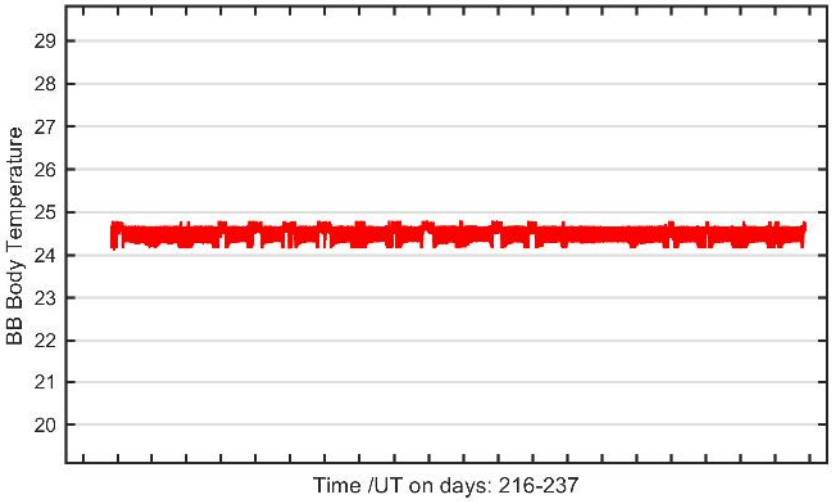

Calibration Matrix fn; Model sdisortPMODmsO3; f0=1.5332

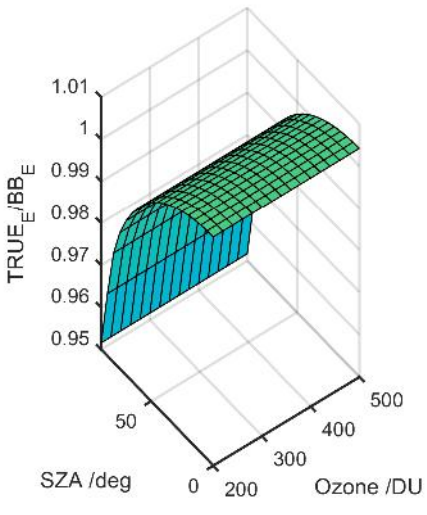

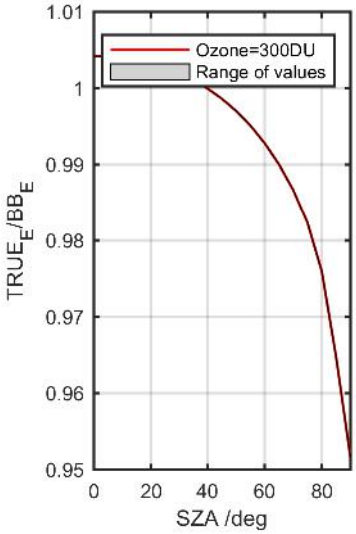

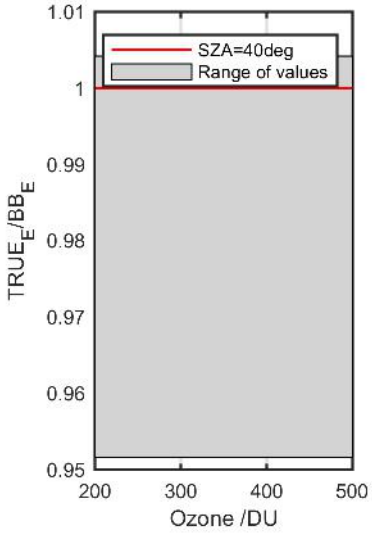

Calibration Results of SL2876 (UVA)

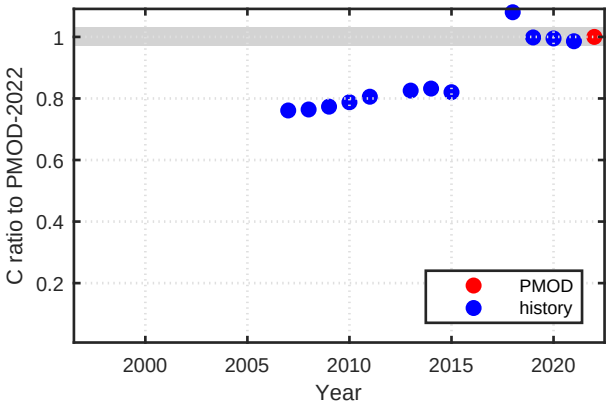

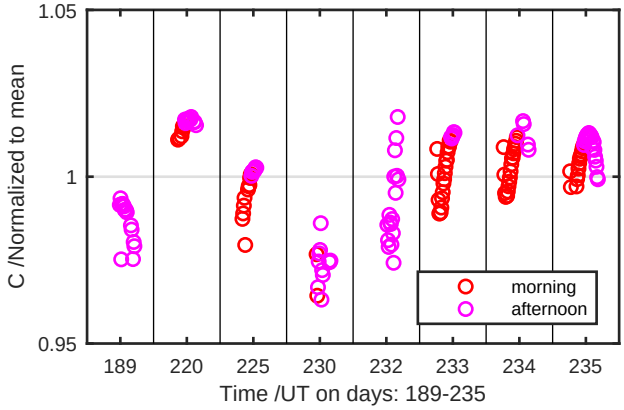

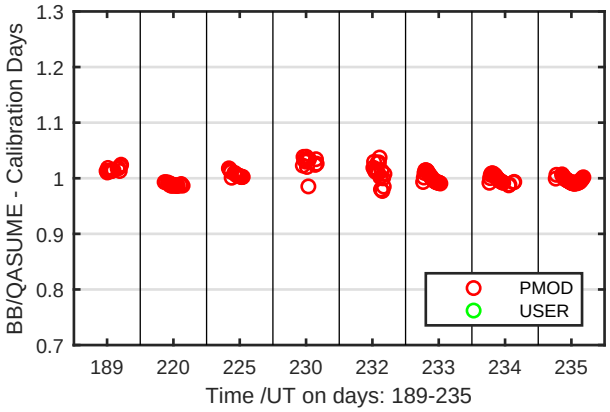

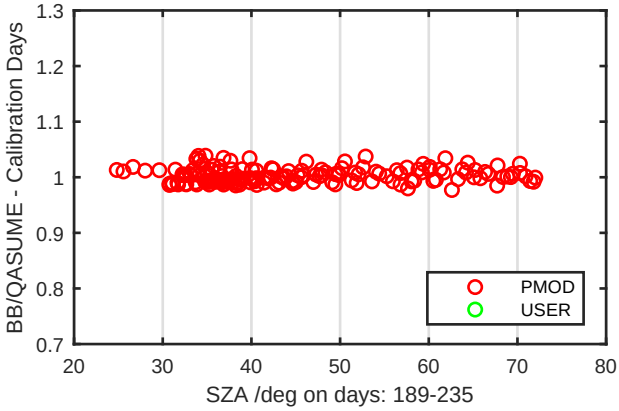

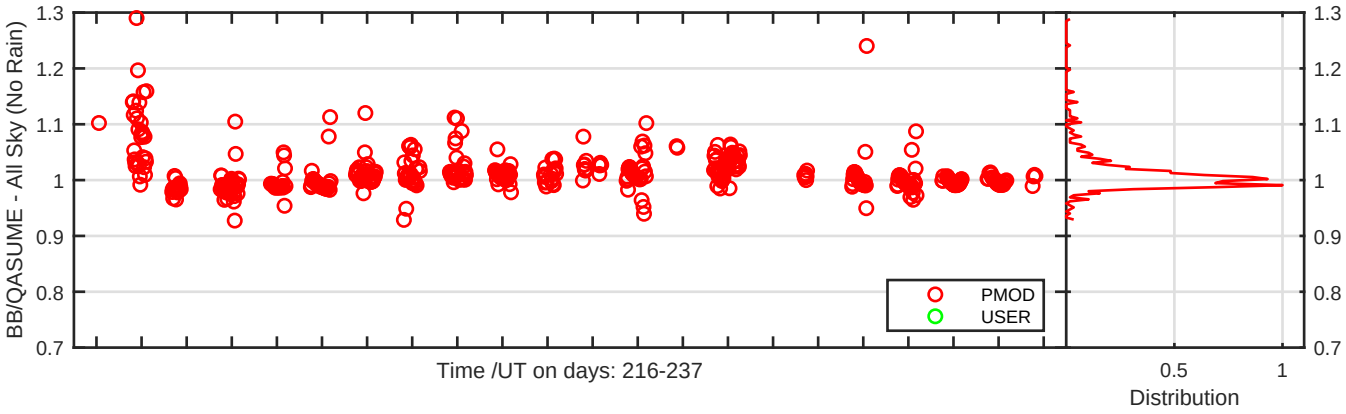

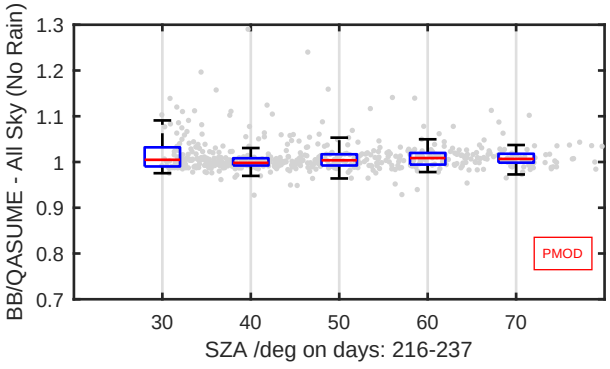

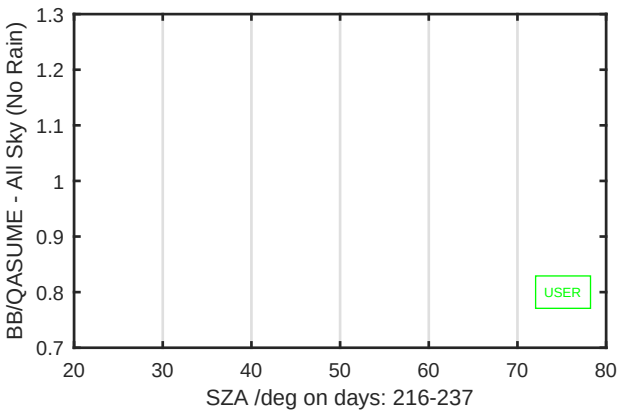

Calibration Results of SL2877 (UVA)

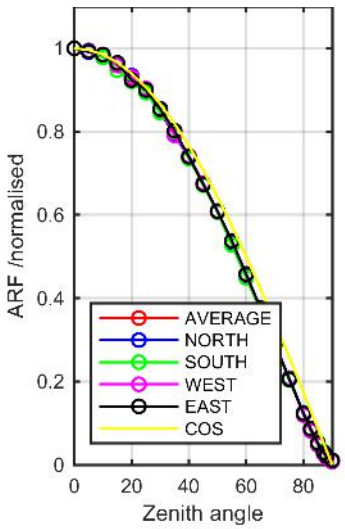

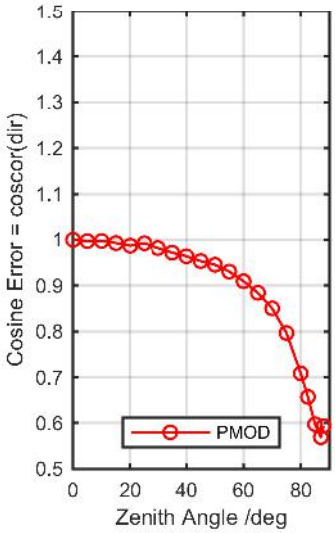

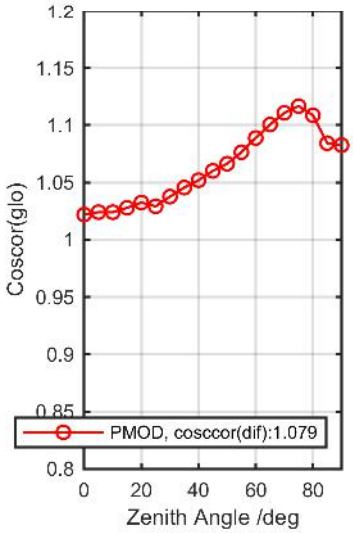

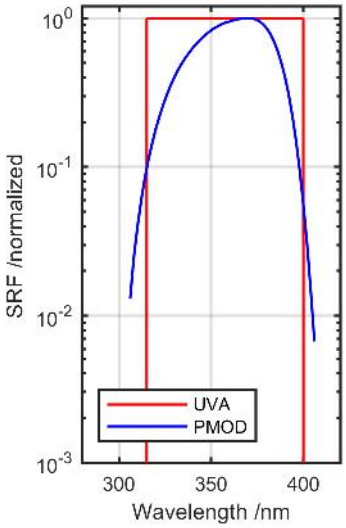

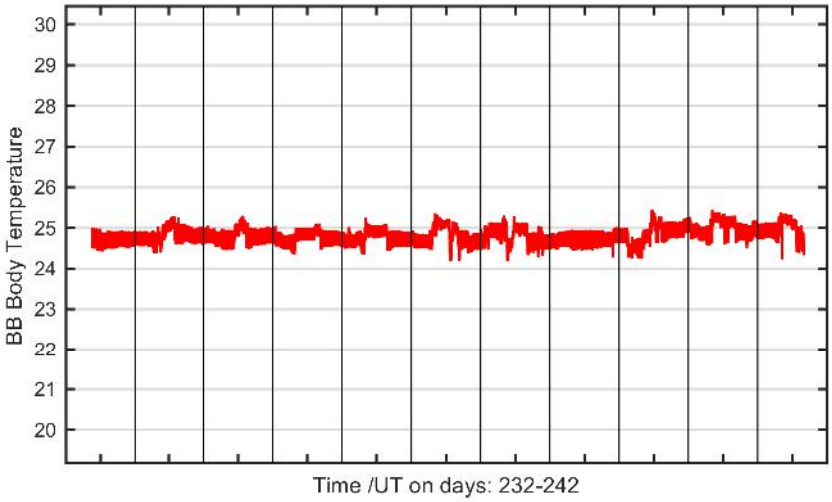

Calibration Matrix fn; Model sdisortPMODmsO3; f0=1.5246

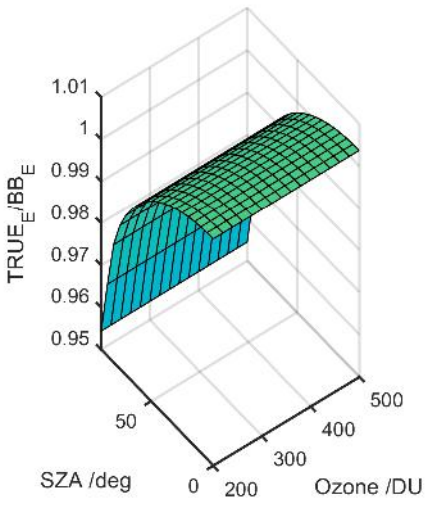

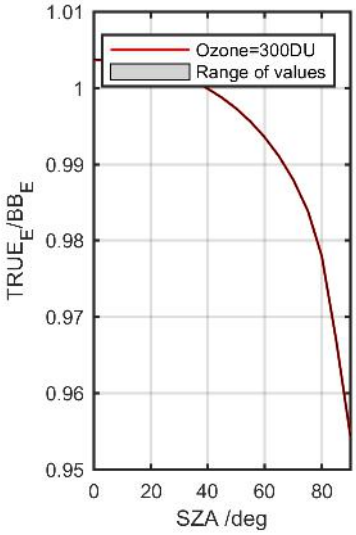

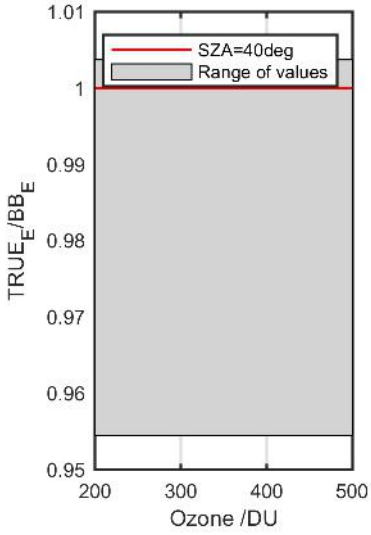

Calibration Results of SL2877 (UVA)

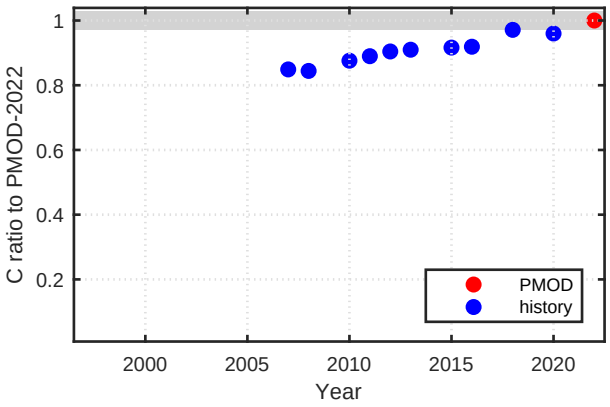

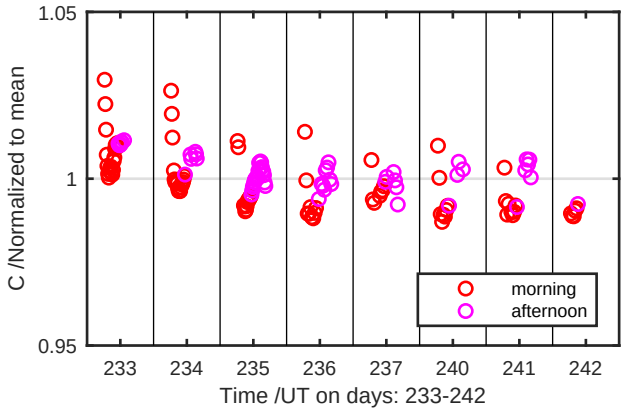

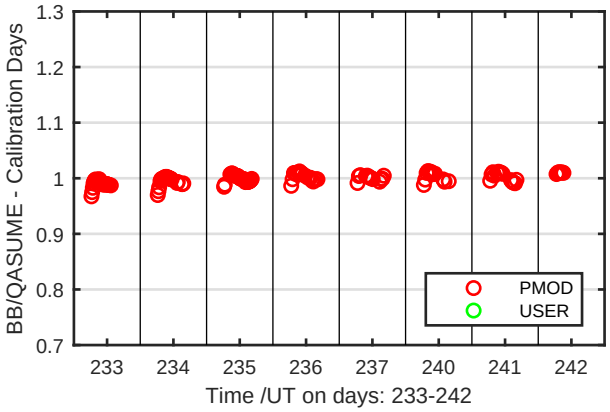

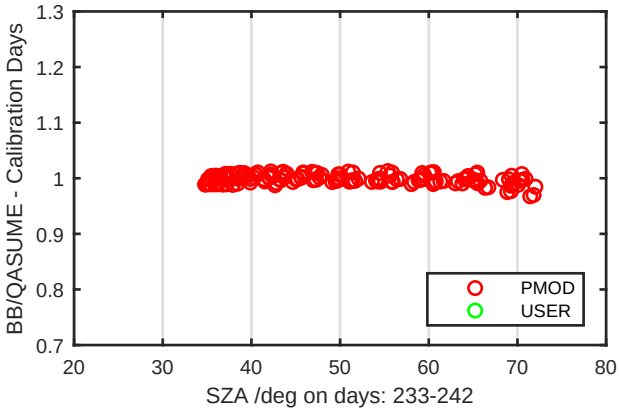

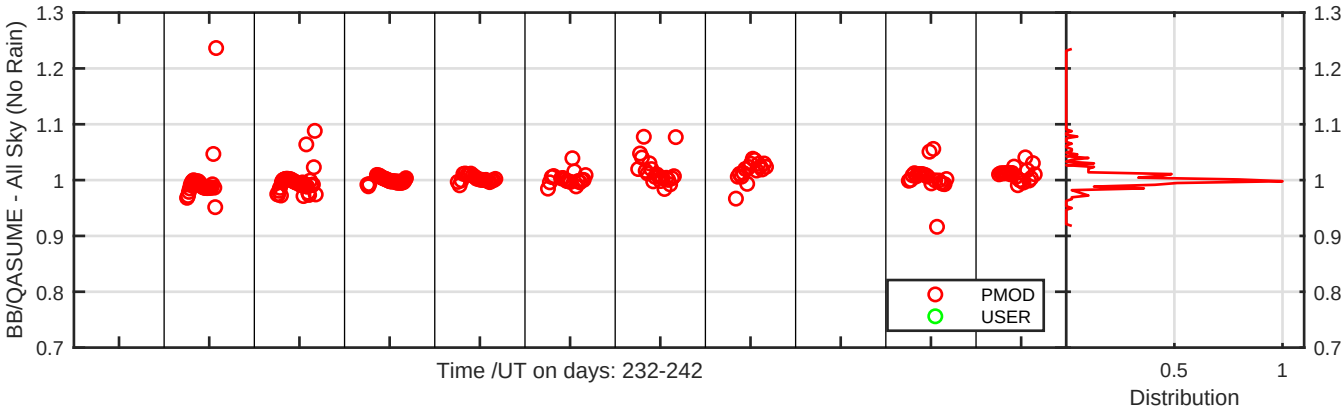

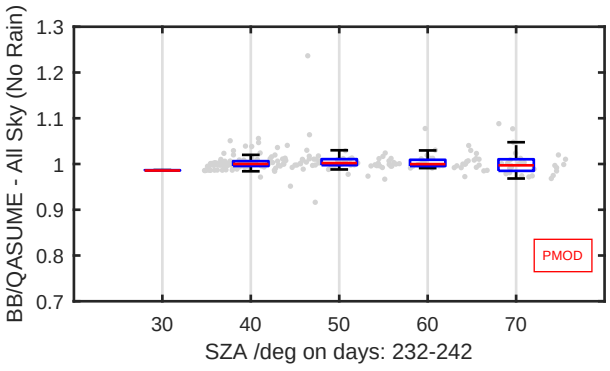

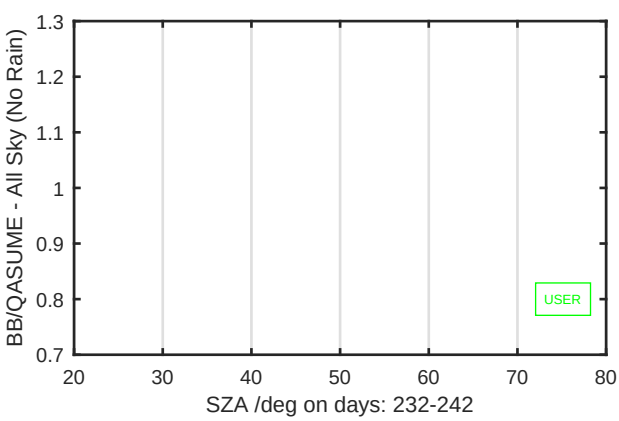

Calibration Results of SL0922 (UVE)

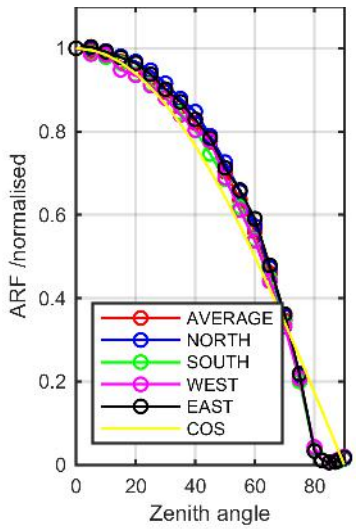

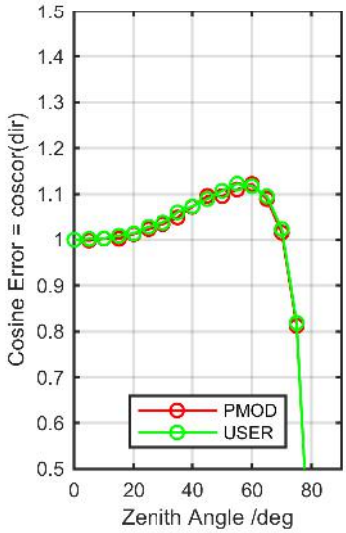

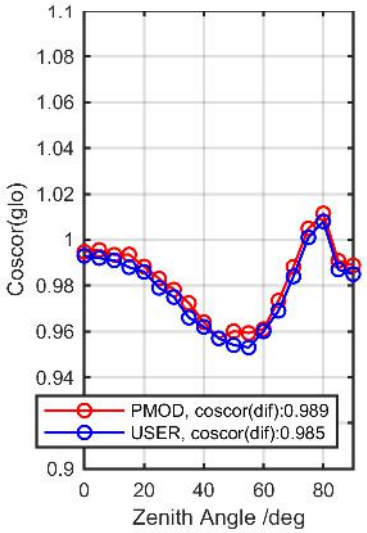

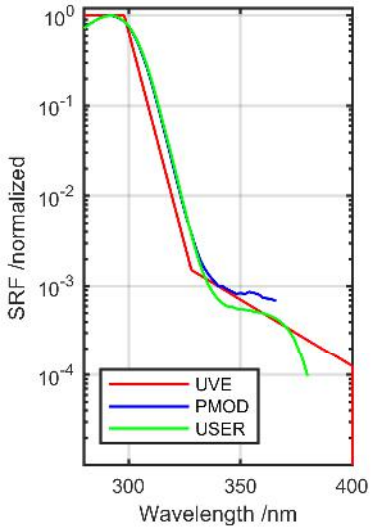

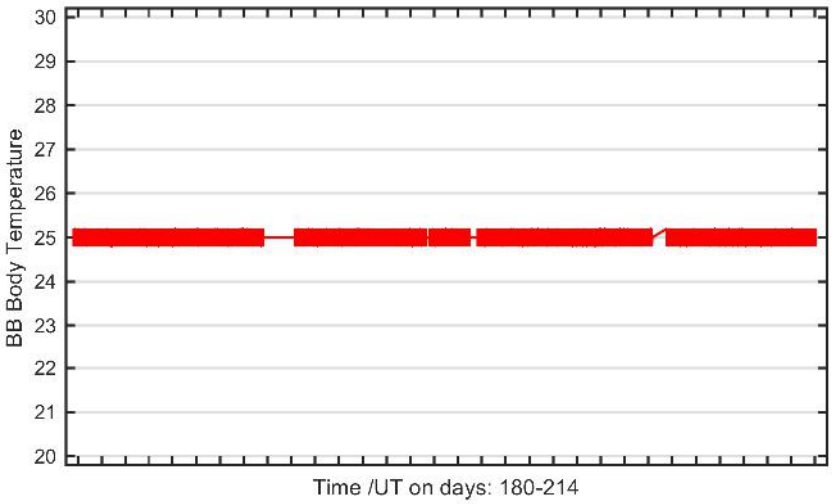

Calibration Matrix fn; Model sdisortREFms2009; f0=0.4862

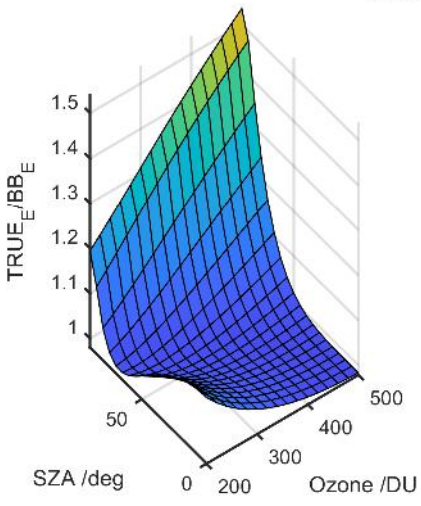

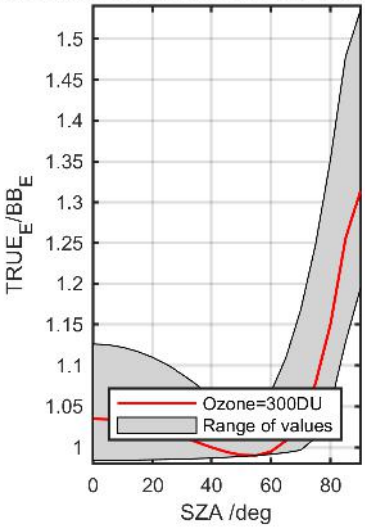

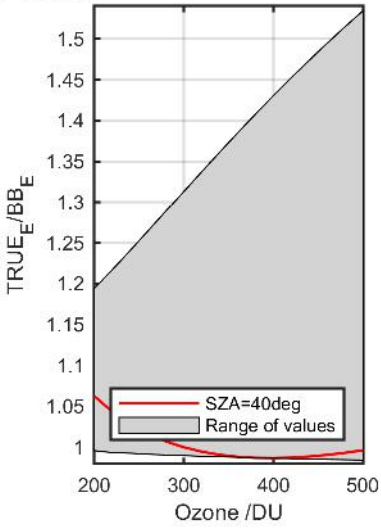

Calibration Results of SL0922 (UVE)

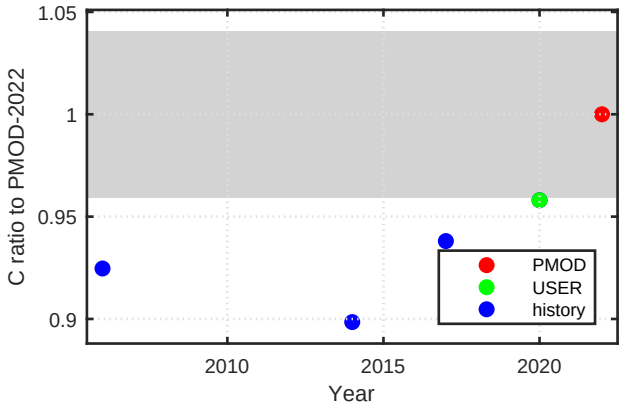

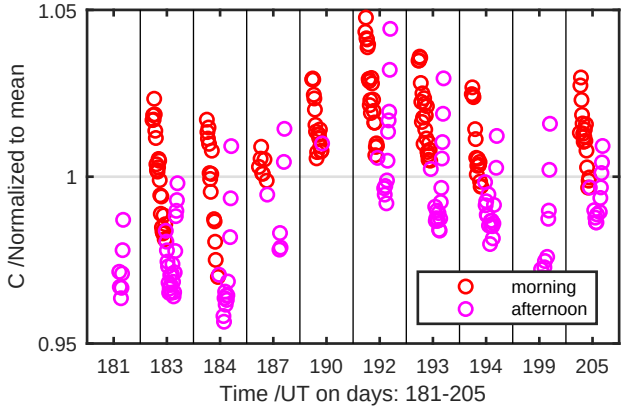

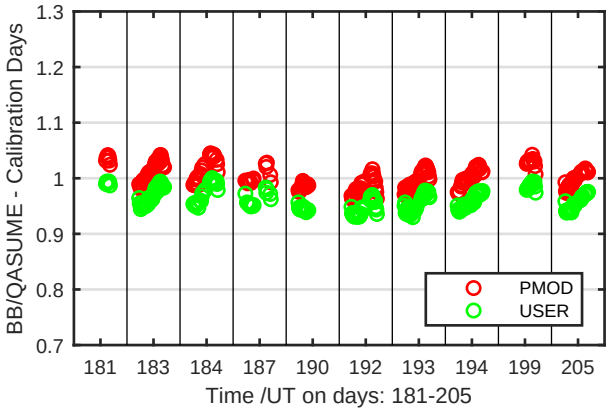

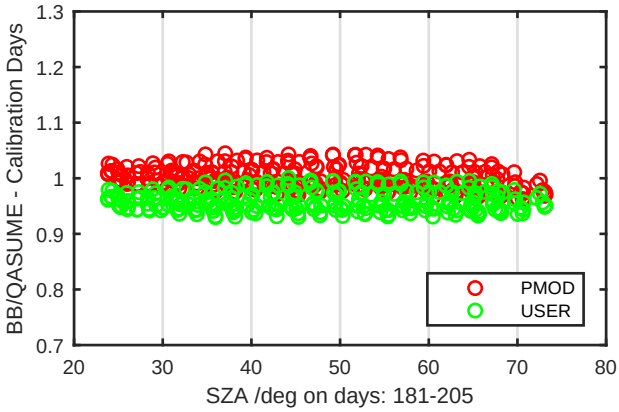

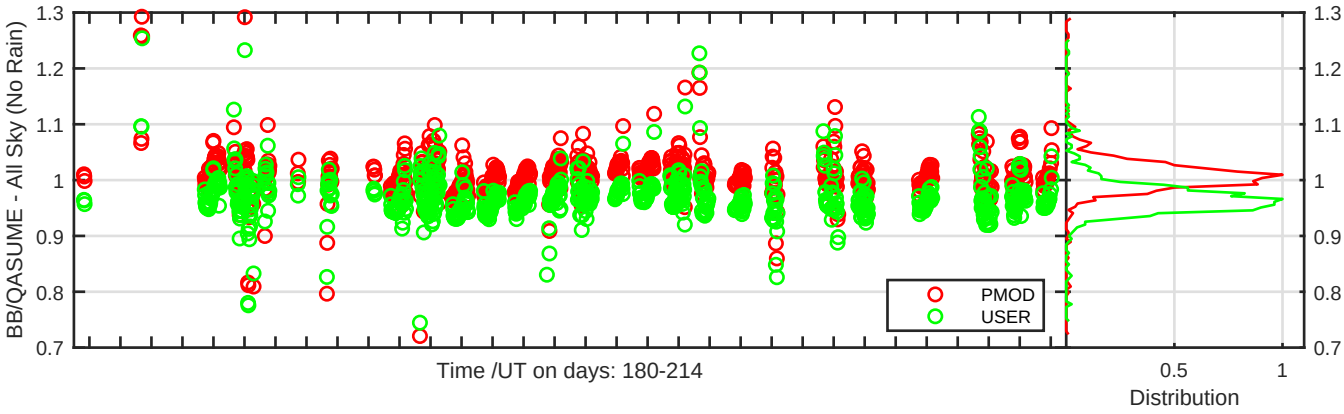

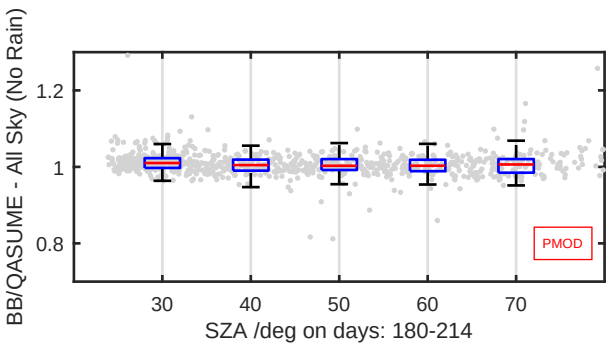

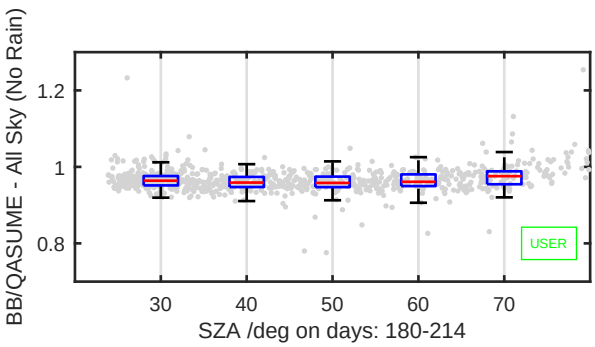

Calibration Results of SL0936 (UVE)

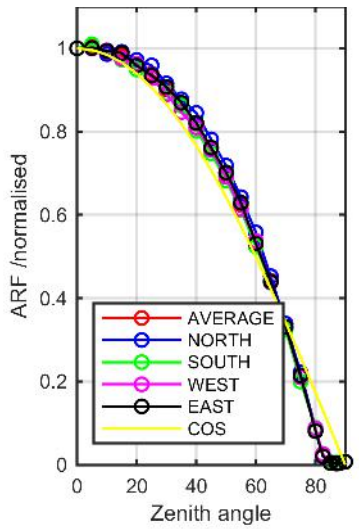

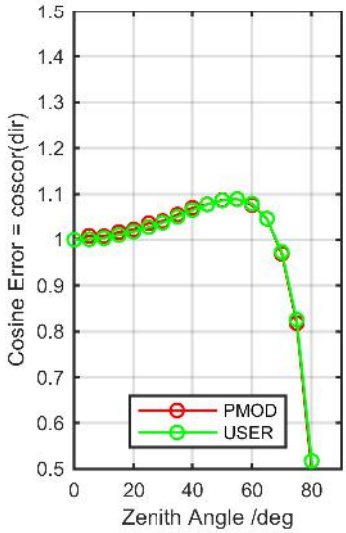

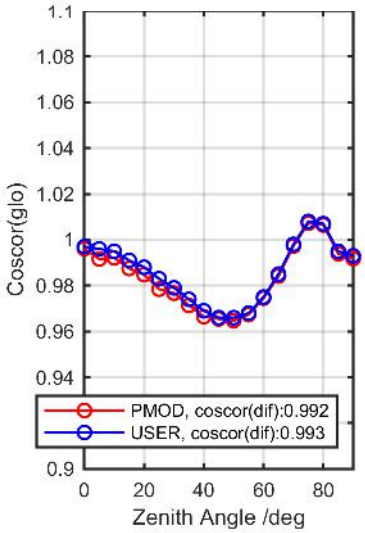

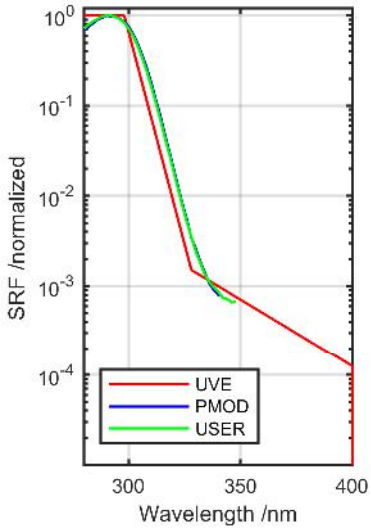

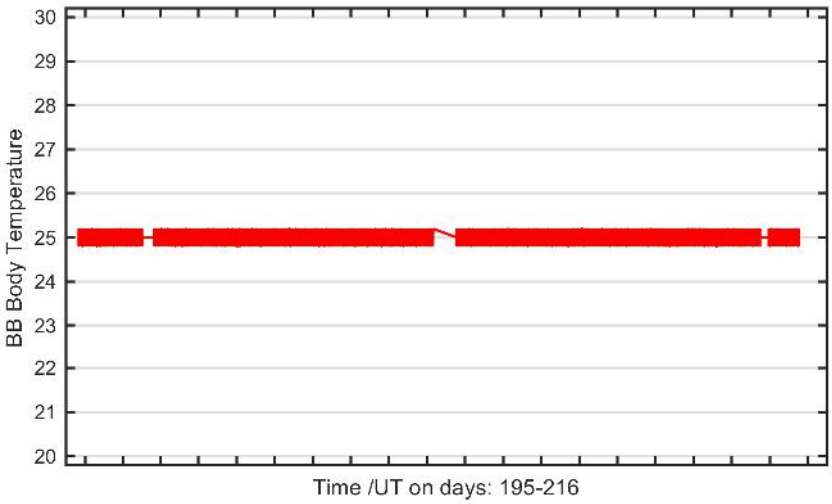

Calibration Matrix fn; Model sdisortREFms2009; f0=0.5171

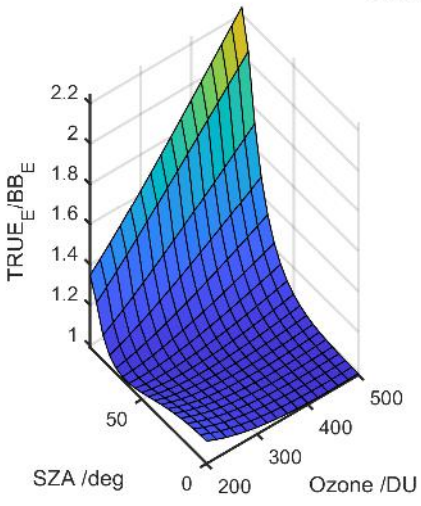

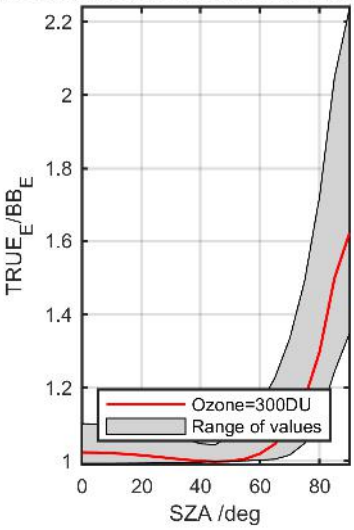

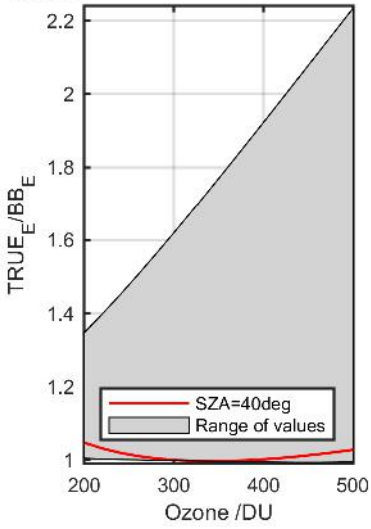

Calibration Results of SL0936 (UVE)

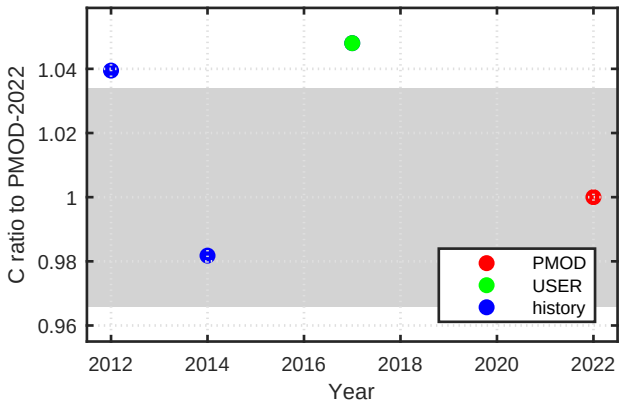

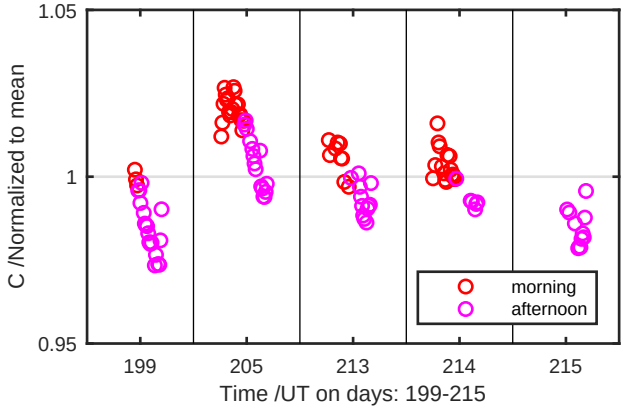

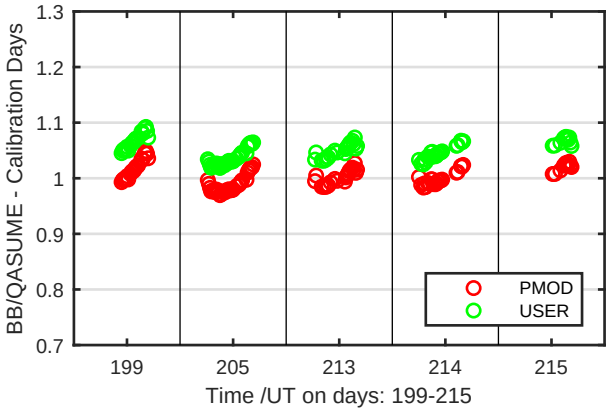

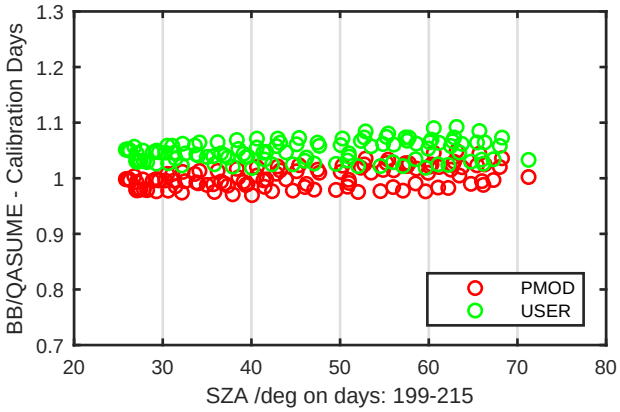

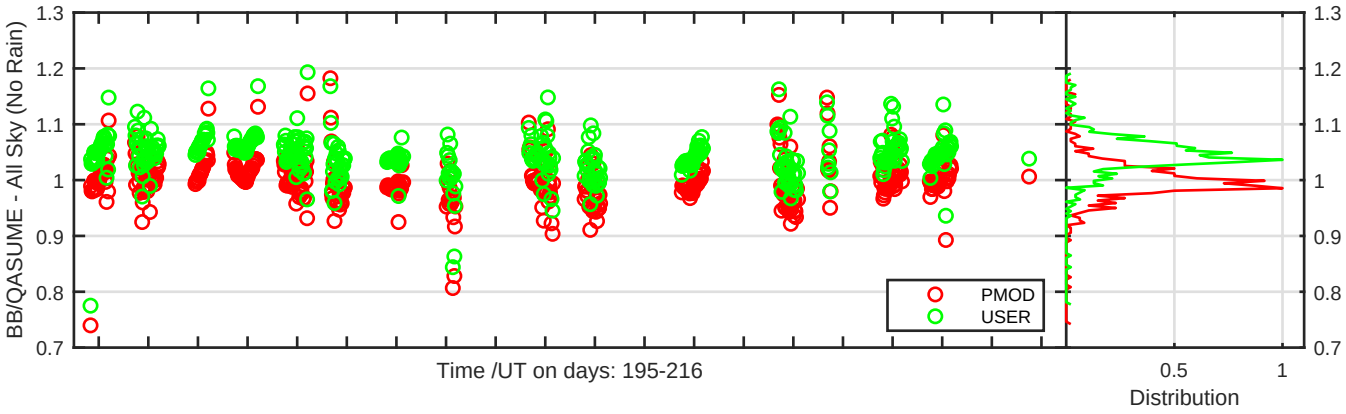

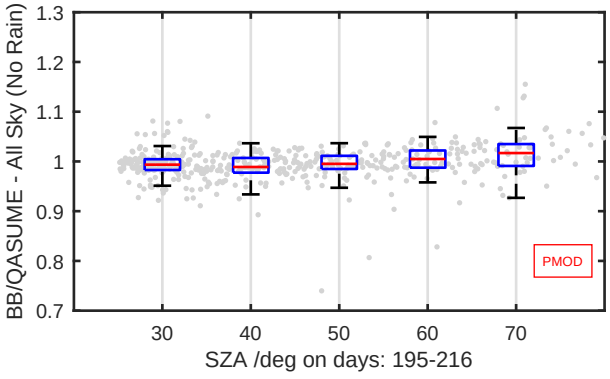

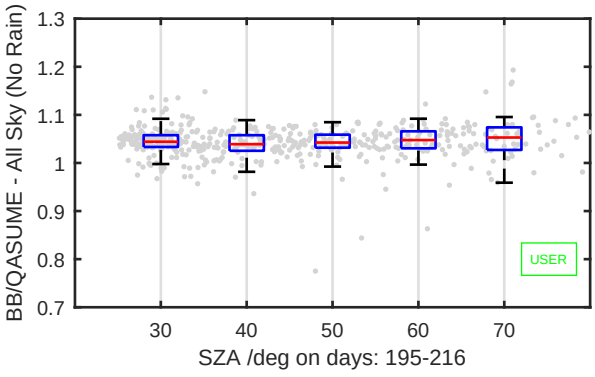

Calibration Results of SL1120 (UVE)

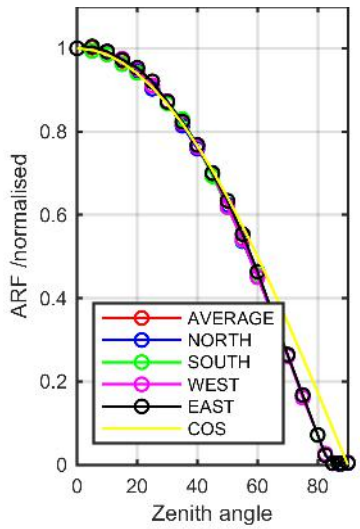

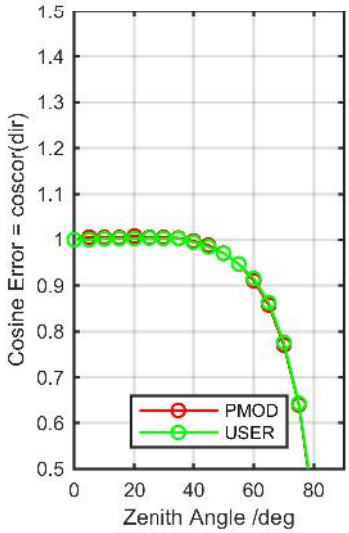

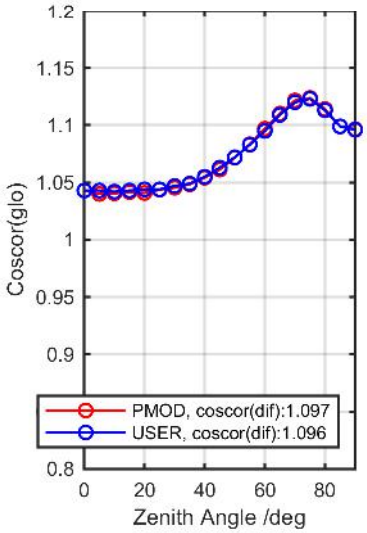

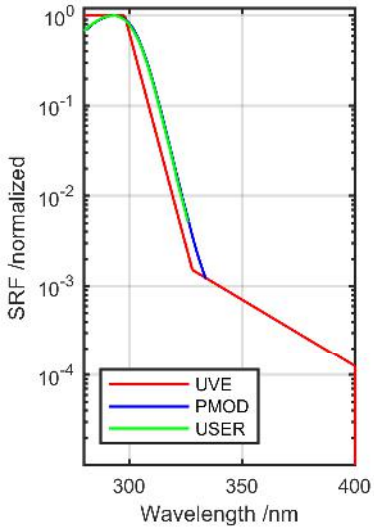

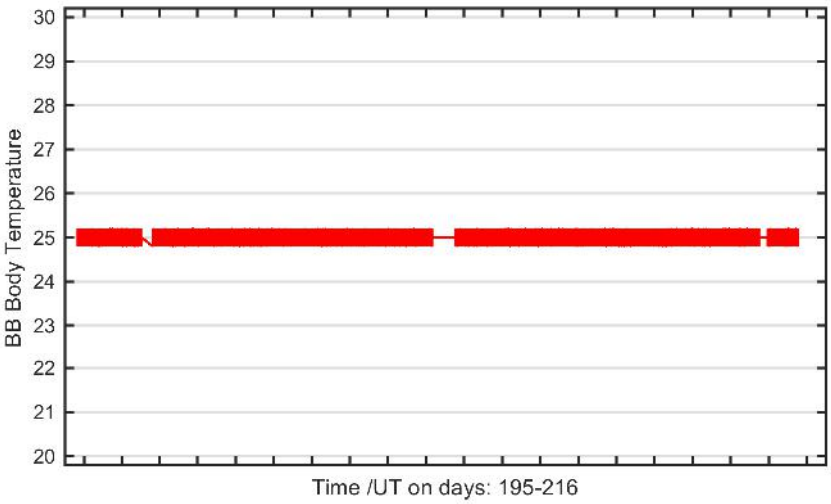

Calibration Matrix fn; Model sdisortREFms2009; f0=0.4645

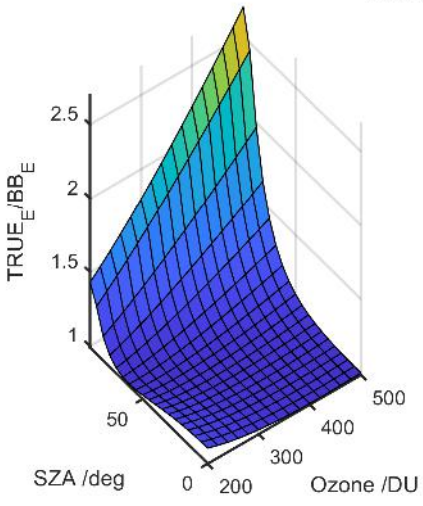

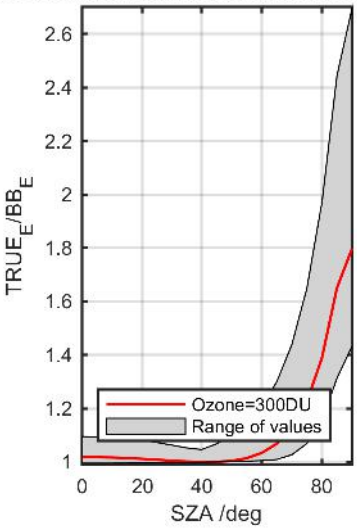

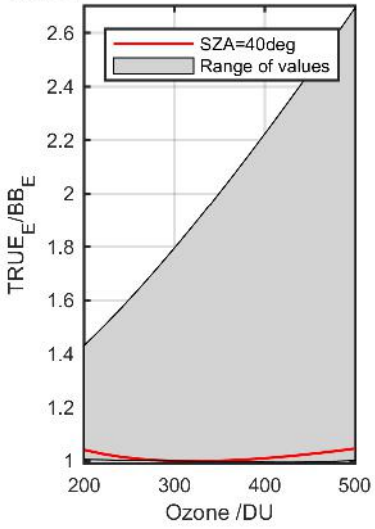

Calibration Results of SL1120 (UVE)

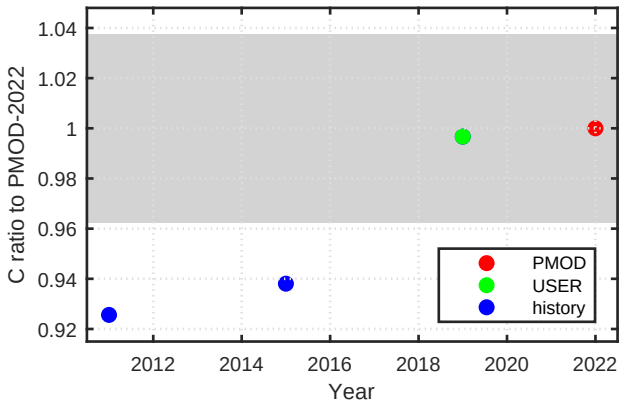

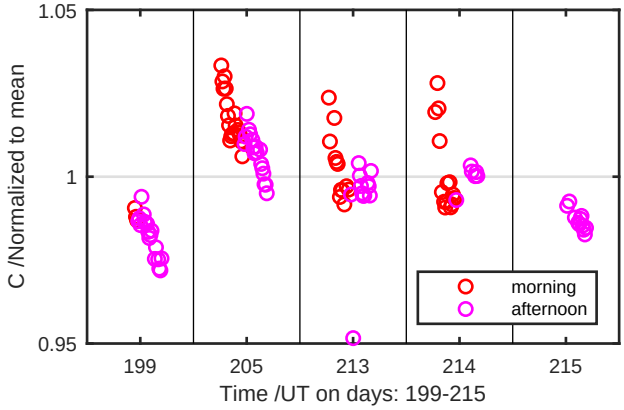

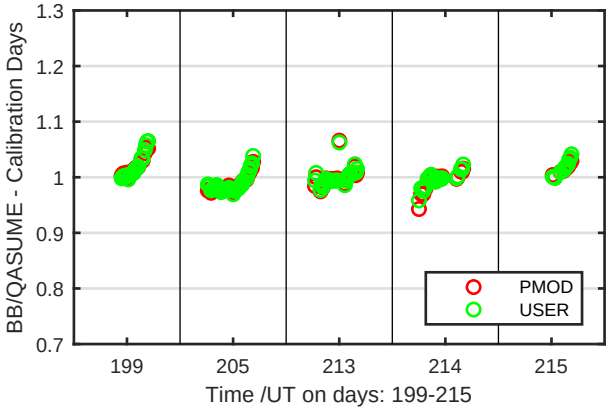

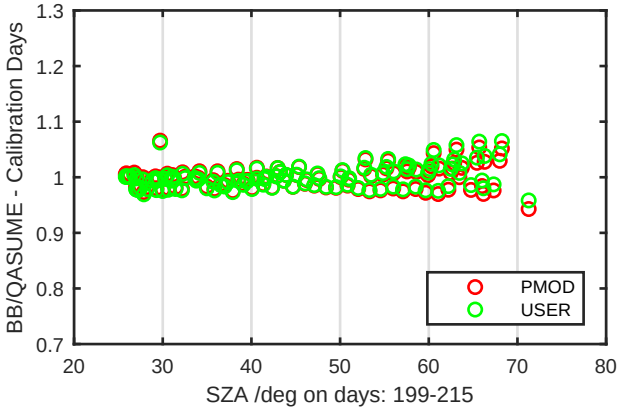

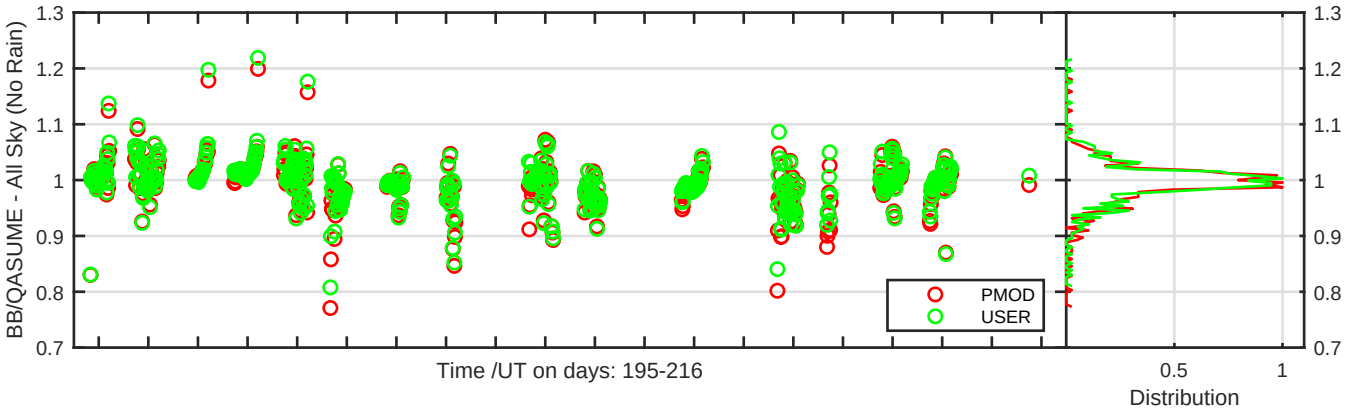

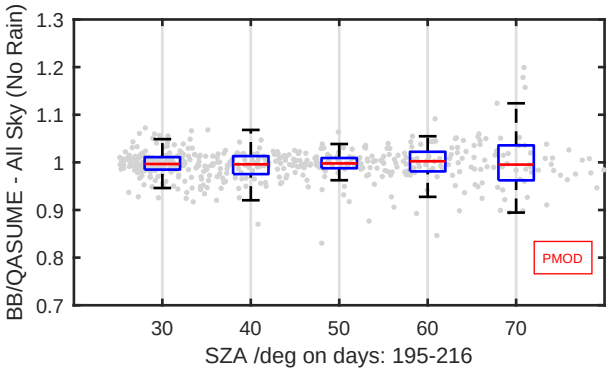

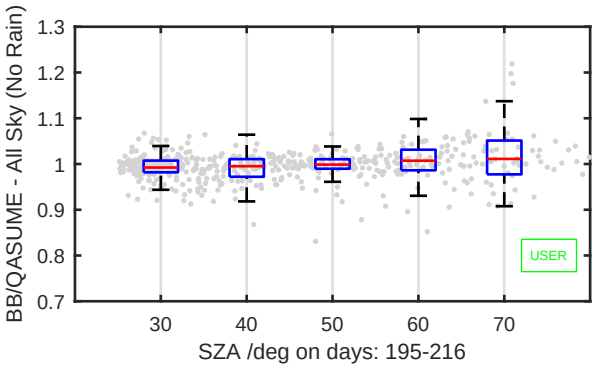

Calibration Results of SL2733 (UVE)

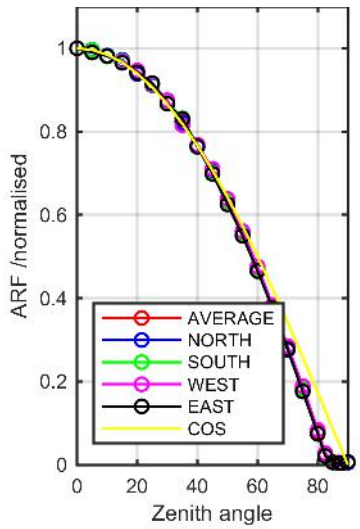

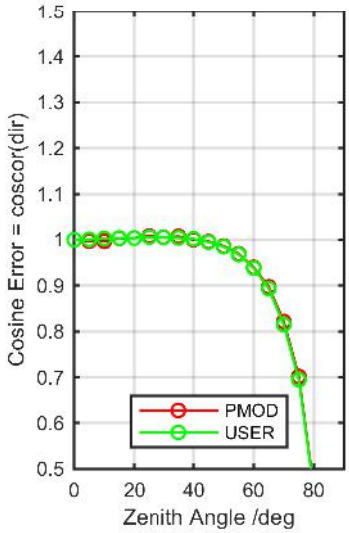

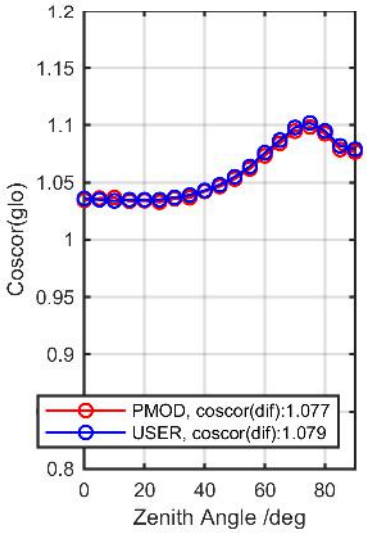

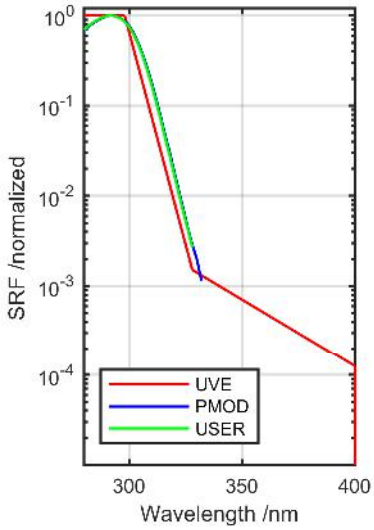

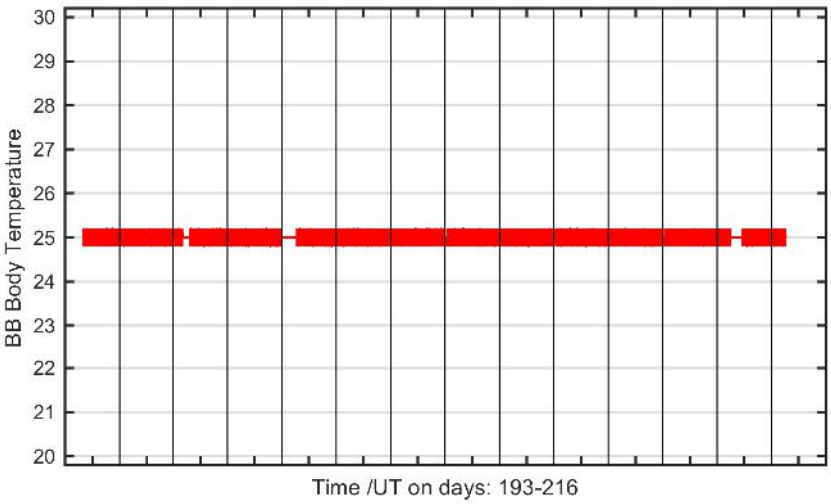

Calibration Matrix fn; Model sdisortREFms2009; f0=0.5398

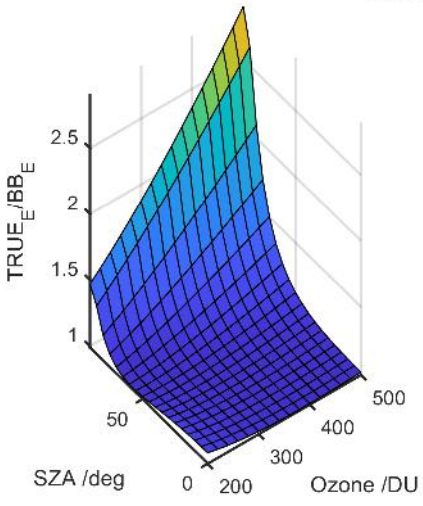

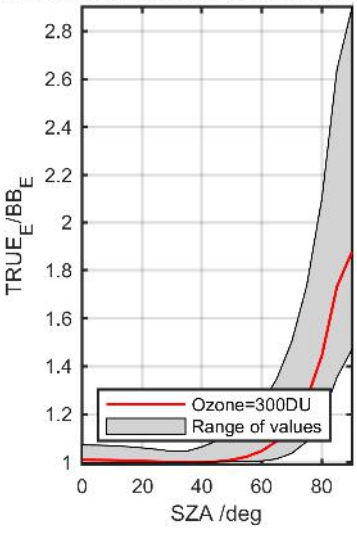

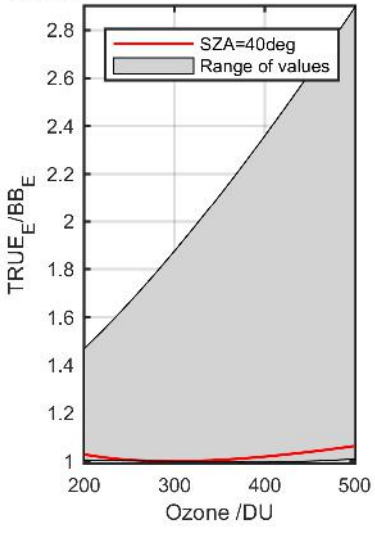

Calibration Results of SL2733 (UVE)

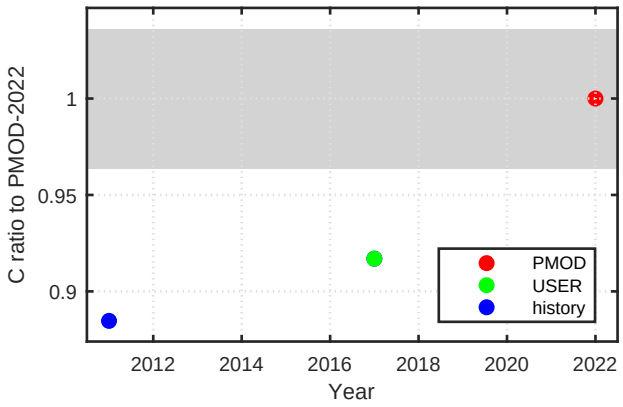

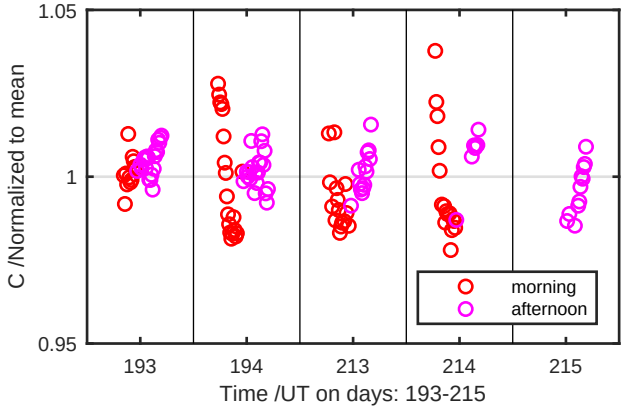

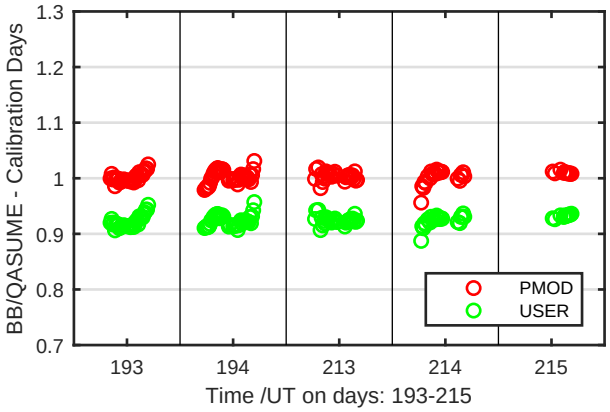

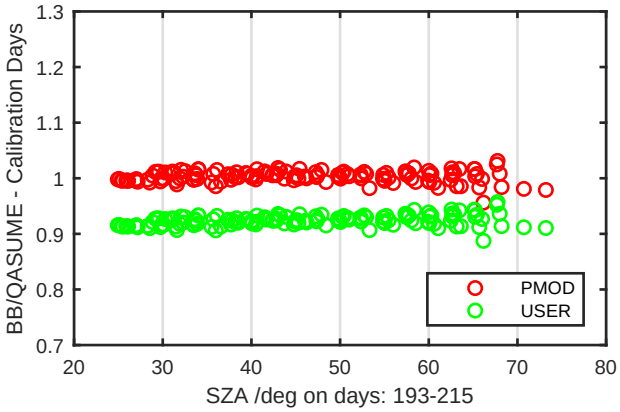

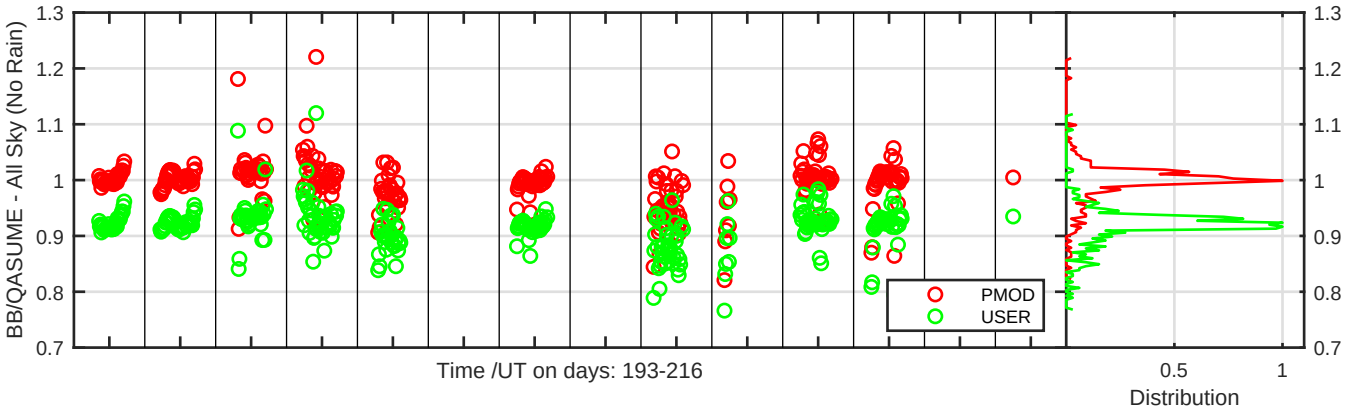

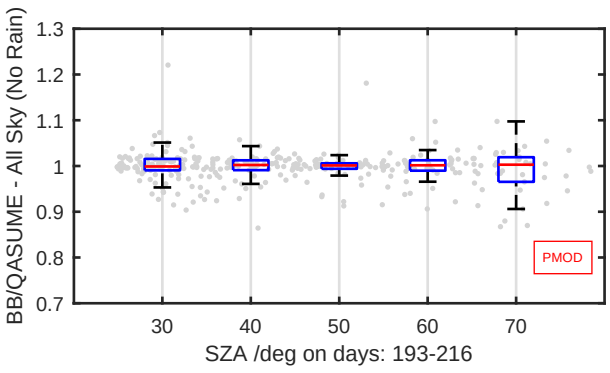

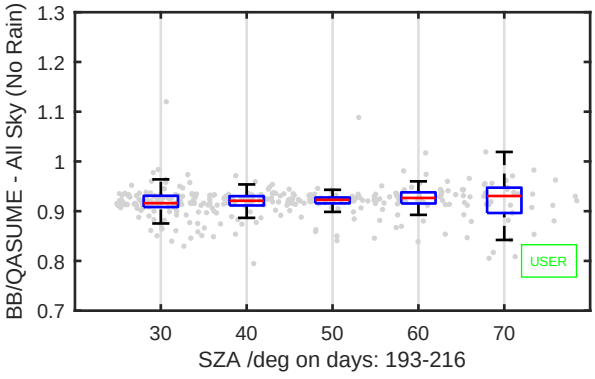

Calibration Results of SL4811 (UVE)

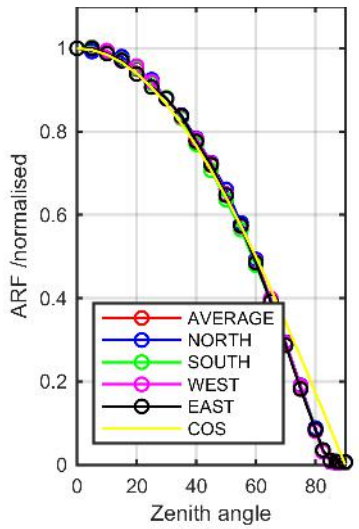

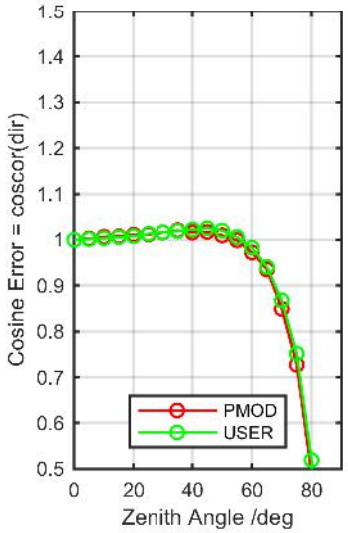

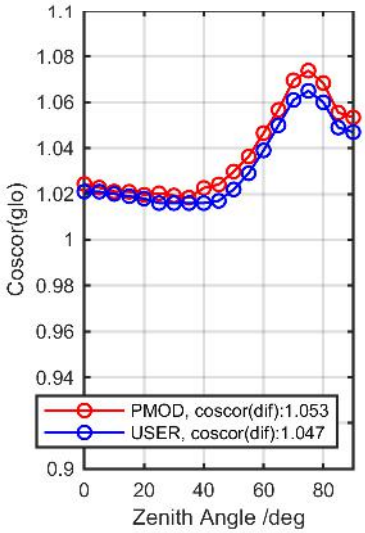

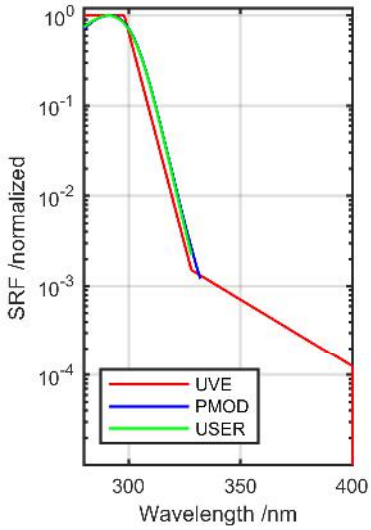

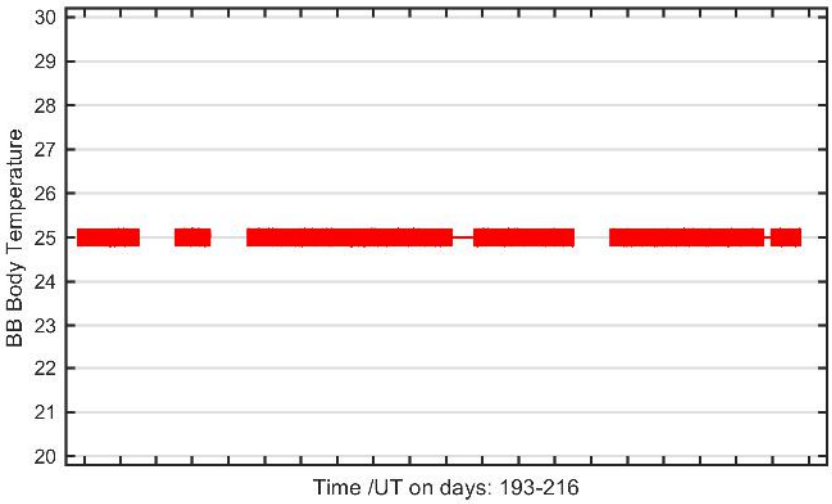

Calibration Matrix fn; Model sdisortREFms2009; f0=0.6133

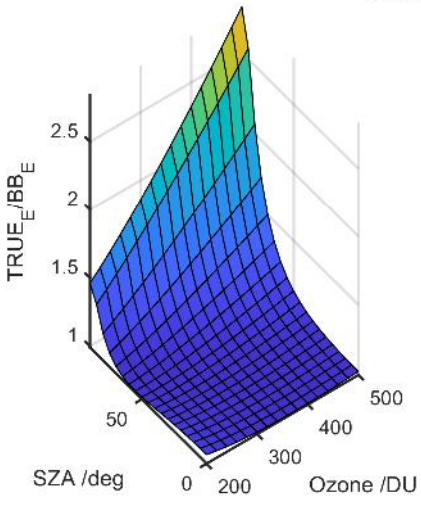

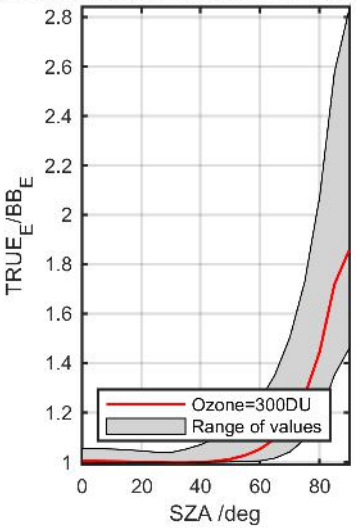

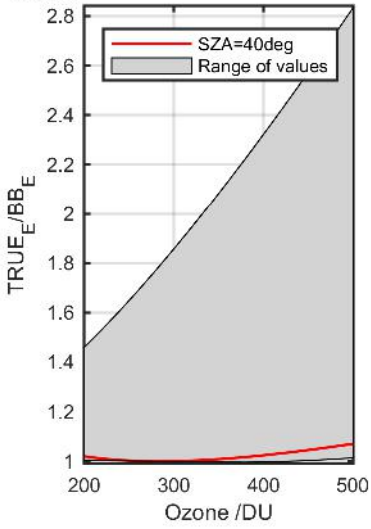

Calibration Results of SL4811 (UVE)

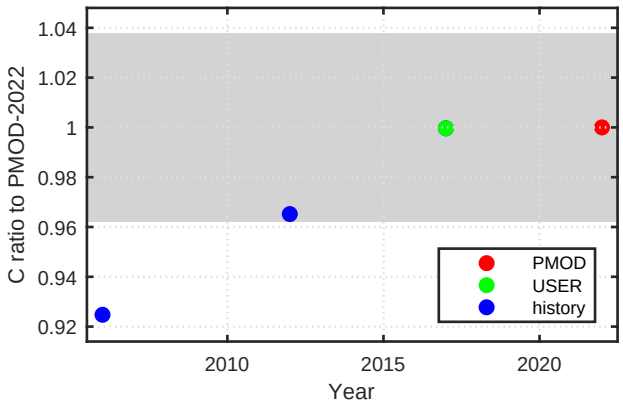

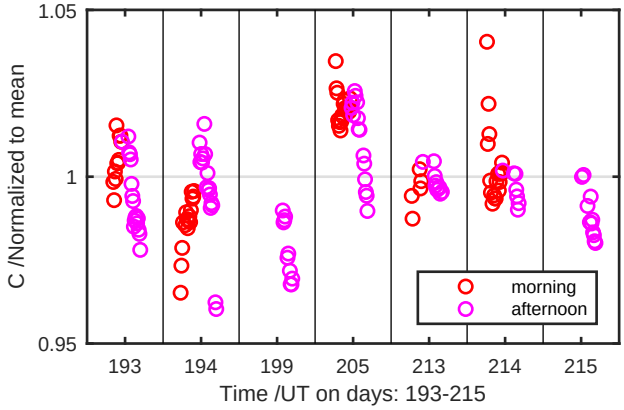

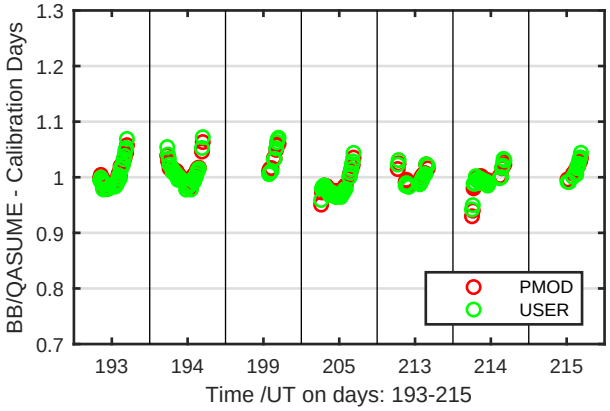

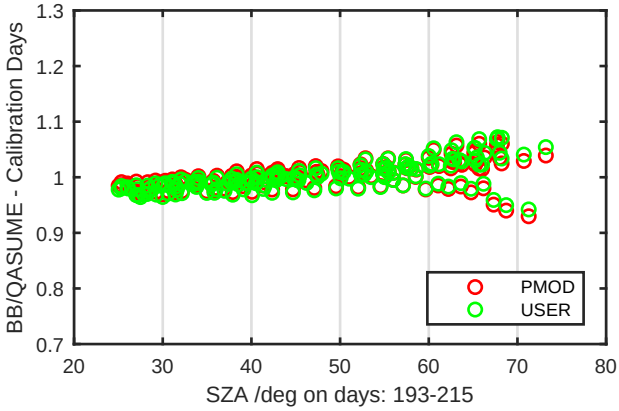

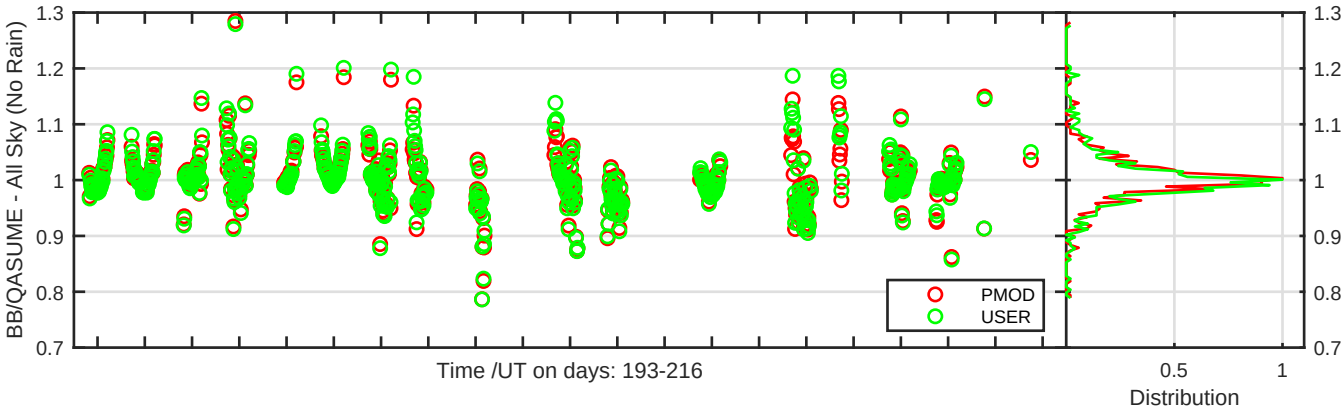

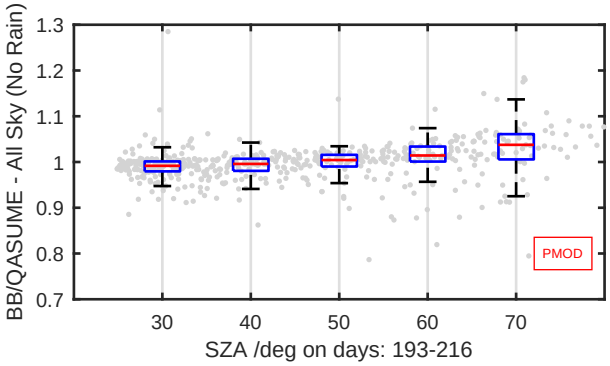

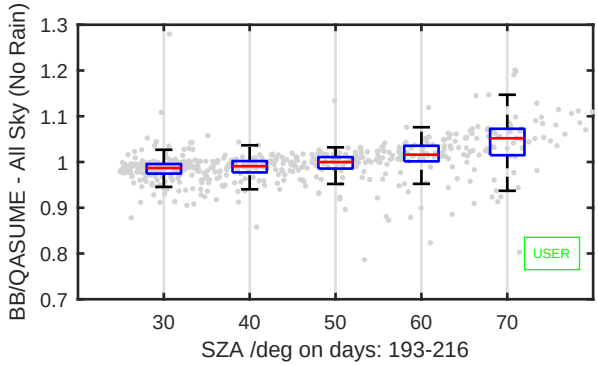

Calibration Results of SL16723 (UVE)

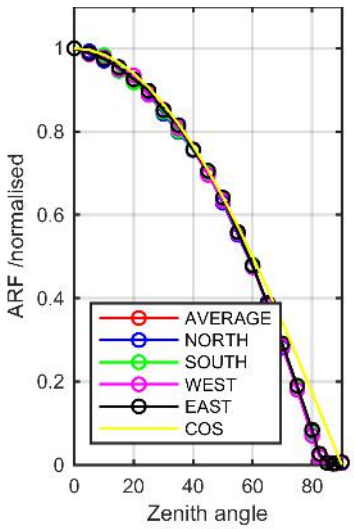

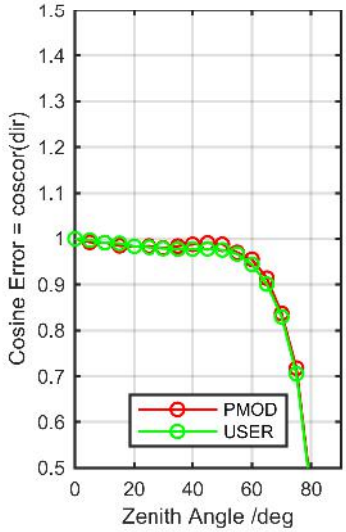

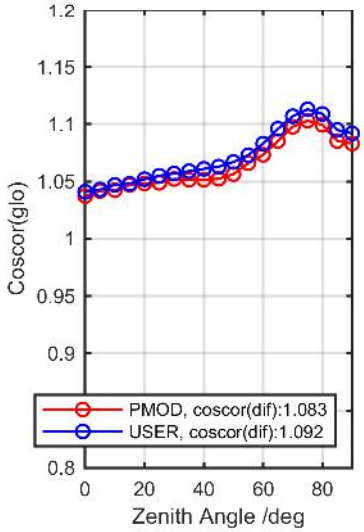

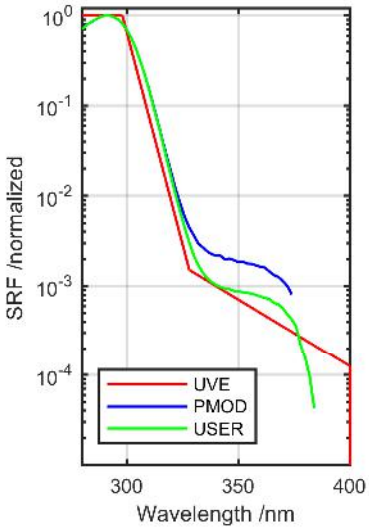

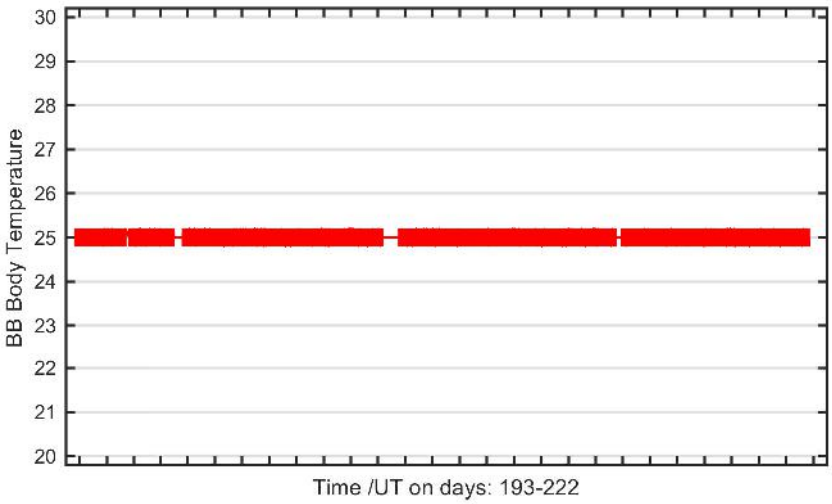

Calibration Matrix fn; Model sdisortREFms2009; f0=0.5230

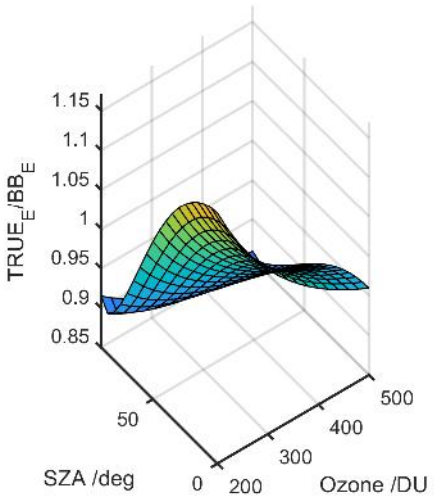

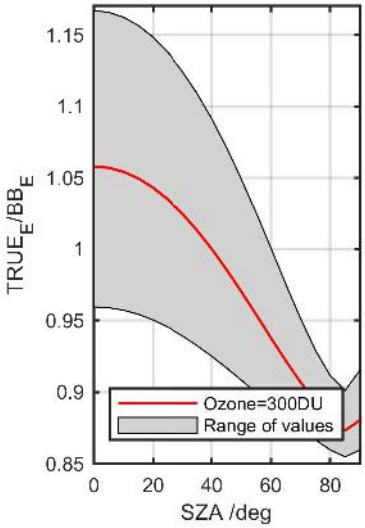

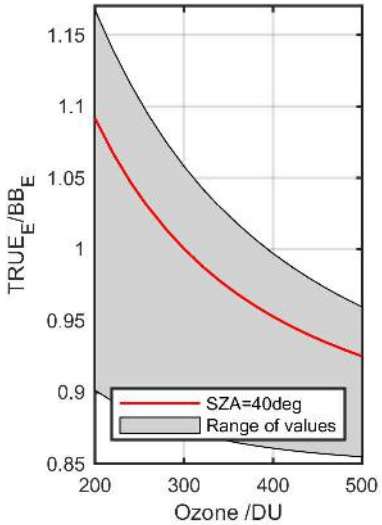

Calibration Results of SL16723 (UVE)

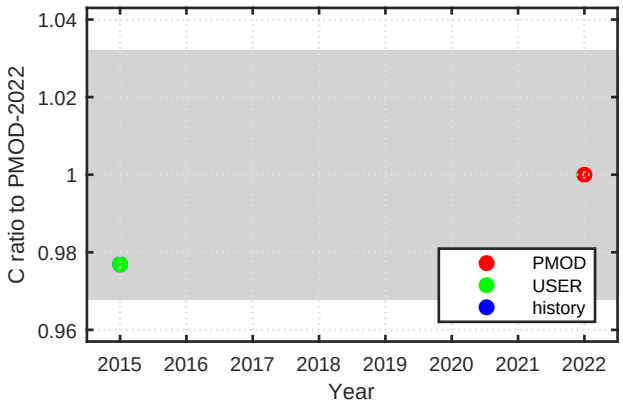

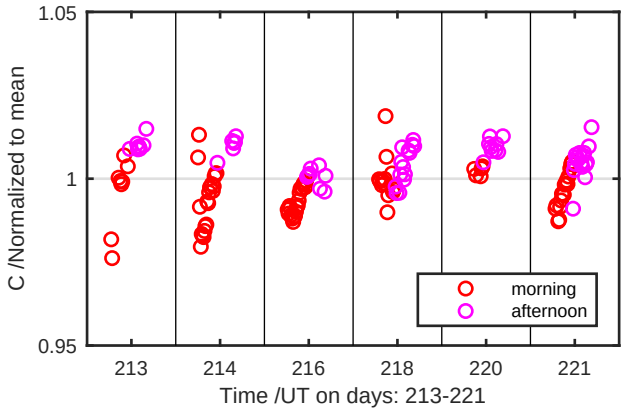

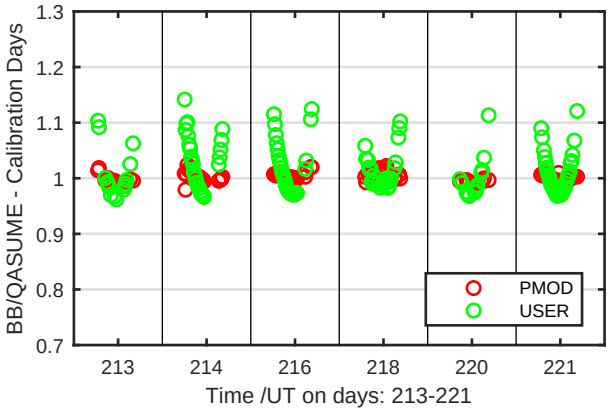

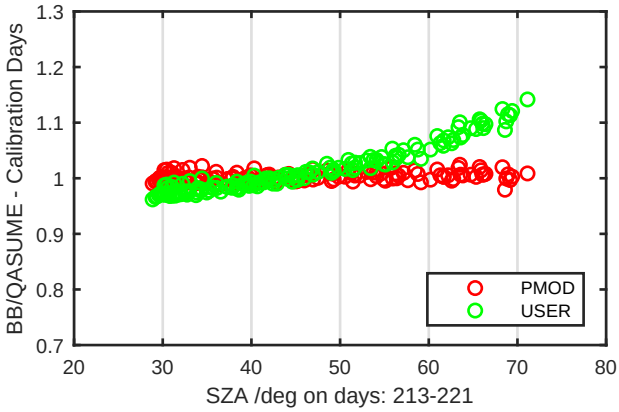

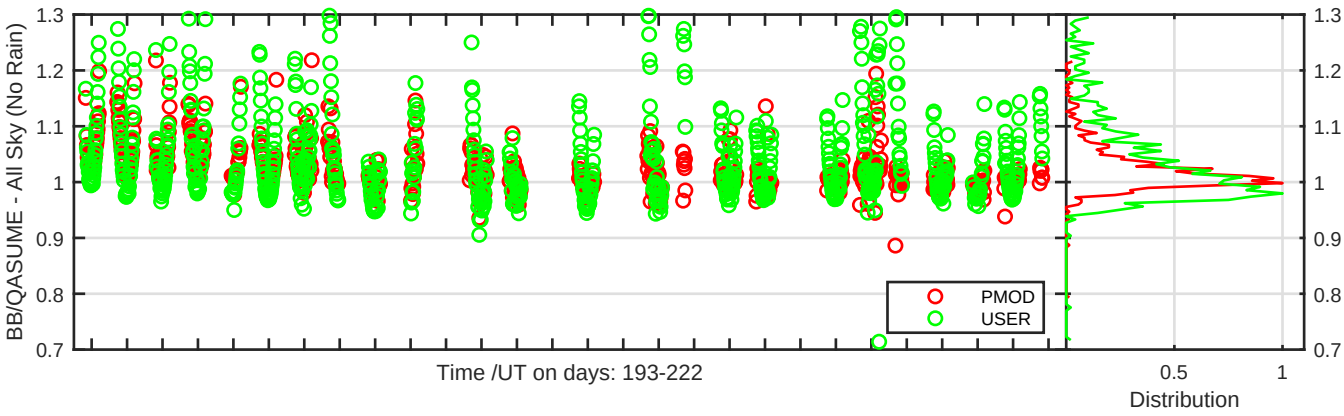

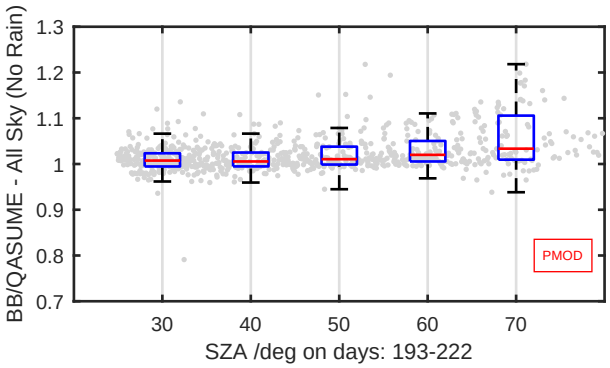

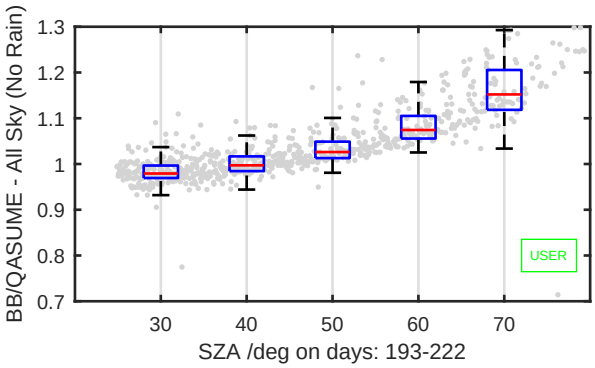

Calibration Results of SL21883 (UVE)

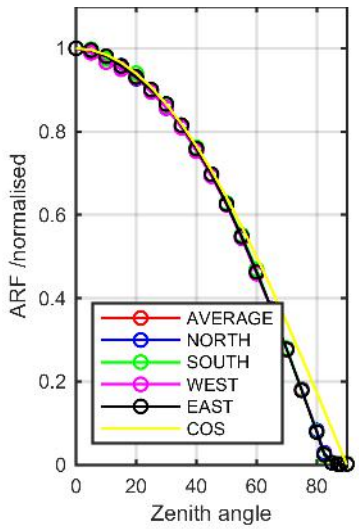

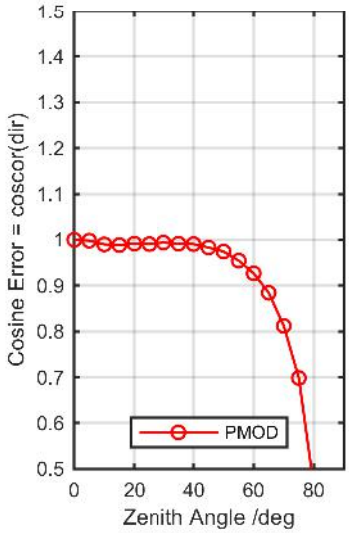

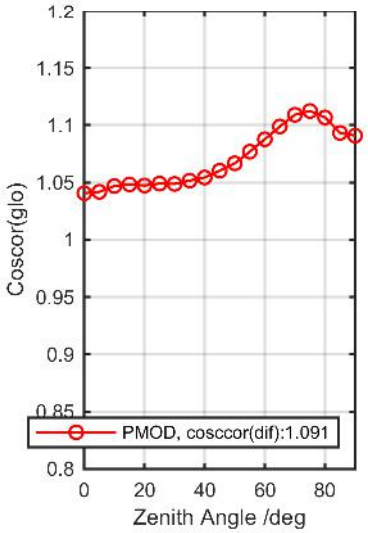

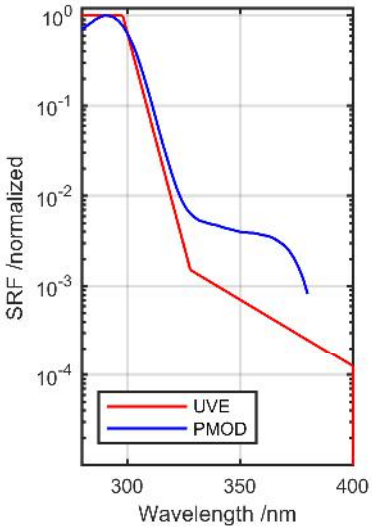

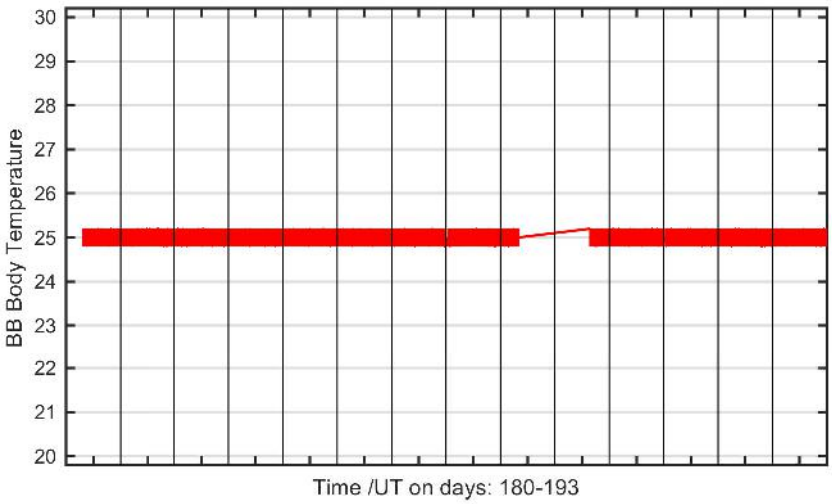

Calibration Matrix fn; Model sdisortREFms2009; f0=0.4764

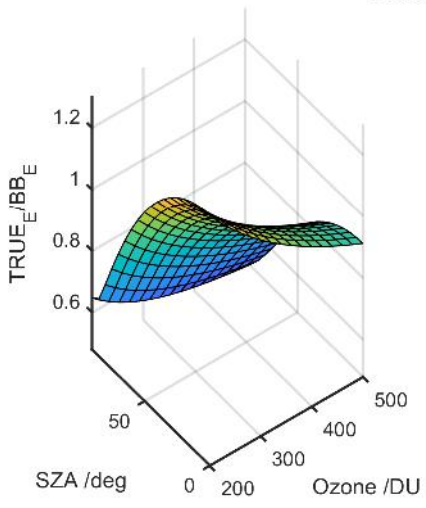

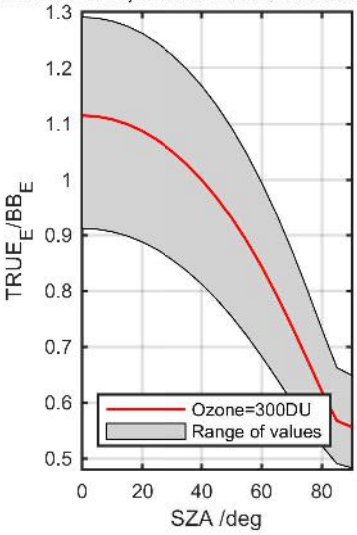

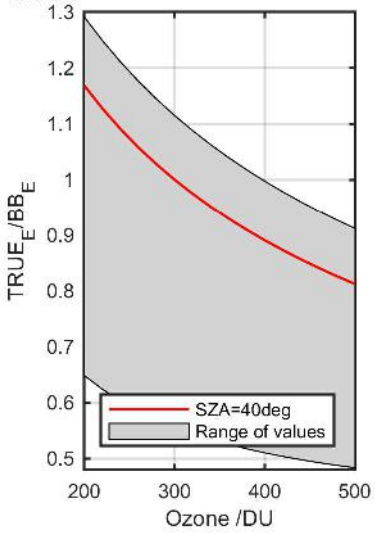

Calibration Results of SL21883 (UVE)

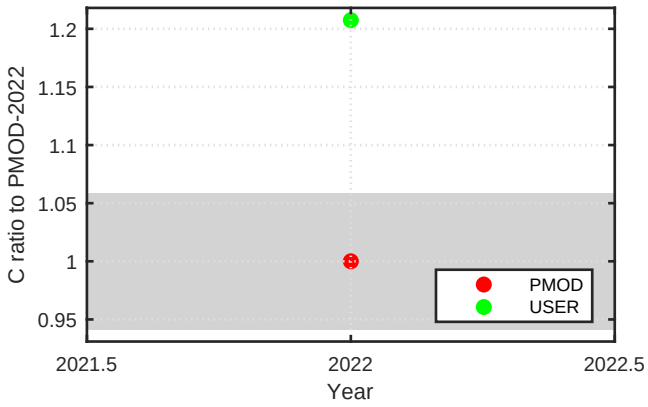

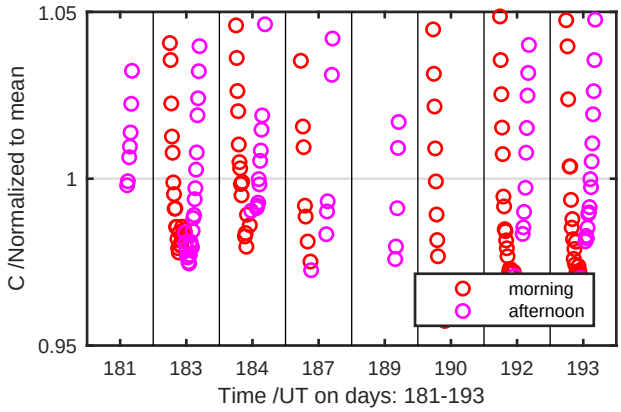

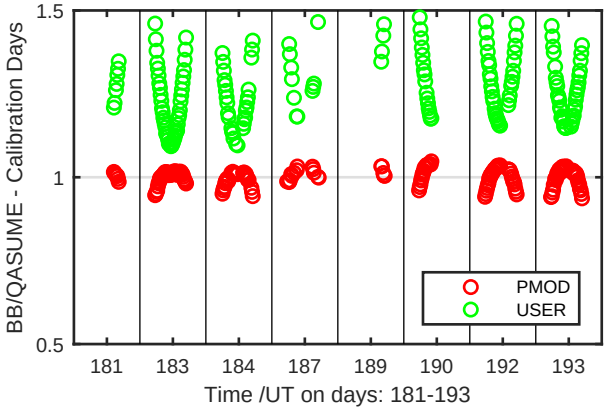

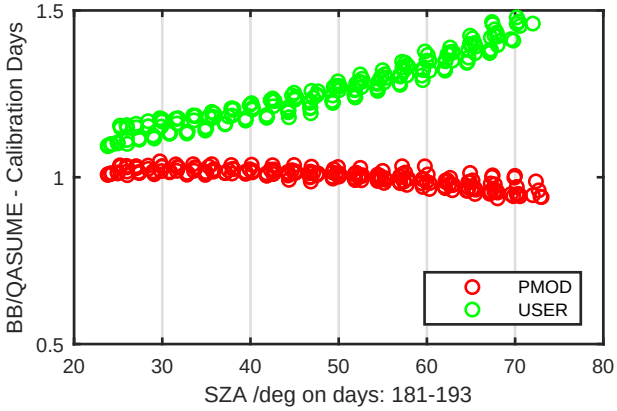

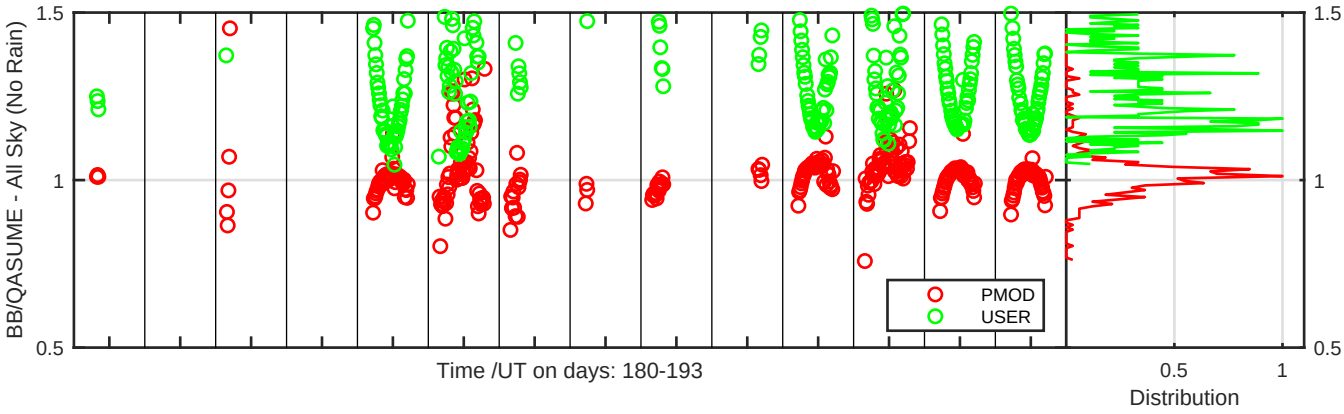

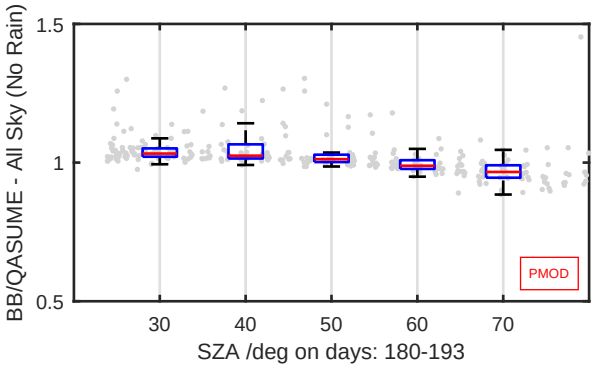

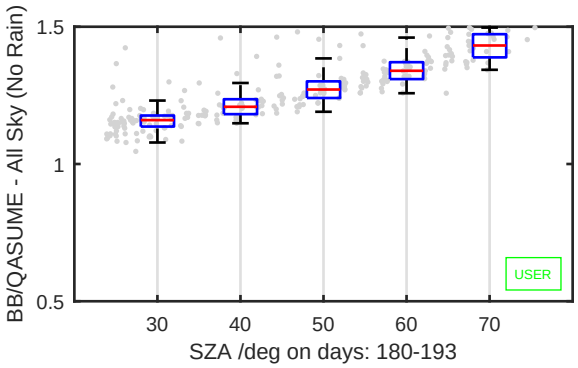

Calibration Results of SL16724 (UVA)

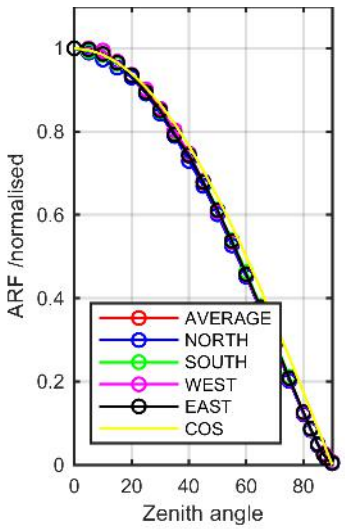

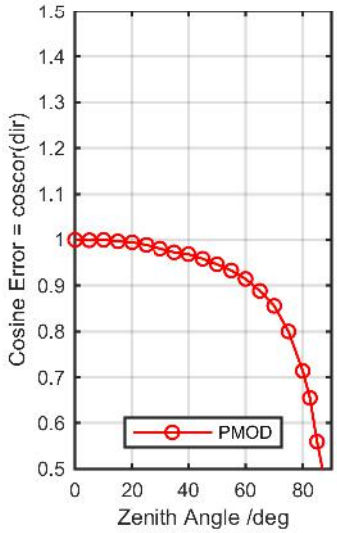

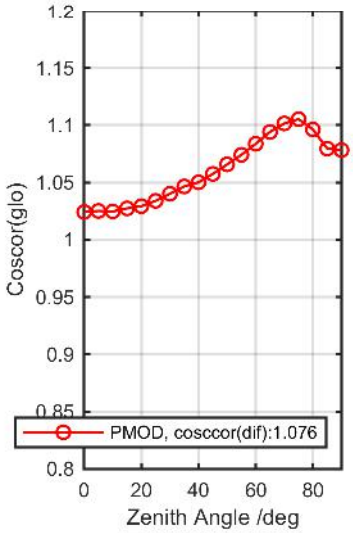

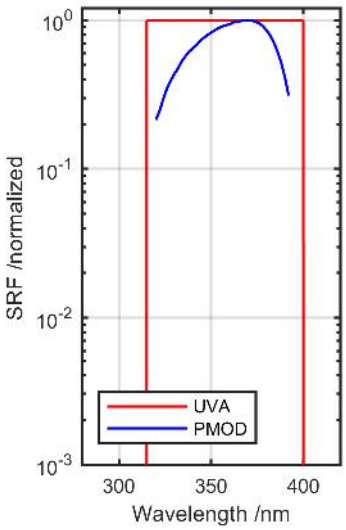

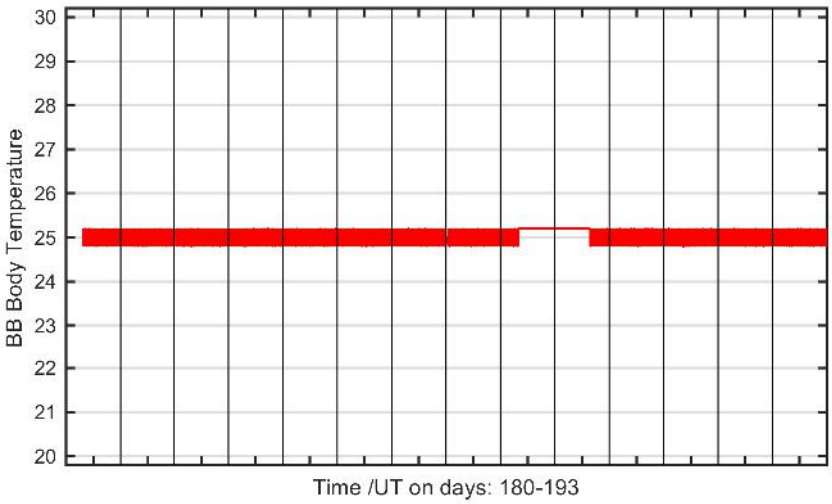

Calibration Matrix fn; Model sdisortREFms2009; f0=1.5457

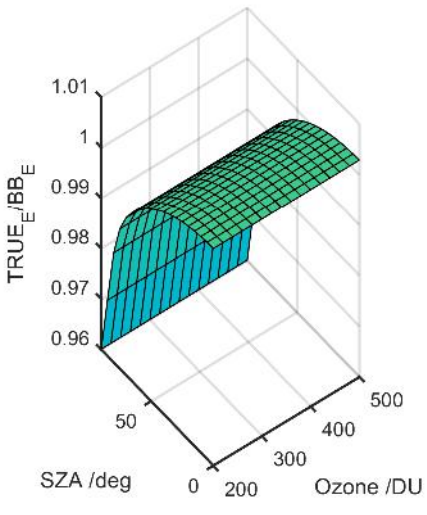

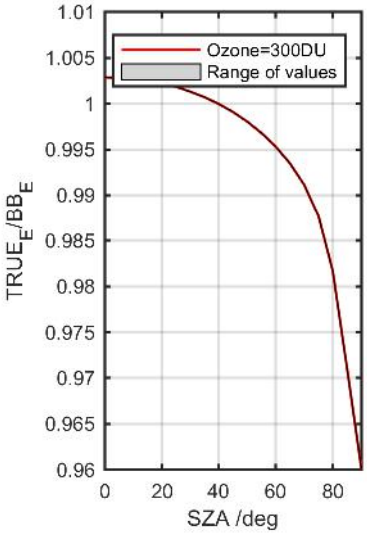

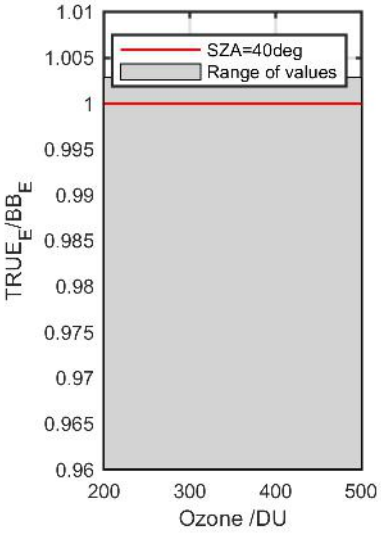

Calibration Results of SL16724 (UVA)

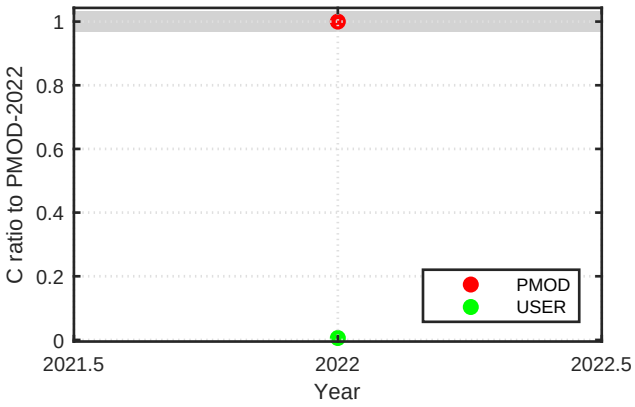

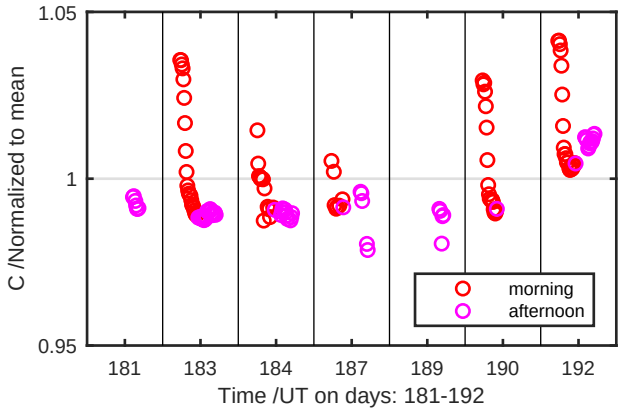

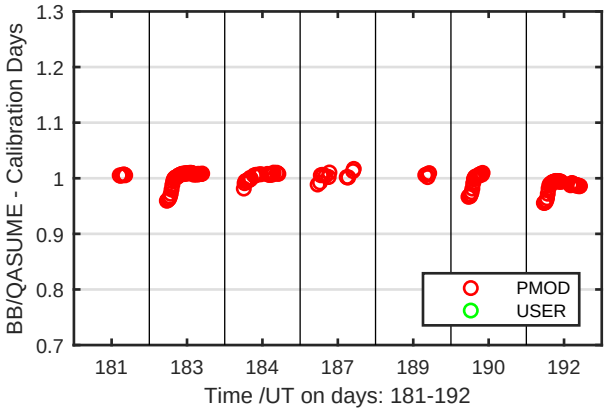

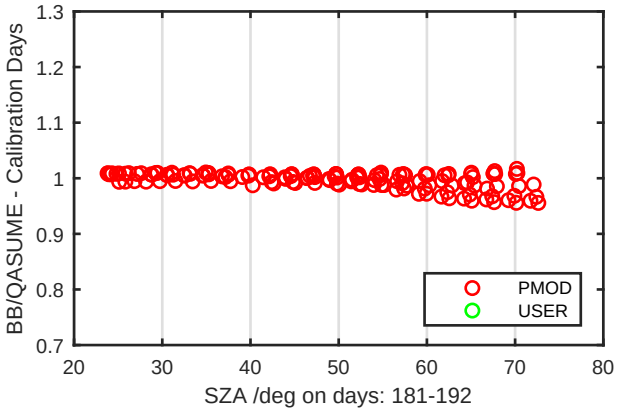

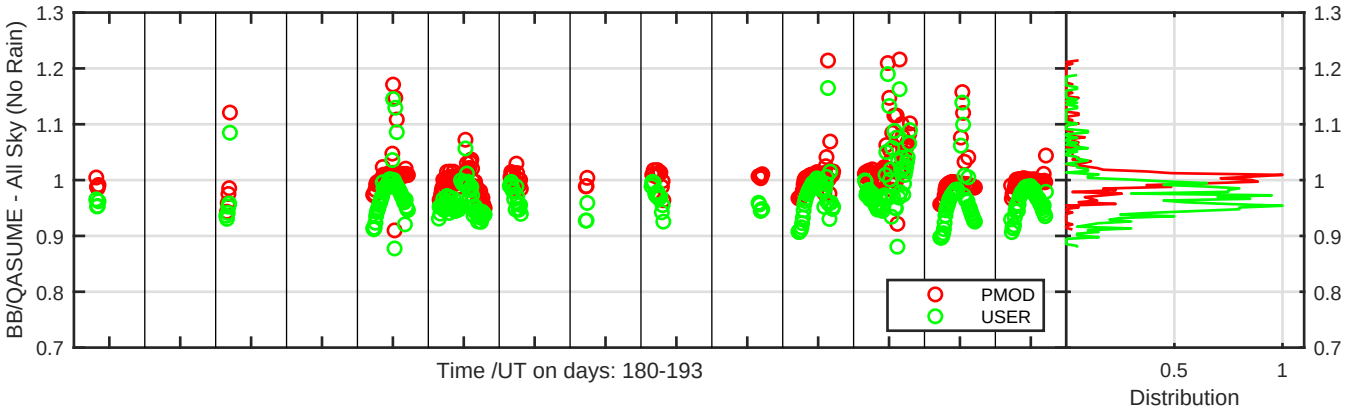

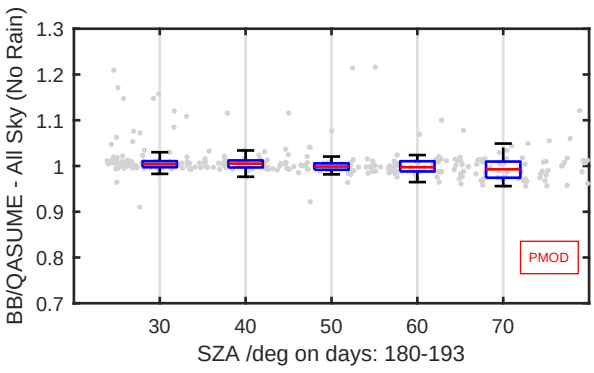

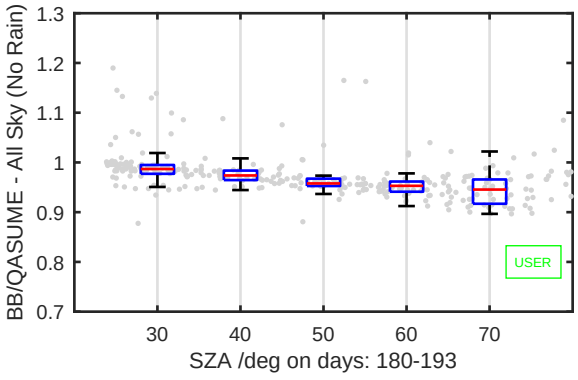

Calibration Results of SL16725 (UVA)

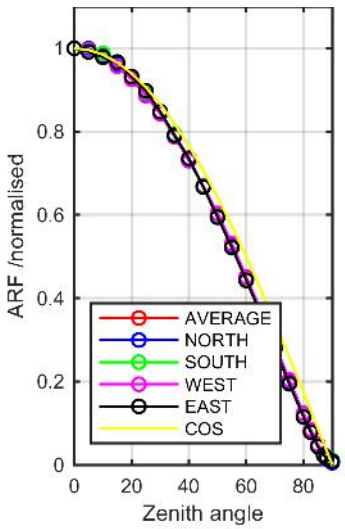

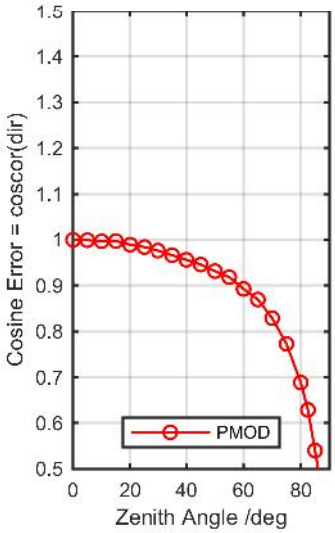

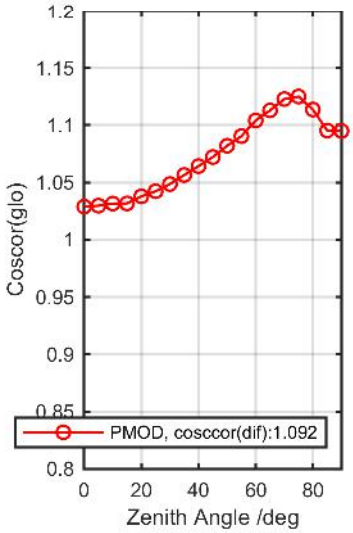

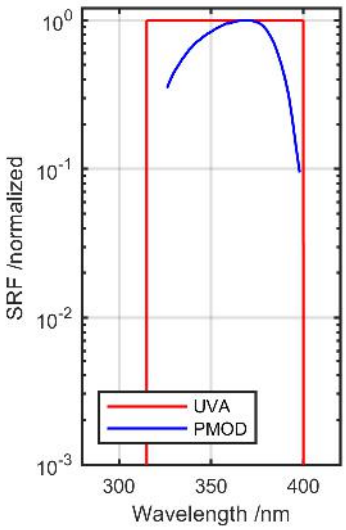

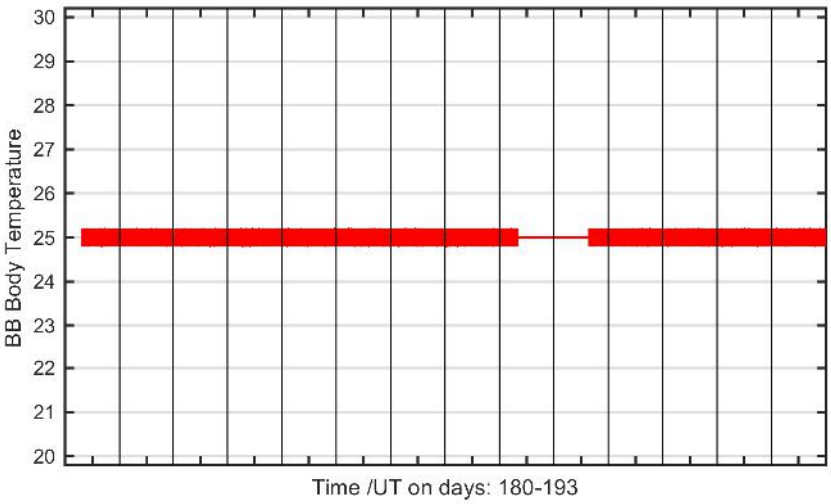

Calibration Matrix fn; Model sdisortREFms2009; f0=1.5145

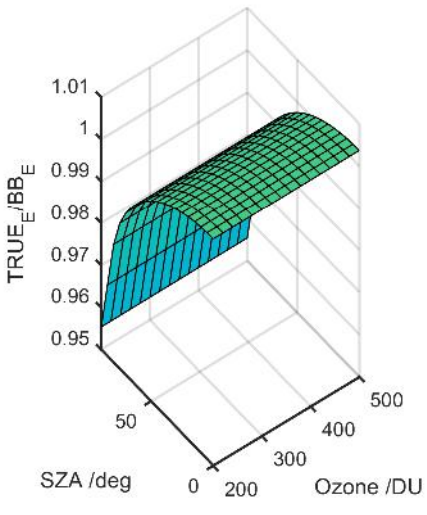

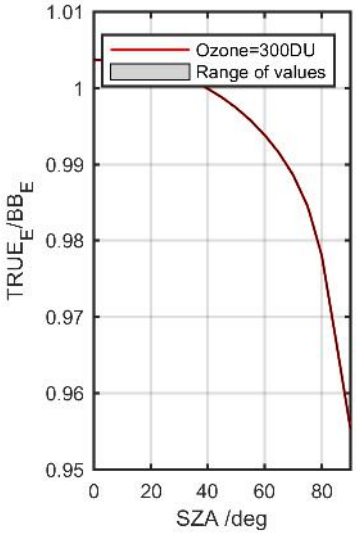

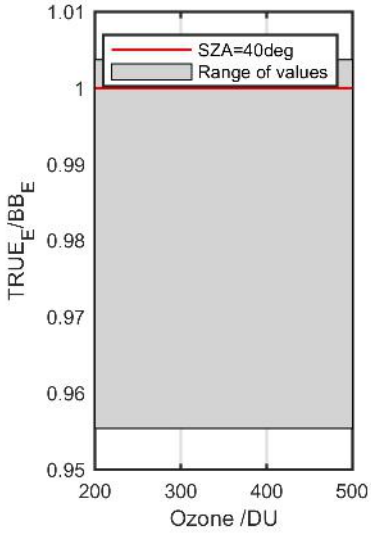

Calibration Results of SL16725 (UVA)

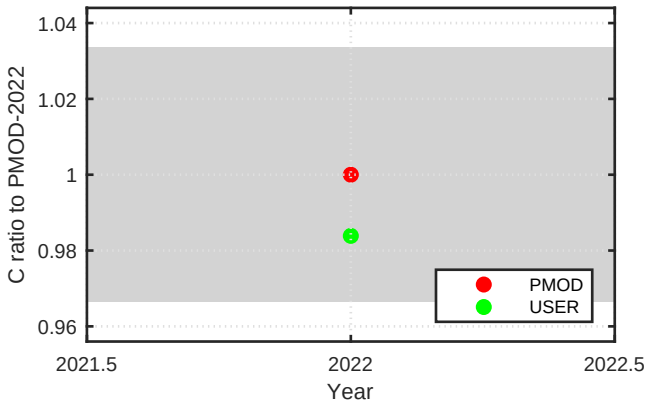

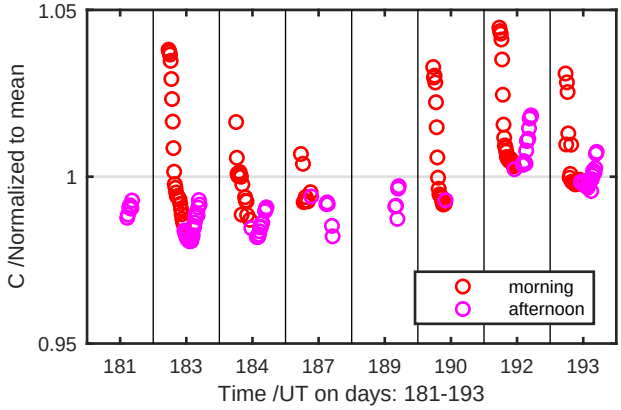

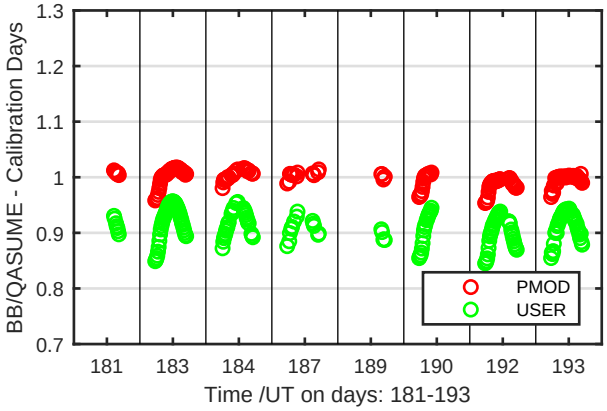

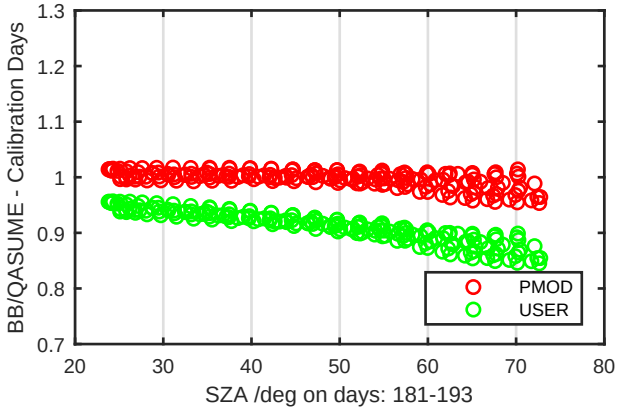

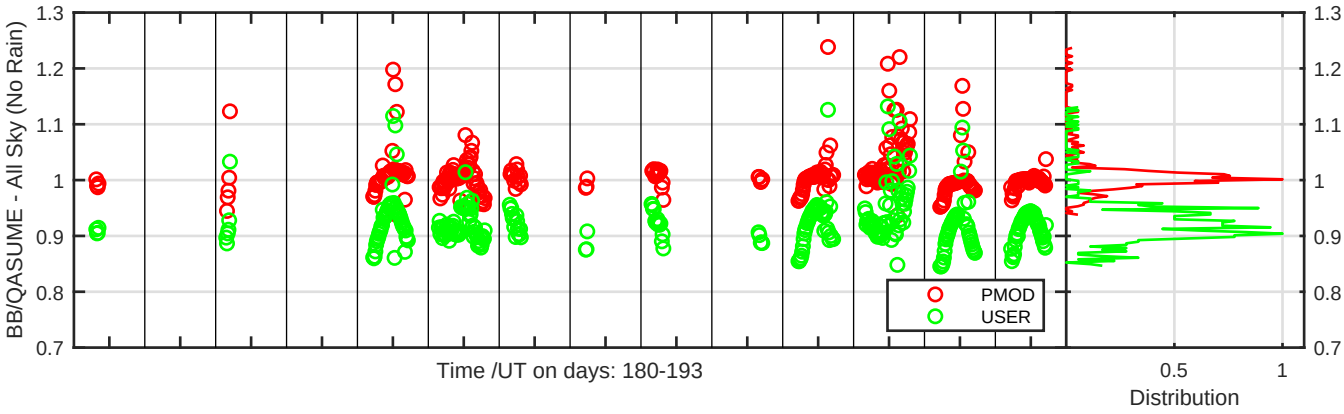

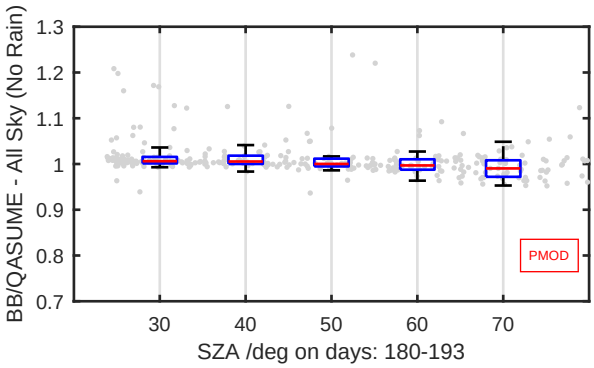

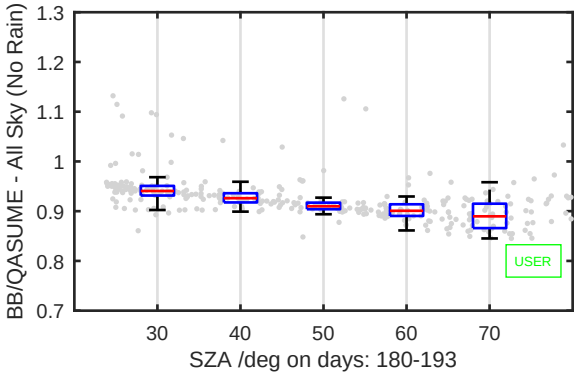

Calibration Results of SL21904 (UVA)

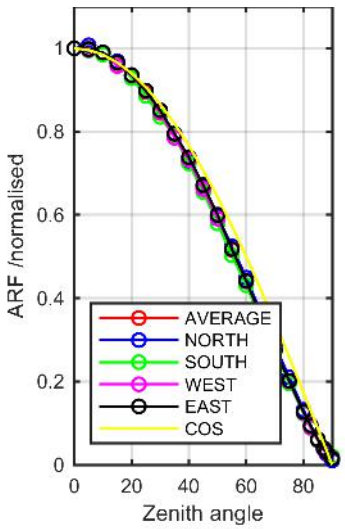

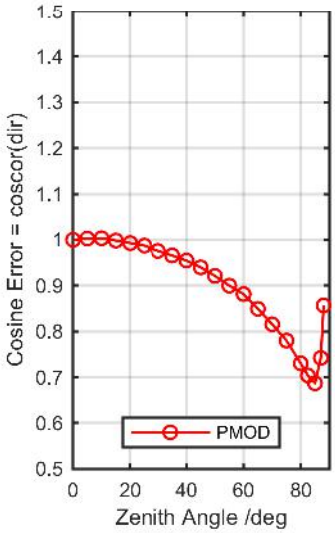

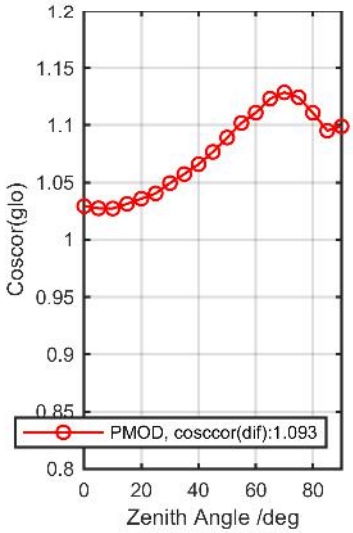

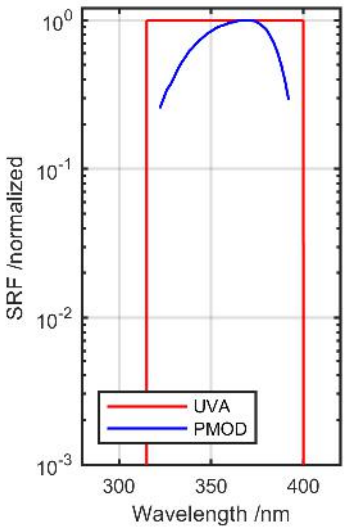

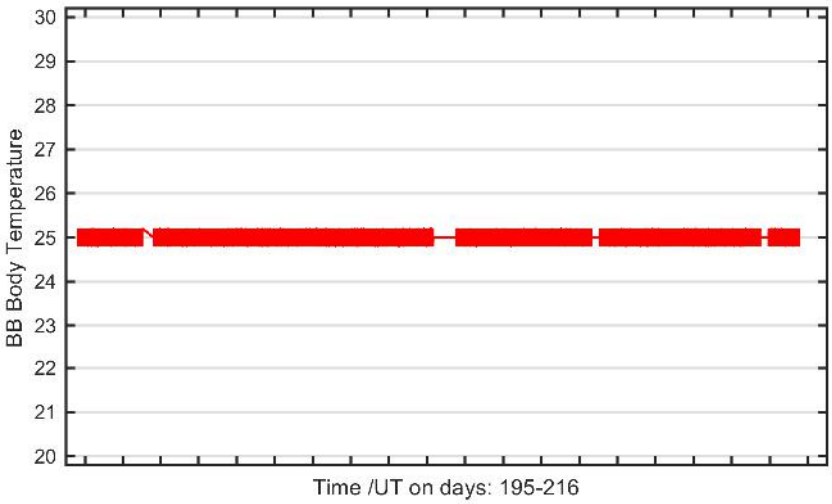

Calibration Matrix fn; Model sdisortREFms2009; f0=1.5443

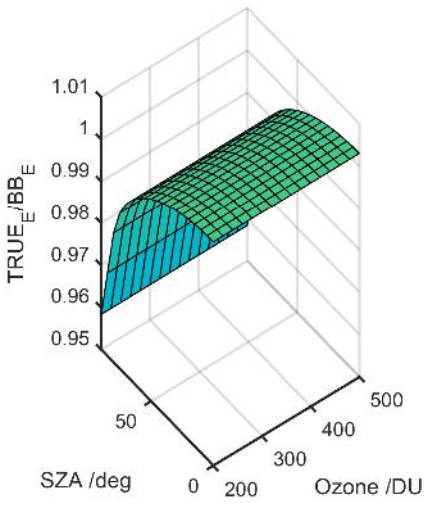

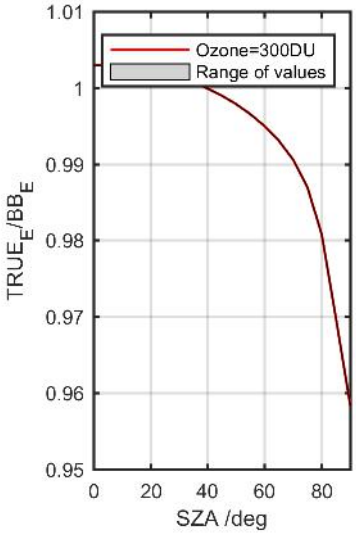

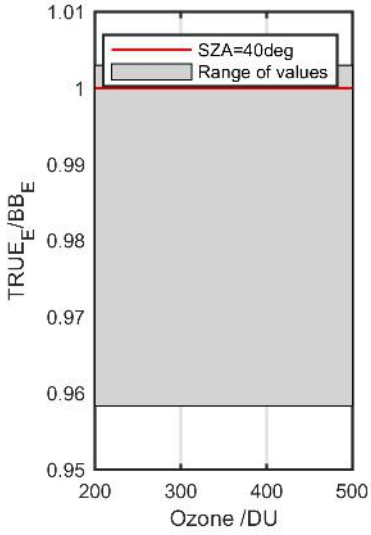

Calibration Results of SL21904 (UVA)

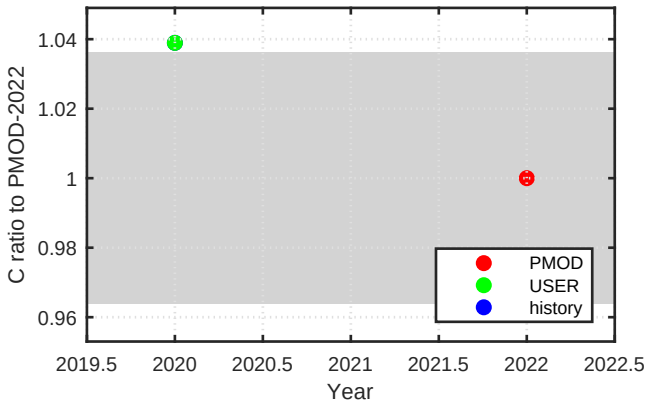

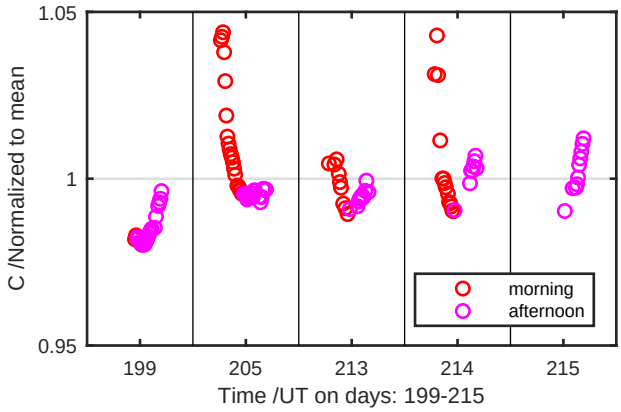

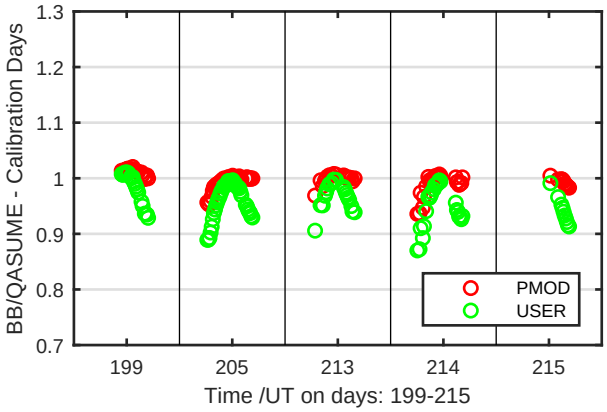

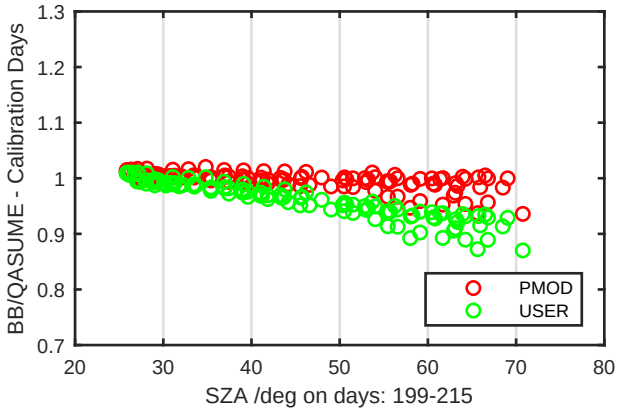

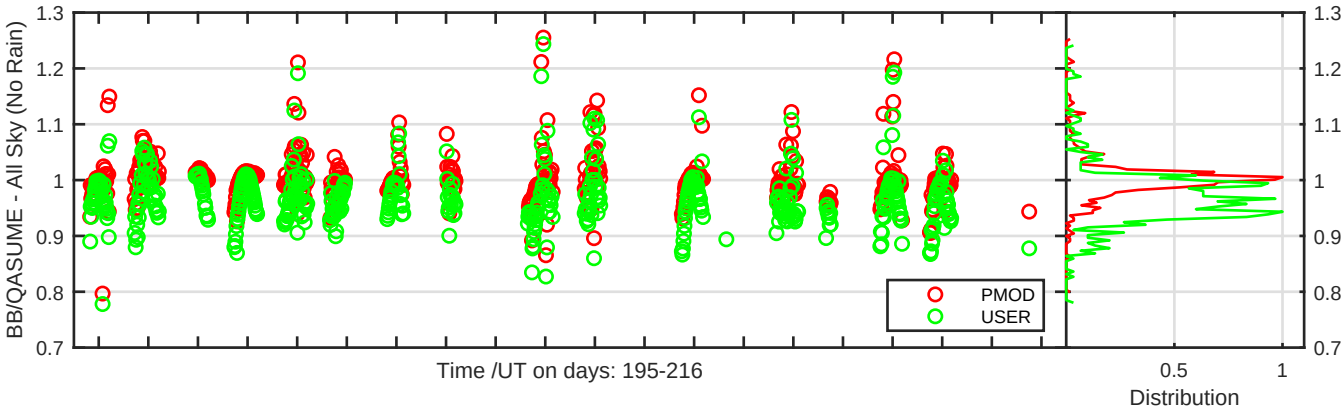

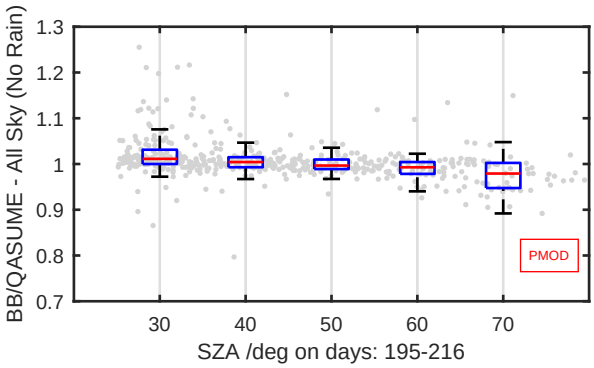

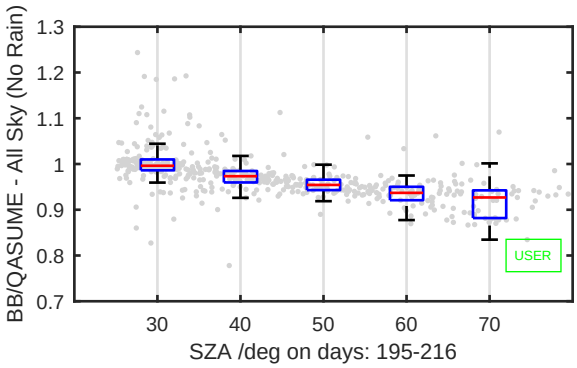

Calibration Results of YES000904 (UVE)

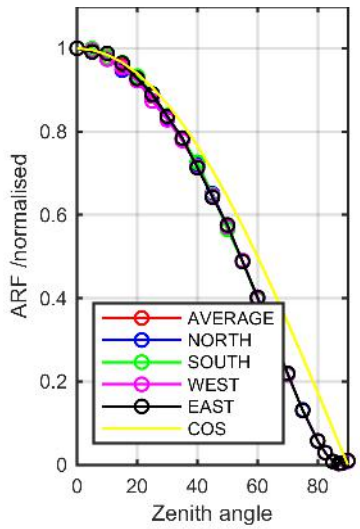

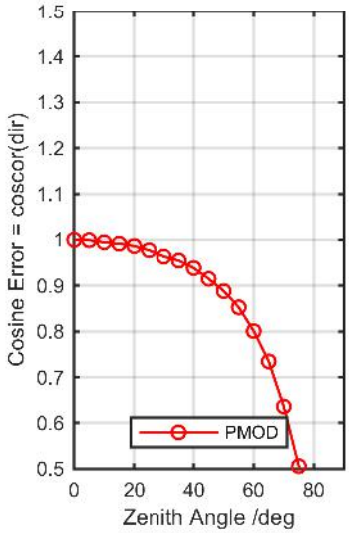

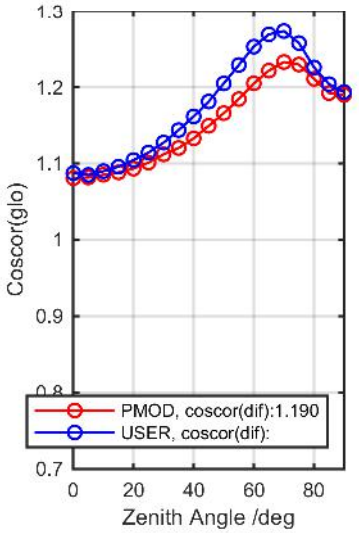

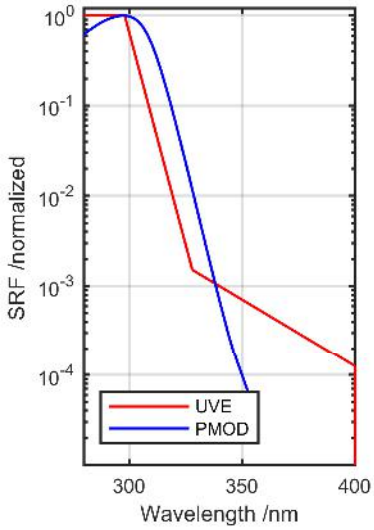

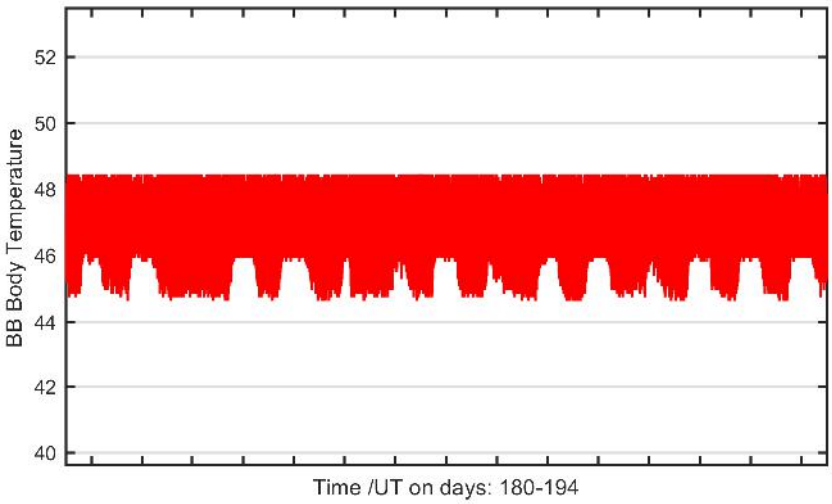

Calibration Matrix fn; Model sdisortREFms2009; f0=0.1969

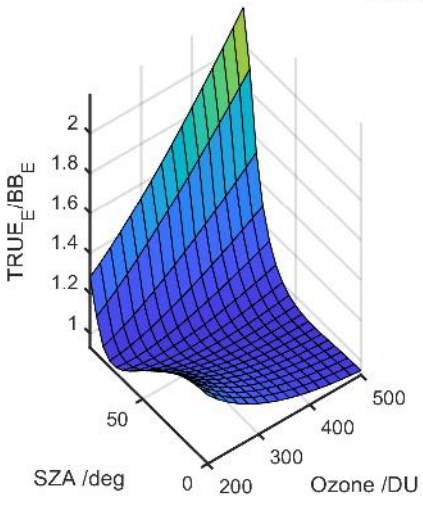

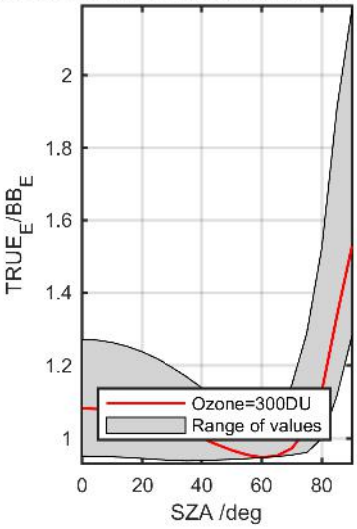

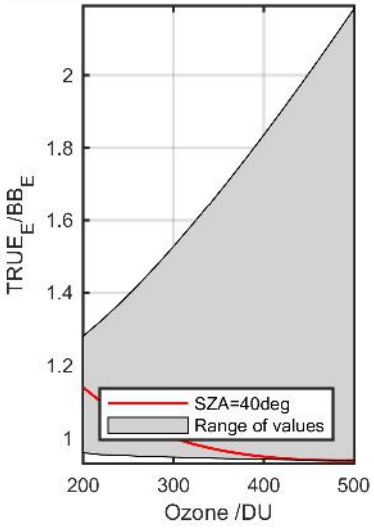

Calibration Results of YES000904 (UVE)

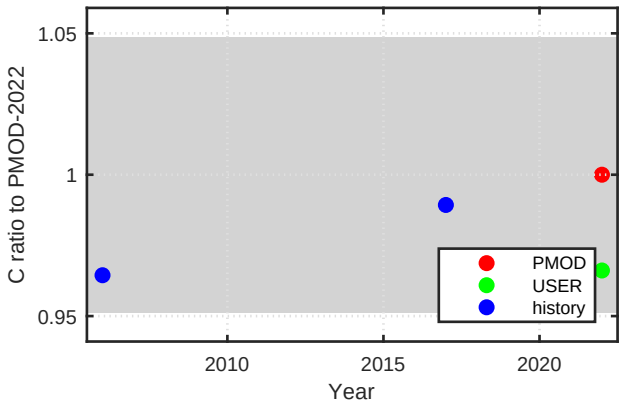

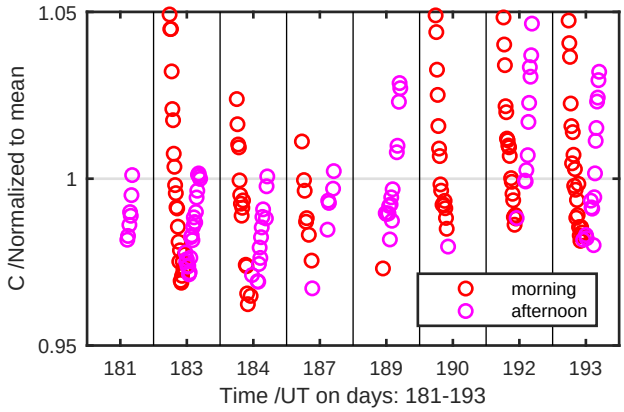

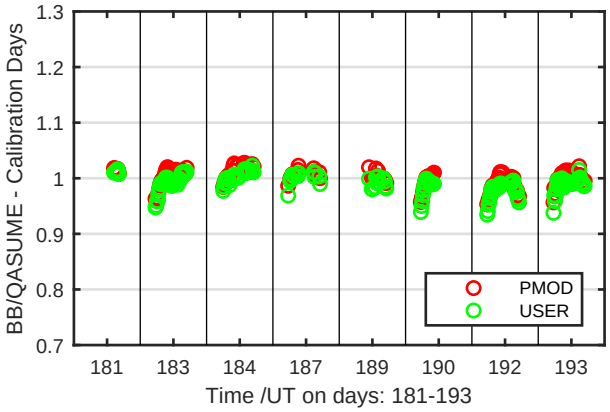

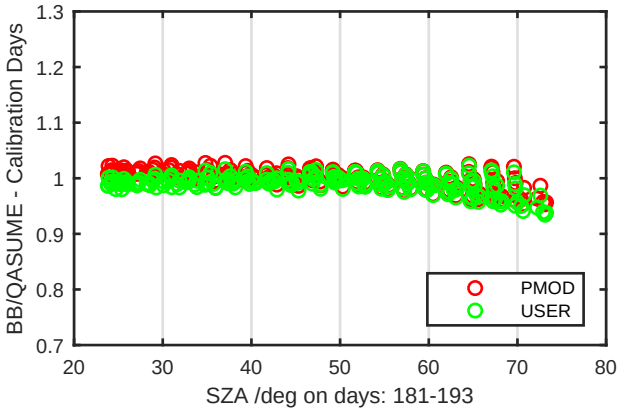

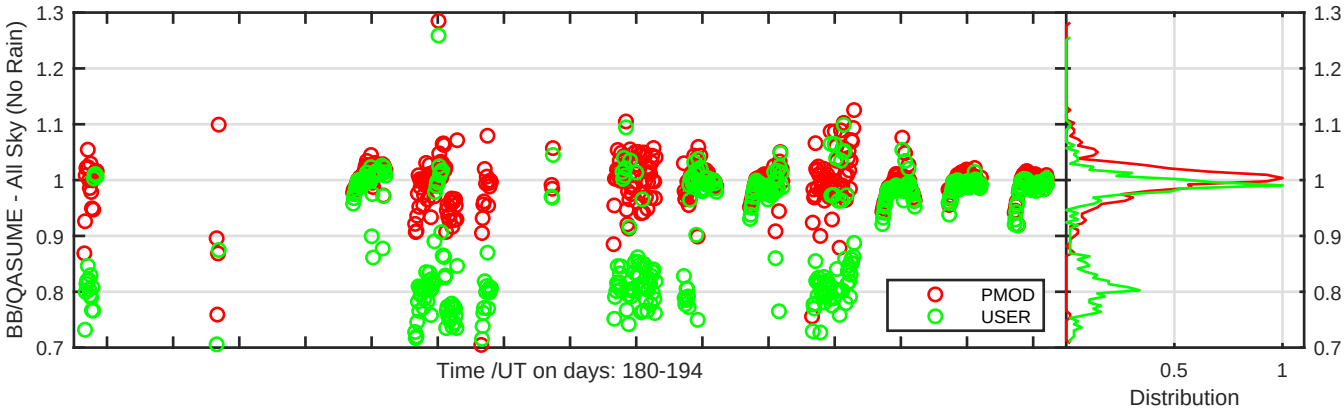

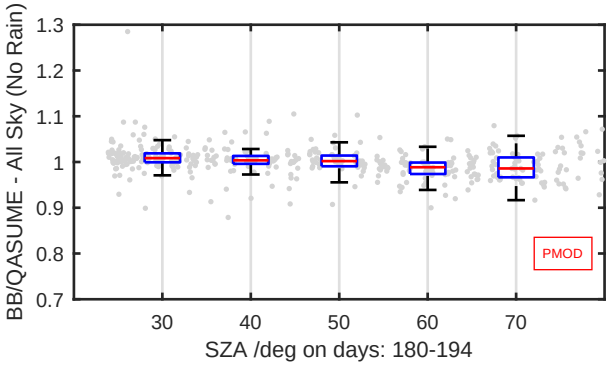

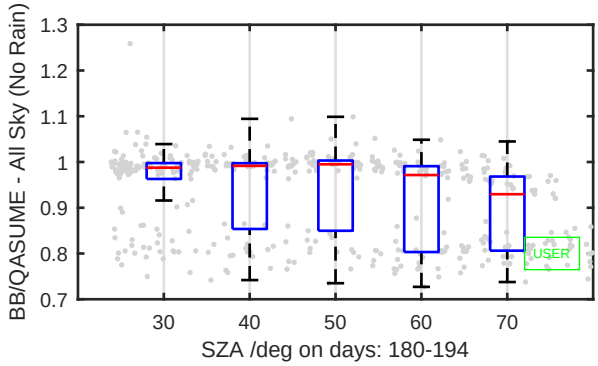

Calibration Results of YES010938 (UVE)

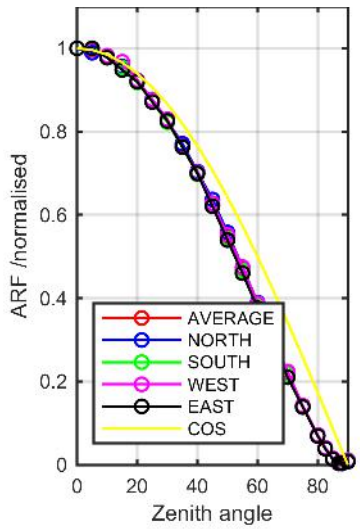

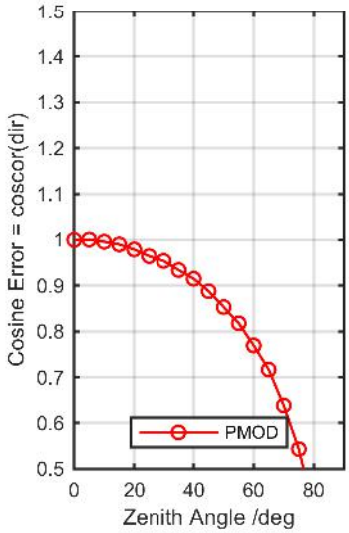

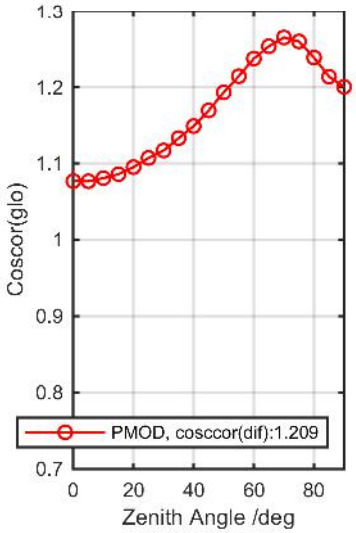

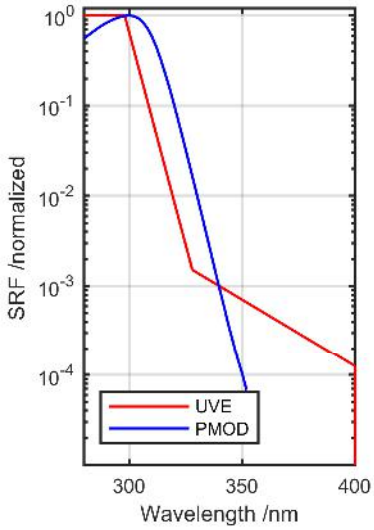

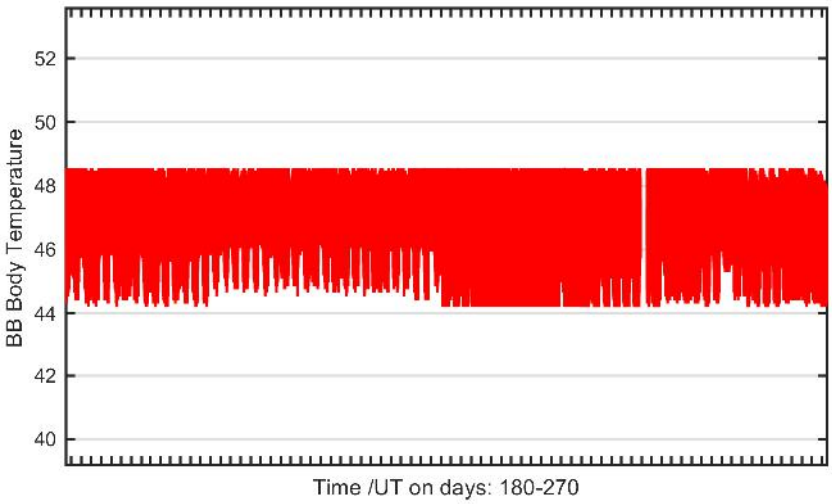

Calibration Matrix fn; Model sdisortPMODmsO3; f0=0.1578

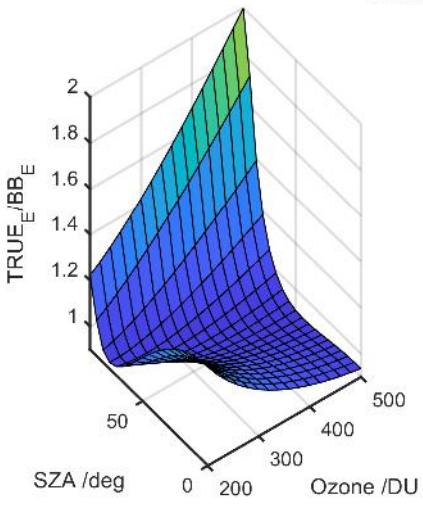

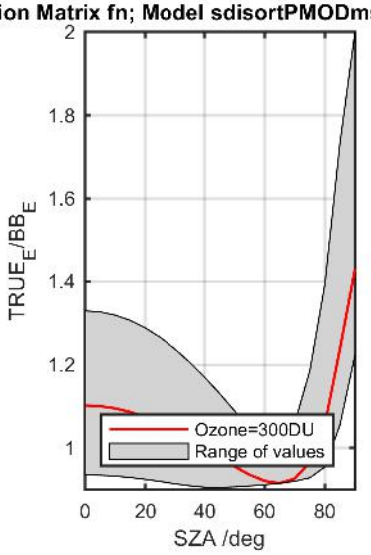

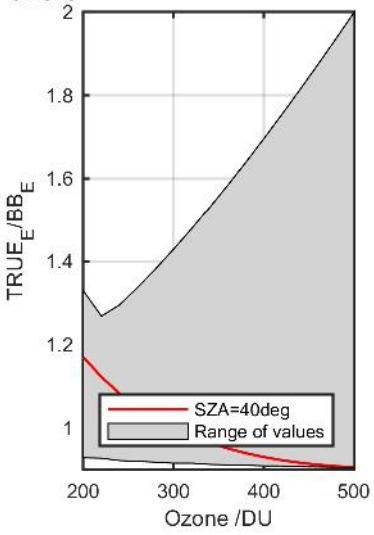

Calibration Results of YES010938 (UVE)

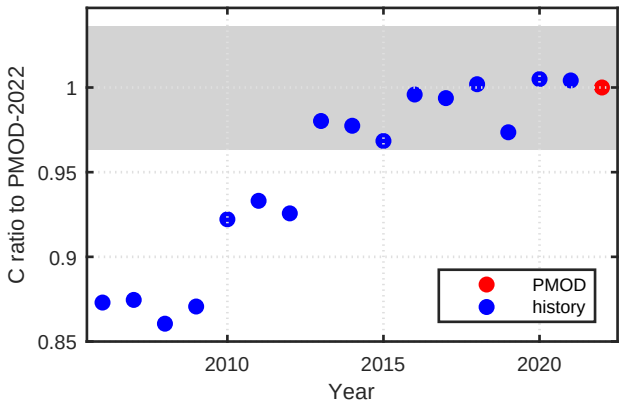

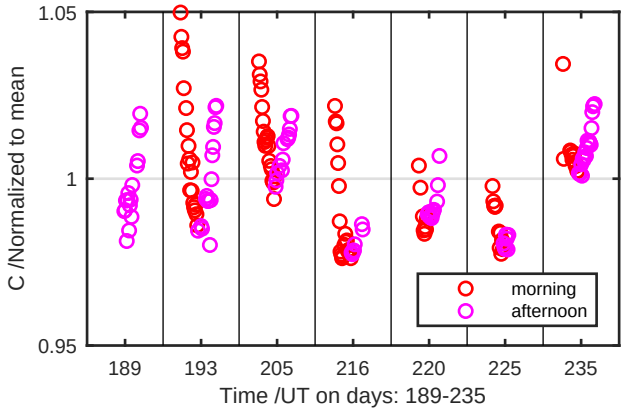

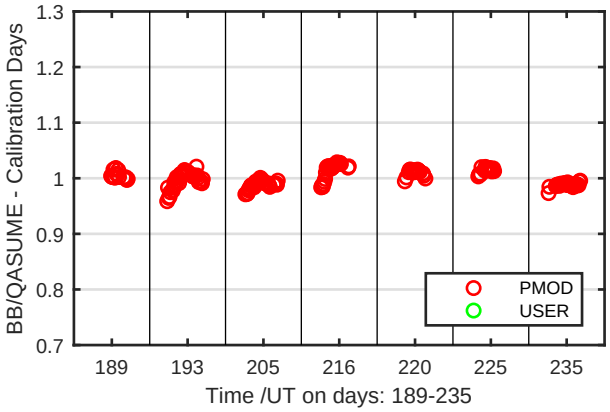

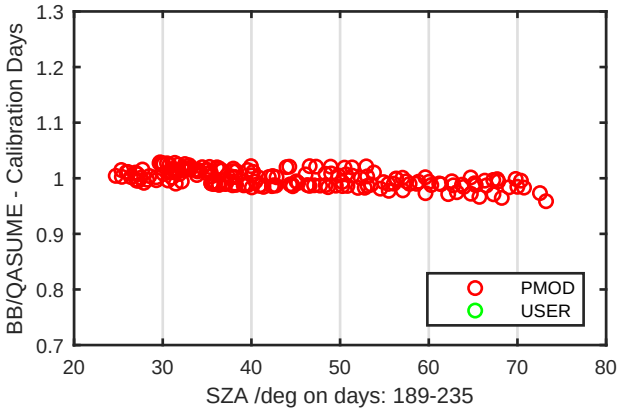

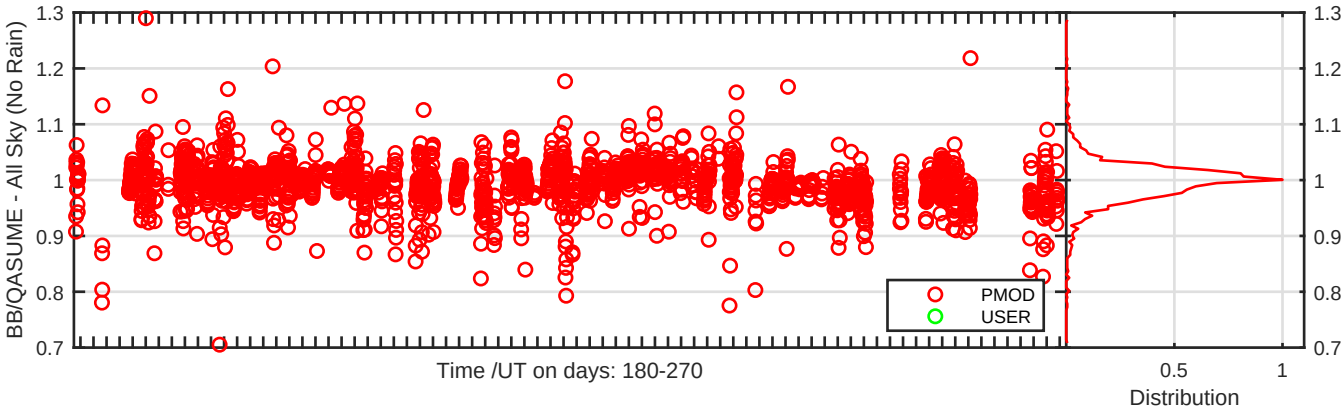

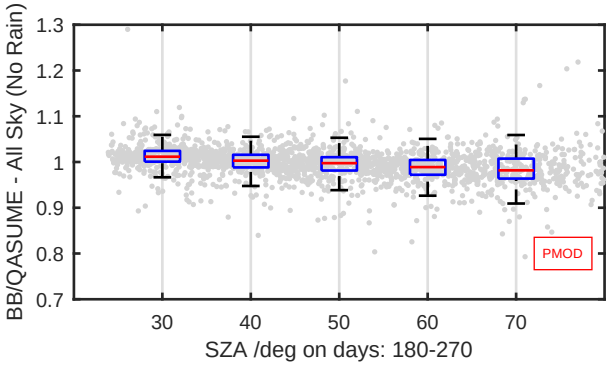

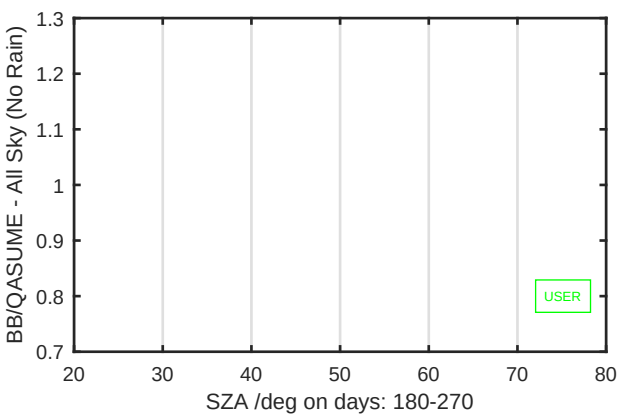

Calibration Results of YES030520 (UVE)

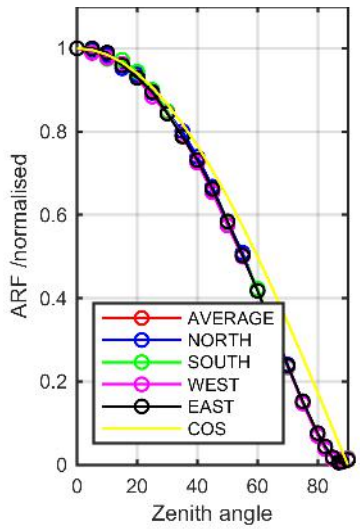

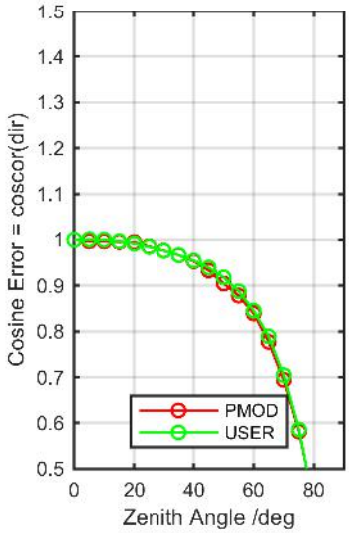

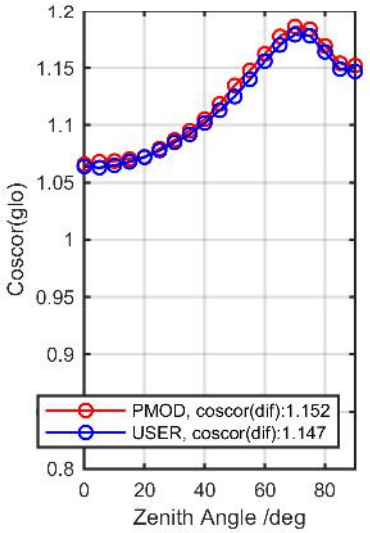

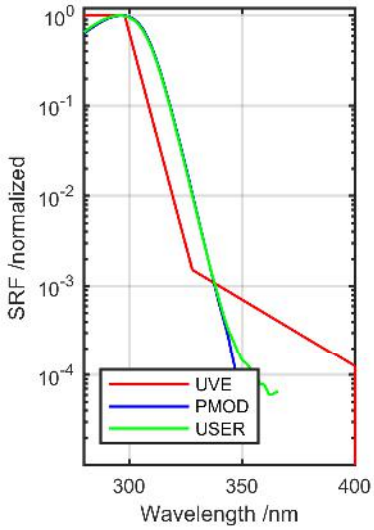

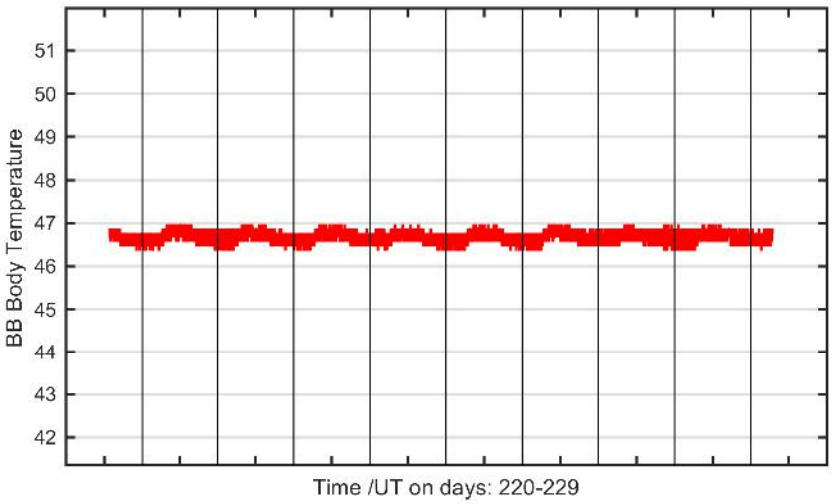

Calibration Matrix fn; Model sdisortREFms2009; f0=0.2128

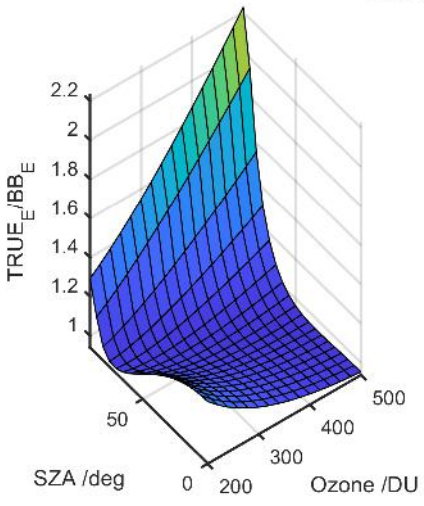

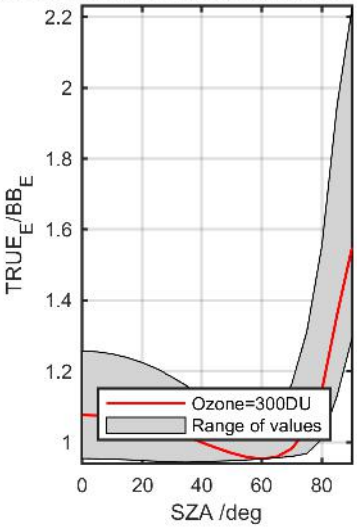

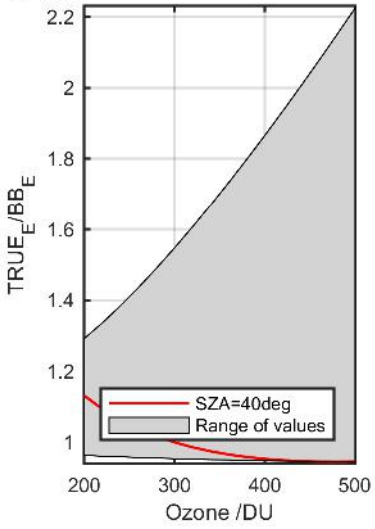

Calibration Results of YES030520 (UVE)

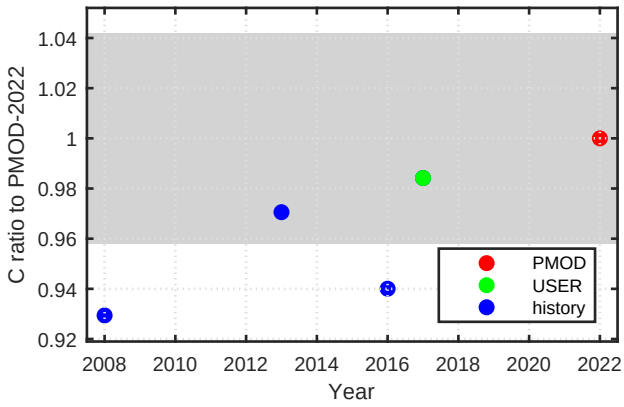

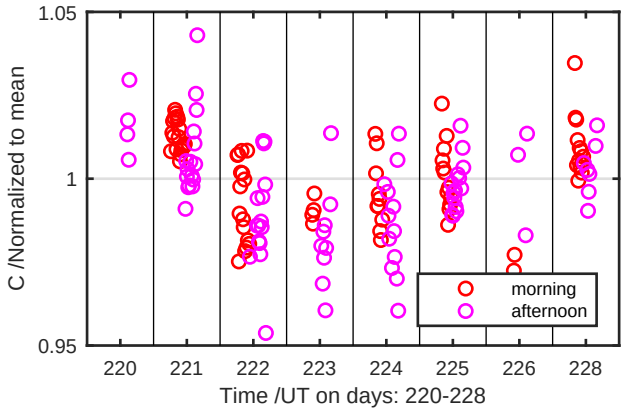

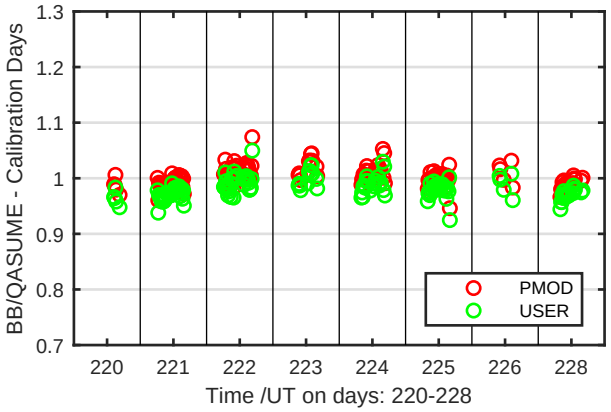

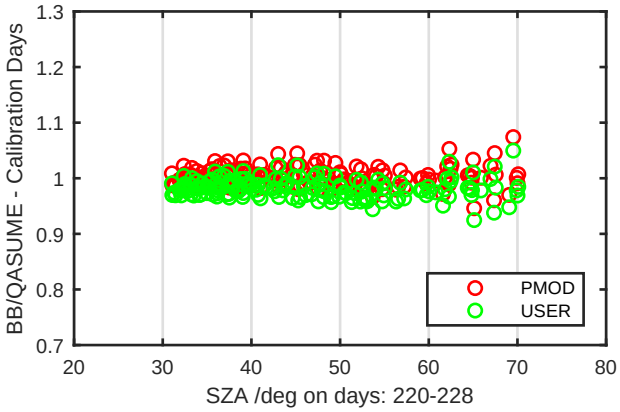

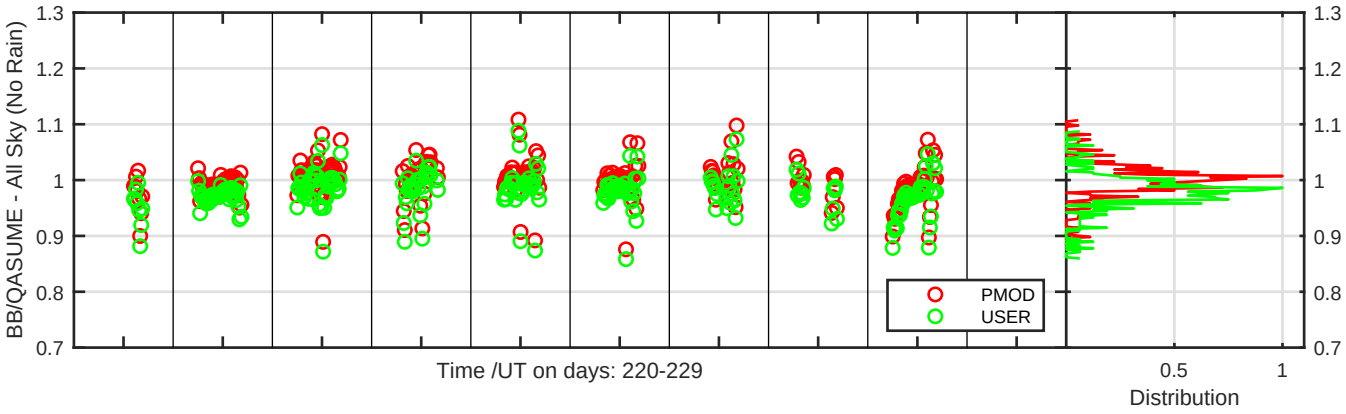

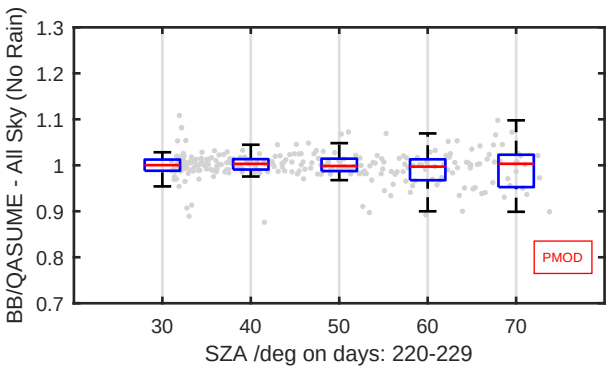

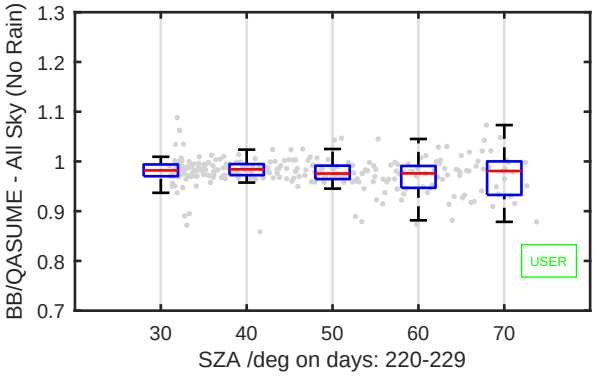

Calibration Results of YES010925 (UVB320)

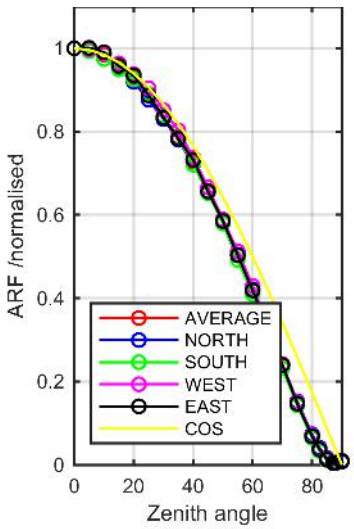

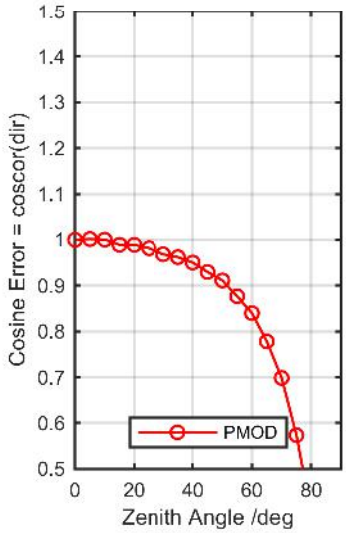

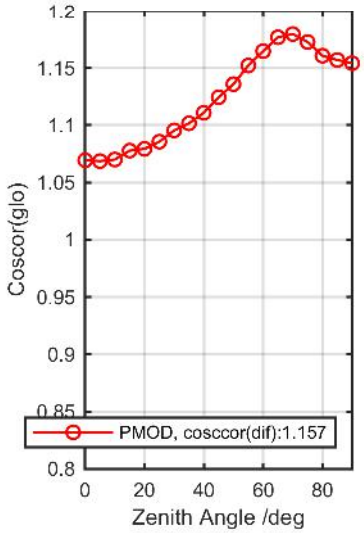

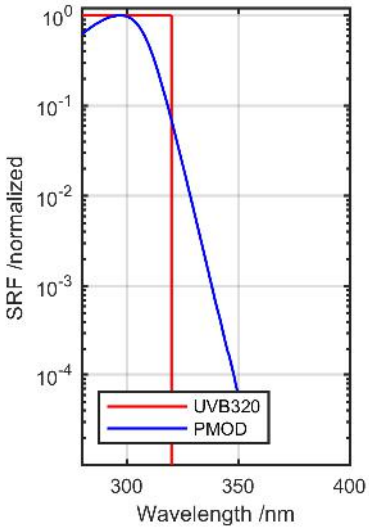

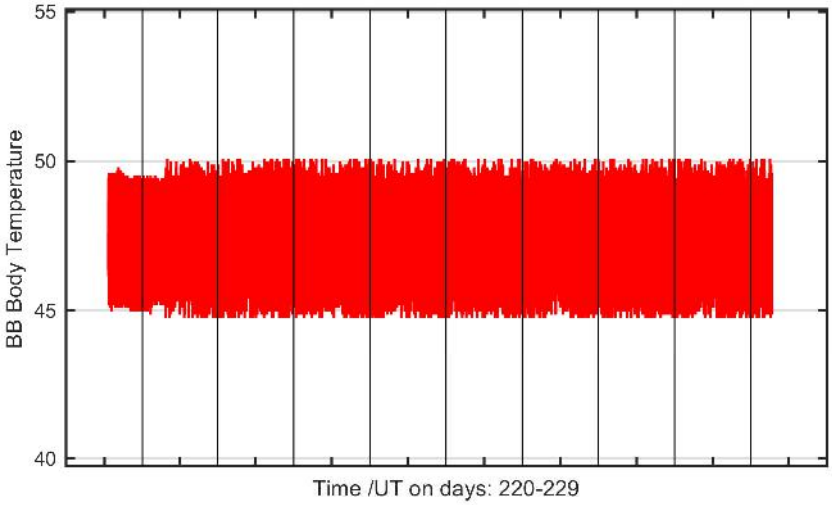

Calibration Matrix fn; Model sdisortREFms2009; f0=3.1073

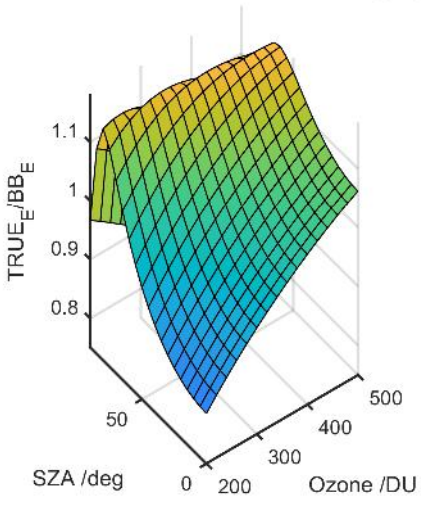

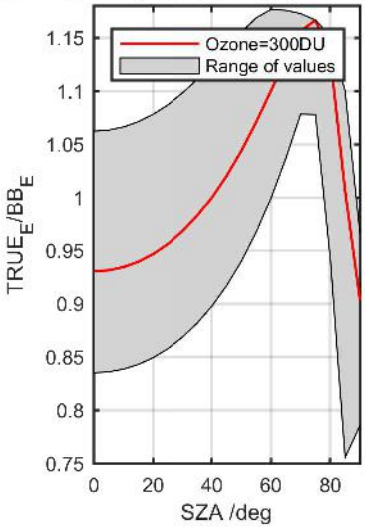

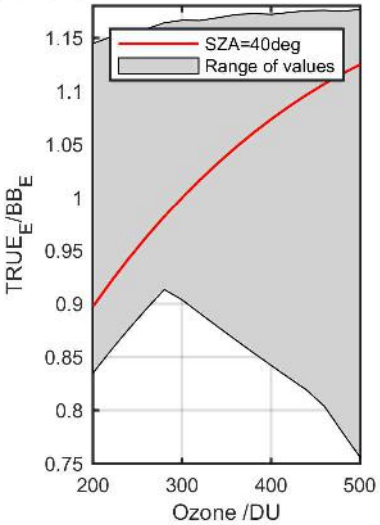

Calibration Results of YES010925 (UVB320)

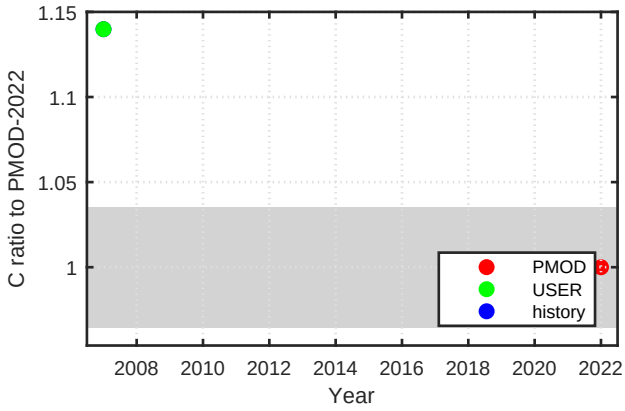

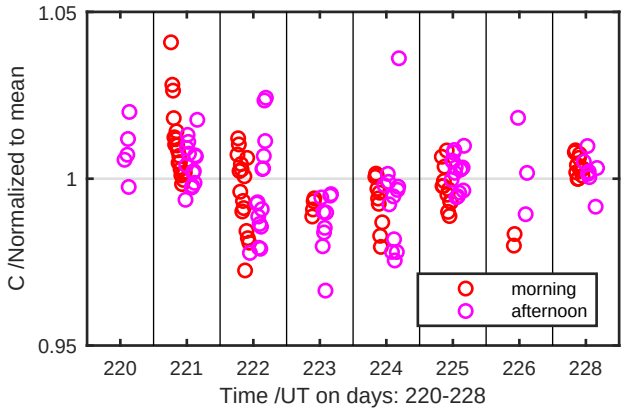

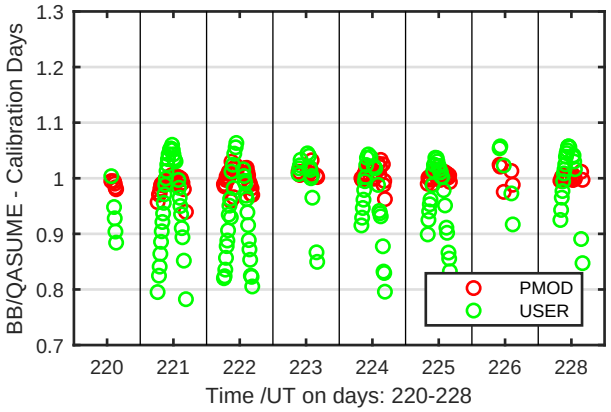

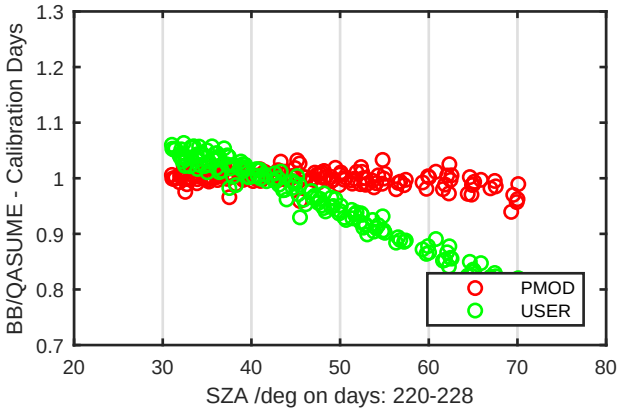

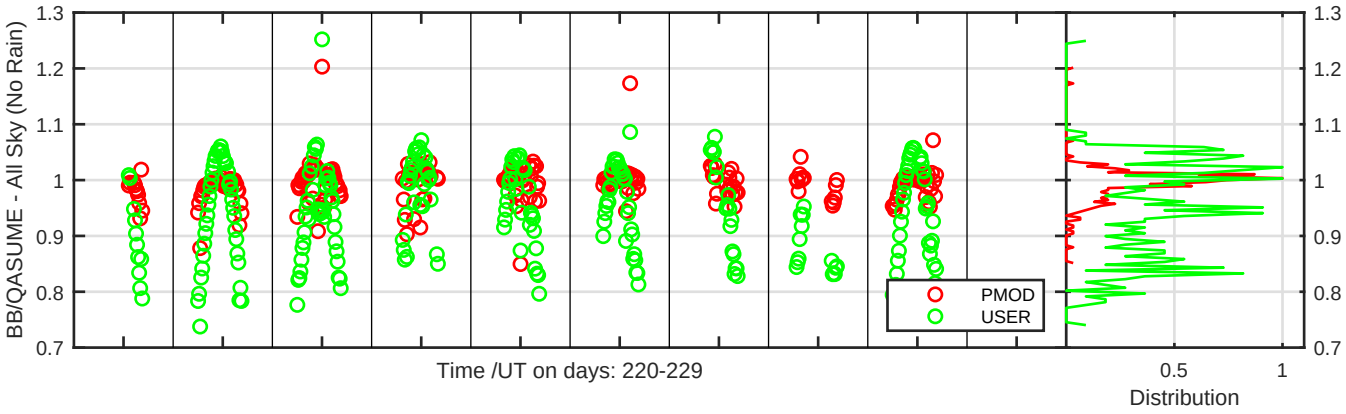

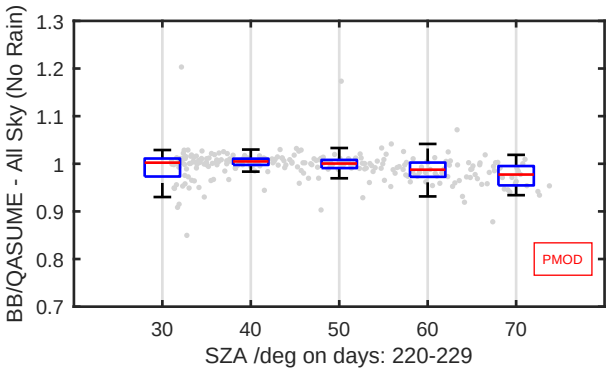

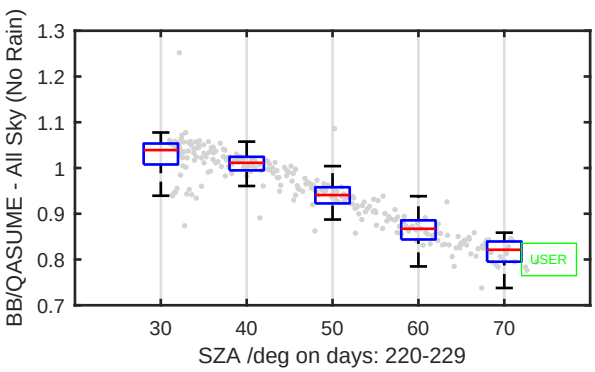

Calibration Results of YES150703 (UVE)

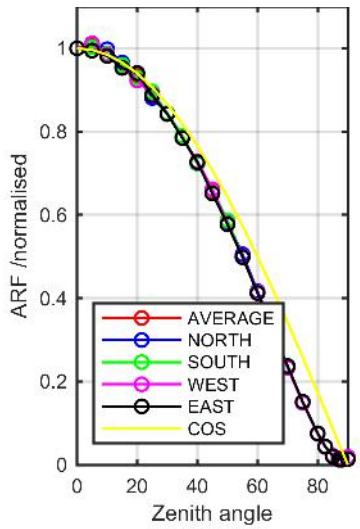

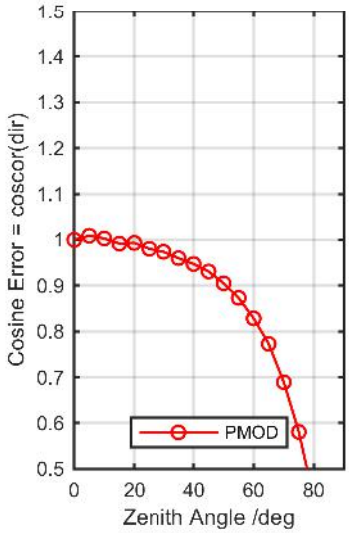

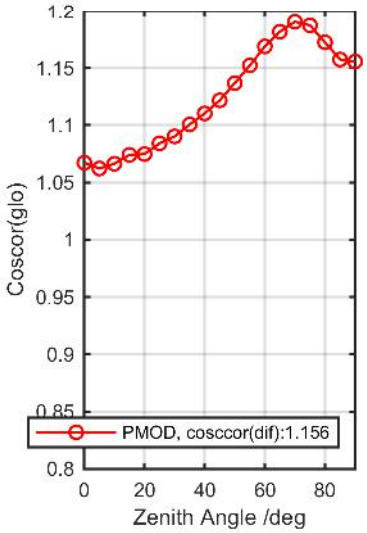

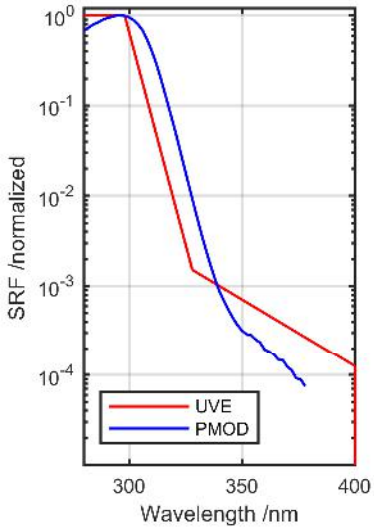

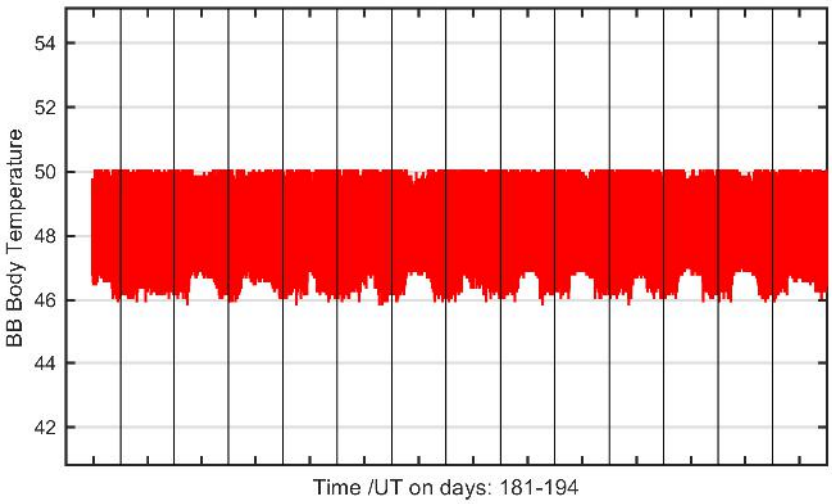

Calibration Matrix fn; Model sdisortREFms2009; f0=0.2349

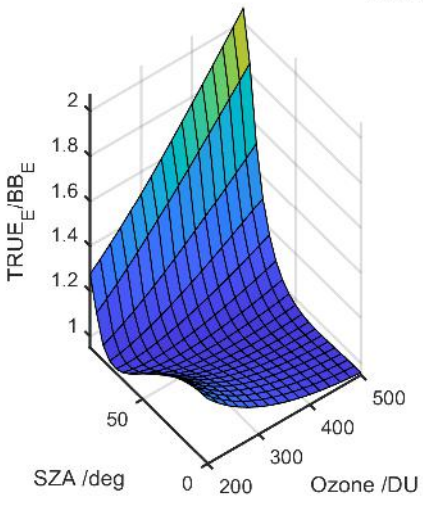

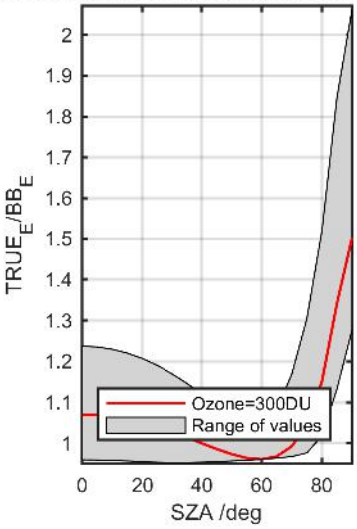

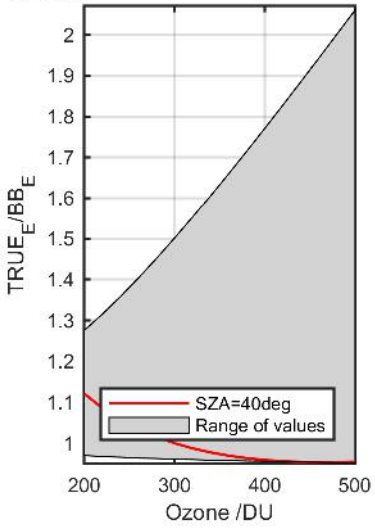

Calibration Results of YES150703 (UVE)

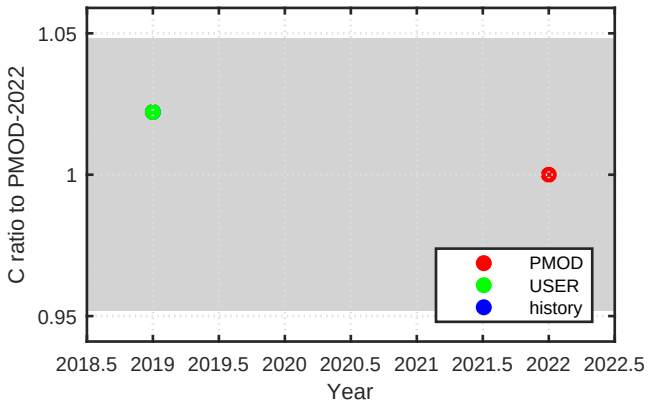

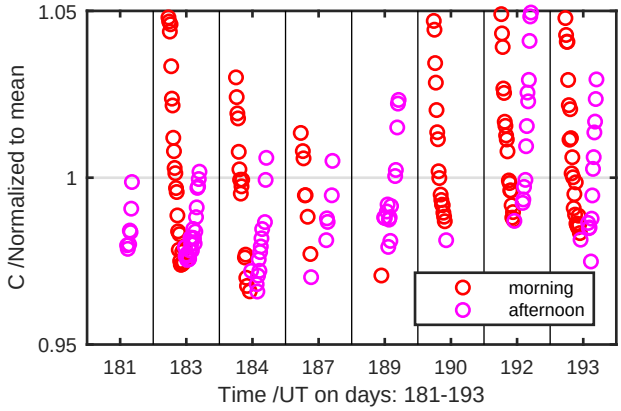

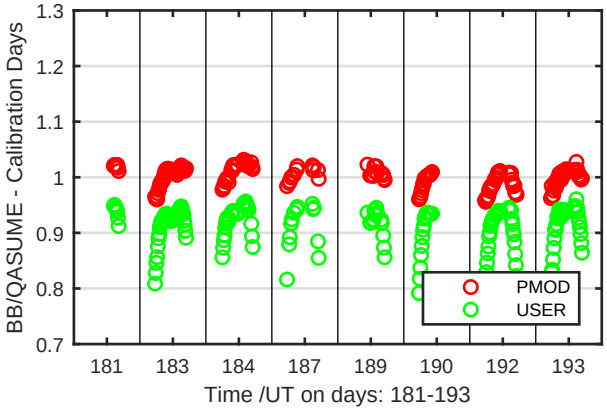

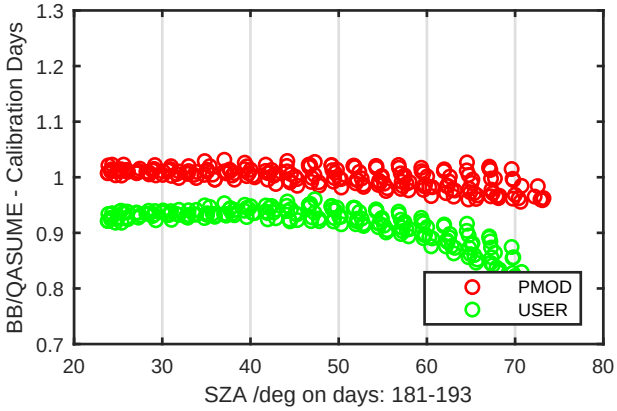

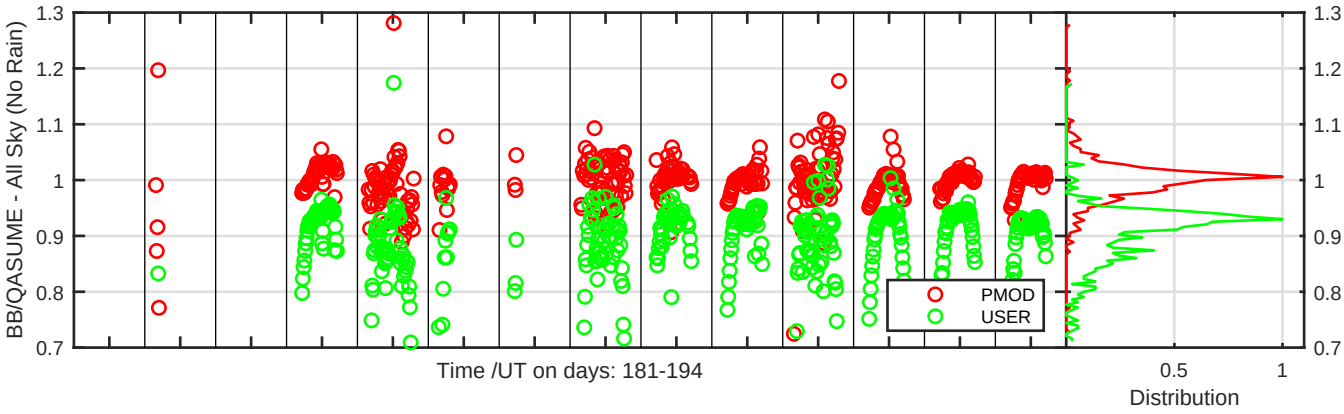

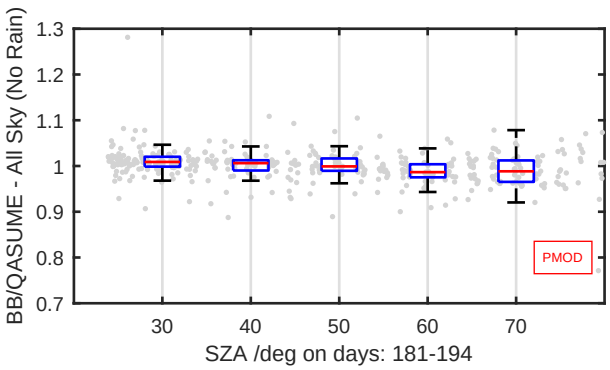

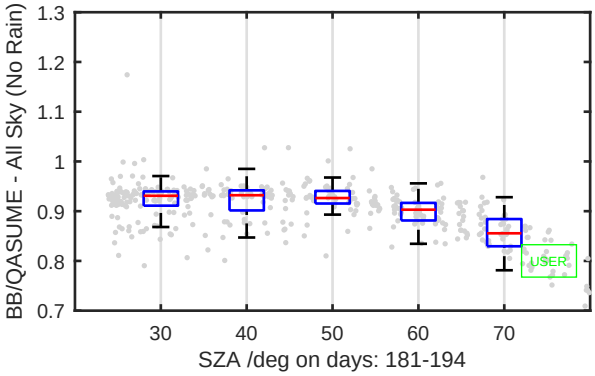

Calibration Results of YES920906 (UVE)

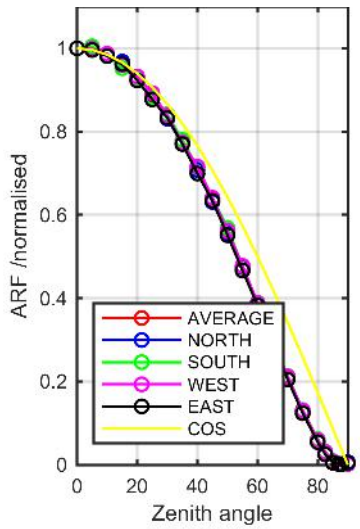

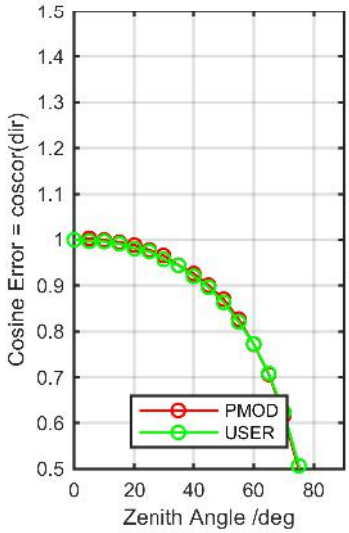

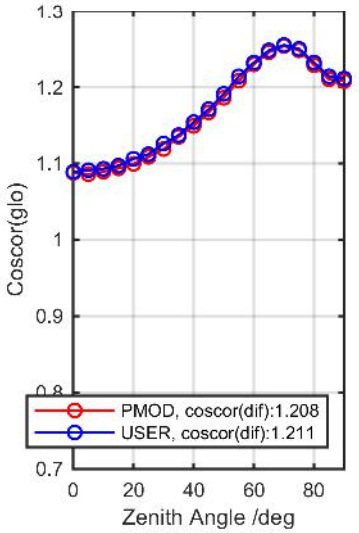

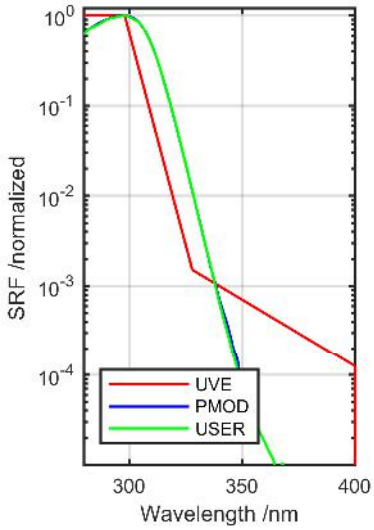

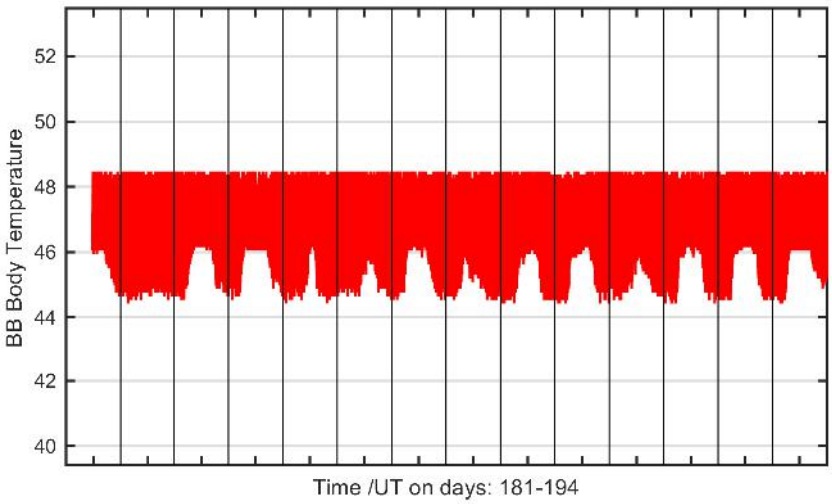

Calibration Matrix fn; Model sdisortREFms2009; f0=0.2009

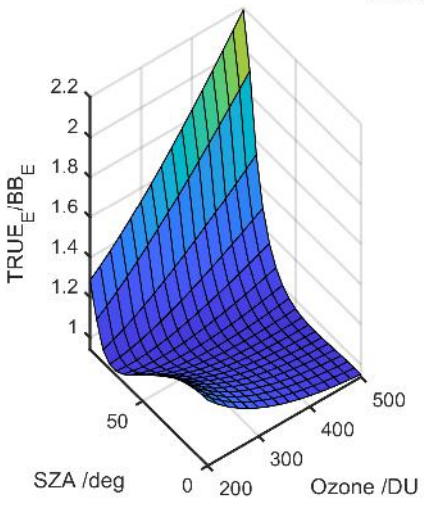

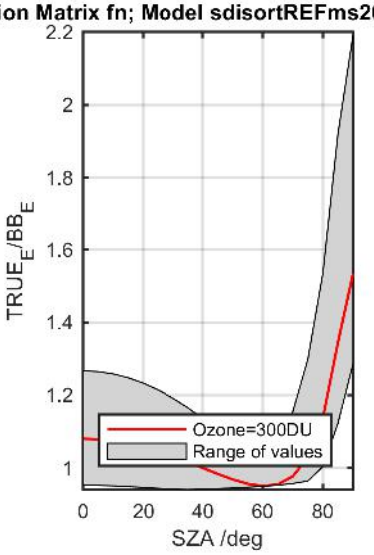

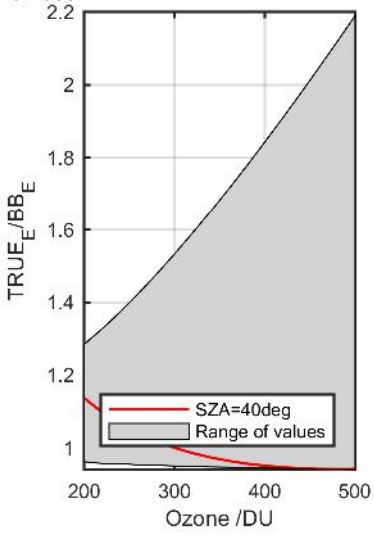

Calibration Results of YES920906 (UVE)

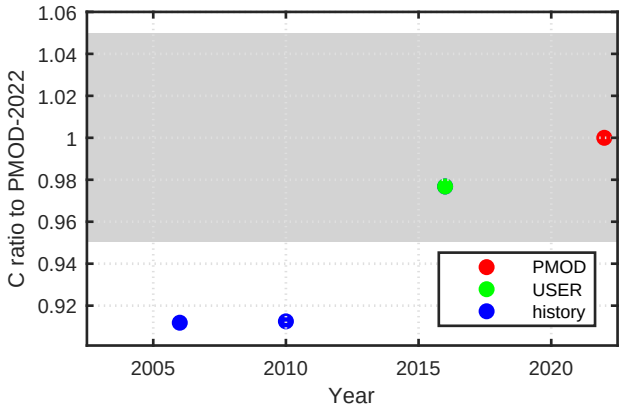

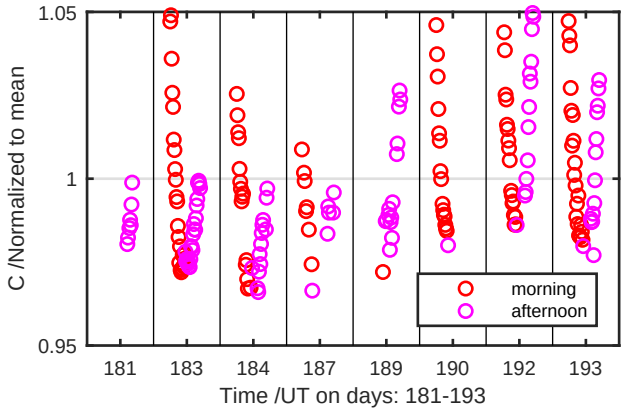

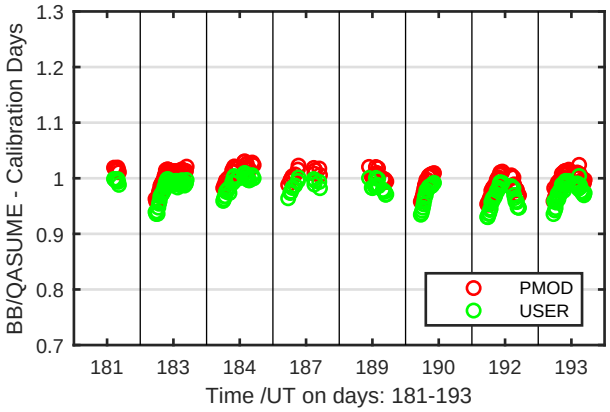

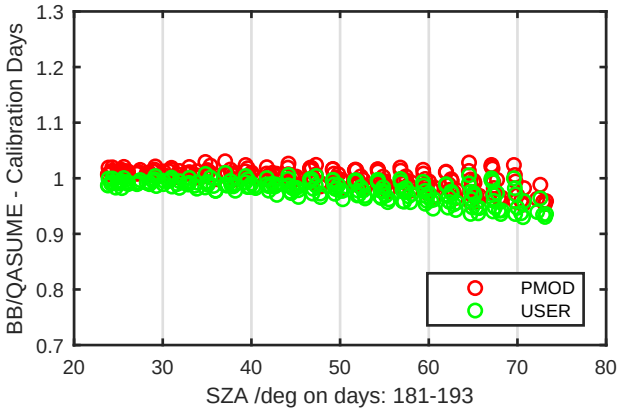

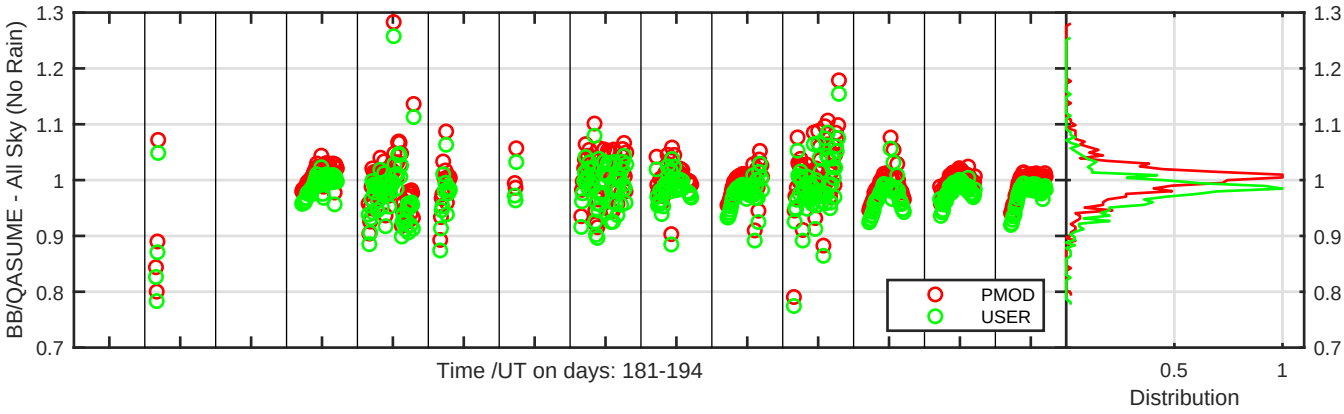

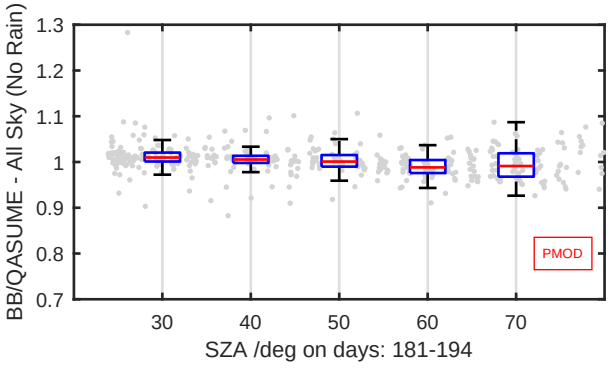

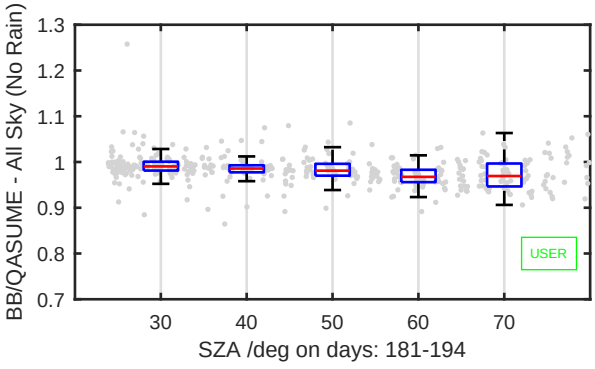

Calibration Results of YES990506 (UVE)

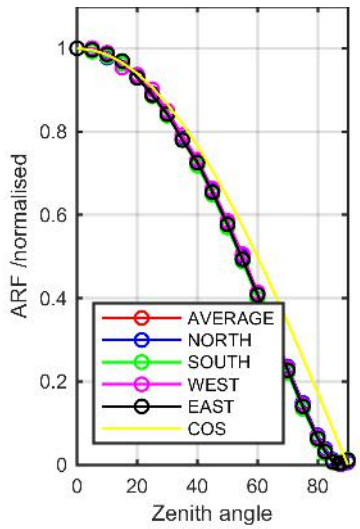

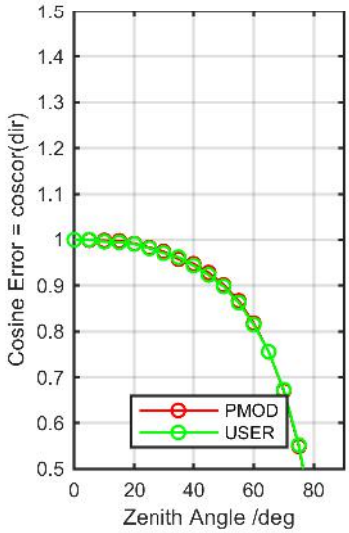

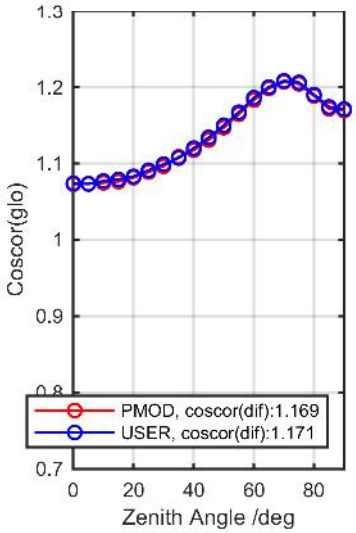

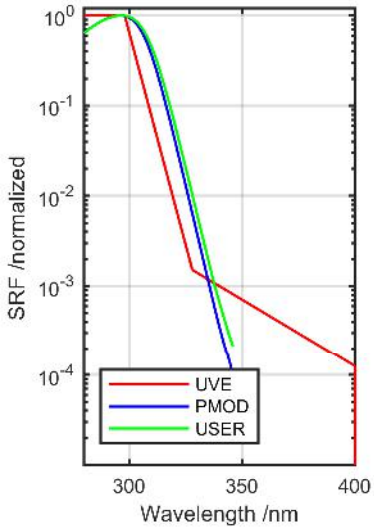

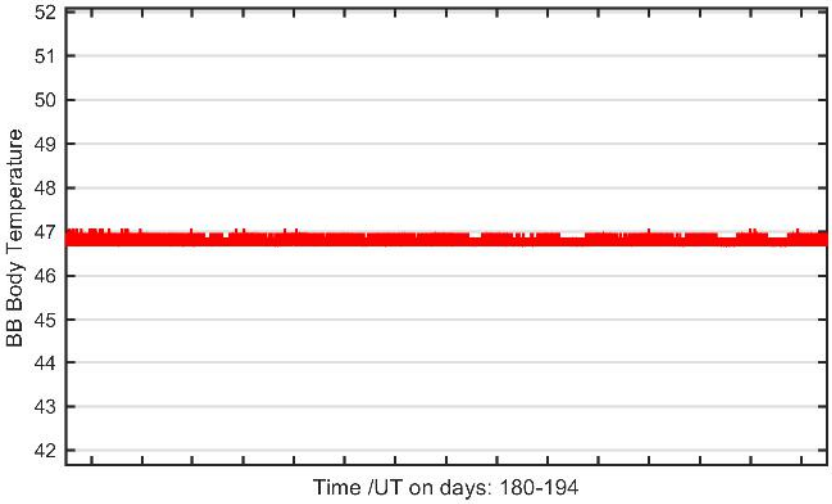

Calibration Matrix fn; Model sdisortREFms2009; f0=0.2757

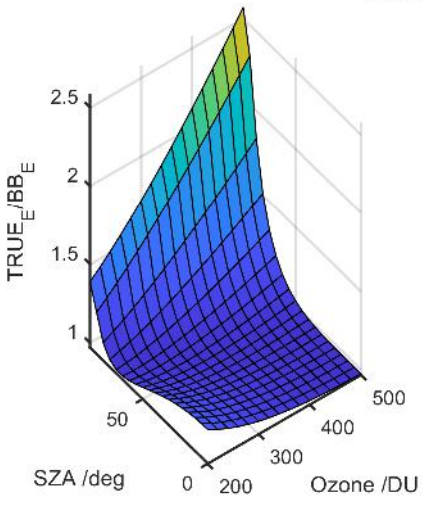

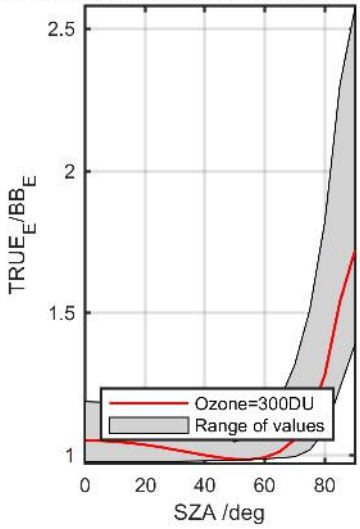

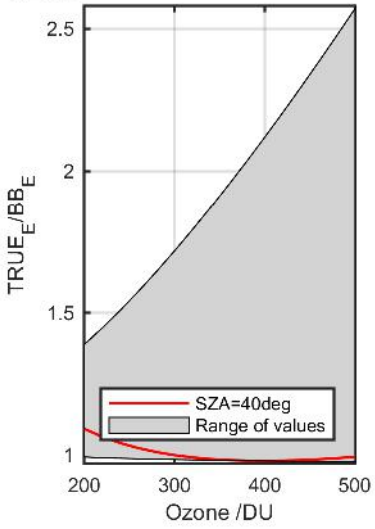

Calibration Results of YES990506 (UVE)

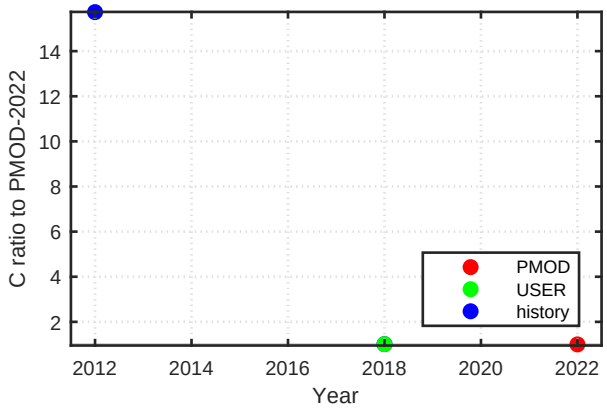

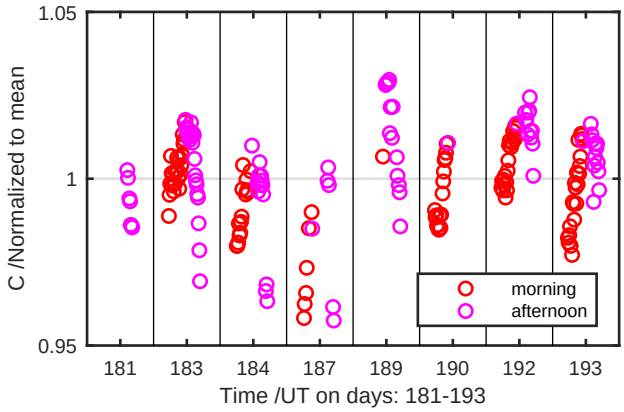

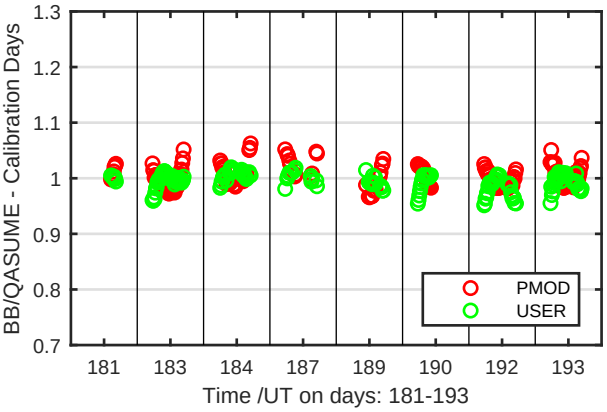

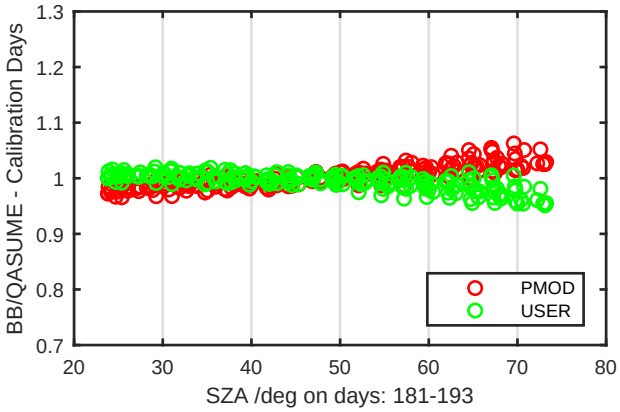

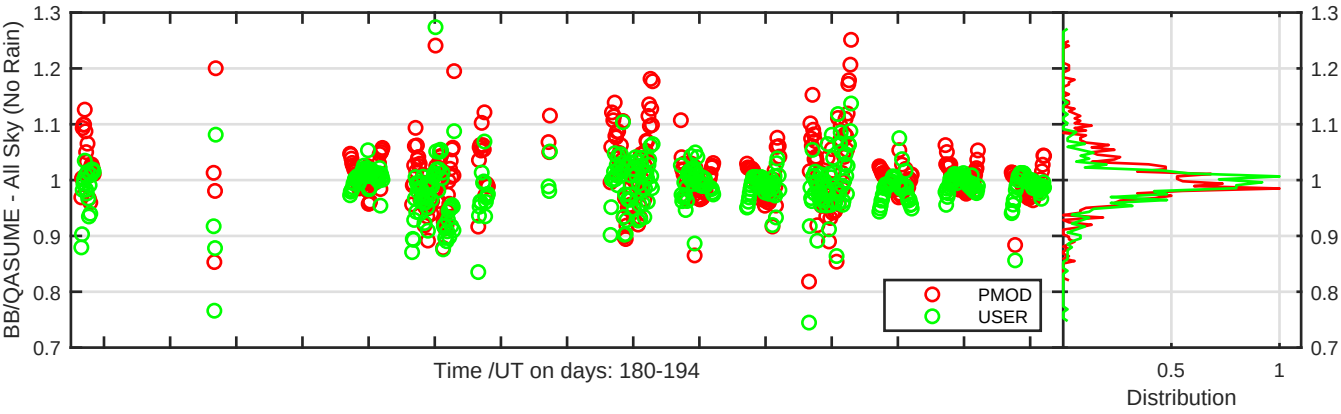

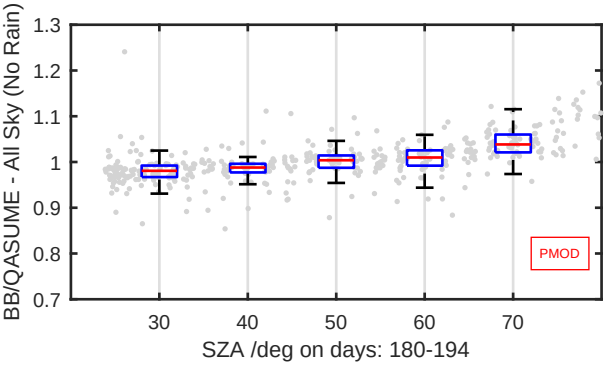

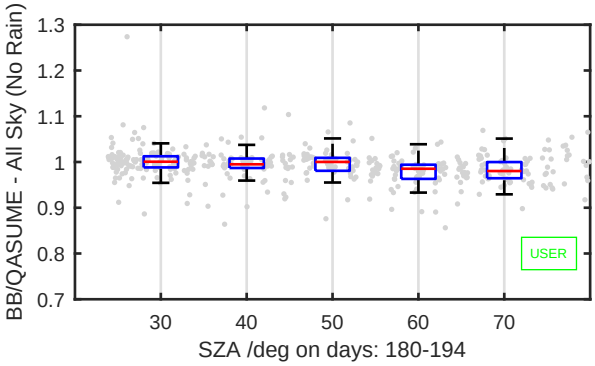

Calibration Results of MS-11S2200102 (UVB)

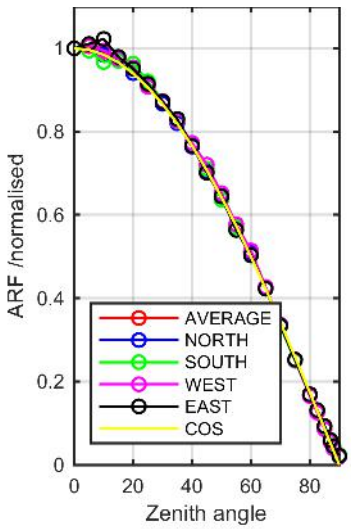

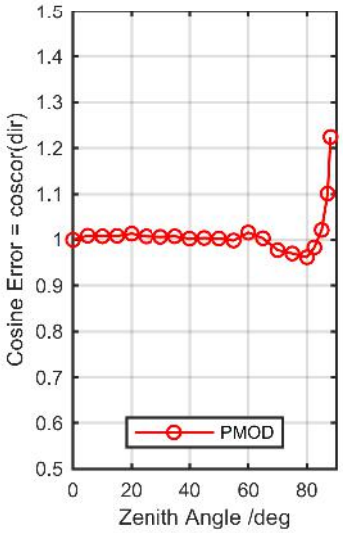

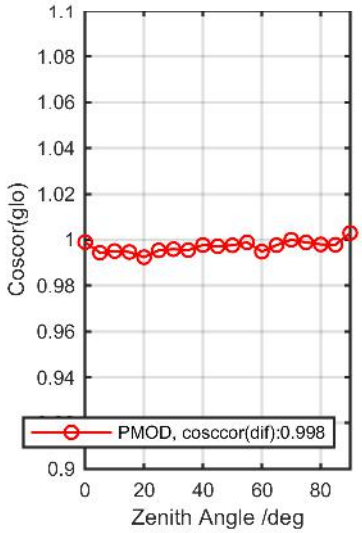

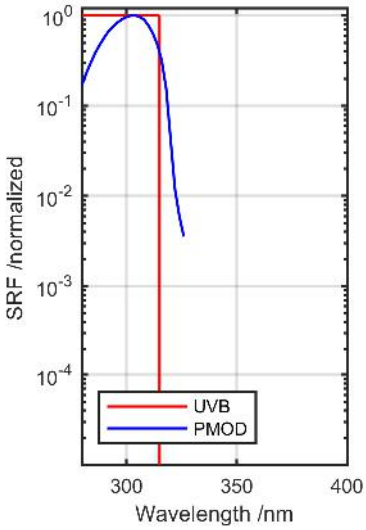

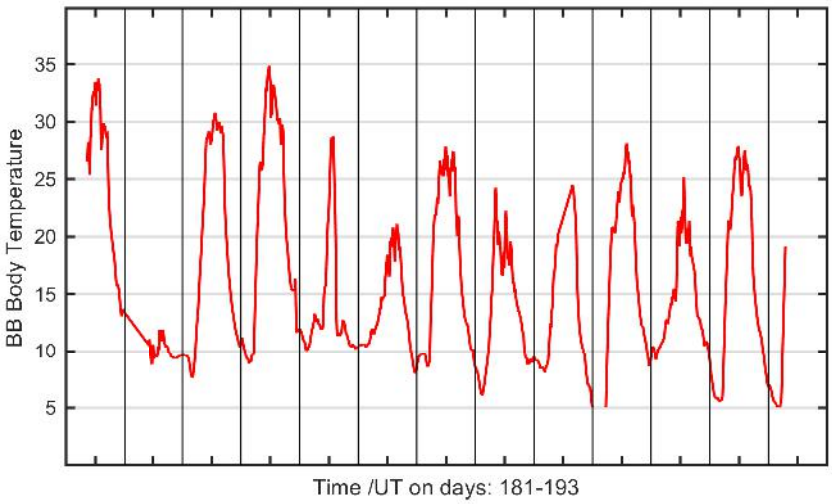

Calibration Matrix fn; Model sdisortREFms2009; f0=1.1290

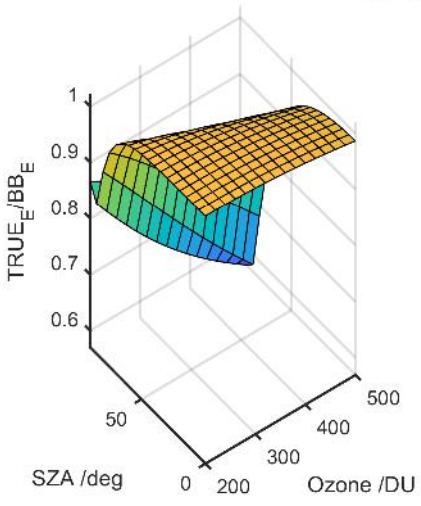

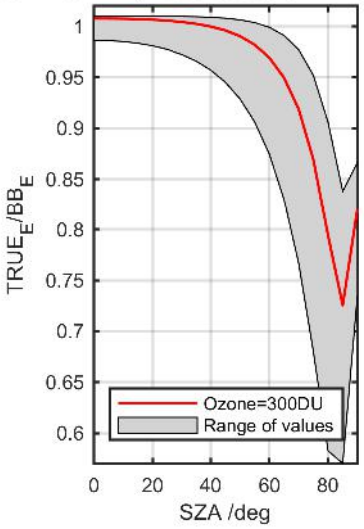

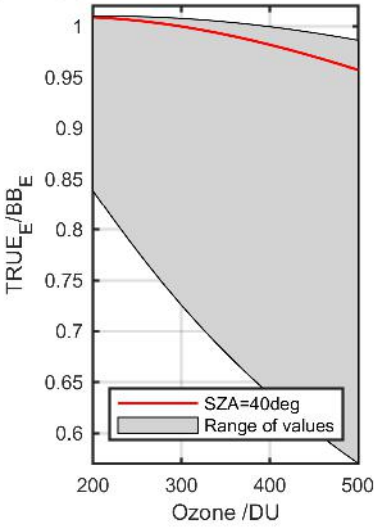

Calibration Results of MS-11S2200102 (UVB)

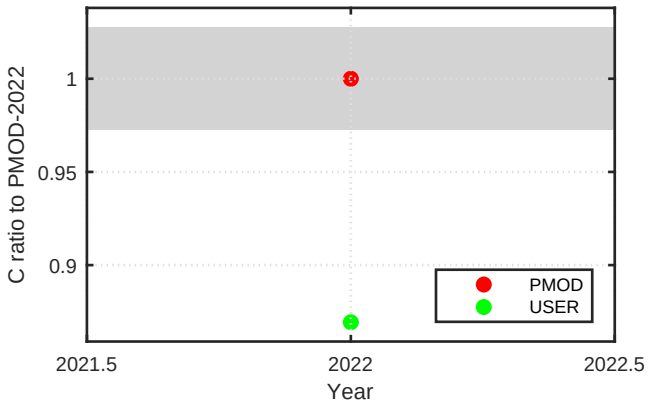

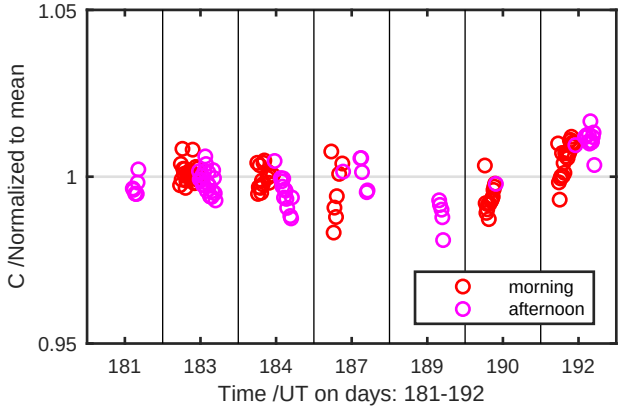

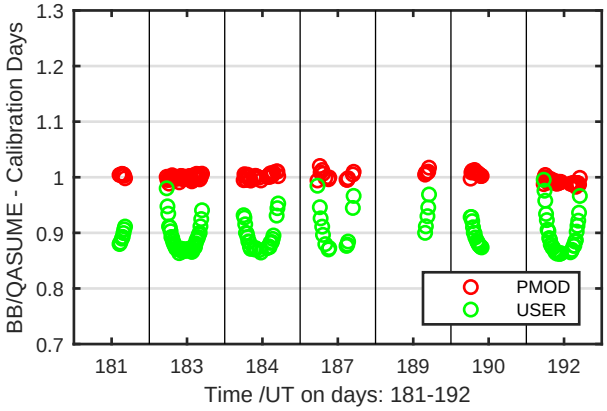

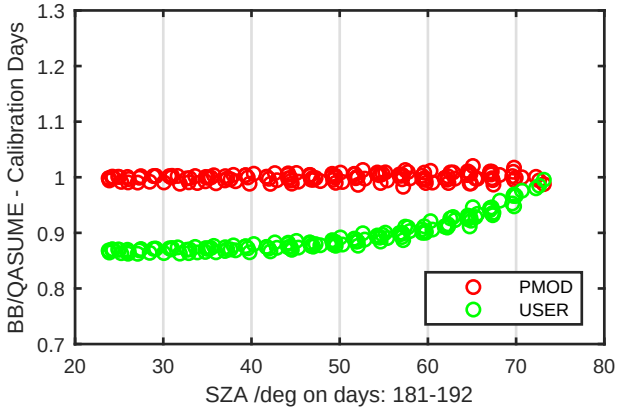

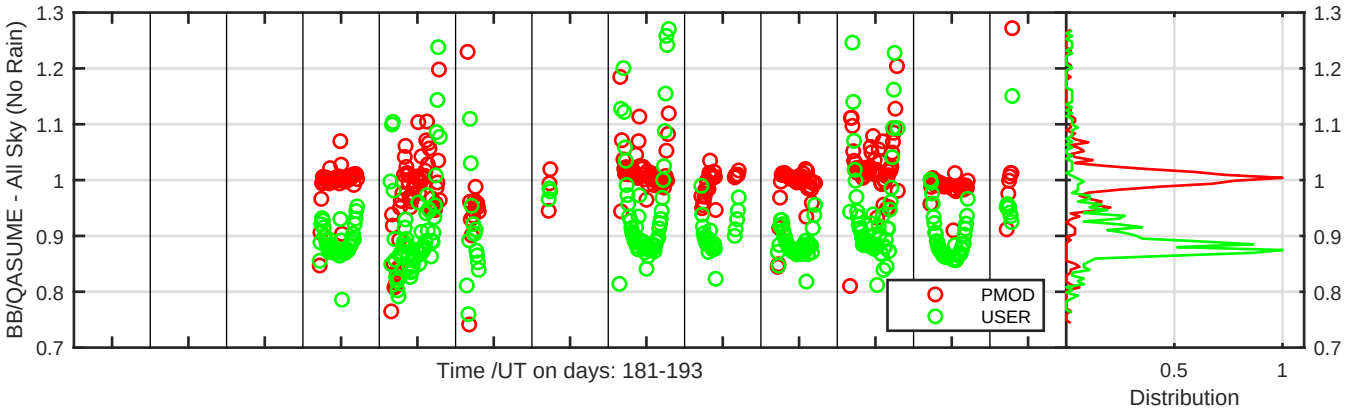

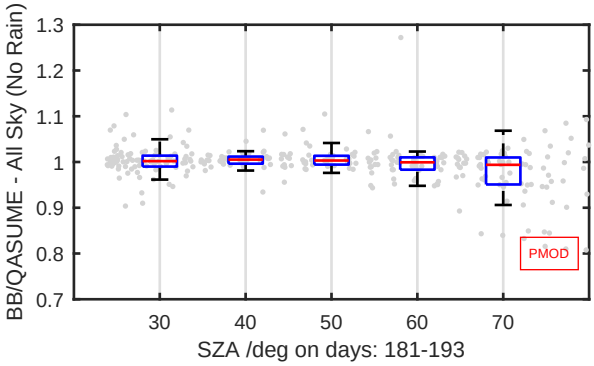

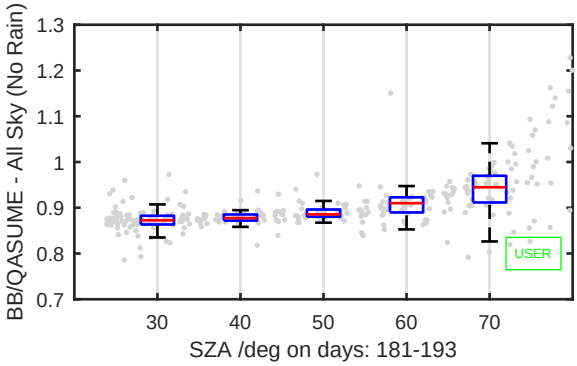

Calibration Results of MS-11S2200103 (UVB)

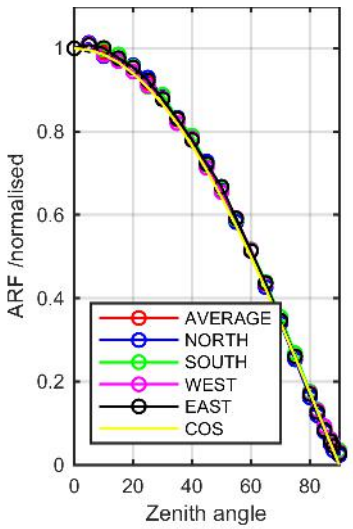

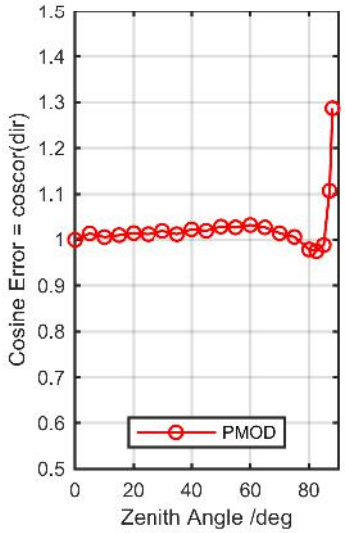

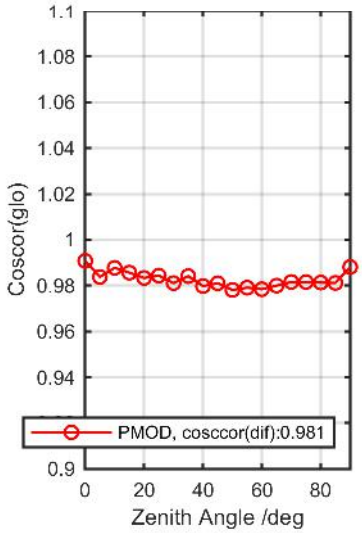

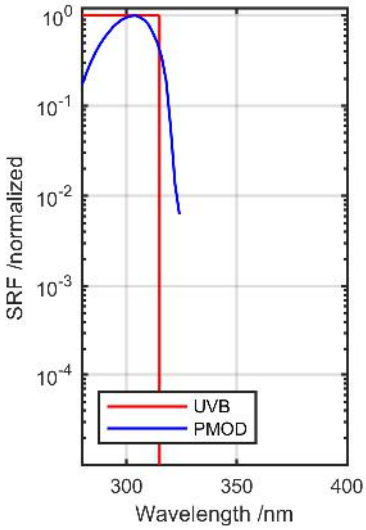

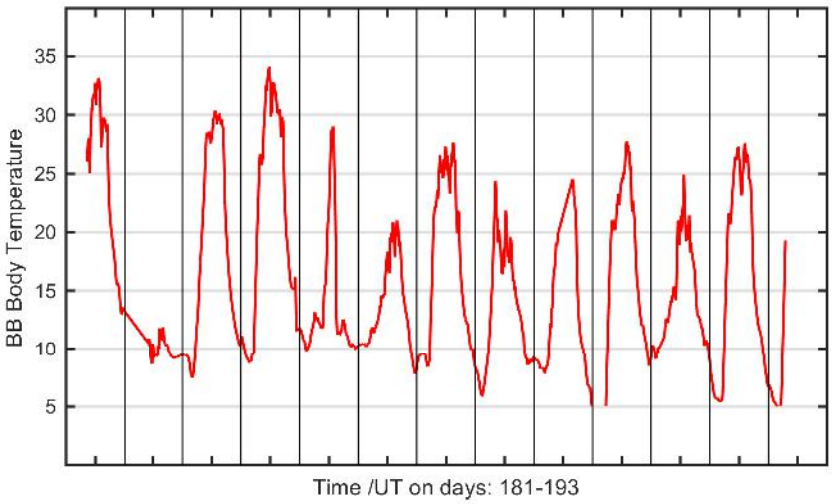

Calibration Matrix fn; Model sdisortREFms2009; f0=1.0776

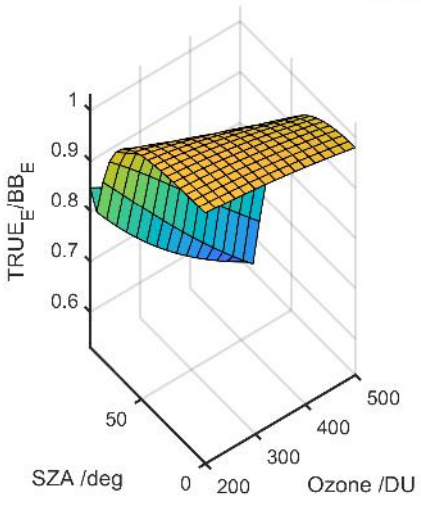

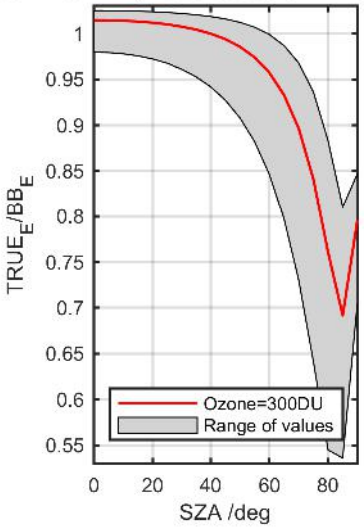

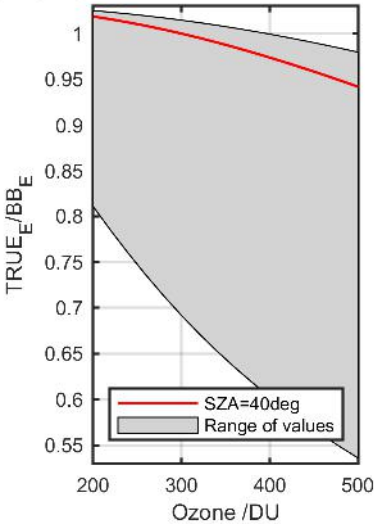

Calibration Results of MS-11S2200103 (UVB)

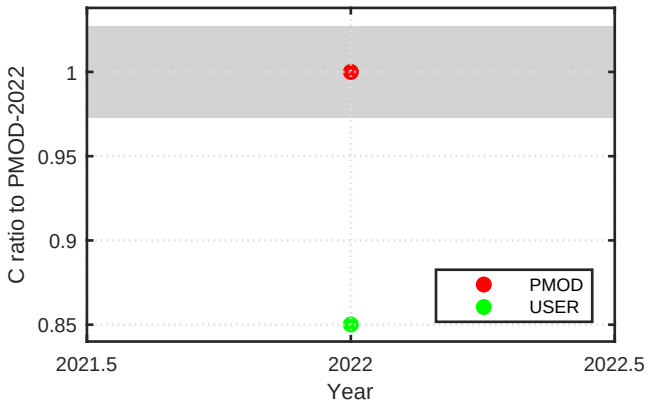

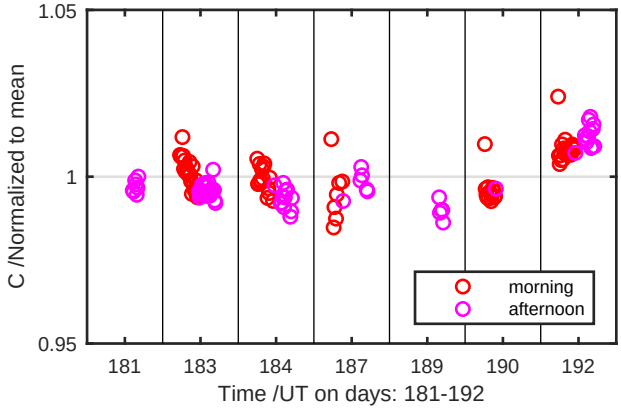

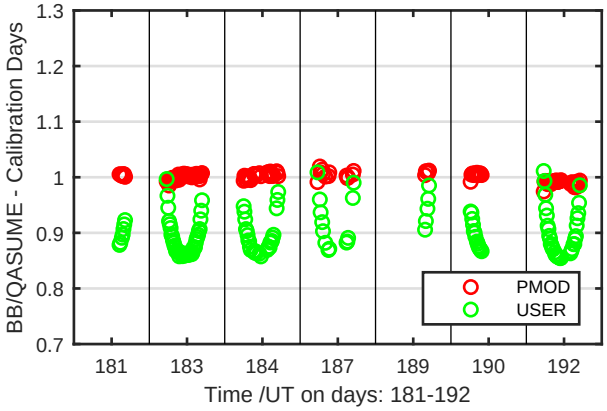

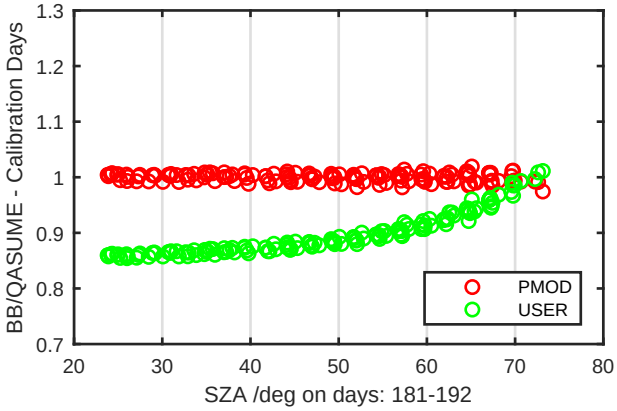

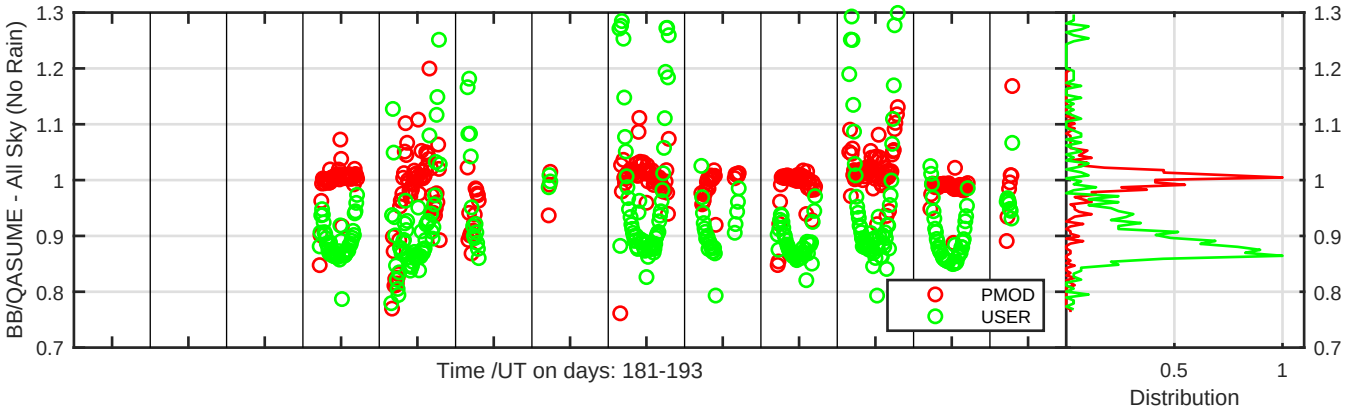

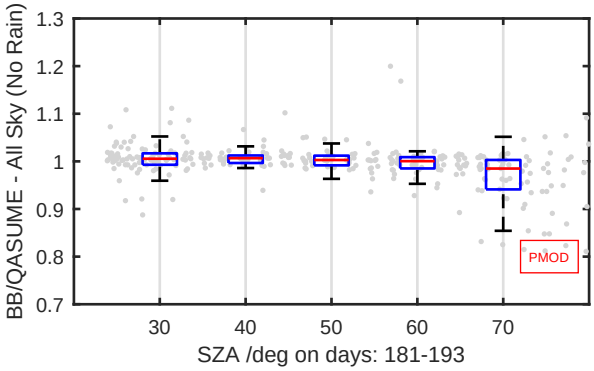

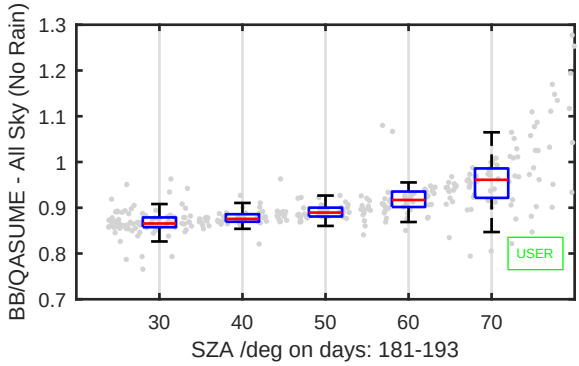

Calibration Results of MS-11S21346007 (UVB)

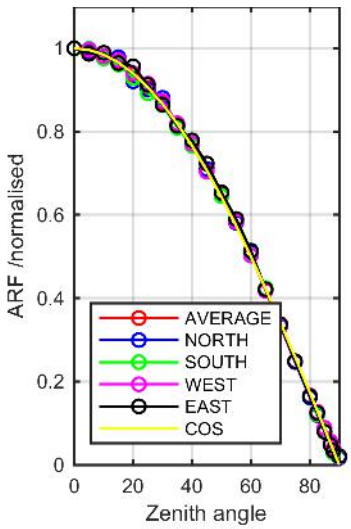

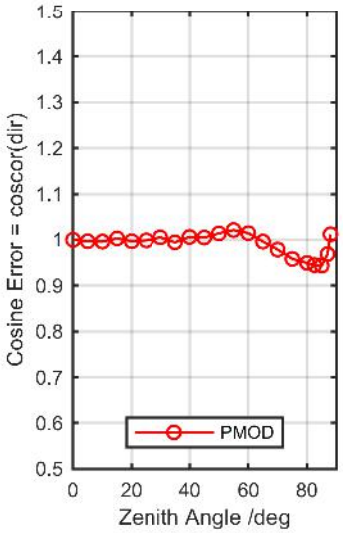

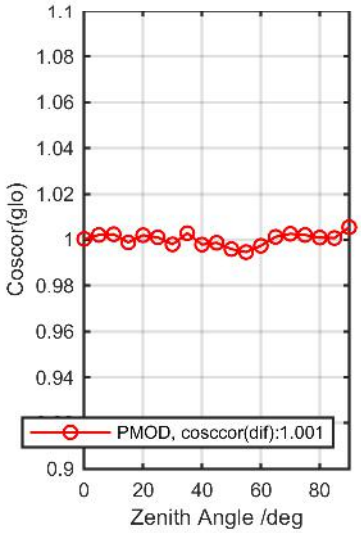

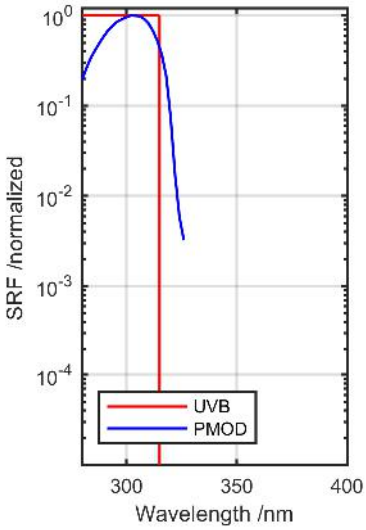

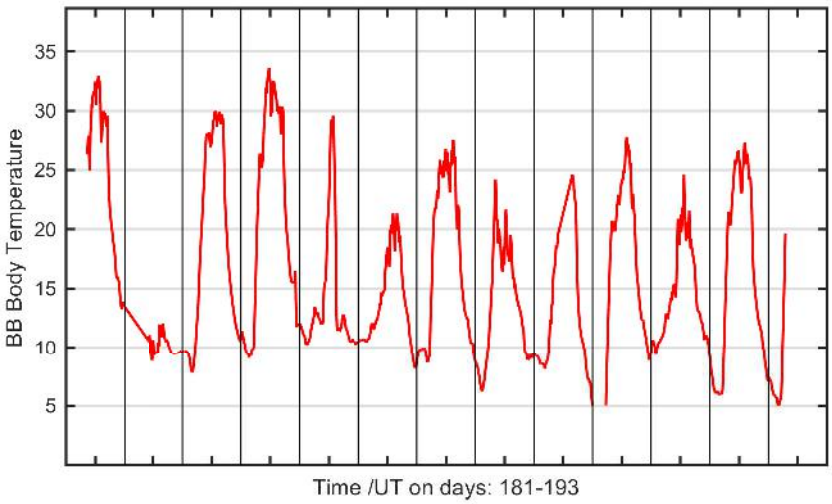

Calibration Matrix fn; Model sdisortREFms2009; f0=1.0194

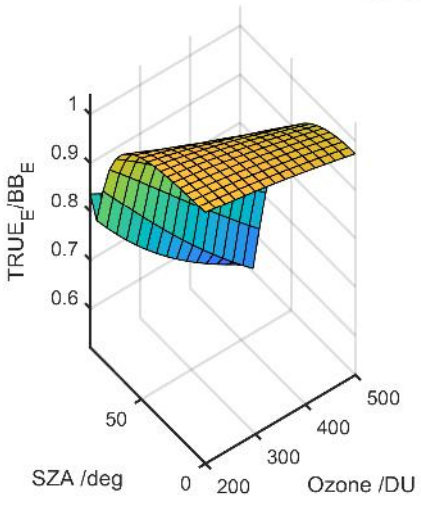

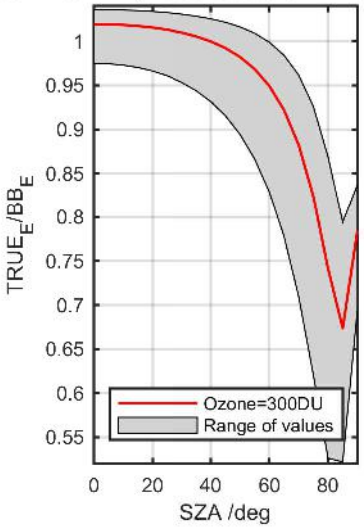

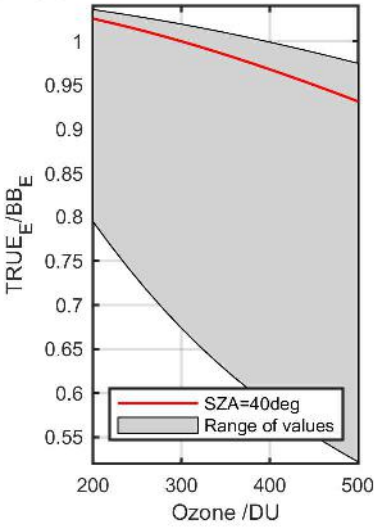

Calibration Results of MS-11S21346007 (UVB)

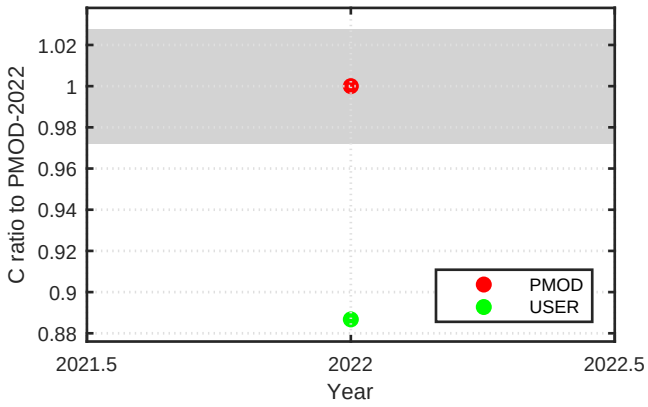

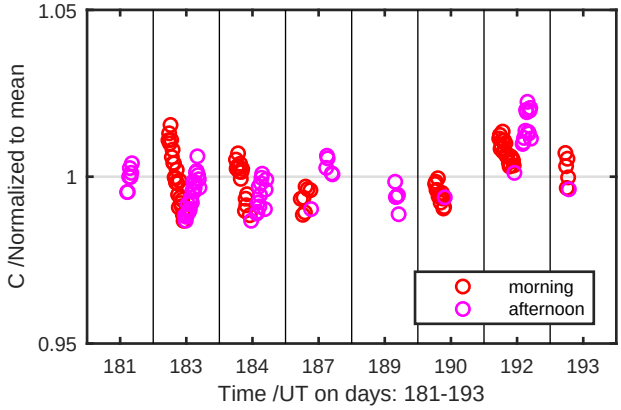

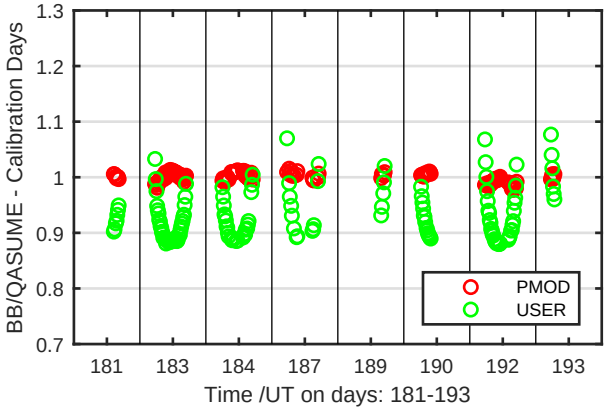

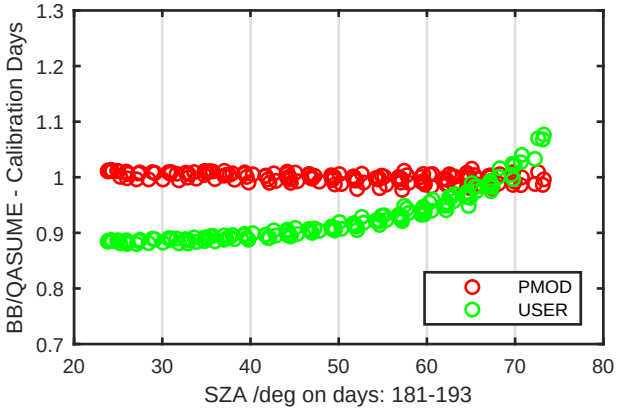

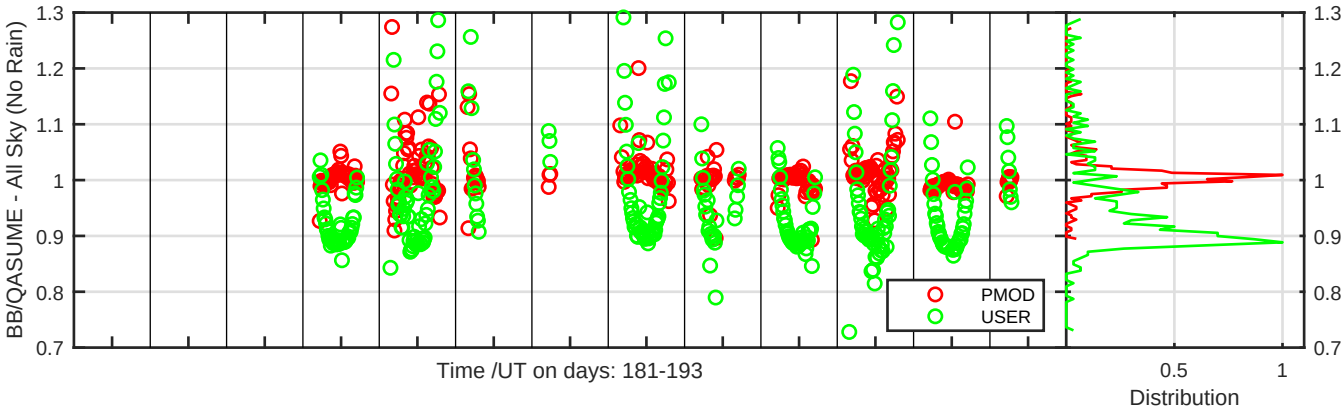

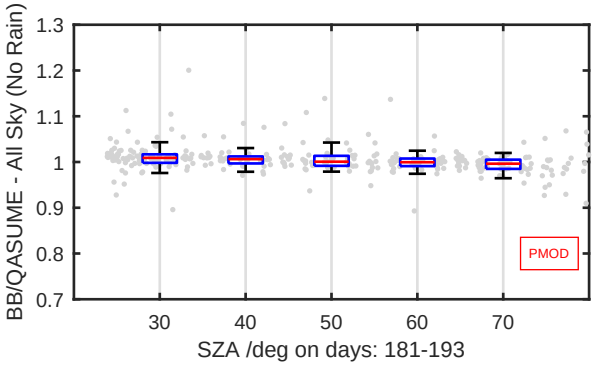

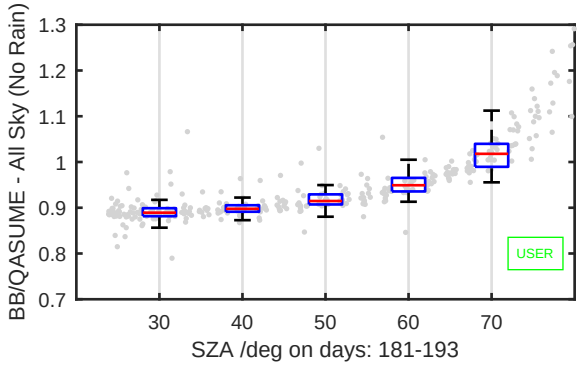

Calibration Results of MS-10S2200108 (UVA)

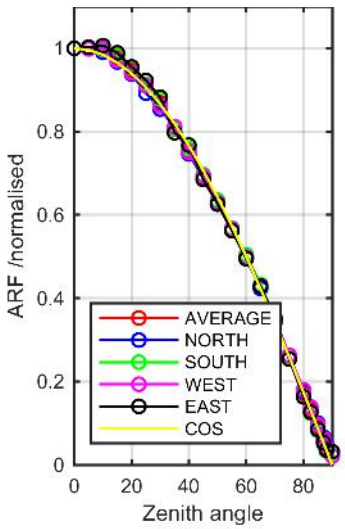

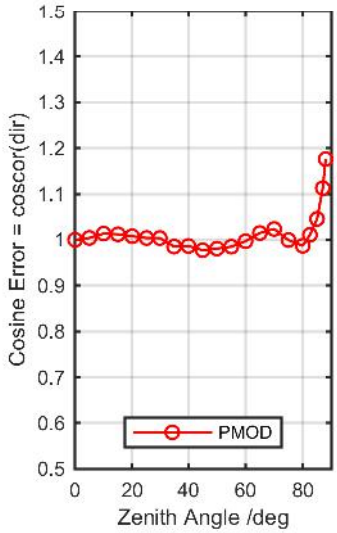

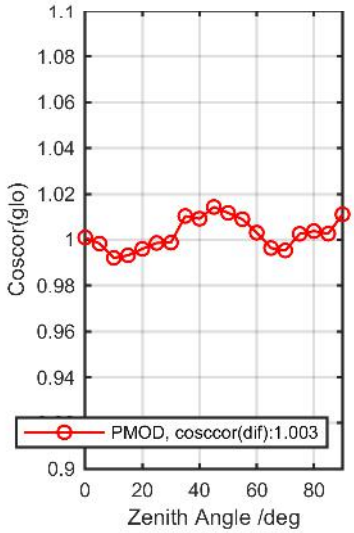

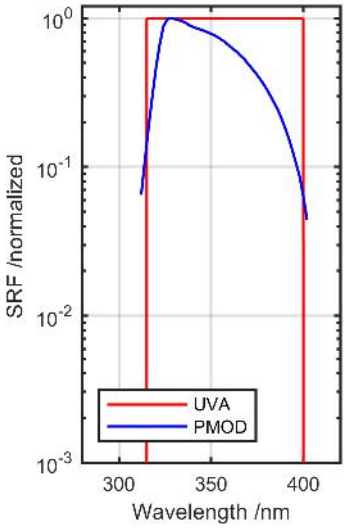

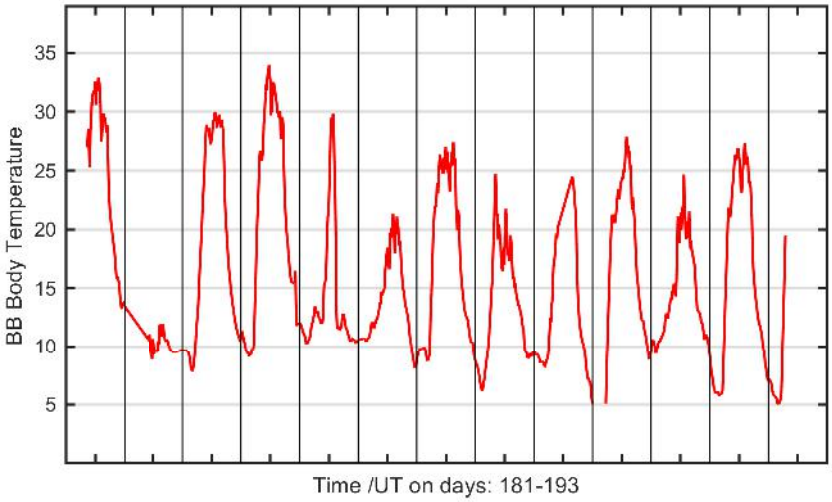

Calibration Matrix fn; Model sdisortREFms2009; f0=1.8435

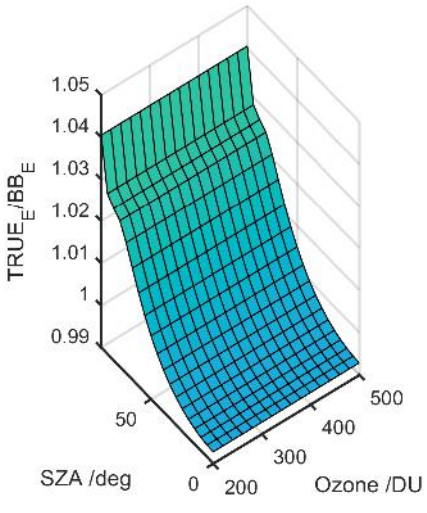

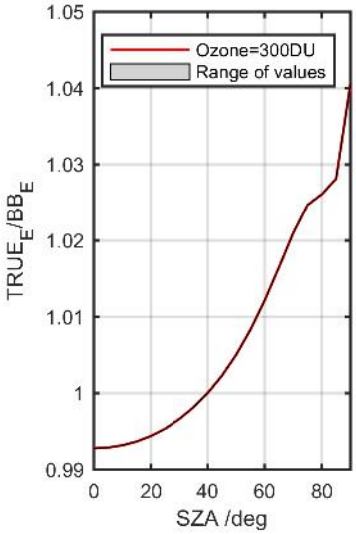

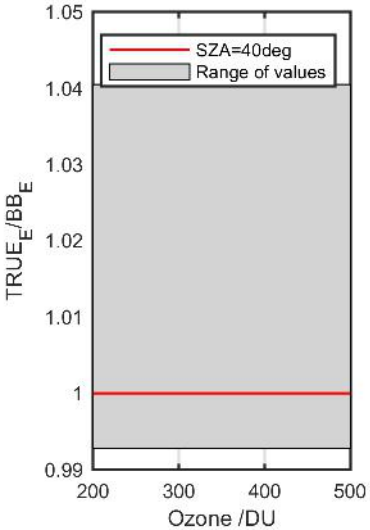

Calibration Results of MS-10S2200108 (UVA)

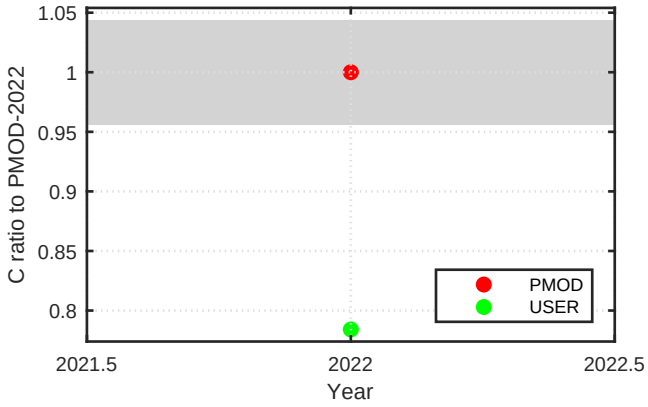

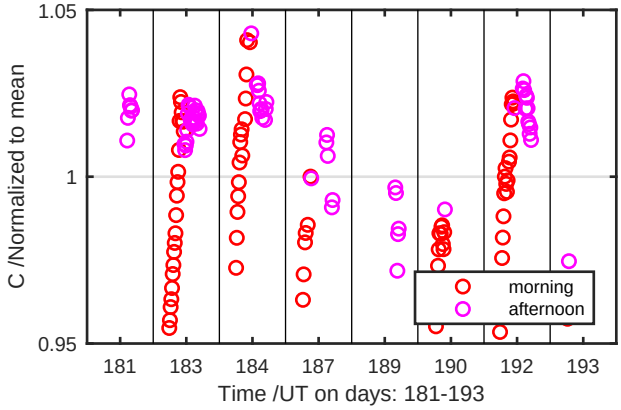

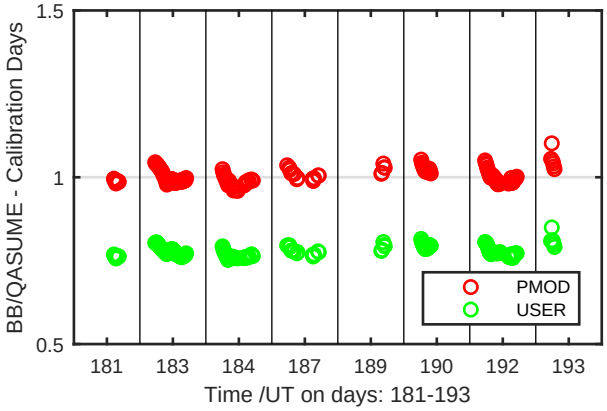

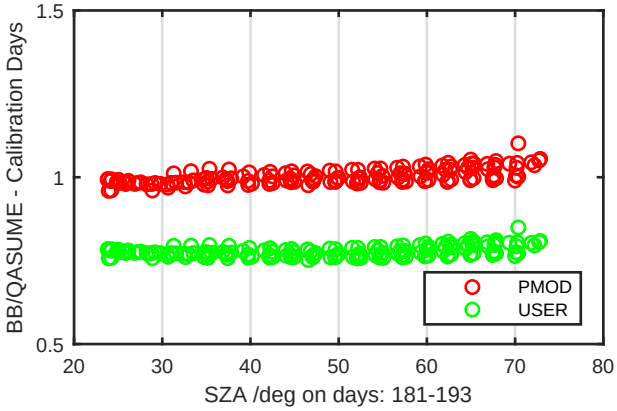

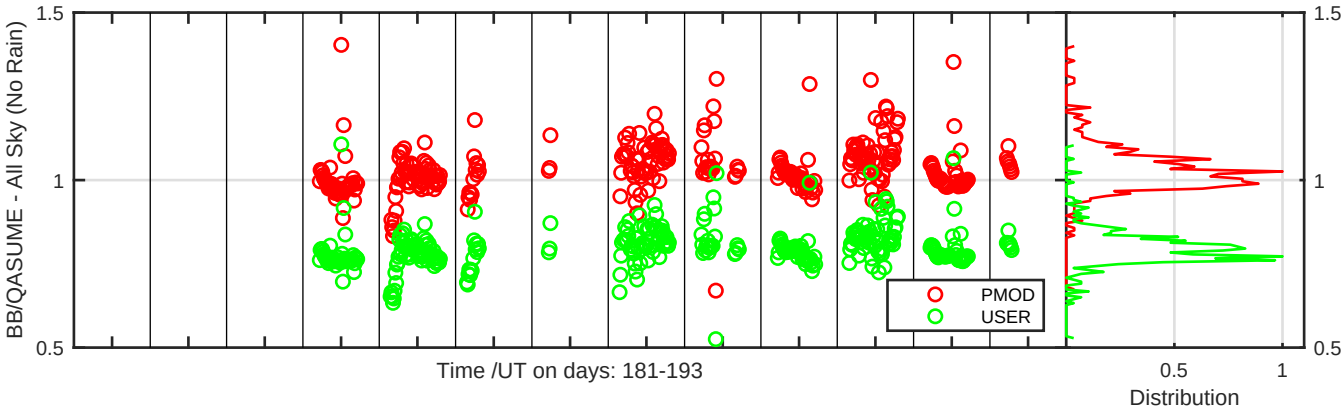

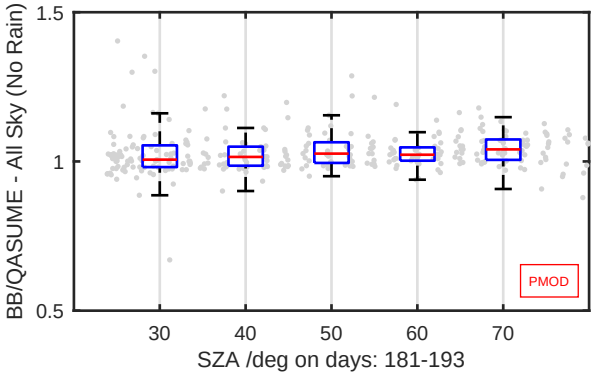

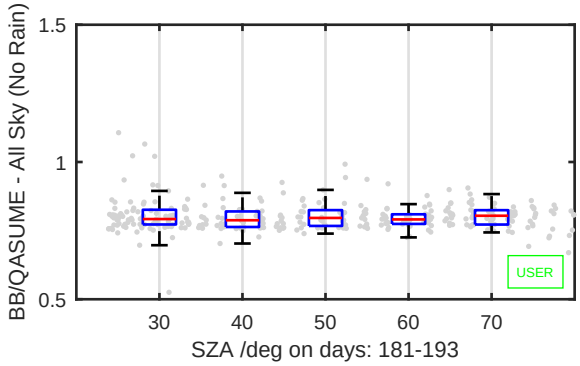

Calibration Results of EKOS11044p01 (UVE)

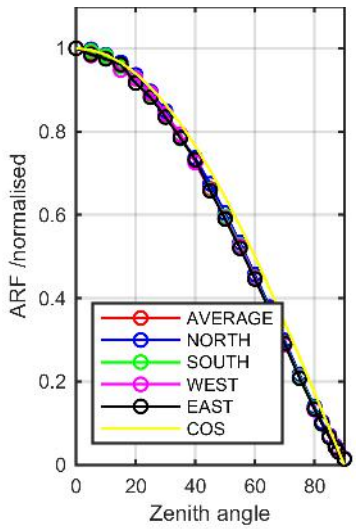

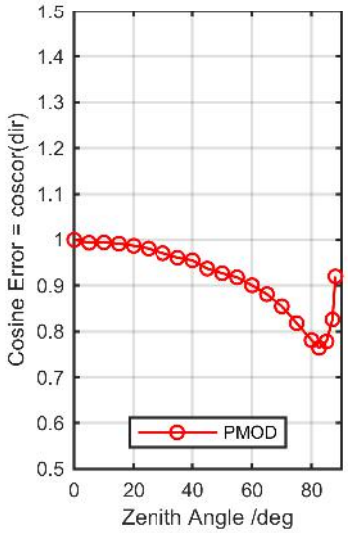

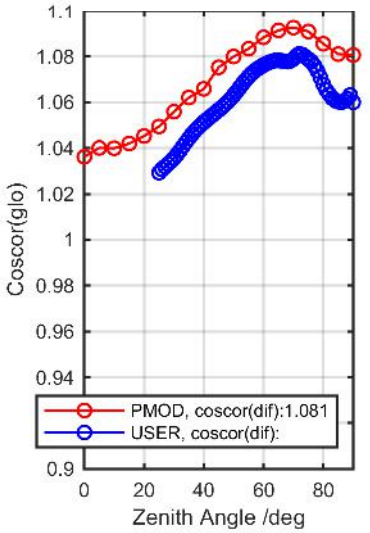

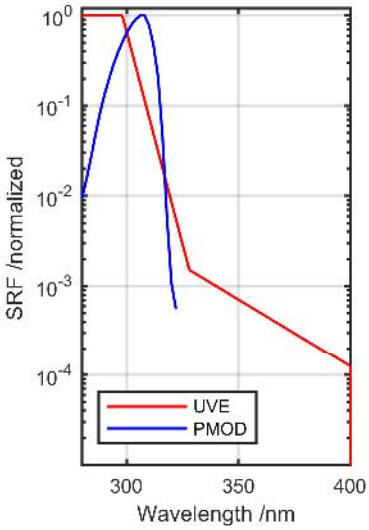

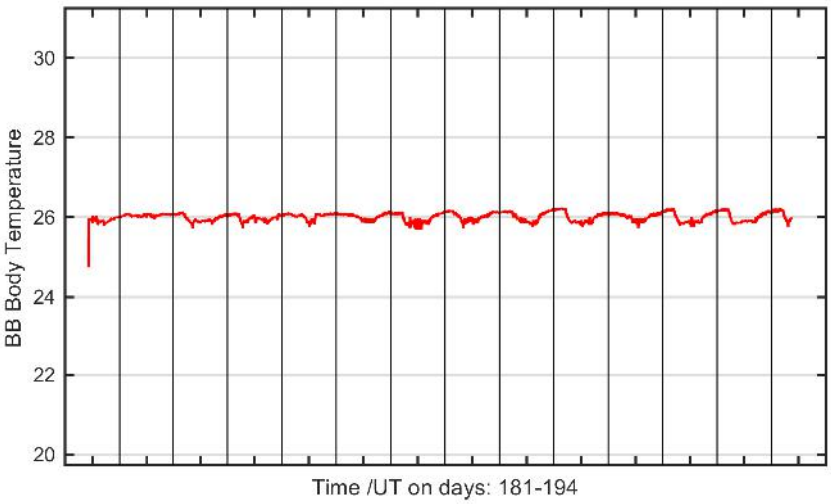

Calibration Matrix fn; Model sdisortREFms2009; f0=0.2223

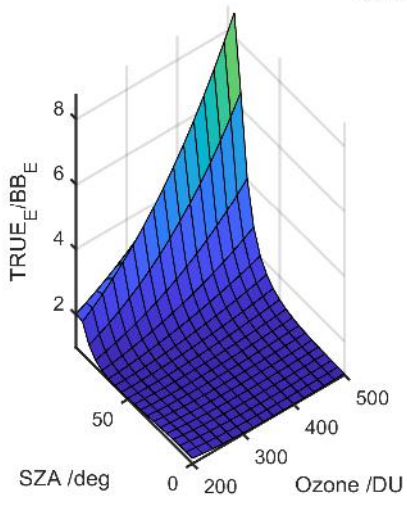

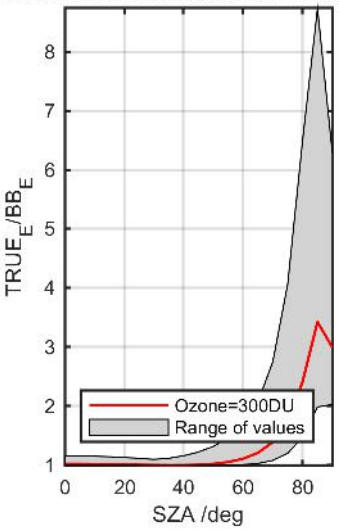

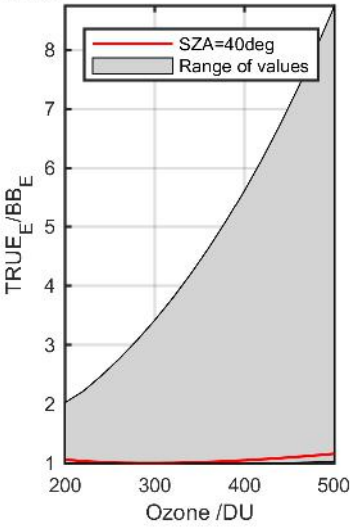

Calibration Results of EKOS11044p01 (UVE)

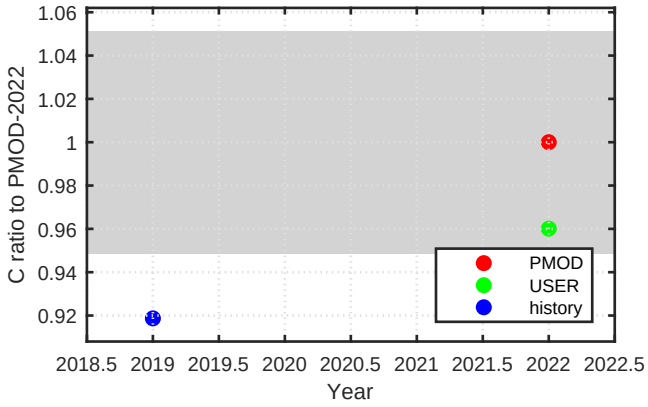

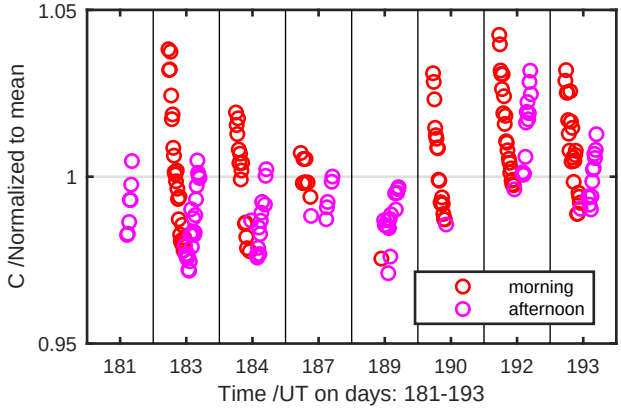

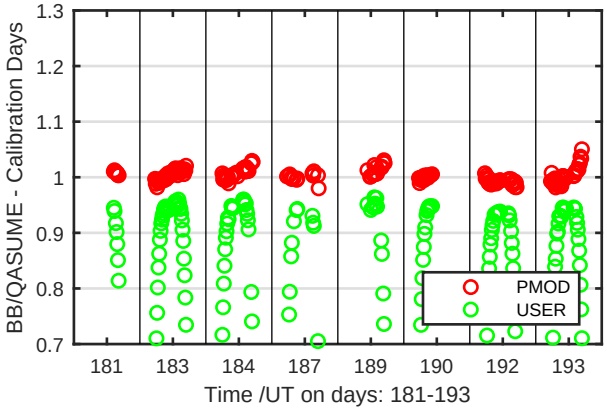

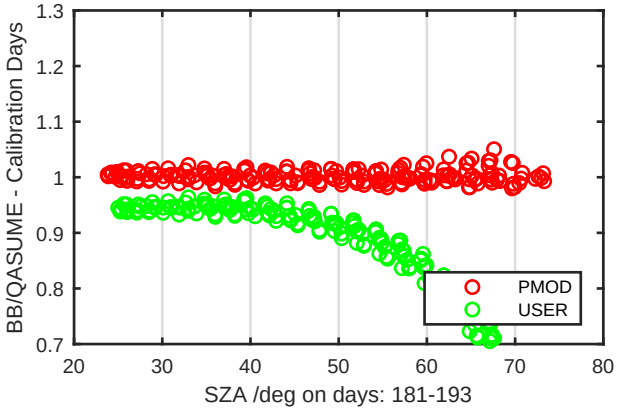

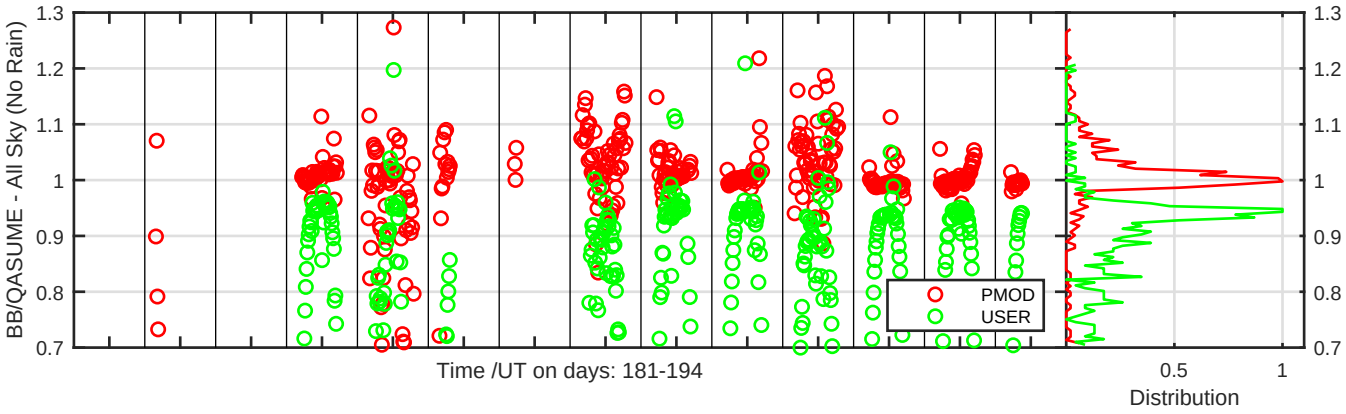

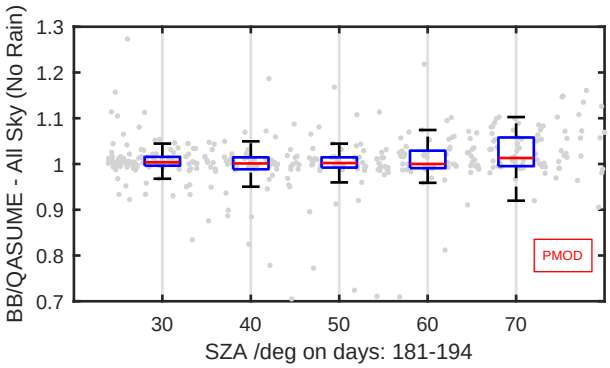

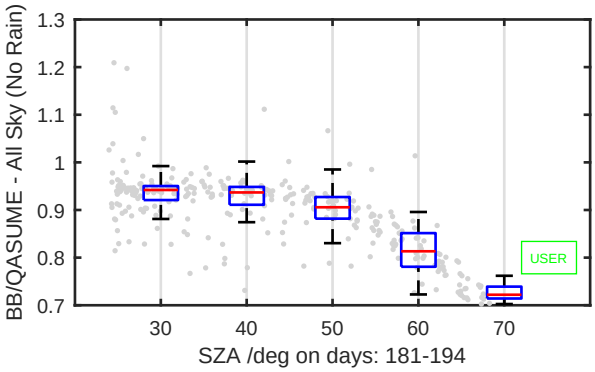

Calibration Results of FS-UVA5239 (UVA)

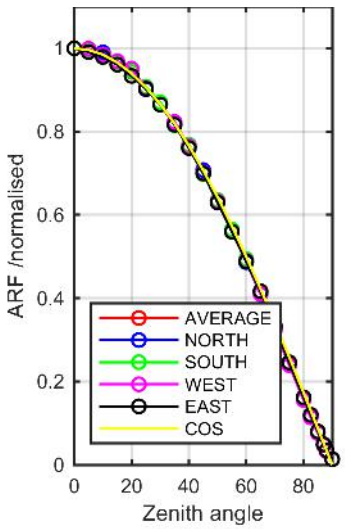

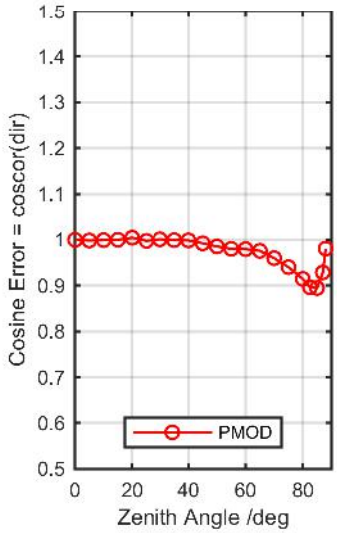

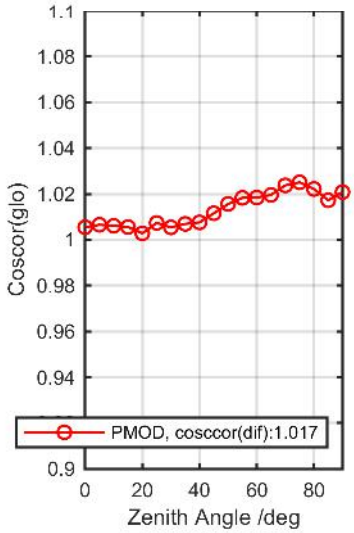

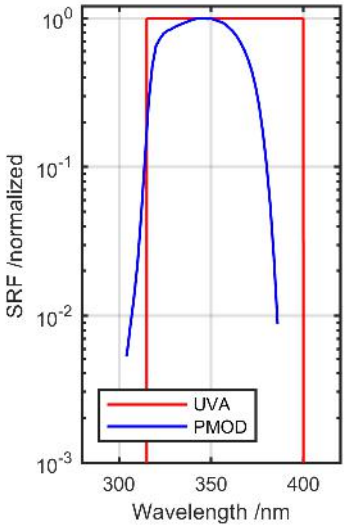

Calibration Matrix fn; Model sdisortREFms2009; f0=1.8865

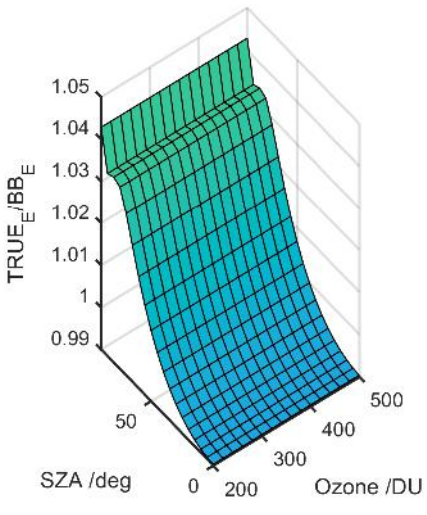

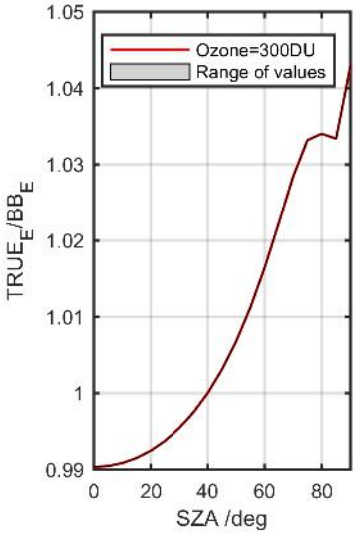

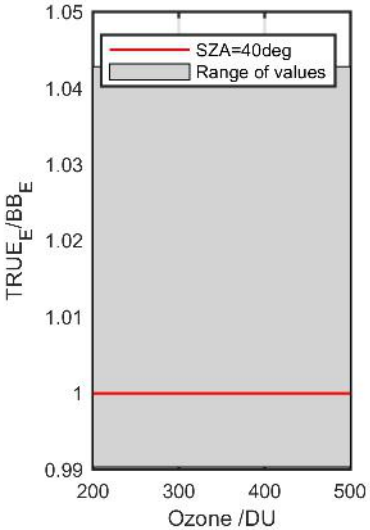

Calibration Results of FS-UVA5239 (UVA)

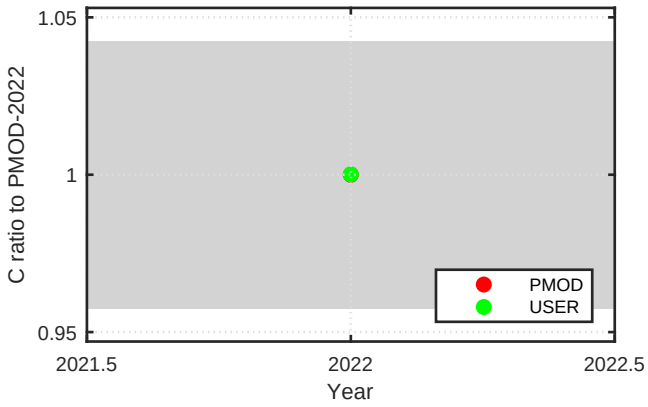

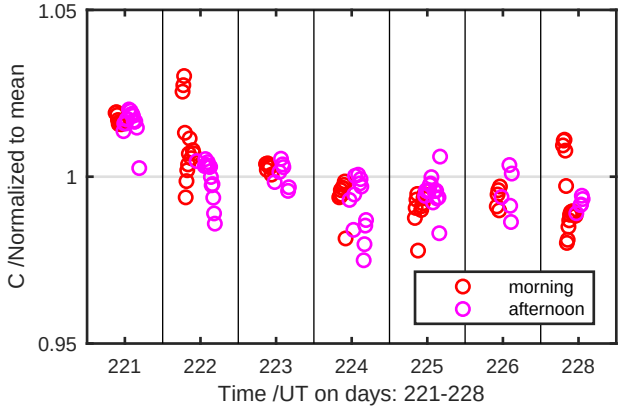

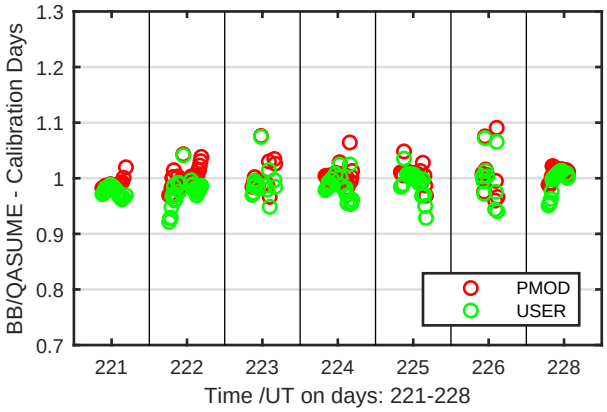

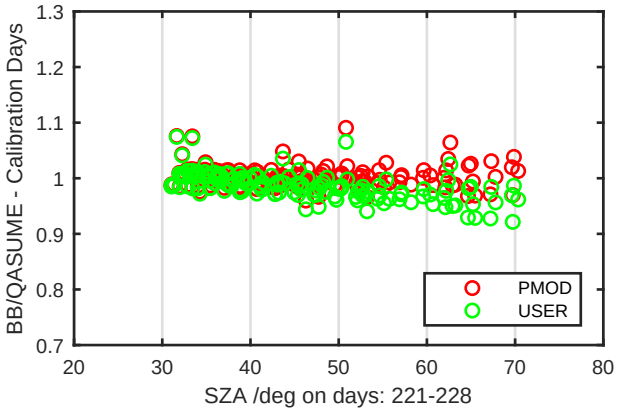

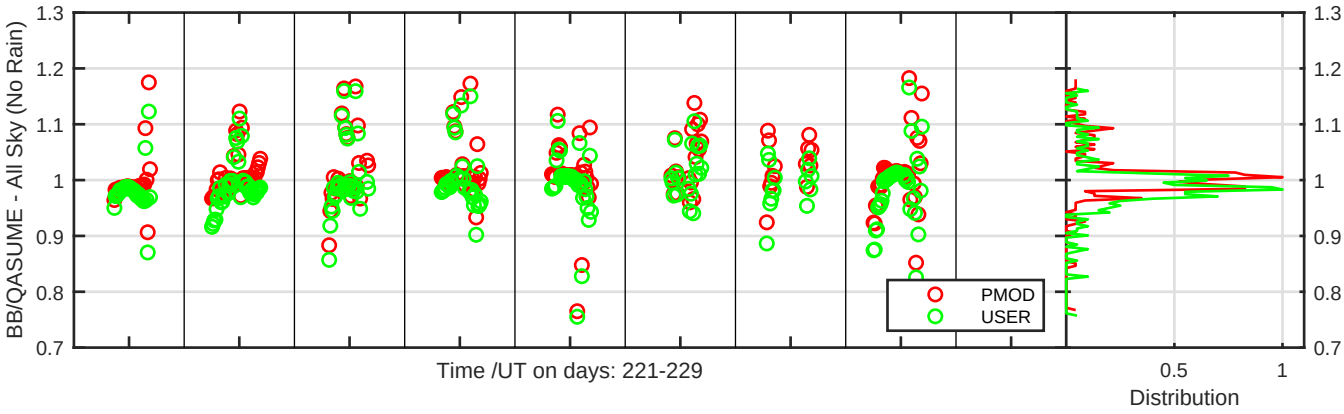

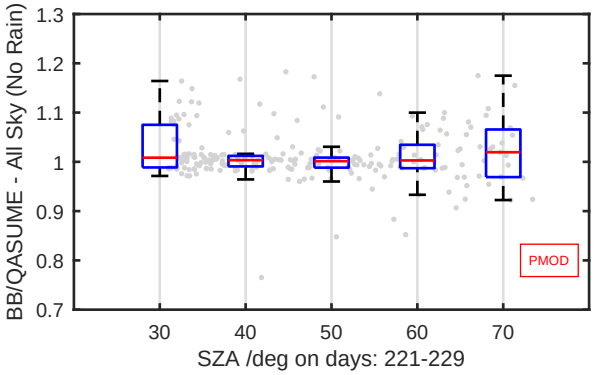

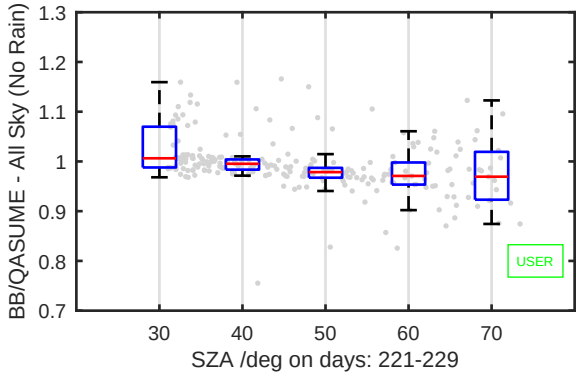

Calibration Results of FS-UVB3214 (UVB)

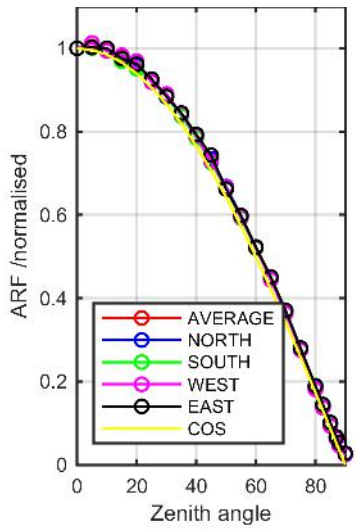

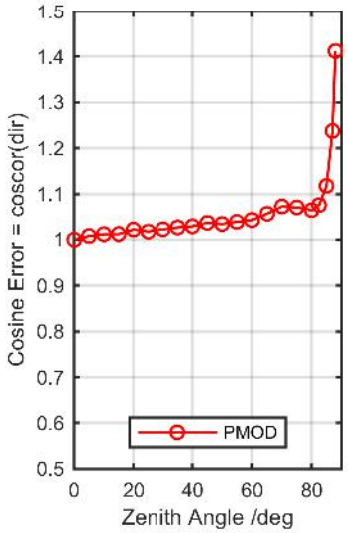

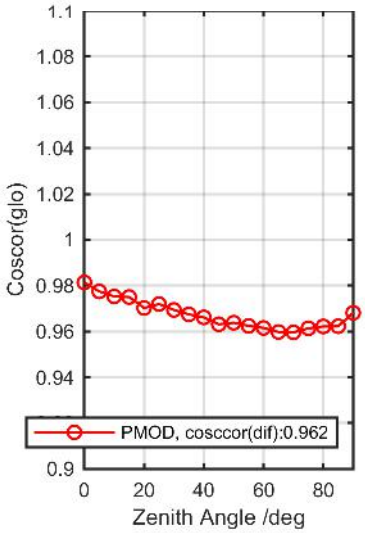

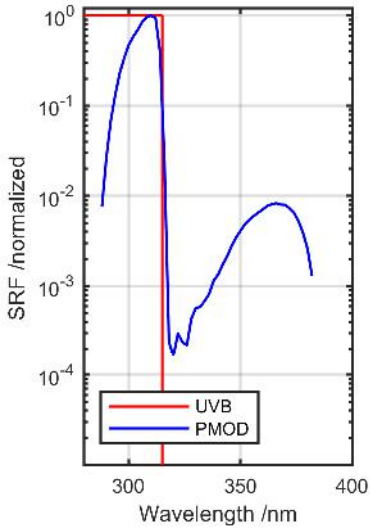

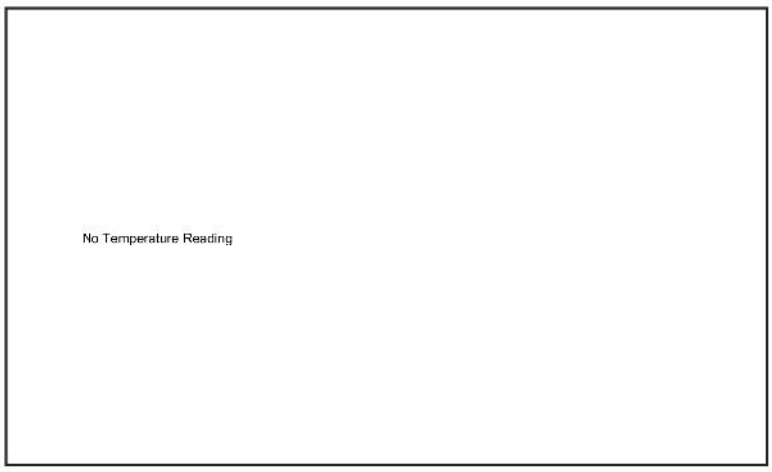

Calibration Matrix fn; Model sdisortREFms2009; f0=1.1853

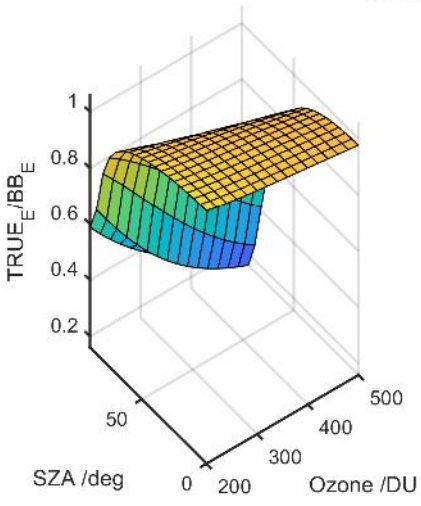

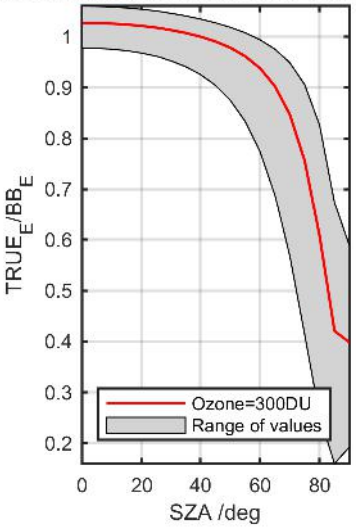

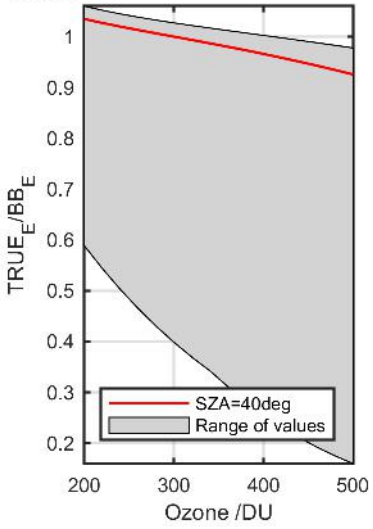

Calibration Results of FS-UVB3214 (UVB)

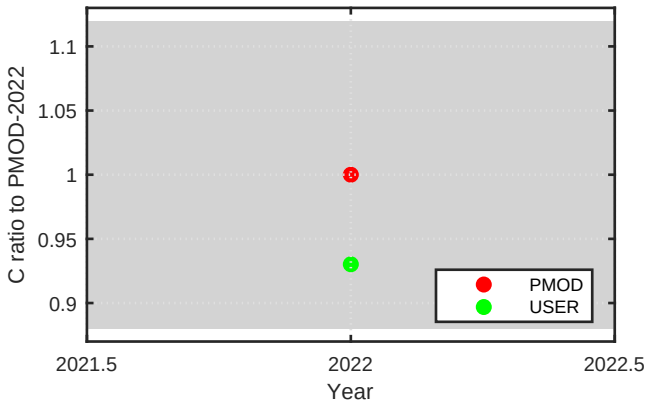

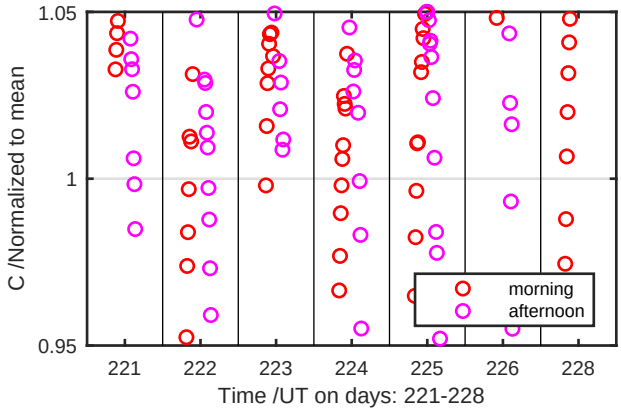

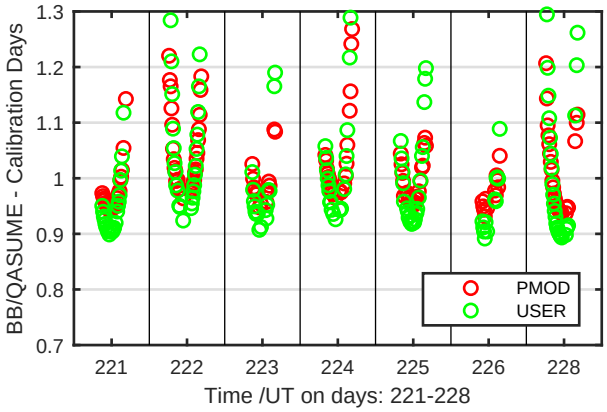

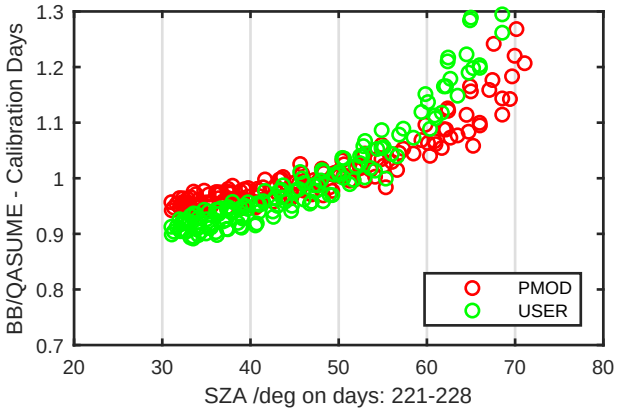

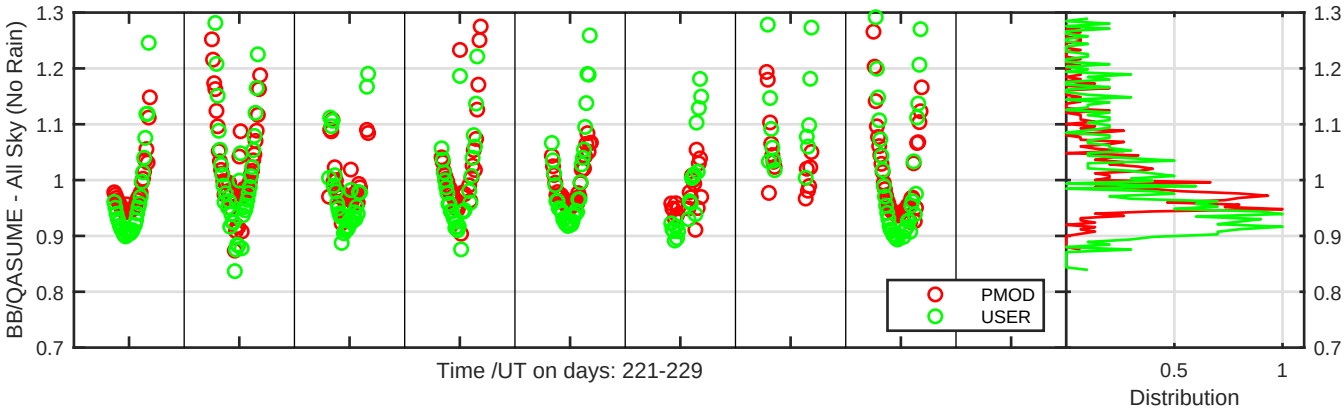

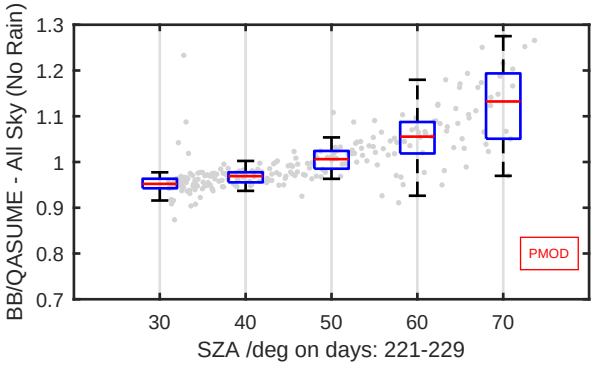

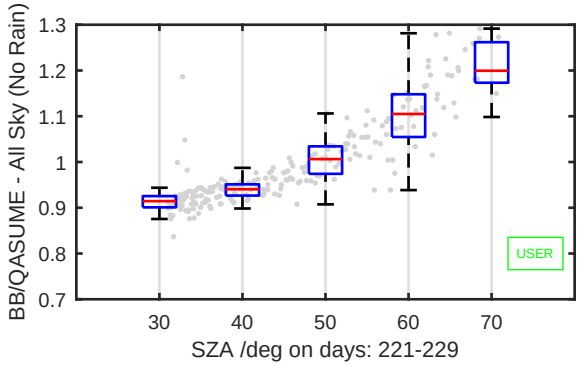

Calibration Results of CMS16113 (UVE)

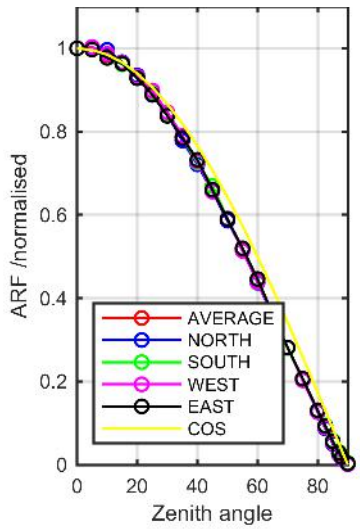

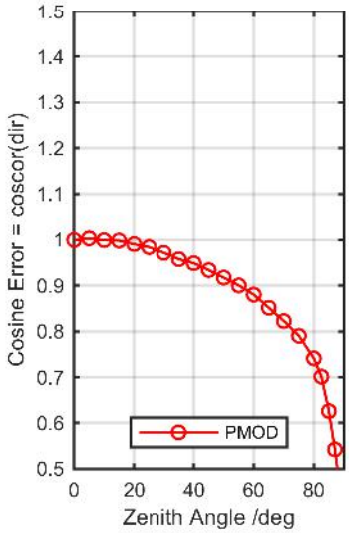

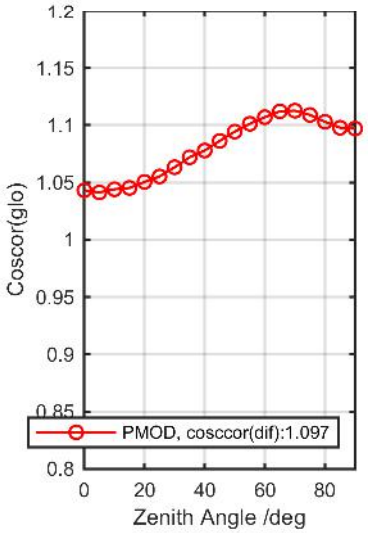

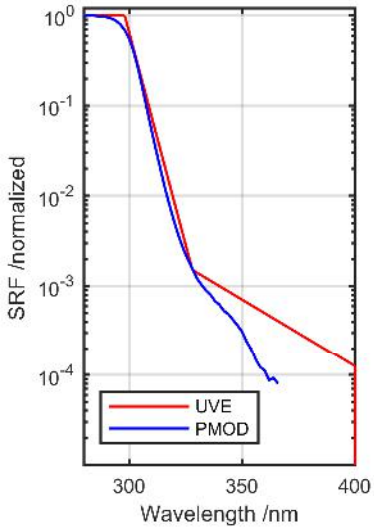

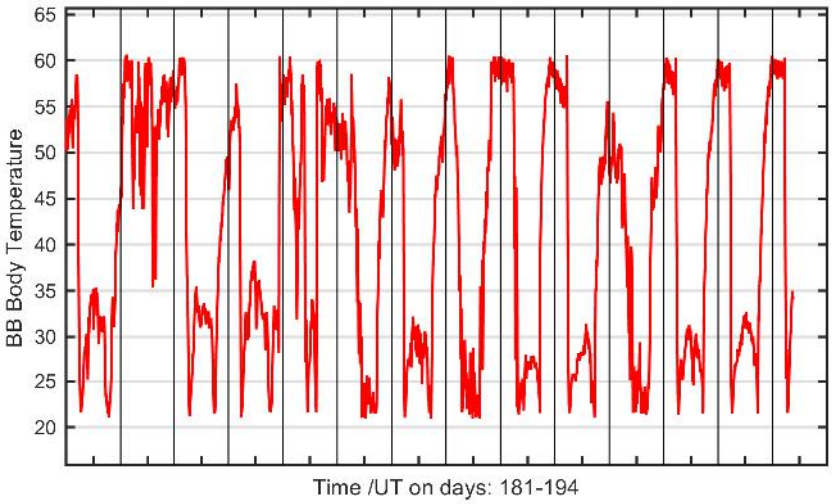

Calibration Matrix fn; Model sdisortREFms2009; f0=1.4028

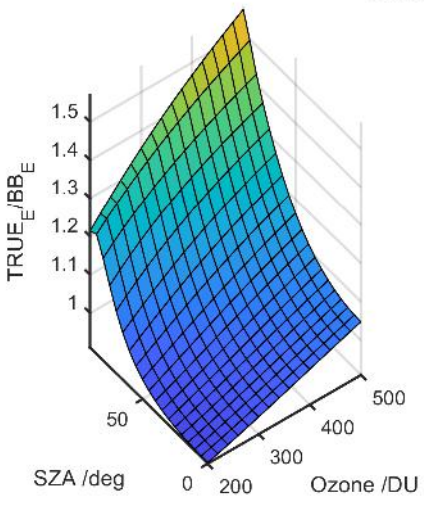

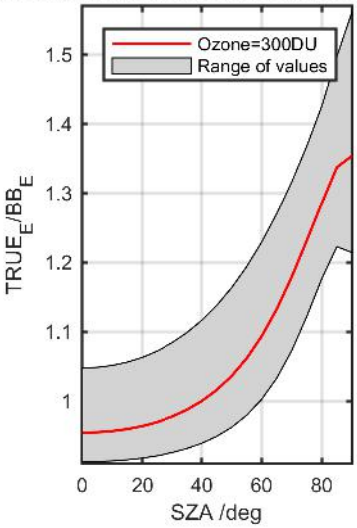

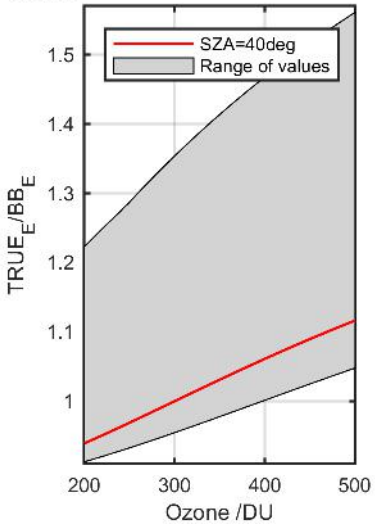

Calibration Results of CMS16113 (UVE)

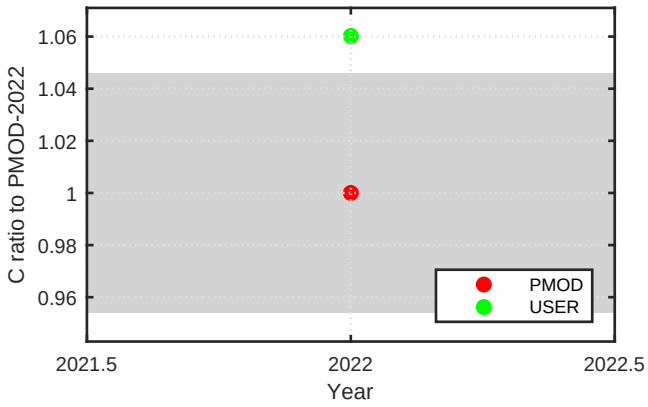

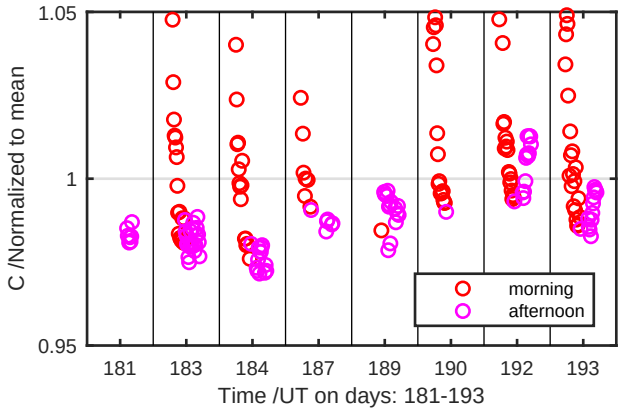

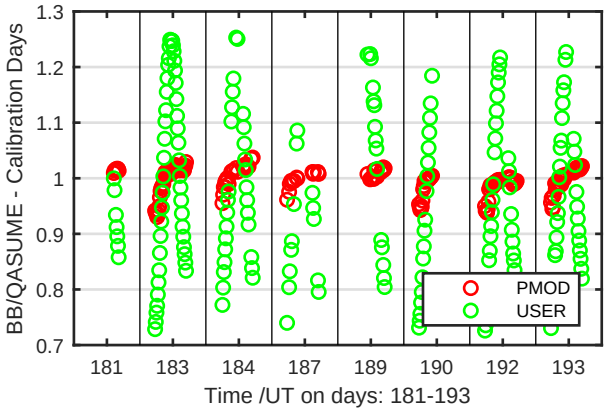

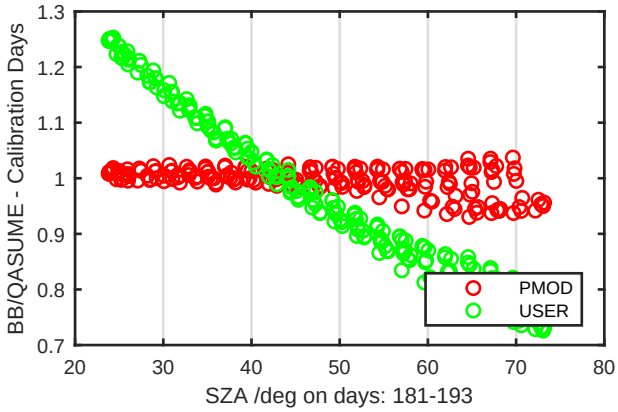

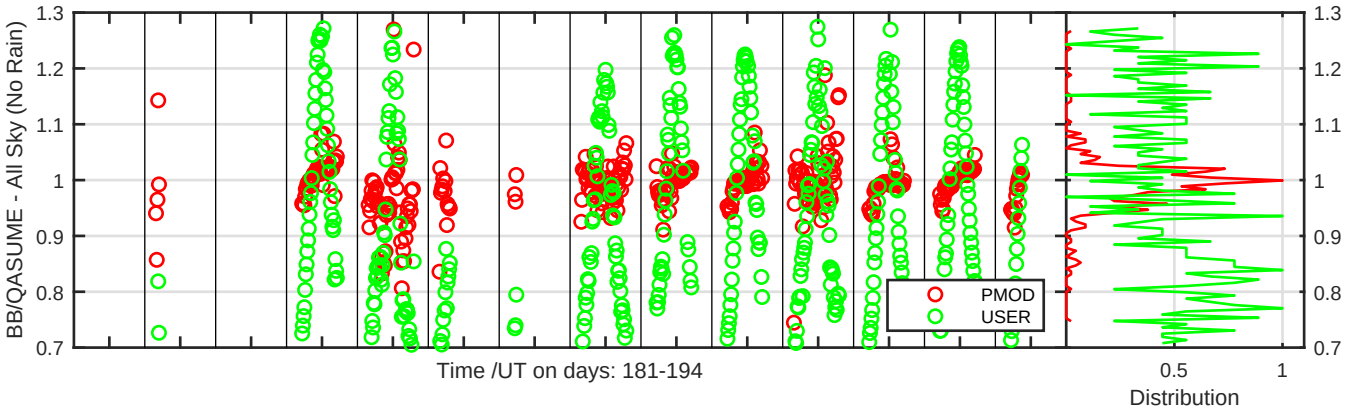

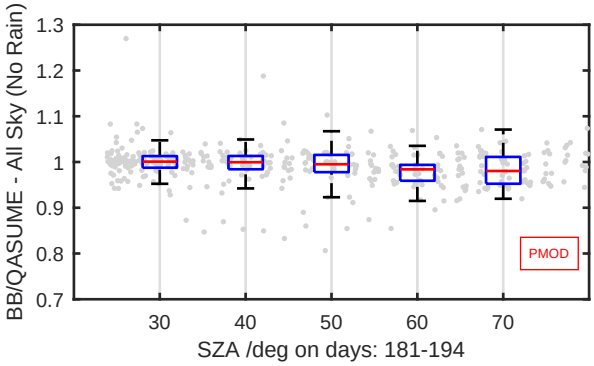

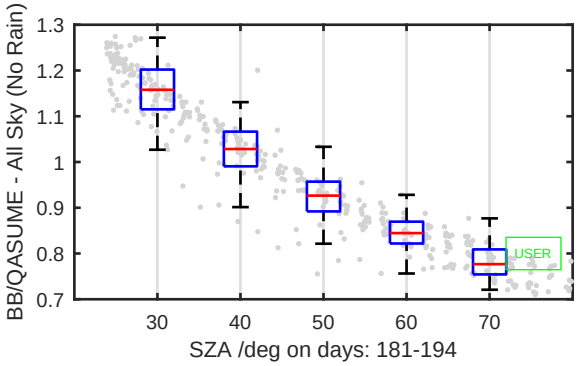

Calibration Results of DELTA11028751 (UVE)

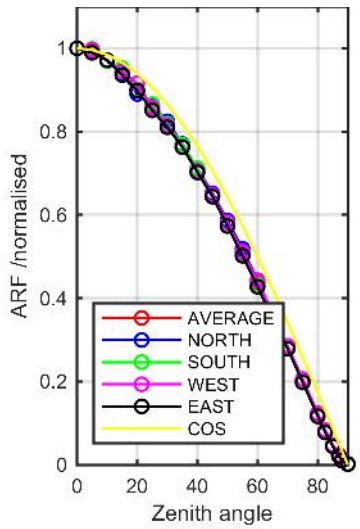

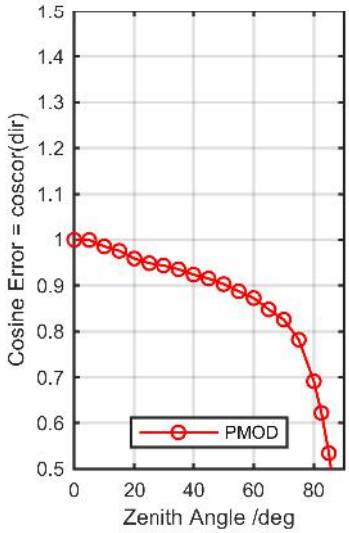

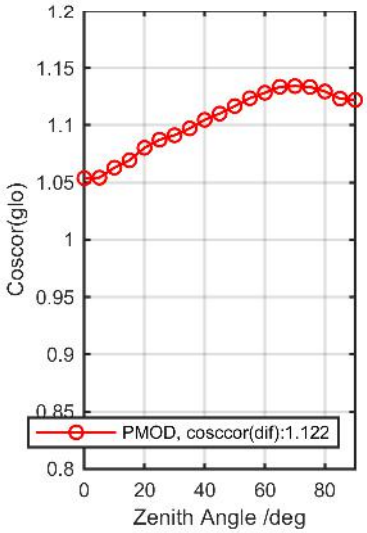

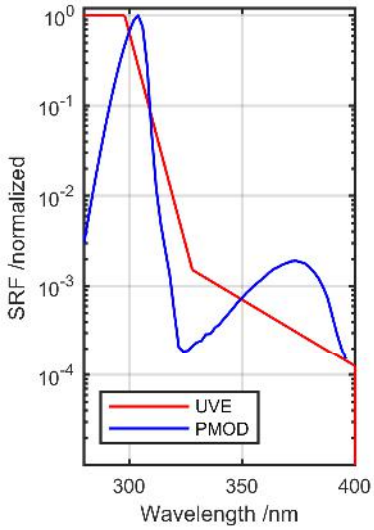

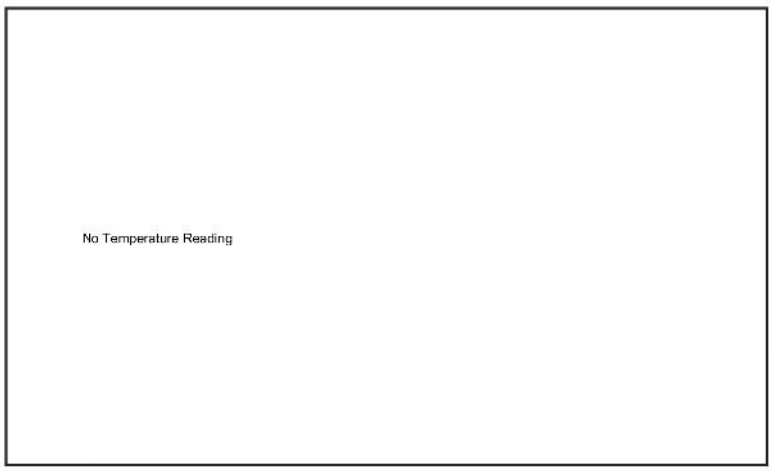

Calibration Matrix fn; Model sdisortREFms2009; f0=0.6441

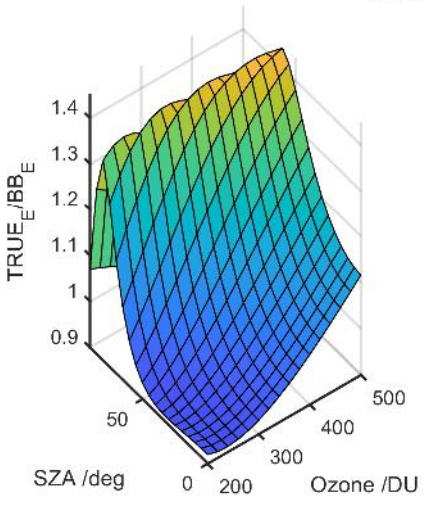

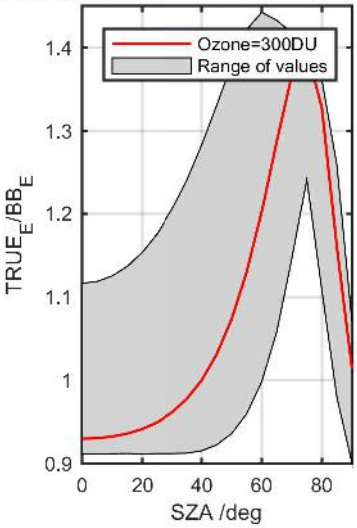

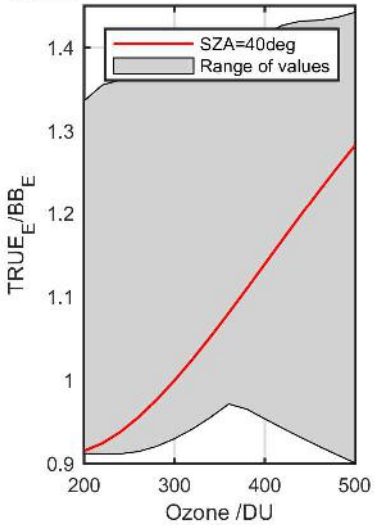

Calibration Results of DELTA11028751 (UVE)

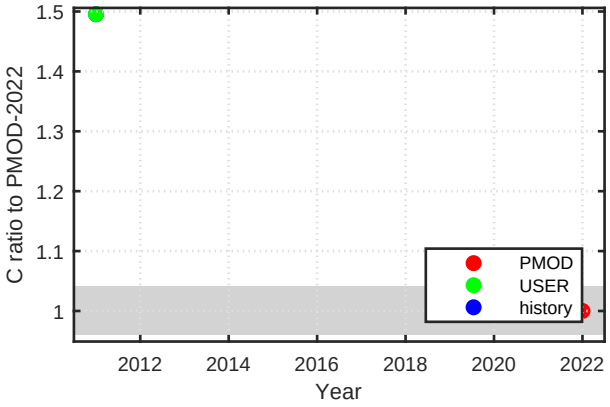

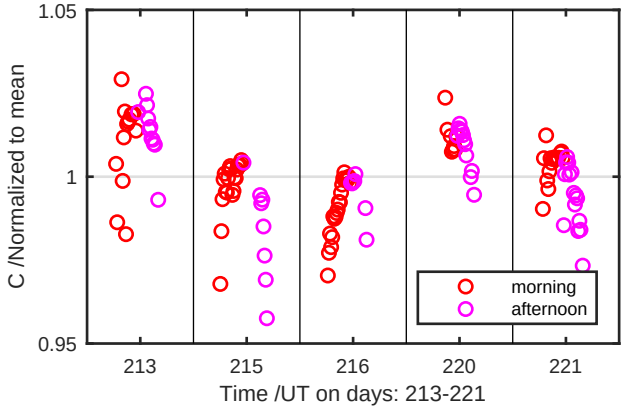

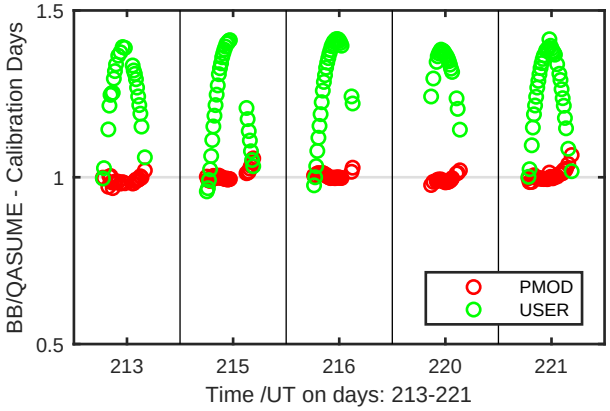

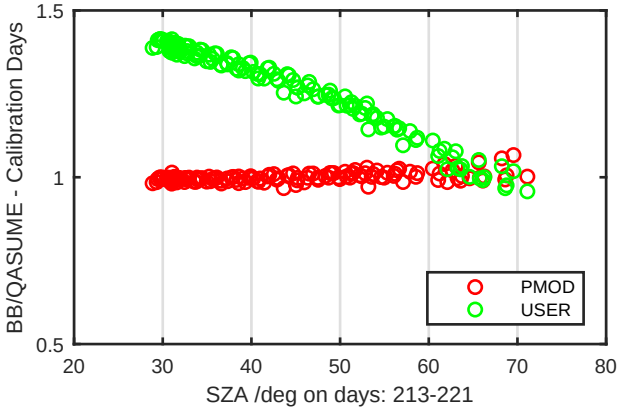

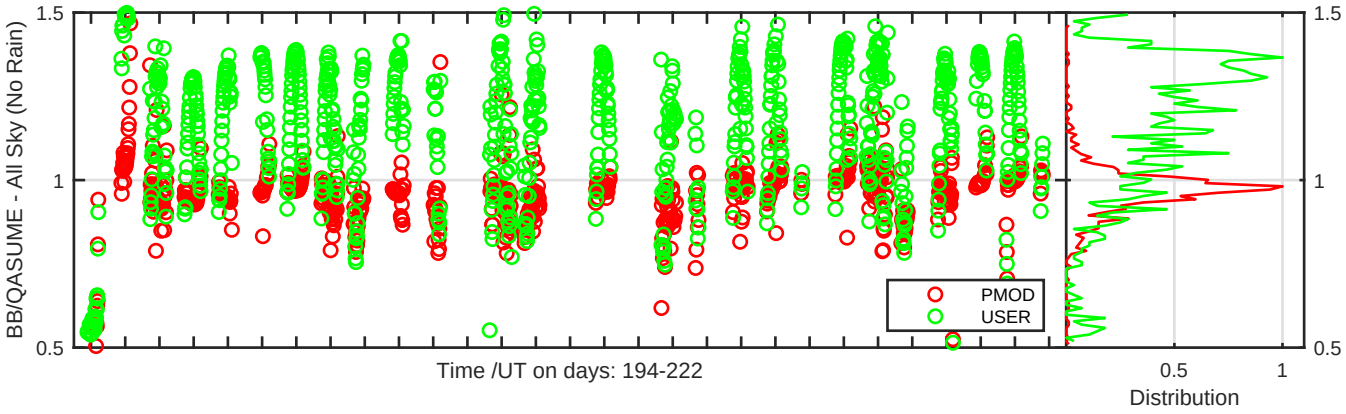

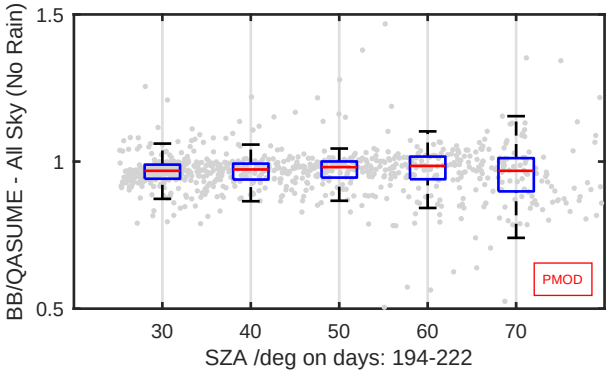

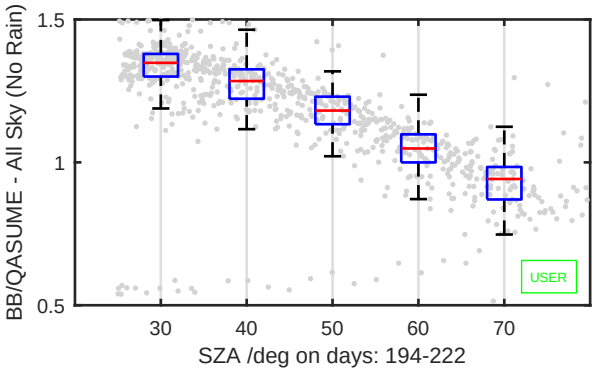

Calibration Results of IS16799s22 (UVE)

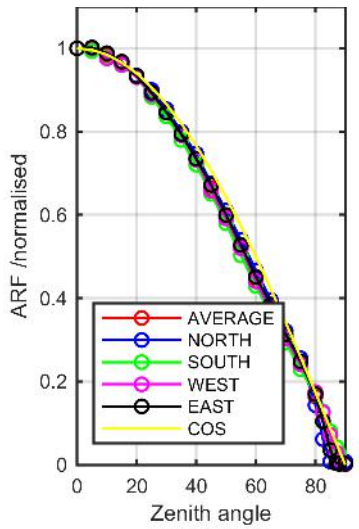

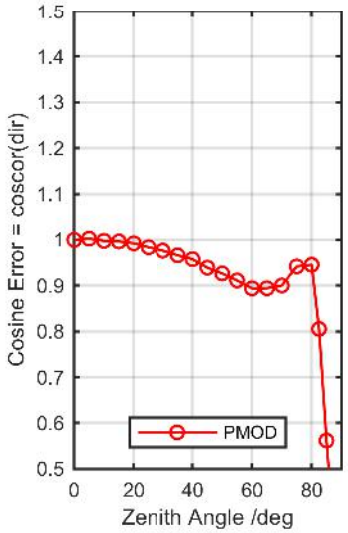

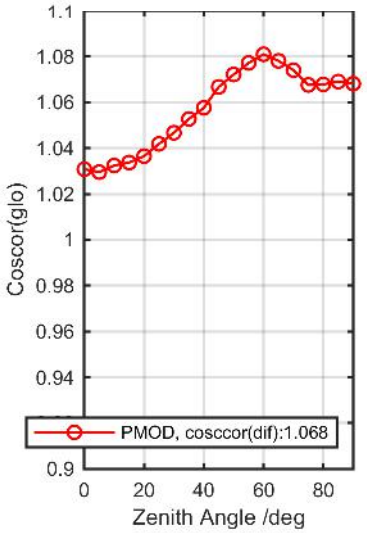

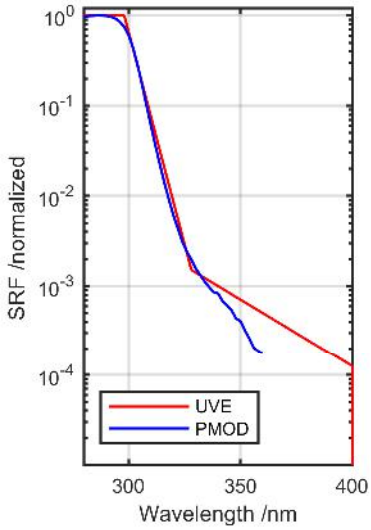

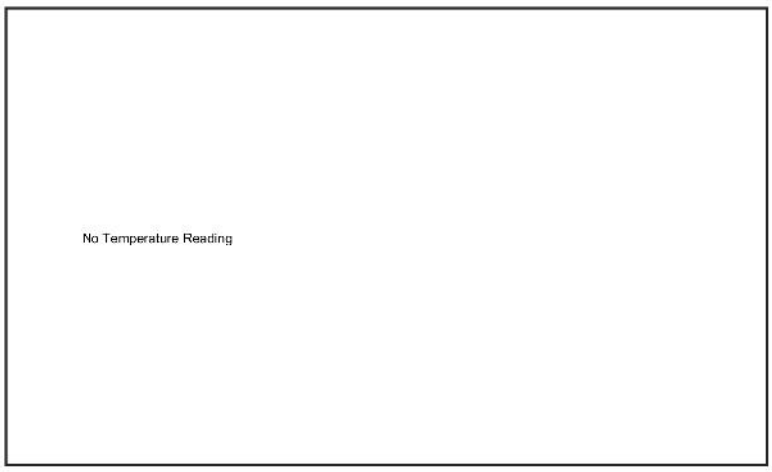

Calibration Matrix fn; Model sdisortREFms2009; f0=1.2418

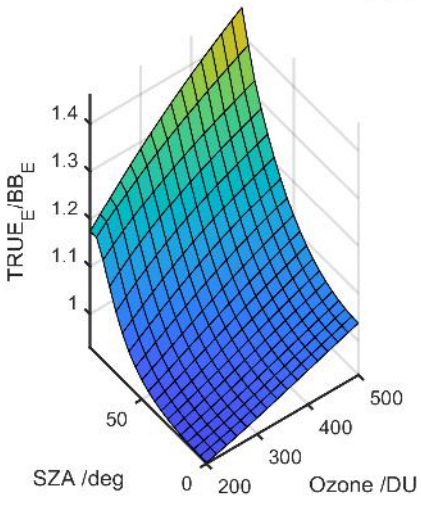

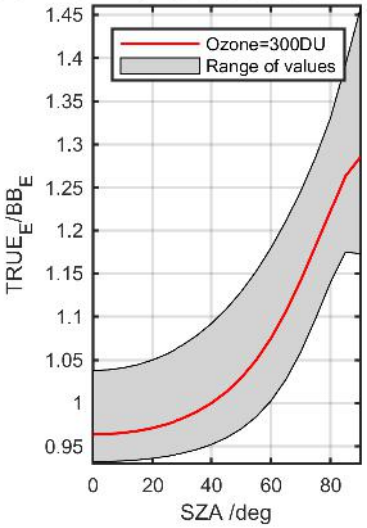

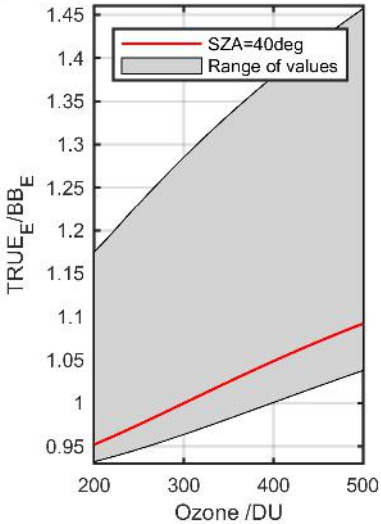

Calibration Results of IS16799s22 (UVE)

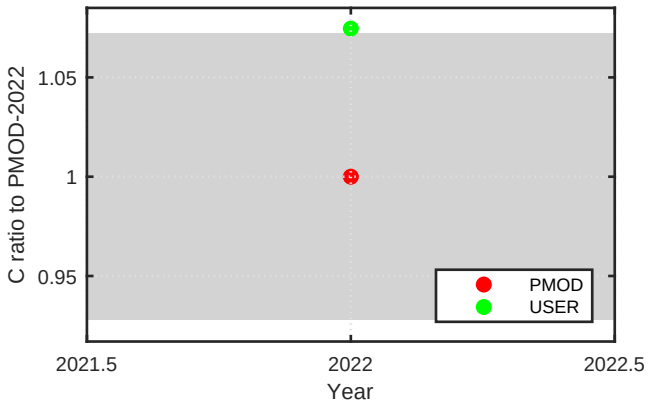

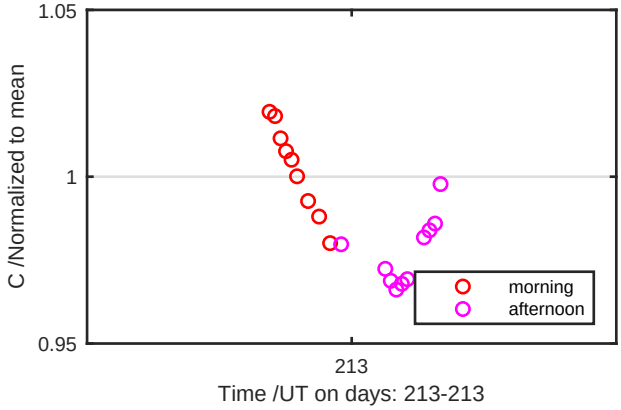

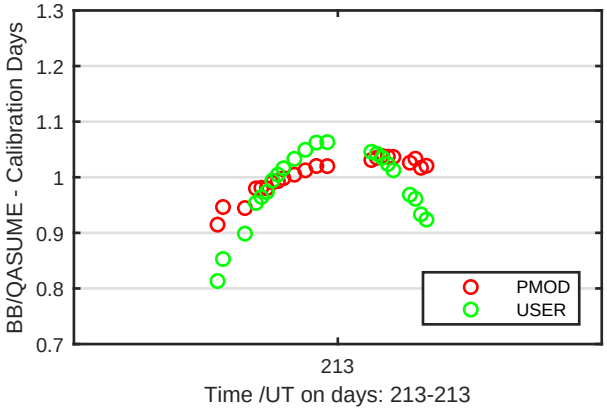

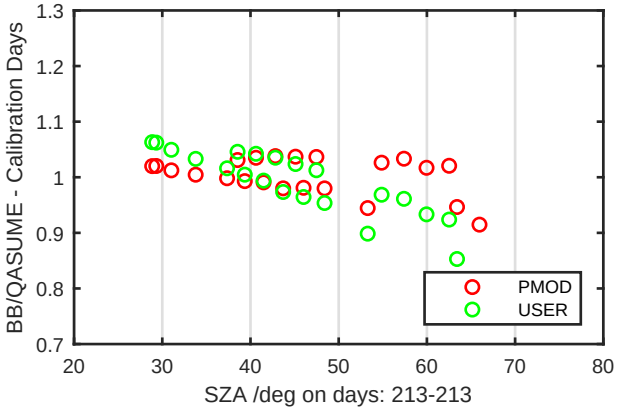

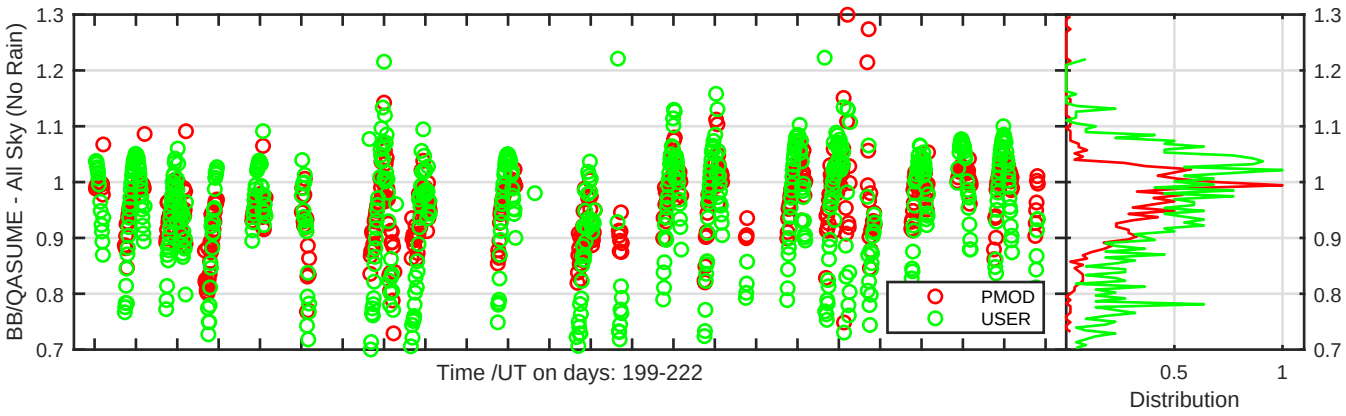

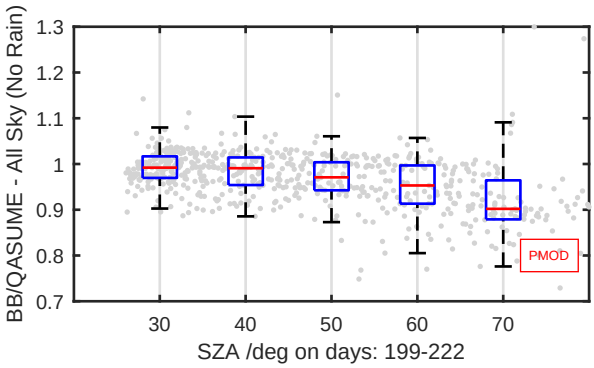

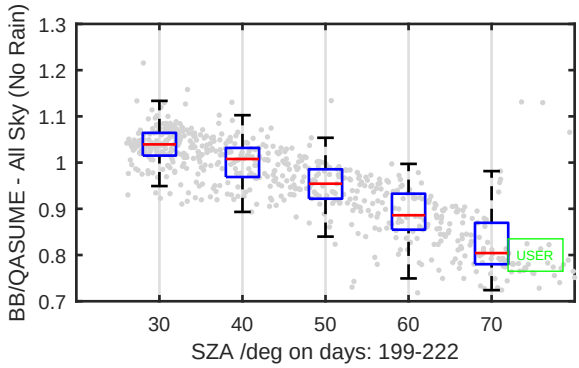

Calibration Results of SGLUX-UVI031 (UVE)

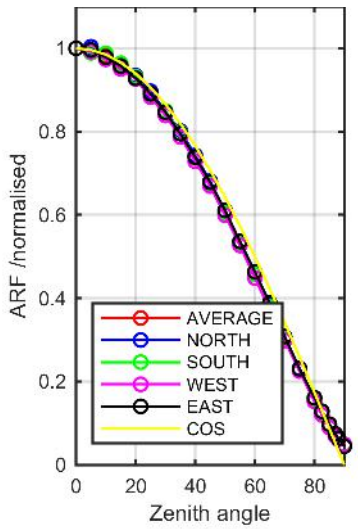

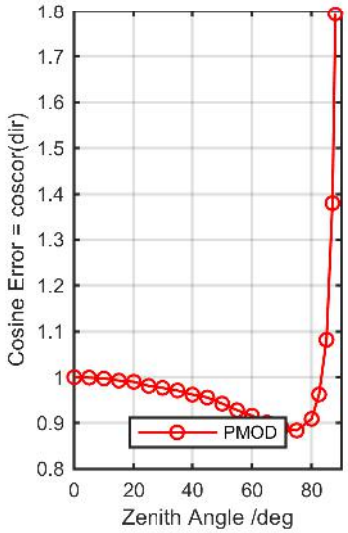

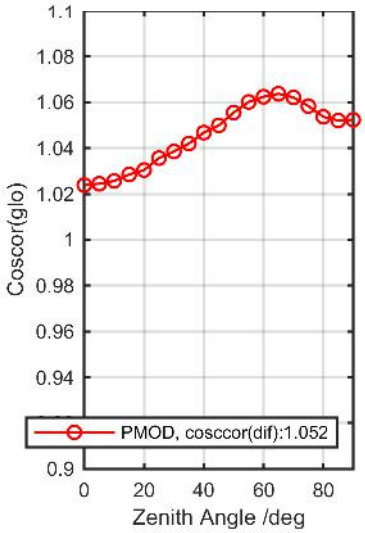

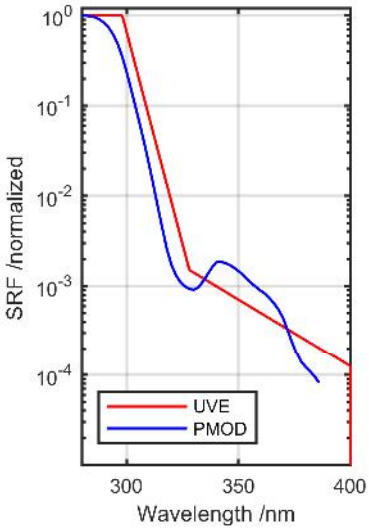

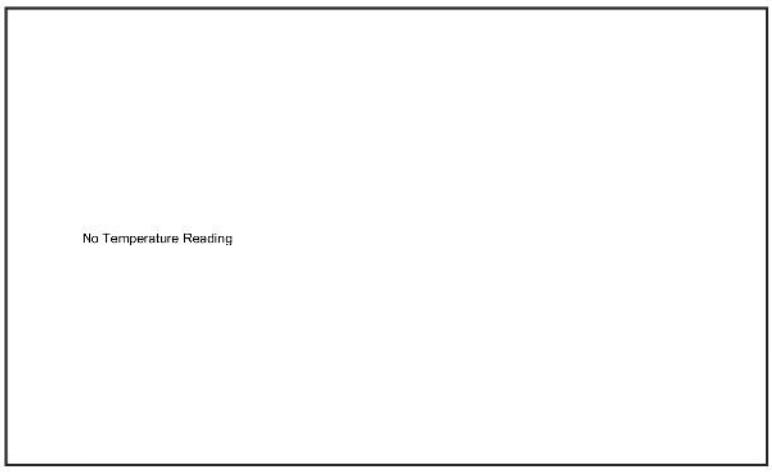

Calibration Matrix fn; Model sdisortREFms2009; f0=2.2673

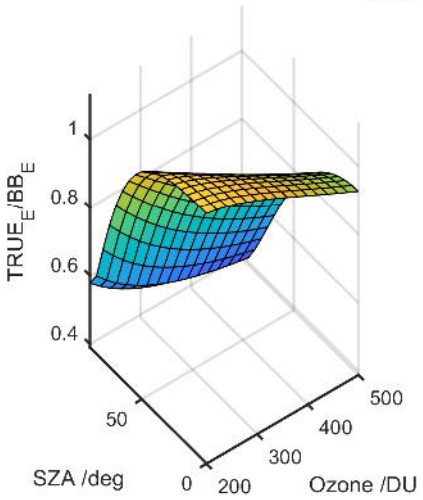

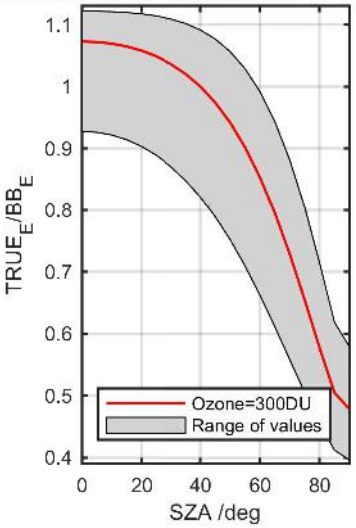

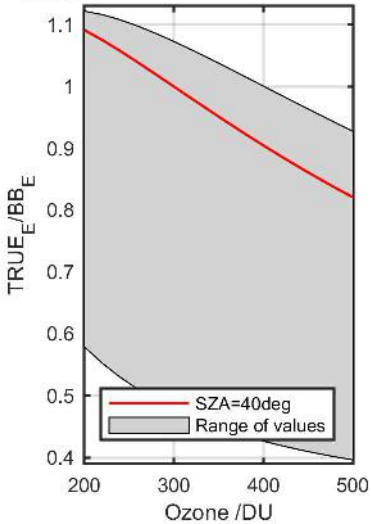

Calibration Results of SGLUX-UVI031 (UVE)

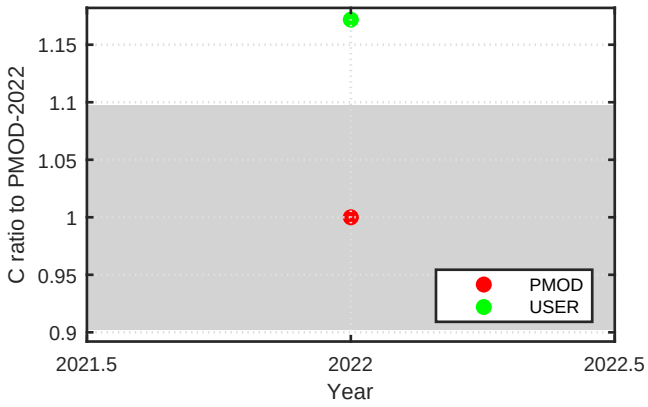

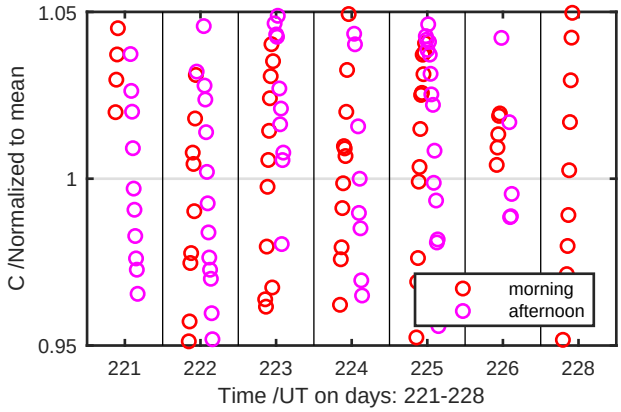

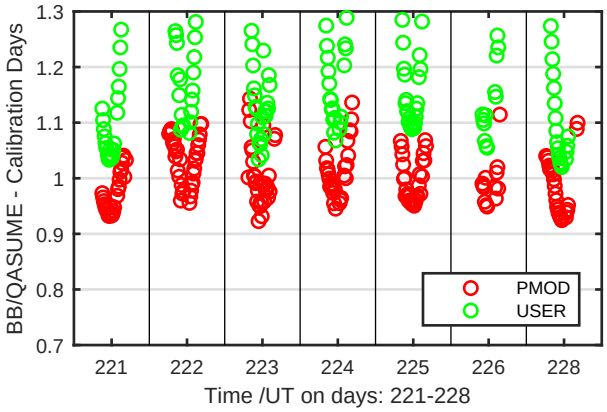

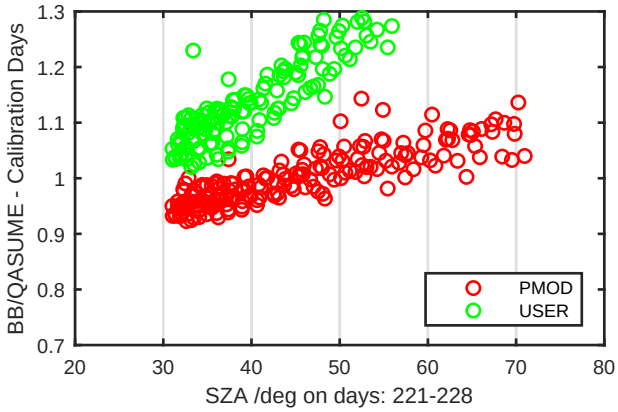

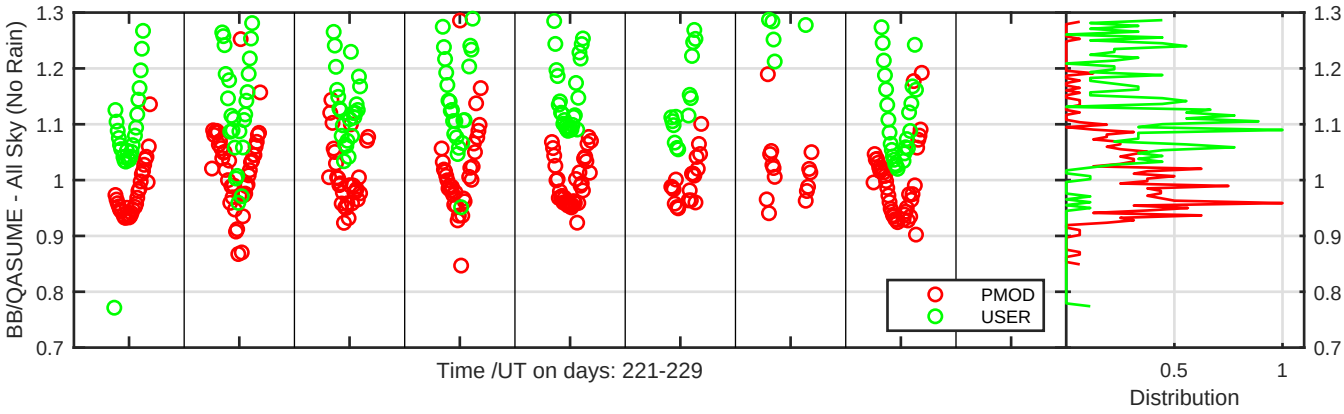

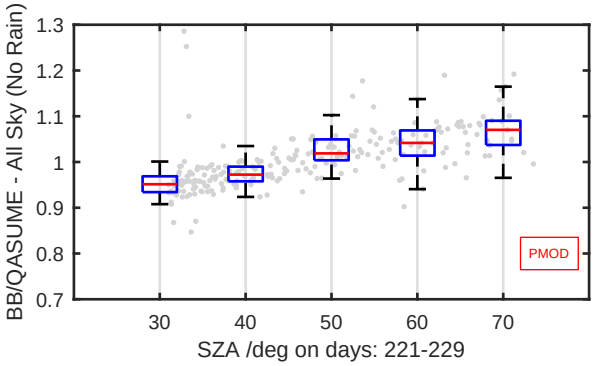

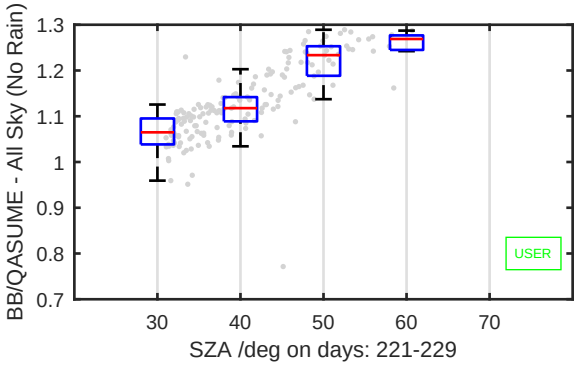

Calibration Results of D3000 (UVE)

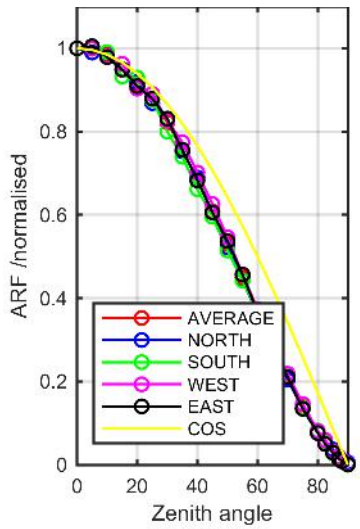

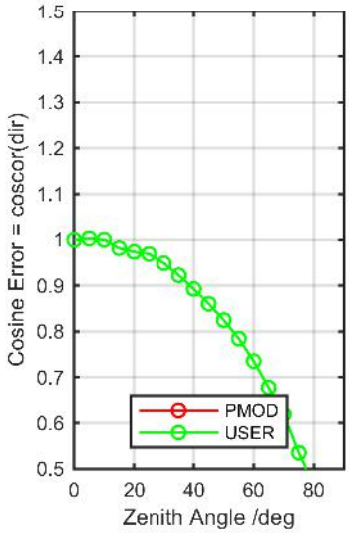

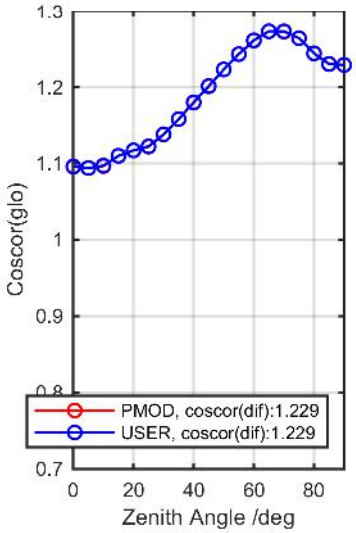

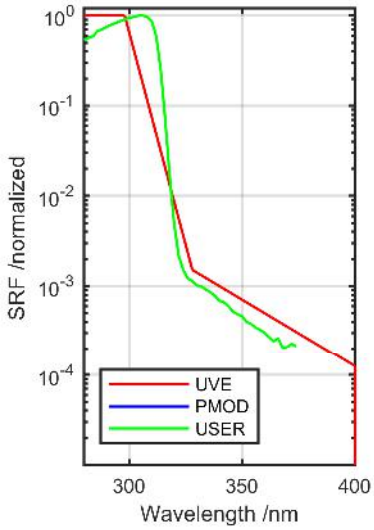

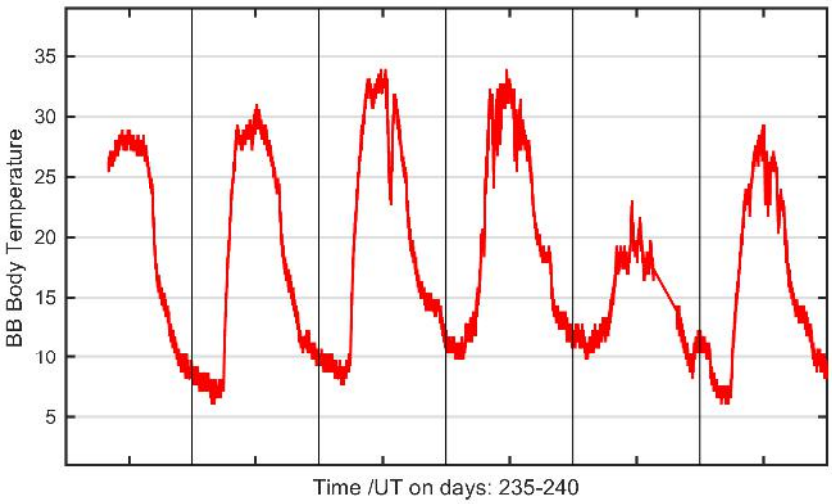

Calibration Matrix fn; Model sdisortREFms2009; f0=0.1485

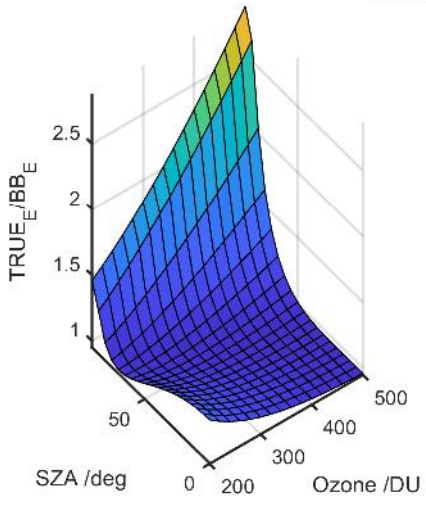

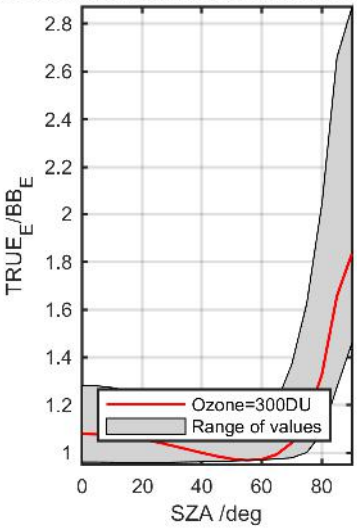

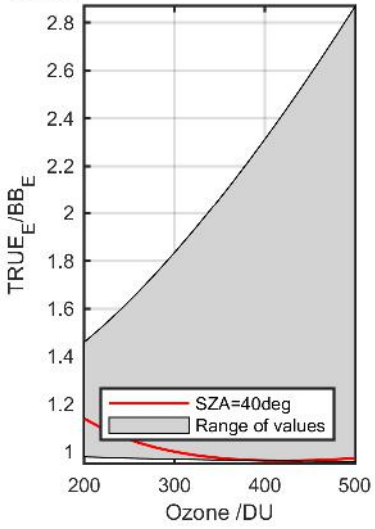

Calibration Results of D3000 (UVE)

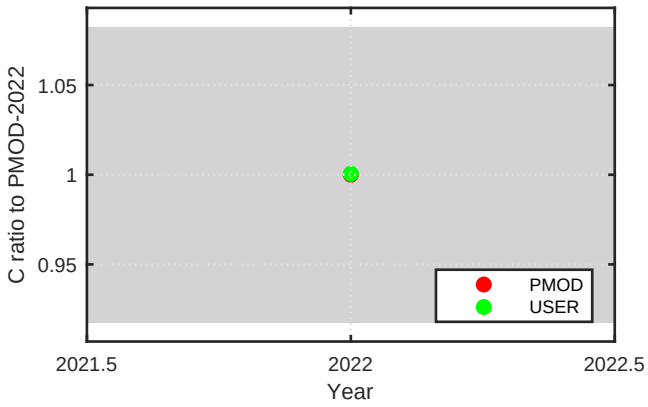

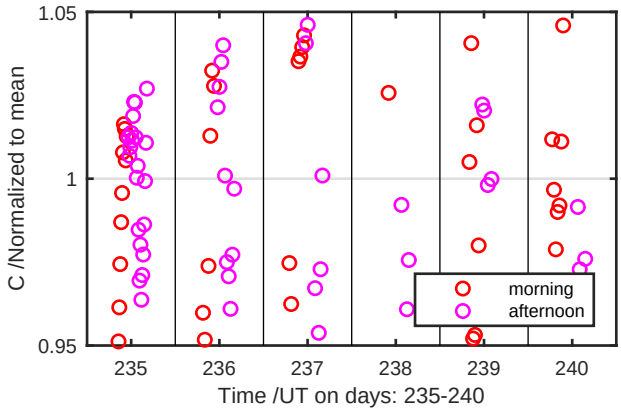

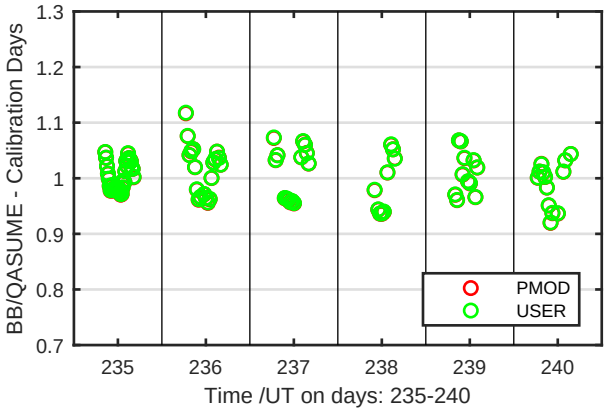

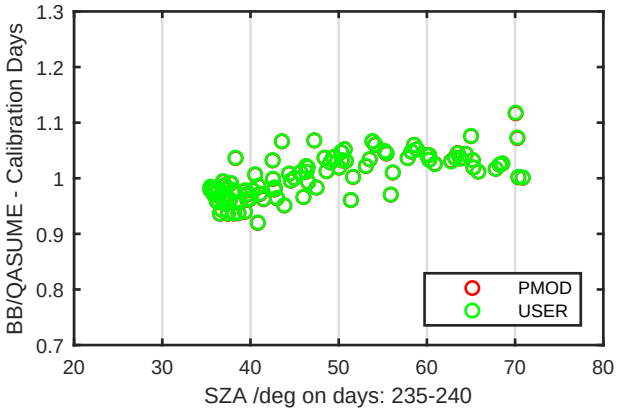

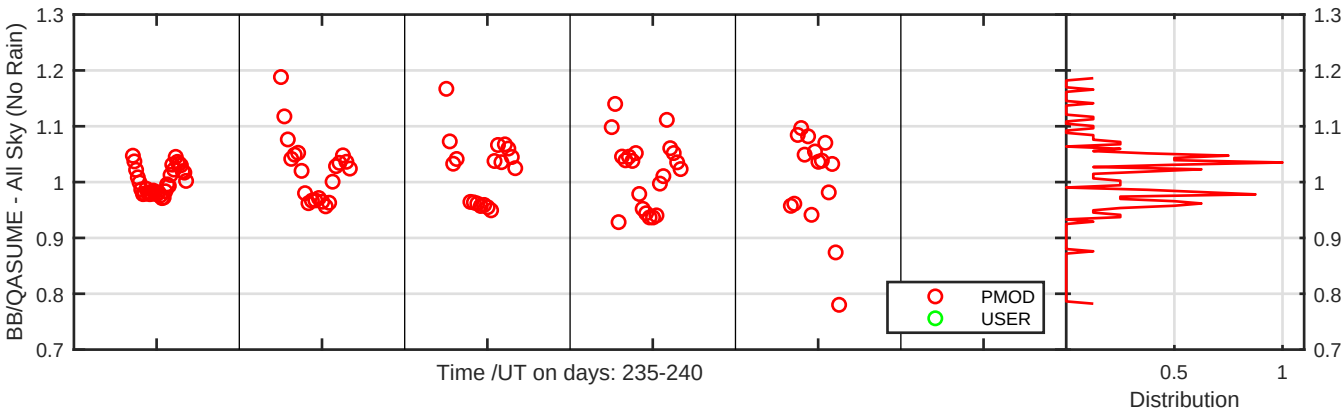

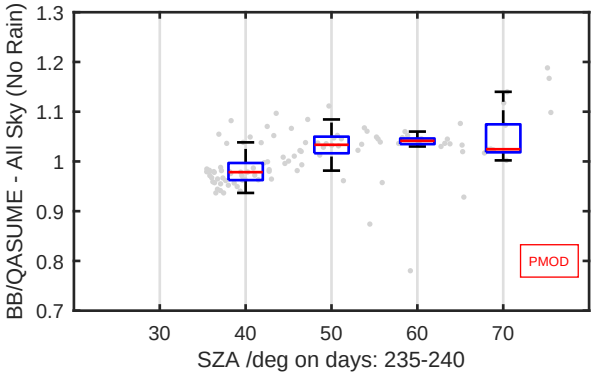

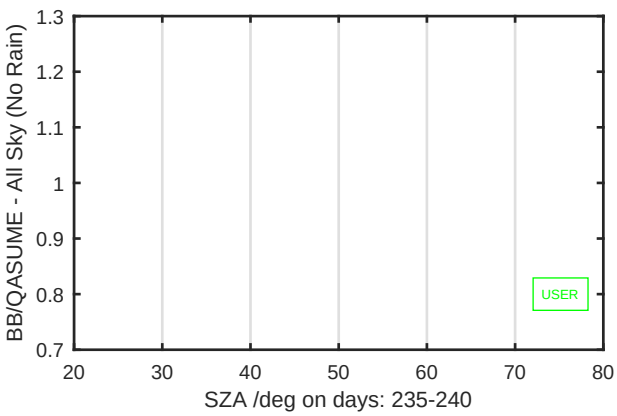

Calibration Results of D3000 (UVA)

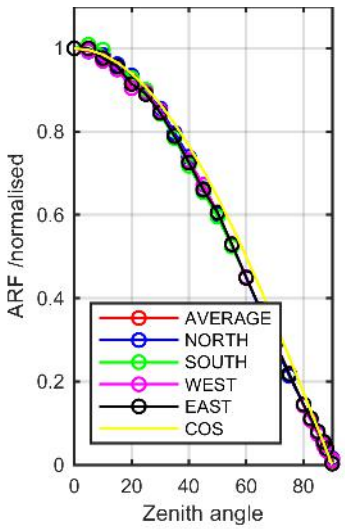

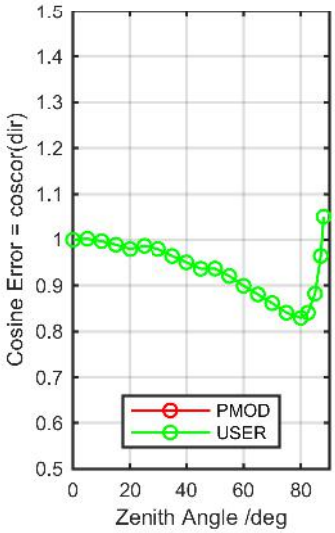

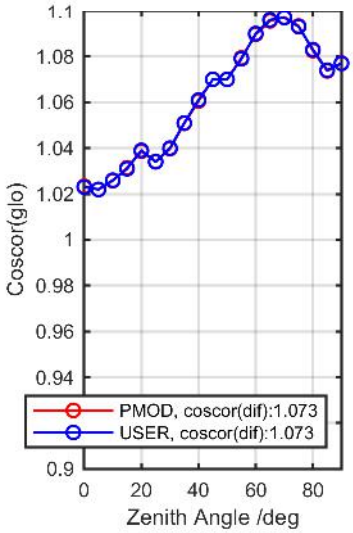

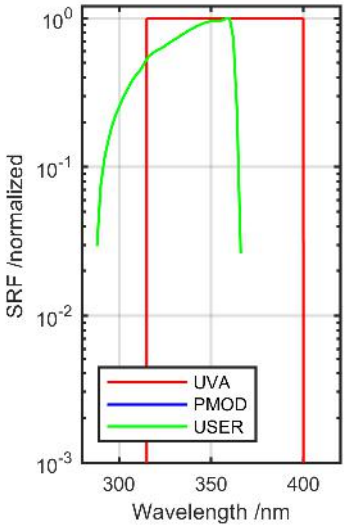

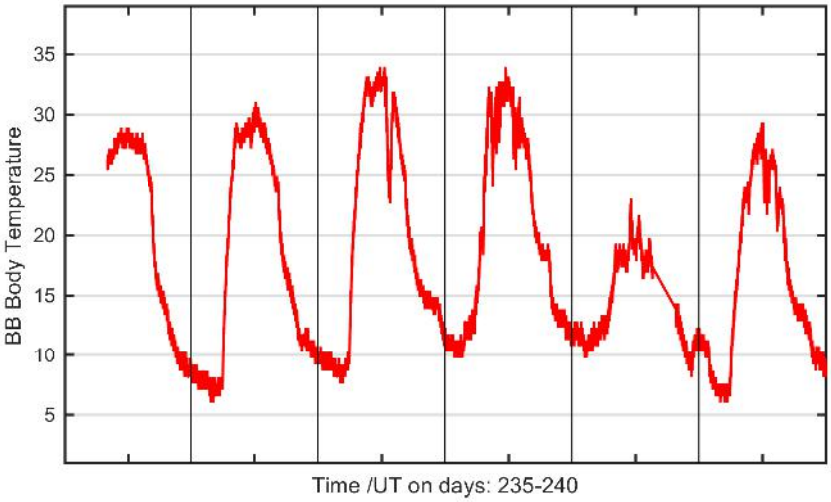

Calibration Matrix fn; Model sdisortREFms2009; f0=2.4524

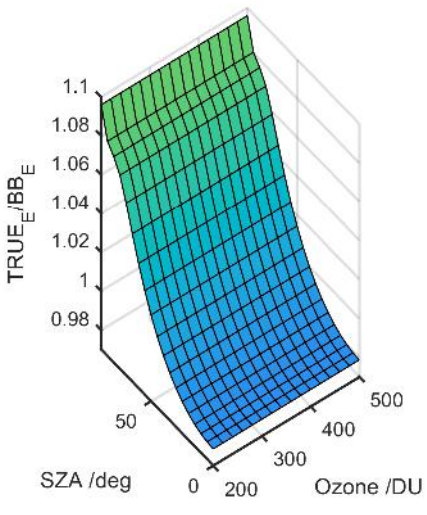

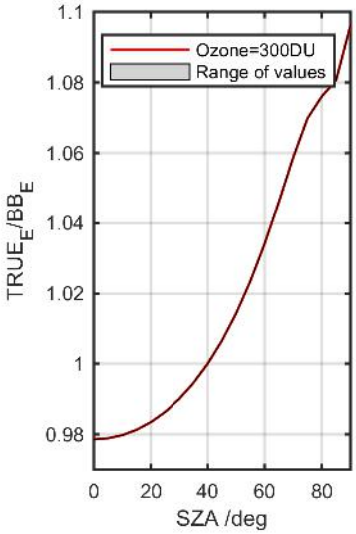

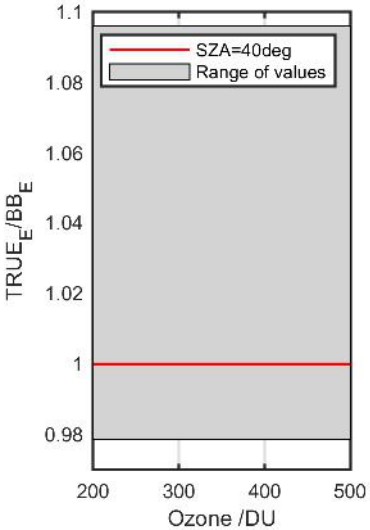

Calibration Results of D3000 (UVA)

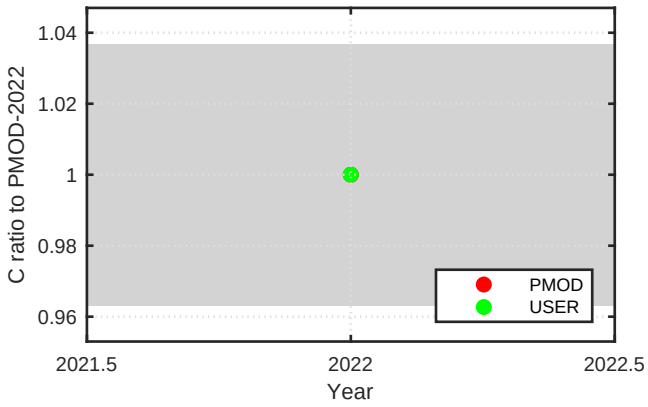

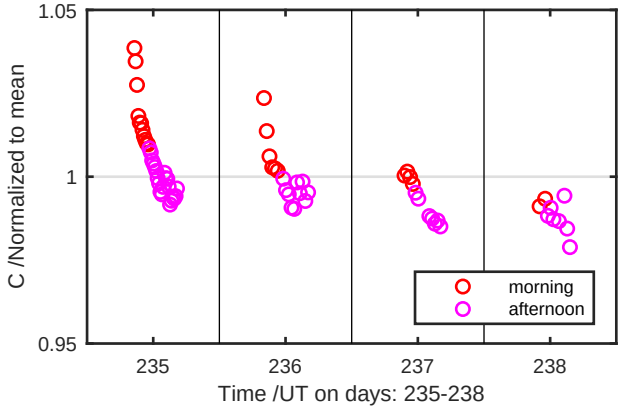

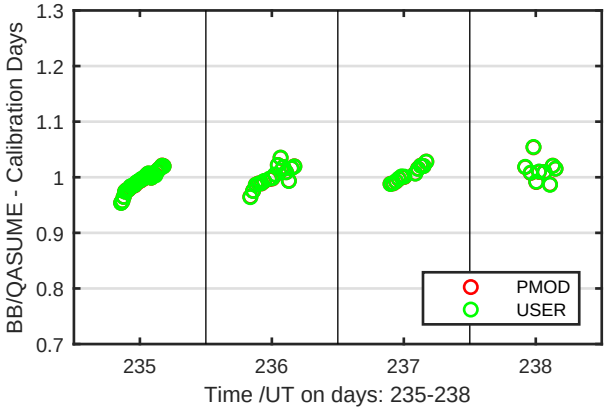

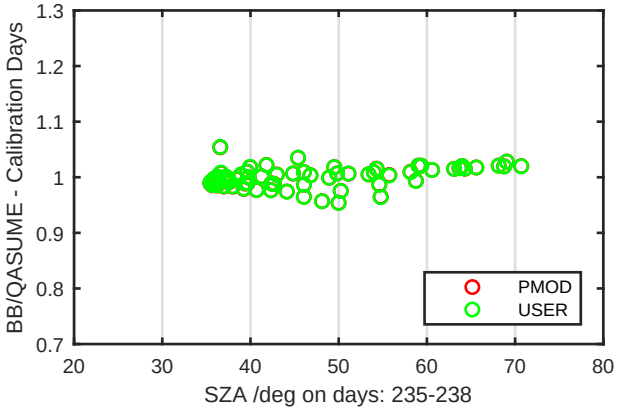

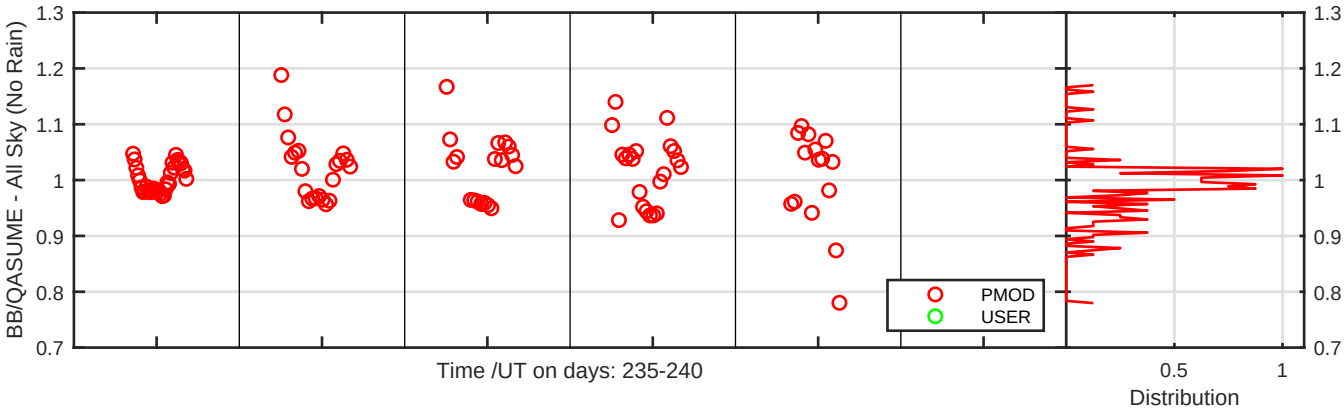

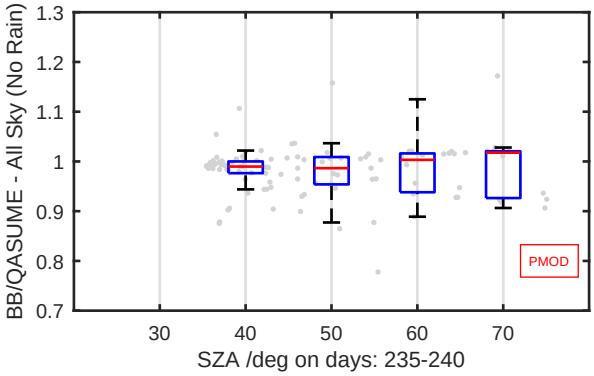

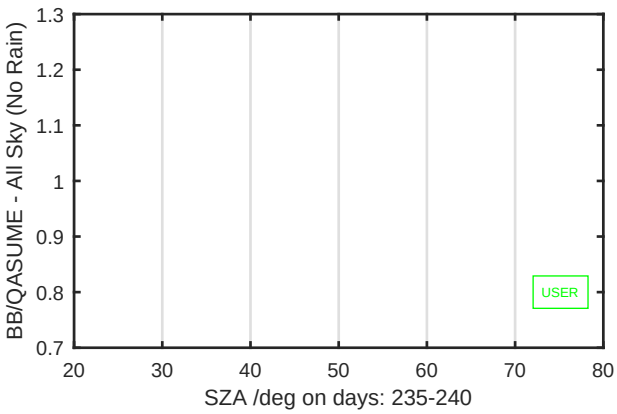

For more information, please contact:

World Meteorological Organization

Science and Innovation Department

7 bis, avenue de la Paix – P.O. Box 2300 – CH 1211 Geneva 2 – Switzerland

Tel.: +41 (0) 22 730 81 11 – Fax: +41 (0) 22 730 81 81

Email: GAW@wmo.int

Website: https://public.wmo.int/en/programmes/global-atmosphere-watch-programme

JN 231052